VOLUME 35 / NUMBER 1 / 1993

Radiocarbon

An International Journal of Cosmogenic Isotope Research

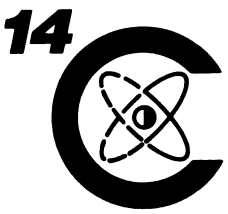

Calibration 1993

Department of Geosciences
The University of Arizona
4717 East Ft. Lowell Road
Tucson, Arizona 85712 USA

ISSN: 0033-8222

ASSOCIATE EDITORS

[RADIOCARBON, VOL. 35, NO. 1, 1993, P. iii]

EDITORIAL COMMENT

This CALIBRATION 1993 volume amends and extends the time series published in the 1986 CALIBRATION ISSUE. Whereas the 1986 issue provided age calibration over nearly 10,000 calibrated (cal) years, the current material more than doubles this age range.

The joint Seattle-Belfast bidecadal, and the Seattle decadal, calibration curves now cover about 8000 cal yr. Minor corrections, explained in the text, had to be applied to previously (1986) published ^{14}C dates of the Belfast and Seattle laboratories. The corrections are in the 10 to 20 ^{14}C-yr range. Most calibration curves are for decadal and bidecadal samples, but finer chronological detail can be found in Pretoria-Groningen (1900–3900 BC) and Seattle (AD 1510–1950) results.

The dendrochronologically dated tree-ring samples in the AD/BC realm cover nearly 10,000 cal yr. The earliest millennia of the German absolute oak chronology are discussed in Hohenheim, Heidelberg and Belfast reports. Heidelberg also reports ^{14}C data for a nearly 1600-yr floating (not connected to the present) pine chronology. A tentative estimate of the gap between the pine and oak chronologies allows the tree-ring chronology to be extended back to 11,400 cal BP.

The tree-ring-derived calibration curves are applicable to samples formed in equilibrium with atmospheric CO_2. To calibrate samples of marine origin, a Seattle curve, derived from the tree-ring information through carbon-reservoir modeling, can be used. A joint Gif sur Yvette/Lamont-Doherty effort allows the continuance of ^{14}C age calibration beyond 11,400 cal yr BP. Here, coral ^{14}C ages and (U/Th) ages are compared, yielding calibration data for the marine environment. As the ^{14}C variations in the oceans are smoothed relative to those in the atmosphere, the inferred approximate atmospheric curve that is obtained by deducting a fixed marine reservoir ^{14}C age from the marine measurements has less century detail than the calibration curve based on tree-ring data. Thus, the calibration of atmospheric samples beyond 10,000 ^{14}C yr is approximate only.

Computerized calibration facilitates age calibration and is discussed in Seattle and Groningen papers. The IBM-compatible computer program, CALIB 3.0, inserted in the back cover, integrates the new data, which can be used for age calibration as well as ^{14}C research. Calibration of decadal and bidecadal atmospheric samples is limited to, respectively, 0–7210 ^{14}C yr BP and 0–18,360 ^{14}C yr BP, whereas the range for marine samples is 460–18,760 ^{14}C yr BP.

To facilitate time-scale calibration by individual researchers, the CALIB 3.0 computer program can be copied freely. A Macintosh version can be obtained from the Quaternary Isotope Laboratory upon request. Proper credit, of course, should be given and the original program should be kept an integral part of this issue. To improve the compatibility of CALIB cal age results with other, existing or future, computerized calibration programs, the use of CALIB data sets is recommended for these programs.

Minze Stuiver

FURTHER EDITORIAL COMMENT

From the vantage point of the *RADIOCARBON* editorial offices, we are well aware of the popularity, and presumed usefulness of the first Radiocarbon Calibration Issue published seven years ago. We continue to receive more requests for this single issue than all other back issues.

Despite the added uncertainty, and often enigmatic calibrated ranges and probability curves, most consumers of ^{14}C data are interested less in "radiocarbon years" than in calendrical years. Radiocarbon calibration schemes were available before the 1986 CALIBRATION ISSUE, which summarized the most recent and best calibration data available at the time. However, like any other technical measurement at the leading edge of possible precision, ^{14}C measurements have their intrinsic uncertainties. CALIBRATION 1993 represents the current state-of-the-art calibration, with improvements, adjustments and extensions. In only a few cases will the user notice minor differences in calibrated results from these new calibrations compared to the 1986 calibrations. The major differences are in the extended calibrated time range and the computer programs for calibration.

Calibration work continues, and this 1993 version is unlikely to be the last one. Anticipated major refinements in the next calibration issue are extensions using datable material other than tree rings, and possibly the confirmation of small regional variations of the ^{14}C calibration.

Austin Long

COVER

The Sun's "rays" were constructed from an 11,000 cal yr residual $\Delta^{14}C$ record (Fig. 11, p. 148). Time (past to present) proceeds clockwise. Approximate cal yr ages of some prominent perturbations (6–3) are, respectively, 8500 BP, 7200 BP, 4800 BP and 2700 BP. The 16th and 18th century Spörer (2) and Maunder (1) $\Delta^{14}C$ maxima complete the recent part of the record.

Design by Minze Stuiver, T. F. Braziunas and Floyd Bardsley.

CONTENTS

[RADIOCARBON, VOL. 35, NO. 1, 1993, P. 1–23]

Radiocarbon

1993

HIGH-PRECISION BIDECADAL CALIBRATION OF THE RADIOCARBON TIME SCALE, AD 1950–500 BC AND 2500–6000 BC

MINZE STUIVER

Department of Geological Sciences and Quaternary Research Center, University of Washington Seattle, Washington 98195 USA

and

GORDON W. PEARSON

Retired from Palaeoecology Centre, The Queen's University of Belfast, Belfast, BT71NN, Northern Ireland

INTRODUCTION

The radiocarbon ages of dendrochronologically dated wood spanning the AD 1950–6000 BC interval are now available for Seattle (10-yr samples, Stuiver & Becker 1993) and Belfast (20-yr samples, Pearson, Becker & Qua 1993; Pearson & Qua 1993). The results of both laboratories were previously combined to generate a bidecadal calibration curve spanning nearly 4500 years (Stuiver & Pearson 1986; Pearson & Stuiver 1986). We now find that minor corrections must be applied to the published data sets, and therefore, give new bidecadal radiocarbon age information for 2500–6000 BC, as well as corrected radiocarbon age averages for AD 1950–500 BC. Corrected average ^{14}C ages for the 500–2500 BC interval are given separately (Pearson & Stuiver 1993). The Seattle corrections (in the 10–30 ^{14}C-yr range) are discussed in Stuiver and Becker (1993), whereas Pearson and Qua (1993) provide information on Belfast corrections (averaging 16 yr). All dates reported here are conventional radiocarbon dates, as defined in Stuiver and Polach (1977). Belfast ^{14}C ages back to 5210 BC were obtained on wood from the Irish oak chronology (Pearson *et al.* 1986). Wood from the German oak chronology (Becker 1993) was used by Belfast for the 5000–6000 BC interval. For the overlapping interval (5000–5210 BC), Belfast reports weighted Irish wood/German wood ^{14}C age averages. The Seattle ^{14}C ages for the AD interval were either on Douglas fir wood from the US Pacific Northwest, or Sequoia wood from California (Stuiver 1982). The BC materials measured in Seattle were mostly part of the German oak chronology. Thirteen samples (5680–5810 BC) from the US bristlecone pine chronology (Ferguson & Graybill 1983) were measured in Seattle as well. Here, the final Seattle decadal ^{14}C ages resulted from averaging German oak and bristlecone pine ages.

Several factors contribute to the uncertainty in the calibration curve for bidecadal cellulose samples. The precision and accuracy of the ^{14}C measuring process is limited, and dendrochronological errors (if any) may result in ^{14}C age differences when materials of different chronologies (and "identical" AD or BC age) are used. And although relatively fast transport in the troposphere causes atmospheric $^{14}CO_2$ to be fairly uniformly mixed near the earth surface, small regional differences remain. General circulation and carbon reservoir model calculations (Braziunas, Fung & Stuiver 1991) predict regional "age" differences of maximally 20 ^{14}C years within the northern hemisphere.

Such inhomogeneity in atmospheric $^{14}CO_2$ alone can induce ^{14}C age offsets on the order of a decade between individual northern hemisphere dendrochronologies.

The Seattle and Belfast results on wood of the same calibrated (cal) age, but not necessarily of the same region, give consistent replication for most of the 8000-yr record. Marginal replication is only encountered for the 5180–5500 BC interval. We first discuss the aspects of replication; detailed calibration curves follow.

SAMPLE AVAILABILITY AND PRETREATMENT

During the earlier phases of the Seattle calibration project, many of the wood samples of AD age were treated with dilute NaOH and HCl solutions to remove resins, sugars and a portion of the lignin (de Vries method, Stuiver & Quay 1980). The samples from the German chronology (and part of our single-year AD Pacific Northwest chronology) were subjected to a more rigorous extraction, yielding alpha cellulose. The cellulose preparation procedure is similar to the ^{13}C sample treatment given in Stuiver, Burk & Quay (1984), with slight modifications due to the bulk of the ^{14}C samples. The de Vries method is less efficient in removing components added after the year of growth, but the influence of the incomplete removal on the ^{14}C ages of the Seattle samples is limited to 2 or 3 ^{14}C years (Stuiver & Quay 1981). All Belfast samples were pretreated to reduce the wood to cellulose (Pearson & Stuiver 1986).

To cover identical bidecades for Belfast and Seattle, we combined pairs of Seattle decadal ^{14}C (weighted mean) to produce appropriate bidecadal results. The sequence is not entirely a rhythmic flow of numbers because there are a few 10-yr gaps in the Belfast bidecadal sequence, some overlapping bidecadal measurements with a 10-yr difference at midpoint, and some missing Seattle and Belfast measurements. Many samples had to be processed, and occasionally, wood was either not available in sufficient quantities (thin rings) for the high-precision ^{14}C measurement, or was lost during sample processing. There are also small differences in midpoint age of the "contemporaneous" 20-yr blocks used for ^{14}C age averaging of up to 2 cal yr. Thus, the listed midpoint cal ages (which are multiples of 10, with exceptions listed below) can differ by up to 1 cal yr from the actual cal age. The following exceptions apply (dates given are midpoints):

AD 1940–1860	Seattle bidecadal data only
AD 1825/AD 1275/AD 1245	Seattle decadal points inserted in Belfast data gaps
AD 1212/AD 1192/AD 952	Averages of bidecades with midpoints 5 yr apart
2450 BC/4150 BC/5150 BC	Belfast data only, as in each case one of the Seattle decadal measurements was missing.

TECHNIQUE AND LABORATORY REPRODUCIBILITY

The radiocarbon community tends to under-report the standard error in a ^{14}C age determination (International Study Group 1982; Scott, Long & Kra 1990). Age errors solely based on the Poisson error in the number of counts accumulated during the ^{14}C activity measurement are lower limits only, and an "error multiplier" K (defined as the actual standard error/quoted standard error) must be applied (*e.g.*, Stuiver 1982). The error multiplier of a specific laboratory may range from 1 to 2 (Scott, Long & Kra 1990). Although the sources of variance are additive (causing K to increase with sample age), K is a convenient expression of the degree to which the quoted error is representative of the overall error in a ^{14}C date.

The quoted standard errors of the Belfast laboratory are based on a study of the parameters contributing to the error in ^{14}C measurements of the liquid scintillation counting system employed (Pearson *et al.* 1986), whereas for Seattle's CO_2 gas counting system, the quoted errors are based on the Poisson standard deviation in the sample count and the largest of 1) the Poisson deviation in the average of multiple standard runs, and 2) the standard deviation from the observed scatter in these multiple runs. Previous replicate analysis of 55 determinations on pairs of wood of the same age yielded $K_{Belfast} = 1.23$ (Pearson *et al.* 1986), whereas the upper limit for $K_{Seattle}$ was estimated at 1.6 (Stuiver & Pearson 1986; Stuiver & Becker 1993).

SYSTEMATIC DIFFERENCES BETWEEN LABORATORIES

Interlaboratory comparisons are needed to identify any offsets, and these lead to independent K information as well. We compared the ^{14}C age results (Kromer *et al.* 1986; Kromer & Becker 1993; de Jong, Becker & Mook 1986; Linick *et al.* 1986; Pearson, Becker & Qua 1993; Pearson & Qua 1993; Stuiver & Becker 1993, Vogel *et al.* 1993) of dendrochronologically dated wood of the same age and different origin, as well as those of the same age and same chronology.

Of the six laboratories involved, three measured either decadal (Tucson and Seattle) or bidecadal samples (Belfast). Groningen, Heidelberg and La Jolla measured samples grown over shorter time intervals (usually 1–3 yr). For comparison purposes, we choose to average the published results over decades or bidecades. Usually only part of the 10 or 20 years will have been measured, and the "decadal" or "bidecadal" ^{14}C ages calculated in this manner need not be identical to the ^{14}C ages that would have been obtained by measuring decadal or bidecadal samples directly. An error multiplier, $K_{Lab\ A\text{-}Lab\ B}$, for interlaboratory comparisons was derived by taking the quotient of the standard deviation, σ_{tot}, in the observed differences and the average standard deviation, σ, of the differences calculated from the quoted errors in the ^{14}C determinations.

A test of internal consistency of ^{14}C data of laboratories measuring wood of the same tree chronology provides insight into the sum total uncertainty tied to procedures of wood allocation, dendro-age determination, sample pretreatment, laboratory ^{14}C determination, regional ^{14}C distribution and ^{14}C differences between individual trees of the same chronology. Often the splitting of samples from wood sections in the dendrochronology laboratories took place several years apart, and wood from identical trees was not necessarily supplied for the same chronology to different ^{14}C laboratories. Here, even the region may be uncertain, because the area of original growth is not well defined for trees collected from alluvial sediments.

Good interlaboratory ^{14}C age agreement (n = number of comparisons, offset = "a" with positive values when Lab A dates are older) is found, *e.g.*, for decadal or bidecadal wood (in some instances, "decadal" or "bidecadal", see above) of the German chronology (Becker 1993) with $K_{Seattle\text{-}Groningen} = 1.8$ and $a = -4 \pm 2$ yr (3210–3910 BC, n = 36), $K_{Seattle\text{-}Pretoria} = 1.2$ and $a = 4 \pm 2$ yr (1930–3350 BC, n = 72), $K_{Seattle\text{-}La\ Jolla} = 1.3$ and $a = -4 \pm 3$ yr (2500–5000 BC, n = 97), and $K_{Seattle\text{-}Belfast} = 1.5$ and $a = -15 \pm 4$ yr (5500–6000 BC, n = 24). Less satisfactory agreement is found in $K_{Seattle\text{-}Belfast} = 1.3$ and $a = -54 \pm 5$ yr (5180–5500 BC, n = 16) and $K_{Seattle\text{-}Heidelberg} = 1.8$ and $a = -41 \pm 4$ yr (4075–5265 BC and 5805–5995 BC, n = 65). The reasons for the larger offsets are, as yet, not well understood.

Comparing decadal or bidecadal ^{14}C dates from the German (measured in Seattle and Belfast) and bristlecone pine (measured in Tucson and Seattle) chronologies for the 5680–5810 BC interval yields excellent agreement with $K_{Seattle\text{-}Seattle} = 1.3$ and $a = -6 \pm 7$ yr (n = 13), $K_{Seattle\text{-}Tucson} = 1.8$ and $a = -3 \pm 7$ yr (n = 15; the 2 additional points are at 6475 and 6360 BC), and $K_{Belfast\text{-}Tucson} = 1.8$ and $a = 6 \pm 7$ (n = 7). A comparison of the joint Northwest Pacific and German chronology measured

in Seattle, and the Irish chronology measured in Belfast, yielded, for bidecadal samples covering the AD 1840–5180 BC interval $K_{Seattle-Belfast} = 1.56$ and $a = 2 \pm 1$ ($n = 344$). The majority of offsets are in the decade (or less) range, and error multipliers for the age differences are 1.8 maximally.

Of crucial importance for the construction of the bidecadal calibration curve are the systematic differences between Seattle and Belfast results for the AD 1840–6000 BC interval. The systematic difference, averaging only -0.8 ± 0.9 yr ($K = 1.7$, $n = 386$) for the full AD 1840–6000 BC interval, can be substantially larger for shorter time units. Systematic differences for successive millennia (first "millennium" is AD 1840–1000, last one 5001–6000 BC) are -0.4 ± 2.3 yr ($K = 1.4$), 0.9 ± 2.6 ($K = 1.4$), 9.9 ± 2.5 ($K = 1.3$), 16.6 ± 2.6 ($K = 1.4$), 2.4 ± 2.4 ($K = 1.8$), -4.3 ± 2.6 ($K = 1.4$), -12.1 ± 2.8 ($K = 1.9$) and -25.2 ± 2.7 ($K = 1.7$). These offsets (applying the corresponding K value) equal, respectively, 0.1, 0.2, 3.0, 4.6, 0.1, 1.2, 2.3 and 5.3 times the standard deviation in the mean. Clearly, the 9.9 (3.0 σ), 16.6 (4.6 σ) and −25.2 (5.3 σ) ^{14}C year offsets are too large to be accounted for solely by statistical considerations of the reproducibility of the measurements. Measurements on four duplicate samples (3130 BC, 3190 BC, 3210 BC and 3230 BC) of the Irish chronology also yielded a substantial offset of 52 ± 8 yr, with Belfast results being older.

Closer inspection of the distribution of the actual ^{14}C age differences of the 3 millennia with statistically unacceptable systematic offsets shows one interval (5180–5500 BC) with substantial Seattle and Belfast ^{14}C age differences ($a = -54 \pm 5$ yr). The offset for the remaining portion of the millennium (5001–5180 BC and 5500–6000 BC) is now -12.2 ± 3.3 yr ($K = 1.5$). This offset equals 2.4 standard deviations of the mean, which is not an abnormally large value. Significant systematic Seattle-Belfast differences are then 9.9 yr (1–1000 BC), 16.6 yr (1001–2000 BC) and −54 yr (5180–5500 BC). The standard deviation given with the calibration curve does not account for offsets. Therefore, for the above intervals, the calibration curve ^{14}C age averages could be subject to systematic errors of, respectively, 5.0, 8.3 and 27 yr. The first two systematic errors are rather insignificant, as they are less than a decade and only a fraction of the curve standard deviation (which averages 12.9 yr). The 27-yr systematic error contribution to the radiocarbon ages of the 5180–5500 BC interval, however, is unacceptably large and warrants further calibration efforts.

CONSTRUCTION OF THE RADIOCARBON AGE CALIBRATION CURVES

When calculating the Seattle-Belfast bidecadal ^{14}C age averages, and their errors, an error multiplier must be assigned to the quoted laboratory error. In our previous papers, we took $K_{Belfast} = 1.23$ and $K_{Seattle} = 1.6$ for results going back to 2500 BC. K tends to increase with sample age (*e.g.*, for the AD 1840–2500 BC interval, $K_{Seattle-Belfast} = 1.44$ ($n = 212$, $a = 7 \pm 1.2$ yr), whereas for the 2500–5000 BC interval, $K_{Seattle-Belfast} = 1.75$ ($n = 124$, $a = -7 \pm 1.6$)). Thus, we selected a larger K value of 1.7 for both Seattle and Belfast for samples older than 2500 BC. A more detailed discussion of this choice can be found elsewhere (Stuiver & Pearson 1992).

The above K values, multiplied with the quoted standard deviation, yield corrected standard deviations (σ) for the individual Belfast and Seattle ^{14}C ages. Using these standard deviations, we find that the calculated standard deviations of the ^{14}C age differences of contemporaneous bidecadal sample pairs of Seattle and Belfast account for 90–100% of the demonstrated standard deviations in ^{14}C age differences of both laboratories for the AD 1940–5180 BC and 5500–6000 BC intervals. The standard deviations of the weighted average ^{14}C ages (Table 1) of sample pairs that form the basis of the ^{14}C calibration curve are based on the above K-corrected standard deviations.

The mean standard deviation of the bidecadal averages of Seattle and Belfast is 12.9 (± 1.6‰ for $\Delta^{14}C$) ^{14}C yr for the AD 1950–6000 BC interval. The standard deviations of the ^{14}C ages associated

with the 5180–5500 BC interval do not fully account for the total uncertainty, as systematic error contributions play a role for this part of the calibration curve (see previous section).

CALIBRATION INSTRUCTIONS

We recommend that users of ^{14}C dates obtain additional information on reproducibility (and systematic error, if any) from the laboratory reporting the ^{14}C date. This information should lead to a realistic standard deviation in the reported age. A systematic error has to be deducted from, or added to, the reported radiocarbon age prior to age calibration.

Only the calibration curve is given in Figure 1; the one-sigma (1σ; standard deviation) uncertainty in the curve is not given. The actual standard deviation (averaging 12.9 ^{14}C yr for the nearly 8000 cal yr bidecadal calibration curve of Seattle-Belfast ^{14}C age averages) is tabulated in Table 1 for each bidecadal midpoint.

Cal BP ages are relative to the year AD 1950, with 0 cal BP equal to AD 1950. The relationship between cal AD/BC and cal BP ages is cal BP = 1950–cal AD, and cal BP = 1949 + cal BC. The switch from 1950 to 1949 when converting BC ages is caused by the absence of the year zero in the AD/BC chronology.

The conversion of a ^{14}C age to a cal age is as follows: 1) draw line A parallel to the bottom axis through the ^{14}C age to be converted; 2) draw vertical line(s) through the intercept(s) of line A and the calibration curve. The cal AD/BC ages can be read at the bottom axis, the cal BP ages at the top.

To convert the standard error in the ^{14}C age into a range of cal AD/BC (BP) ages, determine the sample standard deviation, σ, by multiplying the quoted laboratory standard deviation with the "error multiplier." Unfortunately, information on error multipliers is often lacking. Here, the ^{14}C age user should refer to K values given above, or to Scott, Long & Kra (1990).

Once the sample σ is known, the curve σ should be read from Table 1. The curve σ and sample σ should then be used to calculate total $\sigma = ((\text{sample } \sigma)^2 + (\text{curve } \sigma)^2)^{1/2}$ (Stuiver 1982). Lines parallel to A should now be drawn through the ^{14}C age + total σ, and ^{14}C age – total σ value. The vertical lines drawn through the intercepts now yield the outer limits of possible cal AD/BC (cal BP) ages that are compatible with the sample standard deviation.

The conversion procedure yields 1) single or multiple cal AD/BC (BP) ages that are compatible with a certain ^{14}C age, and 2) the range(s) of cal ages that correspond(s) to the standard deviation in the ^{14}C age (and calibration curve). Here, the user must determine the calibrated ages from Figure 1 graphs by drawing lines, whereas an alternate approach would be to use the computerized calibration (CALIB) program discussed elsewhere in this issue (Stuiver & Reimer 1993).

The probability that a certain cal age is the actual sample age may be quite variable within the cal age range. Higher probabilities are encountered around the intercept ages. The non-linear transform of a near-Gaussian distribution around a ^{14}C age into cal AD/BC (cal BP) age is not a simple matter, and computer programs are needed to derive the complex probability distribution. The CALIB program incorporates such probability distributions.

The calibration data presented here are valid for northern hemispheric samples that were formed in equilibrium with atmospheric $^{14}CO_2$. Systematic age differences are possible for the southern hemisphere, where ^{14}C ages of wood samples tend to be about 40 yr older (Vogel *et al.* 1993). Thus, ^{14}C ages of southern hemispheric samples preceding our era of fossil-fuel combustion should be reduced by 40 yr before conversion into cal AD/BC (BP) ages.

The Figure 1 calibration points are the midpoints of wood samples spanning 20 yr. Samples submitted for dating may cover shorter or longer intervals. The decadal calibration results of the Seattle laboratory (Stuiver & Becker 1993; Stuiver & Reimer 1993) provide a better time resolution, whereas the CALIB program also has an option to use Figure 1 moving averages (*e.g.*, a 5-point or 100-yr moving average of the bidecadal curve). The latter should be used for a sample grown over a 100-yr interval. Samples formed over intervals longer than a decade or bidecade are very desirable, as the ^{14}C "wiggles" of the calibration curve have lesser influence on the (midpoint) cal age when a smoothed (moving average) calibration curve is used (Stuiver 1992).

The calibration curve is only valid for age conversion of samples that were formed in equilibrium with atmospheric CO_2. Conventional ^{14}C ages of materials not in equilibrium with atmospheric reservoirs do not take into account the offset in ^{14}C age that may occur (Stuiver & Polach 1977). An offset, or reservoir deficiency, must be deducted from the reported ^{14}C age before any attempt can be made to convert to cal AD/BC (BP) ages.

The reservoir deficiency is time dependent for the mixed (and deep) layer of the ocean. For the calibration of marine samples, the reader is referred to Stuiver and Braziunas (1993) and, of course, the CALIB program.

ACKNOWLEDGMENTS

The ^{14}C research at Seattle and Belfast was supported, respectively, by a National Science Foundation grant BNS-9004492 and a SERC grant. We thank Dr. B. Becker of the University of Hohenheim, Stuttgart for providing German oak (unified Donau/Main series) samples, Drs. J. R. Pilcher and M. G. Baillie for wood samples of the Irish chronology, and F. Qua, P. J. Reimer and P. J. Wilkinson for crucial technical and analytical support.

REFERENCES

Becker, B. 1993 A 11,000-year German oak and pine dendrochronology for radiocarbon calibration. *Radiocarbon*, this issue.

Braziunas, T. F., Fung, I. Y. and Stuiver, M. 1991 Oceanic and solar forcing of natural geographic variations in atmospheric $\Delta^{14}C$. Abstract. *Radiocarbon* 33(2): 180.

de Jong, A. F. M., Becker, B. and Mook, W. G. 1986 High-precision calibration of the radiocarbon time scale. *In* Stuiver, M. and Kra, R. S., eds., Proceedings of the 12th International Radiocarbon Conference. *Radiocarbon* 28(2B): 939–942.

Ferguson, C. W. and Graybill, D. A. 1983 Dendrochronology of bristlecone pine: A progress report. *In* Stuiver, M. and Kra, R. S., eds., Proceedings of the 11th International Radiocarbon Conference. *Radiocarbon* 25(2): 287–288.

International Study Group 1982 An inter-laboratory comparison of radiocarbon measurements in tree rings. *Nature* 298: 619–623.

Kromer, B. and Becker, B. 1993 German oak and pine ^{14}C calibration, 7200–9400 BC. *Radiocarbon*, this issue.

Kromer, B., Rhein, M., Bruns, M., Schoch-Fischer, H., Münnich, K. O., Stuiver, M. and Becker, B. 1986 Radiocarbon calibration data for the 6th to the 8th millennia BC. *In* Stuiver, M. and Kra, R. S., eds., Proceedings of the 12th International Radiocarbon Conference. *Radiocarbon* 28(2B): 954–960.

Linick, T. W., Long, A., Damon, P. E. and Ferguson, C. W. 1986 High-precision radiocarbon dating of bristlecone pine from 6554 to 5350 BC. *In* Stuiver, M. and Kra, R. S., eds., Proceedings of the 12th International Radiocarbon Conference. *Radiocarbon* 28(2B): 943–953.

Pearson, G. W., Becker, B. and Qua, F. 1993 High-precision ^{14}C measurement of German and Irish oaks to show the natural ^{14}C variations from 7890 to 5000 BC. *Radiocarbon*, this issue.

Pearson, G. W., Pilcher, J. R., Baillie, M. G. L., Corbett, D. M. and Qua, F. 1986 High-precision ^{14}C measurement of Irish Oaks to show the natural ^{14}C variations from AD 1840–5210 BC. *In* Stuiver, M. and Kra, R. S., eds., Proceedings of the 12th International Radiocarbon Conference. *Radiocarbon* 28(2B): 911–934.

Pearson, G. W. and Qua, F. 1993 High-precision ^{14}C measurement of Irish oaks to show the natural ^{14}C variations from AD 1840–5000 BC – A correction. *Radiocarbon*, this issue.

Pearson, G. W. and Stuiver, M. 1986 High-precision calibration of the radiocarbon time scale, 500–2500

BC. *In* Stuiver, M. and Kra, R. S., eds., Proceedings of the 12th International Radiocarbon Conference. *Radiocarbon* 28(2B): 839–862.

Pearson, G. W. and Stuiver, M.1993 High-precision bidecadal calibration of the radiocarbon time scale, 500–2500 BC. *Radiocarbon*, this issue.

Scott, E. M., Long, A. and Kra, R., eds., 1990 Proceedings of the International Workshop on Intercomparison of Radiocarbon Laboratories. *Radiocarbon* 32(3): 253–397.

Stuiver, M. 1982 A high-precision calibration of the AD radiocarbon time scale. *Radiocarbon* 24(1): 1–26.

_____1992 How accurate are our chronologies of the past? I: Time warps caused by the transformation of ^{14}C ages. *Proceedings of the Dahlem Workshop on Global Changes in the Perspective of the Past.* Chichester, John Wiley & Sons, in press.

Stuiver, M. and Becker, B. 1993 High-precision decadal calibration of the radiocarbon time scale AD 1950–6000 BC. *Radiocarbon*, this issue.

Stuiver, M. and Braziunas, T. F. 1993 Modeling radiocarbon ages of marine samples back to 10,000 BC. *Radiocarbon*, this issue.

Stuiver, M., Burk, R. L. and Quay, P. D. 1984 $^{13}C/^{12}C$ ratios in tree rings and the transfer of biospheric carbon to the atmosphere. *Journal of Geophysical Research* 89: 11,731–11,748.

Stuiver, M. and Pearson, G. W. 1986 High-precision calibration of the radiocarbon time scale, AD 1950–500 BC. *In* Stuiver, M. and Kra, R. S., eds., Proceedings of the 12th International Radiocarbon Conference. *Radiocarbon* 28(2B): 805–838.

_____1992 Calibration of the radiocarbon time scale 2500–5000 BC. *In* Taylor, R. E., Long, A. and Kra, R. S., eds., *Radiocarbon After Four Decades: An Interdisciplinary Perspective.* New York: Springer Verlag: 19–33.

Stuiver, M. and Polach, H. 1977 Discussion: Reporting of ^{14}C data. *Radiocarbon* 19(3): 355–363.

Stuiver, M. and Quay, P. D. 1980 Changes in atmospheric carbon-14 attributed to a variable Sun. *Science* 207: 11–19.

_____1981 Atmospheric ^{14}C changes resulting from fossil fuel CO_2 release and cosmic ray flux variability. *Earth and Planetary Science Letters* 53: 349–362.

Stuiver, M. and Reimer, P. J. 1993 Extended ^{14}C data base and revised CALIB radiocarbon age calibration program. *Radiocarbon*, this issue.

Vogel, J. C., Fuls, A., Visser, E. and Becker, B. 1993 Pretoria calibration curve for short-lived samples, 1930–3350 BC. *Radiocarbon*, this issue.

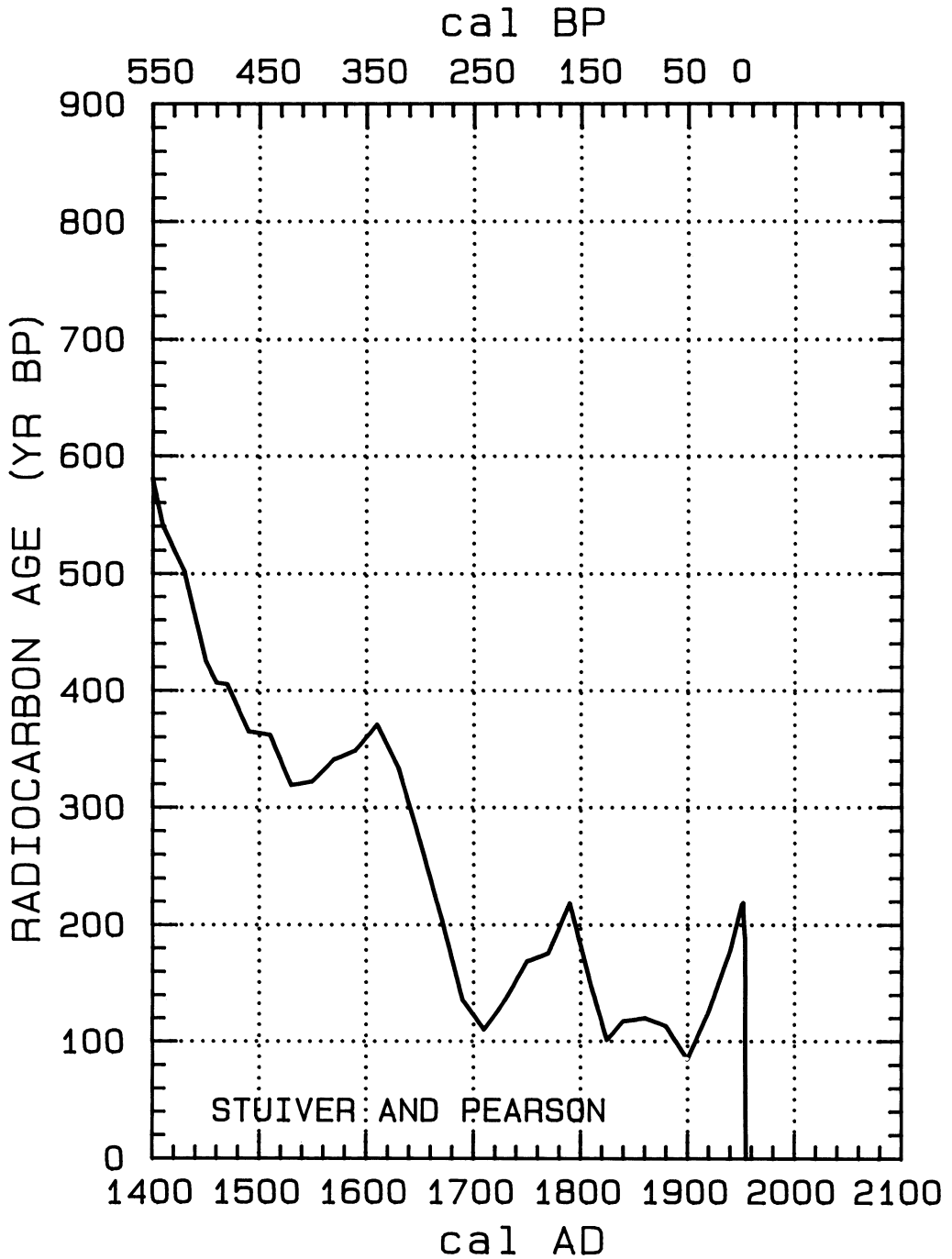

Fig. 1A–L. ^{14}C calibration curve derived from bidecadal samples, with single-year AD 1951–1954 data added to complete the pre-nuclear bomb era

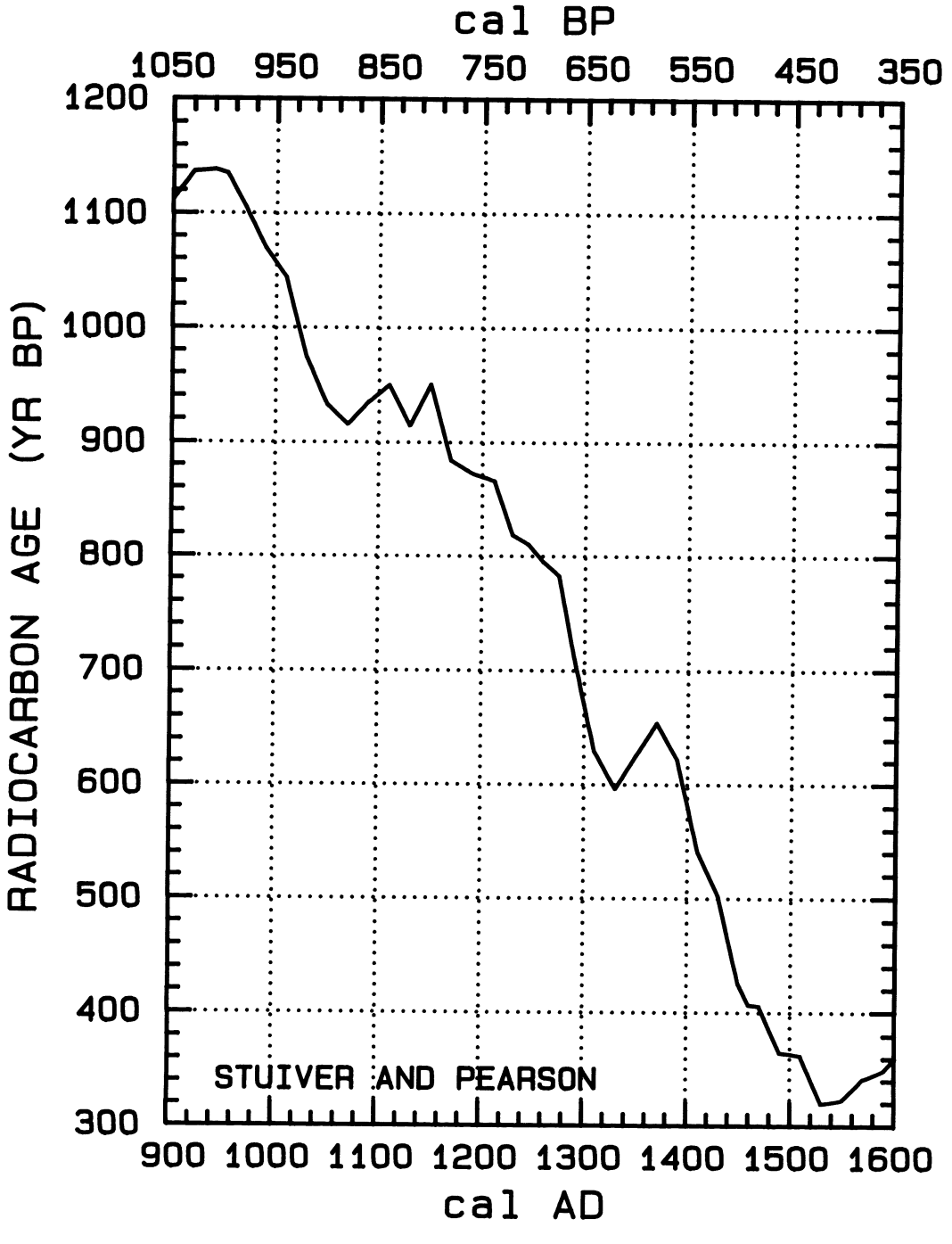
cal BP
1050 950 850 750 650 550 450 350
1200
1100
1000
900
800
700
600
500
400
300
RADIOCARBON AGE (YR BP)
STUIVER AND PEARSON
900 1000 1100 1200 1300 1400 1500 1600
cal AD

Fig. 1B

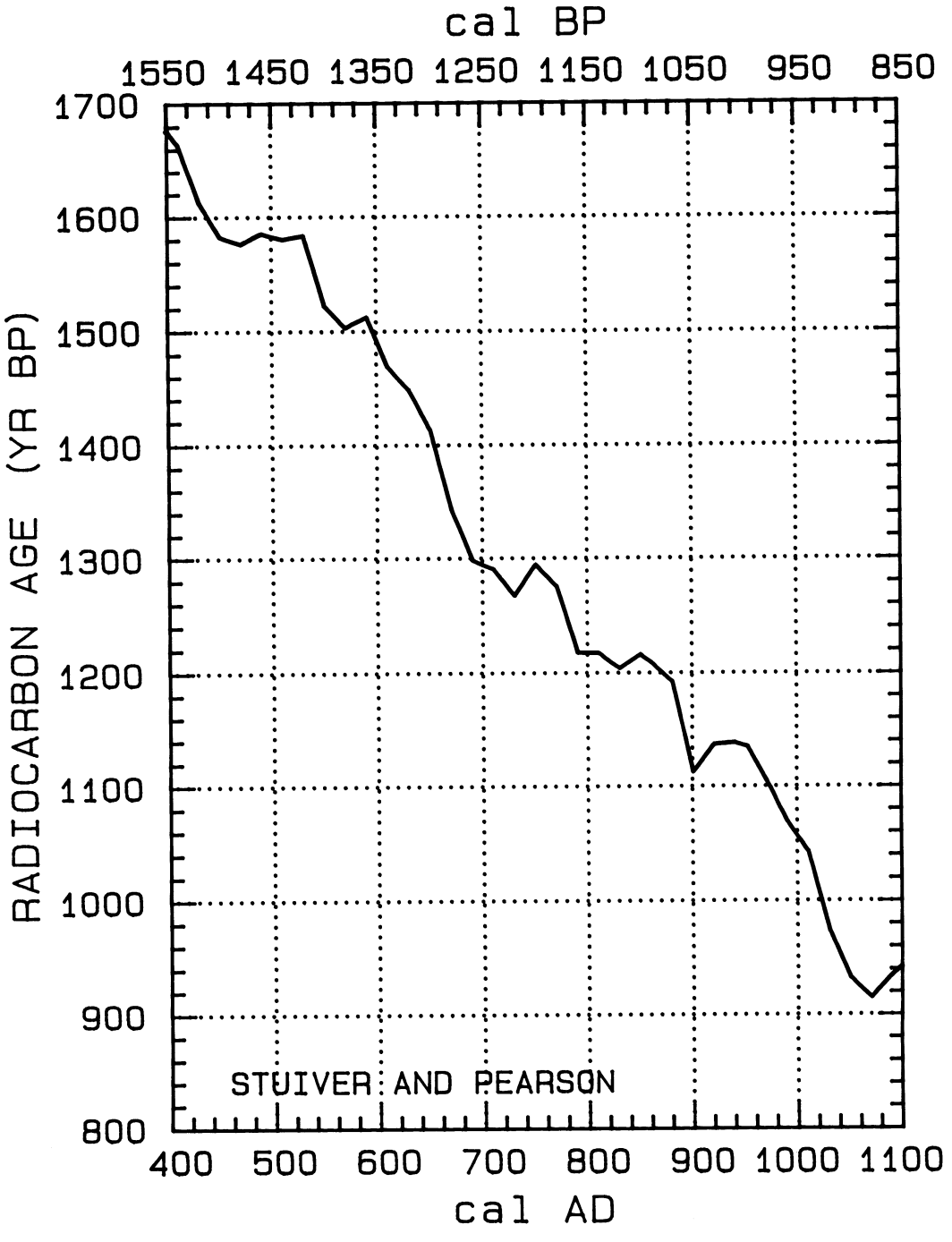
cal BP
1550 1450 1350 1250 1150 1050 950 850
1700
1600
1500
1400
1300
1200
1100
1000
900
800
RADIOCARBON AGE (YR BP)
STUIVER AND PEARSON
400 500 600 700 800 900 1000 1100
cal AD

Fig. 1C

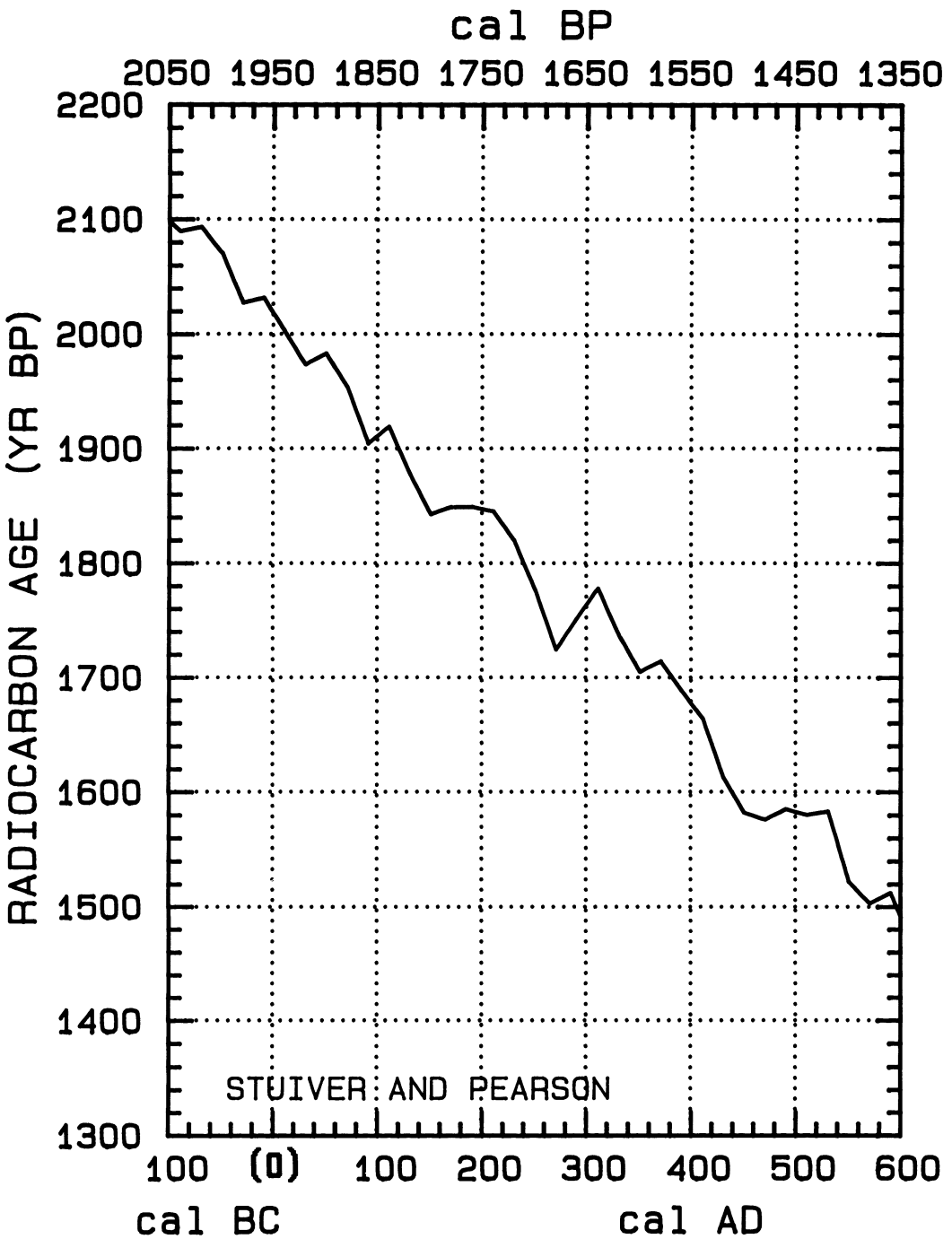
cal BP
2050 1950 1850 1750 1650 1550 1450 1350
2200
2100
2000
1900
1800
1700
1600
1500
1400
1300
RADIOCARBON AGE (YR BP)
STUIVER AND PEARSON
100 (0) 100 200 300 400 500 600
cal BC
cal AD

Fig. 1D

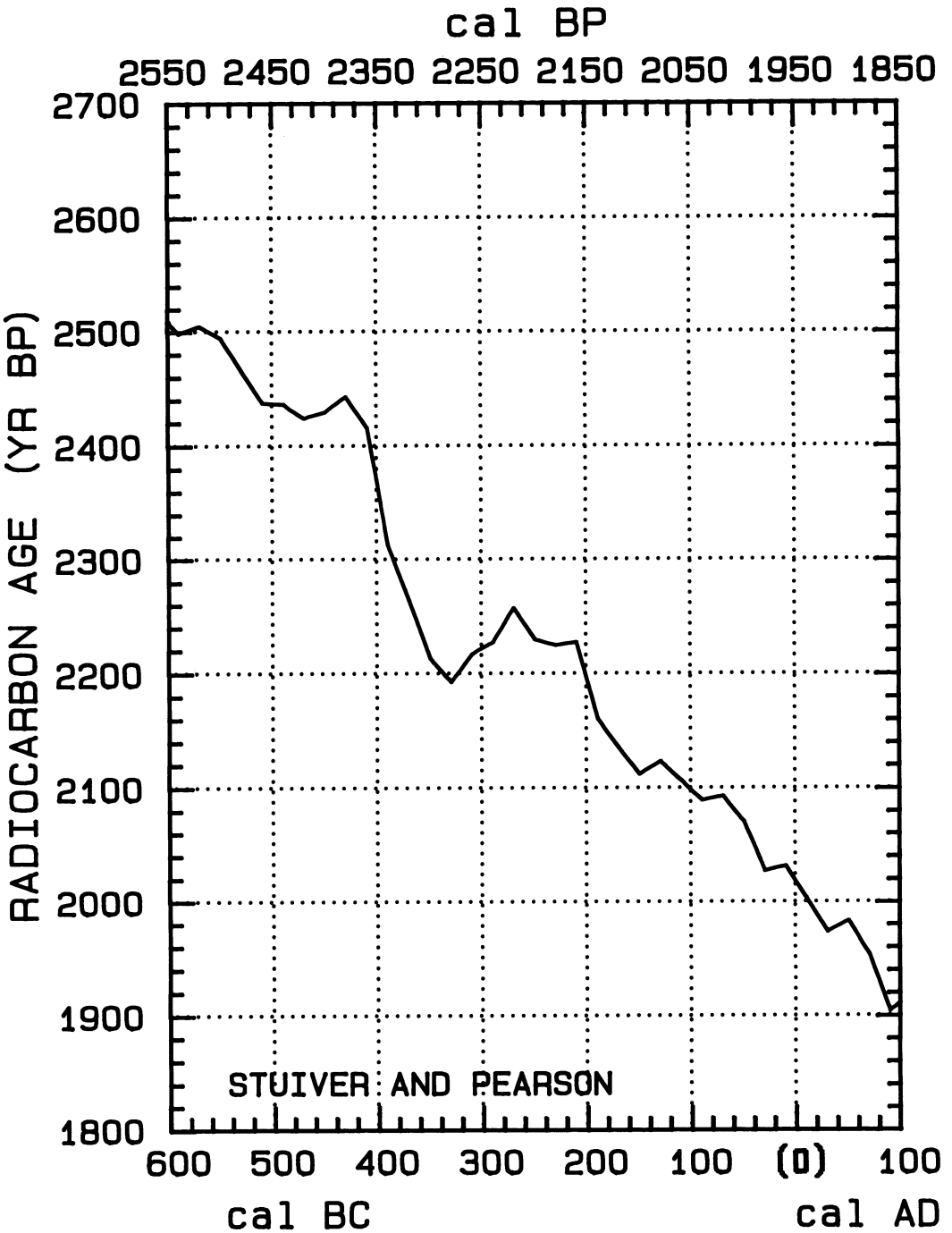
cal BP
2550 2450 2350 2250 2150 2050 1950 1850
2700
2600
2500
2400
2300
2200
2100
2000
1900
1800
RADIOCARBON AGE (YR BP)
STUIVER AND PEARSON
600 500 400 300 200 100 (0) 100
cal BC
cal AD

Fig. 1E

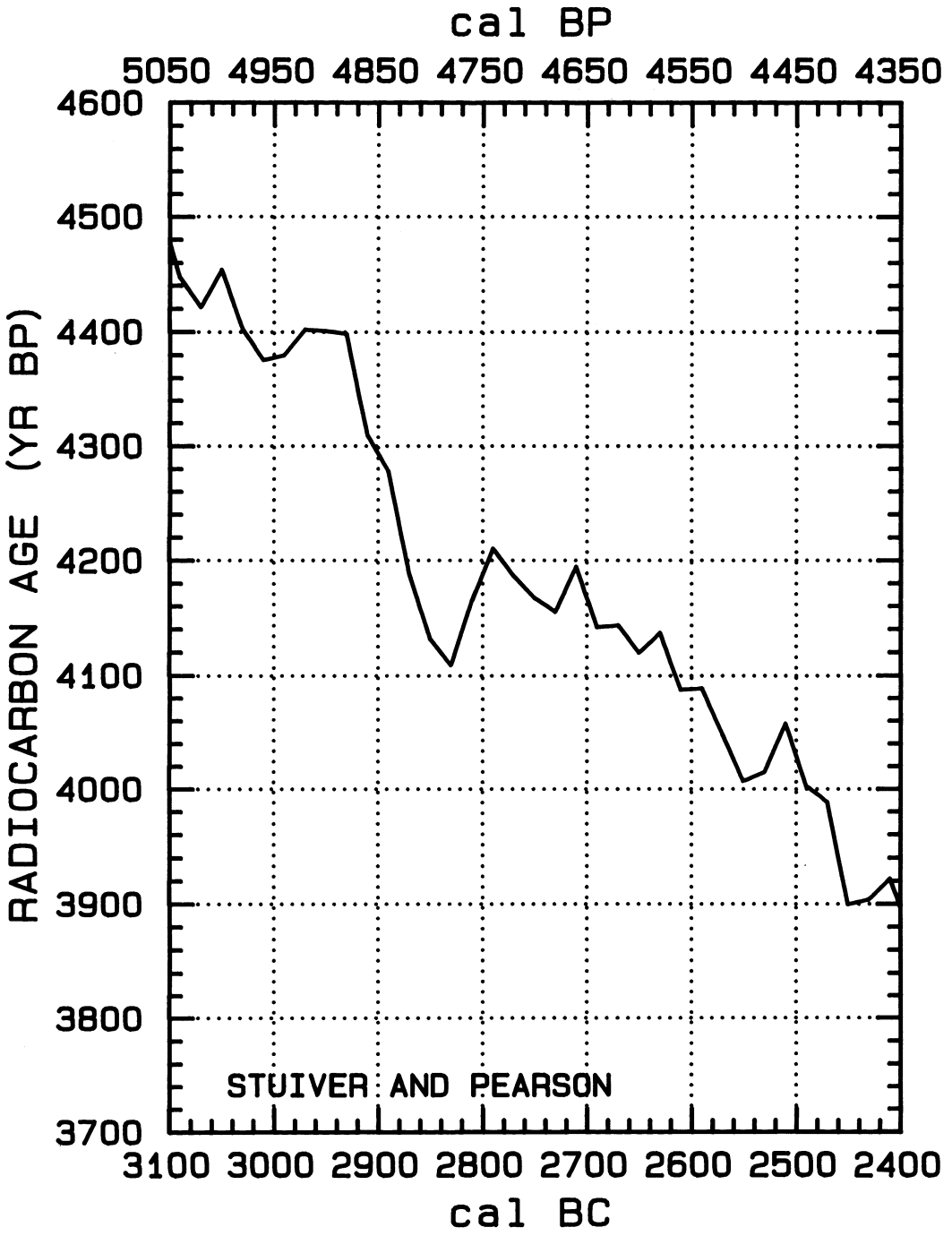
cal BP
5050 4950 4850 4750 4650 4550 4450 4350
4600
4500
4400
4300
4200
4100
4000
3900
3800
3700
RADIOCARBON AGE (YR BP)
STUIVER AND PEARSON
3100 3000 2900 2800 2700 2600 2500 2400
cal BC

Fig. 1F

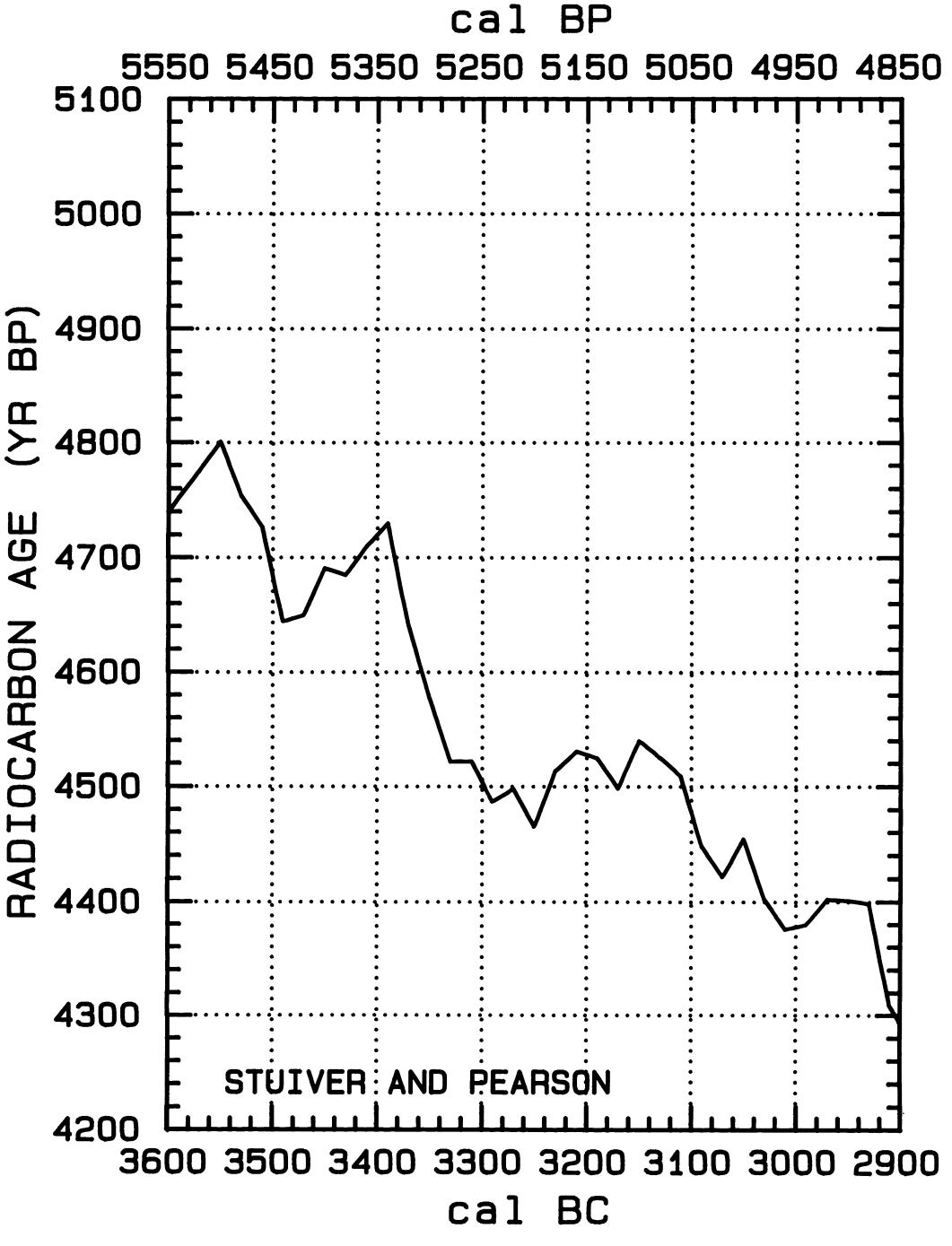
cal BP
5550 5450 5350 5250 5150 5050 4950 4850
5100
5000
4900
4800
4700
4600
4500
4400
4300
4200
RADIOCARBON AGE (YR BP)
STUIVER AND PEARSON
3600 3500 3400 3300 3200 3100 3000 2900
cal BC

Fig. 1G

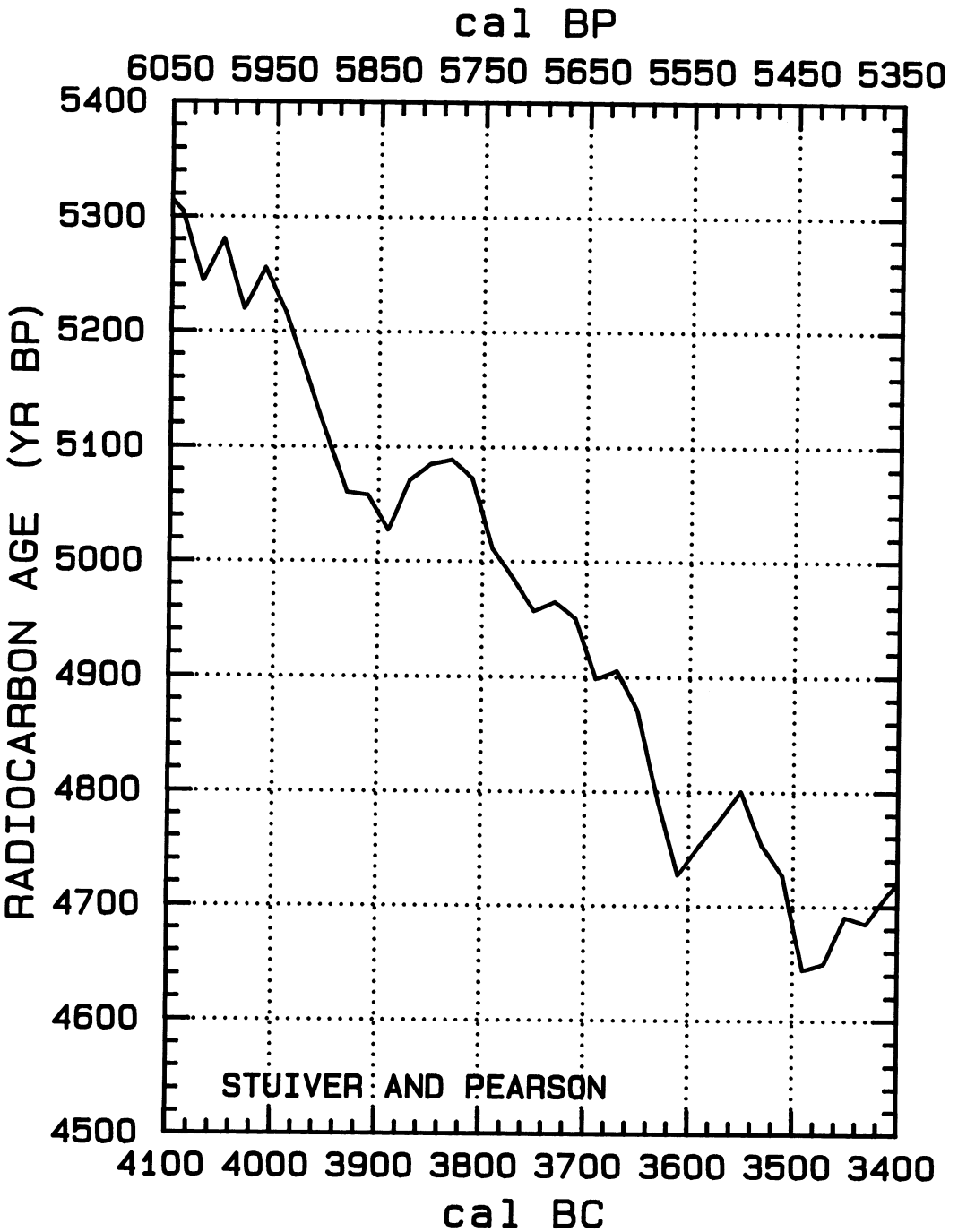
cal BP
6050 5950 5850 5750 5650 5550 5450 5350
5400
5300
5200
5100
5000
4900
4800
4700
4600
4500
RADIOCARBON AGE (YR BP)
STUIVER AND PEARSON
4100 4000 3900 3800 3700 3600 3500 3400
cal BC

Fig. 1H

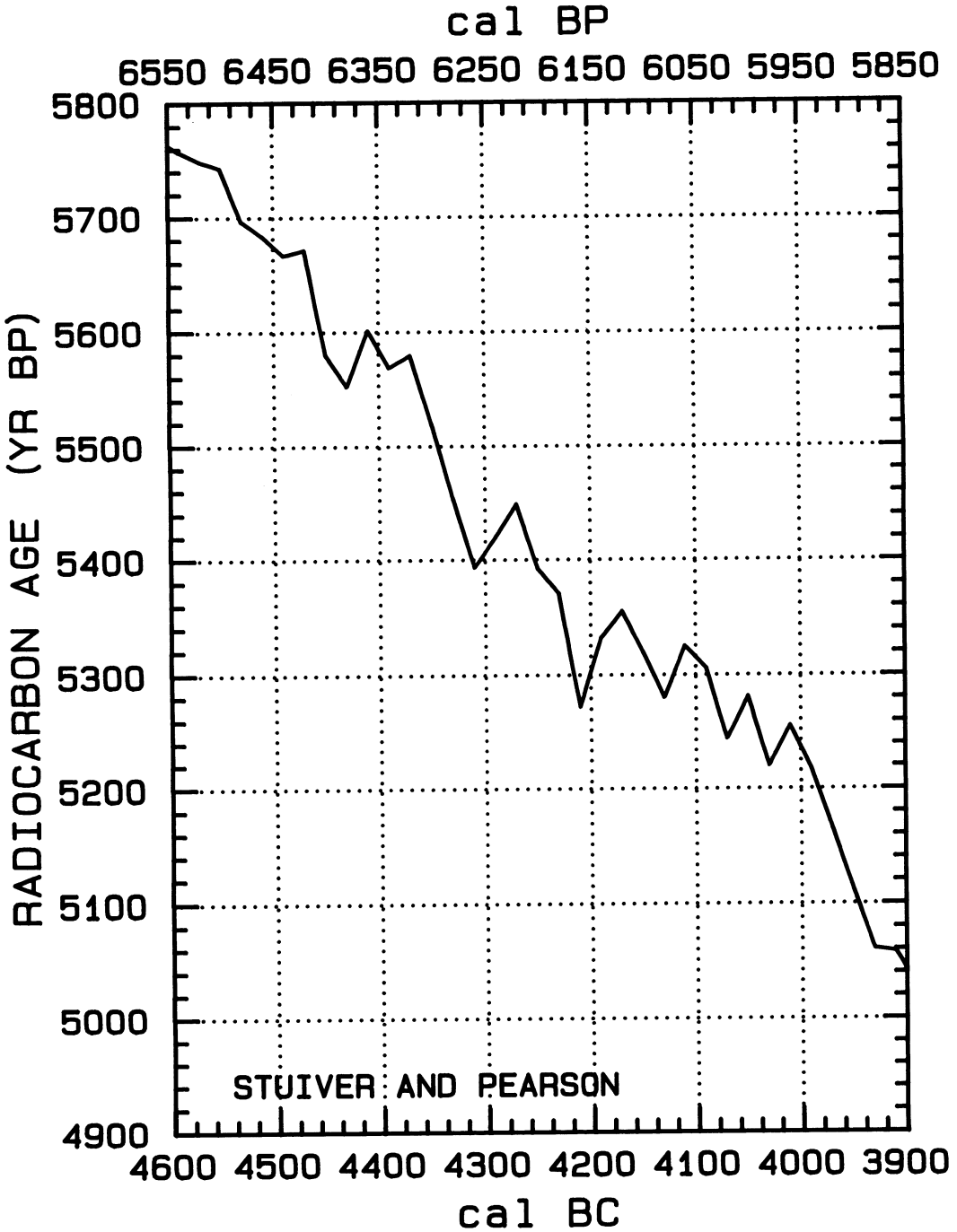
cal BP
6550 6450 6350 6250 6150 6050 5950 5850
5800
5700
5600
5500
5400
5300
5200
5100
5000
4900
RADIOCARBON AGE (YR BP)
STUIVER AND PEARSON
4600 4500 4400 4300 4200 4100 4000 3900
cal BC

Fig. 1I

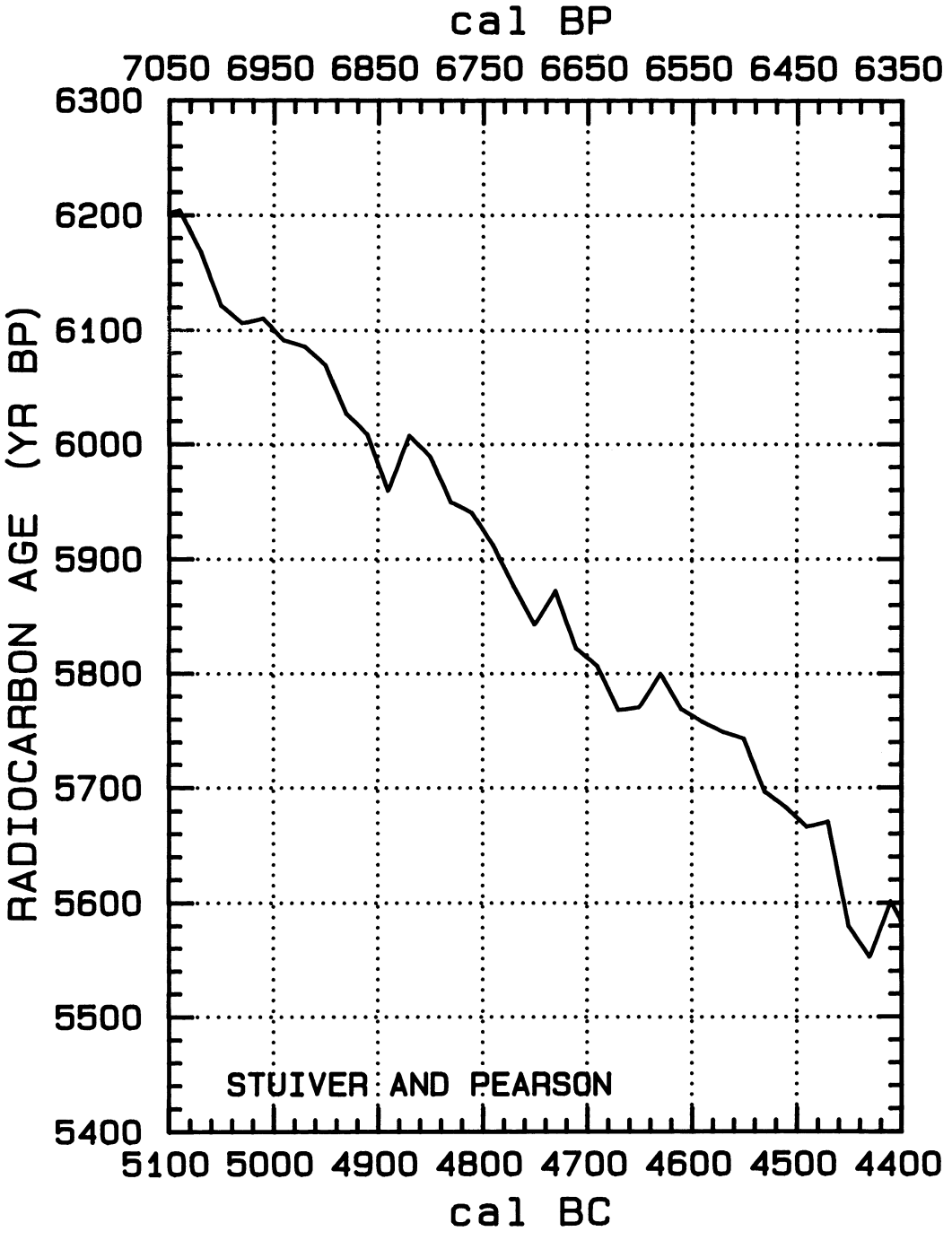
cal BP
7050 6950 6850 6750 6650 6550 6450 6350
6300
6200
6100
6000
5900
5800
5700
5600
5500
5400
RADIOCARBON AGE (YR BP)
STUIVER AND PEARSON
5100 5000 4900 4800 4700 4600 4500 4400
cal BC

Fig. 1J

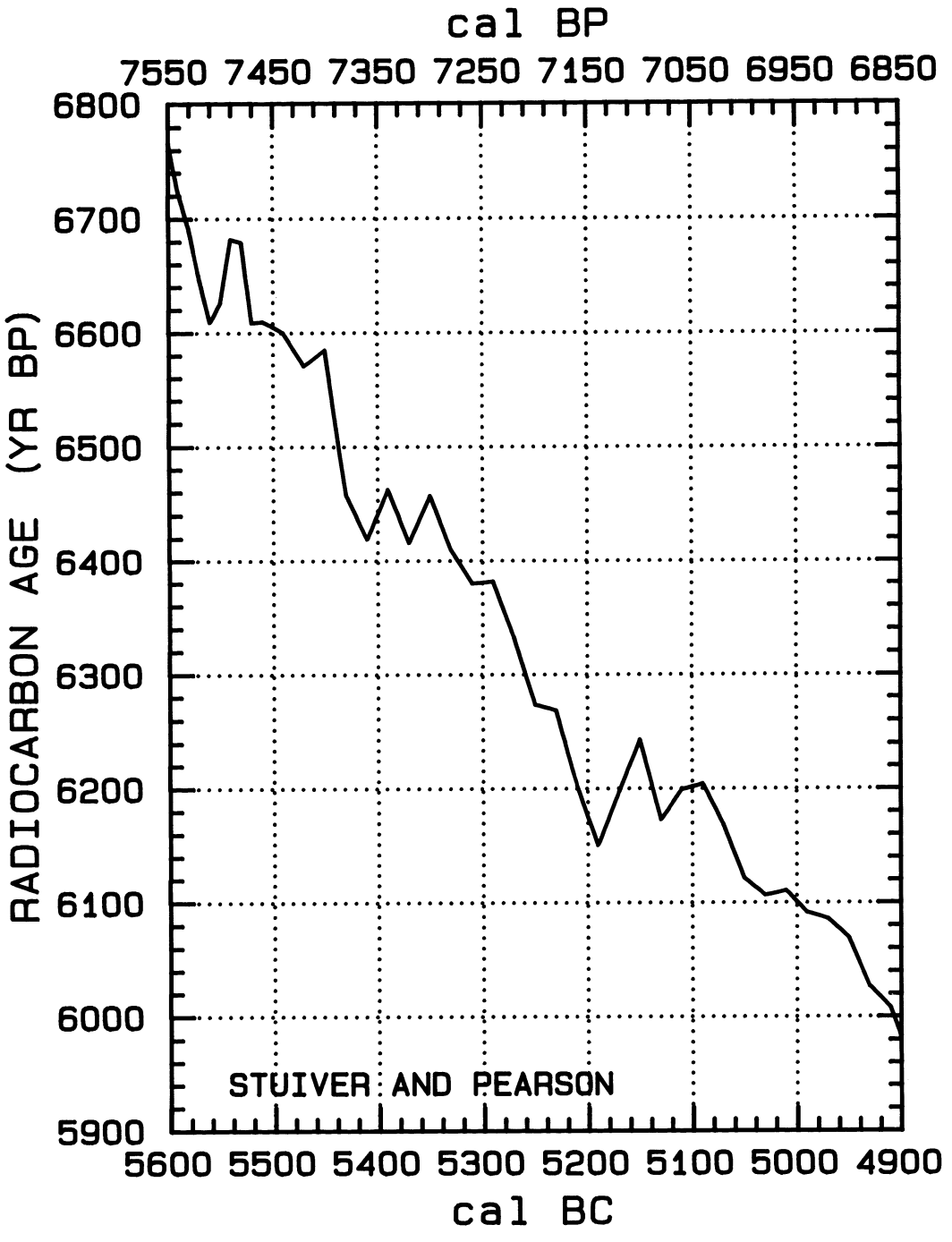
cal BP
7550 7450 7350 7250 7150 7050 6950 6850
6800
6700
6600
6500
6400
6300
6200
6100
6000
5900
RADIOCARBON AGE (YR BP)
STUIVER AND PEARSON
5600 5500 5400 5300 5200 5100 5000 4900
cal BC

Fig. 1K

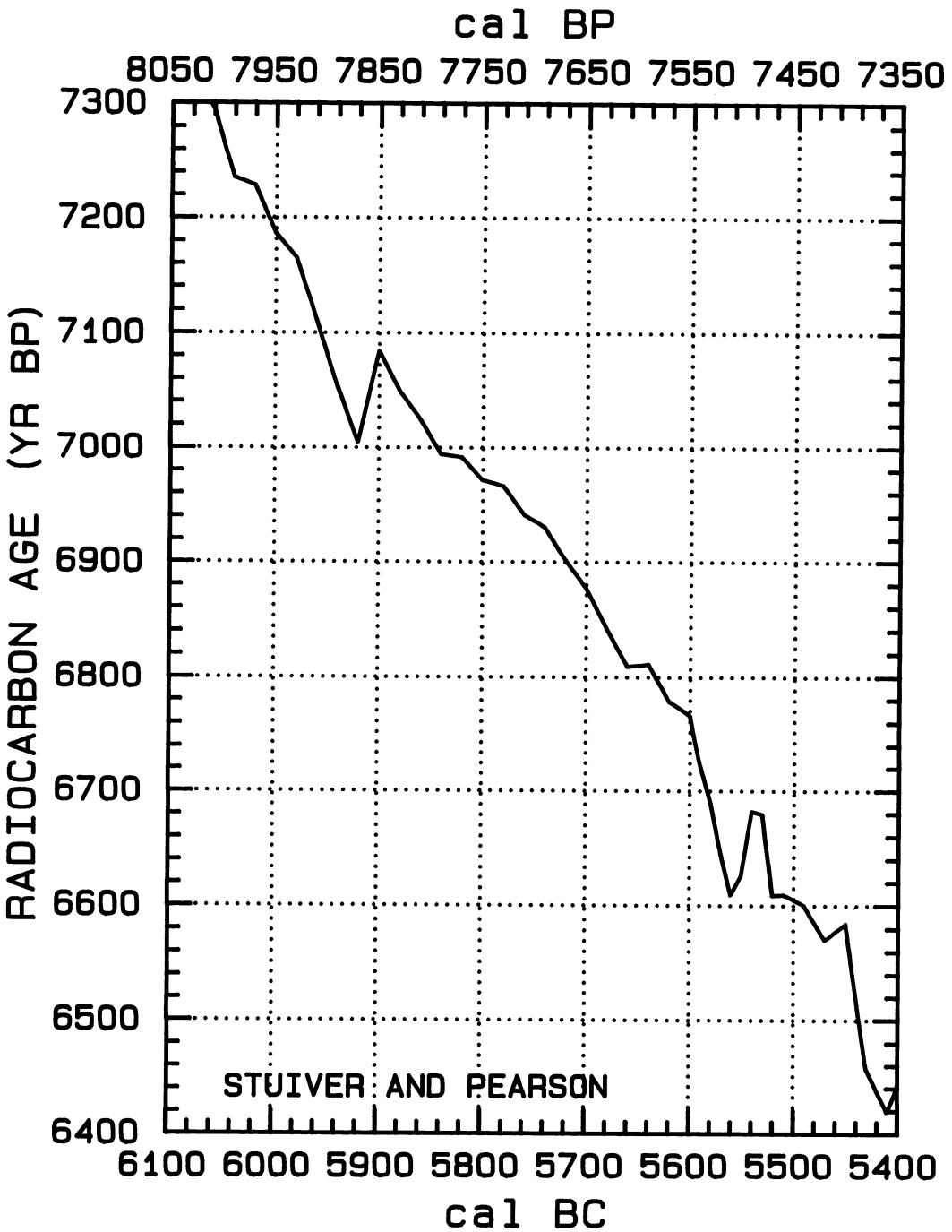
cal BP
8050 7950 7850 7750 7650 7550 7450 7350
7300
7200
7100
7000
6900
6800
6700
6600
6500
6400
RADIOCARBON AGE (YR BP)
STUIVER AND PEARSON
6100 6000 5900 5800 5700 5600 5500 5400
cal BC

Fig. 1L

TABLE 1. Weighted averages of University of Washington (Seattle) and the University of Belfast ^{14}C age determinations. The cal AD/BC (or cal BP) ages represent the midpoints of bidecadal wood sections, except as noted in the text. The standard deviation in the ages and $\Delta^{14}C$ (defined in Stuiver and Polach (1977)) values includes lab error multipliers of 1.23 for Belfast and 1.6 for Seattle after 2500 BC, and 1.7 for both labs prior to 2500 BC.

		^{14}C				^{14}C	
Cal AD/BC	$\Delta^{14}C$ ‰	age (BP)	Cal BP	Cal AD/BC	$\Delta^{14}C$ ‰	age (BP)	Cal BP
AD 1940	−20.7 ± .6	178 ± 5	BP 10	AD 1130	−14.4 ± 1.3	914 ± 10	BP 820
AD 1920	−11.9 ± .5	126 ± 4	BP 30	AD 1110	−16.4 ± 1.1	949 ± 9	BP 840
AD 1900	−4.5 ± .7	85 ± 6	BP 50	AD 1090	−12.2 ± 1.0	935 ± 8	BP 860
AD 1880	−5.6 ± .5	113 ± 4	BP 70	AD 1070	−7.4 ± .9	915 ± 7	BP 880
AD 1860	−4.1 ± .6	120 ± 5	BP 90	AD 1050	−7.1 ± 1.1	932 ± 9	BP 900
AD 1840	−1.3 ± .5	118 ± 4	BP 110	AD 1030	−9.9 ± 1.2	974 ± 10	BP 920
AD 1825	2.5 ± .6	101 ± 5	BP 125	AD 1010	−16.0 ± 1.3	1043 ± 11	BP 940
AD 1810	−1.4 ± .5	148 ± 4	BP 140	AD 990	−16.8 ± 1.2	1069 ± 9	BP 960
AD 1790	−7.8 ± .6	219 ± 5	BP 160	AD 970	−18.9 ± 1.2	1105 ± 10	BP 980
AD 1770	−.1 ± .5	176 ± 4	BP 180	AD 952	−20.3 ± 1.5	1135 ± 12	BP 998
AD 1750	3.1 ± .5	169 ± 4	BP 200	AD 940	−19.4 ± 1.6	1139 ± 13	BP 1010
AD 1730	9.7 ± .5	136 ± 4	BP 220	AD 920	−16.8 ± 1.3	1137 ± 11	BP 1030
AD 1710	15.5 ± .4	110 ± 3	BP 240	AD 900	−11.4 ± 1.2	1112 ± 10	BP 1050
AD 1690	14.7 ± .4	136 ± 3	BP 260	AD 880	−18.9 ± 1.3	1193 ± 11	BP 1070
AD 1670	8.1 ± .5	207 ± 4	BP 280	AD 860	−18.5 ± 1.3	1210 ± 10	BP 1090
AD 1650	2.4 ± .5	272 ± 4	BP 300	AD 850	−18.2 ± 1.3	1216 ± 10	BP 1100
AD 1630	−2.8 ± .5	334 ± 4	BP 320	AD 830	−14.3 ± 1.4	1204 ± 11	BP 1120
AD 1610	−5.0 ± .5	371 ± 4	BP 340	AD 810	−13.6 ± 1.4	1218 ± 11	BP 1140
AD 1590	.1 ± .6	349 ± 5	BP 360	AD 790	−11.2 ± 1.0	1218 ± 9	BP 1160
AD 1570	3.5 ± .6	341 ± 5	BP 380	AD 770	−15.9 ± 1.2	1276 ± 10	BP 1180
AD 1550	8.3 ± .5	322 ± 4	BP 400	AD 750	−15.9 ± 1.0	1295 ± 8	BP 1200
AD 1530	11.1 ± .5	319 ± 4	BP 420	AD 730	−10.1 ± 1.0	1267 ± 8	BP 1220
AD 1510	8.2 ± .7	362 ± 5	BP 440	AD 710	−10.6 ± 1.2	1291 ± 9	BP 1240
AD 1490	10.3 ± 1.4	365 ± 11	BP 460	AD 690	−9.2 ± 1.8	1299 ± 15	BP 1260
AD 1470	7.7 ± 1.6	405 ± 13	BP 480	AD 670	−12.3 ± 1.8	1343 ± 14	BP 1280
AD 1460	8.7 ± 1.1	406 ± 9	BP 490	AD 650	−18.5 ± 1.4	1414 ± 12	BP 1300
AD 1450	7.6 ± 1.3	425 ± 11	BP 500	AD 630	−20.4 ± 1.5	1448 ± 13	BP 1320
AD 1430	.4 ± 1.6	502 ± 13	BP 520	AD 610	−20.6 ± 1.9	1469 ± 15	BP 1340
AD 1410	−1.9 ± 1.4	540 ± 12	BP 540	AD 590	−23.5 ± 1.7	1512 ± 14	BP 1360
AD 1390	−9.6 ± 1.3	622 ± 10	BP 560	AD 570	−20.0 ± 1.8	1503 ± 14	BP 1380
AD 1370	−11.2 ± 1.2	654 ± 10	BP 580	AD 550	−20.0 ± 1.5	1523 ± 13	BP 1400
AD 1350	−5.2 ± 1.4	625 ± 11	BP 600	AD 530	−25.0 ± 1.4	1584 ± 12	BP 1420
AD 1330	.8 ± 1.2	596 ± 10	BP 620	AD 510	−22.3 ± 1.6	1580 ± 13	BP 1440
AD 1310	−.9 ± 1.2	629 ± 9	BP 640	AD 490	−20.6 ± 1.6	1586 ± 13	BP 1460
AD 1290	−8.7 ± 1.4	711 ± 11	BP 660	AD 470	−17.0 ± 1.7	1576 ± 14	BP 1480
AD 1275	−15.6 ± 2.9	782 ± 24	BP 675	AD 450	−15.5 ± 1.7	1583 ± 14	BP 1500
AD 1260	−15.3 ± 1.2	794 ± 10	BP 690	AD 430	−16.8 ± 1.6	1613 ± 13	BP 1520
AD 1245	−15.4 ± 2.8	810 ± 23	BP 705	AD 410	−20.7 ± 1.6	1664 ± 14	BP 1540
AD 1230	−14.6 ± 1.1	818 ± 9	BP 720	AD 390	−21.3 ± 1.4	1689 ± 11	BP 1560
AD 1212	−18.3 ± 1.6	865 ± 13	BP 738	AD 370	−22.1 ± 1.3	1715 ± 11	BP 1580
AD 1192	−16.6 ± 1.6	871 ± 13	BP 758	AD 350	−18.5 ± 1.7	1705 ± 14	BP 1600
AD 1170	−15.5 ± 1.0	883 ± 9	BP 780	AD 330	−20.1 ± 1.7	1737 ± 14	BP 1620
AD 1150	−21.3 ± 1.0	950 ± 9	BP 800	AD 310	−22.7 ± 1.7	1778 ± 14	BP 1640

TABLE 1. (Continued)

Cal AD/BC	$\Delta^{14}C$ ‰	^{14}C age (BP)	Cal BP	Cal AD/BC	$\Delta^{14}C$ ‰	^{14}C age (BP)	Cal BP
AD 290	−17.1 ± 1.6	1752 ± 13	BP 1660	2670 BC	43.9 ± 1.6	4143 ± 12	BP 4619
AD 270	−11.4 ± 1.5	1724 ± 12	BP 1680	2690 BC	46.7 ± 1.7	4141 ± 13	BP 4639
AD 250	−15.4 ± 1.1	1777 ± 9	BP 1700	2710 BC	42.3 ± 1.6	4194 ± 12	BP 4659
AD 230	−18.3 ± 1.5	1820 ± 13	BP 1720	2730 BC	50.0 ± 1.6	4155 ± 12	BP 4679
AD 210	−19.1 ± 1.5	1846 ± 13	BP 1740	2750 BC	51.0 ± 2.0	4167 ± 15	BP 4699
AD 190	−17.2 ± 1.7	1850 ± 14	BP 1760	2770 BC	51.0 ± 2.2	4186 ± 17	BP 4719
AD 170	−14.8 ± 1.8	1849 ± 15	BP 1780	2790 BC	50.4 ± 1.6	4210 ± 13	BP 4739
AD 150	−11.6 ± 1.7	1843 ± 14	BP 1800	2810 BC	58.9 ± 1.8	4165 ± 14	BP 4759
AD 130	−13.6 ± 1.2	1879 ± 10	BP 1820	2830 BC	68.9 ± 1.5	4109 ± 12	BP 4779
AD 110	−16.2 ± 1.8	1919 ± 15	BP 1840	2850 BC	68.5 ± 1.8	4131 ± 14	BP 4799
AD 90	−12.0 ± 1.4	1904 ± 12	BP 1860	2870 BC	63.5 ± 1.8	4188 ± 13	BP 4819
AD 70	−15.7 ± 1.3	1954 ± 11	BP 1880	2890 BC	54.2 ± 2.0	4278 ± 15	BP 4839
AD 50	−16.9 ± 1.1	1984 ± 9	BP 1900	2910 BC	52.7 ± 1.9	4309 ± 15	BP 4859
AD 30	−13.3 ± 1.4	1974 ± 11	BP 1920	2930 BC	43.6 ± 2.1	4398 ± 16	BP 4879
AD 10	−14.6 ± 1.1	2003 ± 9	BP 1940	2950 BC	45.8 ± 1.7	4401 ± 13	BP 4899
10 BC	−15.8 ± 1.1	2032 ± 9	BP 1959	2970 BC	48.2 ± 2.3	4402 ± 17	BP 4919
30 BC	−12.9 ± 1.0	2027 ± 8	BP 1979	2990 BC	53.6 ± 1.8	4380 ± 14	BP 4939
50 BC	−15.9 ± 1.0	2071 ± 8	BP 1999	3010 BC	56.8 ± 2.1	4375 ± 16	BP 4959
70 BC	−16.2 ± 1.2	2093 ± 10	BP 2019	3030 BC	55.8 ± 2.0	4402 ± 15	BP 4979
90 BC	−13.4 ± 1.2	2090 ± 10	BP 2039	3050 BC	51.5 ± 1.6	4454 ± 12	BP 4999
110 BC	−13.1 ± 1.2	2107 ± 9	BP 2059	3070 BC	58.4 ± 1.6	4421 ± 12	BP 5019
130 BC	−12.8 ± 1.3	2124 ± 10	BP 2079	3090 BC	57.5 ± 2.2	4447 ± 17	BP 5039
150 BC	−9.0 ± 1.4	2112 ± 11	BP 2099	3110 BC	52.0 ± 2.1	4509 ± 16	BP 5059
170 BC	−9.5 ± 1.3	2136 ± 10	BP 2119	3130 BC	52.5 ± 2.1	4525 ± 16	BP 5079
190 BC	−10.2 ± 1.3	2161 ± 11	BP 2139	3150 BC	53.1 ± 2.1	4540 ± 16	BP 5099
210 BC	−16.0 ± 1.2	2228 ± 10	BP 2159	3170 BC	61.1 ± 2.0	4498 ± 15	BP 5119
230 BC	−13.3 ± 1.3	2225 ± 10	BP 2179	3190 BC	60.2 ± 1.7	4524 ± 13	BP 5139
250 BC	−11.6 ± 1.5	2230 ± 12	BP 2199	3210 BC	61.9 ± 1.8	4530 ± 14	BP 5159
270 BC	−12.6 ± 1.5	2258 ± 12	BP 2219	3230 BC	66.8 ± 2.0	4513 ± 15	BP 5179
290 BC	−6.4 ± 1.5	2227 ± 12	BP 2239	3250 BC	75.9 ± 2.1	4465 ± 15	BP 5199
310 BC	−2.7 ± 1.5	2217 ± 12	BP 2259	3270 BC	74.0 ± 2.3	4498 ± 17	BP 5219
330 BC	2.7 ± 1.5	2193 ± 12	BP 2279	3290 BC	78.2 ± 2.1	4486 ± 16	BP 5239
350 BC	2.6 ± 1.3	2213 ± 11	BP 2299	3310 BC	76.1 ± 1.9	4521 ± 14	BP 5259
370 BC	−1.4 ± 1.2	2264 ± 10	BP 2319	3330 BC	78.7 ± 1.7	4521 ± 12	BP 5279
390 BC	−5.0 ± 1.4	2313 ± 12	BP 2339	3350 BC	73.9 ± 1.8	4577 ± 14	BP 5299
410 BC	−15.3 ± 1.3	2416 ± 11	BP 2359	3370 BC	68.0 ± 2.4	4640 ± 18	BP 5319
430 BC	−16.2 ± 1.3	2443 ± 11	BP 2379	3390 BC	58.7 ± 2.0	4730 ± 15	BP 5339
450 BC	−12.2 ± 1.6	2430 ± 13	BP 2399	3410 BC	63.9 ± 2.4	4710 ± 18	BP 5359
470 BC	−9.1 ± 1.3	2424 ± 10	BP 2419	3430 BC	69.9 ± 1.9	4685 ± 15	BP 5379
490 BC	−8.3 ± 1.4	2437 ± 11	BP 2439	3450 BC	71.6 ± 2.5	4691 ± 19	BP 5399
2510 BC	34.9 ± 1.5	4058 ± 12	BP 4459	3470 BC	79.7 ± 1.9	4650 ± 14	BP 5419
2530 BC	42.9 ± 1.5	4015 ± 11	BP 4479	3490 BC	83.1 ± 1.9	4644 ± 14	BP 5439
2550 BC	46.5 ± 1.6	4007 ± 12	BP 4499	3510 BC	74.6 ± 1.9	4726 ± 14	BP 5459
2570 BC	43.7 ± 1.5	4048 ± 12	BP 4519	3530 BC	73.6 ± 1.9	4753 ± 14	BP 5479
2590 BC	40.9 ± 1.5	4088 ± 11	BP 4539	3550 BC	69.9 ± 1.9	4801 ± 14	BP 5499
2610 BC	43.7 ± 2.0	4087 ± 15	BP 4559	3570 BC	75.9 ± 1.9	4776 ± 14	BP 5519
2630 BC	39.7 ± 1.4	4137 ± 11	BP 4579	3590 BC	81.6 ± 1.7	4752 ± 13	BP 5539
2650 BC	44.5 ± 2.1	4119 ± 16	BP 4599	3610 BC	87.7 ± 1.6	4726 ± 12	BP 5559

TABLE 1. (Continued)

Cal AD/BC	$\Delta^{14}C$ ‰	^{14}C age (BP)	Cal BP	Cal AD/BC	$\Delta^{14}C$ ‰	^{14}C age (BP)	Cal BP
3630 BC	81.4 ± 2.1	4793 ± 16	BP 5579	4590 BC	77.1 ± 2.1	5757 ± 16	BP 6539
3650 BC	73.6 ± 1.9	4871 ± 14	BP 5599	4610 BC	78.2 ± 2.4	5769 ± 18	BP 6559
3670 BC	71.5 ± 1.7	4905 ± 13	BP 5619	4630 BC	76.7 ± 1.9	5799 ± 14	BP 6579
3690 BC	75.1 ± 1.8	4898 ± 14	BP 5639	4650 BC	83.2 ± 1.7	5770 ± 13	BP 6599
3710 BC	70.7 ± 1.8	4950 ± 14	BP 5659	4670 BC	86.2 ± 2.5	5768 ± 18	BP 6619
3730 BC	71.4 ± 2.1	4965 ± 16	BP 5679	4690 BC	83.7 ± 1.8	5806 ± 13	BP 6639
3750 BC	75.0 ± 1.8	4957 ± 13	BP 5699	4710 BC	84.2 ± 2.1	5821 ± 15	BP 6659
3770 BC	73.8 ± 1.8	4985 ± 14	BP 5719	4730 BC	80.0 ± 2.5	5872 ± 18	BP 6679
3790 BC	73.0 ± 1.7	5011 ± 13	BP 5739	4750 BC	86.6 ± 2.5	5842 ± 18	BP 6699
3810 BC	67.4 ± 2.0	5073 ± 15	BP 5759	4770 BC	84.7 ± 2.5	5876 ± 18	BP 6719
3830 BC	67.8 ± 2.2	5089 ± 16	BP 5779	4790 BC	82.5 ± 2.5	5912 ± 19	BP 6739
3850 BC	70.9 ± 1.6	5085 ± 12	BP 5799	4810 BC	81.3 ± 2.5	5940 ± 19	BP 6759
3870 BC	75.3 ± 1.4	5071 ± 10	BP 5819	4830 BC	82.7 ± 2.2	5949 ± 17	BP 6779
3890 BC	83.9 ± 1.7	5027 ± 13	BP 5839	4850 BC	80.0 ± 2.2	5989 ± 16	BP 6799
3910 BC	82.3 ± 1.6	5058 ± 12	BP 5859	4870 BC	80.1 ± 2.5	6007 ± 19	BP 6819
3930 BC	84.6 ± 1.9	5060 ± 14	BP 5879	4890 BC	89.3 ± 2.3	5959 ± 17	BP 6839
3950 BC	80.4 ± 1.7	5111 ± 13	BP 5899	4910 BC	85.3 ± 1.8	6008 ± 13	BP 6859
3970 BC	75.8 ± 1.3	5165 ± 10	BP 5919	4930 BC	85.4 ± 1.7	6026 ± 13	BP 6879
3990 BC	71.4 ± 1.7	5217 ± 13	BP 5939	4950 BC	82.3 ± 1.5	6069 ± 12	BP 6899
4010 BC	68.9 ± 1.9	5255 ± 15	BP 5959	4970 BC	82.7 ± 1.7	6085 ± 13	BP 6919
4030 BC	76.3 ± 1.7	5219 ± 13	BP 5979	4990 BC	84.6 ± 1.9	6091 ± 14	BP 6939
4050 BC	70.7 ± 2.0	5281 ± 15	BP 5999	5010 BC	84.6 ± 2.4	6110 ± 18	BP 6959
4070 BC	78.3 ± 1.9	5244 ± 15	BP 6019	5030 BC	87.8 ± 2.5	6106 ± 19	BP 6979
4090 BC	72.7 ± 1.8	5305 ± 14	BP 6039	5050 BC	88.4 ± 2.5	6121 ± 18	BP 6999
4110 BC	72.6 ± 2.1	5324 ± 16	BP 6059	5070 BC	84.6 ± 2.2	6168 ± 16	BP 7019
4130 BC	81.3 ± 2.1	5279 ± 16	BP 6079	5090 BC	82.4 ± 1.8	6204 ± 13	BP 7039
4150 BC	78.6 ± 4.8	5319 ± 36	BP 6099	5110 BC	85.7 ± 2.0	6199 ± 15	BP 7059
4170 BC	76.3 ± 2.3	5355 ± 17	BP 6119	5130 BC	91.9 ± 2.0	6172 ± 14	BP 7079
4190 BC	82.1 ± 2.1	5332 ± 16	BP 6139	5150 BC	85.0 ± 2.5	6243 ± 19	BP 7099
4210 BC	92.9 ± 2.4	5271 ± 18	BP 6159	5170 BC	93.8 ± 2.0	6197 ± 15	BP 7119
4230 BC	82.2 ± 1.8	5370 ± 14	BP 6179	5190 BC	103.0 ± 2.1	6150 ± 16	BP 7139
4250 BC	81.8 ± 2.1	5392 ± 16	BP 6199	5210 BC	98.5 ± 2.5	6202 ± 18	BP 7159
4270 BC	76.8 ± 2.2	5449 ± 16	BP 6219	5230 BC	92.2 ± 2.5	6268 ± 18	BP 7179
4290 BC	83.3 ± 2.1	5420 ± 16	BP 6239	5250 BC	94.1 ± 1.9	6273 ± 14	BP 7199
4310 BC	89.6 ± 2.3	5393 ± 17	BP 6259	5270 BC	88.7 ± 2.0	6332 ± 15	BP 7219
4330 BC	84.1 ± 2.1	5453 ± 15	BP 6279	5290 BC	84.7 ± 2.1	6381 ± 16	BP 7239
4350 BC	77.8 ± 2.0	5519 ± 15	BP 6299	5310 BC	87.6 ± 2.2	6379 ± 16	BP 7259
4370 BC	72.4 ± 1.9	5579 ± 15	BP 6319	5330 BC	86.2 ± 2.1	6409 ± 16	BP 7279
4390 BC	76.4 ± 2.4	5568 ± 18	BP 6339	5350 BC	82.4 ± 2.0	6457 ± 15	BP 7299
4410 BC	74.6 ± 2.4	5601 ± 18	BP 6359	5370 BC	90.5 ± 2.5	6416 ± 18	BP 7319
4430 BC	83.9 ± 2.4	5552 ± 18	BP 6379	5390 BC	86.9 ± 2.5	6462 ± 19	BP 7339
4450 BC	82.8 ± 2.4	5579 ± 18	BP 6399	5410 BC	95.4 ± 2.2	6419 ± 16	BP 7359
4470 BC	73.1 ± 2.0	5671 ± 15	BP 6419	5430 BC	92.8 ± 2.2	6457 ± 16	BP 7379
4490 BC	76.4 ± 2.4	5666 ± 18	BP 6439	5450 BC	78.3 ± 2.2	6585 ± 16	BP 7399
4510 BC	76.7 ± 2.4	5683 ± 18	BP 6459	5470 BC	82.8 ± 2.2	6570 ± 16	BP 7419
4530 BC	77.5 ± 2.5	5696 ± 18	BP 6479	5490 BC	81.4 ± 2.5	6600 ± 18	BP 7439
4550 BC	73.9 ± 2.5	5742 ± 18	BP 6499	5500 BC	82.1 ± 2.6	6605 ± 19	BP 7449
4570 BC	75.7 ± 1.9	5748 ± 14	BP 6519	5510 BC	82.8 ± 2.5	6609 ± 18	BP 7459

TABLE 1. (Continued)

Cal AD/BC	$\Delta^{14}C$ ‰	^{14}C age (BP)	Cal BP	Cal AD/BC	$\Delta^{14}C$ ‰	^{14}C age (BP)	Cal BP
5520 BC	84.2 ± 2.6	6608 ± 19	BP 7469	5740 BC	69.8 ± 1.6	6930 ± 12	BP 7689
5530 BC	76.0 ± 2.4	6679 ± 18	BP 7479	5760 BC	70.9 ± 1.6	6941 ± 12	BP 7709
5540 BC	76.9 ± 2.6	6682 ± 19	BP 7489	5780 BC	70.2 ± 1.7	6966 ± 12	BP 7729
5550 BC	85.8 ± 2.2	6626 ± 16	BP 7499	5800 BC	72.1 ± 1.6	6971 ± 12	BP 7749
5560 BC	89.4 ± 2.2	6609 ± 17	BP 7509	5820 BC	72.0 ± 1.6	6991 ± 12	BP 7769
5570 BC	85.7 ± 1.8	6646 ± 13	BP 7519	5840 BC	74.2 ± 1.7	6994 ± 13	BP 7789
5580 BC	81.0 ± 1.8	6691 ± 13	BP 7529	5860 BC	72.8 ± 2.5	7024 ± 19	BP 7809
5590 BC	78.1 ± 2.0	6722 ± 15	BP 7539	5880 BC	72.1 ± 2.5	7049 ± 19	BP 7829
5600 BC	73.5 ± 1.9	6766 ± 14	BP 7549	5900 BC	70.0 ± 2.3	7084 ± 17	BP 7849
5620 BC	74.4 ± 1.6	6778 ± 12	BP 7569	5920 BC	83.3 ± 2.1	7004 ± 15	BP 7869
5640 BC	72.7 ± 1.7	6811 ± 13	BP 7589	5940 BC	79.3 ± 2.7	7053 ± 20	BP 7889
5660 BC	75.6 ± 1.6	6809 ± 12	BP 7609	5960 BC	74.1 ± 2.5	7111 ± 19	BP 7909
5680 BC	73.8 ± 1.8	6842 ± 14	BP 7629	5980 BC	69.5 ± 2.3	7165 ± 17	BP 7929
5700 BC	71.7 ± 1.7	6877 ± 13	BP 7649	6000 BC	69.3 ± 2.3	7186 ± 17	BP 7949
5720 BC	71.0 ± 2.0	6901 ± 15	BP 7669				

[RADIOCARBON, VOL. 35, NO. 1, 1993, P. 25–33]

HIGH-PRECISION BIDECADAL CALIBRATION OF THE RADIOCARBON TIME SCALE, 500–2500 BC

GORDON W. PEARSON

Retired from Palaeoecology Centre, The Queen's University of Belfast, Belfast, BT71NN, Northern Ireland

and

MINZE STUIVER

Department of Geological Sciences and Quaternary Research Center, University of Washington, Seattle, Washington 98195 USA

INTRODUCTION

The sole purpose of this paper is to present a previously published ^{14}C data set to which minor corrections have been applied. All basic information previously given is still applicable (Pearson & Stuiver 1986). The corrections are needed because ^{14}C count-rate influences (radon decay in Seattle, a re-evaluation of the corrections applied for efficiency variation with time previously unrecognized in Belfast) had to be accounted for in more detail. Information on the radon correction is given in Stuiver and Becker (1993). The Belfast corrections were necessary because the original correction for efficiency variations with time was calculated using two suspect standards (these were shown to be suspect by recent observations) that overweighted the correction. A re-evaluation (Pearson & Qua 1993) now shows it to be almost insignificant, and the corrected dates (using the new correction) became older by about 16 years.

Systematic ^{14}C age differences between the current Seattle and Belfast data sets are 9.9, 16.6 and 2.4 ^{14}C yr for, respectively, the 1–1000 BC, 1001–2000 BC and 2001–3000 BC intervals. Reproducibility can be expressed by an error multiplier, $K_{Seattle-Belfast}$, which is defined as the ratio of the actual standard deviation in the age differences and the average standard deviation of the differences calculated from the quoted errors in the ^{14}C determinations. K values for the above intervals are, respectively, 1.3, 1.4 and 1.8. A detailed discussion of the offsets and K values for the AD 1840–6000 BC interval is given in Stuiver and Pearson (1992, 1993). Here we note: 1) the Table 1 Seattle-Belfast bidecadal conventional (Stuiver & Polach 1977) ^{14}C age averages may be subject to systematic errors of 5–8 ^{14}C yr maximally; and 2) the standard deviations given with the bidecadal ^{14}C ages are based on quoted errors multiplied with $K_{Belfast}$ = 1.23 and $K_{Seattle}$ = 1.6, and thus account for 90–100% of the variance encountered in the Seattle-Belfast ^{14}C age differences. Details on K determinations can be found, *e.g.*, in Stuiver and Pearson (1986).

Seattle-Belfast bidecadal ^{14}C age averages for the AD 1840–500 BC and 2500–6000 BC interval are given in a twin paper (Stuiver & Pearson 1993).

CALIBRATION INSTRUCTIONS

We recommend that users of ^{14}C dates obtain additional information on reproducibility (and systematic error, if any) from the laboratory reporting the ^{14}C date. This information should lead to a realistic standard deviation in the reported age. A systematic error has to be deducted from, or added to, the reported ^{14}C age prior to age calibration.

Only the calibration curve is given in Figure 1; the one-sigma (1σ; standard deviation) uncertainty in the curve is not given. The actual standard deviation (averaging 12.9 ^{14}C yr for the nearly 8000 cal yr bidecadal calibration curve of Belfast-Seattle ^{14}C age averages) is tabulated in Table 1 for each bidecadal midpoint.

Cal BP ages are relative to the year AD 1950, with 0 cal BP equal to AD 1950. The relationship between cal AD/BC and cal BP ages is cal BP = 1950 − cal AD, and cal BP = 1949 + cal BC. The switch from 1950 to 1949 when converting BC ages is caused by the absence of the zero year in the AD/BC chronology.

The conversion of a ^{14}C age to a cal age is as follows: 1) draw line A parallel to the bottom axis through the ^{14}C age to be converted; 2) draw vertical line(s) through the intercept(s) of line A and the calibration curve. The cal AD/BC ages can be read at the bottom axis, the cal BP ages at the top.

To convert the standard error in the ^{14}C age into a range of cal AD/BC (BP) ages, determine the sample standard deviation, σ, by multiplying the quoted laboratory standard deviation by the "error multiplier". Unfortunately, information on error multipliers is often lacking. Here, the ^{14}C age user should refer to K values given in Stuiver and Pearson (1992, 1993) or Scott, Long & Kra (1990).

Once the sample σ is known, the curve σ should be read from Table 1. The curve σ and sample σ should then be used to calculate total $\sigma = ((\text{sample } \sigma)^2 + (\text{curve } \sigma)^2)^{1/2}$ (Stuiver 1982). Lines parallel to A should now be drawn through the ^{14}C age + total σ, and ^{14}C age − total σ value. The vertical lines drawn through the intercepts now yield the outer limits of possible cal AD/BC (cal BP) ages that are compatible with the sample standard deviation.

The conversion procedure yields 1) single or multiple cal AD/BC (BP) ages that are compatible with a certain ^{14}C age, and 2) the range(s) of cal ages that correspond(s) to the standard deviation in the ^{14}C age (and calibration curve). Here, the user determines the calibrated ages from the Figure 1 graphs by drawing lines, whereas an alternate approach would be to use the computerized calibration (CALIB) program discussed elsewhere in this issue (Stuiver & Reimer 1993).

The probability that a certain cal age is the actual sample age may be quite variable within the cal age range. Higher probabilities are encountered around the intercept ages. The non-linear transform of a Gaussian standard deviation around a ^{14}C age into cal AD/BC (cal BP) age is not a simple matter, and computer programs are needed to derive the complex probability distribution. The CALIB program incorporates such probability distributions.

The calibration data presented here are valid for northern hemispheric samples that were formed in equilibrium with atmospheric $^{14}CO_2$. Systematic age differences are possible for the southern hemisphere where ^{14}C ages of wood samples tend to be about 40 yr older (Vogel *et al.* 1993). Thus, ^{14}C ages of southern hemispheric samples preceding our era of fossil-fuel combustion should be reduced by 40 yr before being converted into cal AD/BC (BP) ages.

The Figure 1 calibration points are the midpoints of wood samples spanning 20 yr. Samples submitted for dating may cover shorter or longer intervals. The decadal calibration results of the Seattle laboratory (Stuiver & Becker 1993; Stuiver & Reimer 1993) provide a better time resolution, whereas the CALIB program also has an option to use Figure 1 moving averages (*e.g.*, a 5-point or 100-yr moving average of the bidecadal curve). The latter should be used for a sample grown over a 100-yr interval. Samples formed over intervals longer than a decade or bidecade are very desirable as the ^{14}C "wiggles" of the calibration curve have less influence on the (midpoint) cal age when a smoothed (moving average) calibration curve is used (Stuiver 1992).

The calibration curve is valid only for age conversion of samples that were formed in equilibrium with atmospheric CO_2. Conventional ^{14}C ages of materials not in equilibrium with atmospheric reservoirs do not take into account the offset in ^{14}C age that may occur (Stuiver & Polach 1977). This constant offset, or reservoir deficiency, must be deducted from the reported ^{14}C age before any attempt can be made to convert to cal AD/BC (BP) ages.

The reservoir deficiency is time dependent for the mixed (and deep) layer of the ocean. For the calibration of marine samples in this time domain, the reader is referred to Stuiver and Braziunas (1993) and, of course, the CALIB program.

ACKNOWLEDGMENTS

The ^{14}C research at Seattle was supported by a National Science Foundation grant BNS-9004492, and by a SERC grant in Belfast. We thank Dr. B. Becker of the University of Hohenheim, Stuttgart for providing German oak (unified Donau/Main series) samples, Drs. J. R. Pilcher and M. G. Baillie for the wood samples of the Irish chronology, and F. Qua, P. J. Reimer and P. J. Wilkinson for crucial technical and analytical support.

REFERENCES

Pearson, G. W. and Qua, F. 1993 High-precision ^{14}C measurement of Irish oaks to show the natural ^{14}C variations from AD 1840–5000 BC: A correction. *Radiocarbon*, this issue.

Pearson, G. W., and Stuiver, M. 1986 High-precision calibration of the radiocarbon time scale, 500–2500 BC. *In* Stuiver, M. and Kra, R. S., eds., Proceedings of the 12th International Radiocarbon Conference. *Radiocarbon* 28(2B): 839–862.

Scott, E. M., Long, A. and Kra, R., eds. 1990 Proceedings of the International Workshop on Intercomparison of Radiocarbon Laboratories: *Radiocarbon* 32(3): 253–397.

Stuiver, M. 1982 A high-precision calibration of the AD radiocarbon time scale. *Radiocarbon* 24(1): 1–26.

_____1992 How accurate are our chronologies of the past? I: Time warps caused by the transformation of ^{14}C ages. *Proceedings of the Dahlem Workshop on Global Changes in the Perspective of the Past.* Chichester, John Wiley & Sons, in press.

Stuiver, M. and Becker, B. 1993 High-precision decadal calibration of the radiocarbon time scale AD 1950–6000 BC. *Radiocarbon*, this issue.

Stuiver, M. and Braziunas, T. F. 1993 Modeling radiocarbon ages of marine samples back to 10,000 BC. *Radiocarbon*, this issue.

Stuiver, M. and Pearson, G. W. 1986 High-precision calibration of the radiocarbon time scale, AD 1950–500 BC. *In* Stuiver, M. and Kra, R. S., eds., Proceedings of the 12th International Radiocarbon Conference. *Radiocarbon* 28(2B): 805–838.

_____1992 Calibration of the radiocarbon time scale 2500–5000 BC. *In* Taylor, R. E., Long, A. and Kra, R. S., eds., *Radiocarbon After Four Decades: An Interdisciplinary Perspective*. New York, Springer Verlag: 19–33.

_____1993 High-precision bidecadal calibration of the radiocarbon time scale, AD 1950–500 BC and 2500–6000 BC. *Radiocarbon*, this issue.

Stuiver, M. and Polach, H. 1977 Discussion: Reporting of ^{14}C data. *Radiocarbon* 19(3): 355-363.

Stuiver, M. and Reimer, P. J. 1993 Extended ^{14}C database and revised CALIB radiocarbon age calibration program. *Radiocarbon*, this issue.

Vogel, J. C., Fuls, A., Visser, E. and Becker, B. 1993 Pretoria calibration curve for short-lived samples, 1930 BC–3350 BC. *Radiocarbon*, this issue.

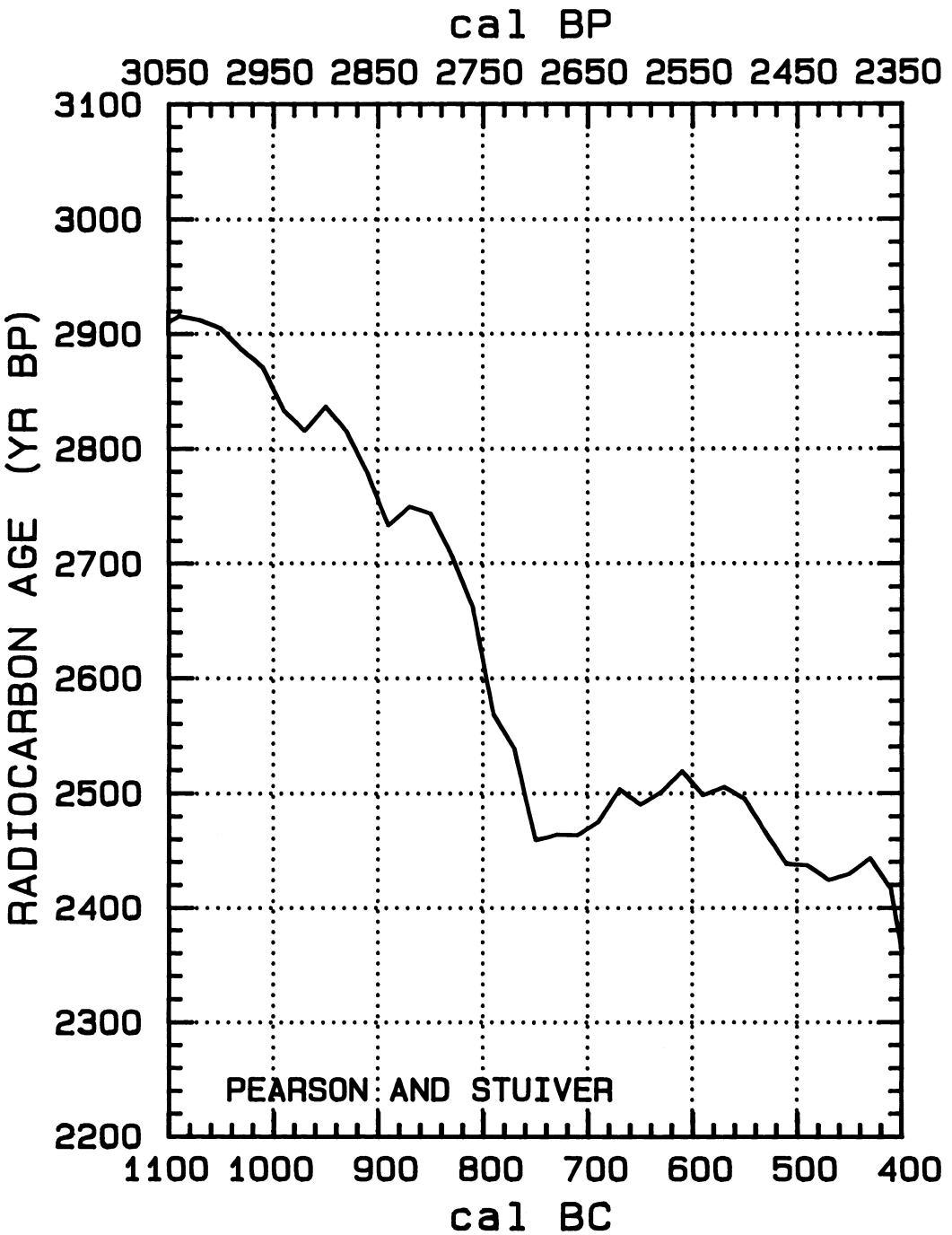

Fig. 1A–D. ^{14}C calibration curve derived from bidecadal samples

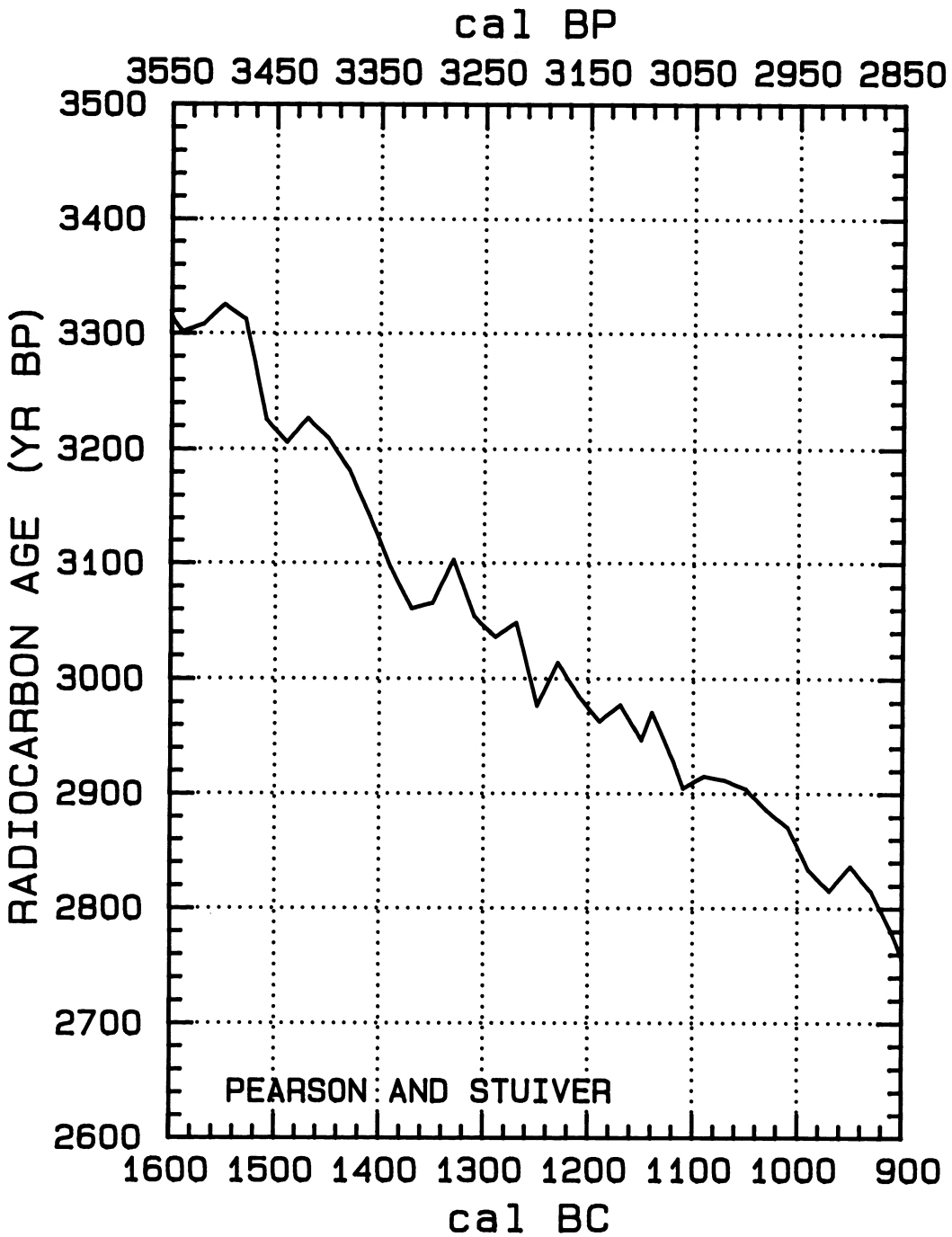
cal BP
3550 3450 3350 3250 3150 3050 2950 2850
3500
3400
3300
3200
3100
3000
2900
2800
2700
2600
RADIOCARBON AGE (YR BP)
PEARSON AND STUIVER
1600 1500 1400 1300 1200 1100 1000 900
cal BC

Fig. 1B

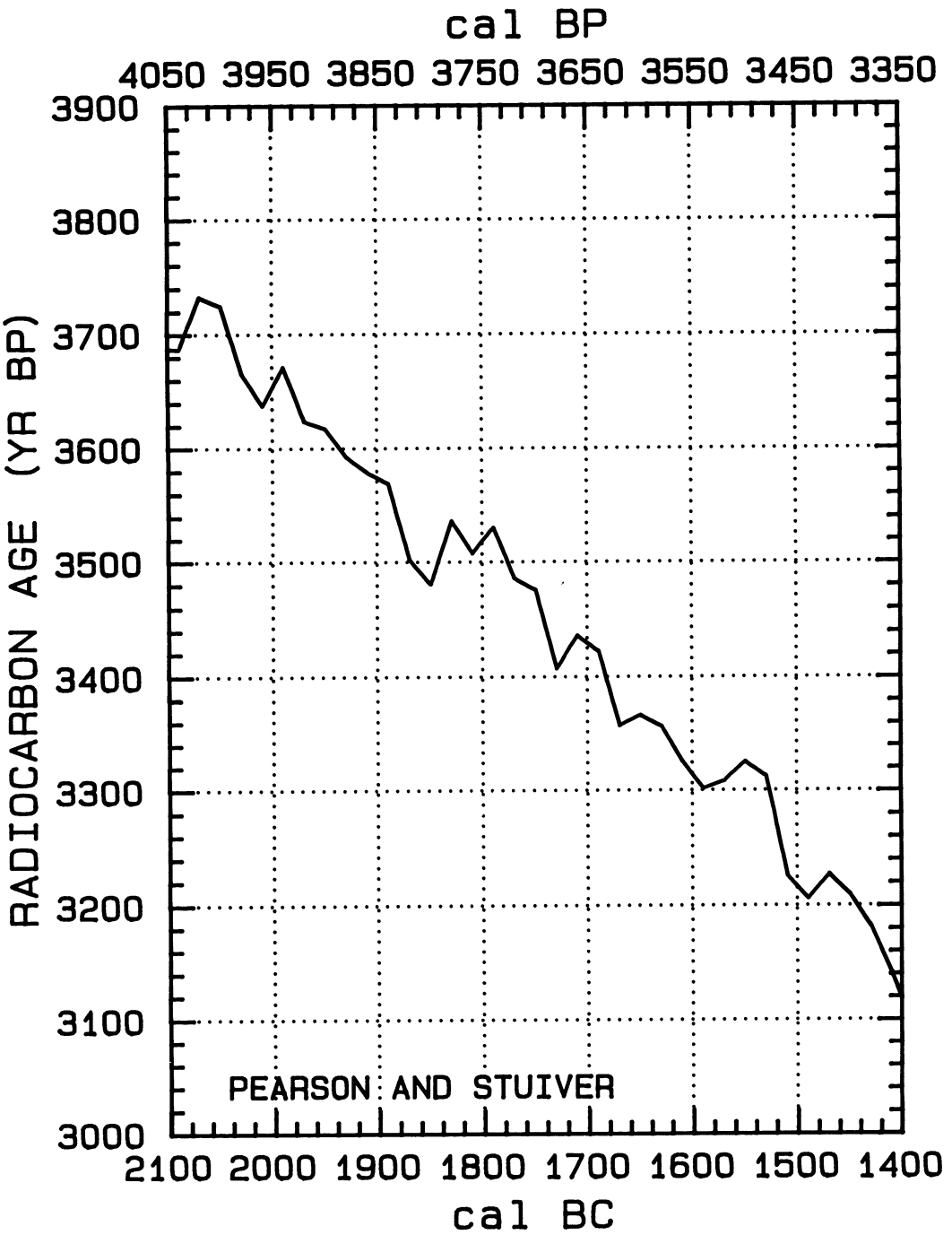
cal BP
4050 3950 3850 3750 3650 3550 3450 3350
3900
3800
3700
3600
3500
3400
3300
3200
3100
3000
RADIOCARBON AGE (YR BP)
PEARSON AND STUIVER
2100 2000 1900 1800 1700 1600 1500 1400
cal BC

Fig. 1C

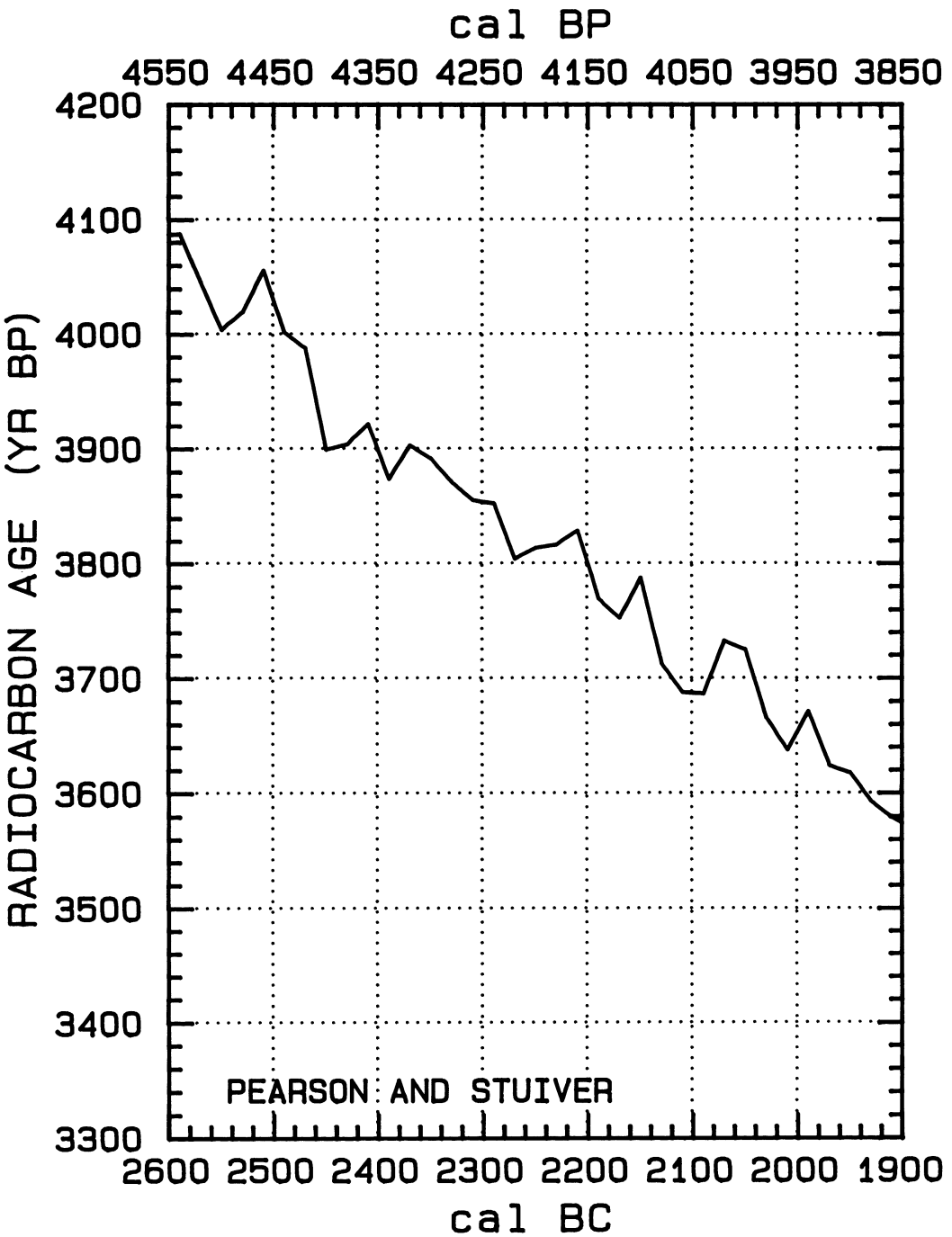
cal BP
4550 4450 4350 4250 4150 4050 3950 3850
4200
4100
4000
3900
3800
3700
3600
3500
3400
3300
RADIOCARBON AGE (YR BP)
PEARSON AND STUIVER
2600 2500 2400 2300 2200 2100 2000 1900
cal BC

Fig. 1D

TABLE 1. Weighted averages of University of Belfast and the University of Washington (Seattle) ^{14}C age determinations. The cal AD/BC (or cal BP) ages represent the midpoints of bidecadal wood sections, except as noted in the text. The standard deviation in the ages and $\Delta^{14}C$ (defined in Stuiver and Polach 1977) values includes lab error multipliers of 1.23 for Belfast and 1.6 for Seattle.

Cal AD/BC	$\Delta^{14}C$ ‰	^{14}C age (BP)	Cal BP	Cal AD/BC	$\Delta^{14}C$ ‰	^{14}C age (BP)	Cal BP
510 BC	−6.0 ± 1.2	2438 ± 10	BP 2459	1350 BC	17.6 ± 1.8	3066 ± 14	BP 3299
530 BC	−7.1 ± 1.1	2466 ± 9	BP 2479	1370 BC	20.7 ± 1.8	3061 ± 14	BP 3319
550 BC	−8.2 ± 1.0	2495 ± 8	BP 2499	1390 BC	18.7 ± 1.5	3096 ± 12	BP 3339
570 BC	−7.1 ± 1.3	2505 ± 11	BP 2519	1410 BC	15.4 ± 1.6	3141 ± 13	BP 3359
590 BC	−3.9 ± 1.3	2498 ± 11	BP 2539	1430 BC	12.7 ± 1.5	3182 ± 12	BP 3379
610 BC	−4.0 ± 1.2	2519 ± 10	BP 2559	1450 BC	11.7 ± 1.1	3210 ± 9	BP 3399
630 BC	0.6 ± 1.2	2501 ± 9	BP 2579	1470 BC	11.9 ± 1.4	3227 ± 11	BP 3419
650 BC	4.4 ± 1.3	2490 ± 10	BP 2599	1490 BC	17.1 ± 1.6	3206 ± 13	BP 3439
670 BC	5.2 ± 1.6	2503 ± 13	BP 2619	1510 BC	17.0 ± 1.7	3226 ± 14	BP 3459
690 BC	11.2 ± 1.8	2475 ± 14	BP 2639	1530 BC	8.5 ± 1.6	3313 ± 13	BP 3479
710 BC	15.1 ± 2.0	2464 ± 16	BP 2659	1550 BC	9.3 ± 1.8	3326 ± 15	BP 3499
730 BC	17.5 ± 1.5	2464 ± 12	BP 2679	1570 BC	14.0 ± 2.1	3308 ± 17	BP 3519
750 BC	20.6 ± 1.7	2459 ± 14	BP 2699	1590 BC	17.3 ± 1.5	3301 ± 12	BP 3539
770 BC	13.1 ± 2.0	2538 ± 16	BP 2719	1610 BC	16.7 ± 1.5	3326 ± 12	BP 3559
790 BC	11.7 ± 1.3	2568 ± 10	BP 2739	1630 BC	15.1 ± 1.6	3357 ± 12	BP 3579
810 BC	2.3 ± 1.6	2662 ± 13	BP 2759	1650 BC	16.3 ± 1.3	3367 ± 10	BP 3599
830 BC	−0.8 ± 1.5	2707 ± 12	BP 2779	1670 BC	20.0 ± 1.7	3357 ± 14	BP 3619
850 BC	−2.9 ± 1.6	2743 ± 13	BP 2799	1690 BC	14.2 ± 1.6	3423 ± 12	BP 3639
870 BC	−1.3 ± 1.6	2750 ± 13	BP 2819	1710 BC	15.0 ± 1.9	3436 ± 15	BP 3659
890 BC	3.2 ± 1.6	2733 ± 13	BP 2839	1730 BC	21.1 ± 1.6	3407 ± 12	BP 3679
910 BC	−0.1 ± 1.5	2779 ± 12	BP 2859	1750 BC	14.9 ± 1.6	3476 ± 12	BP 3699
930 BC	−2.1 ± 1.7	2815 ± 13	BP 2879	1770 BC	16.1 ± 1.4	3486 ± 11	BP 3719
950 BC	−2.4 ± 1.5	2837 ± 12	BP 2899	1790 BC	12.8 ± 1.4	3531 ± 11	BP 3739
970 BC	2.7 ± 1.3	2815 ± 10	BP 2919	1810 BC	18.2 ± 1.5	3508 ± 12	BP 3759
990 BC	2.8 ± 1.4	2833 ± 11	BP 2939	1830 BC	17.0 ± 1.9	3537 ± 15	BP 3779
1010 BC	0.5 ± 1.1	2871 ± 9	BP 2959	1850 BC	26.6 ± 1.7	3481 ± 13	BP 3799
1030 BC	1.1 ± 1.5	2886 ± 12	BP 2979	1870 BC	26.4 ± 1.5	3502 ± 12	BP 3819
1050 BC	1.2 ± 1.3	2905 ± 10	BP 2999	1890 BC	20.3 ± 1.6	3569 ± 12	BP 3839
1070 BC	2.7 ± 1.3	2912 ± 11	BP 3019	1910 BC	21.5 ± 1.9	3579 ± 15	BP 3859
1090 BC	4.7 ± 1.3	2916 ± 11	BP 3039	1930 BC	22.2 ± 1.5	3593 ± 12	BP 3879
1110 BC	8.4 ± 1.4	2905 ± 11	BP 3059	1950 BC	21.5 ± 1.6	3618 ± 13	BP 3899
1120 BC	6.6 ± 1.7	2930 ± 14	BP 3069	1970 BC	23.1 ± 1.8	3624 ± 14	BP 3919
1140 BC	3.8 ± 1.5	2972 ± 12	BP 3089	1990 BC	19.6 ± 1.4	3672 ± 11	BP 3939
1150 BC	8.1 ± 1.7	2947 ± 14	BP 3099	2010 BC	26.4 ± 1.7	3638 ± 13	BP 3959
1170 BC	6.6 ± 1.7	2978 ± 13	BP 3119	2030 BC	25.3 ± 1.5	3666 ± 12	BP 3979
1190 BC	10.9 ± 1.7	2963 ± 14	BP 3139	2050 BC	20.2 ± 1.4	3725 ± 11	BP 3999
1210 BC	10.5 ± 1.4	2986 ± 11	BP 3159	2070 BC	21.7 ± 1.6	3733 ± 13	BP 4019
1230 BC	9.4 ± 1.6	3014 ± 13	BP 3179	2090 BC	30.1 ± 1.7	3687 ± 13	BP 4039
1250 BC	16.5 ± 1.5	2977 ± 12	BP 3199	2110 BC	32.4 ± 1.6	3688 ± 13	BP 4059
1270 BC	9.9 ± 1.8	3049 ± 14	BP 3219	2130 BC	31.8 ± 1.9	3713 ± 15	BP 4079
1290 BC	14.0 ± 1.8	3036 ± 14	BP 3239	2150 BC	24.7 ± 1.3	3788 ± 10	BP 4099
1310 BC	14.1 ± 1.8	3054 ± 15	BP 3259	2170 BC	31.6 ± 1.6	3753 ± 13	BP 4119
1330 BC	10.4 ± 1.7	3103 ± 13	BP 3279	2190 BC	31.9 ± 1.2	3770 ± 9	BP 4139

TABLE 1. (Continued)

Cal AD/BC	$\Delta^{14}C$ ‰	^{14}C age (BP)	Cal BP	Cal AD/BC	$\Delta^{14}C$ ‰	^{14}C age (BP)	Cal BP
2210 BC	26.8 ± 1.4	3829 ± 11	BP 4159	2370 BC	37.2 ± 1.5	3903 ± 11	BP 4319
2230 BC	30.9 ± 1.5	3817 ± 12	BP 4179	2390 BC	43.6 ± 1.7	3874 ± 13	BP 4339
2250 BC	33.7 ± 1.4	3814 ± 11	BP 4199	2410 BC	39.9 ± 1.4	3922 ± 11	BP 4359
2270 BC	37.5 ± 1.9	3804 ± 15	BP 4219	2430 BC	44.7 ± 0.9	3904 ± 7	BP 4379
2290 BC	33.6 ± 1.6	3853 ± 12	BP 4239	2450 BC	48.0 ± 1.7	3899 ± 12	BP 4399
2310 BC	35.8 ± 1.8	3856 ± 14	BP 4259	2470 BC	38.8 ± 1.5	3988 ± 12	BP 4419
2330 BC	36.3 ± 1.5	3872 ± 11	BP 4279	2490 BC	39.5 ± 1.5	4002 ± 12	BP 4439
2350 BC	36.2 ± 1.6	3892 ± 13	BP 4299				

[RADIOCARBON, VOL. 35, NO. 1, 1993, P. 35–65]

HIGH-PRECISION DECADAL CALIBRATION OF THE RADIOCARBON TIME SCALE, AD 1950–6000 BC

MINZE STUIVER

Department of Geological Sciences and Quaternary Research Center, University of Washington Seattle, Washington 98195 USA

and

BERND BECKER

Institute für Botanik, Universität Hohenheim, D-7000 Stuttgart 70 Germany

INTRODUCTION

The radiocarbon ages of dendrochronologically-dated wood samples, each covering 10 years, are now available for the cal AD 1950–6000 BC age range. The decadal calibration curve constructed from these data comprises 1) the previously published AD 1950–2500 BC portion (Stuiver & Becker 1986), to which minor ^{14}C age corrections were applied, and 2) the new 2500–6000 BC extension.

The calibration error (standard deviation in ^{14}C age) is based on 1) an estimate of the reproducibility in the ^{14}C age determination in the Seattle laboratory, and 2) interlaboratory comparisons that provide information on the sum total of uncertainty tied to the processes of wood allocation, dendro-age determination, sample pretreatment, laboratory ^{14}C determination, regional ^{14}C distribution and ^{14}C differences between individual trees of the same chronology (Stuiver & Pearson 1992, 1993). The standard deviations of the Table 1 ^{14}C calibration data for the AD 1950–2500 and 2500–6000 BC intervals are, respectively, equal to 1.6 and 1.7 times the standard deviation derived from the near-Gaussian counting statistics of the accumulated number of counts for the sample and standards.

The ^{14}C ages for the decadal wood samples (Table 1) were used to construct the bidecadal Seattle-Belfast calibration curve reported in this issue (Stuiver & Pearson 1993; Pearson & Stuiver 1993). The ^{14}C age errors are substantially smaller for the bidecadal curve, as most bidecadal data points were obtained by averaging 2 Seattle decadal ^{14}C ages, and 1 Belfast bidecadal ^{14}C age. Thus, the bidecadal curves should be used for most purposes. However, the decadal curve is more important when accounting for the fine structure of ^{14}C age calibration of samples formed during intervals of a decade or less.

DENDROCHRONOLOGY AND SAMPLE TREATMENT

The trees used for the AD interval were mainly from the US Pacific Northwest or California (Table 2 in Stuiver & Becker 1986). Most of the BC material was dendrochronologically dated wood from the German Main-Donau chronology (Becker 1993). Thirteen samples from the US bristlecone pine chronology (Ferguson & Graybill 1983) were ^{14}C dated as well. A limited number of samples from the Irish oak chronology (Pilcher *et al.* 1984) was used near 500 BC. Refer to Stuiver and Becker (1986) for wood pretreatment procedures. Cellulose, isolated from the decadal wood samples, was used for all 2500–6000 BC ^{14}C determinations.

CORRECTIONS

At the start of our time-scale calibration efforts in 1973, the CO_2 samples were stored in pyrex reservoirs for at least four weeks (Procedure 1). Radon decay took place during storage, and as a result, no detectable α particles were present in our α channel. Having never detected tree-ring radon in the α channels, we terminated their use some years later. Unfortunately, laboratory procedures were changed in 1976. Since then, tree-ring samples, after storage for four weeks, were purified on a self-circulating Cu oven (a pyrex reservoir filled with electrolytic copper wire and silver ribbon) at 450 °C before being admitted into the counter (Procedure 2). Small amounts of radon, most likely released from the walls of the heated reservoir, became part of the CO_2 sample. Once the problem was recognized, we determined the count-rate differences (routinely four days of counting) of samples subjected either to Procedure 1 or Procedure 2 for three of our counters to be $\Delta Ra = 0.274 \pm 0.090$, 0.276 ± 0.028 and 0.319 ± 0.090 counts per minute (cpm) (weighted average, 0.279 ± 0.026 cpm). Our radon correction for tree-ring samples (those measured for the 1977–1987 interval) is based on the above incremental four-day sample count-rate increase. As we kept Procedure 1 for routine (as opposed to high-precision) ^{14}C determinations, a radon correction is not needed for these samples.

The radon contribution can also be estimated from a comparison of the first- and last-day count-rate differences of 1) samples (ΔSa), and 2) oxalic acid and background standards (ΔOx and ΔB). Routine sample counts lasted four days; standards were routinely counted for three days. Procedure 2 was followed for all samples during the 1977–1987 period, and Procedure 1 for the standards, except for one counter where the oxalic acid CO_2, after repurification, was subjected to Procedure 2. In this case, the radon contribution was also properly accounted for, but for simplicity, we discuss only the results obtained for Procedure 1 standard counts.

Each counter completes about 50 sample runs per year, as well as 25 runs of oxalic acid and background. Figure 1 gives the yearly averaged ΔSa and ΔB values of the counter longest in operation (LC-4), together with ΔOx values of the LC-5 counter (for LC-4, the oxalic acid treatments did not always follow Procedure 1).

Procedure 1 background runs for 1977–1987 yield $\Delta B = 0.025 \pm 0.017$ cpm; Procedure 2 sample runs over the same interval yield $\Delta Sa = 0.189 \pm 0.049$ cpm. As expected, lower ΔSa values (0.035 ± 0.024 and 0.073 ± 0.081 cpm) are encountered for the 1973–1975 and 1989–1990 periods, when only Procedure 1 was used. Further, oxalic acid runs with Procedure 1 only in counter LC-5 yield a 14-yr ΔOx average of 0.012 ± 0.070 cpm (Fig. 1).

First- and last-day sample count-rate differences, ΔSa, were converted to ΔRa, using the half-life of radon of slightly less than four days. For our tree-ring counters, we determined ΔRa values of 0.285 ± 0.028, 0.247 ± 0.029 and 0.295 ± 0.030 cpm (LC4, 5 and 6, respectively). The weighted average, 0.276 ± 0.016 cpm, is in excellent agreement with the directly measured ΔRa values averaging 0.279 ± 0.026.

The above analysis not only confirms the validity of the radon correction, but can also be used as a test of counting stability. For instance, for the four years, 1984–1987, the scatter standard deviation in the first- to last-day count differences, ΔSa, ΔOx and ΔB (Counter LC-5) are 0.297, 0.315, 0.400 and 0.371 cpm for ΔSa; 0.468, 0.419, 0.459 and 0.372 cpm for ΔOx; and 0.090, 0.075, 0.072, and 0.070 cpm for ΔB. This gives a four-year average scatter standard deviation in the count differences of 0.346 cpm for ΔSa, 0.430 cpm for ΔOx and 0.077 cpm for ΔB. The (average) total counts accumulated during a counting day yields a Poisson standard deviation in the difference of about 0.308 cpm for ΔSa, 0.400 cpm for ΔOx and 0.060 cpm for ΔB. Thus, we

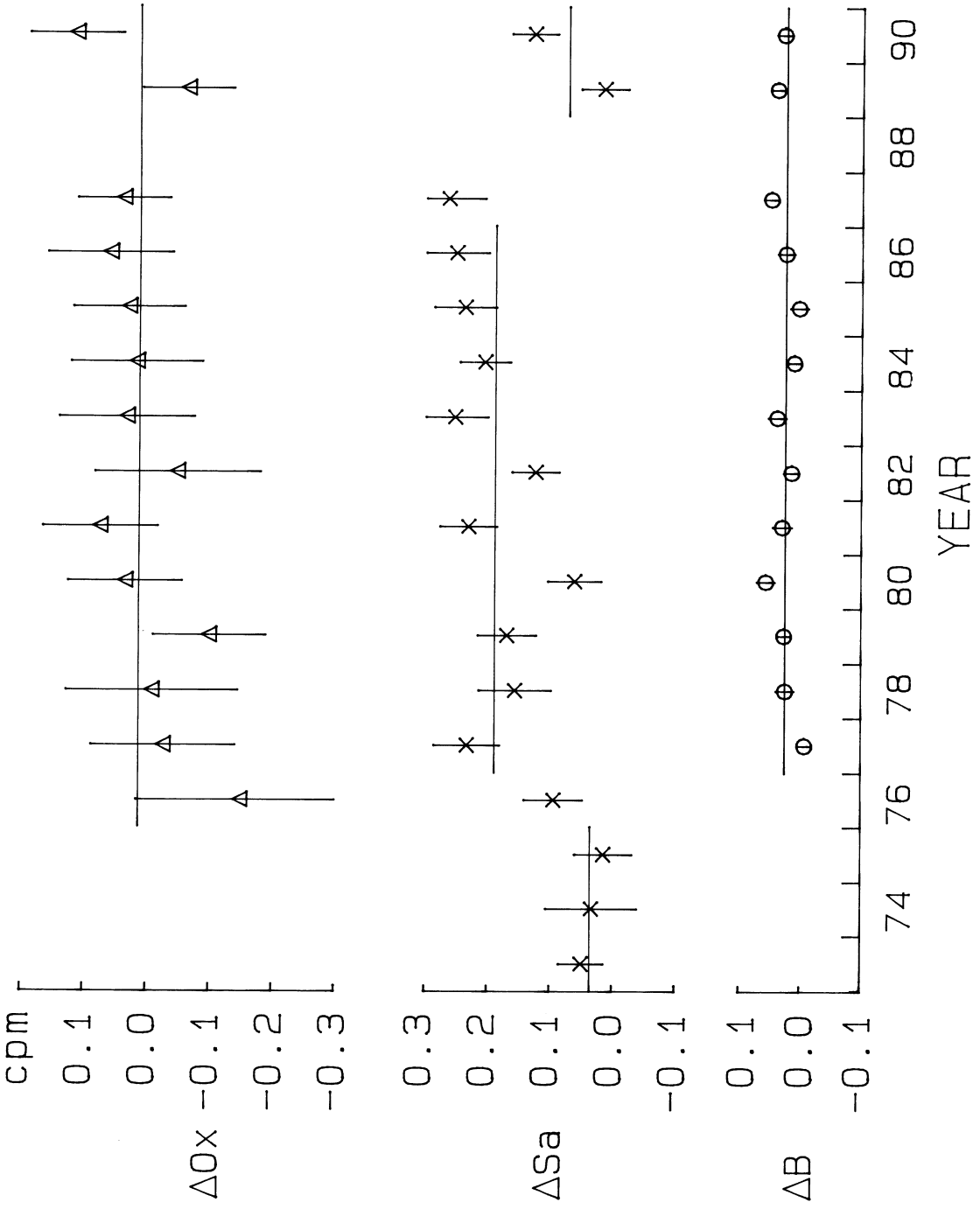

Fig. 1. First- and last-day counting-rate differences of samples (ΔSa, 4-day count) and standards (ΔOx and ΔB; 3-day counts). Sample and background values are yearly averages in Counter LC-4, oxalic acid similarly for Counter LC-5 (see text).

obtain error multipliers for the counting of samples and standards of 0.346/0.308 = 1.12(K_{Sa}), 0.430/0.400 = 1.08(K_{Ox}) and 0.077/0.060 = 1.28(K_B). Results for different years and different counters yield similar results, demonstrating excellent long-term counting stability.

The relative radon count-rate contribution, as a percentage of the observed sample counting rate, decreases when sample counts increase (younger samples). Correcting for the radon contribution results in an age increase of 10 ^{14}C yr for tree-ring samples that are a few hundred years old, and about 30 ^{14}C yr for 4500 yr-old samples.

REPRODUCIBILITY AND SYSTEMATIC DIFFERENCES

The ^{14}C ages reported are conventional ^{14}C ages (Stuiver & Polach 1977). As noted in the introduction, the Poisson-derived standard deviation has been multiplied with an error multiplier, K, of either 1.6 or 1.7. The justification of such a multiplier is given in Stuiver and Pearson (1992, 1993). The standard deviations shown in Table 1 reflect actual reproducibility. The CO_2 gas proportional counters used for the previous study (Stuiver & Becker 1986) also were used for the present one.

A comparison of Table 1 Seattle ^{14}C ages to those obtained by other laboratories confirms the validity of the choice of error multiplier. Systematic differences, although often confined to a decade or less, are more problematic. For the nearly 8000-yr Seattle and Belfast series (nearly 400 bidecadal data points), we find an average offset of <1 ^{14}C yr, but this offset is not uniformly distributed. The offsets found for individual millennia are in the 0–17 ^{14}C-yr range, with the exception of the 5180–5500 BC interval, where the ^{14}C ages differ by an unacceptable 54±5 yr (Stuiver & Pearson 1993). Seattle and Heidelberg (Kromer *et al.* 1986) results differ by 41±4 yr for the 4075–5265 BC and 5805–5995 BC intervals. The reasons for these offsets in the 40–50 yr range are not clear. Several other comparisons, *e.g.,* with Groningen (3210–3910 BC), Tucson (5680–5810 BC), La Jolla (2500–5000 BC), Pretoria (1930–3350 BC) imply the lack of statistically significant offsets (Stuiver& Pearson 1993). It is fair to conclude that systematic offsets in Table 1 are most likely confined to 1 or 2 decades, except for the 5180–5500 BC interval, where an offset up to 54 yr is possible.

CALIBRATION INSTRUCTIONS

We recommend that users of ^{14}C dates obtain additional information on reproducibility (and systematic error, if any) from the laboratory reporting the ^{14}C date. This information should lead to a realistic standard deviation in the reported age. A systematic error has to be deducted from, or added to, the reported ^{14}C age prior to age calibration.

Only the calibration curve is given in Figure 2; the one sigma (1σ; standard deviation) uncertainty in the curve is not given. The standard deviation (averaging 24 ^{14}C yr) is tabulated in Table 1 for each decadal midpoint. Table 1 standard deviations reflect the entire variance in the age determination process.

Cal BP ages are relative to the year AD 1950, with 0 cal BP equal to AD 1950. The relationship between cal AD/BC and Cal BP ages is cal BP = 1950 – cal AD, and cal BP = 1949 + cal BC. The switch from 1950 to 1949 when converting BC ages is caused by the absence of the year zero in the AD/BC chronology.

The conversion of a ^{14}C age to a cal age is as follows: 1) draw line A parallel to the bottom axis through the ^{14}C age to be converted; 2) draw vertical line(s) through the intercept(s) of line A and

the calibration curve. The cal AD/BC ages can be read at the bottom axis, the cal BP ages at the top.

To convert the standard error in the ^{14}C age into a range of cal AD/BC (BP) ages, determine the sample standard deviation, σ, by multiplying the quoted laboratory standard deviation with the "error multiplier". Unfortunately, information on error multipliers is often lacking. Here, the ^{14}C age user should refer to K values given above, or to the Scott, Long and Kra (1990).

Once the sample σ is known, the curve σ should be read from Table 1. The curve σ and sample σ should then be used to calculate total $\sigma = ((\text{sample } \sigma)^2 + (\text{curve } \sigma)^2)^{1/2}$ (Stuiver 1982). Lines parallel to A should now be drawn through the ^{14}C age + total σ, and ^{14}C age – total σ value. The vertical lines drawn through the intercepts now yield the outer limits of possible cal AD/BC (cal BP) ages that are compatible with the sample standard deviation.

The conversion procedure yields 1) single or multiple cal AD/BC (BP) ages that are compatible with a certain ^{14}C age, and 2) the range(s) of cal ages that correspond(s) to the standard deviation in the ^{14}C age (and calibration curve). Here, the user has to determine the calibrated ages from the Figure 2 graphs by drawing lines, whereas an alternate approach would be to use the computerized calibration (CALIB 3.0) program discussed elsewhere in this issue (Stuiver & Reimer 1993).

The probability that a certain cal age is the actual sample age may be quite variable within the cal age range. Higher probabilities are encountered around the intercept ages. The non-linear transform of a near-Gaussian distribution around a ^{14}C age into cal AD/BC (cal BP) age is not a simple matter, and computer programs are needed to derive the complex probability distribution. The CALIB 3.0 program (Stuiver & Reimer 1993) incorporates such probability distributions.

The calibration data presented here are valid for northern hemispheric samples that were formed in equilibrium with atmospheric $^{14}CO_2$. Systematic age differences are possible for the southern hemisphere, where ^{14}C ages of wood samples tend to be about 40 yr older (Vogel *et al.* 1993). Thus, ^{14}C ages of southern hemispheric samples preceding our era of fossil-fuel combustion should be reduced by 40 yr before being converted into cal AD/BC (BP) ages.

The calibration curve is valid only for age conversion of samples that were formed in equilibrium with atmospheric CO_2. Conventional ^{14}C ages of materials not in equilibrium with atmospheric reservoirs do not take into account the offset in ^{14}C age that may occur (Stuiver & Polach 1977). A constant offset, or reservoir deficiency, must be deducted from the reported ^{14}C age before any attempt can be made to convert to cal AD/BC (BP) ages.

The reservoir deficiency is time dependent for the mixed (and deep) layer of the ocean. For the calibration of marine Holocene samples, the reader is referred to Stuiver and Braziunas (1993), and, of course, the CALIB 3.0 program.

ACKNOWLEDGMENTS

The ^{14}C research at Seattle was supported by National Science Foundation grant BNS-9004492. We thank P. J. Reimer and P. J. Wilkinson for crucial technical and analytical support.

REFERENCES

Becker, B. 1993 An 11,000-year German oak and pine dendrochronology for radiocarbon calibration. *Radiocarbon*, this issue.

Ferguson, C. W. and Graybill, D. A. 1983 Dendrochronology of bristlecone pine: A progress report. *In* Stuiver, M. and Kra, R. S., Proceedings of the 11th International Radiocarbon Conference. *Radiocarbon* 25(2): 287–288.

Kromer, B., Rhein, M., Bruns, M., Schoch-Fischer, H., Münnich, K. O., Stuiver, M. and Becker, B. 1986 Radiocarbon calibration data for the 6th to the 8th Millennia BC. *In* Stuiver, M. and Kra, R. S., eds., Proceedings of the 12th International Radiocarbon Conference. *Radiocarbon* 28(2B): 954–960.

Pearson, G. W. and Stuiver, M. 1993 High-precision bidecadal calibration of the radiocarbon time scale, 500–2500 BC. *Radiocarbon*, this issue.

Pilcher, J. R., Baillie, M. G. L., Schmidt, B. and Becker, B. 1984 A 7,272-year tree-ring chronology for western Europe. *Nature* 312: 150–152.

Scott, E. M., Long, A. and Kra, R., eds. 1990 Proceedings of the International Workshop on Intercomparison of Radiocarbon Laboratories. *Radiocarbon* 32(3): 253–397.

Stuiver, M. 1982 A high-precision calibration of the AD radiocarbon time scale. *Radiocarbon* 24(1): 1–26.

Stuiver, M. and Becker, B. 1986 High-precision decadal calibration of the radiocarbon time scale, AD 1950–2500 BC. *In* Stuiver, M. and Kra, R. S., eds., Proceedings of the 12th International Radiocarbon Conference. *Radiocarbon* 28(2B): 863-910.

Stuiver, M. and Braziunas, T. F. 1993 Modeling radiocarbon ages of marine samples back to 10,000 BC. *Radiocarbon*, this issue.

Stuiver, M. and Pearson, G. W. 1992 Calibration of the radiocarbon time scale, 2500–5000 BC. *In* Taylor, R. E., Long, A. and Kra, R. S., eds., *Radiocarbon After Four Decades: An Interdisciplinary Perspective.* New York, Springer Verlag: 19–33.

_____1993 High-precision calibration of the radiocarbon time scale, AD 1950–500 BC and 2500–6000 BC. *Radiocarbon*, this issue.

Stuiver, M. and Polach, H. A. 1977 Discussion: Reporting of ^{14}C data. *Radiocarbon* 19(3): 355–363.

Stuiver, M. and Reimer, P.J. 1993 Extended ^{14}C data base and revised CALIB radiocarbon age calibration program. *Radiocarbon*, this issue.

Vogel, J.C., Fuls, A., Visser, E. and Becker, B. 1993 Pretoria calibration curve for short-lived samples, 1930 BC–3350 BC. *Radiocarbon*, this issue.

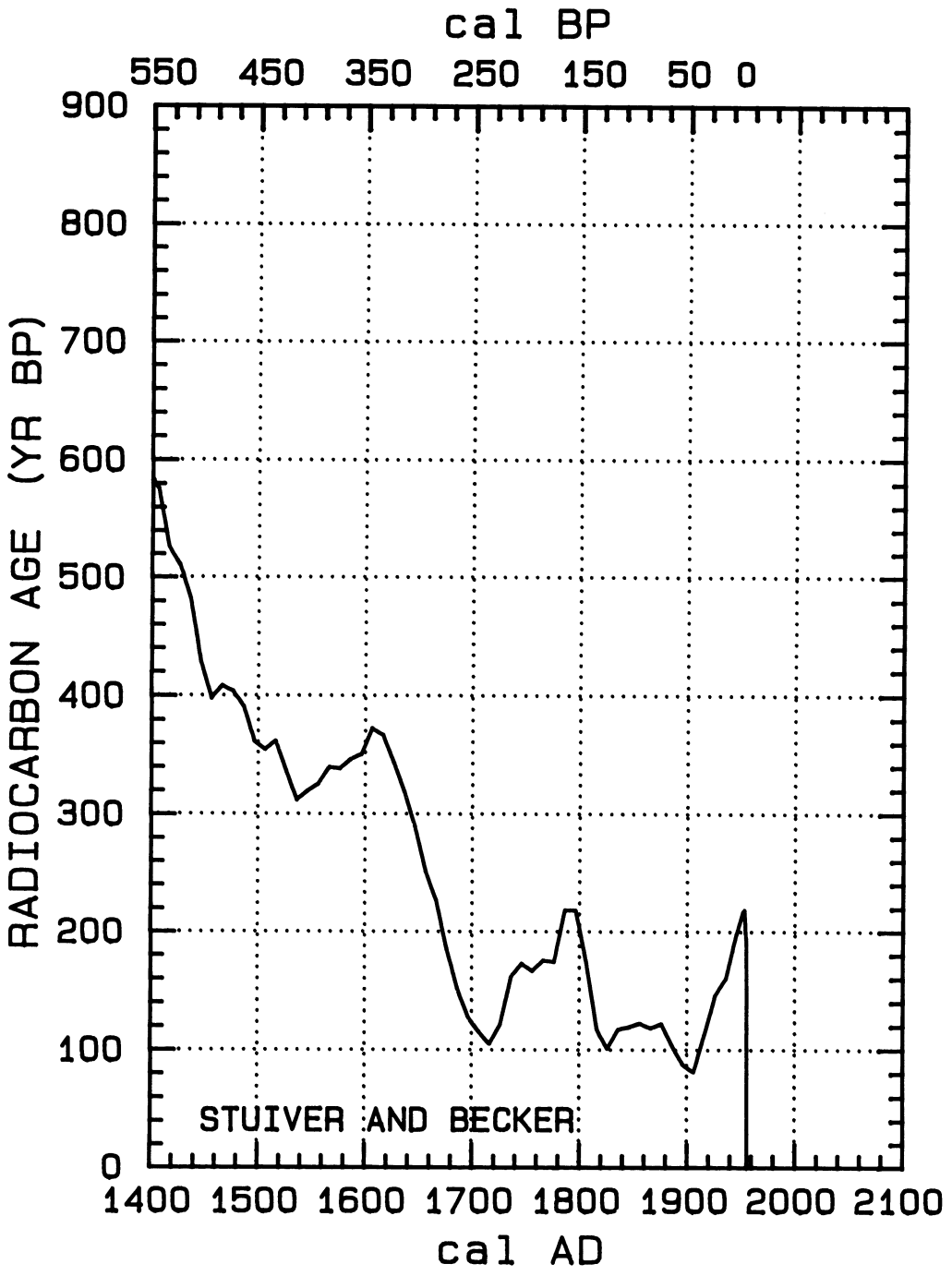

Fig. 2A–P. ^{14}C calibration curve derived from decadal samples

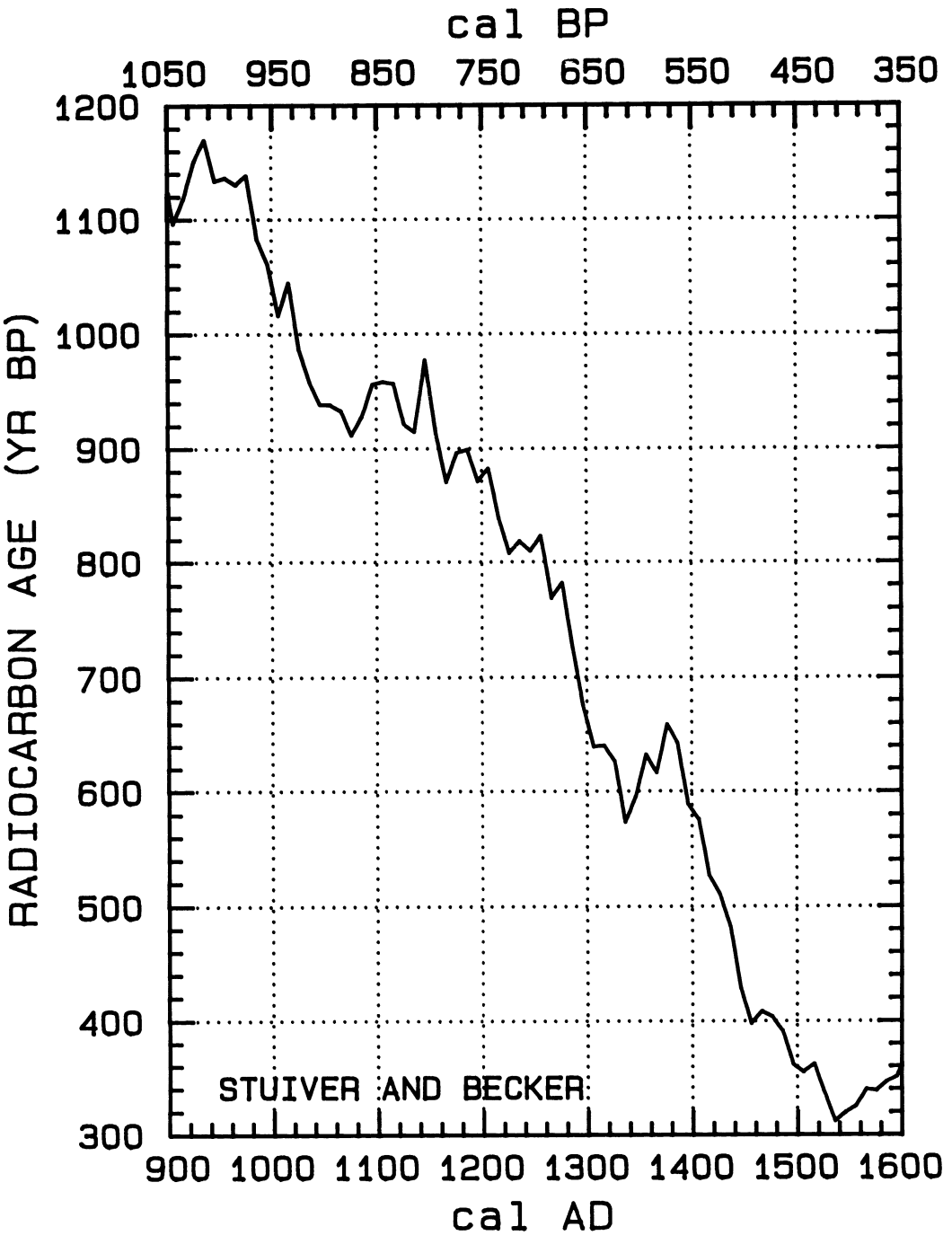
cal BP
1050 950 850 750 650 550 450 350
1200
1100
1000
900
800
700
600
500
400
300
RADIOCARBON AGE (YR BP)
STUIVER AND BECKER
900 1000 1100 1200 1300 1400 1500 1600
cal AD

Fig. 2B

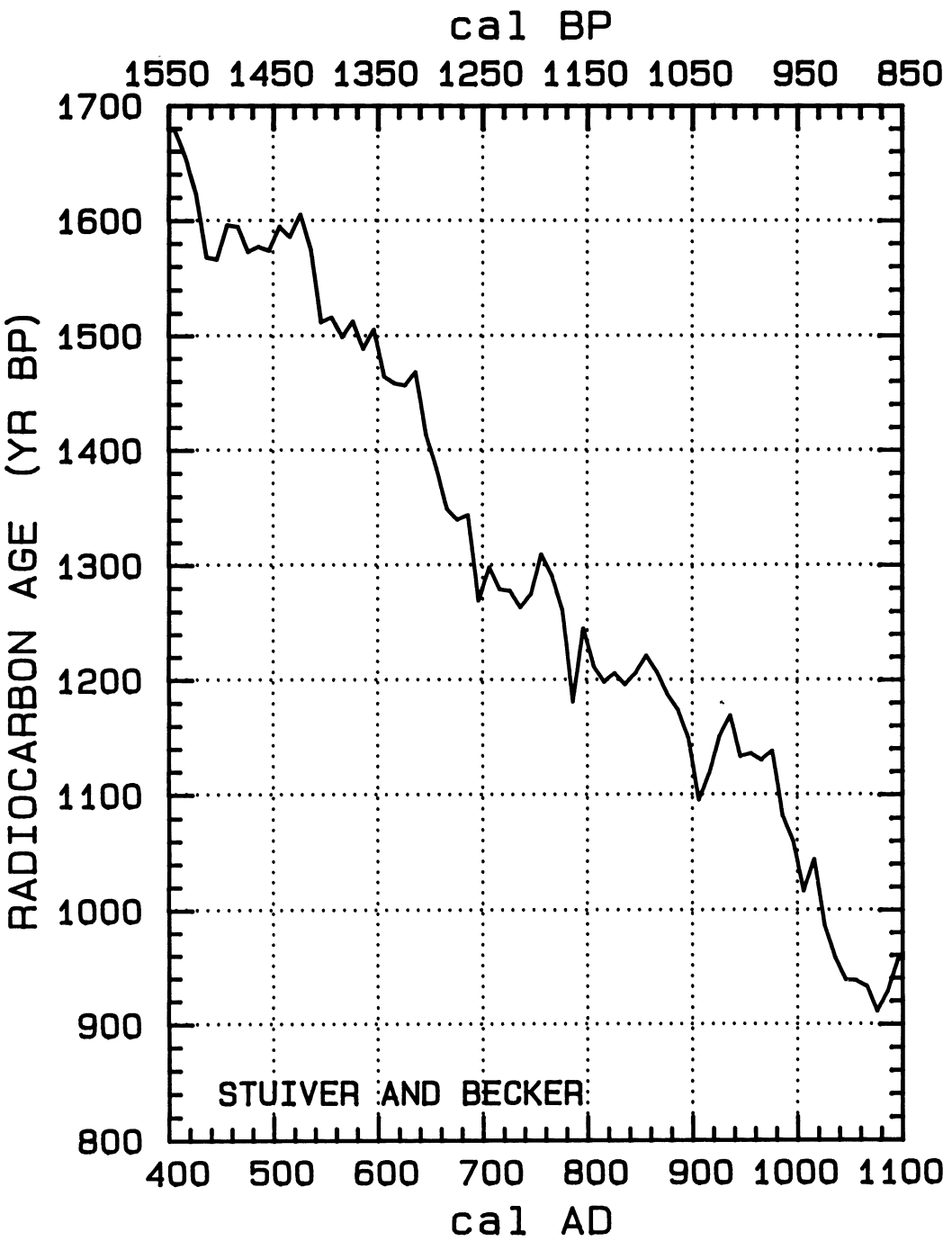
cal BP
1550 1450 1350 1250 1150 1050 950 850
1700
1600
1500
1400
1300
1200
1100
1000
900
800
RADIOCARBON AGE (YR BP)
STUIVER AND BECKER
400 500 600 700 800 900 1000 1100
cal AD

Fig. 2C

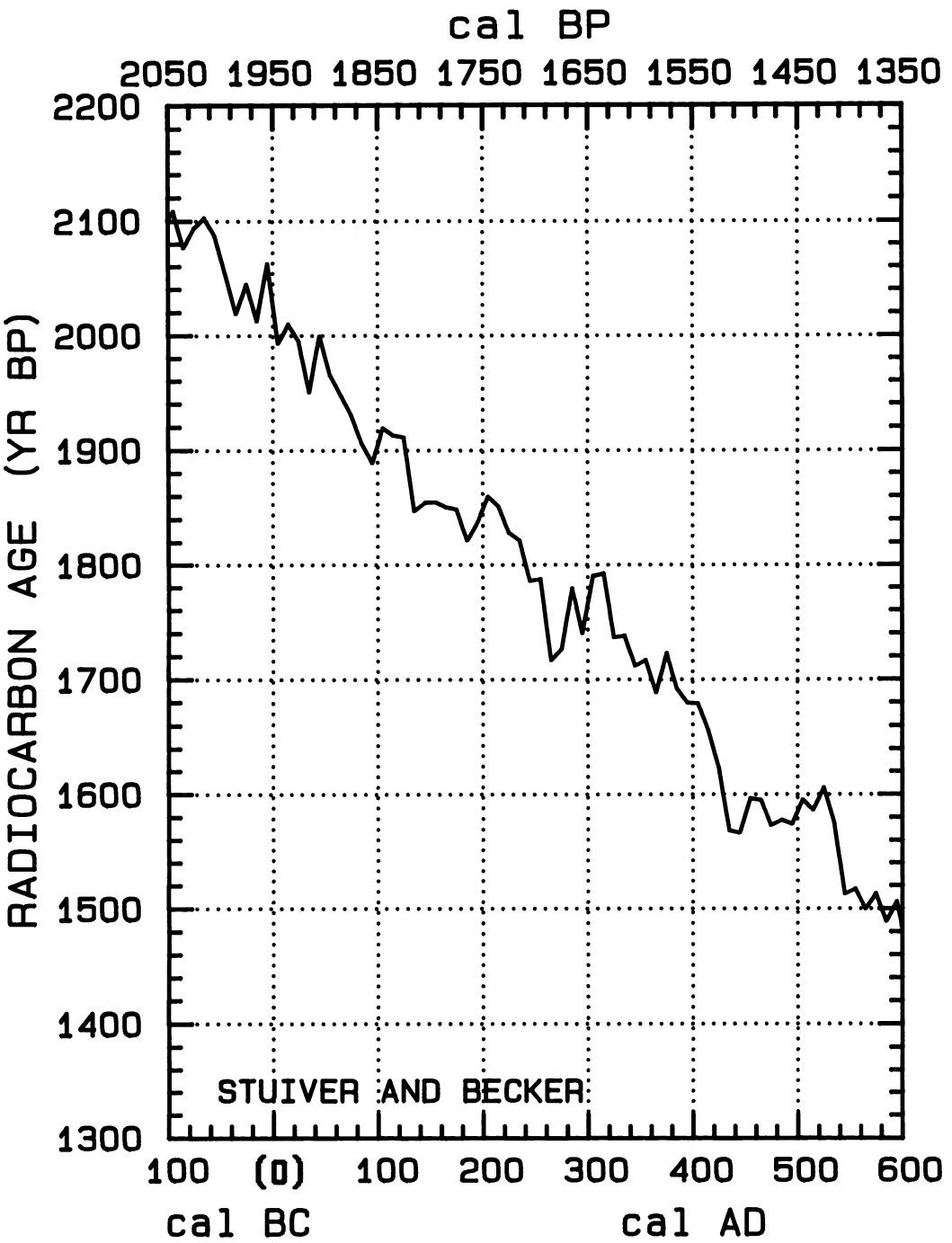
cal BP
2050 1950 1850 1750 1650 1550 1450 1350
2200
2100
2000
1900
1800
1700
1600
1500
1400
1300
RADIOCARBON AGE (YR BP)
STUIVER AND BECKER
100 (0) 100 200 300 400 500 600
cal BC
cal AD

Fig. 2D

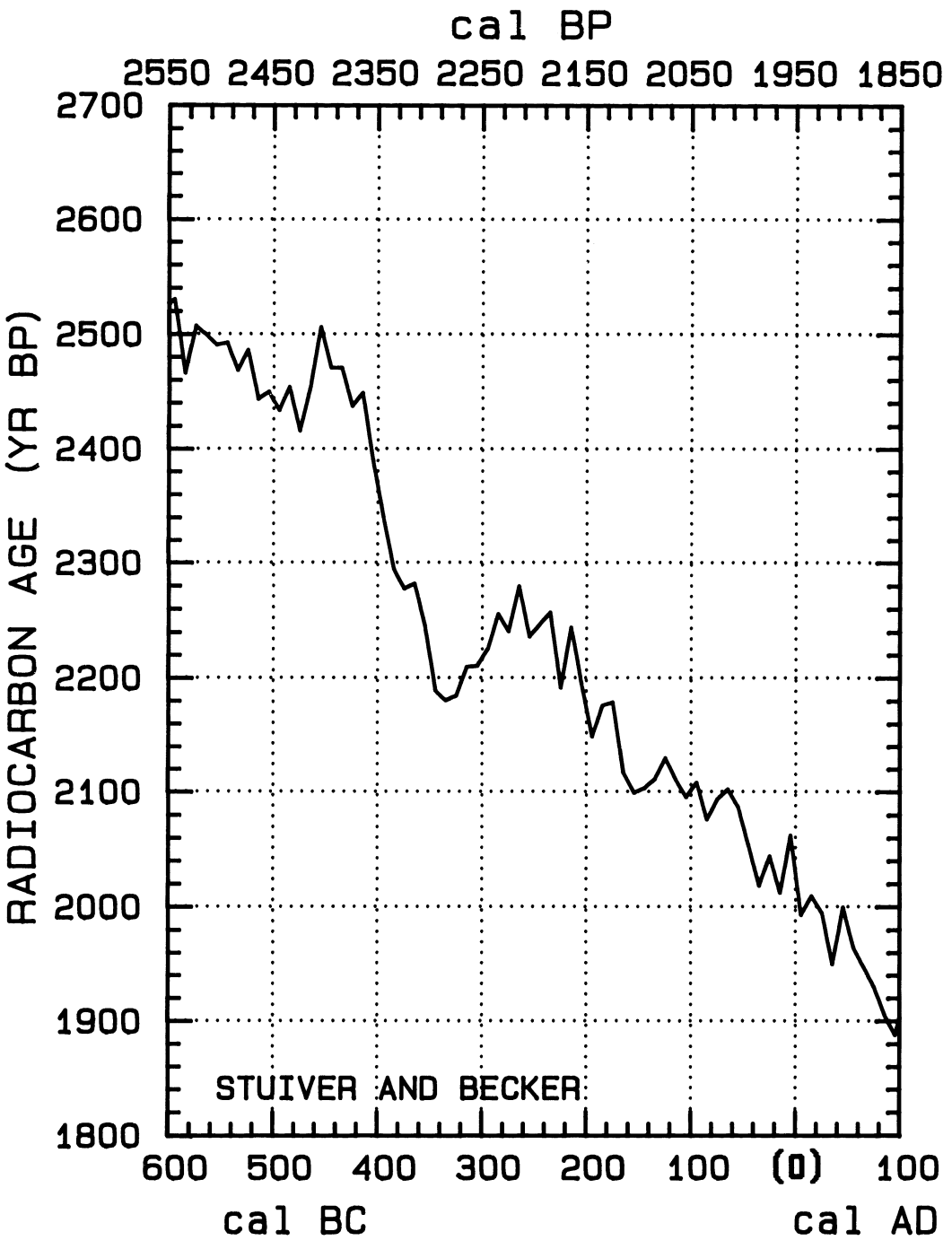
cal BP
2550 2450 2350 2250 2150 2050 1950 1850
2700
2600
2500
2400
2300
2200
2100
2000
1900
1800
RADIOCARBON AGE (YR BP)
STUIVER AND BECKER
600 500 400 300 200 100 (0) 100
cal BC
cal AD

Fig. 2E

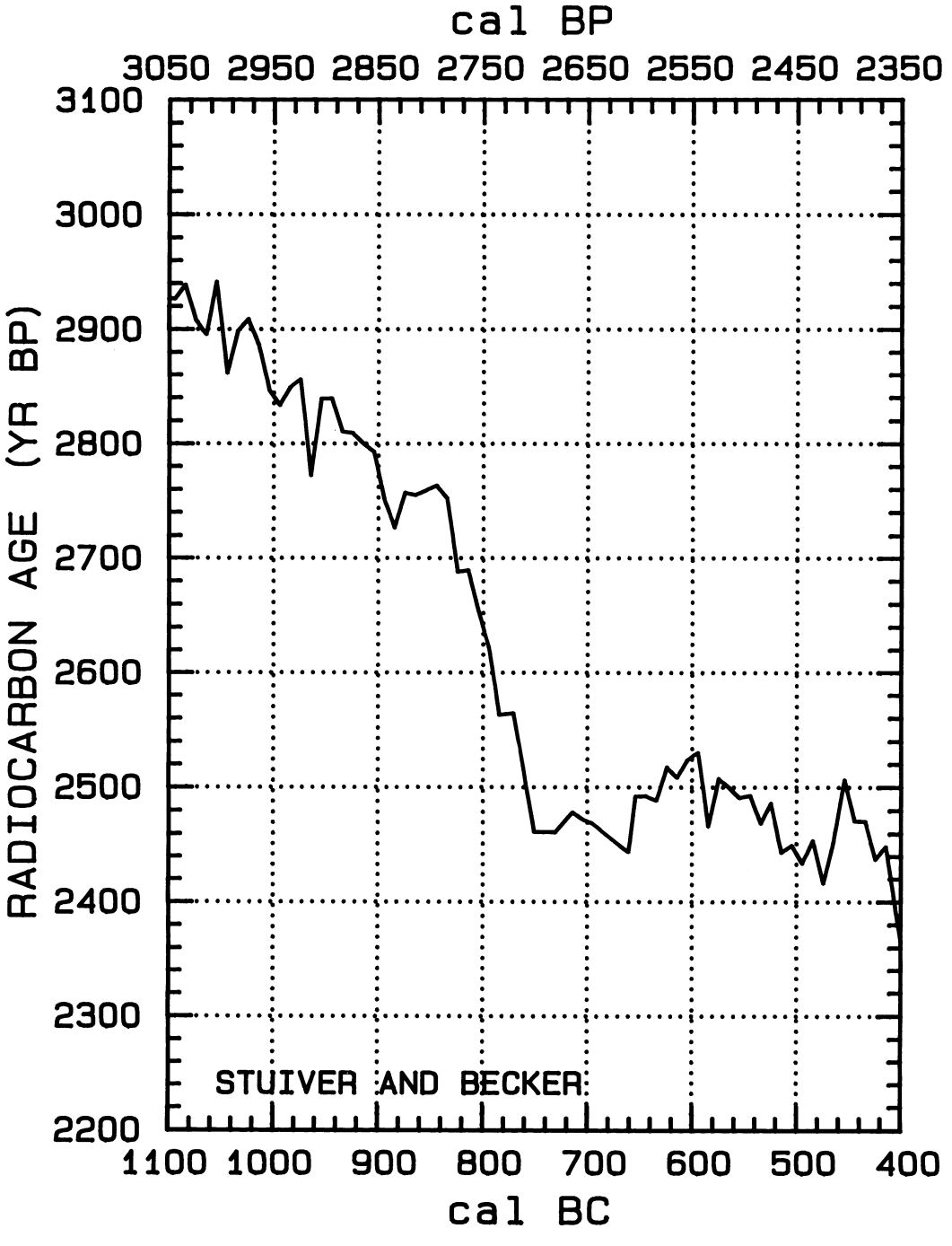
cal BP
3050 2950 2850 2750 2650 2550 2450 2350
3100
3000
2900
2800
2700
2600
2500
2400
2300
2200
RADIOCARBON AGE (YR BP)
STUIVER AND BECKER
1100 1000 900 800 700 600 500 400
cal BC

Fig. 2F

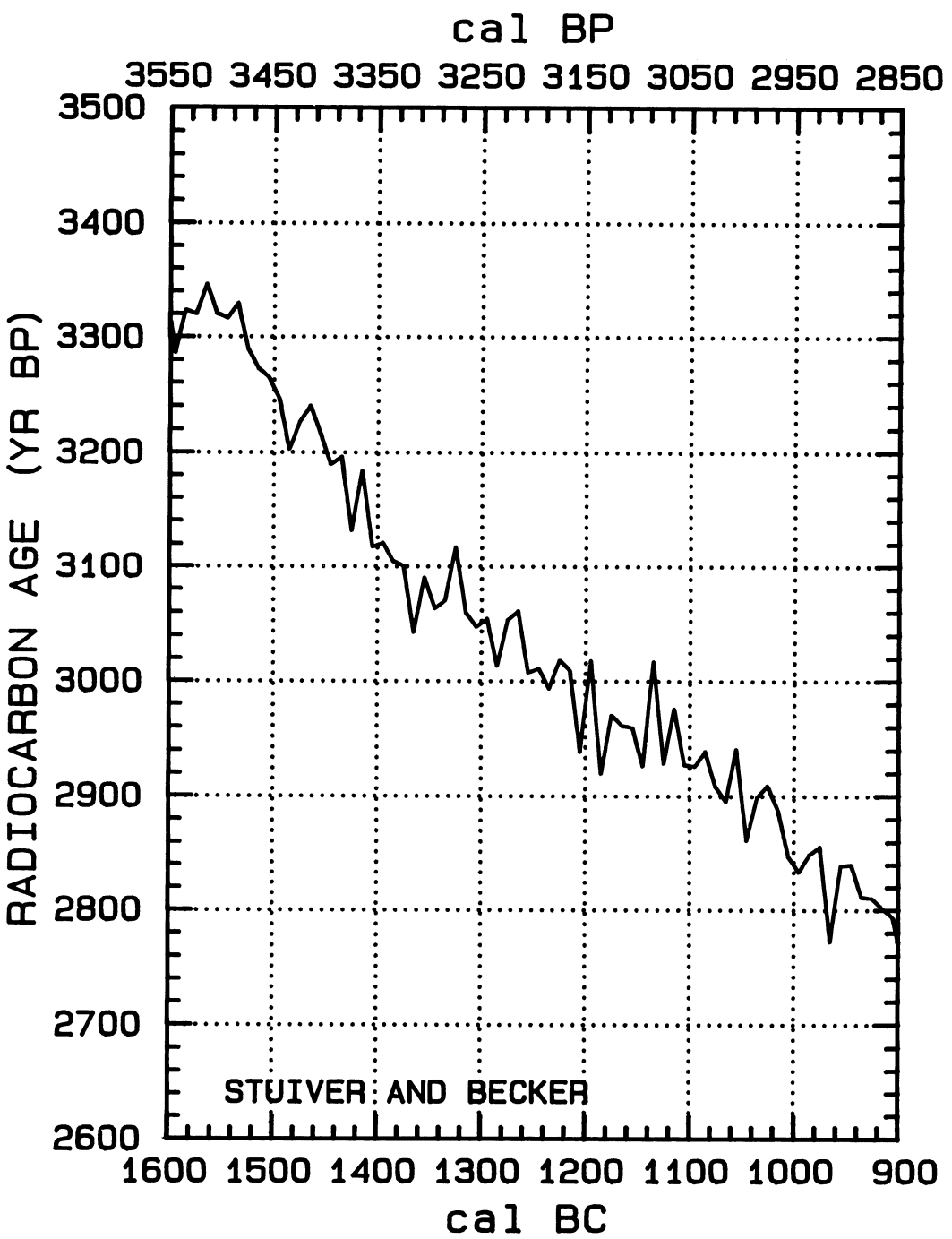
cal BP
3550 3450 3350 3250 3150 3050 2950 2850
3500
3400
3300
3200
3100
3000
2900
2800
2700
2600
RADIOCARBON AGE (YR BP)
STUIVER AND BECKER
1600 1500 1400 1300 1200 1100 1000 900
cal BC

Fig. 2G

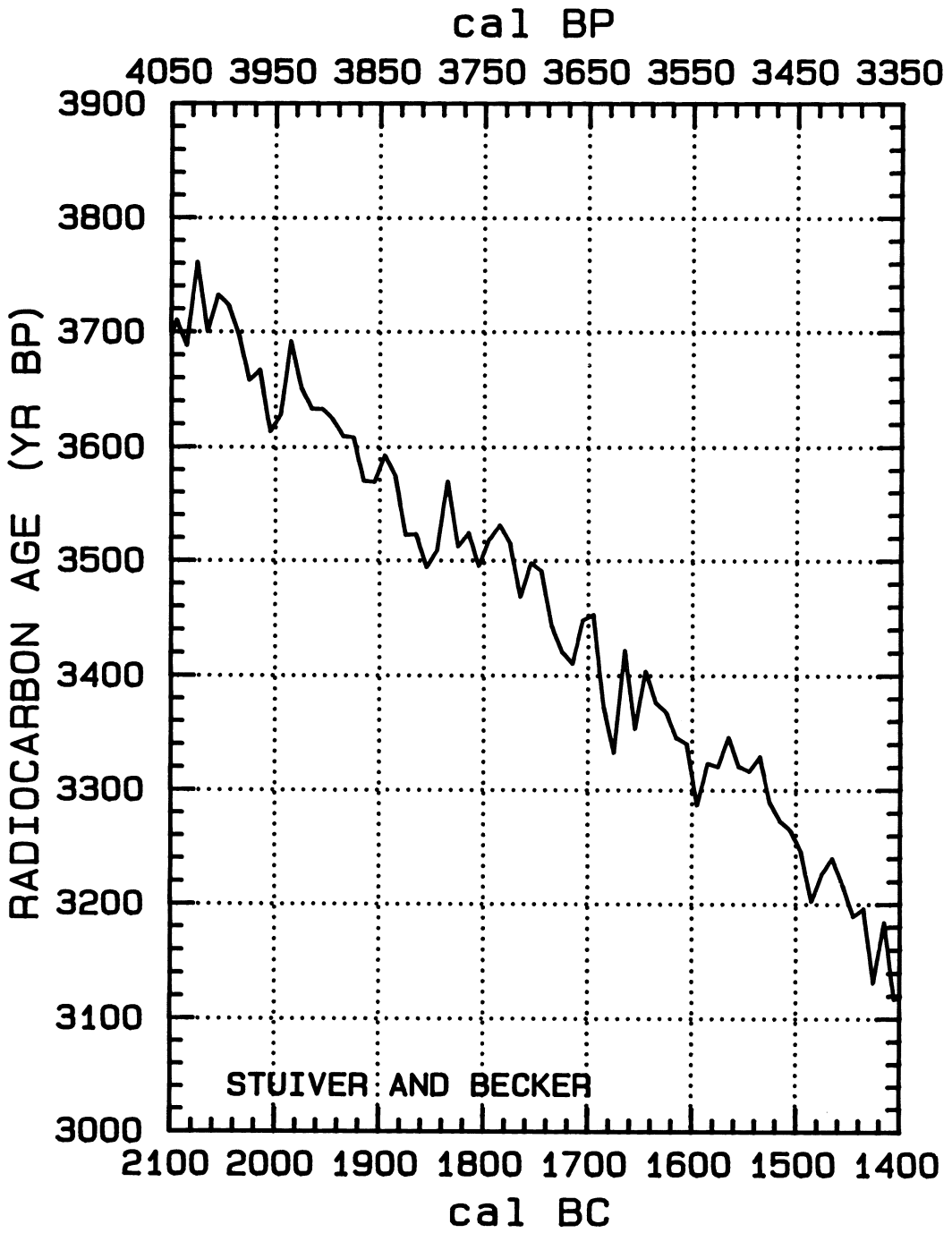
cal BP
4050 3950 3850 3750 3650 3550 3450 3350
3900
3800
3700
3600
3500
3400
3300
3200
3100
3000
RADIOCARBON AGE (YR BP)
STUIVER AND BECKER
2100 2000 1900 1800 1700 1600 1500 1400
cal BC

Fig. 2H

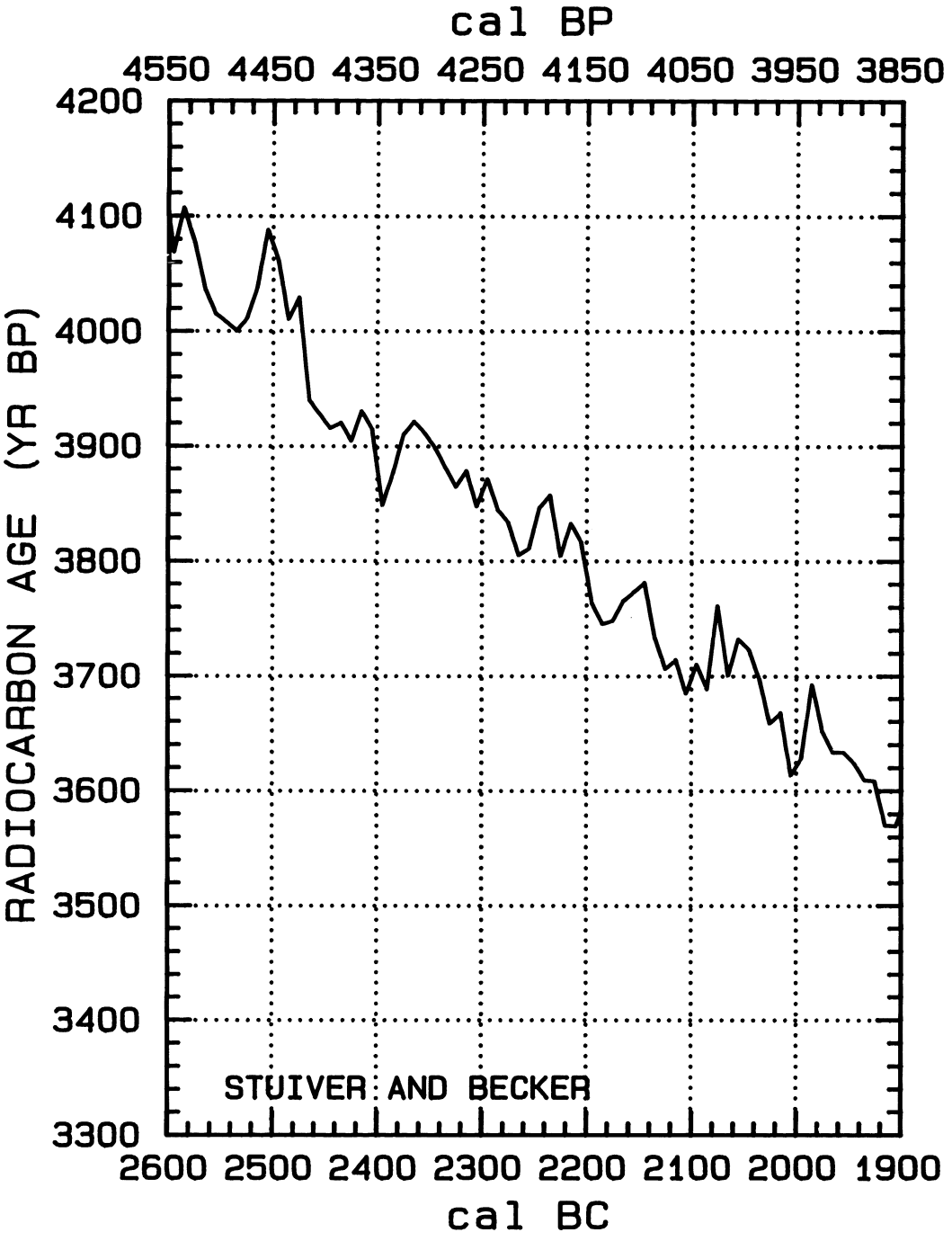
cal BP
4550 4450 4350 4250 4150 4050 3950 3850
4200
4100
4000
3900
3800
3700
3600
3500
3400
3300
RADIOCARBON AGE (YR BP)
STUIVER AND BECKER
2600 2500 2400 2300 2200 2100 2000 1900
cal BC

Fig. 2I

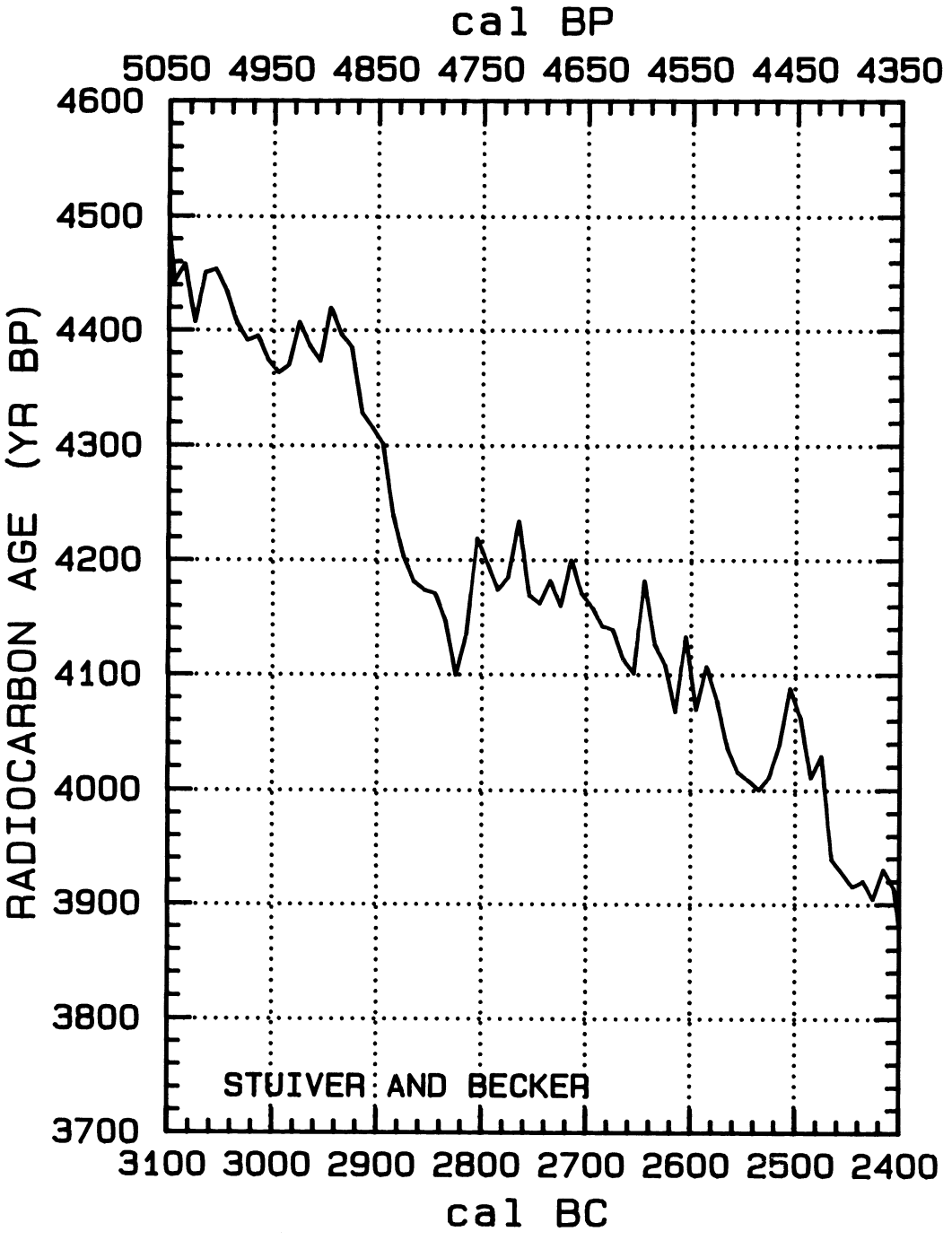
cal BP
5050 4950 4850 4750 4650 4550 4450 4350
4600
4500
4400
4300
4200
4100
4000
3900
3800
3700
RADIOCARBON AGE (YR BP)
STUIVER AND BECKER
3100 3000 2900 2800 2700 2600 2500 2400
cal BC

Fig. 2J

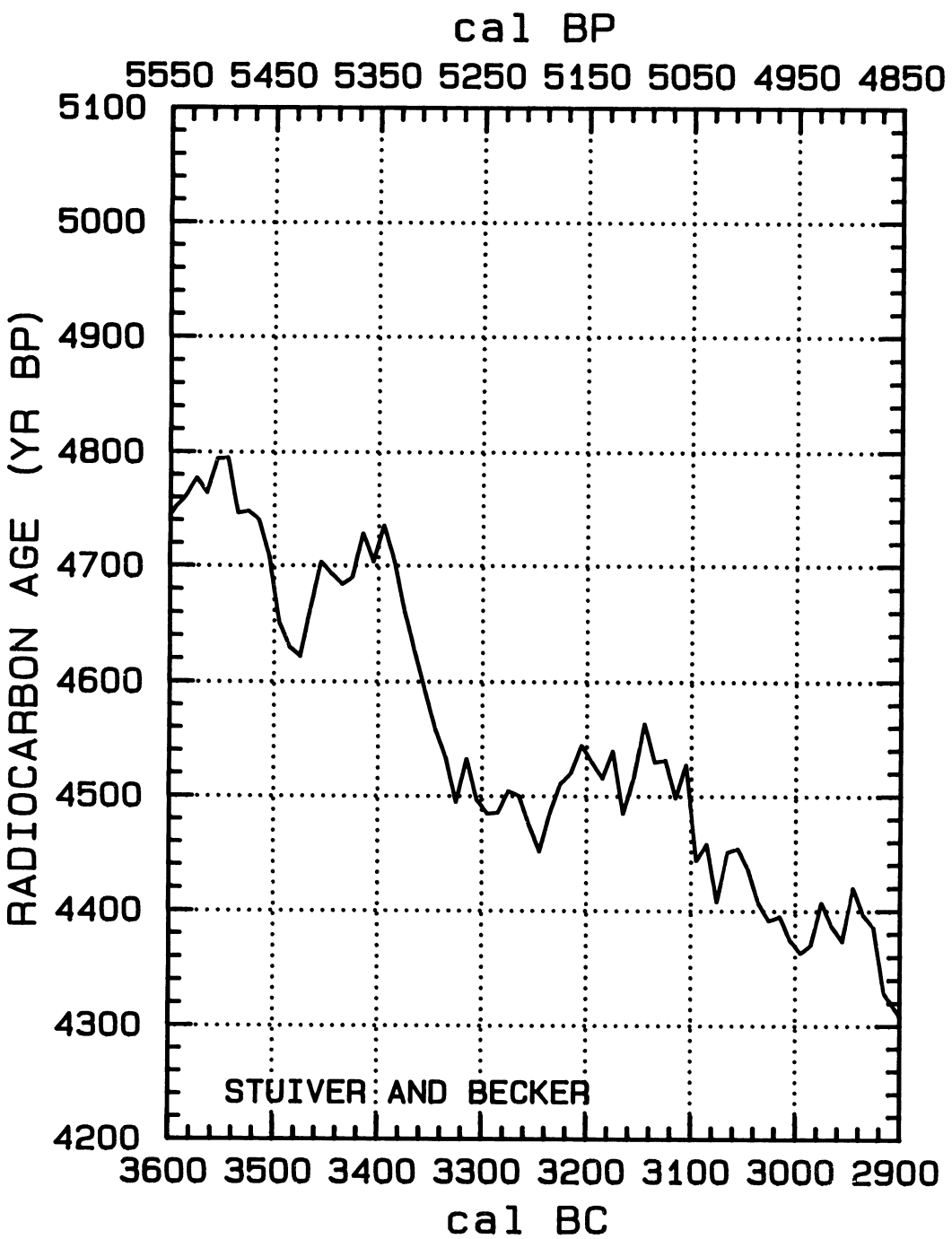
cal BP
5550 5450 5350 5250 5150 5050 4950 4850
5100
5000
4900
4800
4700
4600
4500
4400
4300
4200
RADIOCARBON AGE (YR BP)
STUIVER AND BECKER
3600 3500 3400 3300 3200 3100 3000 2900
cal BC

Fig. 2K

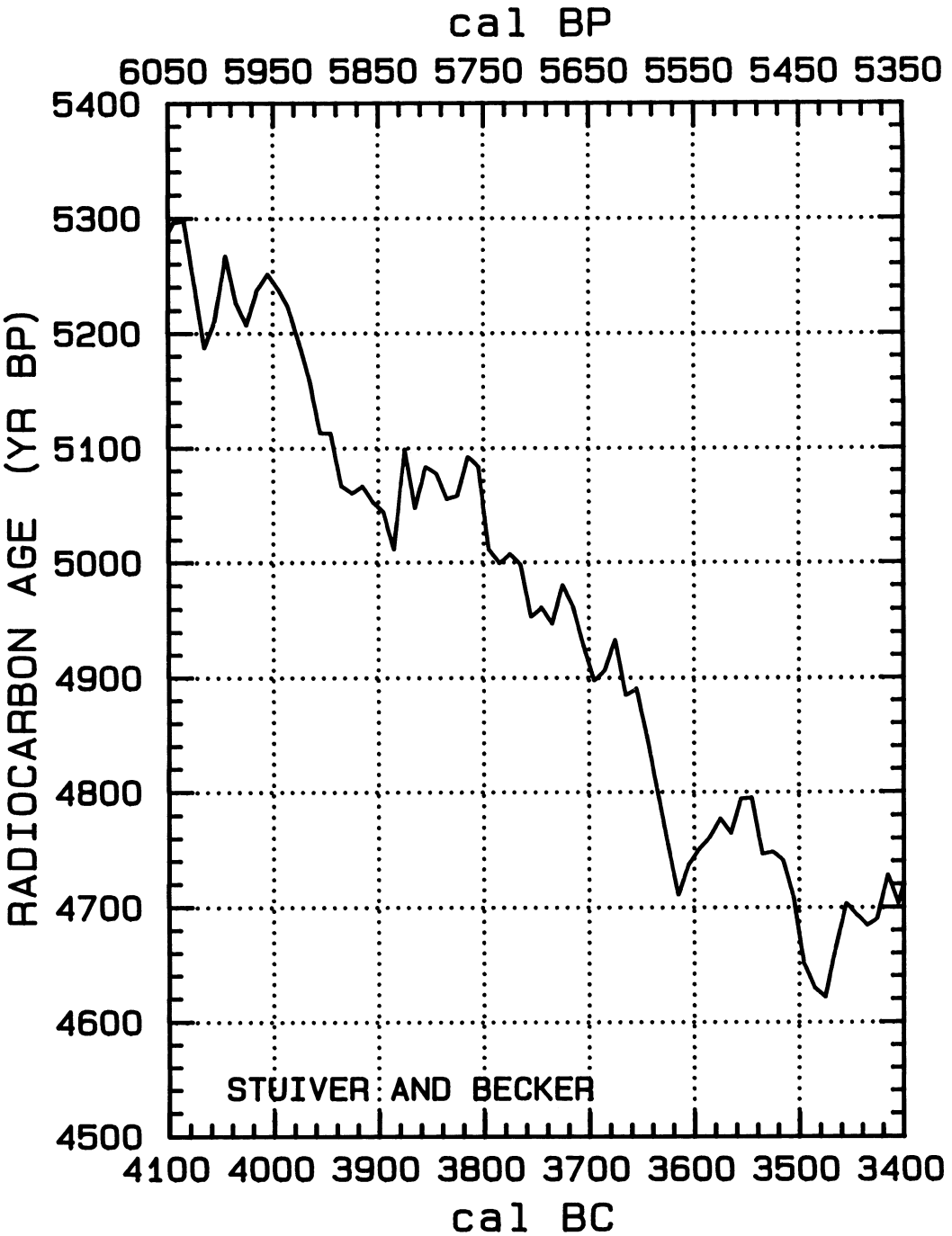
cal BP
6050 5950 5850 5750 5650 5550 5450 5350
5400
5300
5200
5100
5000
4900
4800
4700
4600
4500
RADIOCARBON AGE (YR BP)
STUIVER AND BECKER
4100 4000 3900 3800 3700 3600 3500 3400
cal BC

Fig. 2L

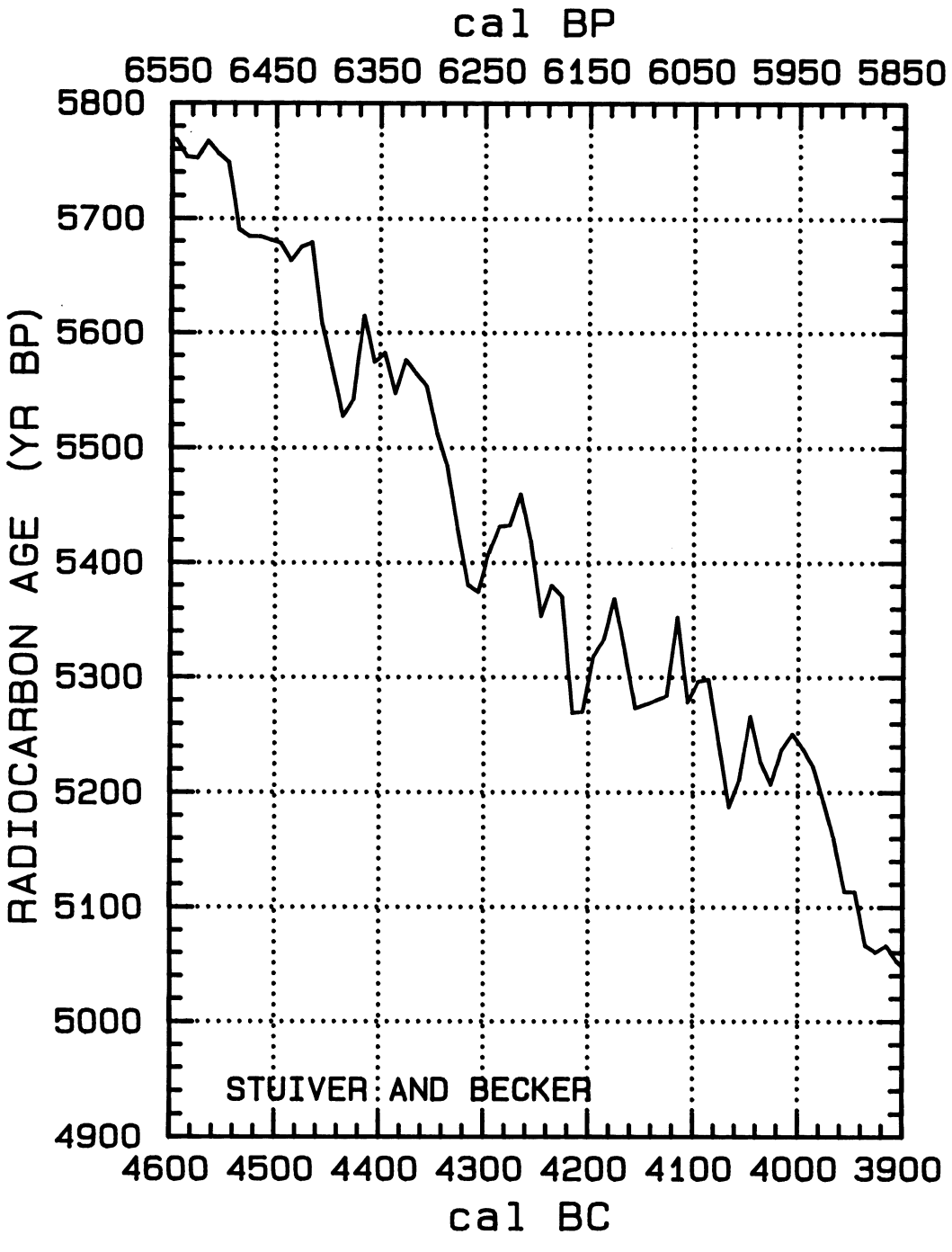
cal BP
6550 6450 6350 6250 6150 6050 5950 5850
5800
5700
5600
5500
5400
5300
5200
5100
5000
4900
RADIOCARBON AGE (YR BP)
STUIVER AND BECKER
4600 4500 4400 4300 4200 4100 4000 3900
cal BC

Fig. 2M

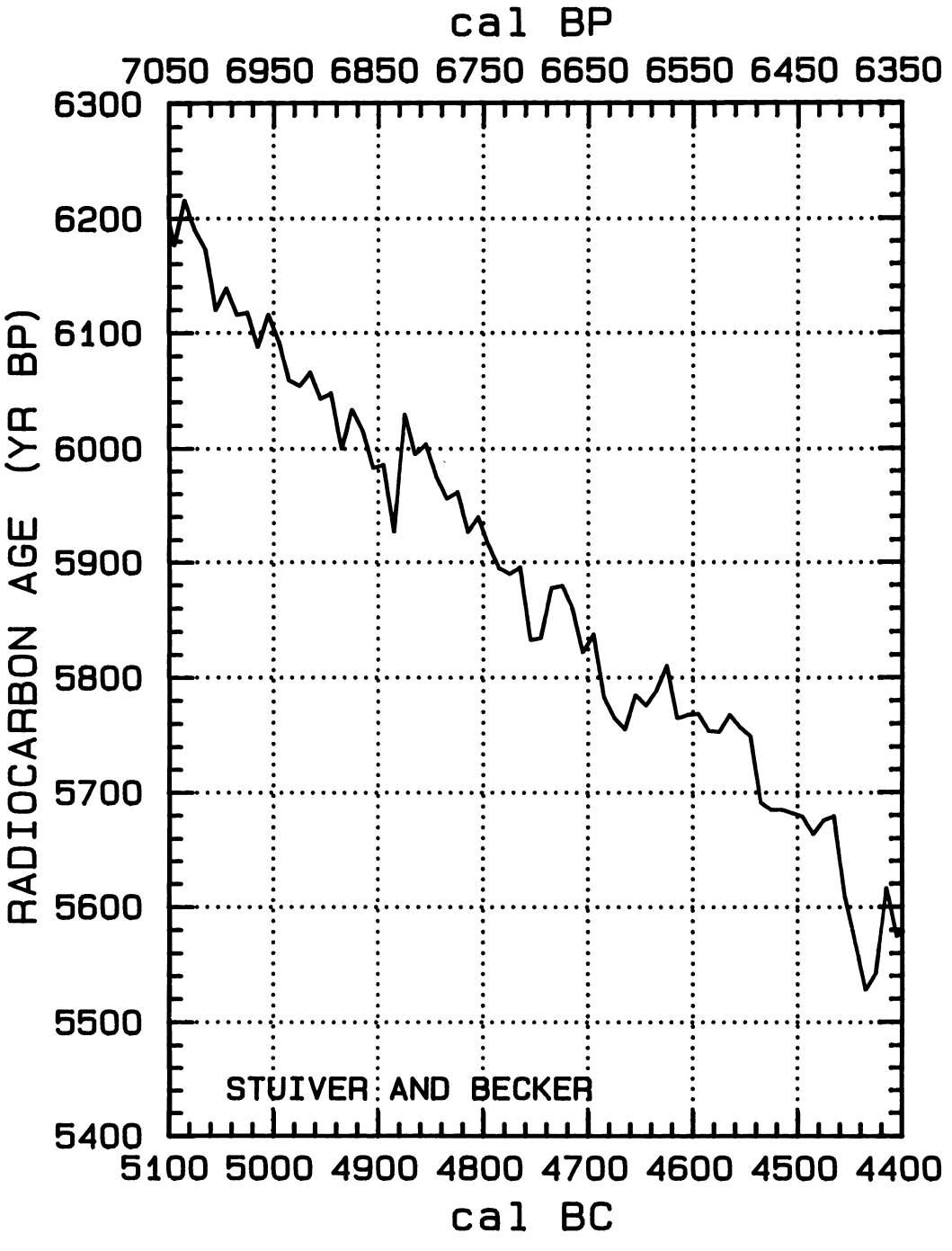
cal BP
7050 6950 6850 6750 6650 6550 6450 6350
6300
6200
6100
6000
5900
5800
5700
5600
5500
5400
RADIOCARBON AGE (YR BP)
STUIVER AND BECKER
5100 5000 4900 4800 4700 4600 4500 4400
cal BC

Fig. 2N

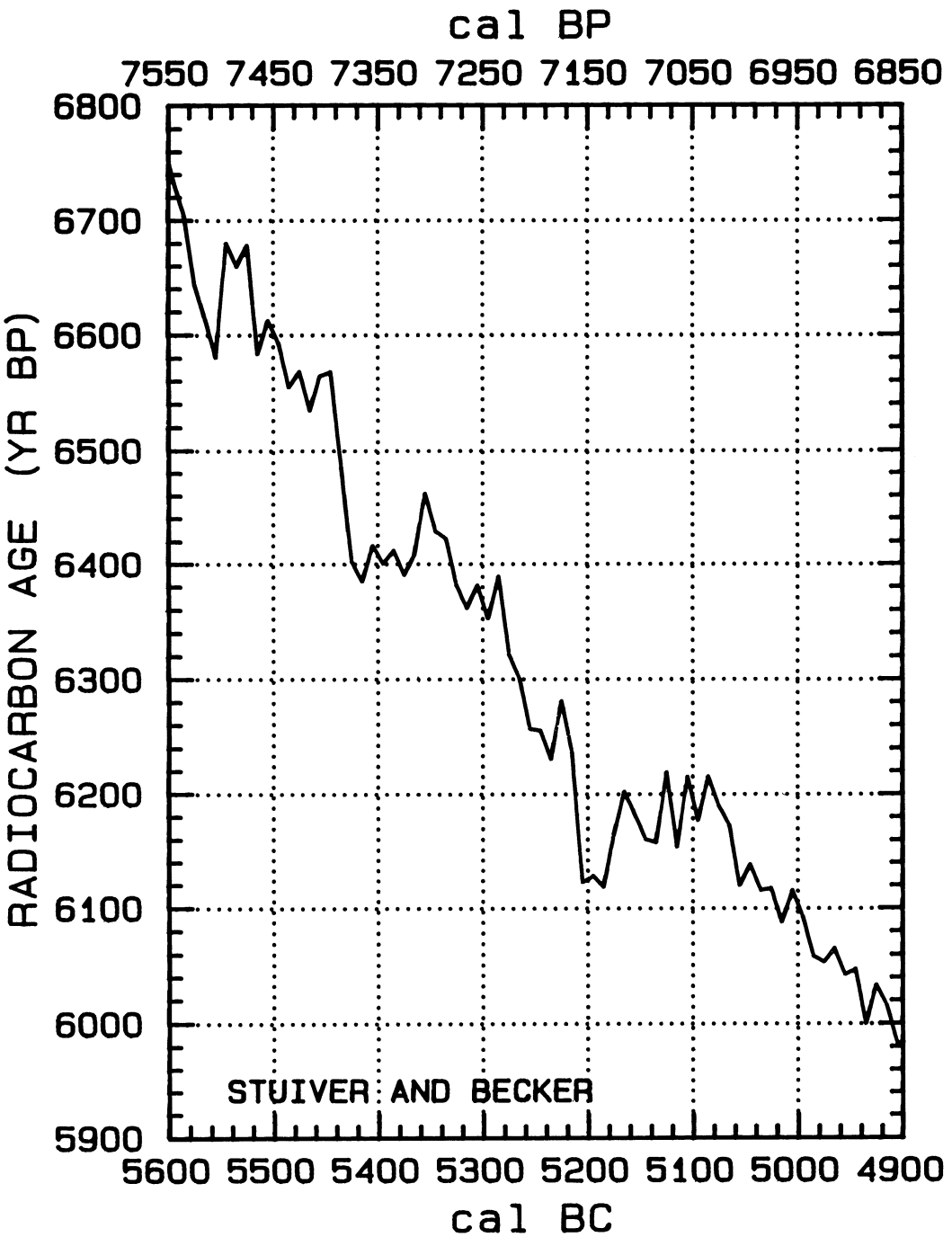
cal BP
7550 7450 7350 7250 7150 7050 6950 6850
6800
6700
6600
6500
6400
6300
6200
6100
6000
5900
RADIOCARBON AGE (YR BP)
STUIVER AND BECKER
5600 5500 5400 5300 5200 5100 5000 4900
cal BC

Fig. 20

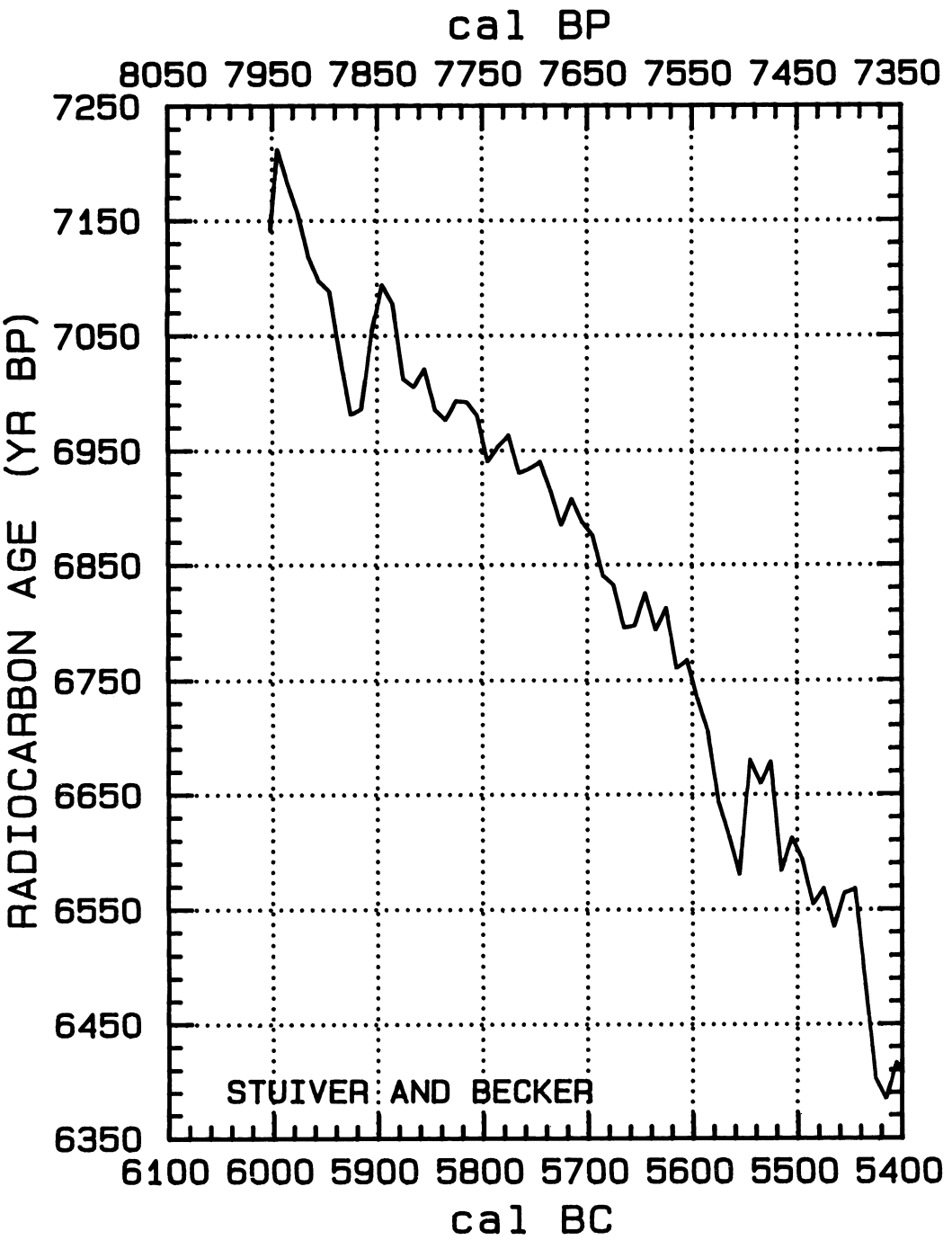
cal BP
8050 7950 7850 7750 7650 7550 7450 7350
7250
7150
7050
6950
6850
6750
6650
6550
6450
6350
RADIOCARBON AGE (YR BP)
STUIVER AND BECKER
6100 6000 5900 5800 5700 5600 5500 5400
cal BC

Fig. 2P

TABLE 1. ^{14}C age determinations made at the University of Washington (Seattle). The cal AD/BC ages (or cal BP) represent the midpoints of 10-yr wood sections, except when 20-yr samples were needed to obtain the quantity of treated wood used for a measurement (661.5, 696.5, 731.5, 751.5 and 771.5 BC). The standard deviation in the age and $\Delta^{14}C$ (defined in Stuiver & Polach (1977)) values includes a 1.6 or 1.7 error multiplier (see text). Overlapping decadal samples with midpoints no greater than 1 yr apart were averaged. Single-year data were averaged with decadal data for the AD 1515–1935 interval, and only single-year data were used for the AD 1945 data point.

Cal AD/BC	$\Delta^{14}C$ ‰	^{14}C age (BP)	Cal BP	Cal AD/BC	$\Delta^{14}C$ ‰	^{14}C age (BP)	Cal BP
AD 1945	−23.7 ± .8	199 ± 7	5	AD 1535	11.5 ± .7	312 ± 5	415
AD 1935	−18.0 ± .8	161 ± 6	15	AD 1525	9.7 ± .8	336 ± 7	425
AD 1925	−15.0 ± .8	146 ± 6	25	AD 1515	7.7 ± .9	362 ± 7	435
AD 1915	−9.8 ± .6	113 ± 5	35	AD 1505	9.8 ± 1.6	355 ± 13	445
AD 1905	−4.7 ± 1.0	81 ± 8	45	AD 1495	10.1 ± 2.0	362 ± 16	455
AD 1895	−4.2 ± 1.1	88 ± 9	55	AD 1485	7.6 ± 2.6	392 ± 21	465
AD 1885	−5.0 ± .7	104 ± 5	65	AD 1475	7.2 ± 2.8	404 ± 23	475
AD 1875	−6.1 ± .7	122 ± 5	75	AD 1465	7.9 ± 2.9	409 ± 23	485
AD 1865	−4.5 ± .7	119 ± 6	85	AD 1455	10.5 ± 2.0	398 ± 16	495
AD 1855	−3.9 ± .9	123 ± 8	95	AD 1445	7.9 ± 2.4	428 ± 19	505
AD 1845	−2.1 ± .8	120 ± 6	105	AD 1435	2.3 ± 2.9	483 ± 23	515
AD 1835	−0.7 ± .7	117 ± 6	115	AD 1425	0.0 ± 2.7	511 ± 21	525
AD 1825	2.6 ± .6	101 ± 5	125	AD 1415	−0.8 ± 2.8	527 ± 22	535
AD 1815	1.7 ± .8	118 ± 7	135	AD 1405	−5.7 ± 2.6	576 ± 21	545
AD 1805	−3.9 ± .8	173 ± 6	145	AD 1395	−6.1 ± 2.8	589 ± 23	555
AD 1795	−8.4 ± .8	219 ± 7	155	AD 1385	−11.6 ± 2.0	643 ± 16	565
AD 1785	−7.3 ± .8	219 ± 7	165	AD 1375	−12.4 ± 2.2	659 ± 18	575
AD 1775	−0.9 ± .7	174 ± 6	175	AD 1365	−5.9 ± 2.1	616 ± 17	585
AD 1765	0.2 ± .8	175 ± 6	185	AD 1355	−6.7 ± 2.3	632 ± 18	595
AD 1755	2.6 ± .6	167 ± 5	195	AD 1345	−0.9 ± 2.3	596 ± 19	605
AD 1745	3.0 ± .7	173 ± 6	205	AD 1335	3.1 ± 2.0	573 ± 16	615
AD 1735	5.5 ± .8	161 ± 6	215	AD 1325	−2.4 ± 2.1	627 ± 17	625
AD 1725	12.0 ± .6	122 ± 5	225	AD 1315	−2.9 ± 2.6	641 ± 21	635
AD 1715	15.2 ± .5	105 ± 4	235	AD 1305	−1.6 ± 1.6	640 ± 13	645
AD 1705	15.2 ± .5	116 ± 4	245	AD 1295	−4.9 ± 2.9	676 ± 24	655
AD 1695	14.8 ± .5	129 ± 4	255	AD 1285	−9.7 ± 2.7	725 ± 22	665
AD 1685	13.1 ± .7	152 ± 6	265	AD 1275	−15.5 ± 2.9	782 ± 24	675
AD 1675	10.4 ± .7	185 ± 6	275	AD 1265	−12.7 ± 2.9	769 ± 23	685
AD 1665	6.3 ± .7	227 ± 6	285	AD 1255	−18.2 ± 2.7	823 ± 22	695
AD 1655	4.5 ± .8	251 ± 6	295	AD 1245	−15.4 ± 2.8	810 ± 23	705
AD 1645	0.9 ± .7	290 ± 6	305	AD 1235	−15.2 ± 2.8	819 ± 23	715
AD 1635	−1.7 ± .7	320 ± 6	315	AD 1225	−12.7 ± 2.0	808 ± 16	725
AD 1625	−3.4 ± .7	344 ± 6	325	AD 1215	−15.4 ± 2.8	839 ± 23	735
AD 1615	−5.1 ± .8	367 ± 6	335	AD 1205	−19.5 ± 2.8	883 ± 23	745
AD 1605	−4.6 ± .7	373 ± 6	345	AD 1195	−16.9 ± 2.8	871 ± 23	755
AD 1595	−0.7 ± .9	351 ± 7	355	AD 1185	−19.1 ± 2.6	899 ± 21	765
AD 1585	1.1 ± .8	346 ± 7	365	AD 1175	−17.6 ± 2.8	896 ± 23	775
AD 1575	3.3 ± .9	338 ± 7	375	AD 1165	−13.2 ± 2.0	870 ± 16	785
AD 1565	4.3 ± .8	340 ± 6	385	AD 1155	−17.4 ± 2.8	914 ± 23	795
AD 1555	7.4 ± .8	325 ± 6	395	AD 1145	−23.9 ± 2.0	977 ± 16	805
AD 1545	9.4 ± .8	319 ± 6	405	AD 1135	−15.2 ± 2.2	915 ± 18	815

TABLE 1. (Continued)

Cal AD/BC	$\Delta^{14}C$ ‰	^{14}C age (BP)	Cal BP	Cal AD/BC	$\Delta^{14}C$ ‰	^{14}C age (BP)	Cal BP
AD 1125	−14.8 ± 2.9	922 ± 24	825	AD 655	−15.5 ± 3.0	1384 ± 25	1295
AD 1115	−17.9 ± 2.1	957 ± 17	835	AD 645	−17.9 ± 3.4	1414 ± 28	1305
AD 1105	−17.0 ± 1.9	958 ± 16	845	AD 635	−23.4 ± 2.3	1468 ± 19	1315
AD 1095	−15.5 ± 2.1	956 ± 17	855	AD 625	−20.8 ± 3.1	1457 ± 25	1325
AD 1085	−10.8 ± 1.5	928 ± 12	865	AD 615	−19.8 ± 6.2	1458 ± 51	1335
AD 1075	−7.6 ± 1.5	911 ± 12	875	AD 605	−19.4 ± 2.9	1465 ± 24	1345
AD 1065	−9.1 ± 1.7	933 ± 14	885	AD 595	−23.2 ± 3.2	1506 ± 27	1355
AD 1055	−8.5 ± 1.8	938 ± 15	895	AD 585	−19.9 ± 3.0	1488 ± 25	1365
AD 1045	−7.4 ± 2.0	939 ± 17	905	AD 575	−21.7 ± 3.4	1513 ± 28	1375
AD 1035	−8.6 ± 2.0	958 ± 16	915	AD 565	−18.8 ± 3.2	1499 ± 26	1385
AD 1025	−10.8 ± 2.8	986 ± 23	925	AD 555	−19.8 ± 3.3	1517 ± 27	1395
AD 1015	−16.7 ± 2.9	1044 ± 24	935	AD 545	−18.1 ± 2.2	1512 ± 18	1405
AD 1005	−12.1 ± 2.9	1016 ± 24	945	AD 535	−24.6 ± 3.1	1575 ± 26	1415
AD 995	−16.3 ± 2.5	1060 ± 21	955	AD 525	−27.1 ± 1.9	1606 ± 16	1425
AD 985	−17.8 ± 2.5	1082 ± 21	965	AD 515	−23.5 ± 2.8	1586 ± 23	1435
AD 975	−23.4 ± 2.9	1138 ± 24	975	AD 505	−23.4 ± 2.9	1595 ± 23	1445
AD 965	−21.2 ± 2.9	1130 ± 24	985	AD 495	−19.7 ± 2.6	1574 ± 21	1455
AD 955	−20.8 ± 3.0	1136 ± 25	995	AD 485	−18.9 ± 3.2	1577 ± 27	1465
AD 945	−19.3 ± 3.0	1133 ± 25	1005	AD 475	−17.1 ± 3.0	1573 ± 25	1475
AD 935	−22.5 ± 3.2	1170 ± 26	1015	AD 465	−18.6 ± 3.2	1595 ± 26	1485
AD 925	−19.3 ± 2.1	1151 ± 17	1025	AD 455	−17.6 ± 3.2	1596 ± 26	1495
AD 915	−13.8 ± 2.9	1118 ± 23	1035	AD 445	−12.7 ± 3.2	1566 ± 26	1505
AD 905	−10.3 ± 1.8	1096 ± 14	1045	AD 435	−11.8 ± 3.2	1568 ± 26	1515
AD 895	−15.3 ± 3.0	1150 ± 25	1055	AD 425	−17.4 ± 2.4	1623 ± 20	1525
AD 885	−17.5 ± 2.2	1175 ± 18	1065	AD 415	−20.1 ± 3.2	1656 ± 26	1535
AD 875	−17.6 ± 2.9	1188 ± 24	1075	AD 405	−21.8 ± 2.9	1679 ± 24	1545
AD 865	−19.2 ± 2.0	1207 ± 16	1085	AD 395	−20.7 ± 2.4	1679 ± 20	1555
AD 855	−19.3 ± 2.2	1222 ± 18	1095	AD 385	−21.0 ± 2.2	1692 ± 18	1565
AD 845	−16.7 ± 2.0	1206 ± 16	1105	AD 375	−23.6 ± 1.8	1723 ± 15	1575
AD 835	−13.9 ± 2.9	1196 ± 23	1115	AD 365	−18.2 ± 2.9	1688 ± 24	1585
AD 825	−14.2 ± 2.0	1206 ± 16	1125	AD 355	−20.5 ± 3.2	1717 ± 26	1595
AD 815	−11.8 ± 2.9	1198 ± 24	1135	AD 345	−18.6 ± 3.0	1711 ± 24	1605
AD 805	−12.6 ± 2.1	1212 ± 17	1145	AD 335	−20.7 ± 3.2	1738 ± 26	1615
AD 795	−15.2 ± 1.7	1246 ± 14	1155	AD 325	−19.3 ± 3.2	1736 ± 27	1625
AD 785	−6.4 ± 1.6	1181 ± 13	1165	AD 315	−25.0 ± 3.2	1792 ± 26	1635
AD 775	−14.7 ± 2.2	1261 ± 18	1175	AD 305	−23.5 ± 3.1	1790 ± 25	1645
AD 765	−17.2 ± 1.7	1291 ± 14	1185	AD 295	−16.1 ± 3.0	1740 ± 24	1655
AD 755	−18.3 ± 1.5	1310 ± 12	1195	AD 285	−19.8 ± 3.1	1779 ± 25	1665
AD 745	−12.8 ± 1.8	1275 ± 14	1205	AD 275	−12.2 ± 3.0	1726 ± 24	1675
AD 735	−10.2 ± 1.6	1264 ± 13	1215	AD 265	−9.7 ± 2.3	1716 ± 18	1685
AD 725	−10.8 ± 1.7	1278 ± 14	1225	AD 255	−17.2 ± 1.7	1787 ± 14	1695
AD 715	−9.8 ± 2.1	1279 ± 17	1235	AD 245	−15.8 ± 1.7	1785 ± 13	1705
AD 705	−10.9 ± 2.2	1299 ± 17	1245	AD 235	−19.0 ± 2.3	1821 ± 19	1715
AD 695	−6.1 ± 3.3	1270 ± 26	1255	AD 225	−18.7 ± 3.2	1828 ± 26	1725
AD 685	−14.2 ± 3.5	1345 ± 28	1265	AD 215	−20.3 ± 3.2	1851 ± 27	1735
AD 675	−12.5 ± 3.3	1340 ± 27	1275	AD 205	−20.1 ± 2.3	1860 ± 19	1745
AD 665	−12.5 ± 3.3	1350 ± 27	1285	AD 195	−16.2 ± 3.2	1837 ± 26	1755

TABLE 1. (Continued)

Cal AD/BC	$\Delta^{14}C$ ‰	^{14}C age (BP)	Cal BP	Cal AD/BC	$\Delta^{14}C$ ‰	^{14}C age (BP)	Cal BP
AD 185	−13.0 ± 2.9	1821 ± 24	1765	285 BC	−10.5 ± 2.9	2256 ± 24	2234
AD 175	−15.1 ± 3.2	1848 ± 26	1775	295 BC	−5.5 ± 2.2	2225 ± 18	2244
AD 165	−14.2 ± 3.5	1850 ± 28	1785	305 BC	−2.5 ± 3.1	2211 ± 25	2254
AD 155	−13.6 ± 3.0	1854 ± 24	1795	315 BC	−1.1 ± 3.1	2210 ± 25	2264
AD 145	−12.3 ± 3.2	1854 ± 26	1805	325 BC	3.2 ± 2.2	2185 ± 18	2274
AD 135	−10.2 ± 2.1	1847 ± 17	1815	335 BC	4.9 ± 3.1	2181 ± 25	2284
AD 125	−16.9 ± 1.7	1911 ± 14	1825	345 BC	5.0 ± 2.2	2189 ± 18	2294
AD 115	−15.9 ± 3.5	1913 ± 28	1835	355 BC	−0.8 ± 2.2	2246 ± 18	2304
AD 105	−15.5 ± 3.3	1919 ± 27	1845	365 BC	−4.1 ± 2.2	2282 ± 18	2314
AD 95	−10.6 ± 1.9	1888 ± 16	1855	375 BC	−2.3 ± 2.2	2278 ± 18	2324
AD 85	−11.5 ± 3.2	1906 ± 26	1865	385 BC	−3.3 ± 3.1	2295 ± 25	2334
AD 75	−13.3 ± 2.2	1930 ± 18	1875	395 BC	−7.8 ± 2.3	2341 ± 19	2344
AD 65	−14.2 ± 2.2	1947 ± 18	1885	405 BC	−12.6 ± 1.8	2390 ± 14	2354
AD 55	−15.2 ± 1.9	1965 ± 15	1895	415 BC	−18.7 ± 3.2	2449 ± 26	2364
AD 45	−18.3 ± 1.6	2000 ± 13	1905	425 BC	−16.0 ± 3.3	2437 ± 27	2374
AD 35	−11.0 ± 2.5	1950 ± 20	1915	435 BC	−18.9 ± 3.1	2471 ± 25	2384
AD 25	−15.3 ± 2.2	1995 ± 18	1925	445 BC	−17.8 ± 5.3	2471 ± 44	2394
AD 15	−15.9 ± 1.8	2010 ± 15	1935	455 BC	−21.0 ± 3.6	2507 ± 30	2404
AD 5	−12.6 ± 1.6	1993 ± 13	1945	465 BC	−13.3 ± 4.0	2454 ± 33	2414
5 BC	−20.2 ± 1.8	2063 ± 15	1954	475 BC	−7.4 ± 2.3	2416 ± 19	2424
15 BC	−12.9 ± 1.6	2012 ± 13	1964	485 BC	−10.9 ± 3.3	2454 ± 26	2434
25 BC	−15.6 ± 2.1	2044 ± 17	1974	495 BC	−7.3 ± 2.5	2434 ± 20	2444
35 BC	−11.2 ± 1.2	2018 ± 10	1984	505 BC	−8.0 ± 3.3	2450 ± 26	2454
45 BC	−14.3 ± 1.7	2053 ± 14	1994	515 BC	−6.1 ± 2.5	2444 ± 20	2464
55 BC	−17.3 ± 1.5	2087 ± 12	2004	525 BC	−10.1 ± 2.7	2487 ± 22	2474
65 BC	−18.0 ± 1.8	2103 ± 15	2014	535 BC	−6.8 ± 1.8	2469 ± 14	2484
75 BC	−15.6 ± 2.3	2094 ± 19	2024	545 BC	−8.6 ± 1.7	2493 ± 13	2494
85 BC	−12.4 ± 1.8	2076 ± 15	2034	555 BC	−7.1 ± 2.9	2491 ± 23	2504
95 BC	−15.1 ± 2.2	2108 ± 18	2044	565 BC	−7.0 ± 3.6	2500 ± 29	2514
105 BC	−12.3 ± 2.0	2095 ± 16	2054	575 BC	−6.7 ± 3.5	2508 ± 28	2524
115 BC	−13.0 ± 1.9	2111 ± 16	2064	585 BC	−0.4 ± 3.5	2466 ± 29	2534
125 BC	−14.2 ± 1.9	2130 ± 16	2074	595 BC	−7.2 ± 2.8	2530 ± 23	2544
135 BC	−10.7 ± 2.3	2111 ± 19	2084	605 BC	−5.1 ± 3.0	2524 ± 24	2554
145 BC	−8.5 ± 1.9	2103 ± 16	2094	615 BC	−2.0 ± 2.6	2508 ± 21	2564
155 BC	−6.7 ± 3.4	2099 ± 27	2104	625 BC	−1.9 ± 2.7	2517 ± 22	2574
165 BC	−7.7 ± 2.2	2117 ± 18	2114	635 BC	2.6 ± 2.3	2488 ± 19	2584
175 BC	−14.2 ± 3.3	2179 ± 27	2124	645 BC	3.6 ± 2.3	2492 ± 19	2594
185 BC	−12.6 ± 3.3	2176 ± 27	2134	655 BC	4.9 ± 2.1	2492 ± 17	2604
195 BC	−8.0 ± 2.2	2149 ± 18	2144	661 BC	11.6 ± 3.2	2444 ± 25	2610
205 BC	−12.6 ± 3.0	2195 ± 25	2154	696 BC	12.7 ± 5.3	2469 ± 42	2645
215 BC	−17.4 ± 1.7	2244 ± 14	2164	705 BC	13.5 ± 5.4	2473 ± 43	2654
225 BC	−9.7 ± 2.4	2192 ± 20	2174	715 BC	14.0 ± 5.4	2479 ± 43	2664
235 BC	−16.6 ± 1.8	2258 ± 15	2184	731 BC	18.1 ± 2.3	2461 ± 18	2680
245 BC	−14.1 ± 2.4	2247 ± 19	2194	751 BC	20.5 ± 3.4	2461 ± 27	2700
255 BC	−11.6 ± 3.2	2236 ± 26	2204	771 BC	9.9 ± 3.2	2565 ± 26	2720
265 BC	−15.8 ± 3.1	2280 ± 25	2214	785 BC	11.9 ± 2.5	2563 ± 20	2734
275 BC	−9.8 ± 2.2	2241 ± 18	2224	795 BC	5.7 ± 2.5	2622 ± 20	2744

TABLE 1. (Continued)

Cal AD/BC	$\Delta^{14}C$ ‰	^{14}C age (BP)	Cal BP	Cal AD/BC	$\Delta^{14}C$ ‰	^{14}C age (BP)	Cal BP
805 BC	3.0 ± 2.5	2654 ± 20	2754	1275 BC	10.2 ± 3.4	3053 ± 27	3224
815 BC	−0.3 ± 3.3	2690 ± 27	2764	1285 BC	16.4 ± 3.6	3013 ± 28	3234
825 BC	1.1 ± 2.6	2688 ± 21	2774	1295 BC	12.5 ± 3.5	3054 ± 28	3244
835 BC	−5.7 ± 2.5	2752 ± 20	2784	1305 BC	14.6 ± 3.7	3047 ± 29	3254
845 BC	−5.8 ± 2.5	2763 ± 20	2794	1315 BC	14.3 ± 3.5	3059 ± 28	3264
855 BC	−4.1 ± 3.3	2759 ± 27	2804	1325 BC	8.2 ± 3.0	3117 ± 24	3274
865 BC	−2.3 ± 3.2	2755 ± 26	2814	1335 BC	15.3 ± 3.5	3070 ± 27	3284
875 BC	−1.4 ± 3.4	2757 ± 27	2824	1345 BC	17.5 ± 3.6	3063 ± 28	3294
885 BC	3.6 ± 3.4	2727 ± 27	2834	1355 BC	15.3 ± 3.5	3090 ± 27	3304
895 BC	1.7 ± 3.3	2752 ± 27	2844	1365 BC	22.6 ± 3.3	3042 ± 26	3314
905 BC	−2.3 ± 3.2	2793 ± 26	2854	1375 BC	16.6 ± 3.2	3100 ± 25	3324
915 BC	−2.0 ± 3.3	2801 ± 27	2864	1385 BC	17.3 ± 3.3	3104 ± 26	3334
925 BC	−1.9 ± 3.3	2810 ± 27	2874	1395 BC	16.4 ± 2.4	3121 ± 19	3344
935 BC	−0.9 ± 2.5	2811 ± 20	2884	1405 BC	18.1 ± 3.3	3117 ± 26	3354
945 BC	−3.2 ± 2.4	2840 ± 19	2894	1415 BC	10.8 ± 3.3	3184 ± 26	3364
955 BC	−2.0 ± 2.6	2839 ± 21	2904	1425 BC	18.8 ± 3.4	3131 ± 27	3374
965 BC	7.7 ± 3.4	2772 ± 27	2914	1435 BC	11.8 ± 2.4	3196 ± 19	3384
975 BC	−1.6 ± 2.4	2856 ± 19	2924	1445 BC	13.8 ± 2.4	3189 ± 19	3394
985 BC	0.4 ± 3.2	2849 ± 25	2934	1455 BC	11.6 ± 2.3	3216 ± 18	3404
995 BC	3.6 ± 3.2	2833 ± 25	2944	1465 BC	9.9 ± 2.4	3240 ± 19	3414
1005 BC	3.2 ± 3.3	2847 ± 27	2954	1475 BC	12.9 ± 2.4	3226 ± 19	3424
1015 BC	−0.6 ± 3.2	2887 ± 26	2964	1485 BC	17.2 ± 2.6	3202 ± 21	3434
1025 BC	−2.2 ± 3.5	2909 ± 28	2974	1495 BC	12.8 ± 3.7	3246 ± 29	3444
1035 BC	0.3 ± 3.4	2899 ± 27	2984	1505 BC	11.8 ± 3.3	3264 ± 26	3454
1045 BC	6.2 ± 3.5	2861 ± 28	2994	1515 BC	12.0 ± 3.5	3272 ± 28	3464
1055 BC	−2.6 ± 3.2	2941 ± 26	3004	1525 BC	11.1 ± 3.2	3289 ± 25	3474
1065 BC	4.4 ± 3.6	2895 ± 29	3014	1535 BC	7.2 ± 3.4	3329 ± 27	3484
1075 BC	4.0 ± 3.5	2908 ± 28	3024	1545 BC	10.0 ± 3.5	3316 ± 28	3494
1085 BC	1.4 ± 3.6	2939 ± 29	3034	1555 BC	10.8 ± 3.3	3320 ± 27	3504
1095 BC	4.1 ± 2.3	2926 ± 19	3044	1565 BC	8.8 ± 5.8	3346 ± 46	3514
1105 BC	5.3 ± 2.5	2927 ± 20	3054	1575 BC	13.2 ± 5.8	3320 ± 46	3524
1115 BC	0.4 ± 3.8	2976 ± 30	3064	1585 BC	14.2 ± 3.6	3323 ± 28	3534
1125 BC	7.5 ± 3.4	2928 ± 27	3074	1595 BC	20.1 ± 2.8	3286 ± 22	3544
1135 BC	−2.3 ± 2.3	3017 ± 18	3084	1605 BC	14.5 ± 2.6	3340 ± 20	3554
1145 BC	10.3 ± 3.4	2926 ± 27	3094	1615 BC	15.1 ± 2.8	3345 ± 22	3564
1155 BC	7.4 ± 3.5	2959 ± 28	3104	1625 BC	13.5 ± 2.7	3367 ± 21	3574
1165 BC	8.3 ± 3.3	2961 ± 26	3114	1635 BC	13.5 ± 3.6	3376 ± 28	3584
1175 BC	8.4 ± 4.2	2970 ± 33	3124	1645 BC	11.3 ± 2.0	3404 ± 16	3594
1185 BC	16.0 ± 3.5	2919 ± 28	3134	1655 BC	19.0 ± 2.6	3353 ± 21	3604
1195 BC	4.9 ± 3.2	3018 ± 26	3144	1665 BC	11.5 ± 3.7	3422 ± 30	3614
1205 BC	16.1 ± 3.6	2938 ± 28	3154	1675 BC	24.1 ± 3.5	3332 ± 28	3624
1215 BC	8.3 ± 1.9	3009 ± 15	3164	1685 BC	20.2 ± 3.5	3372 ± 28	3634
1225 BC	8.5 ± 3.3	3018 ± 27	3174	1695 BC	11.2 ± 2.4	3453 ± 20	3644
1235 BC	12.9 ± 3.6	2993 ± 29	3184	1705 BC	13.1 ± 3.6	3448 ± 28	3654
1245 BC	11.9 ± 3.5	3011 ± 28	3194	1715 BC	19.0 ± 3.5	3410 ± 28	3664
1255 BC	14.5 ± 2.7	3007 ± 22	3204	1725 BC	19.1 ± 3.5	3420 ± 28	3674
1265 BC	8.0 ± 3.5	3061 ± 28	3214	1735 BC	17.3 ± 3.5	3443 ± 28	3684

TABLE 1. (Continued)

Cal AD/BC	$\Delta^{14}C$ ‰	^{14}C age (BP)	Cal BP	Cal AD/BC	$\Delta^{14}C$ ‰	^{14}C age (BP)	Cal BP
1745 BC	12.6 ± 3.6	3491 ± 28	3694	2215 BC	27.2 ± 2.5	3832 ± 20	4164
1755 BC	12.9 ± 2.5	3498 ± 20	3704	2225 BC	32.1 ± 2.1	3804 ± 17	4174
1765 BC	17.9 ± 2.8	3468 ± 22	3714	2235 BC	26.6 ± 3.9	3857 ± 31	4184
1775 BC	13.2 ± 2.7	3515 ± 21	3724	2245 BC	29.2 ± 2.6	3846 ± 21	4194
1785 BC	12.4 ± 2.4	3531 ± 19	3734	2255 BC	34.9 ± 2.5	3811 ± 19	4204
1795 BC	15.2 ± 2.4	3518 ± 19	3744	2265 BC	37.0 ± 3.6	3805 ± 28	4214
1805 BC	19.3 ± 2.4	3495 ± 19	3754	2275 BC	34.6 ± 4.3	3833 ± 34	4224
1815 BC	17.0 ± 2.5	3524 ± 20	3764	2285 BC	34.4 ± 3.0	3844 ± 23	4234
1825 BC	19.7 ± 3.6	3512 ± 28	3774	2295 BC	32.2 ± 2.7	3871 ± 21	4244
1835 BC	13.6 ± 3.4	3570 ± 26	3784	2305 BC	36.5 ± 4.0	3847 ± 31	4254
1845 BC	22.6 ± 3.6	3509 ± 28	3794	2315 BC	33.8 ± 3.6	3878 ± 28	4264
1855 BC	25.7 ± 3.6	3494 ± 28	3804	2325 BC	36.8 ± 2.6	3864 ± 20	4274
1865 BC	23.3 ± 3.6	3523 ± 28	3814	2335 BC	35.9 ± 3.6	3881 ± 28	4284
1875 BC	24.7 ± 2.5	3522 ± 19	3824	2345 BC	35.0 ± 2.6	3898 ± 20	4294
1885 BC	19.2 ± 3.4	3575 ± 27	3834	2355 BC	34.6 ± 3.7	3911 ± 29	4304
1895 BC	18.1 ± 3.6	3593 ± 28	3844	2365 BC	34.5 ± 2.6	3921 ± 20	4314
1905 BC	22.4 ± 3.5	3569 ± 28	3854	2375 BC	37.2 ± 3.6	3910 ± 28	4324
1915 BC	23.4 ± 3.5	3570 ± 28	3864	2385 BC	42.8 ± 2.6	3876 ± 20	4334
1925 BC	19.9 ± 2.7	3608 ± 22	3874	2395 BC	47.7 ± 4.1	3848 ± 31	4344
1935 BC	21.0 ± 3.2	3609 ± 25	3884	2405 BC	40.5 ± 2.7	3914 ± 21	4354
1945 BC	20.3 ± 3.7	3624 ± 29	3894	2415 BC	39.6 ± 2.9	3930 ± 22	4364
1955 BC	20.3 ± 3.6	3633 ± 28	3904	2425 BC	44.2 ± 3.6	3904 ± 28	4374
1965 BC	21.7 ± 3.5	3633 ± 28	3914	2435 BC	43.4 ± 1.9	3920 ± 15	4384
1975 BC	20.5 ± 3.5	3651 ± 27	3924	2445 BC	45.3 ± 3.8	3915 ± 29	4394
1985 BC	16.6 ± 3.5	3692 ± 28	3934	2465 BC	44.8 ± 3.7	3939 ± 28	4414
1995 BC	25.9 ± 3.5	3628 ± 27	3944	2475 BC	34.4 ± 2.6	4029 ± 20	4424
2005 BC	29.2 ± 3.6	3613 ± 28	3954	2485 BC	38.1 ± 2.7	4010 ± 21	4434
2015 BC	23.5 ± 3.4	3667 ± 27	3964	2495 BC	32.7 ± 3.9	4062 ± 30	4444
2025 BC	25.9 ± 3.5	3658 ± 28	3974	2505 BC	30.5 ± 2.9	4088 ± 23	4454
2035 BC	22.2 ± 2.2	3697 ± 17	3984	2515 BC	38.2 ± 2.9	4038 ± 22	4464
2045 BC	20.1 ± 2.5	3723 ± 19	3994	2525 BC	43.0 ± 2.0	4011 ± 16	4474
2055 BC	20.1 ± 2.5	3732 ± 20	4004	2535 BC	45.7 ± 2.7	4000 ± 21	4484
2065 BC	25.5 ± 3.5	3700 ± 28	4014	2545 BC	45.9 ± 2.7	4008 ± 21	4494
2075 BC	18.9 ± 2.5	3761 ± 20	4024	2555 BC	46.2 ± 2.5	4015 ± 19	4504
2085 BC	29.5 ± 3.6	3688 ± 28	4034	2565 BC	44.8 ± 2.5	4036 ± 19	4514
2095 BC	27.9 ± 3.5	3710 ± 27	4044	2575 BC	40.8 ± 3.0	4077 ± 23	4524
2105 BC	32.6 ± 2.5	3684 ± 19	4054	2585 BC	38.1 ± 2.4	4107 ± 19	4534
2115 BC	29.9 ± 3.5	3714 ± 27	4064	2595 BC	44.3 ± 2.7	4069 ± 21	4544
2125 BC	32.2 ± 3.5	3706 ± 28	4074	2605 BC	37.2 ± 4.1	4133 ± 32	4554
2135 BC	29.9 ± 3.5	3733 ± 27	4084	2615 BC	47.1 ± 2.7	4067 ± 21	4564
2145 BC	25.1 ± 2.2	3781 ± 17	4094	2625 BC	43.1 ± 2.8	4108 ± 22	4574
2155 BC	27.3 ± 2.3	3773 ± 18	4104	2635 BC	42.0 ± 2.4	4126 ± 18	4584
2165 BC	29.6 ± 3.6	3765 ± 28	4114	2645 BC	36.0 ± 4.0	4182 ± 31	4594
2175 BC	33.0 ± 2.4	3748 ± 18	4124	2655 BC	47.5 ± 4.0	4101 ± 31	4604
2185 BC	34.6 ± 2.0	3745 ± 16	4134	2665 BC	47.2 ± 2.7	4113 ± 21	4614
2195 BC	33.6 ± 2.0	3763 ± 16	4144	2675 BC	45.1 ± 2.7	4139 ± 21	4624
2205 BC	28.1 ± 3.0	3816 ± 24	4154	2685 BC	45.9 ± 2.8	4142 ± 21	4634

TABLE 1. (Continued)

Cal AD/BC	$\Delta^{14}C$ ‰	^{14}C age (BP)	Cal BP	Cal AD/BC	$\Delta^{14}C$ ‰	^{14}C age (BP)	Cal BP
2695 BC	45.0 ± 4.1	4159 ± 31	4644	3165 BC	62.3 ± 2.8	4484 ± 21	5114
2705 BC	44.6 ± 2.2	4171 ± 17	4654	3175 BC	56.3 ± 4.0	4539 ± 31	5124
2715 BC	42.2 ± 4.1	4200 ± 32	4664	3185 BC	60.8 ± 2.9	4515 ± 22	5134
2725 BC	48.7 ± 4.1	4160 ± 32	4674	3195 BC	60.2 ± 2.8	4529 ± 21	5144
2735 BC	47.2 ± 3.3	4182 ± 26	4684	3205 BC	59.5 ± 4.1	4544 ± 31	5154
2745 BC	51.0 ± 4.1	4162 ± 31	4694	3215 BC	64.0 ± 2.5	4520 ± 19	5164
2755 BC	51.4 ± 4.1	4169 ± 31	4704	3225 BC	66.5 ± 4.1	4511 ± 31	5174
2765 BC	44.2 ± 4.3	4234 ± 33	4714	3235 BC	71.2 ± 4.1	4485 ± 31	5184
2775 BC	51.8 ± 3.5	4185 ± 27	4724	3245 BC	77.1 ± 4.2	4451 ± 31	5194
2785 BC	54.6 ± 2.8	4174 ± 21	4734	3255 BC	75.3 ± 4.1	4474 ± 30	5204
2795 BC	52.8 ± 2.8	4197 ± 22	4744	3265 BC	73.1 ± 3.6	4500 ± 27	5214
2805 BC	51.2 ± 3.8	4219 ± 29	4754	3275 BC	73.9 ± 4.4	4504 ± 33	5224
2815 BC	63.5 ± 2.9	4135 ± 22	4764	3285 BC	77.8 ± 4.1	4485 ± 31	5234
2825 BC	69.6 ± 4.3	4099 ± 33	4774	3295 BC	79.2 ± 4.1	4484 ± 31	5244
2835 BC	64.4 ± 3.9	4147 ± 30	4784	3305 BC	78.8 ± 4.2	4496 ± 31	5254
2845 BC	62.6 ± 3.8	4171 ± 29	4794	3315 BC	75.4 ± 3.0	4532 ± 22	5264
2855 BC	63.5 ± 4.0	4174 ± 30	4804	3325 BC	81.8 ± 2.9	4494 ± 22	5274
2865 BC	63.8 ± 3.7	4181 ± 28	4814	3335 BC	77.8 ± 2.6	4533 ± 20	5284
2875 BC	62.2 ± 2.7	4203 ± 21	4824	3345 BC	75.8 ± 2.7	4557 ± 20	5294
2885 BC	58.7 ± 3.8	4239 ± 29	4834	3355 BC	72.6 ± 4.2	4591 ± 32	5304
2895 BC	51.9 ± 4.0	4301 ± 30	4844	3365 BC	69.3 ± 4.1	4625 ± 31	5314
2905 BC	51.2 ± 4.0	4315 ± 30	4854	3375 BC	66.0 ± 4.1	4660 ± 31	5324
2915 BC	50.9 ± 3.8	4328 ± 29	4864	3385 BC	61.5 ± 4.1	4704 ± 31	5334
2925 BC	44.7 ± 4.0	4385 ± 30	4874	3395 BC	58.7 ± 3.1	4735 ± 23	5344
2935 BC	44.5 ± 4.4	4396 ± 34	4884	3405 BC	64.1 ± 4.1	4703 ± 31	5354
2945 BC	42.7 ± 3.8	4420 ± 29	4894	3415 BC	62.2 ± 4.5	4728 ± 34	5364
2955 BC	50.0 ± 2.7	4373 ± 21	4904	3425 BC	68.5 ± 3.4	4690 ± 26	5374
2965 BC	49.6 ± 3.8	4386 ± 29	4914	3435 BC	70.6 ± 2.9	4684 ± 22	5384
2975 BC	48.1 ± 4.0	4407 ± 30	4924	3445 BC	70.7 ± 4.9	4693 ± 37	5394
2985 BC	54.2 ± 2.7	4370 ± 21	4934	3455 BC	70.6 ± 4.5	4703 ± 34	5404
2995 BC	56.5 ± 4.0	4363 ± 31	4944	3465 BC	77.2 ± 3.0	4664 ± 22	5414
3005 BC	56.3 ± 4.0	4374 ± 31	4954	3475 BC	84.3 ± 2.9	4621 ± 21	5424
3015 BC	54.9 ± 3.9	4395 ± 30	4964	3485 BC	84.4 ± 2.9	4629 ± 22	5434
3025 BC	56.7 ± 3.9	4391 ± 30	4974	3495 BC	82.9 ± 3.0	4650 ± 23	5444
3035 BC	55.9 ± 4.1	4406 ± 31	4984	3505 BC	76.4 ± 3.0	4708 ± 23	5454
3045 BC	53.3 ± 2.6	4435 ± 20	4994	3515 BC	73.5 ± 2.9	4740 ± 22	5464
3055 BC	52.2 ± 2.8	4454 ± 21	5004	3525 BC	73.8 ± 3.0	4748 ± 22	5474
3065 BC	53.9 ± 4.0	4451 ± 31	5014	3535 BC	75.3 ± 3.0	4746 ± 22	5484
3075 BC	61.0 ± 2.1	4407 ± 16	5024	3545 BC	70.0 ± 3.0	4795 ± 22	5494
3085 BC	55.5 ± 4.1	4458 ± 31	5034	3555 BC	71.5 ± 3.1	4794 ± 23	5504
3095 BC	58.7 ± 4.1	4443 ± 31	5044	3565 BC	76.8 ± 3.0	4764 ± 22	5514
3105 BC	49.0 ± 4.1	4527 ± 31	5054	3575 BC	76.4 ± 3.0	4777 ± 22	5524
3115 BC	54.1 ± 2.9	4498 ± 22	5064	3585 BC	79.7 ± 3.0	4761 ± 22	5534
3125 BC	51.1 ± 4.0	4531 ± 30	5074	3595 BC	82.5 ± 2.4	4751 ± 18	5544
3135 BC	52.5 ± 3.9	4529 ± 29	5084	3605 BC	85.7 ± 2.6	4737 ± 20	5554
3145 BC	49.3 ± 4.0	4563 ± 30	5094	3615 BC	90.6 ± 2.3	4710 ± 17	5564
3155 BC	56.8 ± 4.0	4516 ± 31	5104	3625 BC	85.9 ± 4.3	4754 ± 32	5574

TABLE 1. (Continued)

Cal AD/BC	$\Delta^{14}C$ ‰	^{14}C age (BP)	Cal BP	Cal AD/BC	$\Delta^{14}C$ ‰	^{14}C age (BP)	Cal BP
3635 BC	80.9 ± 2.9	4801 ± 22	5584	4105 BC	78.3 ± 4.2	5278 ± 31	6054
3645 BC	75.8 ± 3.0	4849 ± 22	5594	4115 BC	69.4 ± 2.9	5353 ± 22	6064
3655 BC	71.7 ± 2.9	4890 ± 22	5604	4125 BC	80.1 ± 4.3	5284 ± 32	6074
3665 BC	73.8 ± 2.9	4884 ± 22	5614	4135 BC	81.9 ± 3.0	5280 ± 23	6084
3675 BC	68.5 ± 2.4	4933 ± 18	5624	4155 BC	85.4 ± 4.3	5273 ± 32	6104
3685 BC	73.4 ± 2.9	4906 ± 21	5634	4165 BC	80.0 ± 4.2	5323 ± 31	6114
3695 BC	75.8 ± 2.9	4897 ± 22	5644	4175 BC	75.2 ± 4.4	5369 ± 33	6124
3705 BC	73.1 ± 2.9	4928 ± 22	5654	4185 BC	81.2 ± 4.3	5333 ± 32	6134
3715 BC	69.9 ± 2.9	4961 ± 22	5664	4195 BC	84.7 ± 3.0	5318 ± 22	6144
3725 BC	68.6 ± 4.6	4980 ± 35	5674	4205 BC	92.5 ± 4.1	5270 ± 30	6154
3735 BC	74.4 ± 3.0	4947 ± 23	5684	4215 BC	93.9 ± 4.4	5269 ± 33	6164
3745 BC	73.8 ± 2.6	4961 ± 20	5694	4225 BC	81.5 ± 3.0	5370 ± 23	6174
3755 BC	76.2 ± 2.9	4953 ± 22	5704	4235 BC	81.5 ± 3.0	5380 ± 22	6184
3765 BC	71.4 ± 2.9	4998 ± 22	5714	4245 BC	86.4 ± 3.0	5353 ± 22	6194
3775 BC	71.5 ± 3.0	5007 ± 22	5724	4255 BC	78.8 ± 5.0	5419 ± 37	6204
3785 BC	74.0 ± 2.4	4999 ± 18	5734	4265 BC	74.8 ± 3.2	5460 ± 24	6214
3795 BC	73.7 ± 3.1	5011 ± 23	5744	4275 BC	79.5 ± 5.0	5433 ± 37	6224
3805 BC	65.3 ± 2.8	5083 ± 21	5754	4285 BC	81.2 ± 3.0	5432 ± 23	6234
3815 BC	65.4 ± 3.9	5092 ± 30	5764	4295 BC	85.4 ± 4.5	5409 ± 33	6244
3825 BC	71.3 ± 3.9	5058 ± 29	5774	4305 BC	91.5 ± 4.3	5374 ± 32	6254
3835 BC	73.0 ± 4.1	5055 ± 31	5784	4315 BC	92.0 ± 4.4	5380 ± 33	6264
3845 BC	71.3 ± 4.1	5077 ± 31	5794	4325 BC	86.6 ± 4.4	5430 ± 33	6274
3855 BC	71.7 ± 2.4	5083 ± 18	5804	4335 BC	80.8 ± 3.0	5484 ± 23	6284
3865 BC	78.0 ± 2.1	5047 ± 16	5814	4345 BC	78.2 ± 3.1	5512 ± 23	6294
3875 BC	72.2 ± 2.2	5099 ± 17	5824	4355 BC	73.9 ± 4.3	5553 ± 33	6304
3885 BC	85.3 ± 2.7	5011 ± 20	5834	4365 BC	73.7 ± 4.2	5564 ± 32	6314
3895 BC	82.3 ± 3.5	5044 ± 26	5844	4375 BC	68.8 ± 4.3	5576 ± 22	6324
3905 BC	82.5 ± 2.9	5052 ± 21	5854	4385 BC	78.6 ± 4.5	5547 ± 33	6334
3915 BC	81.9 ± 2.8	5066 ± 21	5864	4395 BC	75.3 ± 4.4	5582 ± 33	6344
3925 BC	84.4 ± 3.1	5060 ± 23	5874	4405 BC	77.5 ± 4.4	5574 ± 33	6354
3935 BC	84.5 ± 4.2	5066 ± 31	5884	4415 BC	73.2 ± 4.4	5616 ± 33	6364
3945 BC	79.9 ± 2.4	5113 ± 18	5894	4425 BC	84.5 ± 4.6	5542 ± 35	6374
3955 BC	80.9 ± 5.2	5113 ± 39	5904	4435 BC	87.8 ± 4.6	5527 ± 34	6384
3965 BC	76.3 ± 1.8	5159 ± 13	5914	4445 BC	83.5 ± 4.4	5569 ± 32	6394
3975 BC	72.9 ± 2.6	5192 ± 19	5924	4455 BC	79.6 ± 4.6	5608 ± 34	6404
3985 BC	70.1 ± 2.7	5222 ± 20	5934	4465 BC	71.4 ± 3.0	5679 ± 22	6414
3995 BC	69.3 ± 3.0	5238 ± 22	5944	4475 BC	73.3 ± 4.4	5675 ± 33	6424
4005 BC	68.8 ± 3.0	5251 ± 23	5954	4485 BC	76.1 ± 4.6	5663 ± 35	6434
4015 BC	71.9 ± 4.1	5237 ± 31	5964	4495 BC	75.4 ± 4.4	5678 ± 33	6444
4025 BC	77.3 ± 3.2	5207 ± 24	5974	4505 BC	76.3 ± 4.3	5681 ± 32	6454
4035 BC	76.0 ± 2.7	5226 ± 20	5984	4515 BC	77.2 ± 4.4	5684 ± 33	6464
4045 BC	72.0 ± 4.2	5267 ± 31	5994	4525 BC	78.6 ± 4.7	5684 ± 35	6474
4055 BC	80.7 ± 3.7	5211 ± 28	6004	4535 BC	79.0 ± 4.2	5690 ± 32	6484
4065 BC	85.3 ± 3.0	5187 ± 22	6014	4545 BC	72.5 ± 4.7	5748 ± 35	6494
4075 BC	79.0 ± 4.2	5243 ± 31	6024	4555 BC	72.8 ± 4.4	5756 ± 33	6504
4085 BC	73.0 ± 3.5	5298 ± 26	6034	4565 BC	72.6 ± 3.2	5767 ± 24	6514
4095 BC	74.5 ± 3.0	5296 ± 22	6044	4575 BC	75.9 ± 3.0	5752 ± 23	6524

TABLE 1. (Continued)

Cal AD/BC	$\Delta^{14}C$ ‰	^{14}C age (BP)	Cal BP	Cal AD/BC	$\Delta^{14}C$ ‰	^{14}C age (BP)	Cal BP
4585 BC	77.1 ± 3.1	5753 ± 23	6534	5055 BC	89.3 ± 4.1	6119 ± 33	7004
4595 BC	76.4 ± 4.4	5768 ± 33	6544	5065 BC	83.4 ± 4.0	6172 ± 32	7014
4605 BC	77.9 ± 4.3	5767 ± 32	6554	5075 BC	82.4 ± 4.2	6189 ± 34	7024
4615 BC	79.6 ± 4.7	5764 ± 35	6564	5085 BC	80.3 ± 4.1	6215 ± 33	7034
4625 BC	74.7 ± 2.7	5810 ± 21	6574	5095 BC	86.9 ± 2.9	6176 ± 24	7044
4635 BC	78.9 ± 3.7	5788 ± 28	6584	5105 BC	82.9 ± 4.1	6215 ± 33	7054
4645 BC	81.9 ± 2.3	5775 ± 17	6594	5115 BC	92.6 ± 4.0	6153 ± 32	7064
4655 BC	82.1 ± 3.1	5784 ± 23	6604	5125 BC	85.0 ± 4.0	6219 ± 32	7074
4665 BC	87.4 ± 4.4	5754 ± 32	6614	5135 BC	94.8 ± 3.9	6157 ± 31	7084
4675 BC	87.3 ± 4.8	5764 ± 35	6624	5145 BC	95.6 ± 3.0	6160 ± 24	7094
4685 BC	86.2 ± 2.6	5782 ± 19	6634	5165 BC	92.6 ± 4.1	6202 ± 33	7114
4695 BC	80.1 ± 3.2	5837 ± 24	6644	5175 BC	99.0 ± 4.0	6164 ± 32	7124
4705 BC	83.6 ± 3.0	5821 ± 23	6654	5185 BC	106.7 ± 2.9	6118 ± 24	7134
4715 BC	79.8 ± 4.3	5859 ± 32	6664	5195 BC	106.7 ± 4.0	6128 ± 33	7144
4725 BC	78.4 ± 4.4	5879 ± 33	6674	5205 BC	108.9 ± 4.3	6122 ± 34	7154
4735 BC	80.0 ± 4.3	5877 ± 32	6684	5215 BC	94.6 ± 4.2	6236 ± 34	7164
4745 BC	87.1 ± 4.4	5834 ± 33	6694	5225 BC	89.7 ± 4.3	6281 ± 35	7174
4755 BC	88.7 ± 4.4	5832 ± 32	6704	5235 BC	98.1 ± 4.2	6230 ± 34	7184
4765 BC	81.6 ± 4.3	5895 ± 32	6714	5245 BC	96.0 ± 2.9	6255 ± 24	7194
4775 BC	83.7 ± 4.4	5889 ± 33	6724	5255 BC	97.1 ± 2.9	6256 ± 23	7204
4785 BC	84.3 ± 4.3	5894 ± 32	6734	5265 BC	92.4 ± 4.0	6300 ± 32	7214
4795 BC	82.8 ± 4.3	5914 ± 32	6744	5275 BC	90.9 ± 2.7	6321 ± 22	7224
4805 BC	80.9 ± 4.6	5939 ± 34	6754	5285 BC	83.0 ± 2.8	6389 ± 23	7234
4815 BC	83.8 ± 4.5	5926 ± 34	6764	5295 BC	89.3 ± 4.2	6352 ± 34	7244
4825 BC	80.5 ± 4.4	5961 ± 33	6774	5305 BC	86.7 ± 4.3	6381 ± 35	7254
4835 BC	82.6 ± 4.3	5955 ± 32	6784	5315 BC	90.7 ± 3.0	6361 ± 24	7264
4845 BC	81.3 ± 4.6	5974 ± 34	6794	5325 BC	89.3 ± 3.0	6381 ± 24	7274
4855 BC	78.8 ± 3.1	6003 ± 23	6804	5335 BC	85.1 ± 4.0	6422 ± 32	7284
4865 BC	81.3 ± 4.4	5994 ± 33	6814	5345 BC	85.7 ± 3.0	6428 ± 24	7294
4875 BC	77.8 ± 4.5	6029 ± 33	6824	5355 BC	82.4 ± 3.0	6462 ± 24	7304
4885 BC	93.1 ± 4.6	5926 ± 34	6834	5365 BC	91.0 ± 4.2	6408 ± 34	7314
4895 BC	86.4 ± 3.3	5985 ± 25	6844	5375 BC	94.7 ± 4.4	6390 ± 36	7324
4905 BC	88.1 ± 2.6	5982 ± 19	6854	5385 BC	93.1 ± 4.9	6412 ± 39	7334
4915 BC	85.0 ± 3.5	6015 ± 26	6864	5395 BC	96.0 ± 4.2	6400 ± 34	7344
4925 BC	83.8 ± 4.5	6033 ± 33	6874	5405 BC	95.2 ± 4.2	6416 ± 34	7354
4935 BC	89.8 ± 3.2	5999 ± 24	6884	5415 BC	100.9 ± 3.0	6384 ± 24	7364
4945 BC	84.4 ± 2.3	6047 ± 17	6894	5425 BC	99.8 ± 3.1	6402 ± 25	7374
4955 BC	86.4 ± 3.1	6042 ± 23	6904	5435 BC	89.7 ± 4.1	6485 ± 33	7384
4965 BC	84.8 ± 3.3	6065 ± 24	6914	5445 BC	79.8 ± 3.1	6568 ± 25	7394
4975 BC	87.8 ± 3.1	6053 ± 23	6924	5455 BC	81.7 ± 4.3	6564 ± 34	7404
4985 BC	88.3 ± 3.3	6058 ± 25	6934	5465 BC	87.1 ± 3.0	6534 ± 24	7414
4995 BC	85.1 ± 4.3	6092 ± 32	6944	5475 BC	83.7 ± 4.3	6568 ± 35	7424
5005 BC	83.3 ± 4.1	6115 ± 33	6954	5485 BC	86.9 ± 4.4	6554 ± 35	7434
5015 BC	88.4 ± 4.2	6087 ± 34	6964	5495 BC	83.0 ± 4.3	6593 ± 35	7444
5025 BC	85.6 ± 4.1	6117 ± 33	6974	5505 BC	81.8 ± 4.3	6612 ± 35	7454
5035 BC	87.2 ± 4.3	6115 ± 34	6984	5515 BC	87.0 ± 4.3	6583 ± 35	7464
5045 BC	85.4 ± 4.3	6138 ± 34	6994	5525 BC	75.5 ± 4.2	6678 ± 34	7474

TABLE 1. (Continued)

Cal AD/BC	$\Delta^{14}C$ ‰	^{14}C age (BP)	Cal BP	Cal AD/BC	$\Delta^{14}C$ ‰	^{14}C age (BP)	Cal BP
5535 BC	79.4 ± 4.4	6659 ± 35	7484	5775 BC	69.2 ± 2.9	6969 ± 22	7724
5545 BC	77.9 ± 4.4	6680 ± 35	7494	5785 BC	72.8 ± 2.2	6953 ± 17	7734
5555 BC	89.8 ± 3.3	6604 ± 25	7504	5795 BC	75.1 ± 2.4	6947 ± 18	7744
5565 BC	90.7 ± 3.3	6606 ± 25	7514	5805 BC	71.3 ± 2.4	6982 ± 19	7754
5575 BC	83.5 ± 2.4	6670 ± 18	7524	5815 BC	69.9 ± 2.1	7004 ± 17	7764
5585 BC	77.7 ± 3.3	6721 ± 25	7534	5825 BC	75.8 ± 2.5	6969 ± 20	7774
5595 BC	76.1 ± 3.4	6742 ± 26	7544	5835 BC	75.2 ± 2.6	6983 ± 20	7784
5605 BC	70.8 ± 2.5	6793 ± 19	7554	5845 BC	76.8 ± 2.6	6981 ± 21	7794
5615 BC	74.9 ± 2.2	6774 ± 17	7564	5855 BC	70.7 ± 4.7	7035 ± 38	7804
5625 BC	74.9 ± 2.7	6780 ± 21	7574	5865 BC	76.0 ± 3.9	7005 ± 31	7814
5635 BC	70.8 ± 2.4	6822 ± 19	7584	5875 BC	76.3 ± 4.2	7012 ± 34	7824
5645 BC	75.2 ± 2.6	6799 ± 20	7594	5885 BC	68.9 ± 4.2	7077 ± 34	7834
5655 BC	76.4 ± 2.8	6800 ± 21	7604	5895 BC	68.0 ± 4.6	7094 ± 37	7844
5665 BC	75.8 ± 2.1	6815 ± 16	7614	5905 BC	74.8 ± 3.1	7053 ± 25	7854
5675 BC	75.2 ± 2.7	6828 ± 20	7624	5915 BC	85.0 ± 3.2	6986 ± 26	7864
5685 BC	71.7 ± 3.1	6863 ± 24	7634	5925 BC	87.0 ± 3.0	6981 ± 24	7874
5695 BC	71.2 ± 2.7	6875 ± 21	7644	5935 BC	81.5 ± 5.2	7032 ± 42	7884
5705 BC	70.9 ± 2.5	6885 ± 20	7654	5945 BC	75.3 ± 4.2	7088 ± 34	7894
5715 BC	69.5 ± 3.3	6907 ± 26	7664	5955 BC	75.3 ± 4.1	7097 ± 33	7904
5725 BC	73.7 ± 3.1	6884 ± 24	7674	5965 BC	73.9 ± 4.4	7118 ± 35	7914
5735 BC	69.4 ± 2.5	6929 ± 19	7684	5975 BC	70.2 ± 5.0	7155 ± 40	7924
5745 BC	70.2 ± 2.3	6933 ± 18	7694	5985 BC	67.8 ± 2.8	7182 ± 23	7934
5755 BC	70.8 ± 2.6	6938 ± 20	7704	5995 BC	65.2 ± 4.8	7212 ± 36	7944
5765 BC	73.1 ± 2.2	6931 ± 17	7714	6000 BC	75.6 ± 3.3	7141 ± 25	7949

[RADIOCARBON, VOL. 35, NO. 1, 1993, P. 67–72]

A NOTE ON SINGLE-YEAR CALIBRATION OF THE RADIOCARBON TIME SCALE, AD 1510–1954

MINZE STUIVER

Department of Geological Sciences and Quaternary Research Center, University of Washington, Seattle, Washington 98195 USA

INTRODUCTION

Most data in this Calibration Issue are based on radiocarbon age determinations of tree-ring samples with dendrochronologically determined calibrated (cal) ages. For high-precision measurements, substantial sample amounts are needed, and the processed wood usually spans 10 or 20 tree rings. Thus, the calibration curve data points usually have decadal, or bidecadal, spacing. These curves, to be used for the calibration of samples formed over 1 or 2 decades, may not be fully applicable to samples (leaves, twigs, *etc.*) formed in a single growing season.

The determination of a calibration curve with single-year spacing over many thousands of years requires an order of magnitude larger calibration effort than made so far. For instance, the counting time for producing the 440-yr single-year series reported here is identical to that needed for a 8800-yr bidecadal chronology. Fortunately, the production of a single-year calibration curve for the Holocene is not urgent, as the gains from such an effort are limited.

^{14}C determinations of either the cellulose or de Vries component of Douglas and Noble fir wood from the US Pacific Northwest (Table 1) form the basis for the Figures 1 and 2 calibration curves. All measurements are for single-year samples, except for AD 1890.5–1910.5 (2-yr data) and AD 1913–1916 (3-yr data). The average laboratory standard deviation in the measurements is 12.8 ^{14}C yr. The AD 1510–1625 and AD 1820–1950 data, published previously (Stuiver 1982; Stuiver & Quay 1981), have been corrected for minor amounts of radon in the counting process (Stuiver & Becker 1993).

The time span over which a sample is formed is important in limiting the cal age uncertainty introduced by wiggles in the calibration curve. The wiggles in a curve produced, for instance, by a 100-yr moving average of decadal calibration data are smoothed relative to those of the original decadal calibration curve. In areas of major cal age uncertainty (the horizontal portions of the curve), the ^{14}C age conversion for a sample formed over 100 yr, using the 100-yr moving-average curve, yields a cal age range smaller than the range obtained from the decadal (or single-year) calibration curve. The cal age range derived for the 100-yr sample, of course, represents the midpoint of the 100-yr time span. This approach is valid only when the growth rate of the specimen is reasonably constant, as the amount of material formed during the first 50 yr must approximate that of the second 50 yr.

Figures 1 and 2 detail the calibration curves for, respectively, single-year samples and 3-, 5-, and 10-yr moving averages. With an average standard deviation (for 1.0 error multiplier) in the single-year calibration curve of 12.8 ^{14}C yr, the uncertainties in the 3-, 5- and 10-yr moving averages are, respectively, 7.2, 5.6 and 4.1 yr.

In Figure 3, we compare the cal ages and ranges derived for three high-precision ^{14}C dates (120 ± 15, 180 ± 15 and 260 ± 15 ^{14}C yr BP). The calibration curves used are the Figure 1 single-year curve, its derivatives obtained through moving averages (3-, 5- and 10-yr), and the decadal (Stuiver

& Becker 1993) and bidecadal (Stuiver & Pearson 1993) curves. The 10-yr curves differ slightly, as a 10-yr moving average produces a continuous curve, whereas the decadal Stuiver and Becker calibration curve connects decadal midpoints by a straight line.

For regions of major cal-age uncertainty (^{14}C ages of 120 and 180 yr BP), the number of intercepts (Fig. 3) increases by an order of magnitude when moving from the decadal to the single-year curve. The cal age ranges around most intercepts derived from the single-year curve overlap, however, and do not improve time separation within the larger cal age ranges. Two-sigma cal age ranges (Fig. 3) usually increase for single-year-curve calibration, and additional segments appear. The calibration of a single-year sample against a single-year calibration curve leads to larger cal-age uncertainty than the calibration of a 10-yr sample against a decadal curve.

Materials grown over decades will provide better cal-age control than single-year samples. Of course, single-year samples may be the only ones available for a specific site. As the current single-year calibration curve is only for the post-AD 1510 interval, the calibration of these samples (against a decadal or bidecadal curve) will, in most instances, lead to underestimated cal-age uncertainty.

Single-year ^{14}C age records may differ between regions. Pacific Northwest Δ^{14}C values (derived from the Fig. 1 ^{14}C ages) contain an 11-yr cycle with an average amplitude of 1.40 ± 0.16 ‰ (*ca.* 11 ± 1 ^{14}C yr). This amplitude differs significantly from the 11-yr cycle amplitude of 4.8 ± 0.6 ‰ (*ca.* 39 ± 5 ^{14}C yr) found in Russian trees (Kocharov 1992) between AD 1600 and AD 1950. Confirmation of the Russian data set would imply Pacific Northwest-Russia ^{14}C age differences of at least 20 ^{14}C yr for parts of the single-year record. ^{14}C age differences of about 10 ^{14}C yr appear to be an upper limit for regional offsets in decadal or bidecadal calibration curves (Stuiver & Pearson 1992).

ACKNOWLEDGMENTS

This work was supported by National Science Foundation grant BNS-9004492. P. J. Reimer and P. J. Wilkinson provided crucial technical and analytical support.

REFERENCES

Kocharev, G. E. 1992 Radiocarbon and astrophysical-geophysical phenomena. *In* Taylor, R. E., Long, A. and Kra, R. S., eds., *Radiocarbon After Four Decades: An Interdisciplinary Perspective*. New York, Springer Verlag: 130–145.

Stuiver, M. 1982 A high-precision calibration of the AD radiocarbon time scale, *Radiocarbon* 24(1): 1–26.

Stuiver, M. and Becker, B. 1993 High-precision decadal calibration of the radiocarbon time scale AD 1950-6000 BC. *Radiocarbon*, this issue.

Stuiver, M. and Pearson, G. W. 1992 Calibration of the radiocarbon time scale 2500–5000 BC. *In* Taylor, R. E., Long, A. and Kra, R. S., eds., *Radiocarbon After Four Decades: An Interdisciplinary Perspective*. New York, Springer Verlag: 19–33.

_____1993 High-precision calibration of the radiocarbon time scale, AD 1950–500 BC and 2500–6000 BC. *Radiocarbon*, this issue.

Stuiver, M. and Quay, P. D. 1981 Atmospheric ^{14}C changes resulting from fossil fuel CO_2 release and cosmic ray flux variability. *Earth and Planetary Science Letters* 53: 349–362.

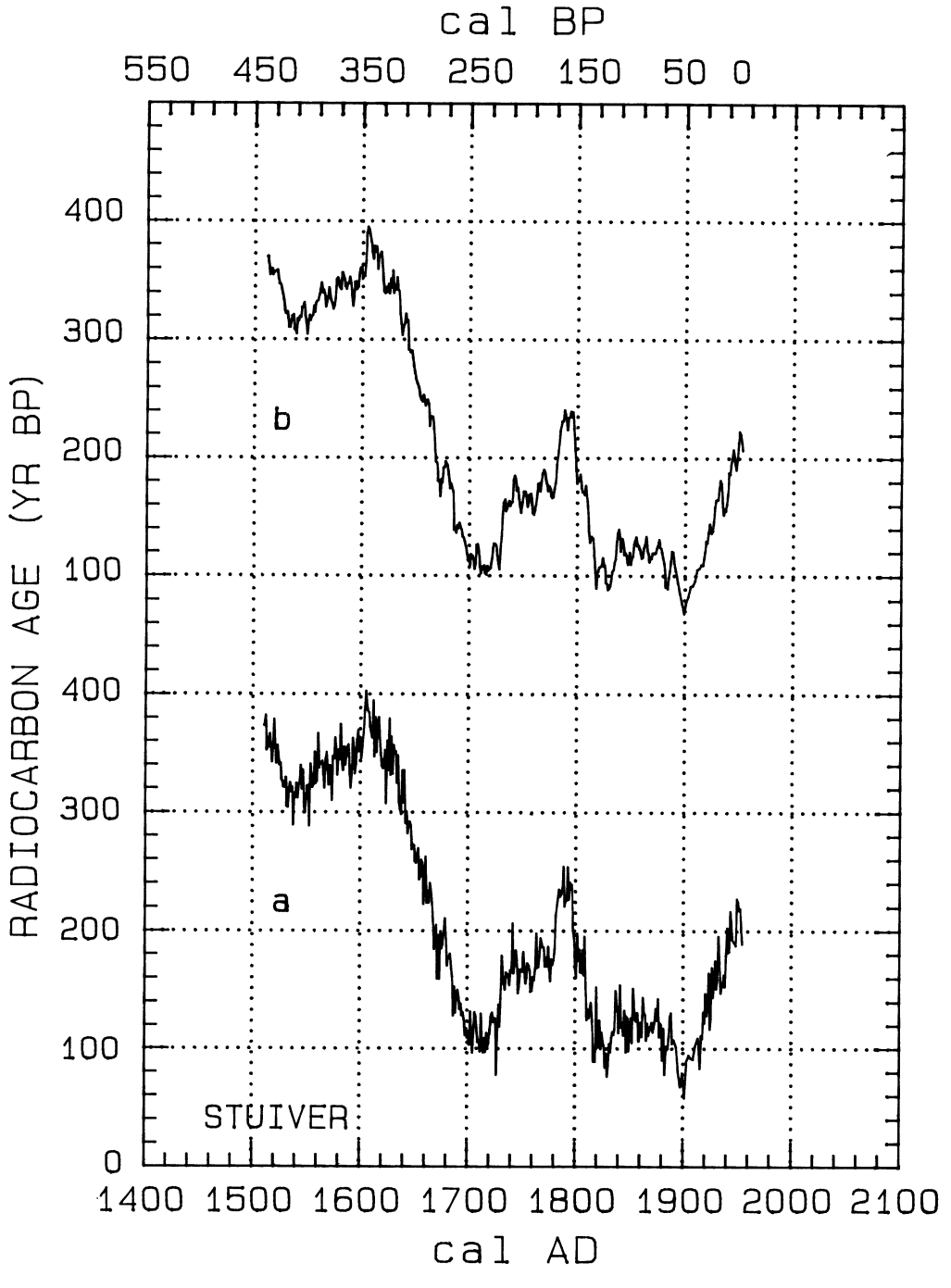

Fig. 1. ^{14}C age *vs.* cal age for single-year samples (a) and 3-yr moving averages (b)

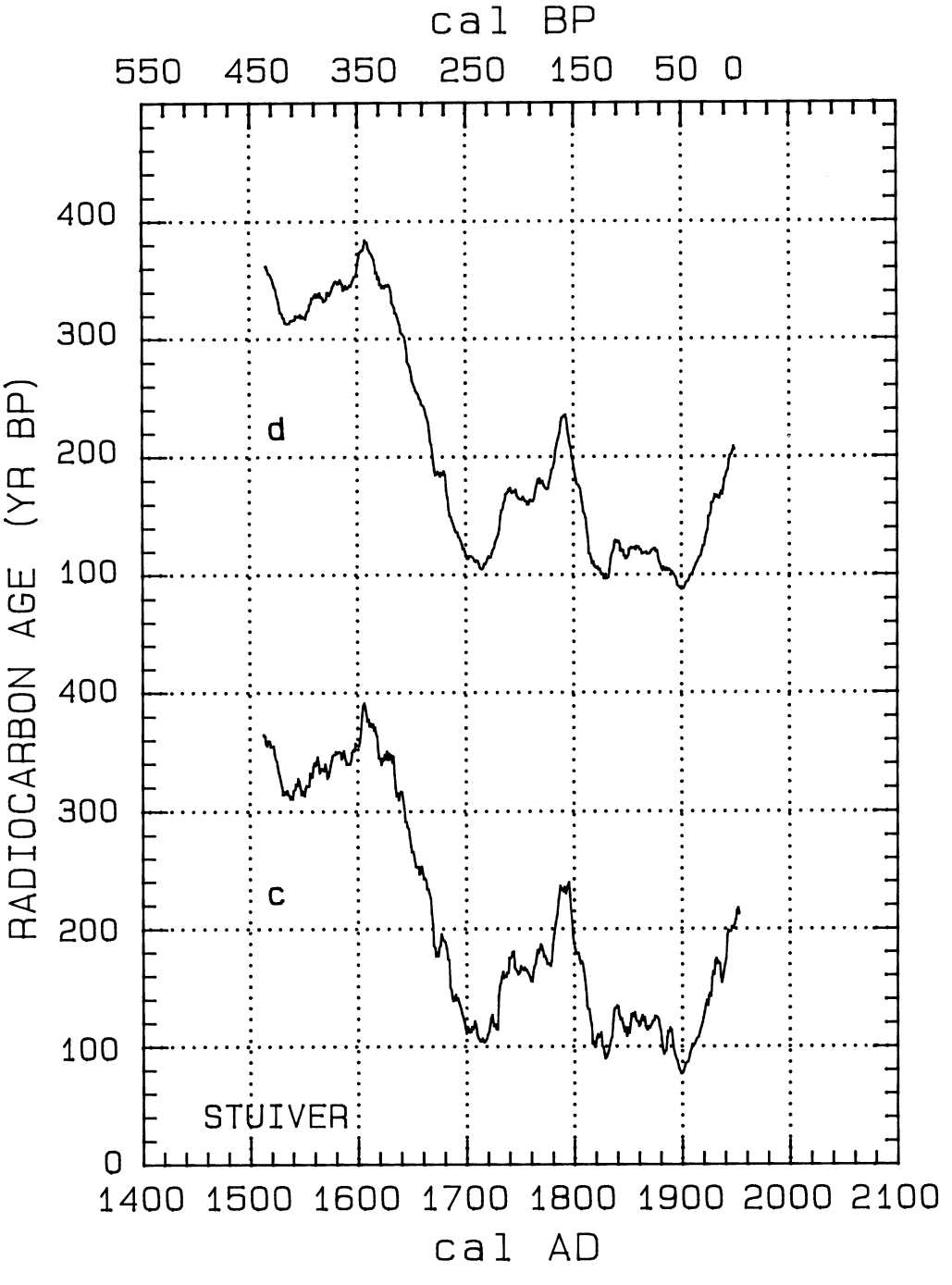

Fig. 2. ^{14}C age *vs.* cal age for 5-yr (c) and 10-yr (d) moving averages of single-year results depicted in Figure 1

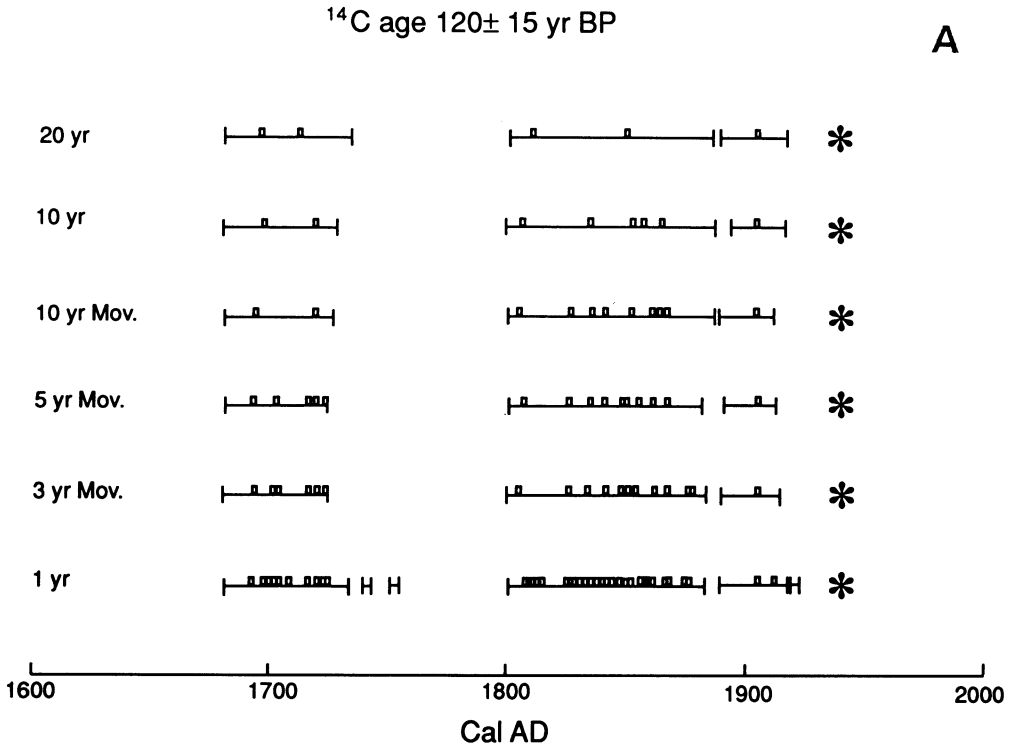

Fig. 3A–C. Cal age results for three ^{14}C ages (120 ± 15, 180 ± 15, and 260 ± 15 ^{14}C yr BP). Cal age intercepts (▫) were derived from the Figure 1 single-year calibration curve, the 3-, 5- and 10-yr moving averages, the Stuiver and Becker (1993) decadal curve, and the Stuiver and Pearson (1993) bidecadal curve. | = 2 σ cal age ranges. ✻ = nuclear bomb intercepts near AD 1954–1955.

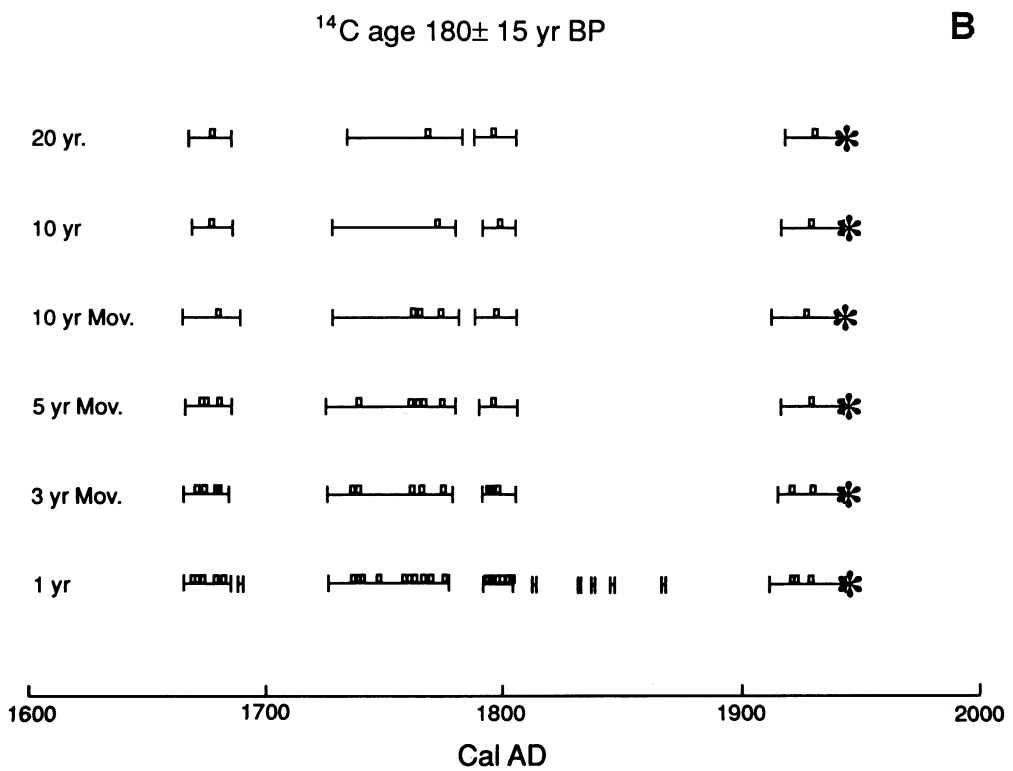

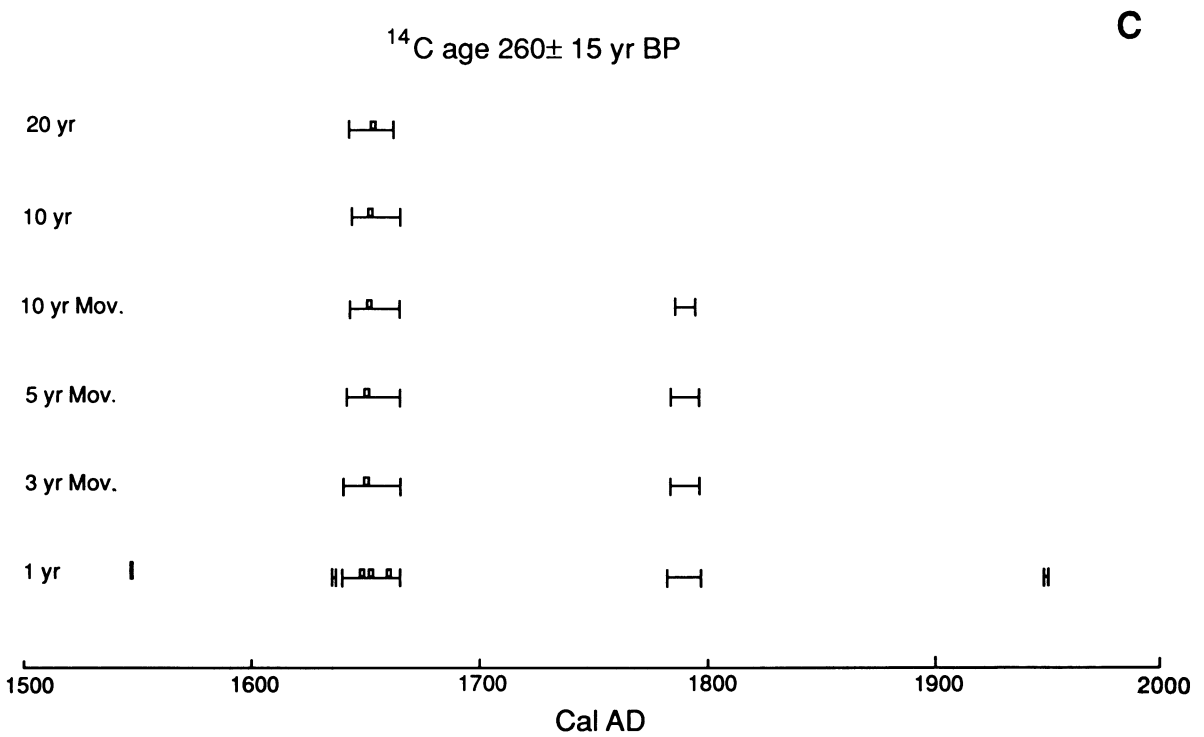

TABLE 1. ^{14}C determinations of either the cellulose or de Vries component of Douglas and Noble fir wood from the US Pacific Northwest

Year AD	Tree	Location	Species	Wood Treatment
1916–1954	C	Olympic Peninsula (47°46′N, 124°06′W)	Douglas fir	CL*
1820–1919	A	Olympic Penninsula (47°46′N, 124°06′W)	Douglas fir	DV**
1690–1725 1755–1759 1784–1822	B	Mt. Rainier, Washington (46°45′N, 121°45′W)	Douglas fir	DV
1686–1781	DW	Cougar, Washington (46°4′N, 122°17′W)	Noble fir	CL
1510–1700	F	Coos Bay, Oregon (43°7′N, 123°40′W)	Douglas fir	CL

*CL = cellulose
**DV = de Vries-treated wood

[RADIOCARBON, VOL. 35, NO. 1, 1993, P. 73–85]

PRETORIA CALIBRATION CURVE FOR SHORT-LIVED SAMPLES, 1930–3350 BC

J. C. VOGEL, ANNEMARIE FULS, EBBIE VISSER

Quaternary Dating Research Unit, CSIR, P.O. Box 395, Pretoria 0001, South Africa

and

BERND BECKER

Institut für Botanik, Universität Hohenheim, D-7000 Stuttgart 70 Germany

The high-precision radiocarbon calibration curve for short-lived samples (1–4 yr) of the early historical period (3rd millennium BC) presented previously (Vogel *et al.* 1986) has been further substantiated and extended to link with a similar curve produced by de Jong for part of the 4th millennium BC (de Jong & Mook 1980). The precise dendrochronological age of the sample set measured by de Jong has finally been fixed (de Jong, Mook & Becker 1989), so that the two sets now cover the period 1930–3900 BC, *i.e.*, the Early Bronze Age and Late Chalcolithic periods of the Middle East. The standard calibration curve for the two sets is presented by Vogel and van der Plicht (1993).

In all, we analyzed 173 samples of 1–4 annual tree rings of the south-central European subfossil oak sequence (Becker 1979). The method of pretreatment and measurement has remained the same, as Vogel *et al.* (1986) briefly described previously. Table 1 lists the results. Because we made certain retrospective adjustments to the 89 analyses presented in our previous paper (Vogel *et al.* 1986), we include them here. For the most part, the corrections are less than 4 yr, but in a few cases, re-evaluation has resulted in larger changes.

The construction of a calibration curve from these data requires some discussion. On the one hand, the individual data points, of necessity, have to scatter on both sides of the actual correlation curve to the degree prescribed by the uncertainty of the measurements. A line connecting successive points would thus show erratic variations that do not correspond to the actual changes in ^{14}C, and some smoothing is necessary. On the other hand, the smoothing procedure should not dampen or eliminate the real "wiggles" in the curve. We feel that the best compromise in this situation is to use a spline curve with "tightness", S = 1, *i.e.*, a curve that passes within 1 σ from 68% of all the data points, but smooths out unsubstantiated variations (Talma & Vogel 1993).

The resulting calibration curve is presented in Figure 1A–C. In Figure 2, the Groningen data (de Jong, Mook & Becker 1989) are added to the Pretoria measurements to show the compatibility of the two sets for the region of overlap. The combined data produce a continuous curve for the period, 1930 to 3900 BC, specifically for calibrating short-lived ^{14}C samples. We consider the 68% confidence level of the curve to be better than the 1 σ errors of individual points, because the adjacent measurements contribute to the estimate of the spline at each point. The validity of our data set has been checked in different ways:

1. We analyzed a set of 13 samples of the bristlecone pine dendrochronological series (Ferguson 1970) in the same counter to verify the tree-ring dating of our series. The samples were chosen from a period when the ^{14}C level was changing rapidly (2830–2960 BC) to achieve maximum sensitivity. Table 2 gives the results of the analyses. The comparison is made by determining the distance on the x axis that the eight samples on the steep part of the calibration curve between 2830 and 2930 BC deviate from the corresponding spline values

through our South German data points. The average deviation is 1.1±4.1 yr, so that we can safely accept that the South German tree-ring dates at 2900 BC correspond to those of the bristlecone pine chronology.

2. It is especially difficult to achieve precise intercalibration among laboratories, and systematic differences of 20–30 yr are probably not unusual between laboratories. With the present data set, we can make very accurate comparisons with other high-precision laboratories. First, we can assess the compatibility of the Groningen data set (de Jong, Mook & Becker 1989) with ours for the period of overlap between 3200 and 3350 BC. By comparing the 25 points of our set in this time range with the corresponding values of the spline through the Groningen data, we find an offset of −7.1 ± 6.4 yr. If the one apparent outlier of our set at 3342 BC is excluded, the difference reduces to −4.2 ± 6.0 yr, *i.e.*, our dates are, on average, 4.2 yr older than those of Groningen. The two sets are thus highly compatible and can be joined without reservation.

3. A similar comparison can be made with the newly adjusted and extended measurements of the Seattle laboratory (Stuiver & Becker 1993). If the 173 points of the Pretoria series are compared with the corresponding values of a spline (S = 1) through the Seattle data, we find an offset of 2.9 ± 1.8 yr, σ = 24.1 yr, indicating that our dates are, on average, 2.9 yr younger than those of Seattle. This means that the calibration of the two laboratories is nearly identical. The standard deviation of 24.1 yr shows that the fluctuations around the spline are of the size to be expected for a sample error of just under 20 yr and an error of ~15 yr in the spline.

We have made more analyses to quantify the difference in ^{14}C ages between the northern and southern hemispheres (Vogel *et al.* 1986). In all, we made 14 comparisons of 1–2 annual rings, covering the 19th century, of an oak grown in Norg, The Netherlands, and a pine grown in Cape Town, South Africa. Table 3 lists the results. The average difference in ^{14}C content between the two sets is 5.1 ±0.6 ‰, which translates to 41 ± 5 yr, a value slightly larger than that reported previously. This value is now used to create a calibration curve for midlatitudes in the southern hemisphere, using the data of Stuiver and Pearson (1993) for the northern hemisphere.

Finally, we measured more precisely the extent of the industrial dilution of ^{14}C (Suess effect) in southern Africa. For this, we secured two pine trees planted in the 1940s in state forests far removed from local city pollution. One tree, planted in 1942, derives from the Jonkershoek forest outside Stellenbosch (33°57′S, 18°57′E). The second, planted in 1947, is from the Mac Mac forest in the eastern Transvaal (25°05′S, 30°47′E). For these measurements, we prepared pure cellulose from the inner annual rings, according to the technique described by Tans, de Jong & Mook (1978), because of the presence of mobile organic substances of later years contaminated by atomic bomb ^{14}C. We also made two analyses on the horn of a Kudu antelope shot in the Erongo Mountains, Namibia (21°39′S, 15°45′E) in 1952. These samples of horn core and horn sheath from the base of the horn should accurately represent the ^{14}C level of vegetation grown in 1950–1952. The ^{14}C analyses of these samples are presented in Table 4. The average ^{14}C depletion, with respect to NBS oxalic acid $\Delta^{14}C$, for the samples dating to 1950–1953, is $\Delta^{14}C$ = −24.7 ± 0.9 ‰. This is almost exactly equal to the value for annual tree rings of the years, 1950–1954, of a Douglas fir, reported by Stuiver & Quay (1981). Because ^{14}C in southern Africa during the 19th century was 5.1‰ lower than in the northern hemisphere (Table 3), the ^{14}C dilution in the southern hemisphere was only about 15‰ between 1860 and 1950, compared to the 20‰ obtained for the northern hemisphere by Stuiver and Quay (1981).

The high-precision calibration curves now available make it possible to produce remarkably accurate age determinations with ^{14}C. However, to obtain the maximum benefit from the technique, great care must be taken with the selection of samples. An accurate historic age can be obtained only if the sample consists of material that is undoubtedly contemporaneous with the event to be dated. This means that emphasis should be placed on short-lived organic matter, such as, *e.g.*, charred food remains associated with a specific destruction level. For the time being, the samples should also be large enough, at least 25 g, so that thorough chemical pretreatment can be undertaken. Such an approach, pursued with vigor, would lead to a new phase of ^{14}C dating in which the early and protohistoric periods could be provided with a more precise chronology.

ACKNOWLEDGMENTS

We thank Siep Talma for providing accurate ^{13}C analyses of all the samples, and especially for producing and debugging the computer programs used in the laboratory. We are indebted to D. Liebenberg, Forestek, CSIR, Stellenbosch and E. J. P. Malan, Department of Water Affairs and Forestry, Pretoria, for supplying disks of the Jonkershoek pine and the Mac Mac pine, respectively.

REFERENCES

Becker, B. 1979 Holocene tree-ring series from southern central Europe for archaeology dating, radiocarbon calibration, and stable isotope analysis. *In* Berger, R. and Suess, H. E., eds., *Radiocarbon Dating*, Proceedings of the 9th International ^{14}C Conference. Berkeley/Los Angeles, University of California Press: 554–565.

de Jong, A. F. M. and Mook, W. G. 1980 Medium-term atmospheric ^{14}C variations. *In* Stuiver, M. and Kra, R. S., eds., Proceedings of the 10th International ^{14}C conference. *Radiocarbon* 22(2): 267–272.

de Jong, A. F. M., Mook, W. G. and Becker, B. 1989 Corrected calibration of the radiocarbon time scale, 3904–3203 cal BC. *Radiocarbon* 31(2): 201–210.

Ferguson, C. W. 1970 Dendrochronology of bristlecone pine, *Pinus aristata*: Establishment of a 7484-year chronology in the White Mountains of eastern-central California. *In* Olsson, I. U., ed., *Radiocarbon Variations and Absolute Chronology*, Proceedings of the 12th Nobel Symposium. New York, John Wiley & Sons: 237–245.

Stuiver, M. and Becker, B. 1993 High-precision decadal calibration of the radiocarbon time scale, AD 1950–6000 BC. *Radiocarbon*, this issue.

Stuiver, M. and Pearson, G. W. 1993 High-precision calibration of the radiocarbon time scale, AD 1950–500 BC and 2500–6000 BC. *Radiocarbon*, this issue.

Stuiver, M. and Quay, P. D. 1981 Atmospheric ^{14}C changes resulting from fossil fuel CO_2 release and cosmic ray flux variability. *Earth and Planetary Science Letters* 53: 349–362.

Talma, A. S. and Vogel, J. C. 1993 A simplified approach to the calibration of radiocarbon dates. *Radiocarbon*, in press.

Tans, P. P., de Jong, A. F. M. and Mook, W. G. 1978 Chemical pretreatment and radial flow of ^{14}C in tree rings. *Nature* 271: 234–235.

Vogel, J. C., Fuls, A., Visser, E. and Becker, B. 1986 Radiocarbon fluctuations during the third millennium BC. *In* Stuiver, M. and Kra, R. S., eds., Proceedings of the 12th International ^{14}C Conference. *Radiocarbon* 28(2B): 935–938.

Vogel, J. C. and van der Plicht, J. 1993 Calibration curve for short-lived samples, 1900–3900 BC. *Radiocarbon*, this issue.

TABLE 1. Conventional ^{14}C ages and $\Delta^{14}C$ of tree-ring samples from the South German oak tree-ring sequence

Pta-no.	Cal BC	^{14}C age (yr BP)	$\delta^{13}C$ (‰)	$\Delta^{14}C$ (‰)
Steinheim 7				
2745	1935–36	3580 ± 8	−25.3	+24.5 ± 0.9
2884	1942–45	3596 ± 18	−25.2	+23.5 ± 2.2
2738	1955–56	3618 ± 14	−25.9	+22.3 ± 1.7
3333	1964–65	3639 ± 20	−25.3	+20.7 ± 2.5
2734	1975–76	3608 ± 14	−26.4	+25.9 ± 1.7
3332	1982–83	3645 ± 17	−25.8	+22.2 ± 2.0
2726	1995–96	3644 ± 15	−26.1	+23.8 ± 1.9
Unterleiterbach 19				
3328	2005–06	3619 ± 19	−24.8	+28.2 ± 2.4
2751	2015–16	3636 ± 16	−25.8	+27.2 ± 2.0
3127	2025–26	3658 ± 18	−24.7	+25.8 ± 2.2
2787	2034–35	3689 ± 14	−25.8	+22.8 ± 1.7
4495	2044–45	3699 ± 27	−24.9	+22.9 ± 3.3
2792	2056	3694 ± 15	−25.5	+24.8 ± 1.9
4510	2065	3760 ± 21	−25.5	+17.7 ± 2.6
2799	2075–76	3707 ± 13	−25.4	+25.8 ± 1.6
4503	2085–86	3738 ± 20	−26.0	+23.0 ± 2.4
Vohberg 19				
2856	2093	3705 ± 14	−25.2	+28.2 ± 1.7
3135	2105	3686 ± 20	−26.0	+32.0 ± 2.5
2892	2115	3680 ± 14	−25.5	+34.0 ± 1.7
3132	2124	3698 ± 18	−26.6	+32.8 ± 2.2
2900	2134–35	3707 ± 19	−24.9	+33.1 ± 2.4
3126	2145–46	3760 ± 20	−24.3	+27.6 ± 2.6
4113	2149–50	3731 ± 18	−24.5	+31.8 ± 2.2
2928	2155	3797 ± 14	−24.4	+24.1 ± 1.8
4096	2159–60	3768 ± 19	−24.9	+28.5 ± 2.4
3327	2165	3782 ± 16	−23.7	+27.3 ± 1.9
2983	2175	3779 ± 16	−24.5	+28.8 ± 1.9
3454	2180	3739 ± 16	−24.2	+34.8 ± 1.9
3321	2185	3734 ± 15	−23.5	+35.8 ± 1.9
3469	2190	3713 ± 25	−24.2	+39.4 ± 3.0
2996	2195	3750 ± 18	−25.2	+35.2 ± 2.2
3115	2205	3801 ± 17	−25.3	+29.7 ± 2.1
3006	2215	3855 ± 17	−23.9	+24.2 ± 2.1
Nersingen 40				
4107	2220–21	3821 ± 18	−24.8	+29.1 ± 2.3
4101	2230–31	3832 ± 16	−25.6	+29.0 ± 2.1
3014	2236	3840 ± 16	−25.2	+28.7 ± 1.9
4147	2239	3806 ± 18	−25.4	+33.5 ± 2.3
3338	2245	3867 ± 17	−24.5	+26.4 ± 2.1
3016	2255–56	3834 ± 18	−25.3	+31.7 ± 2.3
3303	2265	3806 ± 20	−24.9	+36.7 ± 2.4
3120	2275	3808 ± 19	−26.0	+37.5 ± 2.4
Hochstadt–Staustufe 3				
3769	2280–82	3830 ± 20	−26.6	+35.5 ± 2.6
Nersingen 40				
3335	2284	3810 ± 18	−25.2	+38.5 ± 2.3

TABLE 1. (Continued)

Pta-no.	Cal BC	^{14}C age (yr BP)	$\delta^{13}C$ (‰)	$\Delta^{14}C$ (‰)
Hochstadt–Staustufe 3				
3846	2290–92	3850 ± 19	−26.9	+34.2 ± 2.4
Nersingen 40				
3123	2295	3854 ± 17	−24.4	+34.2 ± 2.1
Hochstadt–Staustufe 3				
3503	2300–02	3886 ± 17	−26.6	+30.8 ± 2.1
4512	2310–12	3898 ± 18	−27.4	+30.5 ± 2.3
Vohberg 34				
3532	2320–22	3900 ± 21	−26.0	+31.4 ± 2.6
3496	2327–30	3857 ± 13	−26.2	+38.0 ± 1.6
3502	2337–40	3870 ± 14	−25.3	+37.5 ± 1.8
3541	2350–52	3924 ± 15	−25.3	+32.2 ± 1.8
4518	2360–62	3911 ± 24	−25.5	+35.0 ± 2.9
3599	2370–72	3905 ± 15	−25.4	+37.1 ± 2.0
4509	2380–82	3888 ± 19	−26.1	+40.7 ± 2.4
3606	2390–92	3902 ± 22	−26.0	+40.2 ± 2.8
Christiansworth 2				
3514	2407–10	3895 ± 19	−24.9	+43.1 ± 2.4
3519	2417–20	3888 ± 20	−24.6	+45.3 ± 2.4
3525	2427–30	3904 ± 16	−24.6	+44.5 ± 1.9
3539	2437–40	3929 ± 20	−25.6	+42.6 ± 2.4
3552	2447–50	3913 ± 17	−25.5	+45.9 ± 2.1
3568	2467–70	3939 ± 15	−25.6	+45.0 ± 1.8
4524	2480–82	3987 ± 20	−25.3	+40.4 ± 2.5
3593	2490–92	4014 ± 17	−24.6	+38.3 ± 2.1
4525	2500–02	4037 ± 18	−25.2	+36.5 ± 2.3
3607	2510–12	4055 ± 21	−24.9	+35.3 ± 2.6
3613	2510–12	4045 ± 20	−24.5	+36.8 ± 2.5
4533	2520–22	4040 ± 21	−25.6	+38.5 ± 2.6
3619	2530–32	4058 ± 18	−25.6	+37.5 ± 2.2
Pettstadt 48				
4540	2540–42	3995 ± 14	−24.2	+47.0 ± 1.8
3626	2550–52	4031 ± 19	−23.1	+43.6 ± 2.5
4545	2560–62	3982 ± 21	−23.9	+51.1 ± 2.6
3630	2570–72	4051 ± 19	−23.6	+43.5 ± 2.5
4360	2580–82	4107 ± 17	−23.7	+37.4 ± 2.2
3638	2590–92	4112 ± 15	−23.5	+37.9 ± 1.8
3751	2600–02	4116 ± 17	−23.8	+38.9 ± 2.2
3644	2610–12	4069 ± 18	−23.9	+46.1 ± 2.2
3776	2620–22	4113 ± 18	−24.1	+41.7 ± 2.3
3657	2630–32	4092 ± 19	−24.3	+45.8 ± 2.3
4338	2640–42	4142 ± 21	−24.0	+40.2 ± 2.7
Nersingen 51				
3670	2652–55	4121 ± 20	−25.2	+44.6 ± 2.5
4554	2662–65	4143 ± 15	−26.0	+43.2 ± 1.8
3676	2672–75	4131 ± 18	−26.0	+45.8 ± 2.2
4485	2682–85	4176 ± 14	−26.3	+41.4 ± 1.7
3681	2692–95	4148 ± 18	−25.9	+46.4 ± 2.4
4371	2702–05	4175 ± 16	−26.8	+44.1 ± 2.0
Blindheim 37				
4011	2711–14	4145 ± 18	−25.7	+49.1 ± 2.2

TABLE 1. (Continued)

Pta-no.	Cal BC	^{14}C age (yr BP)	$\delta^{13}C$ (‰)	$\Delta^{14}C$ (‰)
Nersingen 51				
3685	2712–15	4195 ± 18	−26.2	+42.7 ± 2.4
Blindheim 37				
4244	2721–24	4153 ± 18	−26.9	+49.4 ± 2.2
3909	2731–34	4149 ± 20	−26.7	+51.1 ± 2.5
Nersingen 51				
3740	2732–35	4125 ± 15	−25.8	+54.3 ± 2.0
Blindheim 37				
4498	2741–44	4129 ± 27	−26.3	+55.1 ± 3.4
3914	2751–54	4170 ± 18	−25.9	+50.9 ± 2.2
Nersingen 51				
3746	2752–55	4149 ± 21	−25.8	+53.6 ± 2.5
Blindheim 37				
4024	2761–64	4193 ± 18	−25.7	+49.3 ± 2.2
3920	2771–74	4172 ± 22	−26.2	+53.2 ± 2.7
4031	2781–84	4214 ± 17	−25.9	+48.9 ± 2.0
4448	2786–89	4175 ± 18	−25.8	+54.8 ± 2.4
3951	2791–94	4165 ± 21	−26.1	+56.6 ± 2.5
4387	2801–04	4180 ± 14	−25.1	+56.1 ± 1.9
3952	2811–14	4146 ± 16	−24.5	+61.7 ± 2.0
4238	2821–24	4114 ± 18	−24.5	+67.4 ± 2.3
3953	2831–34	4124 ± 18	−24.4	+67.4 ± 2.3
4158	2836–39	4172 ± 18	−24.0	+61.3 ± 2.2
3963	2841–44	4163 ± 15	−24.1	+63.2 ± 1.8
4163	2851–54	4170 ± 17	−24.2	+63.7 ± 2.2
3850	2861–64	4202 ± 19	−24.9	+60.9 ± 2.4
4490	2866–69	4181 ± 15	−24.4	+64.1 ± 1.8
4460	2876–79	4222 ± 15	−25.3	+59.9 ± 1.9
3856	2881–84	4300 ± 21	−24.2	+50.3 ± 2.6
4294	2891–94	4284 ± 15	−24.6	+53.7 ± 1.9
3854	2901–04	4308 ± 20	−25.3	+51.9 ± 2.4
4397	2906–09	4342 ± 19	−24.3	+48.0 ± 2.2
4181	2911–14	4350 ± 17	−24.9	+47.7 ± 2.1
4561	2916–19	4358 ± 18	−25.4	+47.2 ± 2.2
Pettstadt 4				
3861	2921–24	4371 ± 21	−25.6	+46.1 ± 2.6
4175	2931–34	4377 ± 19	−25.7	+46.9 ± 2.4
3878	2941–44	4361 ± 18	−25.6	+50.1 ± 2.2
4130	2946–49	4383 ± 20	−24.7	+47.9 ± 2.6
4285	2956–59	4389 ± 16	−25.1	+48.4 ± 1.9
3867	2961–64	4393 ± 19	−25.4	+48.6 ± 2.2
4037	2971–74	4381 ± 19	−25.5	+51.2 ± 2.4
Bamberg 1				
3885	2981–84	4395 ± 25	−25.0	+50.6 ± 3.1
4456	2986–89	4394 ± 17	−24.7	+51.4 ± 2.1
4058	2991–94	4376 ± 20	−24.9	+54.4 ± 2.6
3888	3001–04	4382 ± 16	−24.7	+55.1 ± 2.1
4125	3011–14	4417 ± 20	−24.5	+51.8 ± 2.4
3901	3021–24	4423 ± 19	−24.7	+52.0 ± 2.4
4483	3026–29	4451 ± 19	−24.9	+49.2 ± 2.3

TABLE 1. (Continued)

Pta-no.	Cal BC	^{14}C age (yr BP)	$\delta^{13}C$ (‰)	$\Delta^{14}C$ (‰)
Bamberg 1 (continued)				
4119	3031–34	4511 ± 20	−24.7	+42.0 ± 2.5
4415	3036–39	4451 ± 16	−25.0	+50.3 ± 2.1
3904	3041–44	4459 ± 19	−24.9	+50.0 ± 2.4
4069	3051–54	4424 ± 22	−24.7	+55.8 ± 2.8
3968	3061–64	4414 ± 19	−24.7	+58.4 ± 2.4
4073	3071–74	4407 ± 17	−24.9	+60.7 ± 2.1
3979	3081–84	4423 ± 24	−25.1	+59.8 ± 2.9
4089	3091–94	4439 ± 19	−24.6	+58.9 ± 2.3
3991	3096–99	4480 ± 19	−24.1	+54.3 ± 2.3
Pettstadt 123				
4836	3106–09	4492 ± 20	−25.6	+53.9 ± 2.5
4933	3116–19	4494 ± 19	−26.6	+55.1 ± 2.3
4830	3126–29	4521 ± 18	−25.5	+52.5 ± 2.3
4929	3136–39	4523 ± 19	−25.5	+53.6 ± 2.3
4825	3146–49	4528 ± 18	−25.0	+54.2 ± 2.3
4891	3156–59	4506 ± 19	−24.8	+58.6 ± 2.3
4820	3166–69	4487 ± 19	−25.3	+62.3 ± 2.4
4885	3176–79	4496 ± 16	−25.1	+62.4 ± 1.9
4787	3186–89	4505 ± 20	−25.7	+62.5 ± 2.5
4870	3196–99	4544 ± 19	−26.1	+58.5 ± 2.5
Pettstadt 123 & 127				
4934	3201–04	4527 ± 19	−26.2	+61.4 ± 2.3
4680	3206–09	4514 ± 19	−25.7	+63.8 ± 2.3
4963	3211–14	4511 ± 17	−26.1	+64.9 ± 2.1
Pettstadt 123				
4866	3216–19	4476 ± 18	−25.5	+70.1 ± 2.3
Pettstadt 123 & 127				
4966	3221–24	4481 ± 11	−26.7	+70.3 ± 1.4
Pettstadt 123 & Erlach 43				
4715	3226–29	4551 ± 21	−25.9	+61.5 ± 2.6
Erlach 43				
5125	3231–34	4496 ± 17	−24.8	+69.4 ± 2.1
4859	3236–39	4489 ± 20	−25.0	+71.2 ± 2.4
5130	3241–44	4474 ± 19	−25.3	+73.6 ± 2.4
5135	3246–49	4479 ± 17	−25.0	+73.4 ± 2.1
4709	3251–54	4471 ± 20	−25.7	+75.4 ± 2.4
5147	3256–59	4449 ± 19	−25.0	+78.9 ± 2.4
4853	3261–64	4425 ± 15	−25.0	+82.9 ± 1.9
5142	3266–69	4492 ± 18	−24.8	+74.5 ± 2.3
4691	3271–74	4528 ± 20	−25.1	+70.5 ± 2.5
4810	3276–79	4498 ± 17	−24.9	+75.0 ± 2.1
4848	3281–84	4482 ± 15	−24.7	+77.7 ± 1.9
5152	3286–89	4502 ± 16	−24.9	+75.8 ± 1.9
4702	3291–94	4539 ± 20	−25.2	+71.4 ± 2.5
4958	3296–99	4467 ± 14	−25.1	+81.9 ± 1.7
4781	3301–04	4495 ± 18	−25.2	+78.8 ± 2.3
4774	3311–14	4490 ± 20	−25.1	+80.6 ± 2.4
4840	3321–24	4490 ± 19	−25.1	+81.7 ± 2.4

TABLE 1. (Continued)

Pta-no.	Cal BC	^{14}C age (yr BP)	$\delta^{13}C$ (‰)	$\Delta^{14}C$ (‰)
Erlach 43 (continued)				
4696	3331–34	4501 ± 19	−25.1	+81.7 ± 2.3
4797	3341–44	4591 ± 19	−24.6	+71.1 ± 2.3
4804	3346–49	4534 ± 20	−24.9	+79.3 ± 2.5

TABLE 2. Conventional ^{14}C ages and $\Delta^{14}C$ of decadal tree-ring samples from Stump TRL77-122 of the bristlecone pine tree-ring sequence, California, USA

Pta-no.	Cal BC	^{14}C age (yr BP)	$\delta^{13}C$ (‰)	$\Delta^{14}C$ (‰)
3410	2830–40	4172 ± 17	−20.7	61.0 ± 2.2
3812	2860–70	4198 ± 15	−20.7	61.6 ± 1.9
4216	2870–80	4210 ± 18	−20.9	61.2 ± 2.3
3826	2880–90	4232 ± 20	−20.6	59.5 ± 2.5
4295	2890–2900	4292 ± 15	−20.8	53.0 ± 1.9
3817	2900–10	4326 ± 20	−20.7	49.8 ± 2.4
4315	2910–20	4358 ± 14	−20.5	46.9 ± 1.7
3831	2920–30	4329 ± 25	−20.6	52.0 ± 3.1
4194	2930–40	4391 ± 16	−21.0	45.2 ± 2.0
4190	2940–45	4384 ± 17	−21.2	47.0 ± 2.1
3415	2940–50	4400 ± 18	−21.3	45.2 ± 2.3
4213	2950–60	4419 ± 15	−20.9	44.1 ± 1.9
3830	2960–70	4373 ± 23	−20.7	51.4 ± 2.8

TABLE 3. Comparison of the ^{14}C content of 19th-century wood grown in Norg, The Netherlands and Cape Town, South Africa

Dutch oak		Cape Town pine		
Dendroyear AD	$\Delta^{14}C$ (‰)	Dendroyear AD	$\Delta^{14}C$ (‰)	Difference (‰)
1835	2.4 ± 1.4	1835	−1.5 ± 1.7	3.9 ± 2.2
1840	−4.6 ± 1.7	1840	−9.0 ± 1.9	4.4 ± 2.6
1844–45	−2.7 ± 1.7	1845	−5.0 ± 1.9	2.3 ± 2.6
1850	−3.9 ± 1.7	1850	−7.2 ± 1.4	3.3 ± 2.2
1854–55	−1.7 ± 1.7	1855	−6.9 ± 1.3	5.2 ± 2.1
1860	−4.2 ± 1.8	1860	−9.3 ± 1.6	5.1 ± 2.4
1865	−3.8 ± 1.2	1864	−10.8 ± 1.7	7.0 ± 2.1
1870	−2.5 ± 1.5	1870	−12.7 ± 1.4	10.2 ± 2.1
1874–75	−3.9 ± 1.9	1874–75	−13.0 ± 1.4	9.1 ± 2.4
1880	−5.1 ± 1.6	1879	−10.2 ± 0.9	5.1 ± 1.8
1885	−4.4 ± 1.6	1885–86	−11.6 ± 1.8	7.2 ± 2.4
1890	−7.2 ± 1.6	1890	−11.8 ± 1.1	4.6 ± 1.9
1895	−3.9 ± 2.0	1895	−7.9 ± 1.6	4.0 ± 2.6
1900	−8.6 ± 1.3	1900	−9.1 ± 1.5	0.5 ± 2.0
			Average	5.14 ± 0.59 (41 ± 5 yr)

TABLE 4. ^{14}C analysis of the industrial effect in southern Africa

Pta-no.	Sample	Date (AD)	^{14}C age (yr BP)	$\Delta^{14}C$ (‰)
5643	Mac Mac pine	1950	198 ± 21	−24.3 ± 2.6
5635	Jonkershoek pine	1950	201 ± 19	−24.8 ± 2.3
5639	Jonkershoek pine	1953	207 ± 21	−25.4 ± 2.6
5564	Erongo Kudu horn core	1951	213 ± 11	−26.1 ± 1.4
5556	Erongo Kudu horn sheath	1951	184 ± 13	−22.6 ± 1.6
		Average	201 ± 7	−24.7 ± 0.9

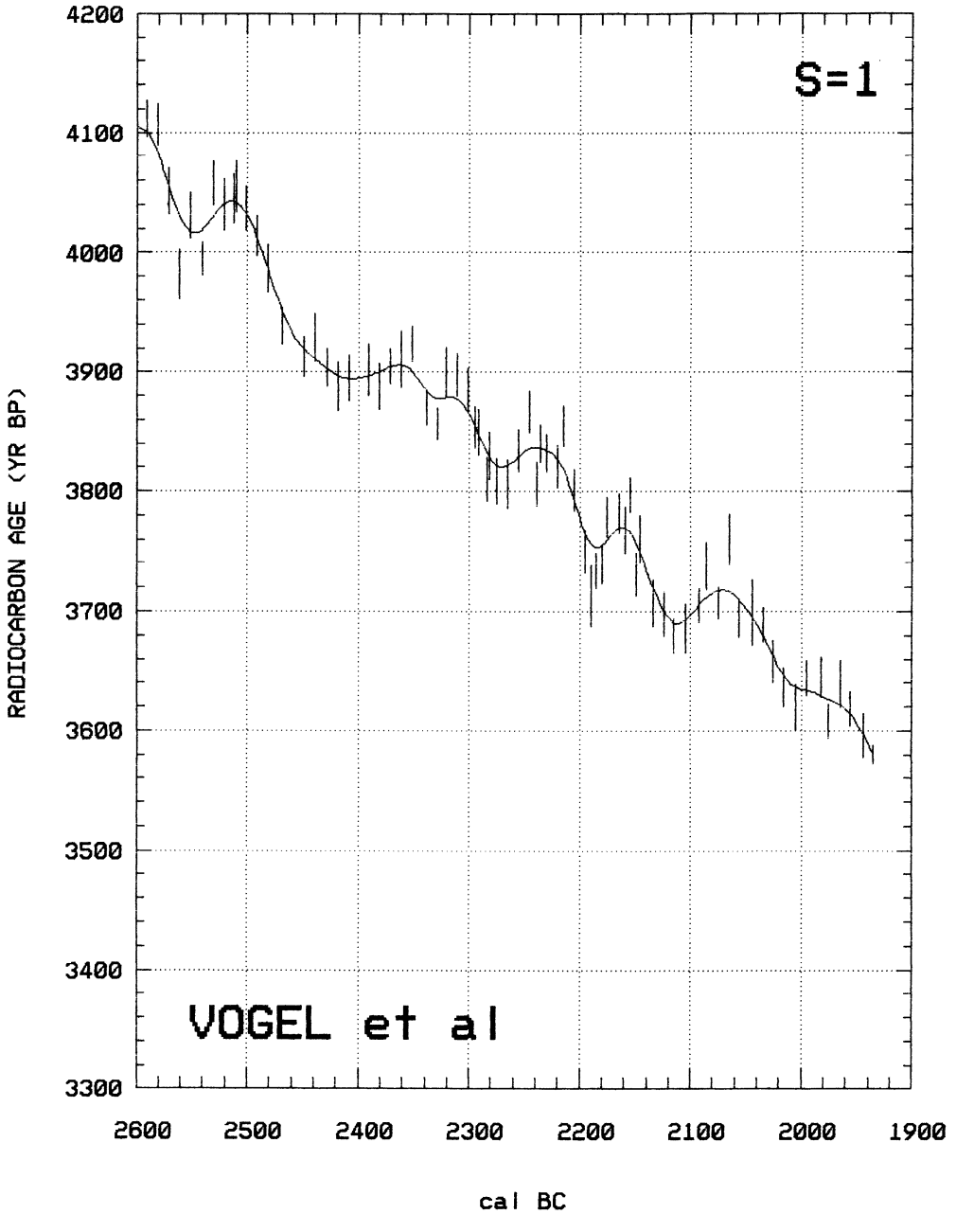

Fig. 1A–C. Pretoria radiocarbon measurements, 1930–3350 BC, with ± 1 σ error bars and a spline drawn through the points with a "tightness", S = 1

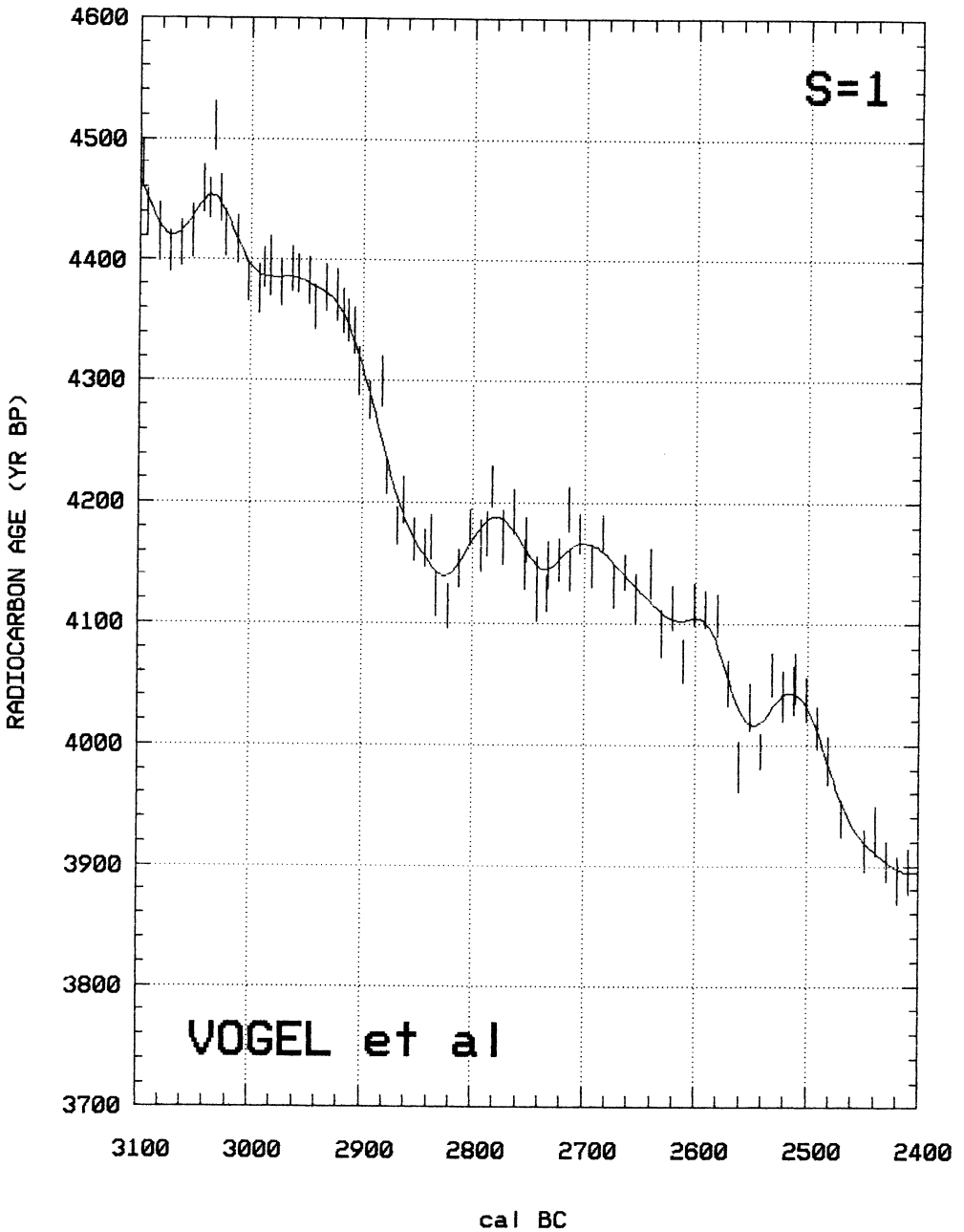
S=1
VOGEL et al
RADIOCARBON AGE (YR BP)
4600
4500
4400
4300
4200
4100
4000
3900
3800
3700
3100
3000
2900
2800
2700
2600
2500
2400
cal BC

Fig. 1B

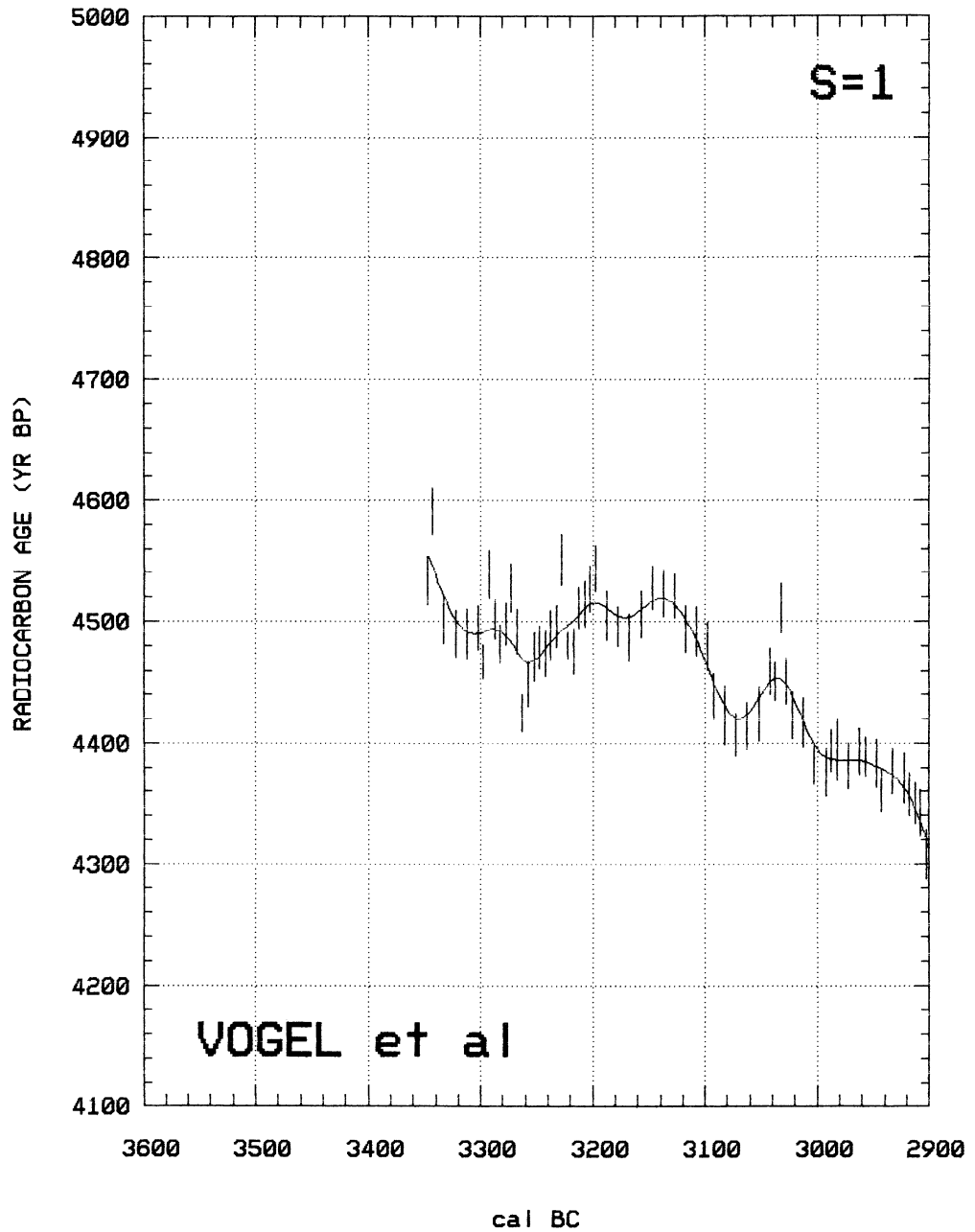
S=1
VOGEL et al
RADIOCARBON AGE (YR BP)
5000
4900
4800
4700
4600
4500
4400
4300
4200
4100
3600
3500
3400
3300
3200
3100
3000
2900
cal BC

Fig. 1C

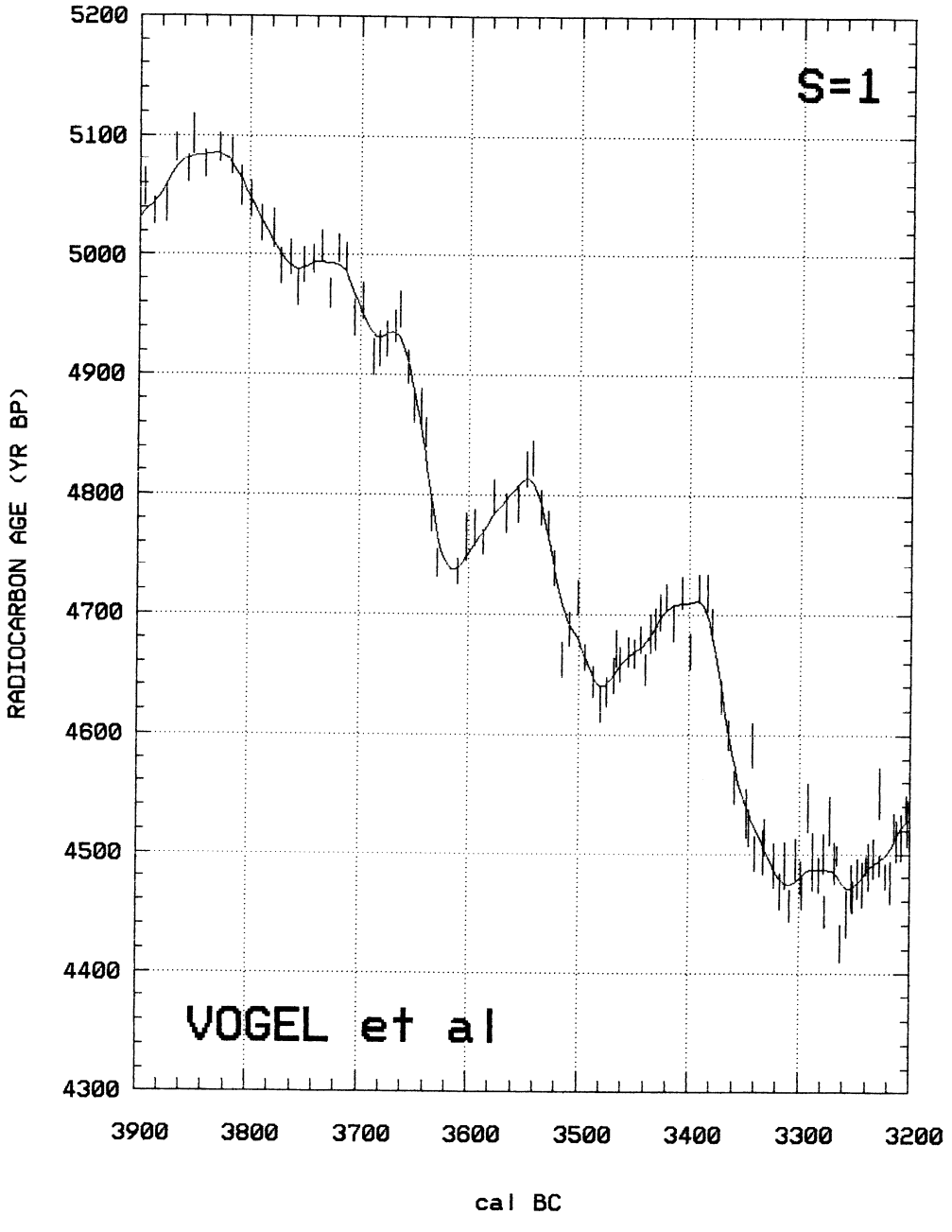

Fig. 2. Pretoria radiocarbon measurements, 3200–3350 BC, combined with those of Groningen for 3200–3900 BC. The smoothed curve through the points is the spline (S = 1) calculated for the entire data sets of Pretoria and Groningen, and differs only very slightly from that in Figure 1C for the overlap period.

[RADIOCARBON, VOL. 35, NO. 1, 1993, P. 87–91]

CALIBRATION CURVE FOR SHORT-LIVED SAMPLES, 1900–3900 BC

J. C. VOGEL

Quaternary Dating Research Unit, CSIR, P. O. Box 395, Pretoria 0001, South Africa

and

JOHANNES VAN DER PLICHT

Centre for Isotope Research, University of Groningen, Nijenborgh 4, 9747 AG Groningen, The Netherlands

Both the Pretoria and the Groningen radiocarbon laboratories performed high-precision analyses on 1–4 annual tree-ring samples made available by Bernd Becker from his South German oak dendrochronological series (Vogel *et al.* 1986; de Jong, Becker & Mook 1986). The Pretoria measurements were extended to overlap the Groningen set, and now cover the range from 1930 to 3350 BC (Vogel *et al.* 1993). The tree-ring dating of the Groningen samples has been adjusted and now ranges from 3200 to 3900 BC (de Jong, Mook & Becker 1989). Taken together, the data provide a calibration curve over two millennia, which is especially suitable for short-lived samples. The curve is shown in Figures 1A–D.

Comparison of the overlap period shows that the activity standards used in the two laboratories are nearly identical. On average, the Pretoria dates are 7.1 ± 6.4 yr older than the Groningen dates, or, if one apparent outlier is excluded, the difference reduces to 4.2 ± 6.0 yr (Vogel *et al.* 1993). Inclusion of this outlier, however, produces a better fit of the combined sets with the revised data of Stuiver and Becker (1993), so that it is not discarded. The whole set is highly compatible with the new and adjusted values of Stuiver and Becker (1993). For the range, 1900–3350 BC, the Pretoria dates average 2.9 ± 1.8 yr younger than the Seattle dates (Stuiver & Becker 1993). In addition to demonstrating compatibility, this analysis shows that little detail is sacrificed by using ten annual tree rings per sample, as was done in the Seattle laboratory.

REFERENCES

de Jong, A. F. M., Becker, B. and Mook, W. G. 1986 High-precision calibration of the radiocarbon time scale, 3930–3230 cal BC. *In* Stuiver, M. and Kra, R. S., eds., Proceedings of the 12th International ^{14}C Conference. *Radiocarbon* 28(2B): 939–941.

de Jong, A. F. M., Mook, W. G. and Becker, B. 1989 Corrected calibration of the radiocarbon time scale, 3904–3203 cal BC. *Radiocarbon* 31(2): 201–210.

Stuiver, M. and Becker, B. 1993 High-precision decadal calibration of the radiocarbon time scale, AD 1950–6000 BC. *Radiocarbon*, this issue.

Vogel, J. C., Fuls, A., Visser, E. and Becker, B. 1986 Radiocarbon fluctuations during the third millennium BC. *In* Stuiver, M. and Kra, R. S., eds., Proceedings of the 12th International ^{14}C Conference. *Radiocarbon* 28(2B): 935–938.

_____ 1993 Pretoria calibration curve for short-lived samples, 1930–3350 BC. *Radiocarbon*, this issue.

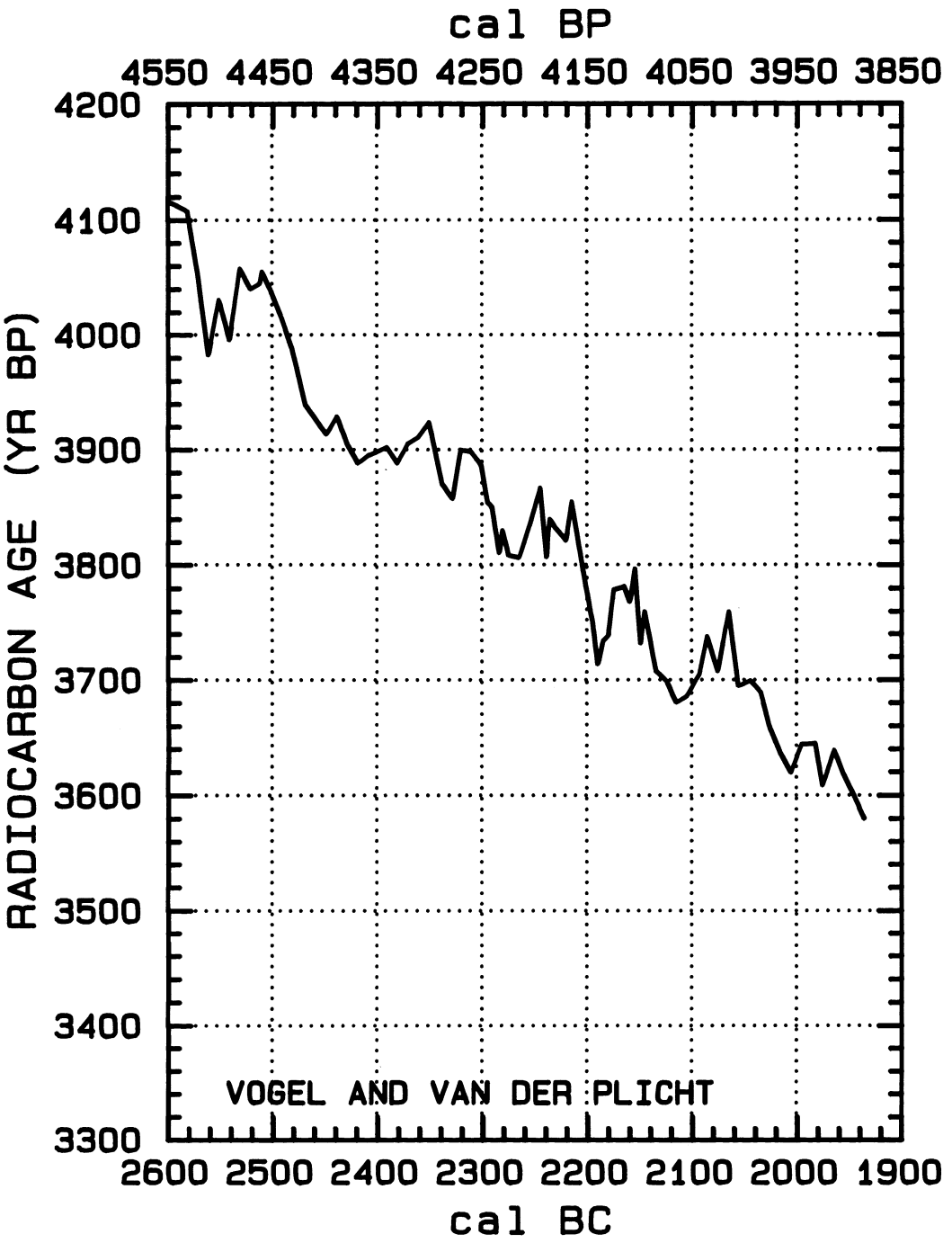

Fig. 1A–D. Combined Pretoria-Groningen calibration curve for radiocarbon dates of short-lived samples

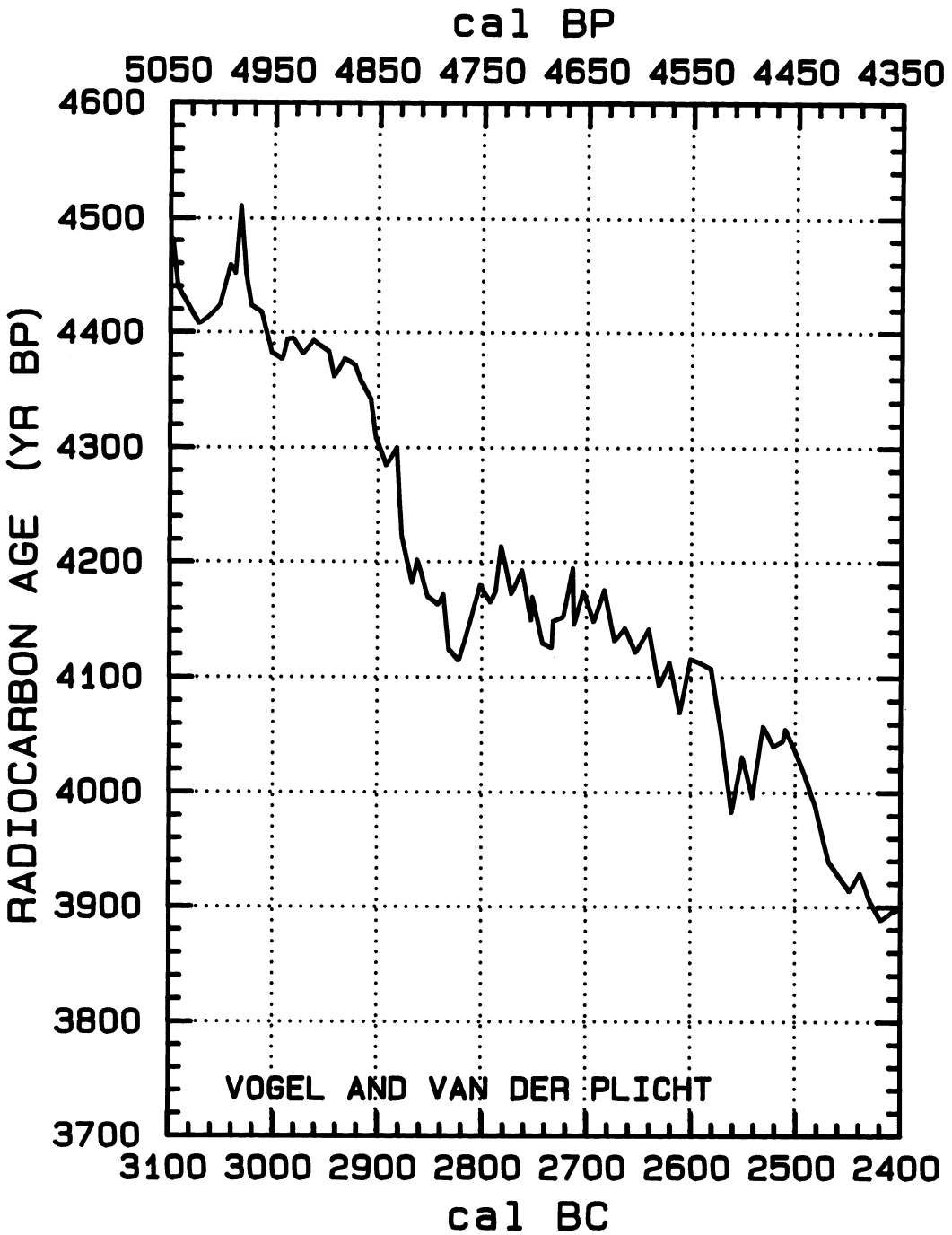
cal BP
5050 4950 4850 4750 4650 4550 4450 4350
4600
4500
4400
4300
4200
4100
4000
3900
3800
3700
RADIOCARBON AGE (YR BP)
VOGEL AND VAN DER PLICHT
3100 3000 2900 2800 2700 2600 2500 2400
cal BC

Fig. 1B

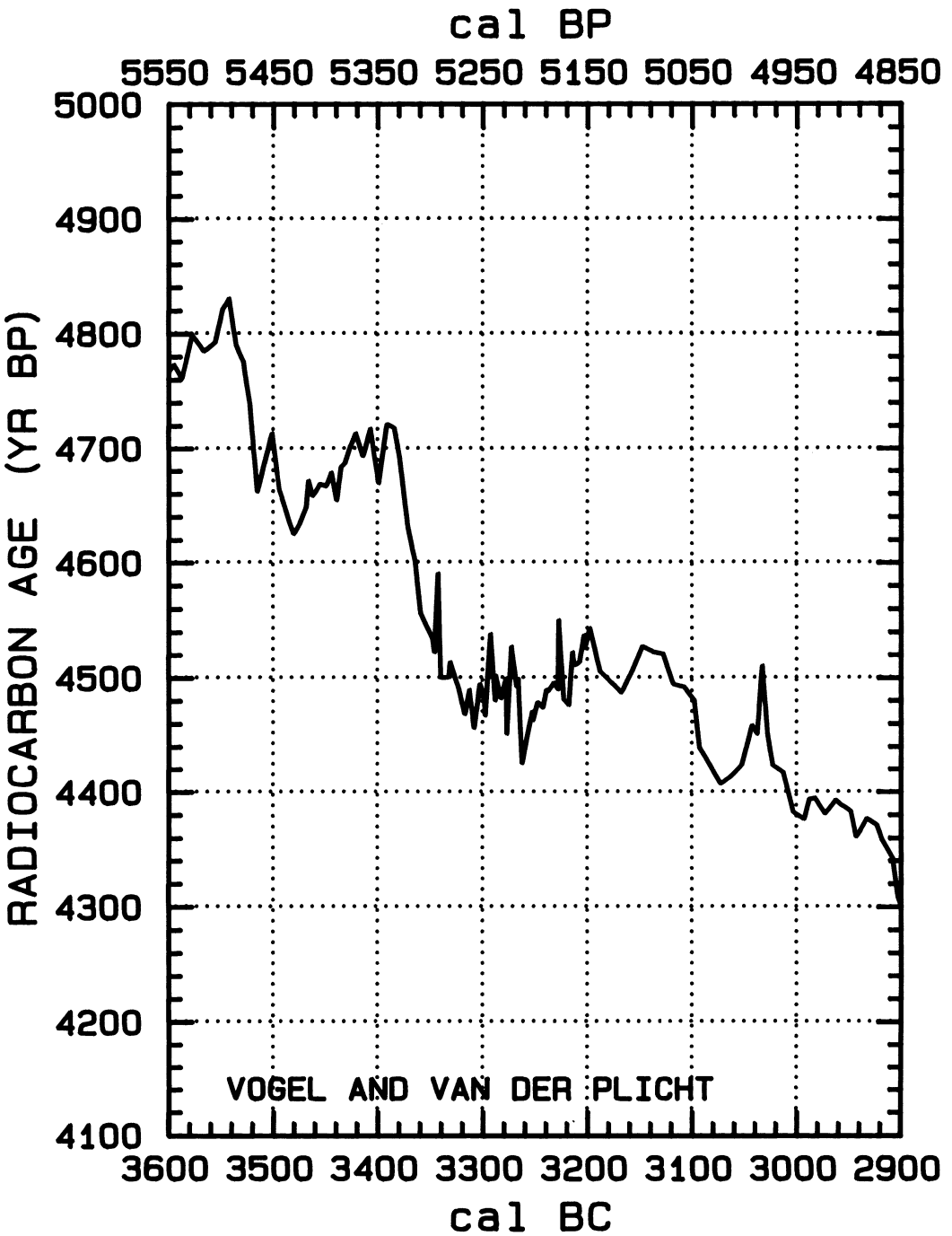
cal BP
5550 5450 5350 5250 5150 5050 4950 4850
5000
4900
4800
4700
4600
4500
4400
4300
4200
4100
RADIOCARBON AGE (YR BP)
VOGEL AND VAN DER PLICHT
3600 3500 3400 3300 3200 3100 3000 2900
cal BC

Fig. 1C

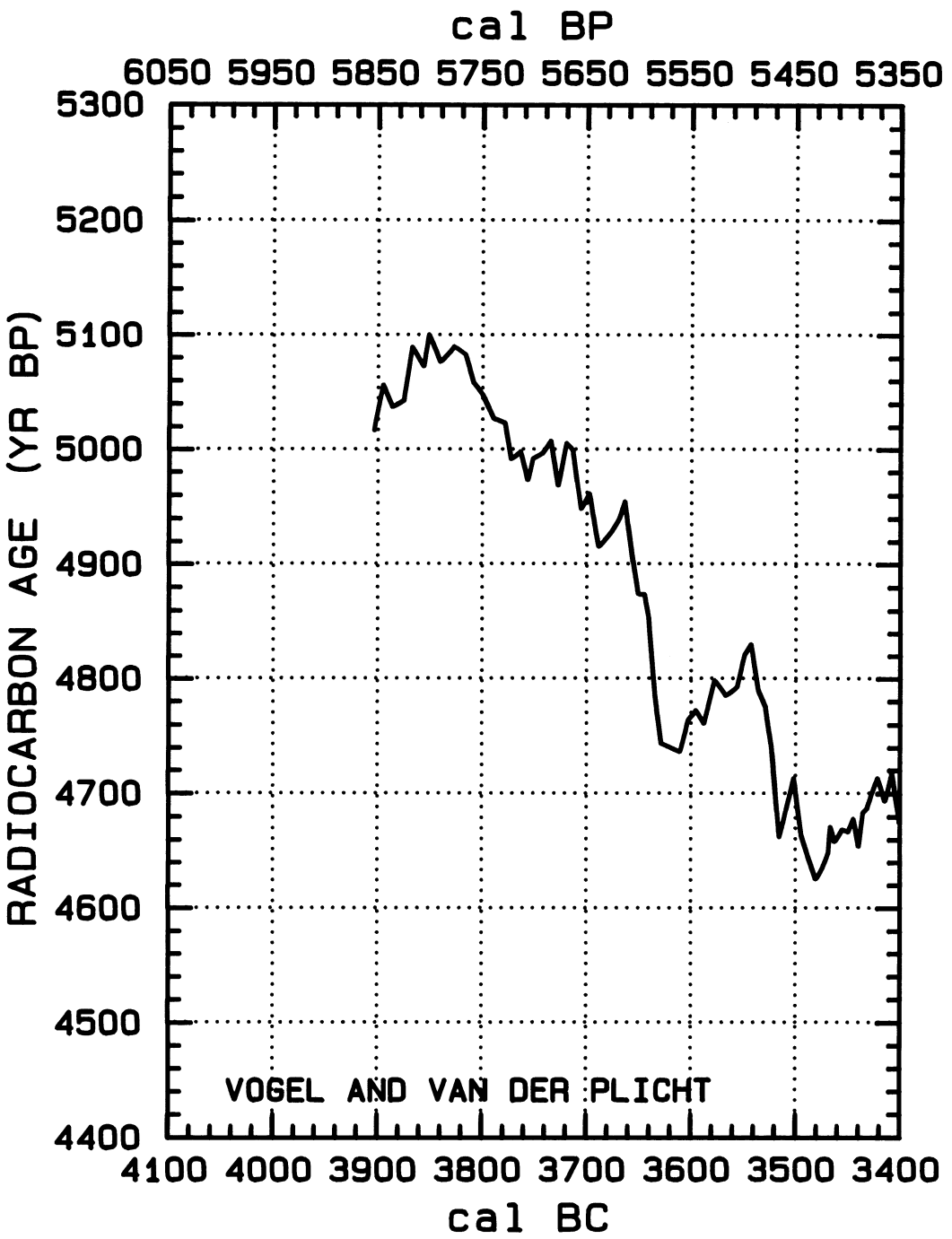
cal BP
6050 5950 5850 5750 5650 5550 5450 5350
5300
5200
5100
5000
4900
4800
4700
4600
4500
4400
RADIOCARBON AGE (YR BP)
VOGEL AND VAN DER PLICHT
4100 4000 3900 3800 3700 3600 3500 3400
cal BC

Fig. 1D

[RADIOCARBON, VOL. 35, NO. 1, 1993, P. 93–104]

HIGH-PRECISION ^{14}C MEASUREMENT OF GERMAN AND IRISH OAKS TO SHOW THE NATURAL ^{14}C VARIATIONS FROM 7890 TO 5000 BC

GORDON W. PEARSON[1], BERND BECKER[2] and FLORENCE QUA[1]

INTRODUCTION

The availability of absolutely (dendrochronologically) dated German oak has allowed the Belfast laboratory to extend its published high-precision ^{14}C measurements of Irish oak (Pearson *et al.* 1986) by 2680 yr. The samples were selected at contiguous 20-yr intervals, following a precedent adopted and considered satisfactory in previous publications. All samples were measured for at least 200,000 counts within the ^{14}C channel. The statistical counting error, together with the error on standards, backgrounds and applied corrections, give a realistic precision quoted on each sample of ± 2.5‰ (± 20 yr). This error is considered high-precision for sample ages of 7000–8000 BP.

In May 1986, the Palaeoecology Centre at The Queen's University of Belfast moved into a new, specially designed building with *ca.* 300 m^2 of laboratory space, plus an additional 75 m^2 of underground counting room (overhead shielding of 1.5 m of high-density concrete). The counting room is temperature-controlled to ± 1°C, and is isolated electrically from the main laboratory. Two LKB Wallac Quantulus counters, modified to the authors' specifications, were purchased in 1987, and were used for the high-precision ^{14}C measurements presented in this paper. Details of counter adjustments, methods of quality control and the corrections applied to the ^{14}C measurements will be discussed elsewhere; some relevant details are given below.

We performed duplicate analyses (Table 1) of six samples to confirm internal consistency. In 1986, the University of Arizona Laboratory of Isotope Geochemistry, Tucson, presented high-precision ^{14}C measurements of decadal bristlecone pine samples (Linick *et al.* 1986). Comparison of some of the Arizona measurements, covering a period of 300 yr, to the Belfast data, shows no significant bias between the mean values of the two data sets.

HIGH-PRECISION ^{14}C MEASUREMENT

The techniques used for the combustion of sample carbon and its conversion to benzene have remained essentially the same in our new laboratory, although completely new, redesigned combustion and synthesis lines have been installed. The methods are detailed in previous publications (Pearson 1979, 1980, 1983; Pearson & Baillie 1983; Pearson *et al.* 1986). The fundamental requirements for high-precision ^{14}C measurement do not change; they are to measure only pure uncontaminated sample carbon under known stable and standardized counting conditions. Many variables that had to be resolved by correction in our old laboratory, using a Phillips counter (now > 15 yr old), have been reduced to an insignificant level, using LKB Wallac 'Quantulus' counters. The efficiency of the ^{14}C counting channel is approximately the same as before (*ca.* 70%), but the background for a 15-ml benzene blank has reduced from > 9 cpm to *ca.* 1.2 cpm, using the same glass vials. This benefit has been achieved in proportion by *ca.* 2–3 cpm from the increased overhead shielding, and the remainder from the advantageous design and critical operation of the 'Quantulus' counters.

[1]Retired from Palaeoecology Centre, The Queen's University of Belfast, Belfast BT7 1NN, Northern Ireland
[2]Institute für Botanik, Universität Hohenheim, D-7000 Stuttgart 70 Germany

The ratio of modern to background count rate is *ca.* 100:1, which, together with long-term stability necessary to give constant counting conditions, now makes high-precision ^{14}C measurement very much easier than with the older system. Detailed analysis of background has shown that the backgrounds used for ^{14}C age calculations could be underestimated by *ca.* 0.10 cpm. This would make all the Belfast dates a few years older at 8000 BC, but only 1 or 2 years different for modern samples. Because this is a variable quantity, and presently not accurately quantifiable (due to contamination of lithium metal used in benzene synthesis), we have not considered it in these age calculations. We re-evaluated one correction (efficiency variation with time) used in the analysis of previously published Belfast data, which significantly changes some dates (average is *ca.* 16 yr older). The published dates presented earlier have been corrected accordingly. A full list of corrected data is also presented (Pearson & Qua 1993).

TABLE 1. Full Replicate Analyses of Calibration Samples

Cal BC*	Date measured	^{14}C age BP**	Published dates – present dates (yr)
3130	Feb/Mar 1980	4506 ± 15	−22
3130	Mar/Apr 1988	4528 ± 20	
3150	Dec 1976/Jan 1977	4553 ± 14	28
3150	Mar/Apr 1988	4525 ± 20	
3170	Feb/Mar 1980	4496 ± 18	21
3170	Mar/Apr 1988	4475 ± 16	
3190	Dec 1976/Jan 1977	4540 ± 15	18
3190	Jan/Feb 1980		
3190	Mar/Apr 1988	4522 ± 20	
3210	Dec 1976/Jan 1977	4560 ± 16	35
3210	Mar/Apr 1988	4525 ± 20	
3230	Jan/Feb 1977	4528 ± 12	2
3230	Oct/Nov 1979		
3230	Mar/Apr 1988	4526 ± 20	
			Mean difference = 13.6

*Cal BC = midpoint of bidecadal sample
**^{14}C age BP = age of bidecadal sample + 1σ

To help justify a claim to accuracy, and at the same time, help to determine a laboratory error multiplier, both replicate analysis and interlaboratory comparisons are necessary. We measured six contiguous samples to give an overall precision of ± 20 yr on each sample. They gave a mean age difference of *ca.* 13 yr, when compared to the same samples (some already duplicated) measured some 8–11 yr before (Table 1). This difference is considered reasonable, although just at the acceptable limit of statistical expectation. We compared recent replicate analysis of Irish oak samples from 5170–5090 BC to German oak, and the mean values differed by <10 yr. A comparison of German oak with previously reported Belfast data, corrected as above, suggested a significant bias between both data sets. However, taking these new measurements into account,

we now consider that both data sets are within statistical expectations. This is consistent with the fact that both the German and Irish oak chronologies are absolute.

RADIOCARBON TIME-SCALE CALIBRATION

The longest single unbroken record of high-precision ^{14}C measurements of dendrochronologically-dated wood was published in the special *RADIOCARBON* Calibration Issue (Pearson *et al.* 1986). Some 7000 yr of decadal and bidecadal measurements of Irish oak were presented graphically, and are used as a 'Radiocarbon Time-Scale Calibration'. These curves are now extended by another 2680 yr, forming a complete sequence back to 7980 BC, giving almost 10,000 yr of high-precision time-scale calibration.

At the Twelfth ^{14}C Conference (1985) in Trondheim, it was agreed that definitive calibration would be published by combining data for time periods that had been duplicated independently by different laboratories, provided they showed agreement within statistical expectation. Two papers resulted (Stuiver & Pearson 1986; Pearson & Stuiver 1986), which covered a time period of some 4500 yr between 2500 BC and the present. The mean difference between the Belfast and Seattle data sets was 0.6 yr with a standard deviation of 25.6 yr (Stuiver & Pearson 1986).

When the data set errors were multiplied by their respective error multiplier of 1.23 (Belfast) and 1.6 (Seattle), the resultant standard deviation was found to be 22.9 yr. Thus, the laboratory precision accounted for almost all variability between the data sets.

We compared data presented here with those of Linick *et al.* (1986) covering a 700-yr period. No significant consistent bias is apparent between both data sets, although the agreement is outside of statistical expectation, based on quoted errors. Thus, before these data can be combined, appropriate error multipliers must be determined to provide realistic standard deviations. We hope that this can be accomplished in the near future. The same conclusions are reached when Belfast data are compared with those of the Heidelberg Laboratory (Kromer *et al.* 1986). However, because the Heidelberg samples are not contiguous, and quite often only one annual growth ring has been measured, it is much more difficult to compare realistically both data sets. More work is needed before these data sets can be combined.

Figure 1A–F shows the natural ^{14}C variations over the time period, 7890–5000 BC. Table 2 gives individual ^{14}C ages in yr BP and Δ ^{14}C values, together with respective precisions.

CONCLUSION

We consider the measurements carried out in our new laboratory with LKB Wallac Quantulus counters as accurate as any of our previous measurements. We expect that the quoted precisions underestimate the true standard deviation, because additional errors in background have not been taken into account. We also expect that an error multiplier between 1.2 and 1.4 would be required to provide a realistic estimate of the true standard deviation. If this is so, and if it is taken that the dendrochronology is absolute, then some conclusions drawn by Linick *et al.* (1986), particularly in the suggested positions of maxima and minima, are suspect, and give cause for re-evaluation. However, because the comparison between Linick *et al.* (1986) and the Belfast data gives only a small difference in the mean values, it supports an assumption of accuracy for each laboratory's measurements, albeit with erroneous precision. Further, if the accuracy (*i.e.*, no significant bias) is assumed genuine, and if additional laboratory cross-checks on identical material (to establish meaningful error multipliers) can explain the observed larger-than-statistically-valid differences, then we must conclude that the German oak and bristlecone pine chronologies are in agreement

over this period. The agreement between Irish and German oak measurements also supports this conclusion. The six replicated analyses of identical samples in the Belfast lab showed good agreement and consistency in analysis.

There appears to be nothing unusual about this 2680-yr extension to the Radiocarbon Time Scale Calibration. Quite small calendrical band-width increases will be encountered when calibrating conventional ^{14}C ages over much of this 2600-yr extension of the ^{14}C timescale; however, a flattening of the curve between 6700 and 7000 BC presents substantial increases in the calendrical band-width of calibrated dates.

ACKNOWLEDGMENTS

G. W. Pearson and Florence Qua would like to thank all members of the ^{14}C laboratory, especially Fiona Sharpe and Stephen Hoper, who performed the routine sample analyses. Thanks are also given to the Science Based Archaeological Committee of SERC for a grant to G. W. Pearson to carry out this research.

REFERENCES

Becker, B. and Schmidt, B. 1990 Extension of the European oak chronology to the past 9224 years. *In* Mook, W. G. and Waterbolk, H. T., eds., Proceedings of the 2nd International Symposium, ^{14}C and Archaeology. *PACT* 29: 37–50.

Kromer, B., Rhein, M., Bruns, M., Schoch-Fischer, H., Münnich, K. O., Stuiver, M. and Becker, B. 1986 Radiocarbon calibration data for the 6th to the 8th millennia BC. *In* Stuiver, M. and Kra, R. S., eds., Proceedings of the 12th International ^{14}C Conference. *Radiocarbon* 28(2B): 954–960.

Linick, T. W., Long, A., Damon, P. E. and Ferguson, C. W. 1986 High-precision radiocarbon dating of bristlecone pine from 6554 to 5350 BC. *In* Stuiver, M. and Kra, R. S., eds., Proceedings of the 12th International ^{14}C Conference. *Radiocarbon* 28(2B): 943–953.

Pearson, G. W. 1979 Precise ^{14}C measurement by liquid scintillation counting. *Radiocarbon* 21(1): 1–21.

_____1980 High-precision radiocarbon dating by liquid scintillation counting applied to radiocarbon timescale calibration. *In* Stuiver, M. and Kra, R. S., eds., Proceedings of the 10th International ^{14}C Conference. *Radiocarbon* 22(2): 337–345.

_____(ms.) 1983 The development of high-precision ^{14}C measurement and its application to archaeological time-scale problems. Ph.D. dissertation, The Queen's University of Belfast.

Pearson, G. W. and Baillie, M. G. L. 1983 High-precision ^{14}C measurement of Irish oaks to show the natural atmospheric ^{14}C variations of the AD time period. *In* Stuiver, M. and Kra, R. S., eds., Proceedings of the 11th International ^{14}C Conference. *Radiocarbon* 25(2): 187–196.

Pearson, G. W., Pilcher, J. R., Baillie, M. G. L., Corbett, D. M. and Qua, F. 1986 High-precision ^{14}C measurement of Irish oaks to show the natural ^{14}C variations from AD 1840–5210 BC. *In* Stuiver, M. and Kra, R. S., eds., Proceedings of the 12th International ^{14}C Conference. *Radiocarbon* 28(2B): 911–934.

Pearson, G. W. and Qua, F. 1993 High-precision ^{14}C measurement of Irish oaks to show the natural ^{14}C variations from AD 1840–5000 BC: A correction. *Radiocarbon*, this issue.

Pearson, G. W. and Stuiver, M. 1986 High-precision calibration of the radiocarbon time scale, AD 1950–2500 BC. *In* Stuiver, M. and Kra, R. S., eds., Proceedings of the 12th International ^{14}C Conference. *Radiocarbon* 28(2B): 839–862.

Stuiver, M. and Pearson, G. W. 1986 High-precision calibration of the radiocarbon time scale, AD 1950–500 BC. *In* Stuiver, M. and Kra, R. S., eds., Proceedings of the 12th International ^{14}C Conference. *Radiocarbon* 28(2B): 805–838.

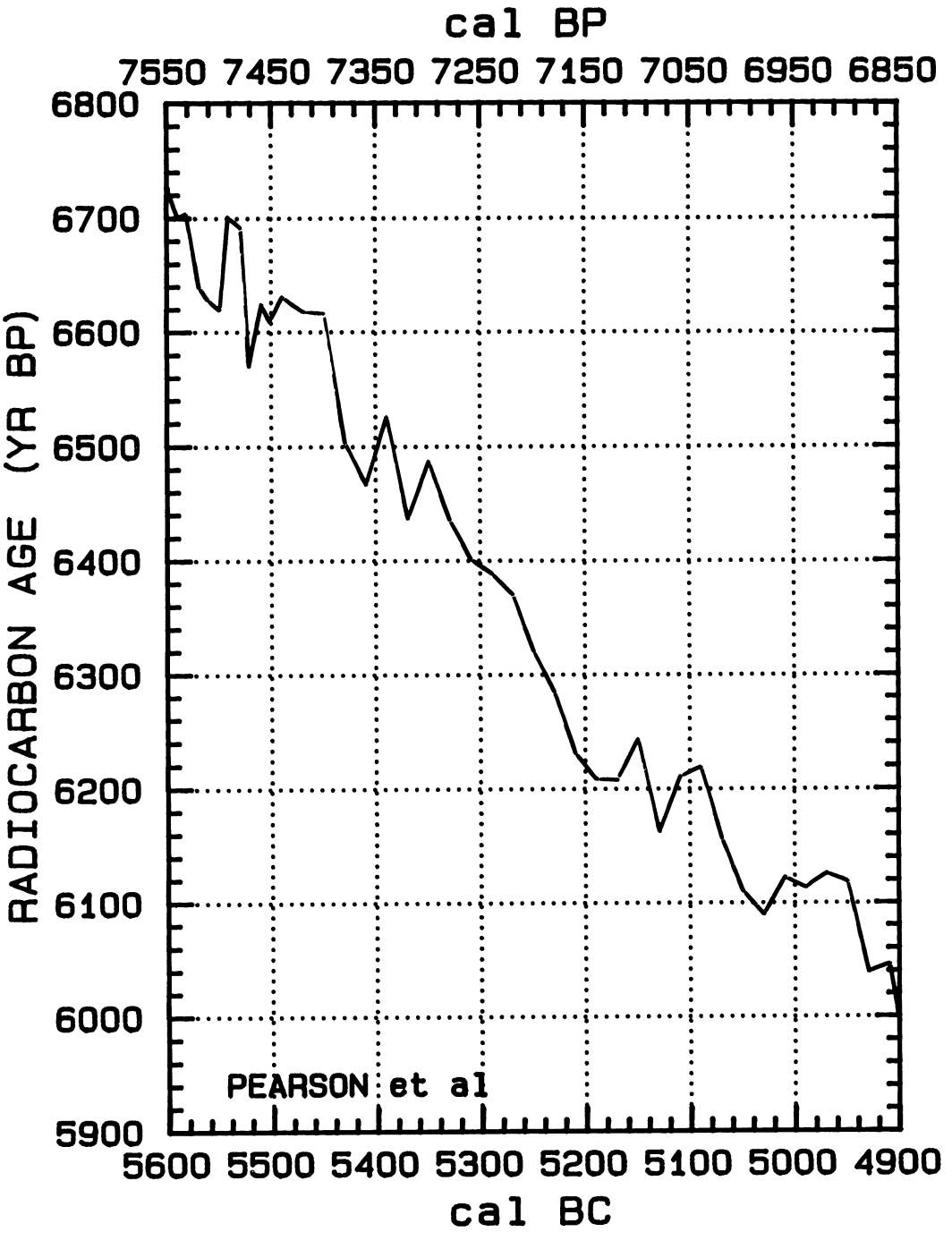

Fig. 1A–F. Calibration curve derived from bidecadal samples

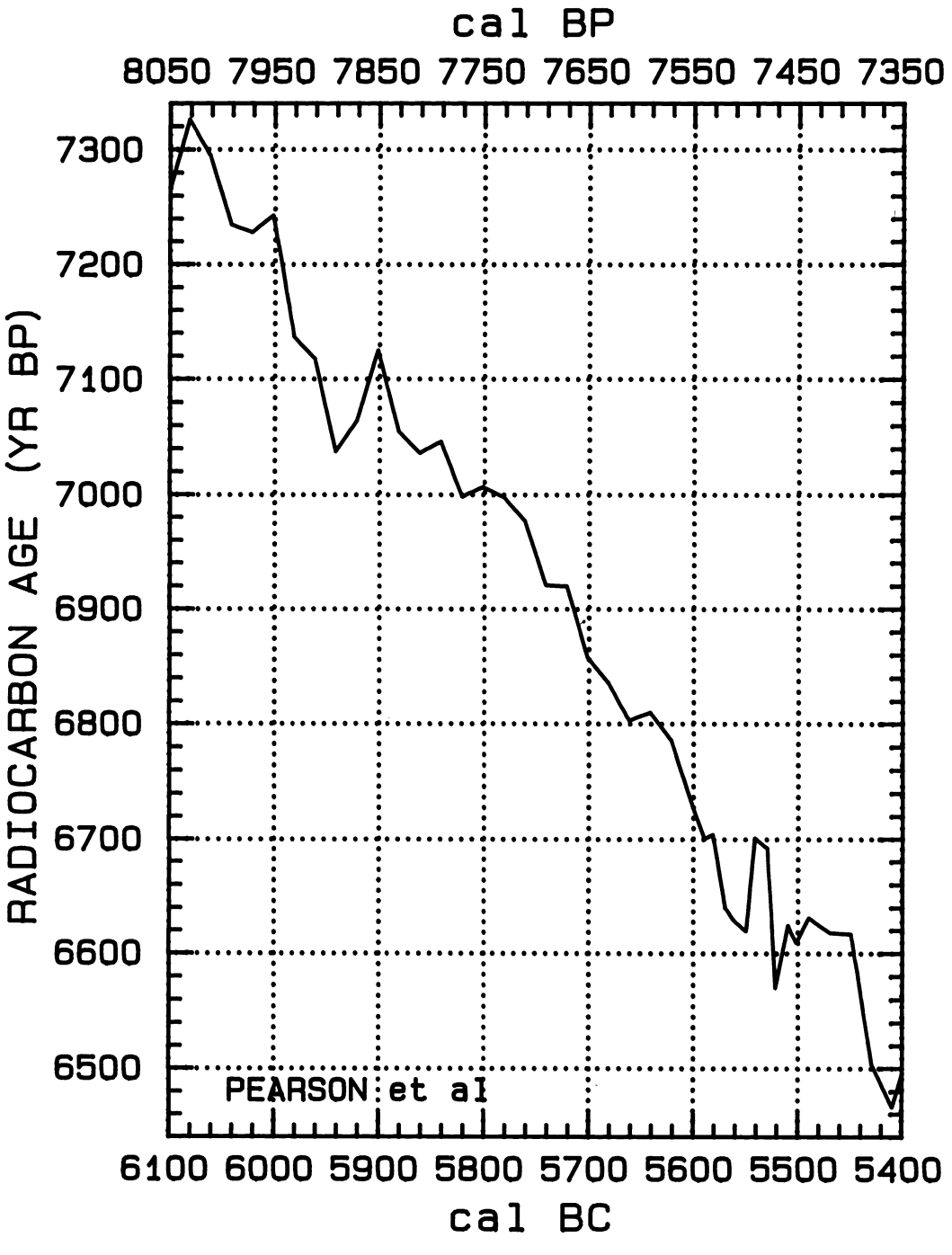
cal BP
8050 7950 7850 7750 7650 7550 7450 7350
7300
7200
7100
7000
6900
6800
6700
6600
6500
RADIOCARBON AGE (YR BP)
PEARSON et al
6100 6000 5900 5800 5700 5600 5500 5400
cal BC

Fig. 1B

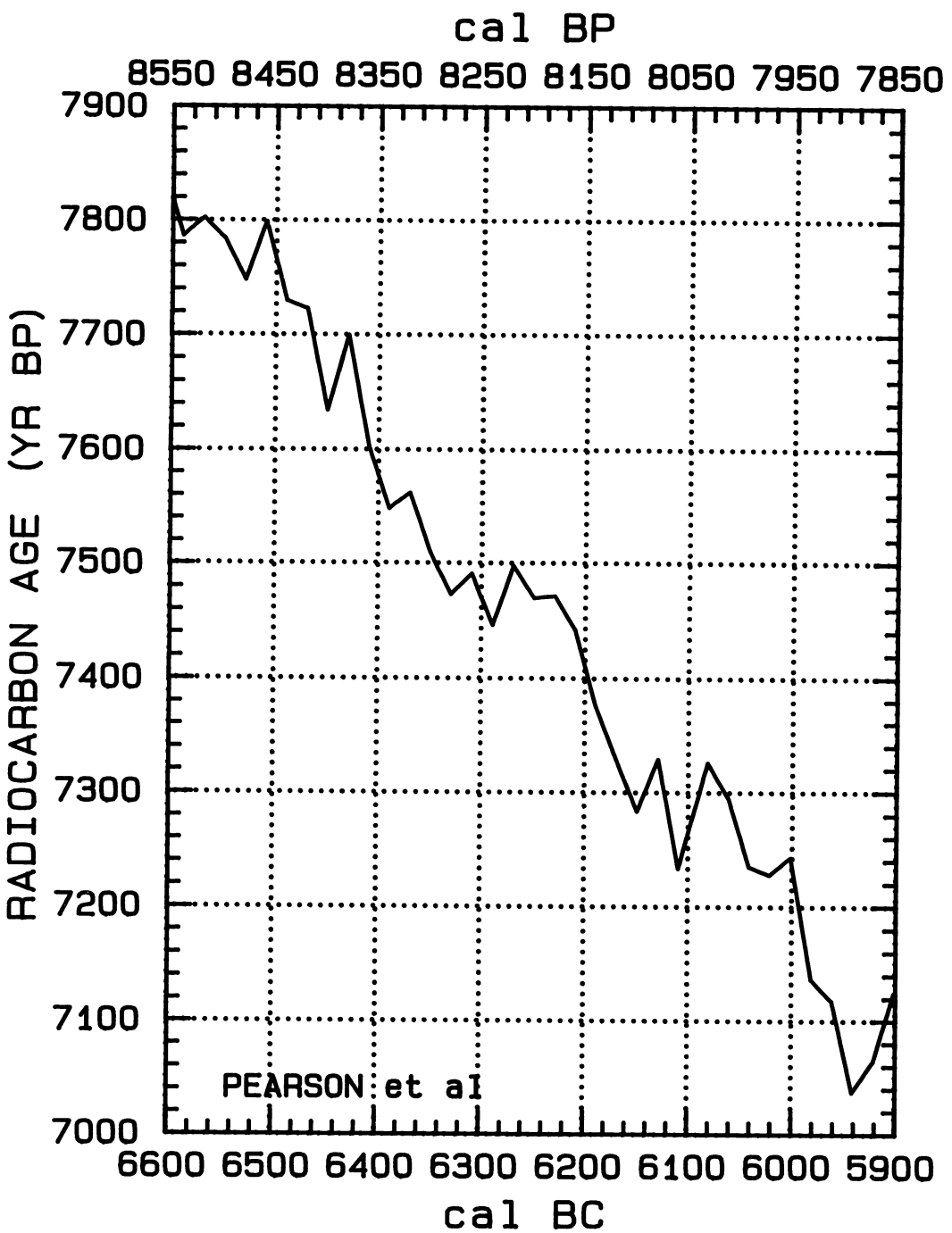
cal BP
8550 8450 8350 8250 8150 8050 7950 7850
7900
7800
7700
7600
7500
7400
7300
7200
7100
7000
RADIOCARBON AGE (YR BP)
PEARSON et al
6600 6500 6400 6300 6200 6100 6000 5900
cal BC

Fig. 1C

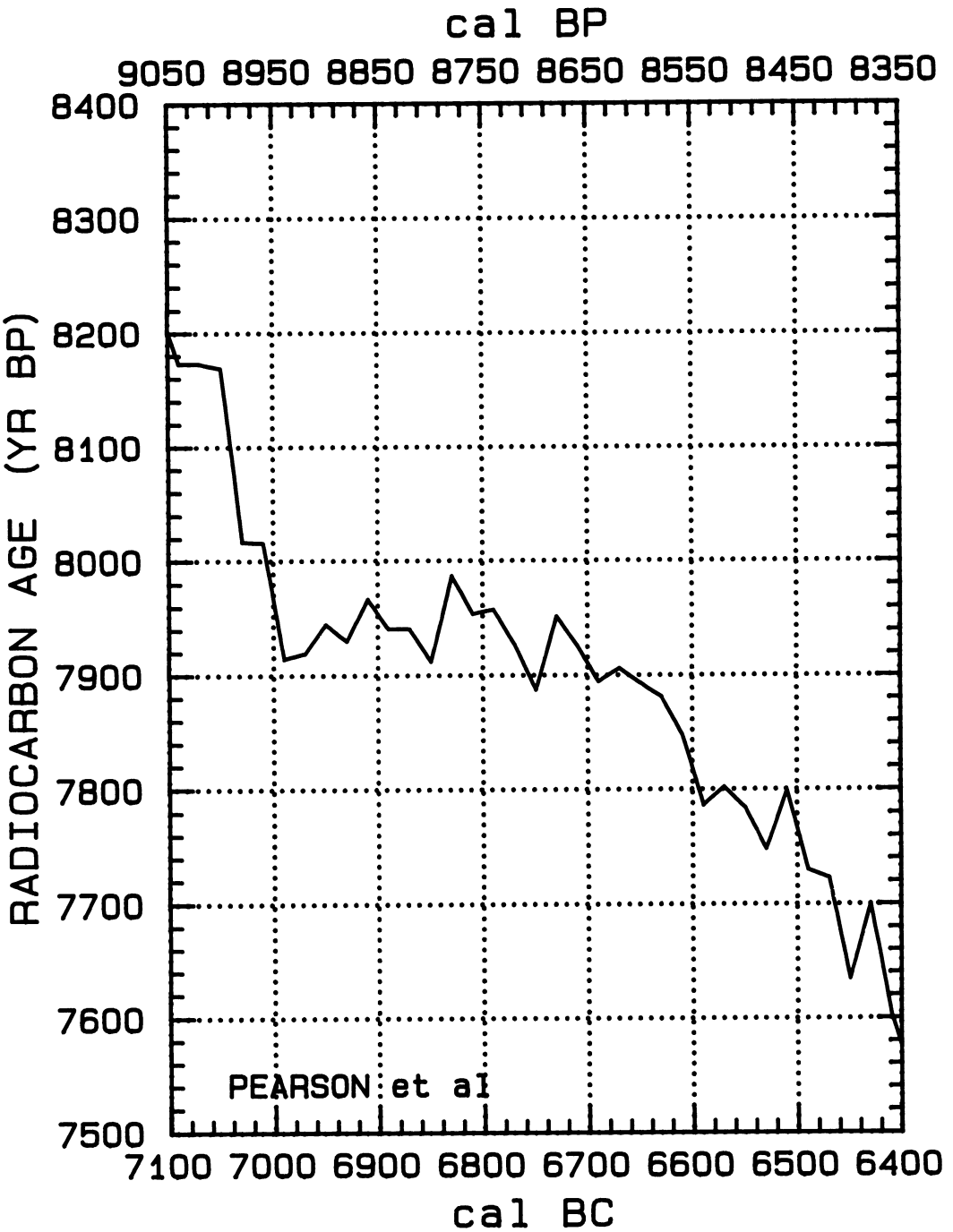
cal BP
9050 8950 8850 8750 8650 8550 8450 8350
8400
8300
8200
8100
8000
7900
7800
7700
7600
7500
RADIOCARBON AGE (YR BP)
PEARSON et al
7100 7000 6900 6800 6700 6600 6500 6400
cal BC

Fig. 1D

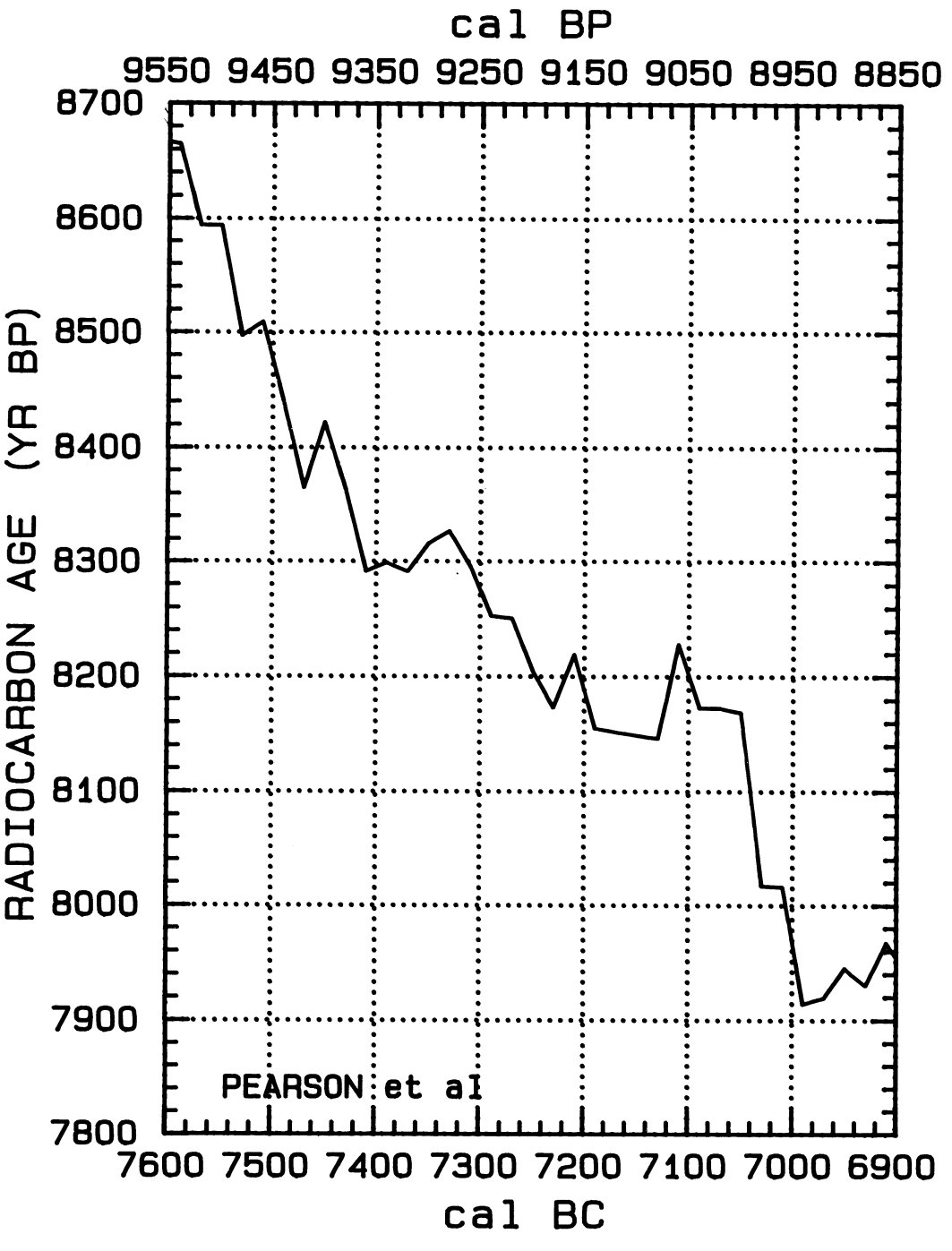
cal BP
9550 9450 9350 9250 9150 9050 8950 8850
8700
8600
8500
8400
8300
8200
8100
8000
7900
7800
RADIOCARBON AGE (YR BP)
PEARSON et al
7600 7500 7400 7300 7200 7100 7000 6900
cal BC

Fig. 1E

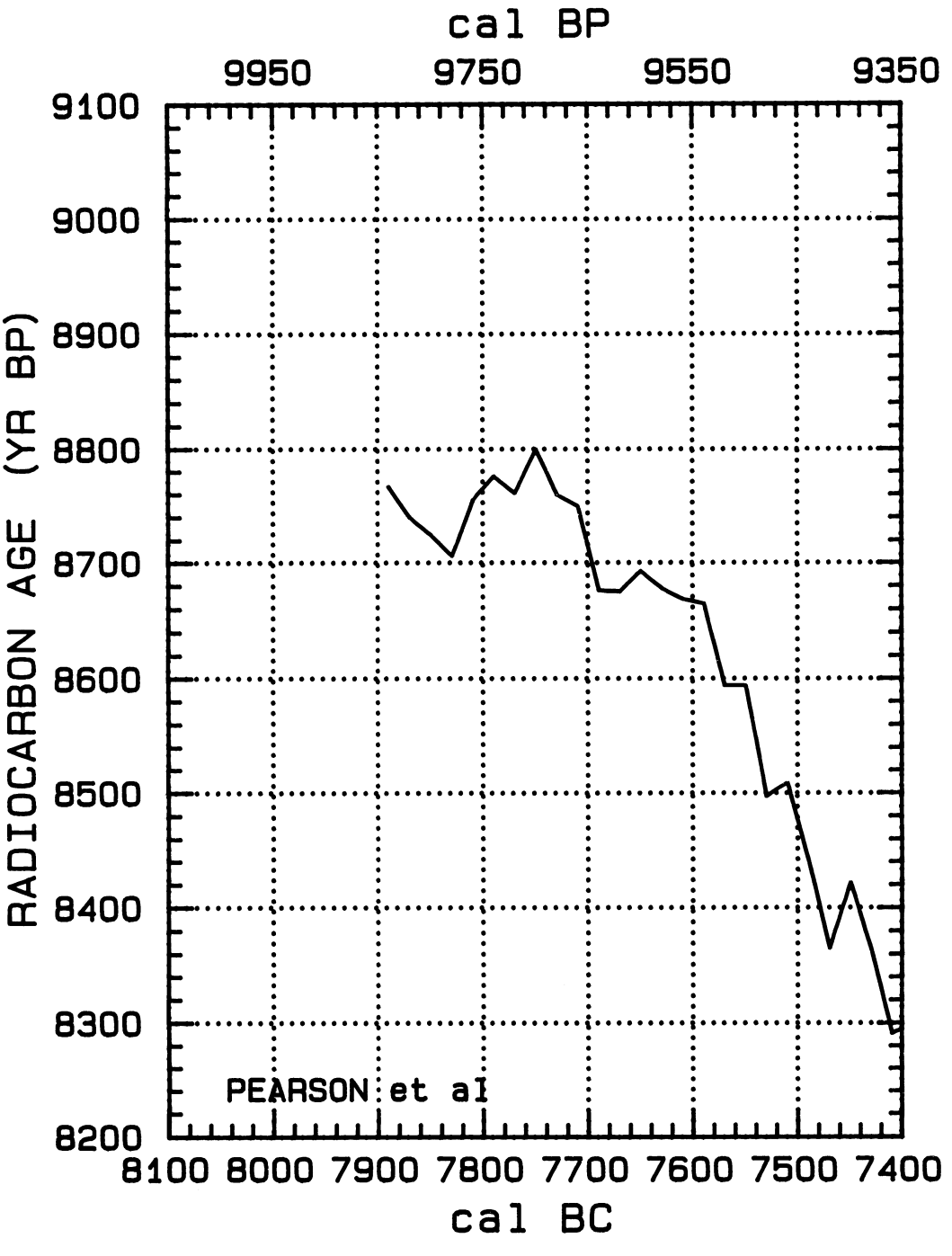
cal BP
9950
9750
9550
9350
9100
9000
8900
8800
8700
8600
8500
8400
8300
8200
RADIOCARBON AGE (YR BP)
PEARSON et al
8100 8000 7900 7800 7700 7600 7500 7400
cal BC

Fig. 1F

TABLE 2. ^{14}C Ages Over the Time Period, 7890–5000 BC

Cal AD/BC	$\Delta^{14}C$ ‰	^{14}C age (BP)	Cal BP	Cal AD/BC	$\Delta^{14}C$ ‰	^{14}C age (BP)	Cal BP
5010 BC	83.1 ± 2.2	6122 ± 16	BP 6960	5842 BC	67.6 ± 2.4	7046 ± 18	BP 7792
5030 BC	90.2 ± 2.5	6089 ± 18	BP 6980	5862 BC	71.5 ± 2.4	7036 ± 18	BP 7812
5050 BC	89.9 ± 2.4	6110 ± 17	BP 7000	5882 BC	71.6 ± 2.4	7055 ± 18	BP 7832
5070 BC	86.2 ± 1.7	6157 ± 13	BP 7020	5902 BC	64.9 ± 2.4	7125 ± 18	BP 7852
5090 BC	80.5 ± 1.5	6219 ± 11	BP 7040	5922 BC	75.6 ± 2.5	7064 ± 18	BP 7872
5110 BC	84.3 ± 1.5	6210 ± 11	BP 7060	5942 BC	81.8 ± 2.5	7037 ± 18	BP 7892
5130 BC	93.4 ± 1.5	6162 ± 11	BP 7080	5962 BC	73.5 ± 2.5	7118 ± 18	BP 7912
5150 BC	85.1 ± 1.5	6243 ± 11	BP 7100	5982 BC	73.6 ± 2.6	7137 ± 19	BP 7932
5170 BC	92.6 ± 1.5	6207 ± 11	BP 7120	6002 BC	62.1 ± 2.6	7243 ± 19	BP 7952
5190 BC	95.1 ± 2.2	6208 ± 16	BP 7140	6022 BC	66.7 ± 2.6	7228 ± 19	BP 7972
5210 BC	94.6 ± 2.2	6231 ± 16	BP 7160	6042 BC	68.3 ± 2.6	7235 ± 19	BP 7992
5230 BC	89.9 ± 2.2	6285 ± 16	BP 7180	6062 BC	62.9 ± 2.6	7295 ± 19	BP 8012
5250 BC	87.7 ± 2.2	6321 ± 16	BP 7200	6082 BC	61.4 ± 2.6	7326 ± 19	BP 8032
5270 BC	83.6 ± 2.2	6371 ± 16	BP 7220	6102 BC	72.7 ± 2.6	7260 ± 19	BP 8052
5290 BC	83.7 ± 2.2	6389 ± 16	BP 7240	6110 BC	77.4 ± 2.6	7233 ± 19	BP 8060
5310 BC	84.6 ± 2.2	6402 ± 16	BP 7260	6130 BC	67.2 ± 2.6	7329 ± 19	BP 8080
5330 BC	82.7 ± 2.2	6436 ± 16	BP 7280	6150 BC	75.9 ± 2.6	7283 ± 19	BP 8100
5350 BC	78.4 ± 2.2	6487 ± 16	BP 7300	6170 BC	72.5 ± 2.3	7328 ± 17	BP 8120
5370 BC	87.9 ± 2.2	6436 ± 16	BP 7320	6190 BC	68.8 ± 2.3	7375 ± 17	BP 8140
5390 BC	78.4 ± 2.2	6526 ± 16	BP 7340	6210 BC	62.5 ± 2.3	7442 ± 17	BP 8160
5410 BC	89.1 ± 2.2	6466 ± 16	BP 7360	6230 BC	61.1 ± 2.3	7472 ± 17	BP 8180
5430 BC	86.6 ± 2.2	6504 ± 16	BP 7380	6250 BC	63.9 ± 2.3	7470 ± 17	BP 8200
5450 BC	74.0 ± 2.2	6617 ± 16	BP 7400	6270 BC	62.8 ± 2.4	7498 ± 18	BP 8220
5470 BC	76.5 ± 2.2	6618 ± 16	BP 7420	6290 BC	72.3 ± 2.4	7446 ± 18	BP 8240
5490 BC	77.3 ± 2.2	6631 ± 16	BP 7440	6310 BC	68.9 ± 2.4	7491 ± 18	BP 8260
5502 BC	81.9 ± 2.5	6609 ± 18	BP 7452	6330 BC	73.9 ± 2.4	7473 ± 18	BP 8280
5510 BC	80.9 ± 2.2	6624 ± 16	BP 7460	6350 BC	71.7 ± 2.4	7509 ± 18	BP 8300
5522 BC	89.8 ± 2.5	6570 ± 18	BP 7472	6370 BC	67.2 ± 2.4	7562 ± 18	BP 8320
5530 BC	74.4 ± 2.2	6692 ± 16	BP 7480	6390 BC	71.7 ± 2.4	7548 ± 18	BP 8340
5542 BC	74.7 ± 2.4	6701 ± 18	BP 7492	6410 BC	66.9 ± 2.4	7603 ± 18	BP 8360
5550 BC	86.8 ± 2.2	6619 ± 16	BP 7500	6430 BC	56.7 ± 2.4	7700 ± 18	BP 8380
5562 BC	87.0 ± 3.4	6629 ± 25	BP 7512	6450 BC	68.0 ± 2.8	7634 ± 21	BP 8400
5570 BC	86.6 ± 2.2	6640 ± 16	BP 7520	6470 BC	58.8 ± 2.4	7723 ± 18	BP 8420
5582 BC	79.5 ± 2.5	6704 ± 18	BP 7532	6490 BC	60.4 ± 2.4	7730 ± 18	BP 8440
5590 BC	81.1 ± 2.2	6700 ± 16	BP 7540	6510 BC	53.9 ± 2.4	7799 ± 18	BP 8460
5602 BC	78.5 ± 2.5	6731 ± 18	BP 7552	6530 BC	63.2 ± 2.7	7748 ± 18	BP 8480
5622 BC	73.8 ± 2.4	6786 ± 18	BP 7572	6550 BC	61.0 ± 2.7	7784 ± 19	BP 8500
5642 BC	73.1 ± 2.4	6810 ± 18	BP 7592	6570 BC	61.2 ± 2.7	7802 ± 19	BP 8520
5662 BC	76.7 ± 2.5	6803 ± 18	BP 7612	6590 BC	65.8 ± 2.7	7786 ± 20	BP 8540
5682 BC	74.9 ± 2.4	6836 ± 18	BP 7632	6610 BC	60.2 ± 2.6	7848 ± 19	BP 8560
5702 BC	74.5 ± 2.4	6858 ± 18	BP 7652	6630 BC	58.4 ± 2.6	7881 ± 19	BP 8580
5722 BC	68.8 ± 2.4	6920 ± 18	BP 7672	6650 BC	59.4 ± 2.2	7893 ± 16	BP 8600
5742 BC	71.3 ± 2.4	6921 ± 18	BP 7692	6670 BC	60.3 ± 2.2	7906 ± 16	BP 8620
5762 BC	66.4 ± 2.4	6977 ± 18	BP 7712	6690 BC	64.4 ± 2.2	7894 ± 16	BP 8640
5782 BC	66.2 ± 2.4	6998 ± 18	BP 7732	6710 BC	62.7 ± 2.2	7926 ± 16	BP 8660
5802 BC	67.6 ± 2.4	7007 ± 18	BP 7752	6730 BC	61.9 ± 2.2	7952 ± 16	BP 8680
5822 BC	71.4 ± 2.4	6998 ± 18	BP 7772	6750 BC	73.1 ± 2.6	7887 ± 19	BP 8700

TABLE 2. (Continued)

Cal AD/BC	$\Delta^{14}C$ ‰	^{14}C age (BP)	Cal BP	Cal AD/BC	$\Delta^{14}C$ ‰	^{14}C age (BP)	Cal BP
6770 BC	70.4 ± 2.6	7927 ± 19	BP 8720	7370 BC	99.9 ± 2.5	8291 ± 18	BP 9320
6790 BC	68.8 ± 2.6	7958 ± 19	BP 8740	7390 BC	101.5 ± 2.8	8299 ± 20	BP 9340
6810 BC	71.9 ± 2.6	7954 ± 19	BP 8760	7410 BC	105.3 ± 2.4	8291 ± 17	BP 9360
6830 BC	70.1 ± 2.6	7987 ± 19	BP 8780	7430 BC	97.9 ± 2.4	8364 ± 17	BP 9380
6850 BC	82.8 ± 1.7	7912 ± 12	BP 8800	7450 BC	92.7 ± 2.4	8422 ± 17	BP 9400
6870 BC	81.5 ± 2.7	7941 ± 20	BP 8820	7470 BC	103.1 ± 2.4	8365 ± 17	BP 9420
6890 BC	84.1 ± 2.7	7941 ± 20	BP 8840	7490 BC	95.4 ± 2.4	8441 ± 17	BP 9440
6910 BC	83.2 ± 2.7	7967 ± 20	BP 8860	7510 BC	88.8 ± 2.5	8509 ± 18	BP 9460
6930 BC	90.9 ± 2.8	7930 ± 20	BP 8880	7530 BC	93.0 ± 2.5	8497 ± 18	BP 9480
6950 BC	91.5 ± 2.8	7945 ± 20	BP 8900	7550 BC	82.5 ± 3.4	8594 ± 25	BP 9500
6970 BC	97.7 ± 2.8	7919 ± 20	BP 8920	7570 BC	85.2 ± 2.5	8594 ± 18	BP 9520
6990 BC	101.0 ± 2.8	7914 ± 20	BP 8940	7590 BC	78.2 ± 2.5	8665 ± 18	BP 9540
7010 BC	89.7 ± 2.8	8016 ± 20	BP 8960	7610 BC	80.3 ± 2.5	8669 ± 18	BP 9560
7030 BC	92.2 ± 2.8	8017 ± 20	BP 8980	7630 BC	81.7 ± 2.5	8678 ± 18	BP 9580
7050 BC	74.4 ± 1.7	8169 ± 12	BP 9000	7650 BC	82.3 ± 2.5	8693 ± 18	BP 9600
7070 BC	76.4 ± 2.0	8173 ± 15	BP 9020	7670 BC	87.3 ± 2.5	8675 ± 18	BP 9620
7090 BC	79.0 ± 2.1	8173 ± 15	BP 9040	7690 BC	89.9 ± 2.5	8676 ± 18	BP 9640
7110 BC	74.3 ± 2.0	8228 ± 15	BP 9060	7710 BC	82.5 ± 2.7	8750 ± 20	BP 9660
7130 BC	87.9 ± 2.6	8146 ± 19	BP 9080	7730 BC	83.7 ± 2.7	8760 ± 20	BP 9680
7190 BC	94.6 ± 2.6	8155 ± 19	BP 9140	7750 BC	81.0 ± 2.7	8800 ± 20	BP 9700
7210 BC	88.6 ± 2.6	8219 ± 19	BP 9160	7770 BC	88.9 ± 2.8	8761 ± 20	BP 9720
7230 BC	97.5 ± 2.6	8173 ± 19	BP 9180	7790 BC	89.5 ± 2.8	8776 ± 20	BP 9740
7250 BC	95.8 ± 2.5	8205 ± 18	BP 9200	7810 BC	95.0 ± 2.5	8755 ± 18	BP 9760
7270 BC	92.1 ± 2.5	8251 ± 18	BP 9220	7830 BC	104.3 ± 2.5	8706 ± 18	BP 9780
7290 BC	94.5 ± 2.4	8253 ± 17	BP 9240	7850 BC	104.4 ± 2.5	8725 ± 18	BP 9800
7310 BC	91.3 ± 2.5	8296 ± 18	BP 9260	7870 BC	105.0 ± 2.5	8740 ± 18	BP 9820
7330 BC	89.7 ± 2.8	8327 ± 20	BP 9280	7890 BC	104.0 ± 2.5	8767 ± 18	BP 9840
7350 BC	93.9 ± 2.8	8316 ± 20	BP 9300				

[RADIOCARBON, VOL. 35, NO. 1, 1993, P. 105–123]

HIGH-PRECISION ^{14}C MEASUREMENT OF IRISH OAKS TO SHOW THE NATURAL ^{14}C VARIATIONS FROM AD 1840–5000 BC: A CORRECTION

GORDON W. PEARSON and FLORENCE QUA

Retired from Paleoecology Centre, The Queen's University of Belfast, Belfast BT71NN, Northern Ireland

We present here ^{14}C data representing previously published material (Pearson *et al.* 1986) with minor corrections. All corrections used for calculations published in Pearson *et al.* (1986) have been re-evaluated, and only one was found to be significantly different. This correction, namely, 'the variation of efficiency with time', being additional to all other corrections for changes in efficiency, was more subjective; the others could be checked and accounted for by experimentation.

The initial correction derived from standards measured between 1981 and 1986, and involved relatively few measurements. Two standards gave a much more pronounced variation than the others, which, taken alone, suggested very little variation. These two standards accounted for practically all the evaluated correction. Subsequent standard analysis, including work on the more sensitive Quantulus counter, supported the hypothesis that this correction was probably unnecessary. The efficiency correction was recalculated, omitting the two suspect standards and using more recent information; this correction was found to be insignificant. Thus, it was removed, and the dates were recalculated. Shifts averaging 16 yr older were obtained for the samples reported in 1986.

It is impossible to account for the losses observed in the two standards omitted, but it is probable that scintillant leakage occurred through the tin foil used for vial sealing. This was not detected as a weight loss, since scintillant was absorbed in other vial cap components. No such change has been observed since the vial caps were sealed with indium foil. It is also possible that samples measured with a tin foil seal were subject to a similar loss, possibly giving an error of up to 20 yr. It cannot be determined if, or to what samples, this happened.

Other basic information previously given is still applicable. The corrected data set (Table 1) is plotted as a ^{14}C age calibration curve in Figure 1A–N.

REFERENCE

Pearson, G. W., Pilcher, J. R., Baillie, M. G. L., Corbett, D. M. and Qua, F. 1986 High precision ^{14}C measurement of Irish oaks to show the natural ^{14}C variations from AD 1840–5210 BC. *In* Stuiver, M. and Kra, R. S., eds., Proceedings of the 12th International ^{14}C Conference. *Radiocarbon* 28(2B): 911–934.

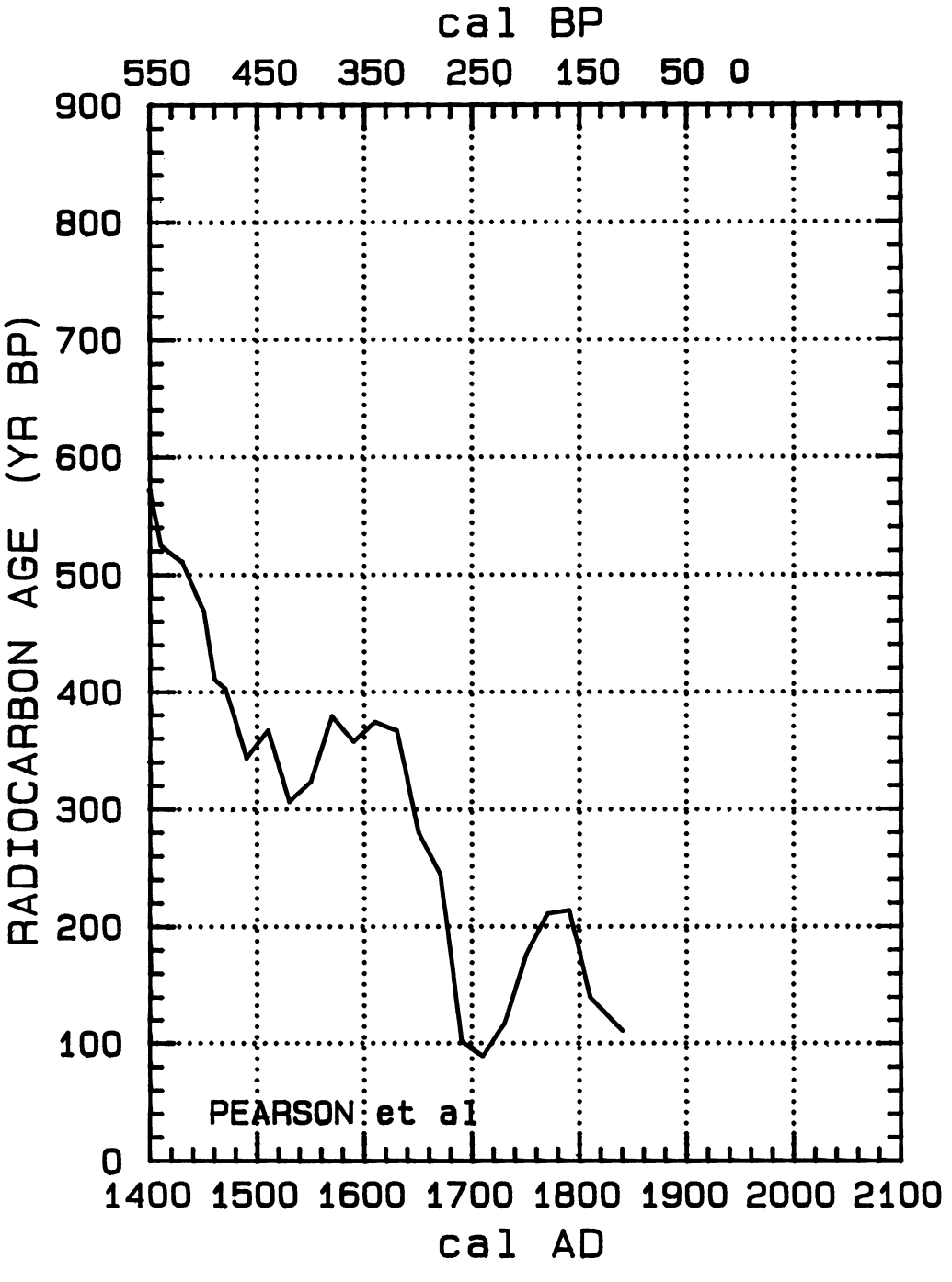

Fig. 1A–N. Calibration curve derived from bidecadal samples

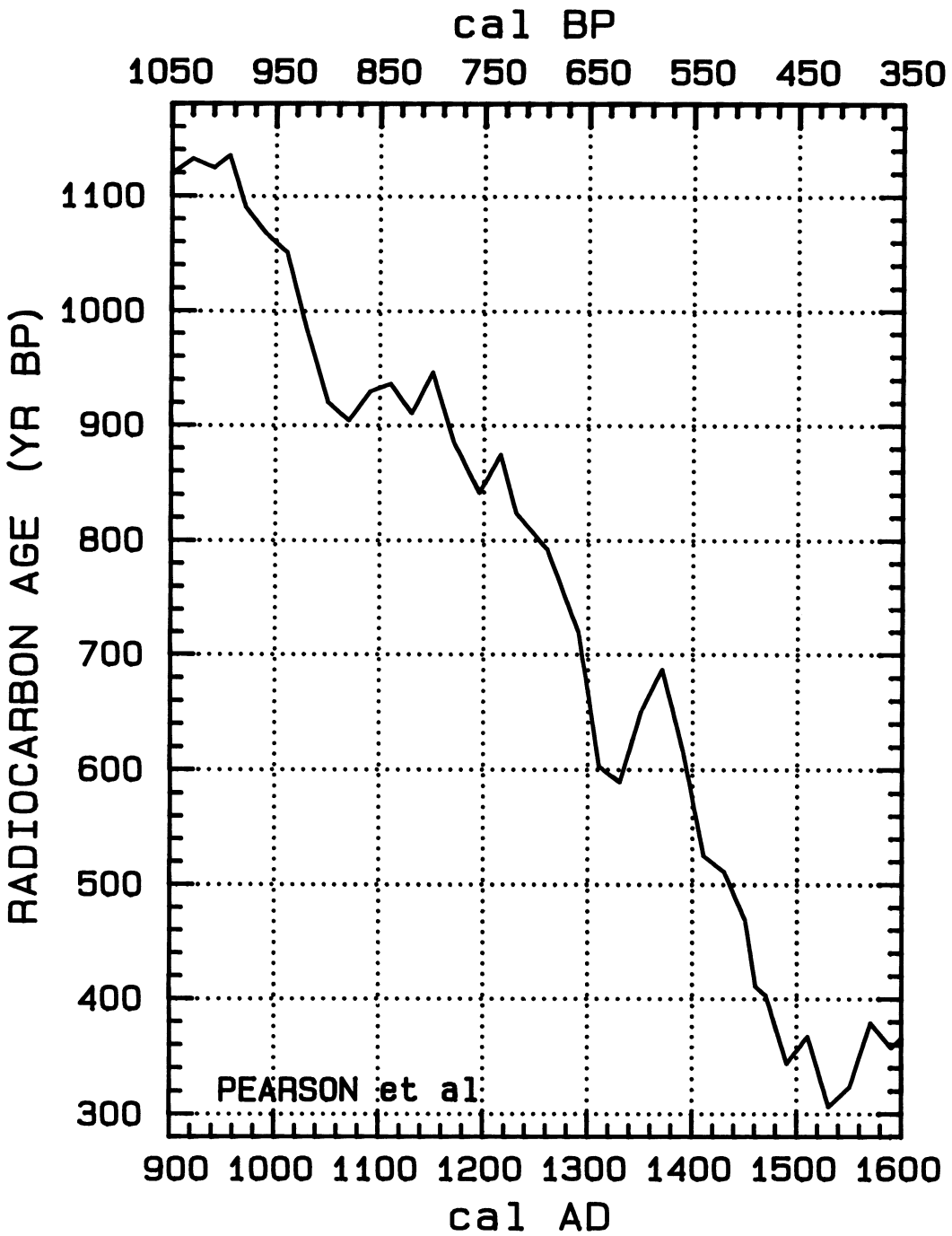
cal BP
1050 950 850 750 650 550 450 350
1100
1000
900
800
700
600
500
400
300
RADIOCARBON AGE (YR BP)
PEARSON et al
900 1000 1100 1200 1300 1400 1500 1600
cal AD

Fig. 1B

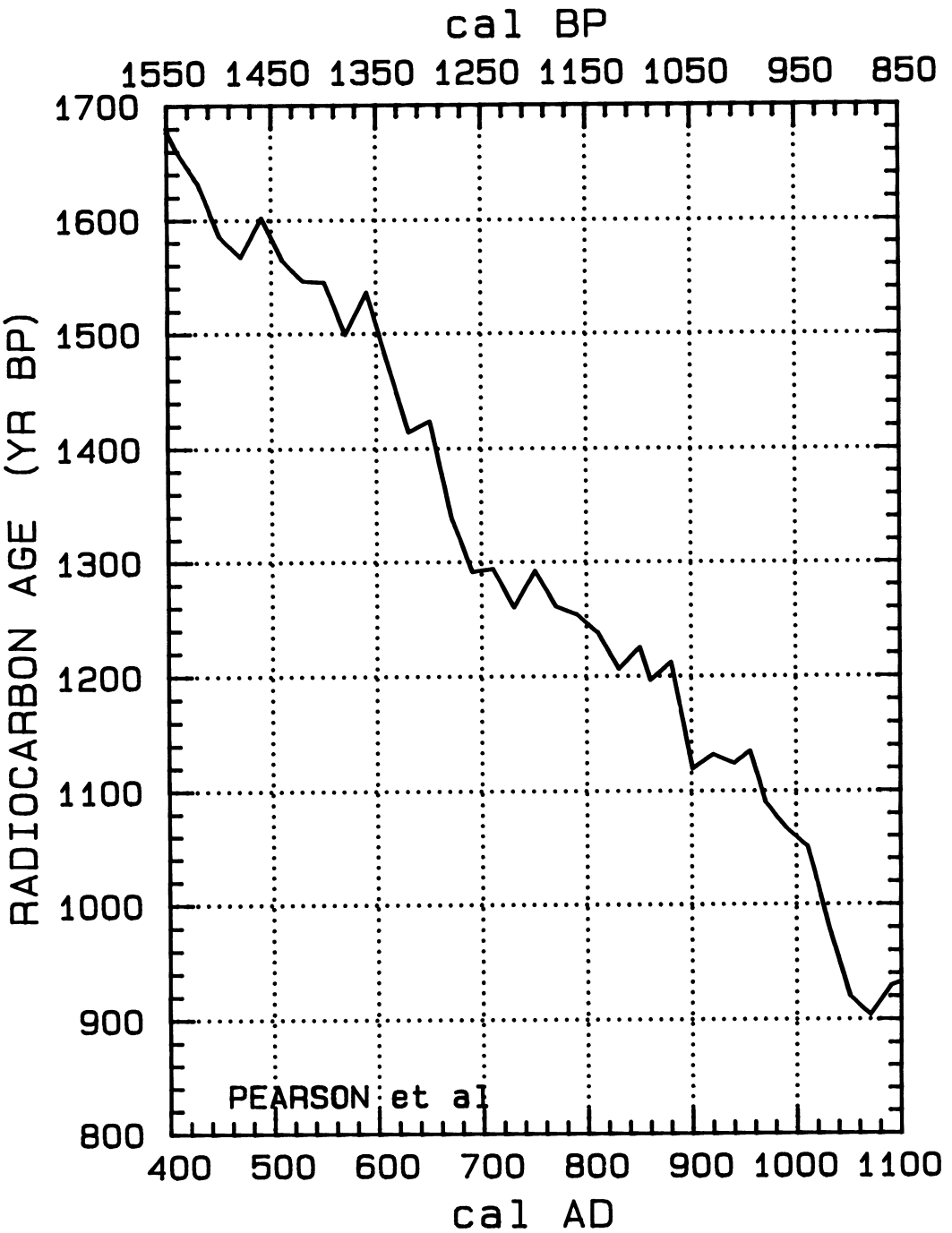
cal BP
1550 1450 1350 1250 1150 1050 950 850
1700
1600
1500
1400
1300
1200
1100
1000
900
800
RADIOCARBON AGE (YR BP)
PEARSON et al
400 500 600 700 800 900 1000 1100
cal AD

Fig. 1C

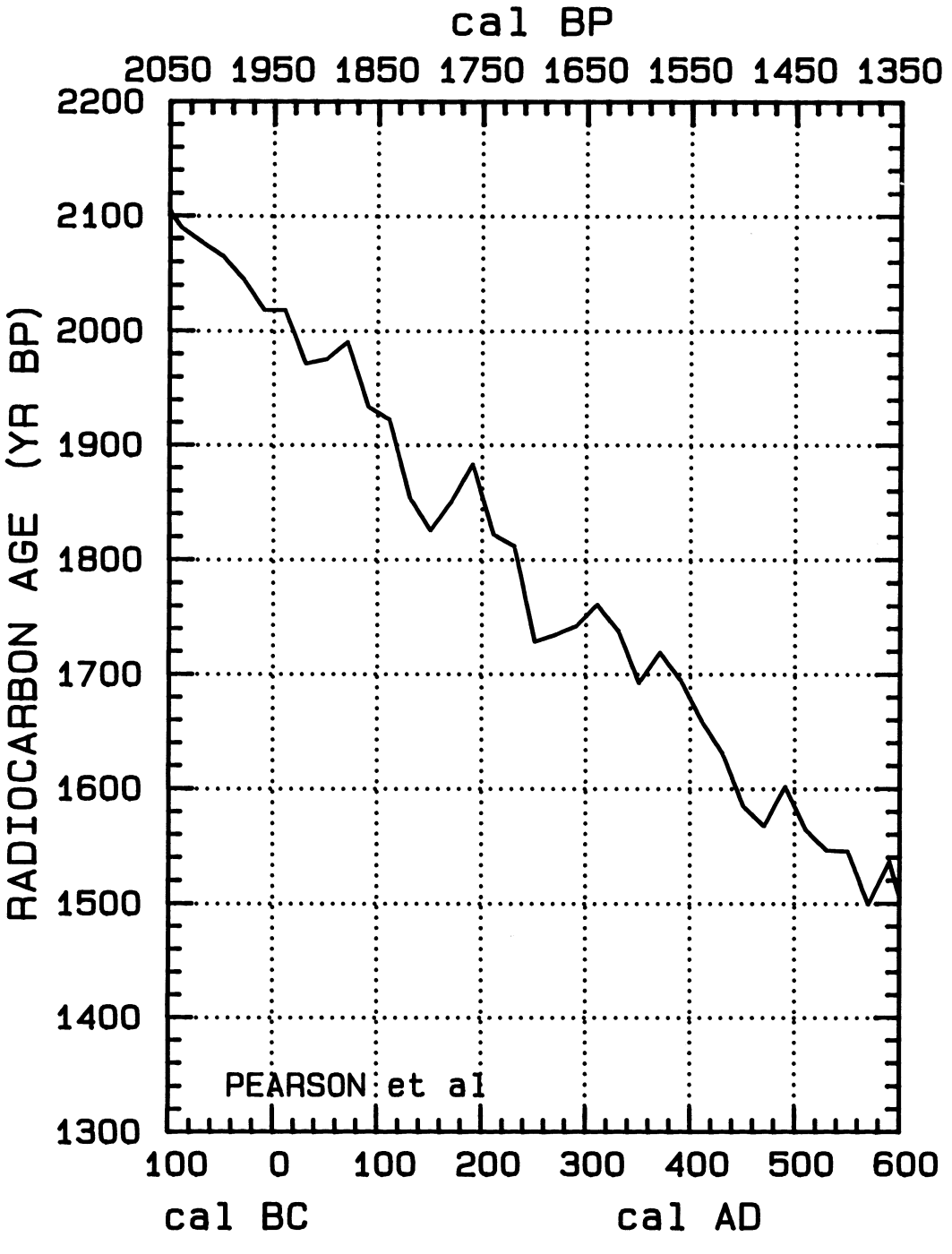
cal BP
2050 1950 1850 1750 1650 1550 1450 1350
2200
2100
2000
1900
1800
1700
1600
1500
1400
1300
RADIOCARBON AGE (YR BP)
PEARSON et al
100 0 100 200 300 400 500 600
cal BC
cal AD

Fig. 1D

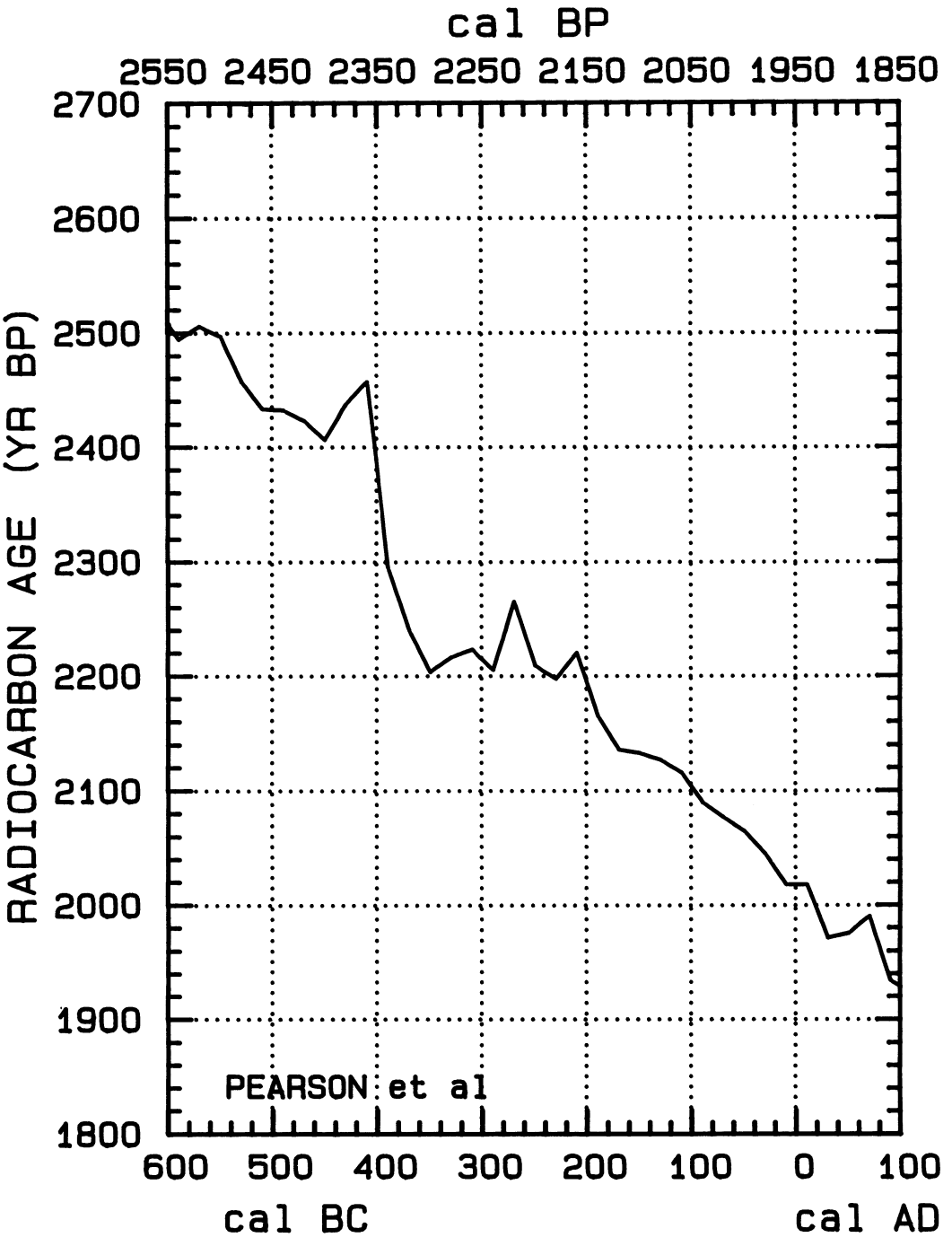
cal BP
2550 2450 2350 2250 2150 2050 1950 1850
2700
2600
2500
2400
2300
2200
2100
2000
1900
1800
RADIOCARBON AGE (YR BP)
PEARSON et al
600 500 400 300 200 100 0 100
cal BC
cal AD

Fig. 1E

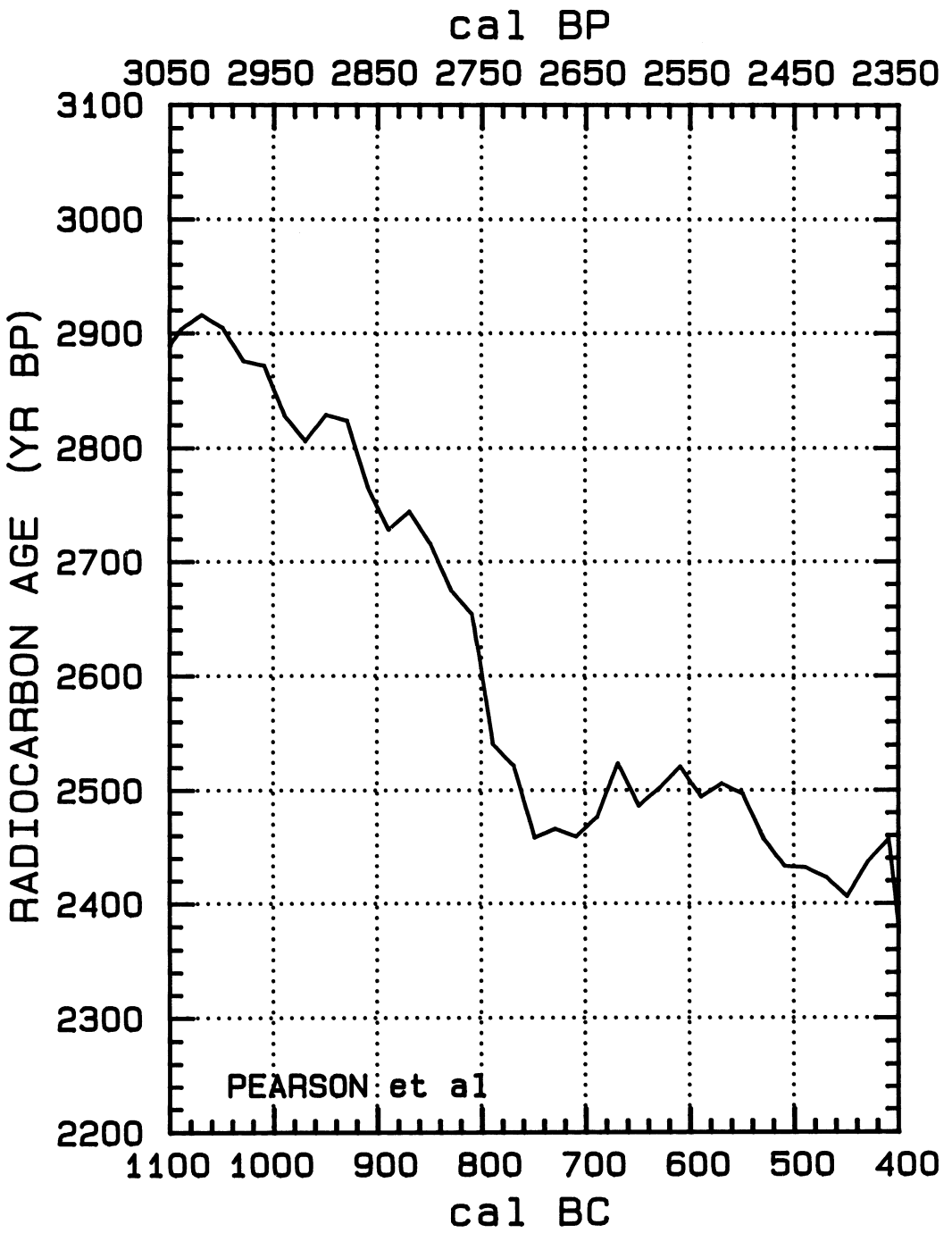
cal BP
3050 2950 2850 2750 2650 2550 2450 2350
3100
3000
2900
2800
2700
2600
2500
2400
2300
2200
RADIOCARBON AGE (YR BP)
PEARSON et al
1100 1000 900 800 700 600 500 400
cal BC

Fig. 1F

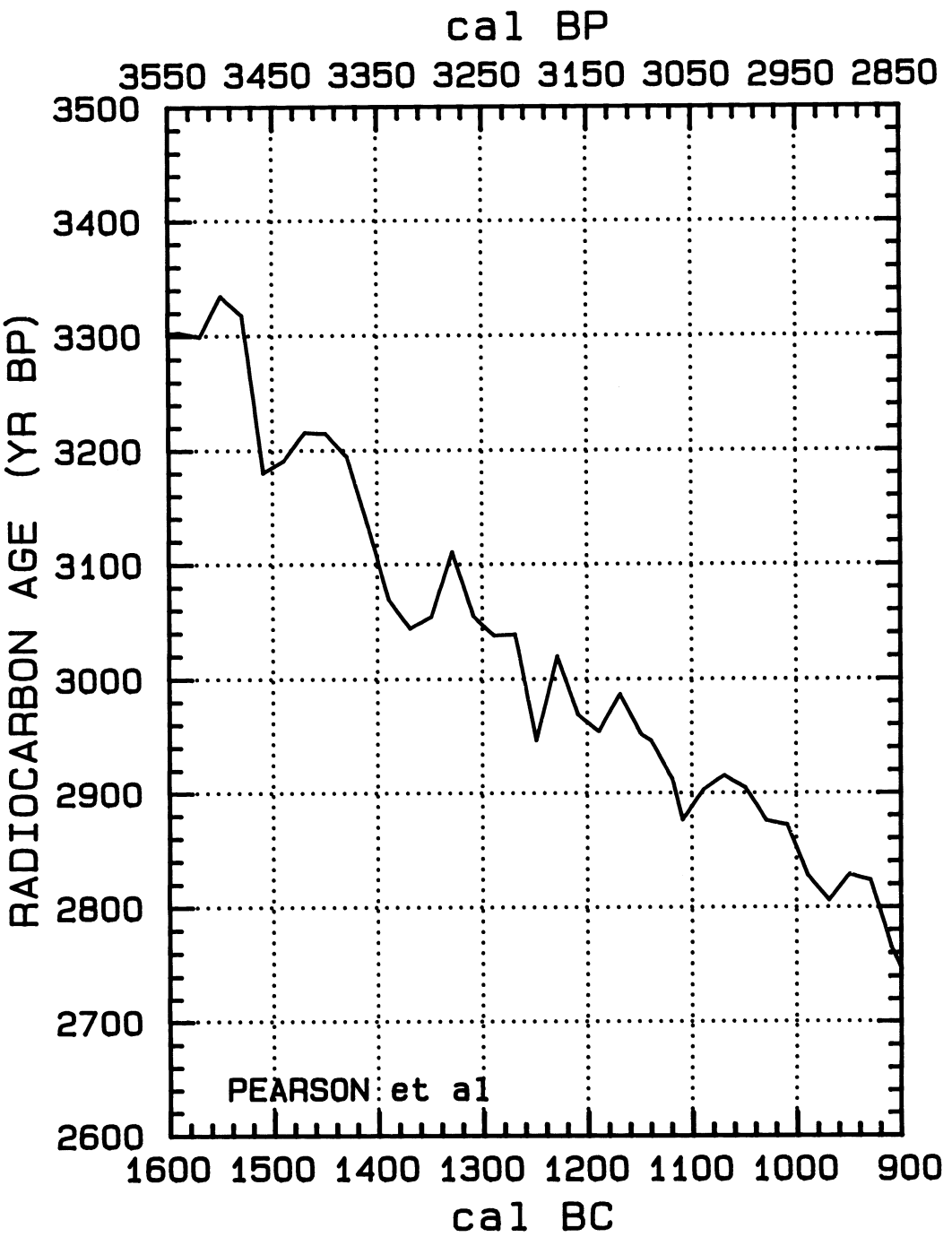
cal BP
3550 3450 3350 3250 3150 3050 2950 2850
3500
3400
3300
3200
3100
3000
2900
2800
2700
2600
RADIOCARBON AGE (YR BP)
PEARSON et al
1600 1500 1400 1300 1200 1100 1000 900
cal BC

Fig. 1G

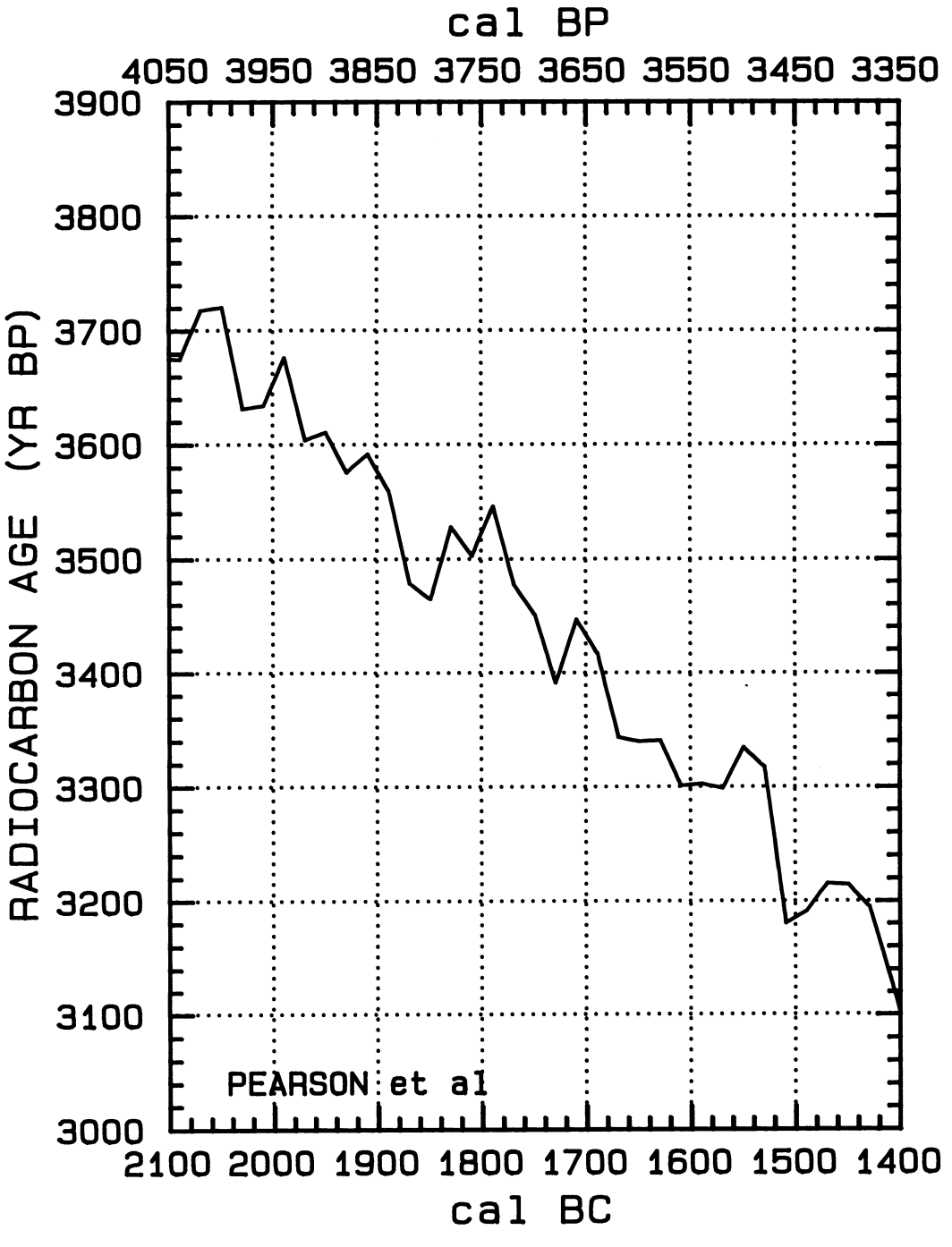
cal BP
4050 3950 3850 3750 3650 3550 3450 3350
3900
3800
3700
3600
3500
3400
3300
3200
3100
3000
RADIOCARBON AGE (YR BP)
PEARSON et al
2100 2000 1900 1800 1700 1600 1500 1400
cal BC

Fig. 1H

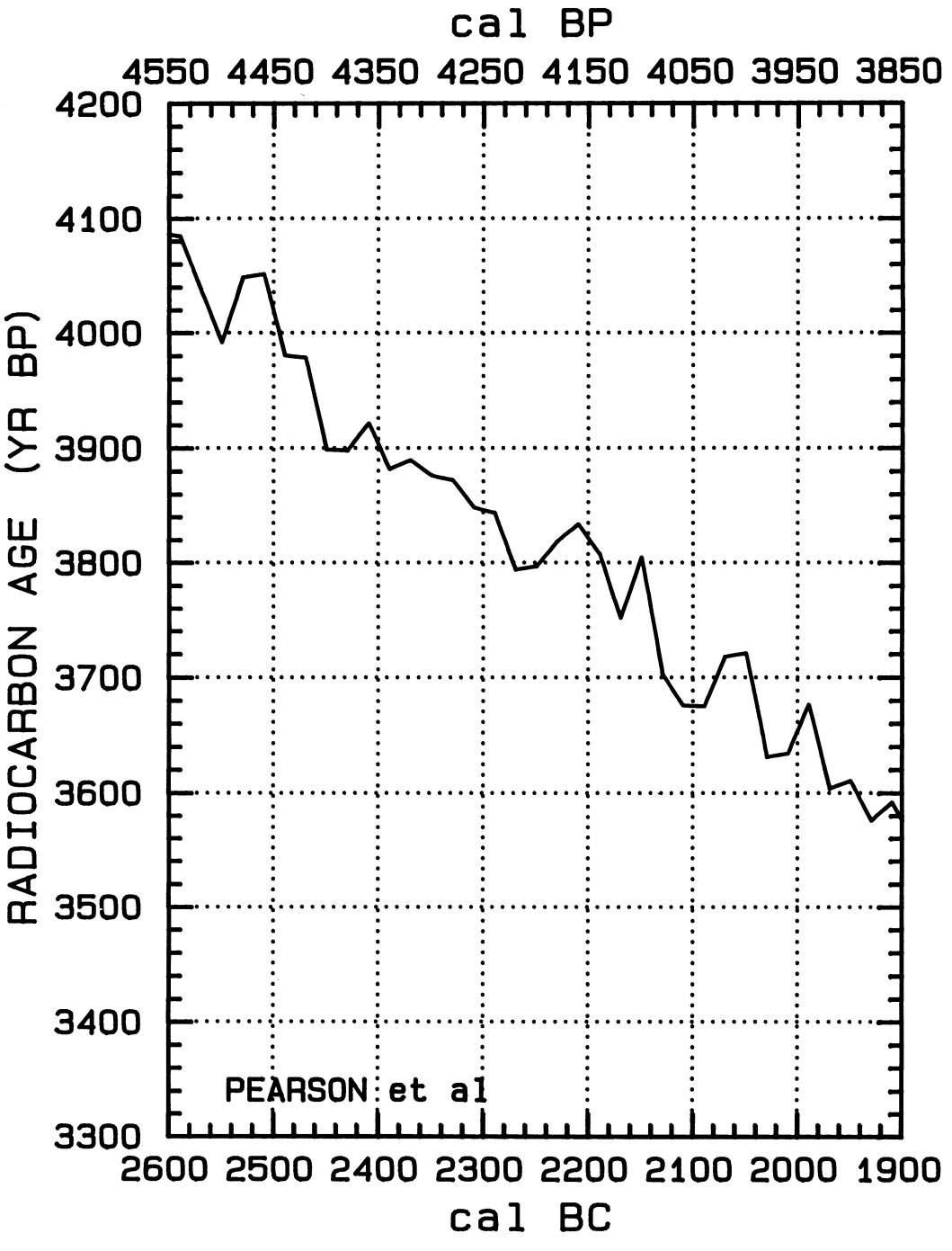
cal BP
4550 4450 4350 4250 4150 4050 3950 3850
4200
4100
4000
3900
3800
3700
3600
3500
3400
3300
RADIOCARBON AGE (YR BP)
PEARSON et al
2600 2500 2400 2300 2200 2100 2000 1900
cal BC

Fig. 1I

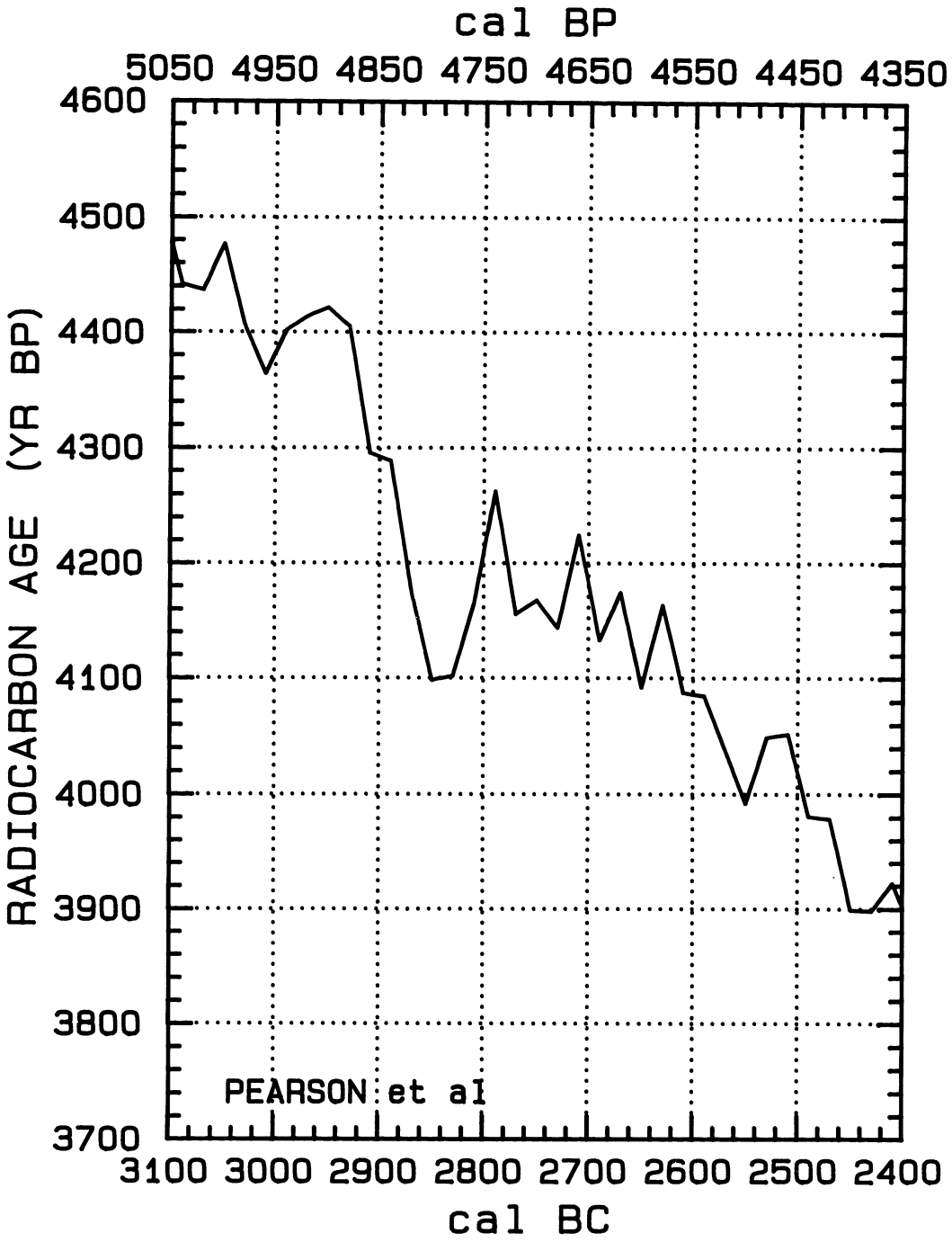
cal BP
5050 4950 4850 4750 4650 4550 4450 4350
4600
4500
4400
4300
4200
4100
4000
3900
3800
3700
RADIOCARBON AGE (YR BP)
PEARSON et al
3100 3000 2900 2800 2700 2600 2500 2400
cal BC

Fig. 1J

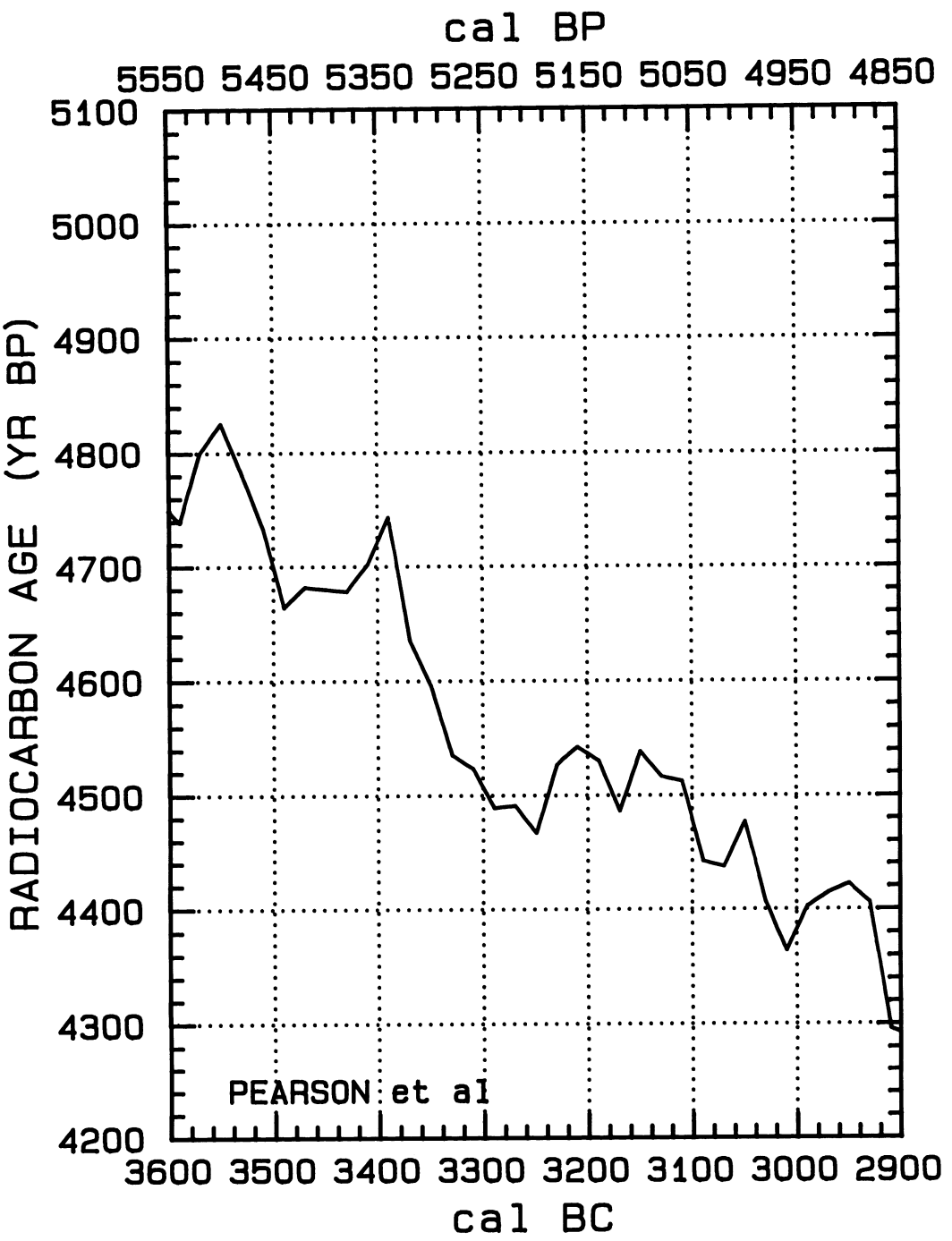
cal BP
5550 5450 5350 5250 5150 5050 4950 4850
5100
5000
4900
4800
4700
4600
4500
4400
4300
4200
RADIOCARBON AGE (YR BP)
PEARSON et al
3600 3500 3400 3300 3200 3100 3000 2900
cal BC

Fig. 1K

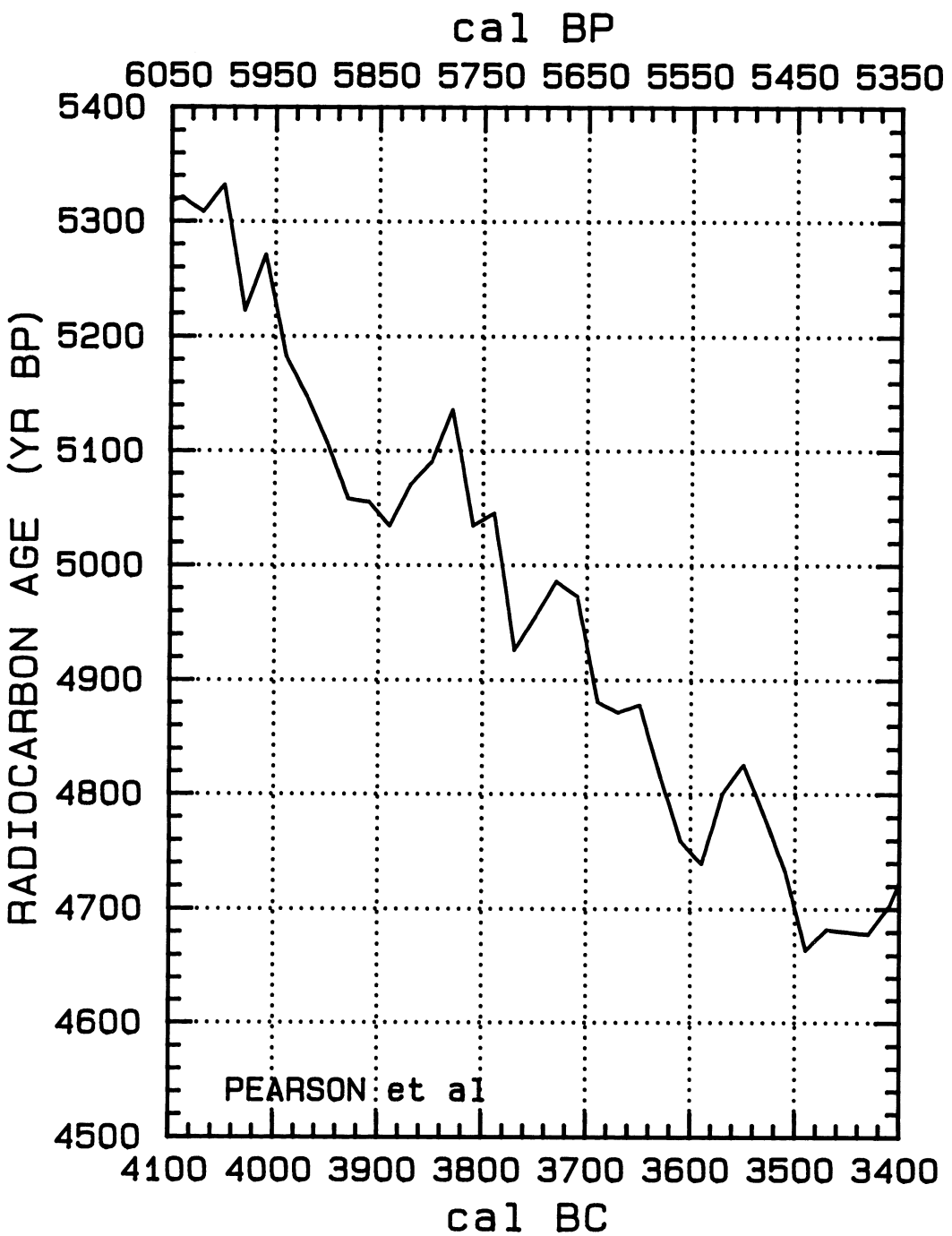
cal BP
6050 5950 5850 5750 5650 5550 5450 5350
5400
5300
5200
5100
5000
4900
4800
4700
4600
4500
RADIOCARBON AGE (YR BP)
PEARSON et al
4100 4000 3900 3800 3700 3600 3500 3400
cal BC

Fig. 1L

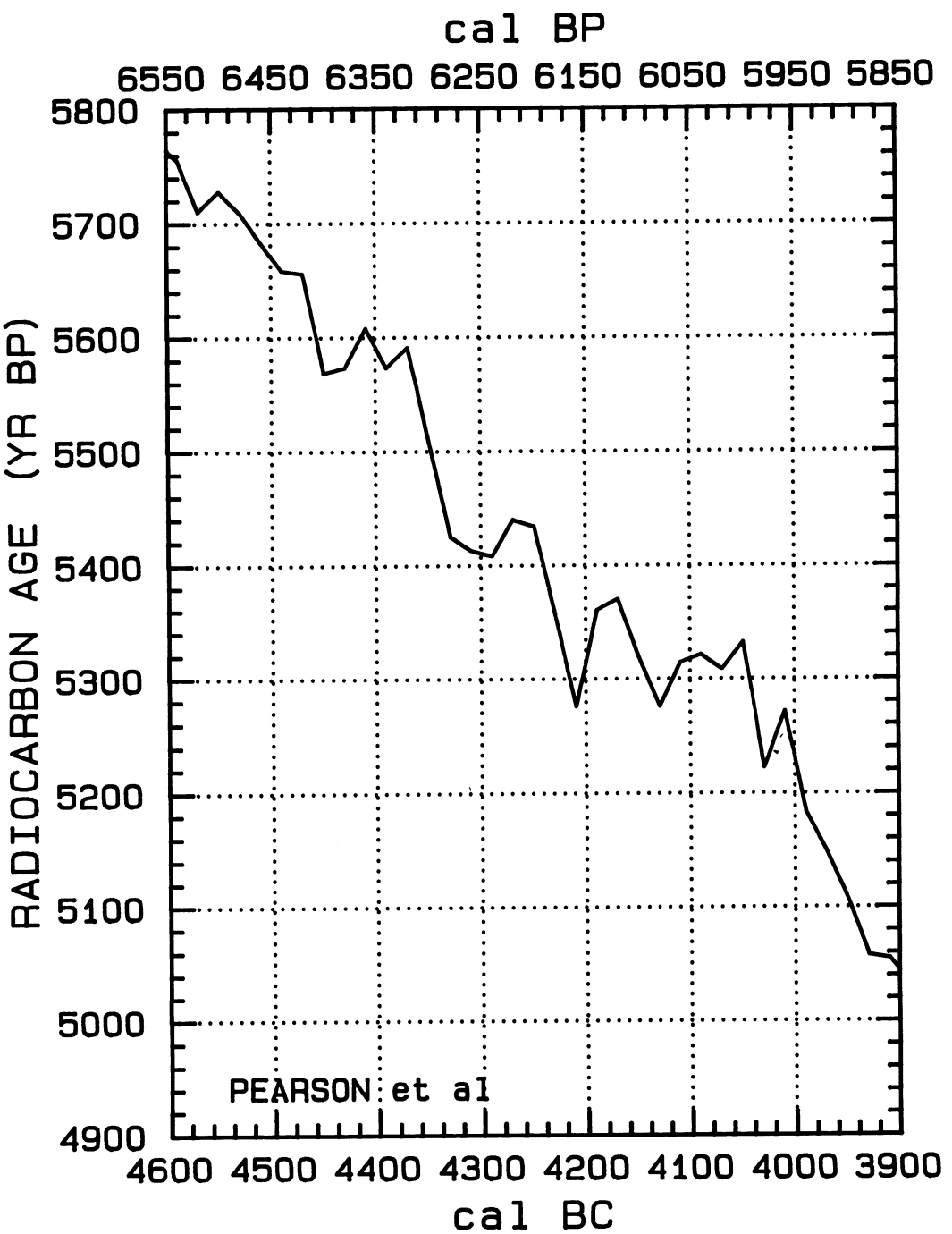
cal BP
6550 6450 6350 6250 6150 6050 5950 5850
5800
5700
5600
5500
5400
5300
5200
5100
5000
4900
RADIOCARBON AGE (YR BP)
PEARSON et al
4600 4500 4400 4300 4200 4100 4000 3900
cal BC

Fig. 1M

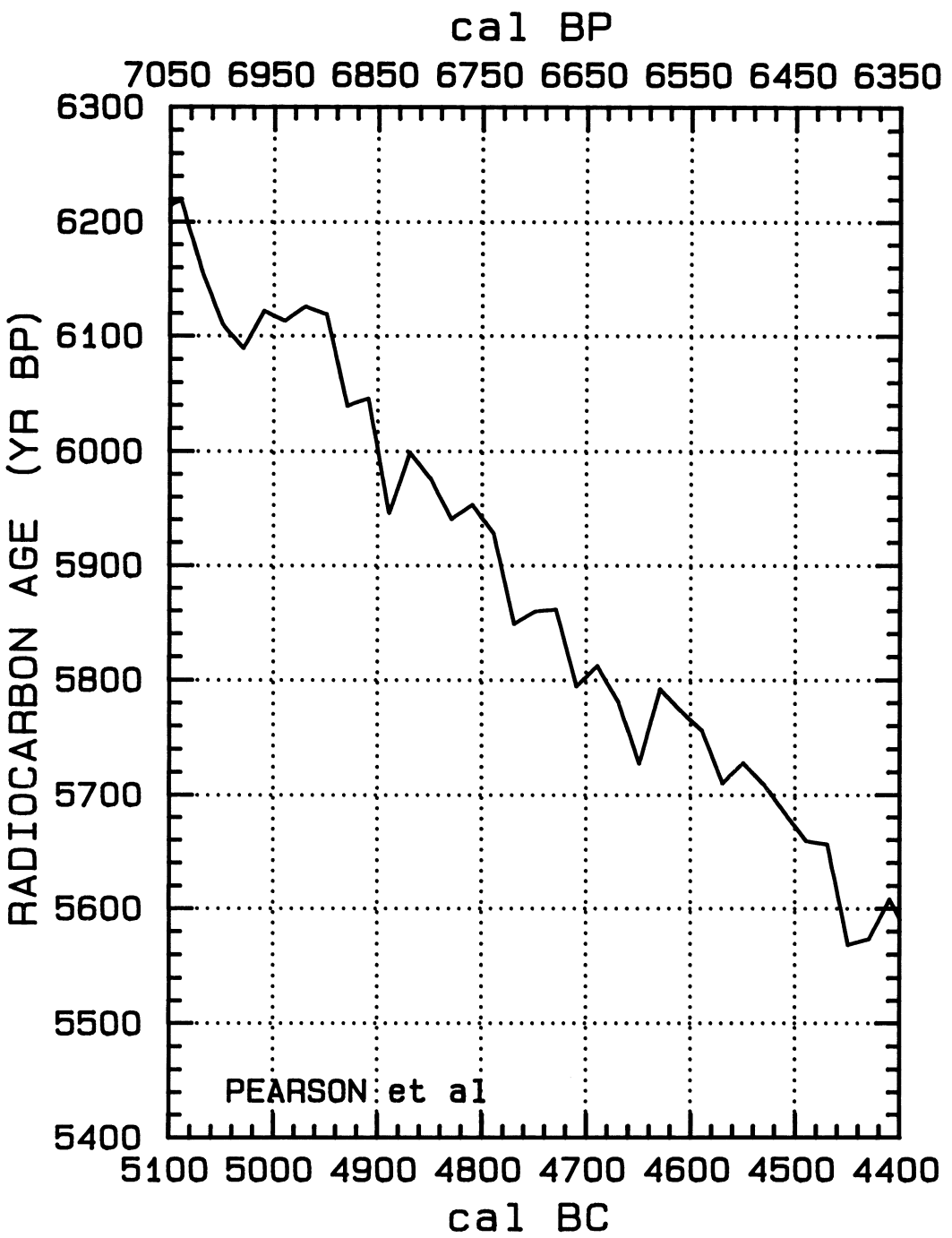
cal BP
7050 6950 6850 6750 6650 6550 6450 6350
6300
6200
6100
6000
5900
5800
5700
5600
5500
5400
RADIOCARBON AGE (YR BP)
PEARSON et al
5100 5000 4900 4800 4700 4600 4500 4400
cal BC

Fig. 1N

TABLE 1. ^{14}C Ages Over the Time Period, AD 1840–5000 BC

Cal AD/BC	$\Delta^{14}C$ ‰	^{14}C age (BP)	Cal BP	Cal AD/BC	$\Delta^{14}C$ ‰	^{14}C age (BP)	Cal BP
AD 1840	0.5 ± 1.3	111 ± 10	BP 110	AD 900	−12.2 ± 1.8	1119 ± 14	BP 1050
AD 1810	1.0 ± 2.2	140 ± 18	BP 140	AD 880	−21.2 ± 1.8	1212 ± 14	BP 1070
AD 1790	−7.3 ± 2.3	214 ± 18	BP 160	AD 860	−16.9 ± 2.1	1196 ± 17	BP 1090
AD 1770	−4.5 ± 2.3	211 ± 18	BP 180	AD 850	−19.3 ± 2.1	1225 ± 17	BP 1100
AD 1750	2.3 ± 2.0	176 ± 16	BP 200	AD 830	−14.5 ± 2.1	1206 ± 17	BP 1120
AD 1730	12.1 ± 2.1	117 ± 16	BP 220	AD 810	−16.1 ± 2.0	1238 ± 16	BP 1140
AD 1710	18.1 ± 1.6	89 ± 12	BP 240	AD 790	−15.7 ± 2.0	1254 ± 16	BP 1160
AD 1690	18.9 ± 2.2	102 ± 17	BP 260	AD 770	−14.1 ± 2.0	1261 ± 16	BP 1180
AD 1670	3.4 ± 2.0	245 ± 16	BP 280	AD 750	−15.6 ± 2.0	1292 ± 16	BP 1200
AD 1650	1.4 ± 1.5	280 ± 12	BP 300	AD 730	−9.3 ± 1.5	1260 ± 12	BP 1220
AD 1630	−7.0 ± 2.2	367 ± 17	BP 320	AD 710	−11.0 ± 1.5	1294 ± 12	BP 1240
AD 1610	−5.4 ± 2.0	374 ± 16	BP 340	AD 690	−8.3 ± 2.3	1291 ± 18	BP 1260
AD 1590	−0.9 ± 1.8	357 ± 14	BP 360	AD 670	−12.0 ± 2.3	1341 ± 18	BP 1280
AD 1570	−1.2 ± 2.0	379 ± 16	BP 380	AD 650	−19.8 ± 1.5	1424 ± 12	BP 1300
AD 1550	8.2 ± 1.4	323 ± 11	BP 400	AD 630	−16.3 ± 2.3	1414 ± 18	BP 1320
AD 1530	12.8 ± 1.3	306 ± 10	BP 420	AD 610	−21.3 ± 2.2	1475 ± 18	BP 1340
AD 1510	7.6 ± 1.2	367 ± 09	BP 440	AD 590	−26.3 ± 2.2	1536 ± 18	BP 1360
AD 1490	13.0 ± 2.2	343 ± 17	BP 460	AD 570	−19.5 ± 2.2	1499 ± 18	BP 1380
AD 1470	7.9 ± 2.3	403 ± 18	BP 480	AD 550	−22.7 ± 2.3	1545 ± 19	BP 1400
AD 1460	8.1 ± 1.3	411 ± 10	BP 490	AD 530	−20.5 ± 2.4	1546 ± 18	BP 1420
AD 1450	2.1 ± 2.2	469 ± 17	BP 500	AD 510	−20.3 ± 2.1	1564 ± 17	BP 1440
AD 1430	−0.7 ± 2.4	511 ± 19	BP 520	AD 490	−22.6 ± 2.1	1602 ± 17	BP 1460
AD 1410	0.0 ± 1.8	525 ± 14	BP 540	AD 470	−15.9 ± 2.1	1567 ± 17	BP 1480
AD 1390	−9.0 ± 1.7	617 ± 13	BP 560	AD 450	−15.7 ± 2.1	1585 ± 17	BP 1500
AD 1370	−15.2 ± 1.8	687 ± 14	BP 580	AD 430	−21.4 ± 2.1	1631 ± 17	BP 1520
AD 1350	−8.3 ± 2.0	650 ± 16	BP 600	AD 410	−20.0 ± 2.1	1659 ± 17	BP 1540
AD 1330	1.7 ± 1.8	589 ± 14	BP 620	AD 390	−22.1 ± 2.1	1695 ± 17	BP 1560
AD 1310	2.4 ± 1.8	603 ± 14	BP 640	AD 370	−22.6 ± 2.1	1719 ± 17	BP 1580
AD 1290	−9.7 ± 1.7	720 ± 13	BP 660	AD 350	−16.9 ± 2.3	1692 ± 18	BP 1600
AD 1260	−15.0 ± 1.3	792 ± 10	BP 690	AD 330	−20.2 ± 2.2	1738 ± 18	BP 1620
AD 1230	−15.4 ± 1.3	824 ± 10	BP 720	AD 310	−20.6 ± 2.1	1761 ± 17	BP 1640
AD 1215	−19.7 ± 2.3	874 ± 18	BP 735	AD 290	−15.9 ± 2.1	1742 ± 17	BP 1660
AD 1195	−13.3 ± 2.3	841 ± 18	BP 755	AD 270	−12.6 ± 2.3	1734 ± 18	BP 1680
AD 1170	−15.8 ± 1.2	886 ± 09	BP 780	AD 250	−9.4 ± 2.3	1728 ± 18	BP 1700
AD 1150	−20 8 ± 1.1	946 ± 09	BP 800	AD 230	−17.4 ± 2.3	1812 ± 18	BP 1720
AD 1130	−14.0 ± 1.5	910 ± 12	BP 820	AD 210	−16.2 ± 2.3	1822 ± 18	BP 1740
AD 1110	−14.8 ± 1.5	936 ± 12	BP 840	AD 190	−21.3 ± 2.2	1883 ± 18	BP 1760
AD 1090	−11.6 ± 1.4	929 ± 11	BP 860	AD 170	−14.9 ± 2.3	1850 ± 18	BP 1780
AD 1070	−6.1 ± 1.3	904 ± 10	BP 880	AD 150	−9.4 ± 2.3	1825 ± 18	BP 1800
AD 1050	−5.6 ± 1.5	920 ± 12	BP 900	AD 130	−10.6 ± 2.3	1854 ± 18	BP 1820
AD 1030	−10.8 ± 1.5	981 ± 12	BP 920	AD 110	−16.7 ± 2.3	1923 ± 18	BP 1840
AD 1010	−17.0 ± 1.4	1051 ± 11	BP 940	AD 90	−15.6 ± 2.3	1934 ± 18	BP 1860
AD 990	−16.6 ± 1.3	1067 ± 10	BP 960	AD 70	−20.0 ± 2.0	1990 ± 16	BP 1880
AD 970	−17.0 ± 1.3	1090 ± 10	BP 980	AD 50	−15.9 ± 2.3	1975 ± 18	BP 1900
AD 955	−20.7 ± 1.8	1135 ± 14	BP 995	AD 30	−13.0 ± 2.0	1971 ± 16	BP 1920
AD 940	−17.7 ± 2.0	1124 ± 16	BP 1010	AD 10	−16.4 ± 2.1	2018 ± 17	BP 1940
AD 920	−16.2 ± 1.8	1132 ± 14	BP 1030	10 BC	−14.0 ± 2.3	2018 ± 18	BP 1960

TABLE 1. (Continued)

Cal AD/BC	$\Delta^{14}C$ ‰	^{14}C age (BP)	Cal BP	Cal AD/BC	$\Delta^{14}C$ ‰	^{14}C age (BP)	Cal BP
30 BC	−15.0 ± 2.3	2045 ± 18	BP 1980	970 BC	−3.6 ± 1.4	2806 ± 11	BP 2920
50 BC	−15.0 ± 2.1	2065 ± 17	BP 2000	990 BC	3.6 ± 1.5	2828 ± 12	BP 2940
70 BC	−14.1 ± 2.0	2077 ± 16	BP 2020	1010 BC	0.5 ± 1.1	2872 ± 8	BP 2960
90 BC	−13.3 ± 2.0	2090 ± 16	BP 2040	1030 BC	2.4 ± 1.5	2876 ± 12	BP 2980
110 BC	−14.1 ± 1.8	2116 ± 14	BP 2060	1050 BC	1.3 ± 1.3	2905 ± 10	BP 3000
130 BC	−13.1 ± 2.0	2127 ± 16	BP 2080	1070 BC	2.3 ± 1.3	2916 ± 10	BP 3020
150 BC	−11.4 ± 2.0	2133 ± 16	BP 2100	1090 BC	6.4 ± 1.6	2903 ± 12	BP 3040
170 BC	−9.4 ± 1.5	2136 ± 12	BP 2120	1110 BC	12.2 ± 1.6	2876 ± 12	BP 3060
190 BC	−10.6 ± 1.5	2165 ± 12	BP 2140	1120 BC	8.8 ± 1.9	2913 ± 15	BP 3070
210 BC	−15.0 ± 1.6	2220 ± 13	BP 2160	1140 BC	7.1 ± 1.9	2946 ± 15	BP 3090
230 BC	−9.7 ± 2.1	2197 ± 17	BP 2180	1150 BC	7.5 ± 2.0	2952 ± 16	BP 3100
250 BC	−8.8 ± 2.0	2209 ± 16	BP 2200	1170 BC	5.6 ± 1.8	2987 ± 14	BP 3120
270 BC	−3.3 ± 2.0	2265 ± 16	BP 2220	1190 BC	12.2 ± 2.0	2954 ± 16	BP 3140
290 BC	−3.5 ± 2.3	2205 ± 18	BP 2240	1210 BC	12.7 ± 2.0	2969 ± 16	BP 3160
310 BC	−3.4 ± 1.7	2223 ± 13	BP 2260	1230 BC	8.8 ± 1.8	3020 ± 14	BP 3180
330 BC	−0.1 ± 2.3	2216 ± 18	BP 2280	1250 BC	20.6 ± 1.8	2946 ± 14	BP 3200
350 BC	4.0 ± 2.0	2203 ± 16	BP 2300	1270 BC	11.3 ± 2.2	3039 ± 17	BP 3220
370 BC	1.8 ± 1.4	2240 ± 13	BP 2320	1290 BC	13.8 ± 2.2	3038 ± 17	BP 3240
390 BC	−2.6 ± 1.9	2295 ± 15	BP 2340	1310 BC	14.1 ± 2.2	3055 ± 17	BP 3260
410 BC	−20.2 ± 2.2	2457 ± 18	BP 2360	1330 BC	9.5 ± 2.0	3111 ± 16	BP 3280
430 BC	−15.4 ± 1.4	2437 ± 11	BP 2380	1350 BC	19.2 ± 2.0	3054 ± 16	BP 3300
450 BC	−9.2 ± 1.5	2406 ± 12	BP 2400	1370 BC	22.9 ± 2.3	3044 ± 18	BP 3320
470 BC	−8.9 ± 1.4	2423 ± 11	BP 2420	1390 BC	22.2 ± 1.9	3069 ± 15	BP 3340
490 BC	−7.6 ± 1.7	2432 ± 13	BP 2440	1410 BC	16.6 ± 1.8	3133 ± 14	BP 3360
510 BC	−5.3 ± 1.3	2433 ± 10	BP 2460	1430 BC	11.2 ± 2.0	3195 ± 16	BP 3380
530 BC	−5.9 ± 1.3	2457 ± 10	BP 2480	1450 BC	11.1 ± 1.3	3215 ± 10	BP 3400
550 BC	−8.4 ± 1.2	2497 ± 9	BP 2500	1470 BC	13.4 ± 1.9	3216 ± 15	BP 3420
570 BC	−7.1 ± 1.3	2506 ± 10	BP 2520	1490 BC	19.1 ± 2.0	3191 ± 16	BP 3440
590 BC	−3.2 ± 1.4	2494 ± 11	BP 2540	1510 BC	22.9 ± 2.0	3180 ± 16	BP 3460
610 BC	−4.2 ± 1.3	2521 ± 10	BP 2560	1530 BC	7.9 ± 1.9	3318 ± 15	BP 3480
630 BC	0.6 ± 1.3	2502 ± 10	BP 2580	1550 BC	8.2 ± 2.3	3335 ± 18	BP 3500
650 BC	5.0 ± 1.8	2486 ± 14	BP 2600	1570 BC	15.2 ± 2.0	3299 ± 16	BP 3520
670 BC	2.7 ± 1.5	2524 ± 12	BP 2620	1590 BC	17.2 ± 1.8	3303 ± 14	BP 3540
690 BC	11.2 ± 1.6	2476 ± 12	BP 2640	1610 BC	19.9 ± 1.9	3301 ± 15	BP 3560
710 BC	15.8 ± 1.6	2459 ± 15	BP 2660	1630 BC	17.3 ± 1.9	3341 ± 15	BP 3580
730 BC	17.3 ± 1.7	2466 ± 13	BP 2680	1650 BC	19.9 ± 1.7	3340 ± 13	BP 3600
750 BC	19.2 ± 1.7	2458 ± 13	BP 2700	1670 BC	21.9 ± 1.9	3344 ± 15	BP 3620
770 BC	15.2 ± 2.1	2522 ± 16	BP 2720	1690 BC	15.0 ± 2.0	3417 ± 16	BP 3640
790 BC	15.2 ± 1.6	2541 ± 12	BP 2740	1710 BC	13.7 ± 2.4	3447 ± 19	BP 3660
810 BC	3.5 ± 2.3	2654 ± 18	BP 2760	1730 BC	23.3 ± 1.7	3391 ± 13	BP 3680
830 BC	3.3 ± 2.3	2675 ± 18	BP 2780	1750 BC	18.1 ± 1.9	3451 ± 15	BP 3700
850 BC	0.6 ± 2.0	2716 ± 16	BP 2800	1770 BC	17.2 ± 1.8	3478 ± 14	BP 3720
870 BC	−0.5 ± 1.8	2744 ± 14	BP 2820	1790 BC	11.0 ± 2.2	3546 ± 17	BP 3740
890 BC	3.9 ± 1.3	2728 ± 14	BP 2840	1810 BC	18.9 ± 2.4	3503 ± 19	BP 3760
910 BC	1.8 ± 1.7	2765 ± 13	BP 2860	1830 BC	18.2 ± 2.4	3528 ± 19	BP 3780
930 BC	−3.2 ± 2.4	2824 ± 19	BP 2880	1850 BC	28.7 ± 1.8	3465 ± 14	BP 3800
950 BC	−1.4 ± 2.4	2829 ± 19	BP 2900	1870 BC	29.4 ± 1.8	3479 ± 14	BP 3820

TABLE 1. (Continued)

Cal AD/BC	$\Delta^{14}C$ ‰	^{14}C age (BP)	Cal BP	Cal AD/BC	$\Delta^{14}C$ ‰	^{14}C age (BP)	Cal BP
1890 BC	21.6 ± 1.7	3560 ± 13	BP 3840	2830 BC	69.9 ± 1.1	4102 ± 8	BP 4780
1910 BC	20.0 ± 2.3	3592 ± 18	BP 3860	2850 BC	73.0 ± 1.5	4098 ± 11	BP 4800
1930 BC	24.5 ± 1.8	3576 ± 14	BP 3880	2870 BC	62.5 ± 1.8	4176 ± 13	BP 4820
1950 BC	22.5 ± 1.7	3611 ± 13	BP 3900	2890 BC	52.9 ± 1.8	4289 ± 13	BP 4840
1970 BC	25.9 ± 2.3	3604 ± 17	BP 3920	2910 BC	54.5 ± 1.6	4296 ± 12	BP 4860
1990 BC	19.0 ± 1.4	3677 ± 11	BP 3940	2930 BC	42.7 ± 1.7	4406 ± 13	BP 4880
2010 BC	27.0 ± 2.0	3634 ± 15	BP 3960	2950 BC	43.1 ± 1.7	4422 ± 13	BP 4900
2030 BC	30.0 ± 2.1	3631 ± 16	BP 3980	2970 BC	46.7 ± 2.4	4414 ± 18	BP 4920
2050 BC	20.9 ± 2.1	3721 ± 16	BP 4000	2990 BC	50.8 ± 2.2	4402 ± 14	BP 4940
2070 BC	23.7 ± 2.3	3718 ± 18	BP 4020	3010 BC	58.4 ± 1.9	4364 ± 14	BP 4960
2090 BC	31.7 ± 2.1	3675 ± 15	BP 4040	3030 BC	55.4 ± 1.8	4406 ± 13	BP 4980
2110 BC	34.1 ± 2.4	3676 ± 18	BP 4060	3050 BC	48.6 ± 1.7	4477 ± 13	BP 5000
2130 BC	33.1 ± 2.3	3703 ± 18	BP 4080	3070 BC	56.4 ± 1.9	4437 ± 14	BP 5020
2150 BC	22.5 ± 1.7	3805 ± 13	BP 4100	3090 BC	58.3 ± 2.2	4442 ± 16	BP 5040
2170 BC	31.8 ± 2.4	3752 ± 18	BP 4120	3110 BC	51.5 ± 2.7	4513 ± 20	BP 5060
2190 BC	27.1 ± 1.8	3808 ± 14	BP 4140	3130 BC	53.6 ± 2.0	4517 ± 15	BP 5080
2210 BC	26.3 ± 1.8	3834 ± 14	BP 4160	3150 BC	53.2 ± 1.9	4539 ± 14	BP 5100
2230 BC	30.7 ± 2.1	3819 ± 16	BP 4180	3170 BC	62.8 ± 2.4	4486 ± 18	BP 5120
2250 BC	36.0 ± 1.7	3797 ± 13	BP 4200	3190 BC	59.4 ± 2.0	4531 ± 15	BP 5140
2270 BC	38.9 ± 2.1	3794 ± 16	BP 4220	3210 BC	60.4 ± 2.2	4543 ± 16	BP 5160
2290 BC	35.0 ± 2.1	3844 ± 16	BP 4240	3230 BC	64.9 ± 1.6	4527 ± 12	BP 5180
2310 BC	36.8 ± 2.1	3849 ± 16	BP 4260	3250 BC	75.7 ± 1.8	4467 ± 13	BP 5200
2330 BC	36.2 ± 1.7	3873 ± 13	BP 4280	3270 BC	75.0 ± 2.3	4491 ± 17	BP 5220
2350 BC	38.2 ± 2.1	3877 ± 16	BP 4300	3290 BC	77.9 ± 1.9	4489 ± 14	BP 5240
2370 BC	39.1 ± 1.7	3890 ± 13	BP 4320	3310 BC	75.8 ± 1.9	4524 ± 14	BP 5260
2390 BC	40.7 ± 2.1	3882 ± 16	BP 4340	3330 BC	76.8 ± 1.9	4536 ± 14	BP 5280
2410 BC	39.9 ± 1.6	3922 ± 12	BP 4360	3350 BC	71.4 ± 1.9	4596 ± 14	BP 5300
2430 BC	45.6 ± 1.0	3898 ± 7	BP 4380	3370 BC	68.7 ± 2.4	4636 ± 18	BP 5320
2450 BC	48.0 ± 1.4	3899 ± 10	BP 4400	3390 BC	57.1 ± 2.2	4743 ± 16	BP 5340
2470 BC	40.1 ± 1.7	3979 ± 13	BP 4420	3410 BC	65.1 ± 2.4	4702 ± 18	BP 5360
2490 BC	42.4 ± 1.7	3981 ± 13	BP 4440	3430 BC	70.8 ± 2.4	4678 ± 18	BP 5380
2510 BC	35.7 ± 1.3	4052 ± 10	BP 4460	3450 BC	73.2 ± 2.3	4680 ± 17	BP 5400
2530 BC	38.6 ± 2.0	4049 ± 15	BP 4480	3470 BC	75.5 ± 2.5	4682 ± 18	BP 5420
2550 BC	48.5 ± 1.9	3992 ± 14	BP 4500	3490 BC	80.5 ± 2.6	4664 ± 19	BP 5440
2570 BC	44.9 ± 1.5	4039 ± 11	BP 4520	3510 BC	73.9 ± 2.6	4733 ± 19	BP 5460
2590 BC	41.5 ± 1.5	4085 ± 11	BP 4540	3530 BC	70.1 ± 2.6	4781 ± 19	BP 5480
2610 BC	43.6 ± 2.4	4088 ± 18	BP 4560	3550 BC	66.7 ± 2.6	4826 ± 19	BP 5500
2630 BC	36.3 ± 1.3	4164 ± 10	BP 4580	3570 BC	72.7 ± 2.7	4800 ± 20	BP 5520
2650 BC	48.2 ± 1.9	4092 ± 14	BP 4600	3590 BC	83.5 ± 2.7	4739 ± 20	BP 5540
2670 BC	39.9 ± 1.6	4175 ± 12	BP 4620	3610 BC	83.4 ± 2.7	4759 ± 20	BP 5560
2690 BC	47.9 ± 1.6	4133 ± 12	BP 4640	3630 BC	78.5 ± 2.7	4815 ± 20	BP 5580
2710 BC	38.5 ± 1.6	4225 ± 12	BP 4660	3650 BC	72.7 ± 2.7	4878 ± 20	BP 5600
2730 BC	51.5 ± 1.2	4144 ± 9	BP 4680	3670 BC	76.2 ± 2.7	4871 ± 18	BP 5620
2750 BC	50.9 ± 1.6	4168 ± 12	BP 4700	3690 BC	77.5 ± 2.4	4881 ± 18	BP 5640
2770 BC	55.0 ± 2.1	4156 ± 16	BP 4720	3710 BC	67.8 ± 2.4	4973 ± 18	BP 5660
2790 BC	43.6 ± 1.7	4263 ± 13	BP 4740	3730 BC	68.6 ± 2.4	4986 ± 18	BP 5680
2810 BC	59.0 ± 1.8	4165 ± 13	BP 4760	3750 BC	75.4 ± 2.5	4955 ± 18	BP 5700

TABLE 1. (Continued)

Cal AD/BC	$\Delta^{14}C$ ‰	^{14}C age (BP)	Cal BP	Cal AD/BC	$\Delta^{14}C$ ‰	^{14}C age (BP)	Cal BP
3770 BC	81.9 ± 2.3	4926 ± 17	BP 5720	4390 BC	75.9 ± 2.2	5573 ± 16	BP 6340
3790 BC	68.5 ± 2.4	5045 ± 18	BP 5740	4410 BC	73.8 ± 2.2	5608 ± 16	BP 6360
3810 BC	72.6 ± 2.3	5034 ± 17	BP 5760	4430 BC	81.1 ± 2.2	5573 ± 16	BP 6380
3830 BC	61.6 ± 2.0	5136 ± 15	BP 5780	4450 BC	84.4 ± 2.2	5568 ± 16	BP 6400
3850 BC	70.3 ± 1.5	5090 ± 11	BP 5800	4470 BC	75.2 ± 2.2	5656 ± 16	BP 6420
3870 BC	75.6 ± 1.8	5070 ± 13	BP 5820	4490 BC	77.4 ± 2.2	5659 ± 16	BP 6440
3890 BC	84.3 ± 1.8	5034 ± 13	BP 5840	4510 BC	76.8 ± 2.3	5683 ± 17	BP 6460
3910 BC	82.8 ± 1.7	5055 ± 12	BP 5860	4530 BC	75.9 ± 2.3	5709 ± 17	BP 6480
3930 BC	85.0 ± 1.7	5058 ± 12	BP 5880	4550 BC	75.9 ± 2.3	5728 ± 17	BP 6500
3950 BC	81.0 ± 1.7	5107 ± 12	BP 5900	4570 BC	81.0 ± 2.5	5710 ± 18	BP 6520
3970 BC	78.1 ± 1.7	5148 ± 12	BP 5920	4590 BC	77.4 ± 2.3	5756 ± 17	BP 6540
3990 BC	76.1 ± 2.1	5183 ± 15	BP 5940	4610 BC	77.7 ± 2.2	5773 ± 16	BP 6560
4010 BC	66.9 ± 1.9	5271 ± 14	BP 5960	4630 BC	77.8 ± 2.2	5792 ± 16	BP 6580
4030 BC	76.0 ± 1.8	5222 ± 13	BP 5980	4650 BC	89.2 ± 2.6	5727 ± 19	BP 6600
4050 BC	64.0 ± 1.8	5332 ± 13	BP 6000	4670 BC	84. ± 2.3	5781 ± 17	BP 6620
4070 BC	69.8 ± 1.9	5308 ± 14	BP 6020	4690 BC	82.9 ± 2.2	5812 ± 16	BP 6640
4090 BC	70.6 ± 1.9	5321 ± 14	BP 6040	4710 BC	88.0 ± 2.2	5794 ± 16	BP 6660
4110 BC	74.1 ± 2.5	5314 ± 18	BP 6060	4730 BC	81.6 ± 2.5	5861 ± 18	BP 6680
4130 BC	82.0 ± 2.5	5275 ± 18	BP 6080	4750 BC	84.5 ± 2.5	5859 ± 18	BP 6700
4150 BC	78.7 ± 2.9	5319 ± 21	BP 6100	4770 BC	88.6 ± 2.5	5848 ± 18	BP 6720
4170 BC	73.9 ± 2.2	5370 ± 16	BP 6120	4790 BC	80.4 ± 2.6	5928 ± 19	BP 6740
4190 BC	78.4 ± 2.6	5360 ± 19	BP 6140	4810 BC	79.7 ± 2.5	5953 ± 18	BP 6760
4210 BC	92.5 ± 2.4	5275 ± 17	BP 6160	4830 BC	84.0 ± 1.9	5940 ± 14	BP 6780
4230 BC	84.2 ± 2.2	5356 ± 16	BP 6180	4850 BC	81.8 ± 2.5	5976 ± 18	BP 6800
4250 BC	76.3 ± 2.2	5434 ± 16	BP 6200	4870 BC	81.3 ± 2.6	5999 ± 19	BP 6820
4270 BC	78.1 ± 2.3	5440 ± 17	BP 6220	4890 BC	91.2 ± 2.5	5945 ± 18	BP 6840
4290 BC	85.0 ± 2.3	5408 ± 17	BP 6240	4910 BC	80.2 ± 2.1	6046 ± 15	BP 6860
4310 BC	87.0 ± 2.1	5413 ± 15	BP 6260	4930 BC	83.8 ± 1.4	6039 ± 10	BP 6880
4330 BC	88.0 ± 2.2	5425 ± 16	BP 6280	4950 BC	75.6 ± 1.6	6119 ± 12	BP 6900
4350 BC	75.9 ± 2.1	5507 ± 15	BP 6300	4970 BC	77.3 ± 1.6	6126 ± 12	BP 6920
4370 BC	70.9 ± 1.9	5591 ± 14	BP 6320	4990 BC	81.7 ± 1.6	6113 ± 12	BP 6940

[RADIOCARBON, VOL. 35, NO. 1, 1993, P. 125–135]

GERMAN OAK AND PINE ^{14}C CALIBRATION, 7200–9439 BC

BERND KROMER

Institut für Umweltphysik, Universität Heidelberg, D-6900 Heidelberg, Germany

and

BERND BECKER

Institut für Botanik, Universität Hohenheim, D-7000 Stuttgart 70 Germany

INTRODUCTION

Radiocarbon calibration data derived from German oak chronologies, ranging back to 7200 BC, have been published in the previous Calibration Issue (Stuiver & Kra 1986). In recent years, the German oak chronology has been extended to 7938 BC (Becker, this issue). For earlier intervals, tree-ring chronologies must be based on pine, because oak re-emigrated to central Europe at the Preboreal/Boreal transition, at about 8000 BC. We have established a 1784-yr pine chronology centered in the Preboreal, and have linked it tentatively to the absolutely dated oak master. We present here calibration data based on this link, for the age range, 7145–9439 BC.

CHRONOLOGIES

The age range, 7145–7875 BC, is represented by the oak chronology, 'Main 9'. The ^{14}C analyses are spaced unevenly, as some of them were performed on floating sections, which later were integrated into the absolute chronology. The age range, 7833–9439 BC, is covered by the 1784-yr pine chronology. In an earlier publication, we derived a minimum absolute age of this series with respect to the absolute oak master by inspection of the century-type ^{14}C oscillation at the respective ends of the chronologies (Becker, Kromer & Trimborn 1991). Since then, a tentative link based on ring-width pattern has been found (see Becker 1992) leading to a shift of 74 yr toward older ages with respect to the minimum position. We calculated the calibration data based on this tentative link (Fig. 1, Table 1).

WOOD PRETREATMENT

All wood samples were chopped to 2–4 mm pieces and pretreated using the acid-alkali-acid (AAA) procedure; for the pine samples, resins were removed prior to the AAA treatment by an overnight soxhlet extraction (cyclohexane/methanol 2:1). Our adaption of the AAA sequence is as follows: 4% NaOH solution at 80°C overnight, 4% HCl at 80°C for 30 min, rinsing with hot water, 4% NaOH at 80°C for 30 min (rinsing and NaOH steps repeated up to three times until the solution becomes sufficiently transparent), 4% HCl at 80°C for 30 min and, finally, rinsing to pH 7. The yield of this procedure is between 40 to 60% by weight. Generally, we used 2–10 rings for a sample.

MEASUREMENTS

The samples (4g C) were counted in CO_2 proportional counters for 7–10 days. All ages are normalized to oxalic acid and are corrected for isotope fractionation (Stuiver & Polach 1977). Generally, the 1 σ error is between 20 and 30 yr.

CALIBRATION CURVES

Calibration curves based on the German oak and pine chronologies are shown in Figure 1A–E. As explained above, the calibrated ages prior to 7800 BC are tentative, as more trees are needed to improve the link of the two chronologies.

Throughout the age interval covered by the series, strong ^{14}C oscillations are apparent; the corresponding ^{14}C age plateaus occur at 8250, 8750, 9600 and 10,000 BP. The latter corresponds to the end of the Younger Dryas event, preventing an accurate calibration of this important transition to the Holocene. However, from stable isotope measurements of the pine series (Becker, Kromer & Trimborn 1991) and based on the link discussed above, we obtain an age of 11,050 cal BP for the beginning of climatic amelioration in central Europe.

ACKNOWLEDGMENTS

C. Junghans performed the ^{13}C analyses. P. Reimer drafted the calibration curves. We thank M. Stuiver for stimulating discussions.

REFERENCES

Becker, B. 1992. A 11,000 year long German oak and pine dendrochronology for radiocarbon calibration. *Radiocarbon*, this issue.

Becker, B., Kromer, B. and Trimborn, P. 1991 A stable isotope tree-ring timescale of the Late Glacial/Holocene boundary. *Nature* 353: 647–649.

Stuiver, M. and Kra, R. S., eds., 1986 Calibration Issue. *In* Stuiver, M. and Kra, R. S., eds., Proceedings of the 12th International ^{14}C Conference. *Radiocarbon* 28(2B): 805–1030.

Stuiver, M. and Polach, H. 1977 Discussion: Reporting of ^{14}C data. *Radiocarbon* 19(3): 355–363.

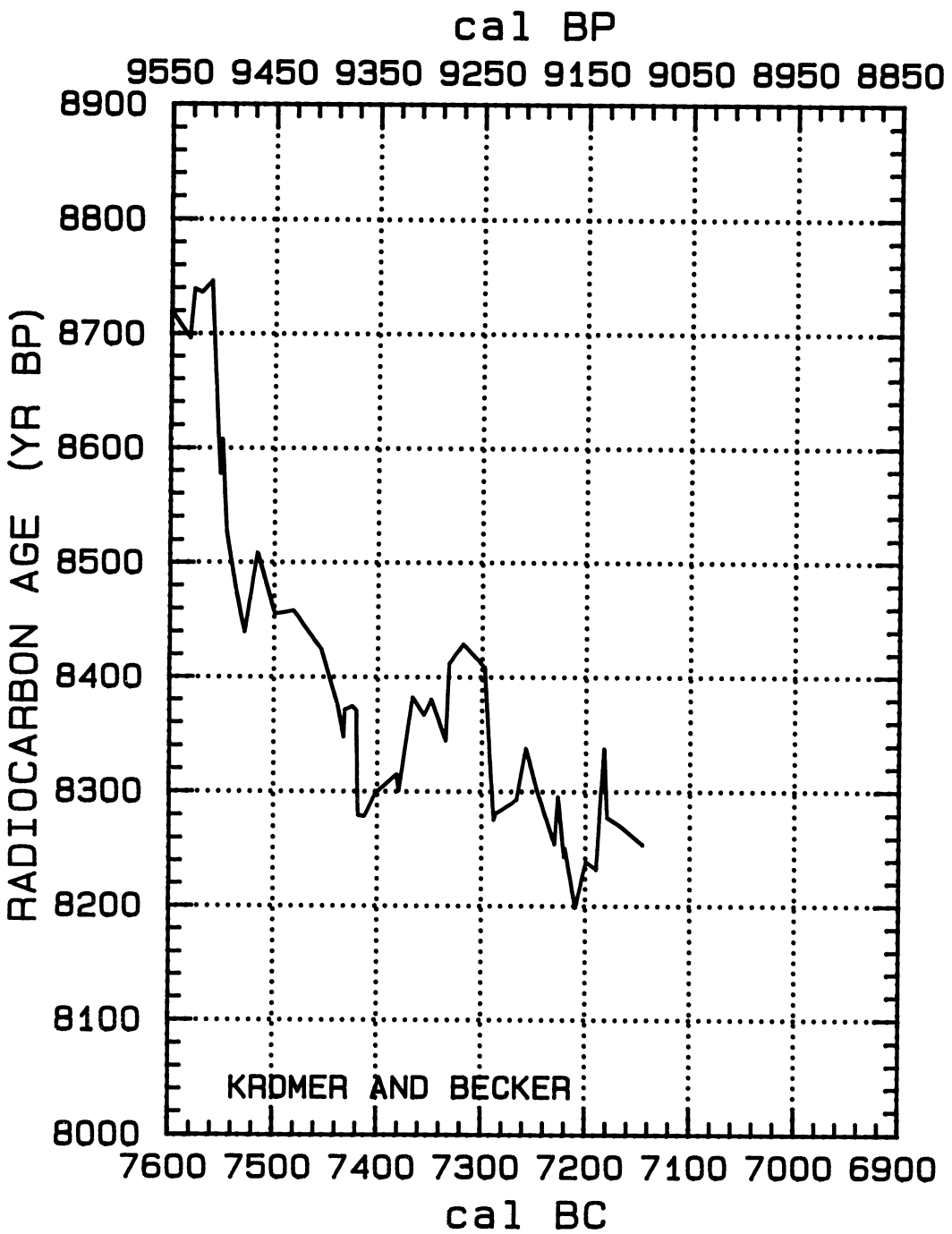

Fig. 1A–E. Calibration curves based on the German oak and pine chronologies

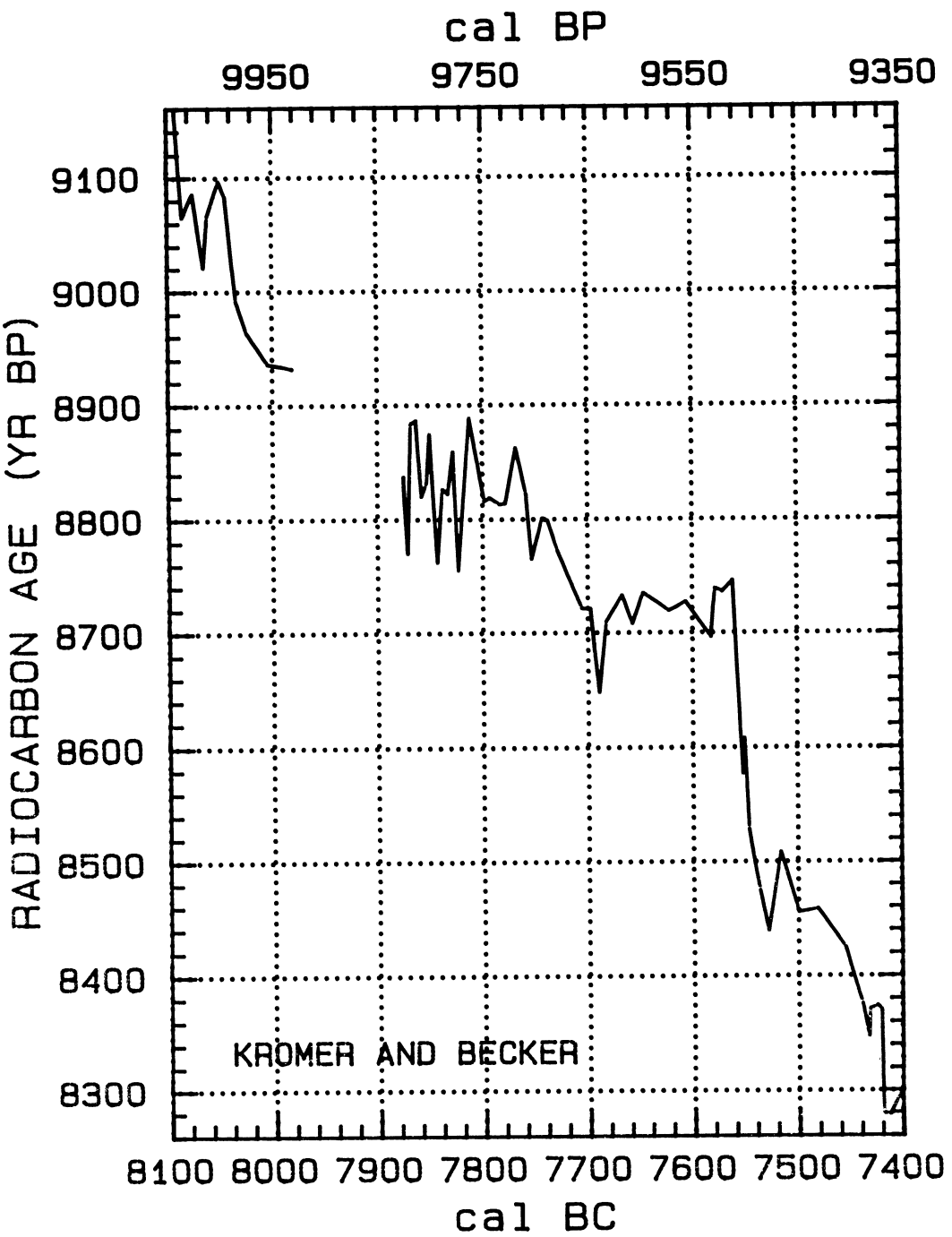
cal BP
9950
9750
9550
9350
9100
9000
8900
8800
8700
8600
8500
8400
8300
RADIOCARBON AGE (YR BP)
KROMER AND BECKER
8100 8000 7900 7800 7700 7600 7500 7400
cal BC

Fig. 1B

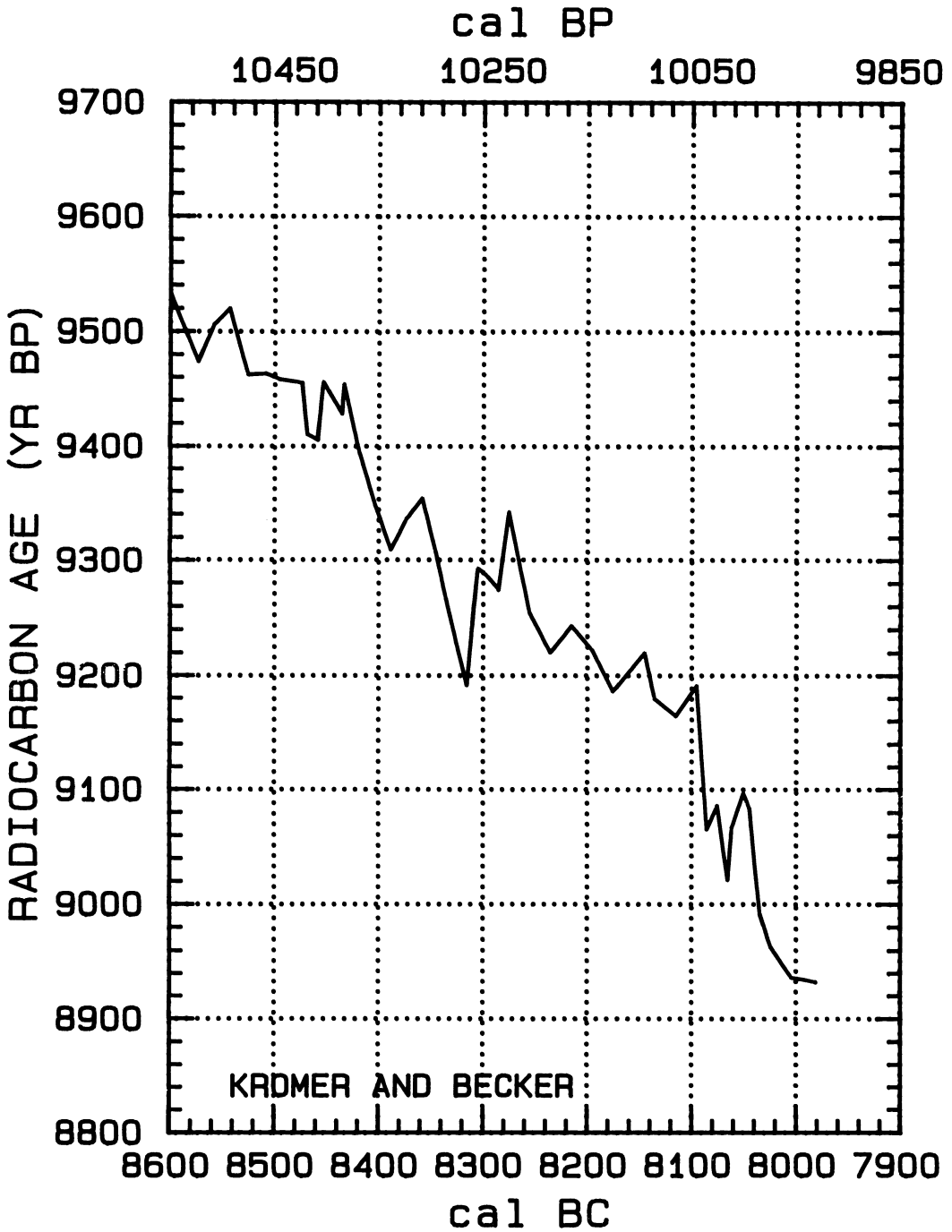
cal BP
10450
10250
10050
9850
9700
9600
9500
9400
9300
9200
9100
9000
8900
8800
RADIOCARBON AGE (YR BP)
KROMER AND BECKER
8600 8500 8400 8300 8200 8100 8000 7900
cal BC

Fig. 1C

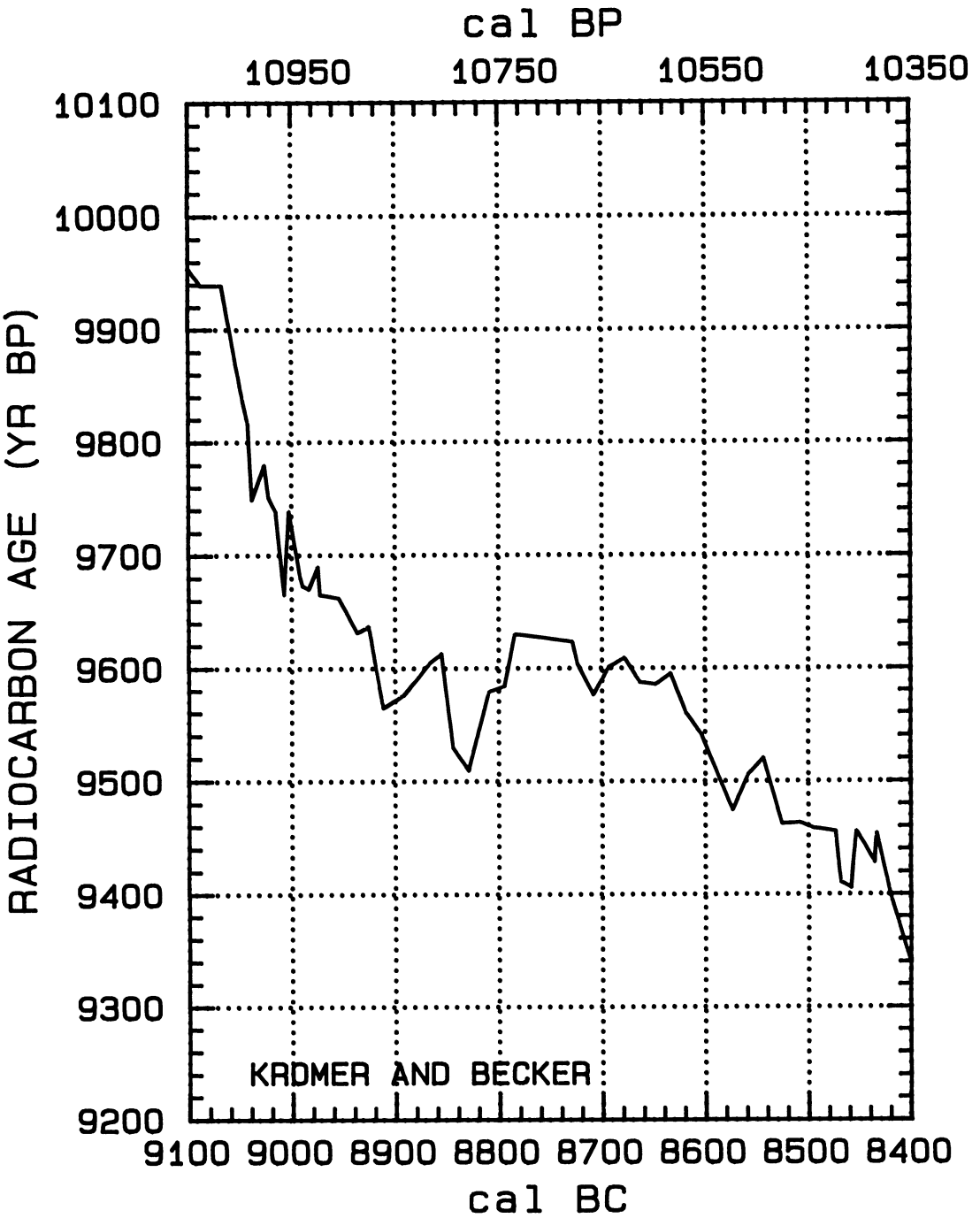
cal BP
10950
10750
10550
10350
10100
10000
9900
9800
9700
9600
9500
9400
9300
9200
RADIOCARBON AGE (YR BP)
KROMER AND BECKER
9100 9000 8900 8800 8700 8600 8500 8400
cal BC

Fig. 1D

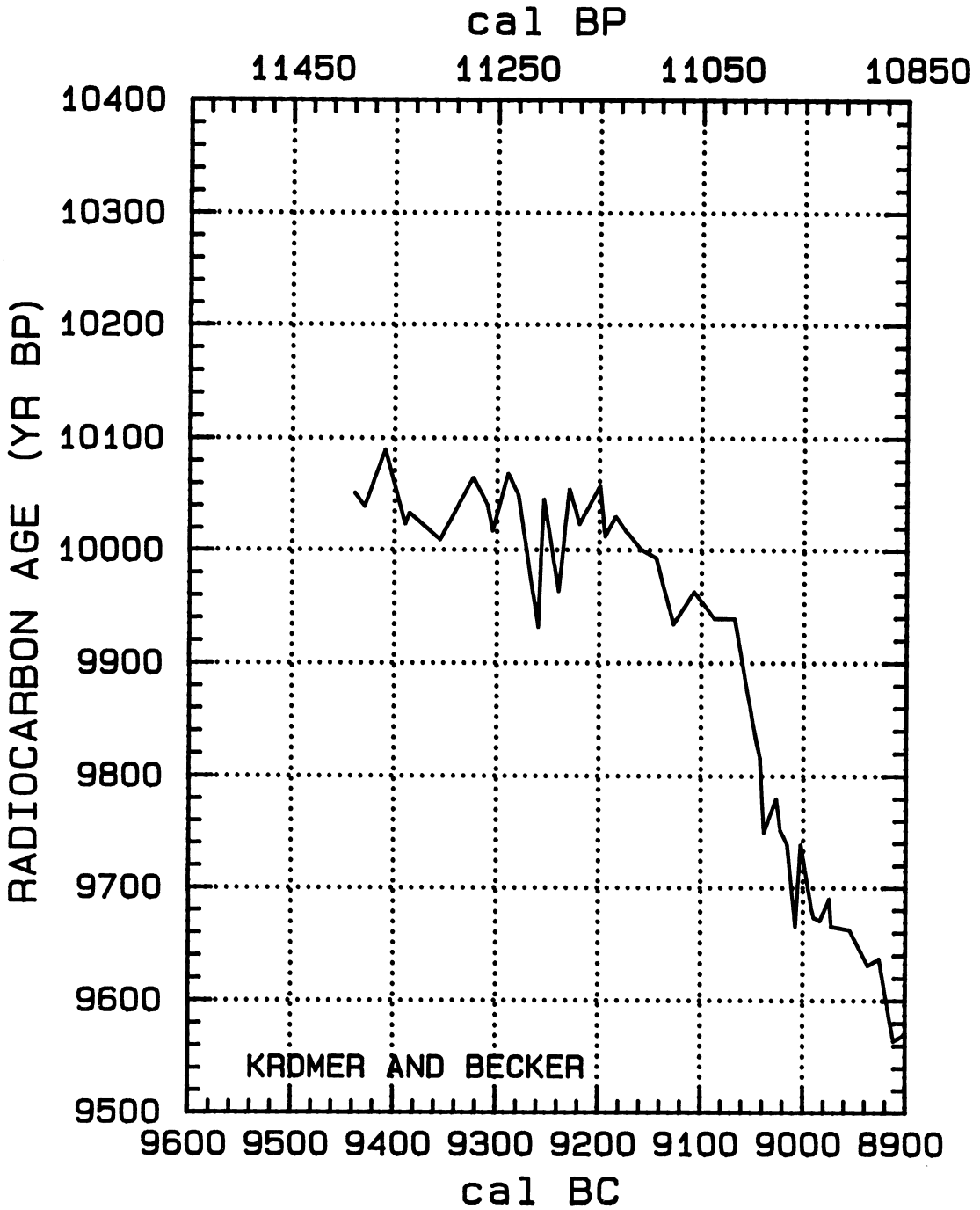
cal BP
11450
11250
11050
10850
10400
10300
10200
10100
10000
9900
9800
9700
9600
9500
RADIOCARBON AGE (YR BP)
KRDMER AND BECKER
9600 9500 9400 9300 9200 9100 9000 8900
cal BC

Fig. 1E

TABLE 1. Calibration data for the age range, 7200–9400 BC. The calibrated ages prior to 7800 BC are tentative (see text).

Lab. no.	Cal BC	^{14}C BP	±	Δ^{14}C	±
13511	−9439	10051	32	135	4
13512	−9429	10039	24	135	3
13525	−9409	10090	28	125	4
13526	−9389	10023	28	132	4
10567	−9385	10033	33	130	4
10568	−9355	10009	35	129	4
12888	−9323	10065	30	117	4
12945	−9309	10040	33	119	4
12959	−9304	10017	32	121	4
12960	−9289	10069	27	112	3
12964	−9279	10049	29	113	4
12987	−9259	9931	35	127	4
14220	−9254	10046	23	110	3
12988	−9239	9963	29	120	4
14159	−9229	10055	25	106	3
12999	−9219	10023	23	109	3
13000	−9199	10058	31	101	4
12967	−9194	10012	36	107	5
12968	−9184	10030	29	103	4
12981	−9174	10017	28	104	4
9097	−9159	9950	26	111	3
12982	−9159	10055	27	96	3
9098	−9144	9993	22	103	3
9118	−9127	9934	26	109	3
9119	−9107	9963	26	102	3
9126	−9087	9939	20	103	3
9127	−9067	9939	30	100	4
9134	−9047	9837	26	111	3
9810	−9042	9816	23	114	3
9969	−9038	9749	20	122	3
9811	−9026	9780	22	117	3
9135	−9022	9751	31	120	4
9970	−9015	9738	20	121	3
9807	−9007	9665	26	130	3
9153	−9002	9739	27	119	3
9808	−8991	9680	26	126	3
13009	−8989	9673	30	126	4
9836	−8983	9670	22	126	3
13010	−8974	9690	31	122	4
9837	−8972	9665	26	125	3
13059	−8954	9662	27	123	3
13087	−8936	9631	33	125	4
9844	−8925	9637	27	123	3
9853	−8911	9564	26	131	3
9864	−8891	9576	26	127	3
13088	−8866	9605	31	119	4
9865	−8855	9613	20	117	3

TABLE 1. (Continued)

Lab no.	Cal BC	^{14}C BP	±	$\Delta^{14}C$	±
13094	−8844	9529	21	127	3
13016	−8829	9509	35	128	4
13017	−8809	9579	35	115	4
13018	−8794	9584	23	112	3
14231	−8784	9630	22	105	3
9005	−8728	9623	16	98	2
8826	−8723	9603	23	100	3
8835	−8708	9576	19	102	2
8836	−8693	9601	18	97	2
8867	−8678	9609	19	93	2
8868	−8663	9587	20	94	3
8876	−8648	9585	20	93	3
8877	−8633	9595	20	89	3
8889	−8618	9559	25	92	3
8890	−8603	9540	20	93	3
8911	−8573	9474	34	98	4
8904	−8558	9506	34	92	4
8905	−8543	9520	34	88	4
8977	−8525	9462	25	93	3
8957	−8508	9463	34	91	4
8978	−8495	9458	24	90	3
8970	−8473	9455	34	87	4
9026	−8468	9410	19	93	2
8971	−8458	9405	34	92	4
9007	−8453	9456	15	85	2
8989	−8435	9428	18	86	2
9064	−8433	9454	27	82	3
9154	−8418	9394	26	88	3
9160	−8403	9348	25	93	3
9161	−8388	9309	25	96	3
9191	−8373	9336	26	90	3
9192	−8358	9354	32	86	4
9199	−8345	9307	30	91	4
10001	−8335	9266	24	95	3
10002	−8315	9191	27	102	3
10191	−8305	9293	29	87	4
10003	−8295	9285	20	87	3
10191	−8285	9274	28	87	4
10004	−8275	9342	22	77	3
10010	−8255	9254	25	86	3
10011	−8235	9220	25	88	3
10035	−8215	9243	25	82	3
10036	−8195	9222	25	82	3
10090	−8175	9186	22	85	3
10091	−8145	9220	22	76	3
10097	−8135	9179	21	80	3
10098	−8115	9164	21	80	3

TABLE 1. (Continued)

Lab no.	Cal BC	^{14}C BP	±	Δ^{14}C	±
10115	−8095	9191	23	73	3
10337	−8085	9065	25	89	3
10116	−8075	9086	25	85	3
10338	−8065	9021	25	92	3
10127	−8050	9097	25	80	3
9031	−8061	9067	23	86	3
9035	−8044	9083	26	81	3
8676	−8034	8991	28	92	4
9036	−8024	8963	23	95	3
9067	−8004	8936	25	96	3
9088	−7981	8932	22	93	3
11354	−7875	8883	48	86	6
14065	−7871	8770	22	101	3
12920	−7850	8875	40	84	5
9769	−7833	8856	22	84	3
9513	−7875	8820	30	95	4
14075	−7868	8884	20	85	3
9502	−7863	8887	30	84	4
14076	−7858	8820	21	92	3
9501	−7853	8832	30	90	4
14077	−7848	8842	26	88	3
9492	−7843	8762	30	98	4
14079	−7838	8827	23	89	3
9491	−7833	8760	30	97	4
14112	−7828	8860	21	83	3
9486	−7823	8755	30	97	4
9273	−7812	8889	30	77	4
9264	−7798	8816	30	85	4
14088	−7793	8819	22	84	3
9258	−7783	8813	30	83	4
14106	−7778	8814	23	83	3
9257	−7768	8863	30	75	4
14171	−7758	8822	23	79	3
9256	−7753	8765	30	86	4
9255	−7743	8801	30	80	4
14160	−7738	8799	23	79	3
14172	−7728	8772	22	82	3
8510	−7705	8721	30	86	4
8511	−7697	8721	30	85	4
8518	−7689	8648	30	94	4
8519	−7682	8710	30	84	4
8524	−7667	8733	30	79	4
8525	−7657	8708	30	81	4
8544	−7647	8735	30	76	4
8141	−7622	8719	30	75	4
8140	−7606	8727	33	72	4
8144	−7582	8696	30	73	4

TABLE 1. (Continued)

Lab no.	Cal BC	^{14}C BP	±	$\Delta^{14}C$	±
8091	−7578	8739	30	67	4
8286	−7571	8736	30	66	4
8145	−7561	8746	30	64	4
8295	−7552	8577	30	85	4
8244	−7550	8608	30	81	4
8127	−7546	8528	30	91	4
8151	−7536	8474	30	97	4
7758	−7528	8439	30	101	4
8171	−7516	8509	30	89	4
7759	−7499	8455	30	95	4
8273	−7481	8458	30	92	4
5768	−7454	8424	34	93	4
5173	−7438	8375	35	97	4
5429	−7432	8347	34	100	4
8304	−7431	8371	30	97	4
5453	−7424	8374	35	96	4
5430	−7420	8370	35	96	4
7760	−7418	8279	30	108	4
5057	−7412	8278	39	107	5
5058	−7401	8299	44	103	6
8086	−7381	8315	30	98	4
7757	−7379	8300	30	100	4
8306	−7366	8382	30	87	4
5469	−7355	8366	33	88	4
8117	−7348	8380	30	85	4
5494	−7334	8344	34	88	4
5400	−7331	8412	34	78	4
5115	−7318	8429	41	74	5
5170	−7297	8408	37	75	5
8247	−7288	8275	25	91	3
5121	−7286	8281	36	90	5
5264	−7266	8293	37	86	5
8248	−7257	8338	25	79	3
8190	−7247	8303	25	82	3
8191	−7229	8254	25	86	3
8689	−7226	8296	30	80	4
8285	−7220	8243	25	87	3
8717	−7219	8251	30	85	4
8718	−7209	8198	30	91	4
8719	−7199	8239	30	84	4
8720	−7189	8232	30	84	4
8248	−7182	8338	30	69	4
8750	−7179	8277	30	77	4
8751	−7168	8271	30	76	4
8181	−7145	8254	30	75	4

[RADIOCARBON, VOL. 35, NO. 1, 1993, P. 137–189]

MODELING ATMOSPHERIC ^{14}C INFLUENCES AND ^{14}C AGES OF MARINE SAMPLES TO 10,000 BC

MINZE STUIVER and THOMAS F. BRAZIUNAS

Department of Geological Sciences, Quaternary Research Center, and Joint Institute for the Study of the Atmosphere and Ocean (JISAO), University of Washington, Seattle, Washington 98195 USA

INTRODUCTION

The detailed radiocarbon age *vs.* calibrated (cal) age studies of tree rings reported in this Calibration Issue provide a unique data set for precise ^{14}C age calibration of materials formed in isotopic equilibrium with atmospheric CO_2. The situation is more complex for organisms formed in other reservoirs, such as lakes and oceans. Here the initial specific ^{14}C activity may differ from that of the contemporaneous atmosphere. The measured remaining ^{14}C activity of samples formed in such reservoirs not only reflects ^{14}C decay (related to sample age) but also the reservoir ^{14}C activity. As the measured sample ^{14}C activity figures into the calculation of a conventional ^{14}C age (Stuiver & Polach 1977), apparent ^{14}C age differences occur when contemporaneously grown samples of different reservoirs are dated.

A correction for the apparent age anomaly is possible when the reservoir-atmosphere offset in specific ^{14}C activity is known. The offset (*e.g.*, ^{14}C age of marine sample – ^{14}C age of atmospheric sample) is expressed as a reservoir ^{14}C age, R(t), which need not be constant with time. When constant, however, the reservoir sample ^{14}C age, A, can be reconciled with the atmospheric one by deducting R(t) from A. Similar reservoir age corrections would be possible for a variable R(t), but complications arise because information on R time dependency usually is lacking. However, R(t) can be accounted for in the world oceans by using a marine calibration curve derived from carbon reservoir modeling (Stuiver, Pearson & Braziunas 1986). In these calculations, atmospheric ^{14}C change is attributed to solar- and geomagnetic-induced ^{14}C production change. Climate-induced changes in global carbon reservoirs, which may repartition ^{14}C among reservoirs, are not accounted for in these calculations.

Measuring a marine calibration curve is complicated because most marine samples lack the continuity and fine structure of tree rings. The $^{234}U/^{230}Th$ dating of corals (Bard *et al.* 1993) provides a good cal age equivalent, but measuring errors in the $^{234}U/^{230}Th$ ratio and ^{14}C accelerator mass spectrometry (AMS) determinations are such that the (bi)decadal chronological detail achieved for tree rings is not possible. Such detail, however, can be realized by calculating the response of the world oceans to tree-ring derived atmospheric ^{14}C changes.

The long-term trend of the ^{14}C age *vs.* cal age curve for the world oceans parallels that of the atmosphere. Short-term (century) variations, however, are smoothed in the oceans. Thus, whereas a constant, R, could be used for long-term variations, the shorter-term variations cannot be accounted for in this manner. Use of constant, R, and the atmospheric calibration curve assumes that the features of the marine and atmospheric curves are identical. The consequences of the constant R approach are obvious when the cal ages of a marine and atmospheric sample with identical (reservoir-corrected) ^{14}C age + standard deviation are evaluated. Calibration of both *vs.* the atmospheric curve yields identical results, whereas, in fact, the cal age range (and average number of intercepts) should be less for most marine samples because of the smoothed nature of the marine curve.

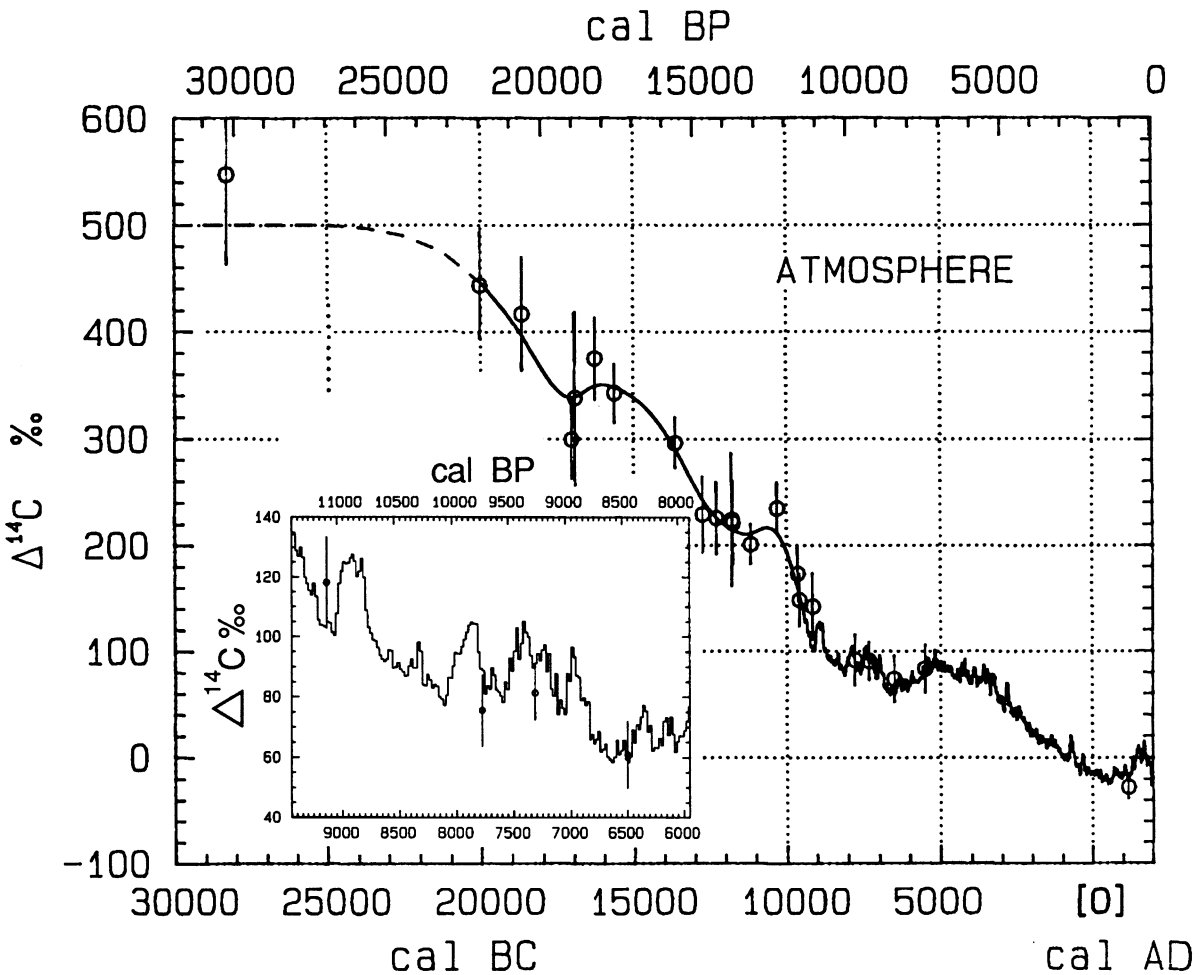

Fig. 1. The atmospheric $\Delta^{14}C$ record as derived from: dendrochronologically calibrated bidecadal tree-ring ^{14}C measurements (—— from 9440 BC to AD 1950), a cubic spline through the $^{234}U/^{230}Th$-calibrated coral ^{14}C averages corrected by 400 ^{14}C yr (—— from 20,000 to 9440 BC), and a smooth transition from an assigned pre-25,000 BC steady-state value of 500‰ (– –). The coral measurements (Bard *et al.* 1993) are shown as circles with 2 σ error bars. For the detailed coral/tree-ring comparison in the inset, the coral ages (1 σ error bars) were converted to cal ages using the marine calibration curve (Fig. 17) with $\Delta R = 0$.

Secular ^{14}C variations in the marine environment are represented by the modeled world ocean marine curve, but a world average curve does not account for the regional oceanic differences in specific ^{14}C activity; this is caused in part by regional variations in upwelling of ^{14}C-deficient waters. Here we define a region-specific ΔR term that represents the ^{14}C activity differences (in ^{14}C yr) of regional and world ocean surface layers. To a first order, the regional difference, ΔR, reflects oceanic mixing processes that contribute to the offset between regional and world ocean ^{14}C ages. Exchange with the atmosphere influences ΔR as well when regional atmospheric ^{14}C activity differs from the observed "global" ^{14}C activity. The ΔR term thus comprises two components: the portion of the shift in regional marine ^{14}C age attributable to a regional atmospheric ^{14}C age difference, and an additional shift in regional marine ^{14}C age, which reflects regional oceanic processes that differ from the parameters in the simulated global ocean.

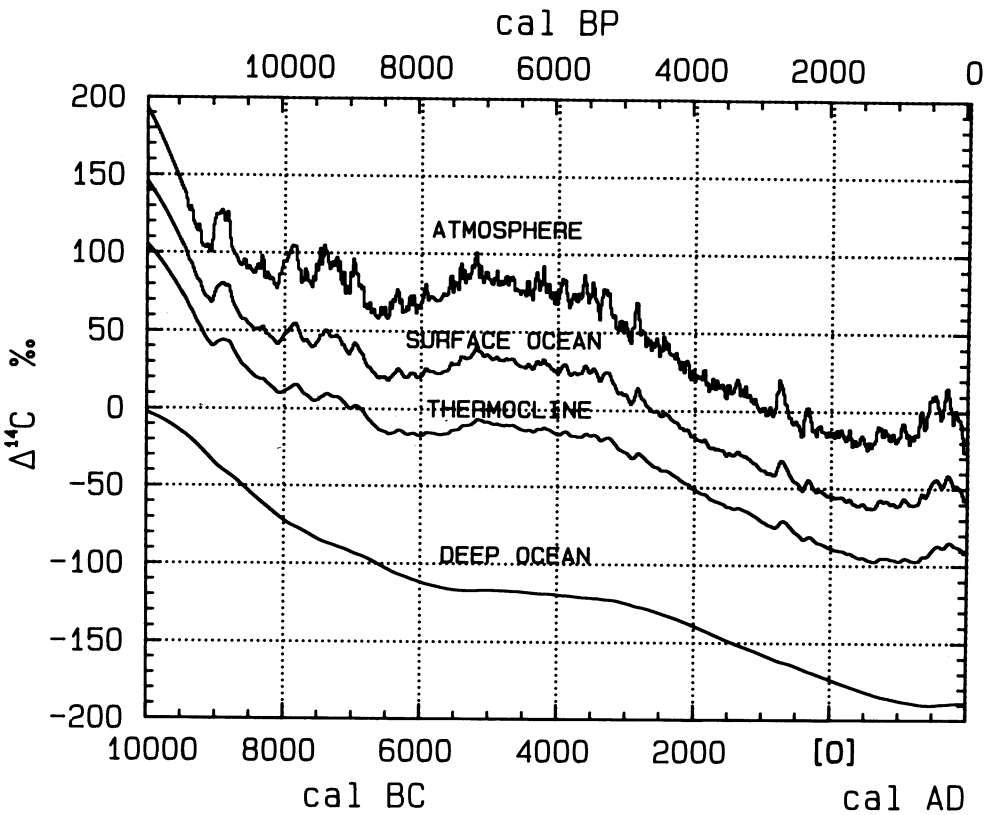

Fig. 2. Atmospheric $\Delta^{14}C$ (bidecadal values) as used for the model calculations and calculated surface ocean (0–75 m), thermocline (75–1000 m), and deep ocean (1000–3800 m) $\Delta^{14}C$ values

The R(t) term (incorporated in the global marine curve) accounts for secular changes, whereas ΔR represents the time-independent (as a first approximation) regional offsets from the world ocean ^{14}C age. The ΔR term corrects for regional activity differences in the calibration process, and can be determined from ^{14}C ages of marine samples of known historical age (Stuiver, Pearson & Braziunas 1986). A regional reservoir age, R′(t), on the other hand, represents a difference in ^{14}C age between the regional atmosphere and regional surface ocean. Thus, R′(t) = global R(t) + ΔR − ΔRa, in which ΔRa is the ^{14}C age difference between the regional atmosphere and our "global" (northern hemisphere tree-ring-based) atmospheric data base.

Previously, we did not consider regional variations in atmospheric ^{14}C activity. Then, ΔRa is zero, and the region-specific shift in marine ^{14}C age, ΔR, is equivalent to the regional reservoir age offset. For southern hemisphere samples, ΔRa = 40 ^{14}C yr (Vogel *et al.* 1993); in the northern hemisphere, ΔRa = 0. The atmospheric ^{14}C variations within each hemisphere representing decade-scale age differences have been neglected. These relations do not affect the calibration process, but the calculation of regional reservoir ages of the southern hemisphere entails the 40-^{14}C-yr adjustment.

The history of ^{14}C variations in the surface layer of the world ocean was previously modeled to about 7000 BC (Stuiver, Pearson & Braziunas 1986). We now use the extended and improved atmospheric record (Stuiver & Reimer 1993; summary of data from Bard *et al.* 1993; Kromer & Becker 1993; Pearson & Stuiver 1993; Pearson, Becker & Qua 1993; Stuiver & Pearson 1993) to

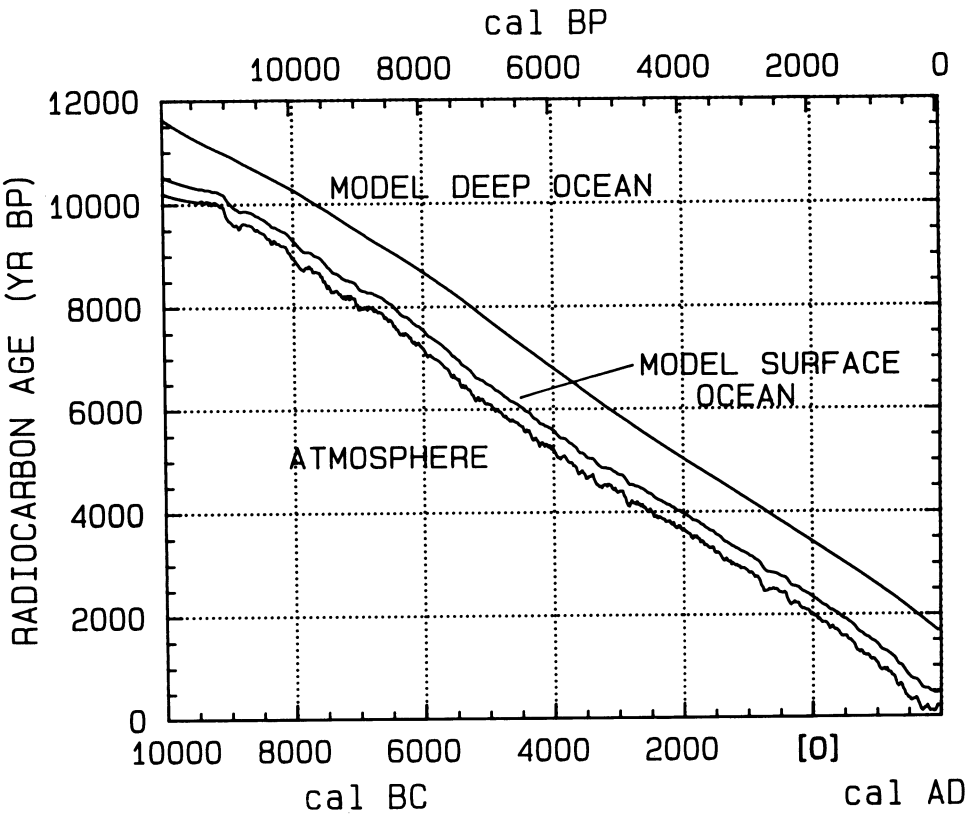

Fig. 3. ^{14}C ages of atmospheric samples (bidecadal values) and calculated conventional ^{14}C ages of the surface (0–75 m) and deep ocean (1000–3800 m)

generate the world ocean marine variations to 10,000 BC (≈10,200 ^{14}C yr BP). Because minor corrections had to be applied to the previously used tree-ring record, the model results are given for the entire AD 1950–10,000 BC interval.

THE GLOBAL CARBON MODEL

The global box-diffusion model, described originally in Oeschger *et al.* (1975), produces globally integrated depth-dependent marine ^{14}C variations in response to changes in atmospheric ^{14}C activity, as represented by the tree-ring (and coral) record. As previously indicated (Stuiver, Pearson & Braziunas 1986), we treat as constant the climate-influenced mixing parameters of the model (F, the air-sea CO_2 gas exchange rate; K_z, the oceanic vertical diffusion coefficient; and B_F, the air-land biospheric carbon uptake and release). We attribute the observed atmospheric $\Delta^{14}C$ (defined in Stuiver & Polach 1977) variability of at least the last 11,650 cal yr to solar (heliomagnetic) and geomagnetic modulation of the ^{14}C production rate, Q, induced by the cosmic-ray flux.

The parameter values and all reservoir CO_2 values remain as described for the earlier model version (Stuiver, Pearson & Braziunas 1986). Ocean exchanges (F = 19 moles m^{-2} yr^{-1} and K_z = 1.26 cm^2 sec^{-1}) are again calibrated to produce a surface ocean $\Delta^{14}C$ close to −50‰ (R ≈ 400 yr) and deep ocean (below 1 km) $\Delta^{14}C$ of −190‰ (R ≈ 1700 yr) for the bidecade centered at AD 1830. We arbitrarily chose the AD 1830 bidecade to use for model calibration; however, the model surface ocean $\Delta^{14}C$ of −46‰ for AD 1700 to AD 1900, which may better represent recent average

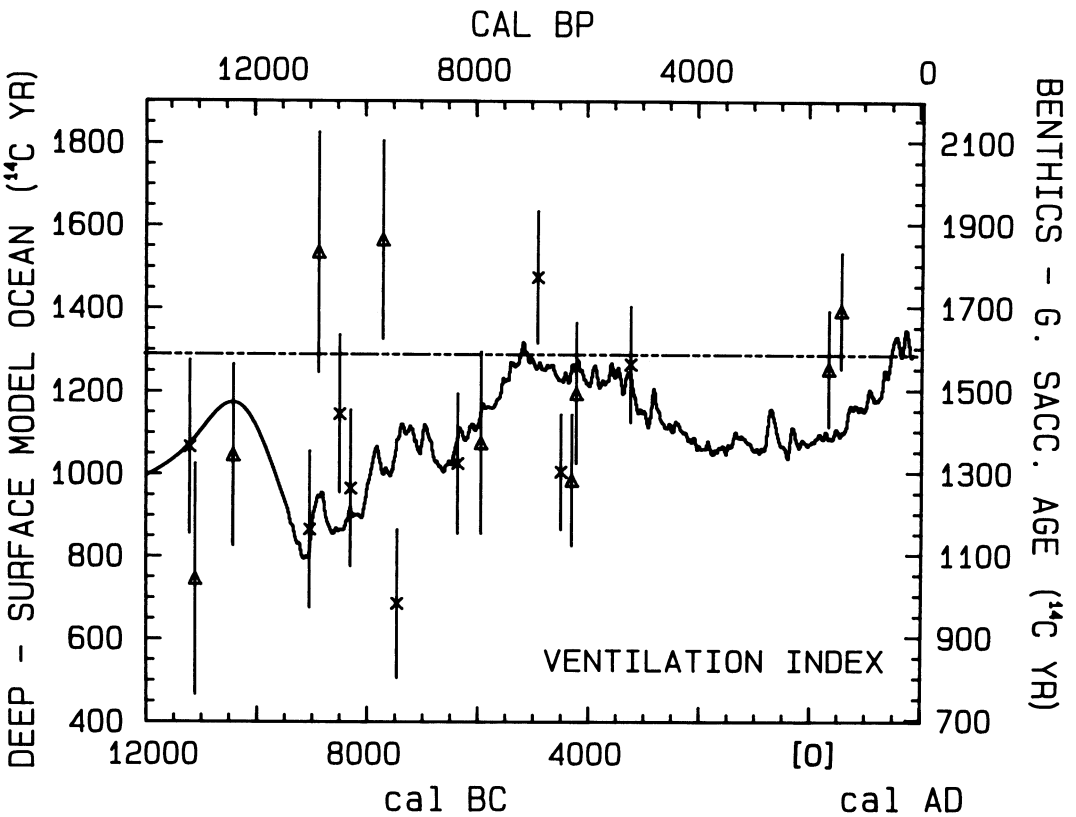

Fig. 4. The calculated deep ocean-surface ocean ^{14}C age differences (——) compared to benthic-planktonic foraminifera differences measured by Andrée *et al.* (1986) for the South China Sea (× = Core V35-6, Δ = Core V35-5). The deep water in the South China Sea is more ^{14}C deficient than our model ocean, causing a shift between the ventilation scales of 1585 (latest pre-anthropogenic age difference in Andrée *et al.* 1986) minus 1290 ^{14}C yr (model AD 1830 value), both indicated by (– – —). Ventilation calculations end in AD 1830, as fossil fuel CO_2 influences the latter part of the $\Delta^{14}C$ record. The planktonic foram age determinations were calibrated by using our marine calibration curve with $\Delta R = 0$.

natural conditions, also coincides with the observed "pre-industrial" estimate of −45 ± 15‰ (Broecker *et al.* 1979; Lassey, Manning & O'Brien 1990).

Emphasis here is on the Holocene time interval, *i.e.*, the last 10,000 ^{14}C yr. The beginning of this interval corresponds to an uncertain cal age, because the atmospheric calibration curve flattens near 10,000 ^{14}C yr BP. Prior to 9440 BC, our model ocean responds to a 10,560-yr history of atmospheric $\Delta^{14}C$ derived from the $^{234}U/^{230}Th$-calibrated coral ^{14}C activities (Bard *et al.* 1993; Stuiver & Reimer 1993). The spline through the coral-based atmospheric $\Delta^{14}C$ determinations (coral dates are corrected by 400 ^{14}C yr) is extrapolated to a pre-25,000 BC steady-state value of 500‰ (Fig. 1). The global model starts at 30,000 BC with this initial atmospheric $\Delta^{14}C$ condition, and calculates both a ^{14}C-production-rate history and an oceanic $\Delta^{14}C$ response curve compatible with the coral and tree-ring ^{14}C time series.

The reliability of the coral *vs.* tree-ring derived atmospheric $\Delta^{14}C$ values was verified by Bard *et al.* (1990) using a constant 400-yr reservoir age correction. More detailed reservoir age corrections are incorporated in the calibration curves of Figure 17. Although application of these curves minimizes coral/tree-ring differences (see Fig. 1 inset), a crucial offset near 11,100 cal BP remains.

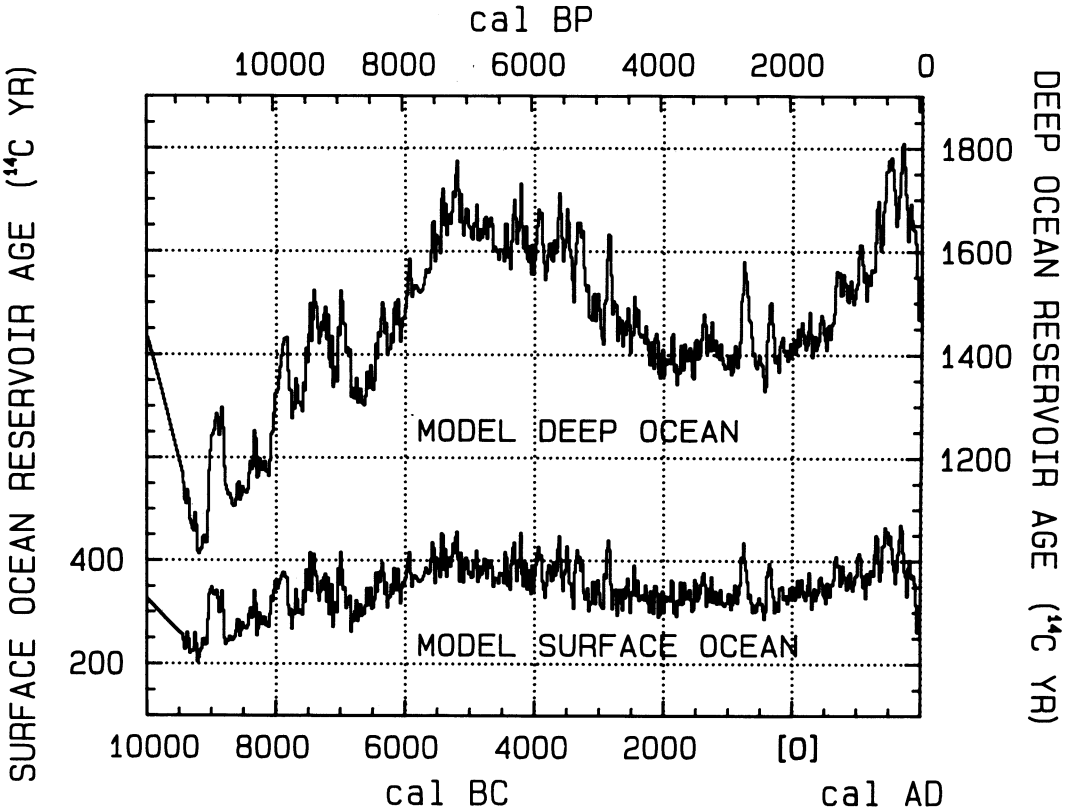

Fig. 5A. Variations in model-calculated reservoir ages R(t) of the surface ocean (bottom curve and left axis) and deep ocean (top curve and right axis) plotted by cal yr.

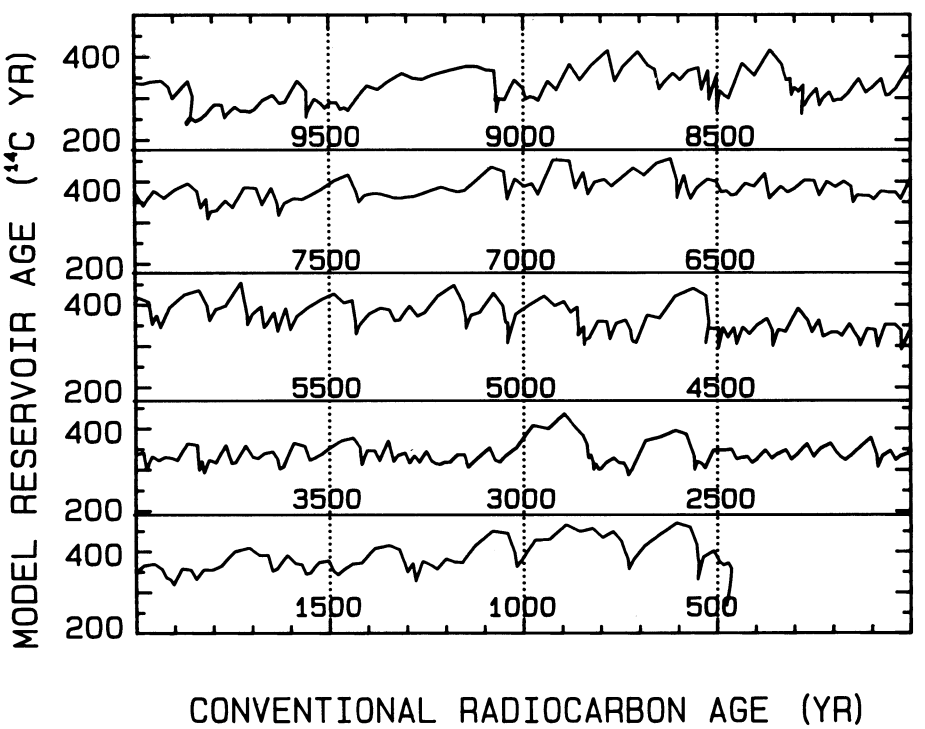

Fig. 5B. Variations in model-calculated surface ocean reservoir age, R(t), plotted *vs.* model-defined conventional ^{14}C age of surface-ocean waters. Each segment covers 2000 ^{14}C yr. Multiple intercepts occasionally occur for individual ^{14}C ages.

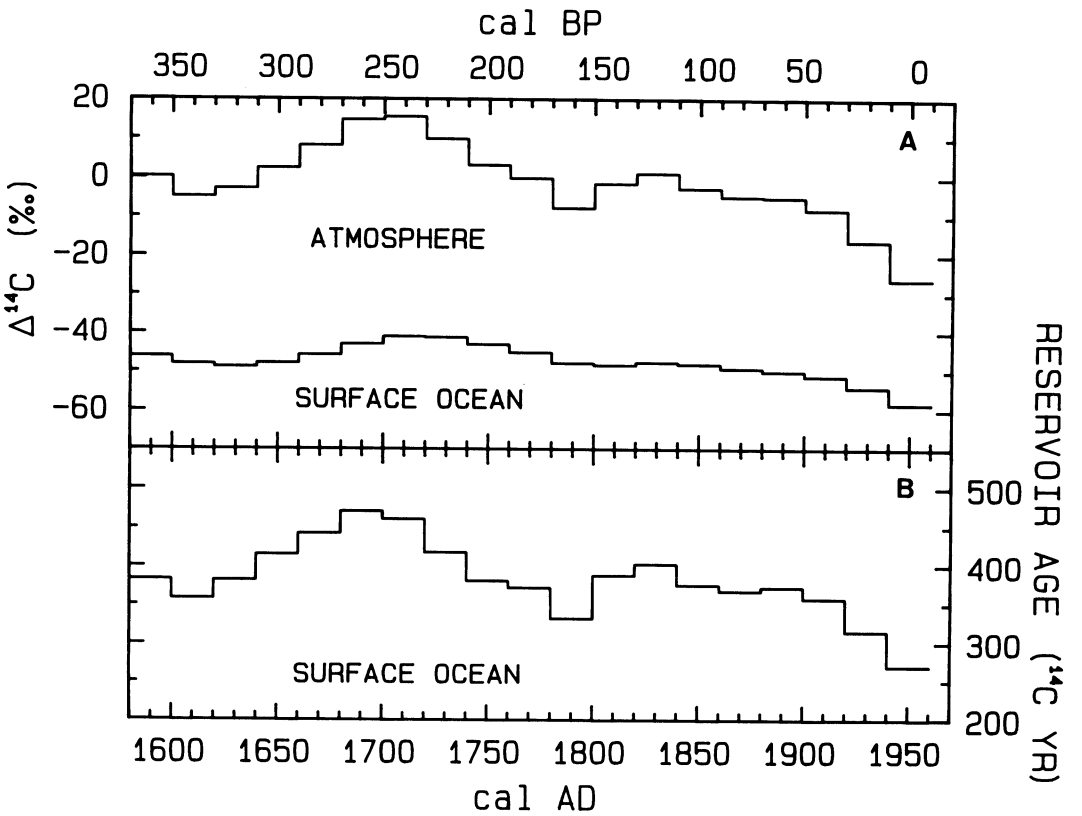

Fig. 6. A. $\Delta^{14}C$ of the atmosphere and surface ocean. B. Surface ocean reservoir ages from AD 1600 to 1950.

As a first approximation, the model exchange parameters are constant during our 32,000-yr simulation, despite significant changes in atmosphere, ocean and terrestrial biosphere dynamics that occurred before 10,000 ^{14}C yr BP; these changes were associated with the glacial-interglacial climate transition (Adams *et al.* 1990; Broecker & Denton 1989). Three lines of evidence suggest that the differences among glacial, deglaciation and interglacial conditions had secondary effects on atmospheric (and oceanic) $\Delta^{14}C$ after 10,000 BC.

First, the model-derived ^{14}C production history agrees with the Q trend expected from documented changes in the geomagnetic dipole over the past 30,000 cal yr, such that no major climatic (oceanic) explanation for millennium-scale atmospheric $\Delta^{14}C$ variations is required (Bard *et al.* 1990; Stuiver *et al.* 1991; Mazaud *et al.* 1991).

Second, carbon model sensitivity tests show that the global-scale ^{14}C reservoirs respond relatively quickly to changes in ocean mixing processes, such that Holocene atmospheric and oceanic $\Delta^{14}C$ levels will have recovered substantially after 2000 cal yr (ocean turnover time) from any pre-Holocene climatic divergences (Braziunas 1990). Such model studies also show that surface ocean ^{14}C closely tracks changes in atmospheric ^{14}C, and that variations in reservoir age for much of the ocean surface generally will not exceed ± 100 ^{14}C yr (Bard 1988). Greater surface-ocean reservoir age variations, up to 200 ^{14}C yr, may also occur in response to sharp Q-induced shifts in atmospheric ^{14}C activity.

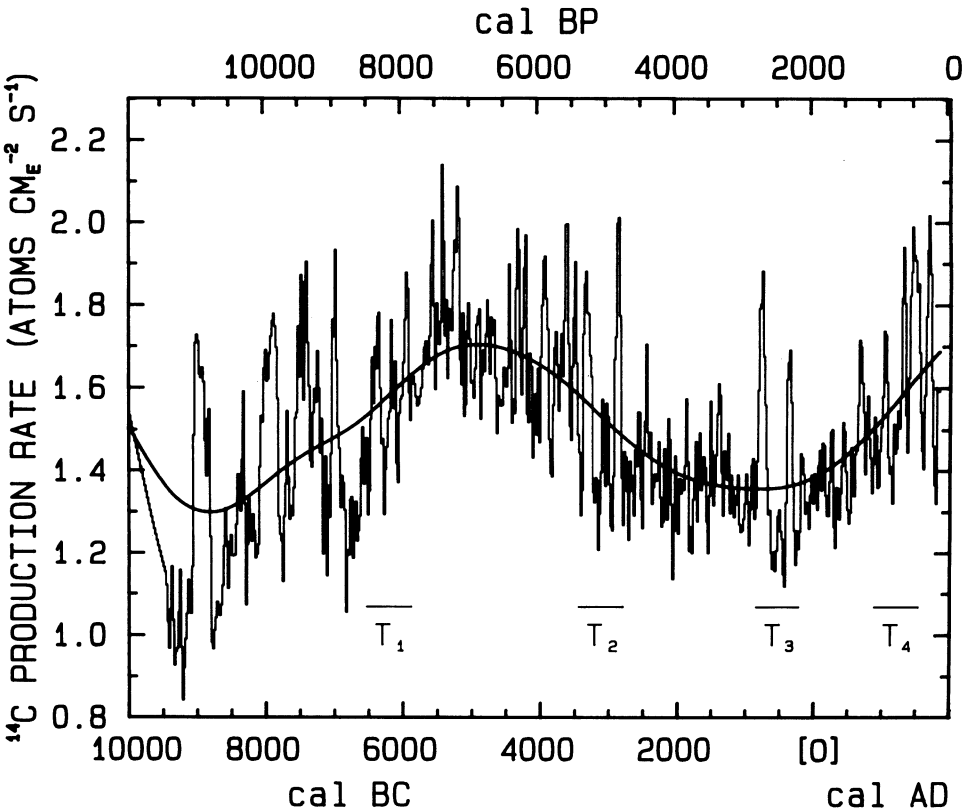

Fig. 7. ^{14}C production rate variations Q back to 10,000 BC. Q was calculated by using atmospheric Δ^{14}C variations (Fig. 1) as carbon reservoir model input. Triplet episodes (Stuiver & Braziunas 1989) are identified as T1–T4. The long-term spline approximates a 2000-yr moving average. The input for the first 500 yr is based on the coral spline, the remaining portion on the tree-ring record.

Finally, the available ^{14}C age differences between contemporaneous deep- and surface-dwelling foraminifera, as measured by AMS, suggest a relatively constant oceanic mixing rate over the past 12,500 ^{14}C yr (see below).

Several factors complicate the simple calculation of global oceanic ^{14}C responses. Distinctions in oceanic mixing between high- and low-latitude ocean regions may lead to dissimilar trends in surface-ocean Δ^{14}C (Toggweiler & Sarmiento 1985; Bard 1988), contrary to our notion of parallel oceanic calibration curves. Also, although the model-derived Q record fits with first-order geomagnetic forcing, uncertainties in the geomagnetic dipole record allow for significant climatic contributions to the atmospheric Δ^{14}C record. We do consider these to be of second-order importance for the Holocene, and note that measurements of pre-Holocene coral (Bard *et al.* 1993) establish a directly measured marine calibration curve for the 10,000–20,000 BC interval.

Despite an identical calibration procedure, our current marine simulation yields Δ^{14}C = −47.7‰ (R = 402 ^{14}C yr) for AD 1830, instead of −49.7‰ (R = 409 ^{14}C yr) reported in Stuiver, Braziunas and Pearson (1986). This difference is related to: 1) slight changes to the atmospheric ^{14}C data base; and 2) an explicit incorporation into the model of reservoir ^{13}C/^{12}C distinctions, rather than simple application of fractionation-corrected ^{14}C activities. Our choices for air-sea and terrestrial fractionation factors (Siegenthaler & Münnich 1981; Keeling 1973) fix δ^{13}C of the atmosphere at

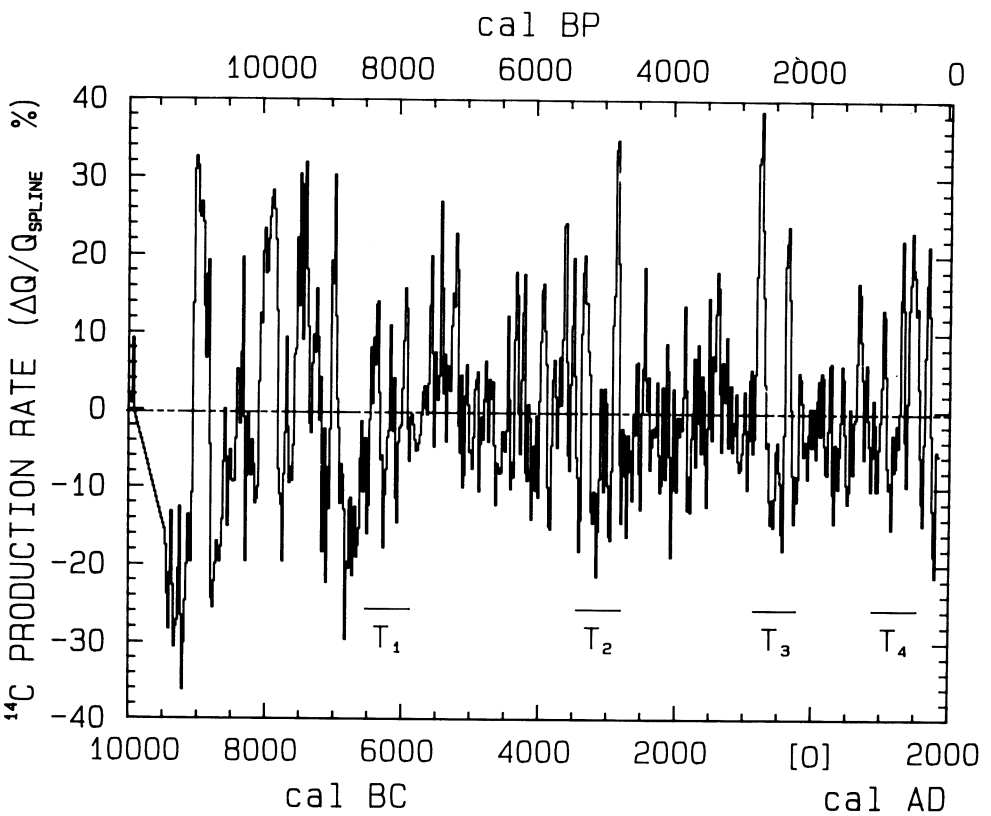

Fig. 8. Relative detrended model calculated ^{14}C production rate variations (for $\Delta Q/Q_{spline}$ definition, see text) for the last 12,000 yr. Triplet episodes are identified as T1–T4. The input for the first 500 yr was based on the Fig. 1 coral spline, that of the remaining interval on the tree-ring record (see Fig. 1).

−7‰, and of the ocean at 0.92‰, with $\delta^{13}C$ of the terrestrial biosphere set at −25‰. Relative to the simpler modeling approach without explicit fractionation, absolute rates of ^{14}C production and decay are elevated ≈ 5%, and ocean $\Delta^{14}C$ levels are affected by 1‰, because absolute oceanic ^{14}C activities are enhanced. The surface-ocean reservoir age of 402 yr also reflects the non-zero atmospheric $\Delta^{14}C$ value of 1.2‰ in AD 1830.

Model Calculations

Figure 2 shows the post-10,000 BC atmospheric (tree-ring) $\Delta^{14}C$ bidecadal record and the model-derived global marine response for surface (0–75 m depth), thermocline (75–1000 m), and deep (1000–3800 m) waters. The corresponding ^{14}C age *vs.* cal age plots are depicted in Figure 3. The 10,000–9440 BC portion of the atmospheric curve derived from the pre- and early Holocene spline representing the coral-based $\Delta^{14}C$ trend (Figure 1). As discussed above, our simulation produces marine $\Delta^{14}C$ and ^{14}C-age time series in response to changes in ^{14}C production rate, rather than climatic variations, because changes in climate during the last deglaciation are not considered in the model. Uncertainties in our model-based ocean reservoir ages that are related to the measure ment standard deviations, σ, *i.e.*, ± 1–8‰ for tree-ring data and ± 10–25‰ for coral data, were estimated by adding ± 1 σ to the Figure 1 data. The later Holocene portions of the oceanic curves generated by the model differ between these extremes (± 1 σ) by generally <20 ^{14}C yr.

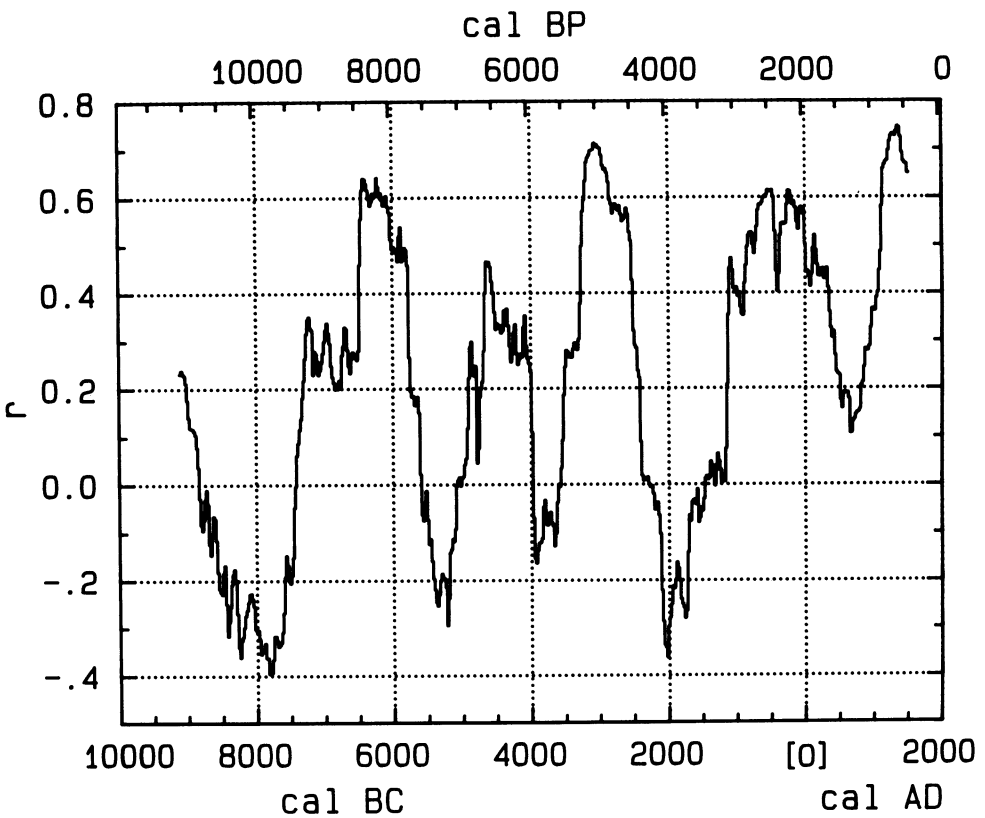

Fig. 9. Correlation coefficient, r, of a 700-yr sliding portion of the ^{14}C production rate with the curve generated from Eq. (1) of Stuiver and Braziunas (1989), as discussed in the text. The 700-yr sliding window results in a loss of 350 yr at either end of the curve.

AMS ^{14}C age measurements on contemporaneous benthic and planktonic foraminifera (Andrée *et al.* 1986; Shackleton *et al.* 1988) suggest that major changes in the rate of deep-ocean ventilation occurred prior to (but not after) 12,500 ^{14}C yr BP. The $\delta^{13}C$ record from a sediment core in the deep Southern Ocean is also consistent with a sharp transition in the influx of ^{13}C-enriched North Atlantic Deep Water at *ca.* 12,500 ^{14}C yr BP, followed by essentially modern conditions for deep-water ventilation (Charles & Fairbanks 1992). In Figure 4, the modeled ^{14}C age differences (ventilation ages) between deep ocean and surface ocean are compared to foraminifera ^{14}C data for the post-12,000 BC era. The foraminifera ^{14}C data were calibrated using the marine calibration curve (part of which is shown in Figure 17, explained below) with $\Delta R = 0$. Such an approximate calibration is needed; otherwise, calendar foraminifera dates may be too young by up to 2000 cal yr. The agreement shown in Figure 4 supports the validity of our modeling approach.

Model reservoir ages are plotted *vs.* cal age in Figure 5A; Figure 5B gives more detail of surface-ocean reservoir ages *vs.* conventional ^{14}C ages. The century-type variations in deep-ocean reservoir ages (Fig. 5A) reflect the atmospheric $\Delta^{14}C$ change relative to a "constant" deep-ocean $\Delta^{14}C$ level; the corresponding surface-ocean reservoir age changes are smaller, because the surface ocean can react on this time scale to the atmospheric $\Delta^{14}C$ change.

For the past 7000 cal yr, the new surface-ocean-model reservoir ages differ by only two decades from those calculated in Stuiver, Braziunas and Pearson (1986). A difference in input for the older

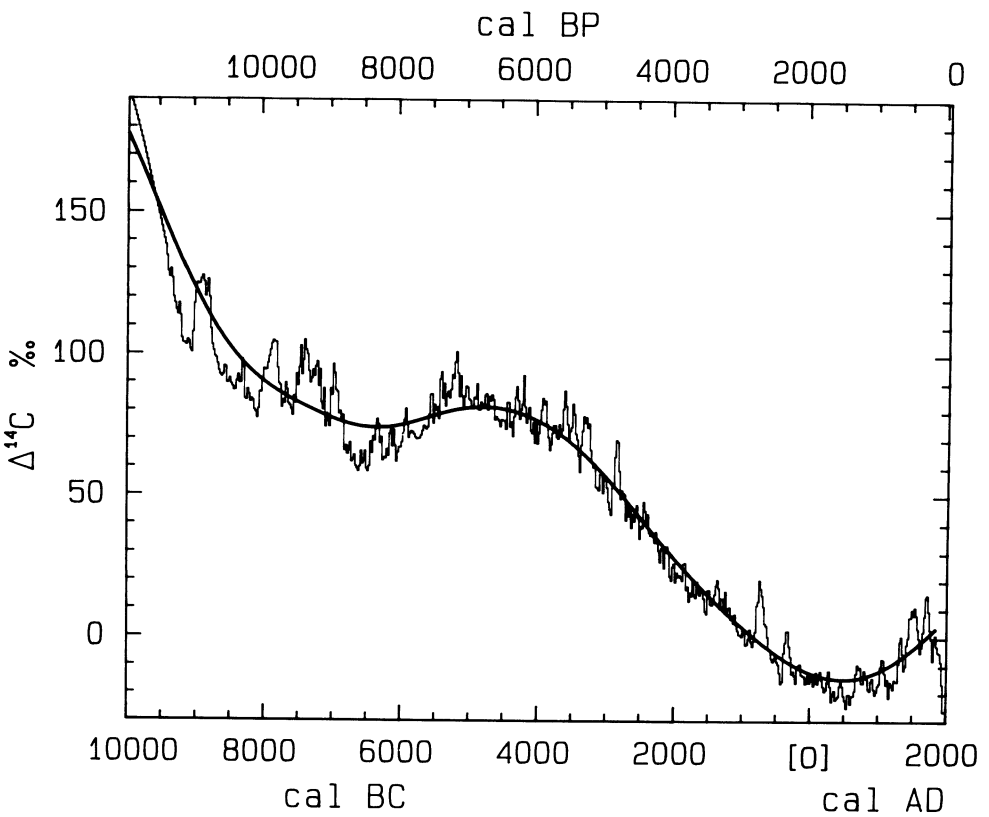

Fig. 10. Atmospheric $\Delta^{14}C$ (coral-derived for the first 500 yr, see Fig. 1) for the past 12,000 yr. The long-term $\Delta^{14}C$ spline was calculated from the Fig. 7 Q spline, but resembles a 2000-yr $\Delta^{14}C$ moving average as well.

part of the record (steady-state in 1986 paper *vs.* coral-based on long-term atmospheric $\Delta^{14}C$ decline now) results in surface-ocean reservoir age discrepancies of generally less than 50 but up to 140 yr for the 7000–9000 cal yr BP interval.

Surface-ocean $\Delta^{14}C$ and reservoir age from AD 1600–1950 are depicted in Figure 6. Alternative pre-Holocene conditions do not change this recent portion of model ocean history. The AD 1950 "bidecade," in effect, does not consider post-AD 1954 nuclear bomb ^{14}C activity changes. It should be noted that the new atmospheric ^{14}C data base and the treatment of the terrestrial biosphere, as well as mixed reservoirs, modifies the results of our calculations compared to earlier studies (*e.g.*, Stuiver *et al.* 1991; Oeschger *et al.* 1975). A change to a model with increased carbon storage in the terrestrial biosphere and ocean (*e.g.*, Damon 1988), balanced by increased (from 1.6 to 2.15 ^{14}C atoms $cm^{-2}sec^{-1}$ averaged over the Holocene) equilibrium Q values more reflective of present neutron flux measurements (*e.g.*, Lingenfelter & Ramaty 1970), yields only slightly different (<15 ^{14}C yr) calibration curves. The calculated Q history does not change in fine structure, and displays only a nearly uniform shift throughout the last 12,000 cal yr.

Spectral Properties and Model-Derived ^{14}C Production Rate *vs.* Oceanic Variations

Model calculations yield information on atmospheric $\Delta^{14}C$ values, production rates, Q, and alternative changes in oceanic mixing rates K_z, and demonstrate the validity of the production modulation approach to calibration.

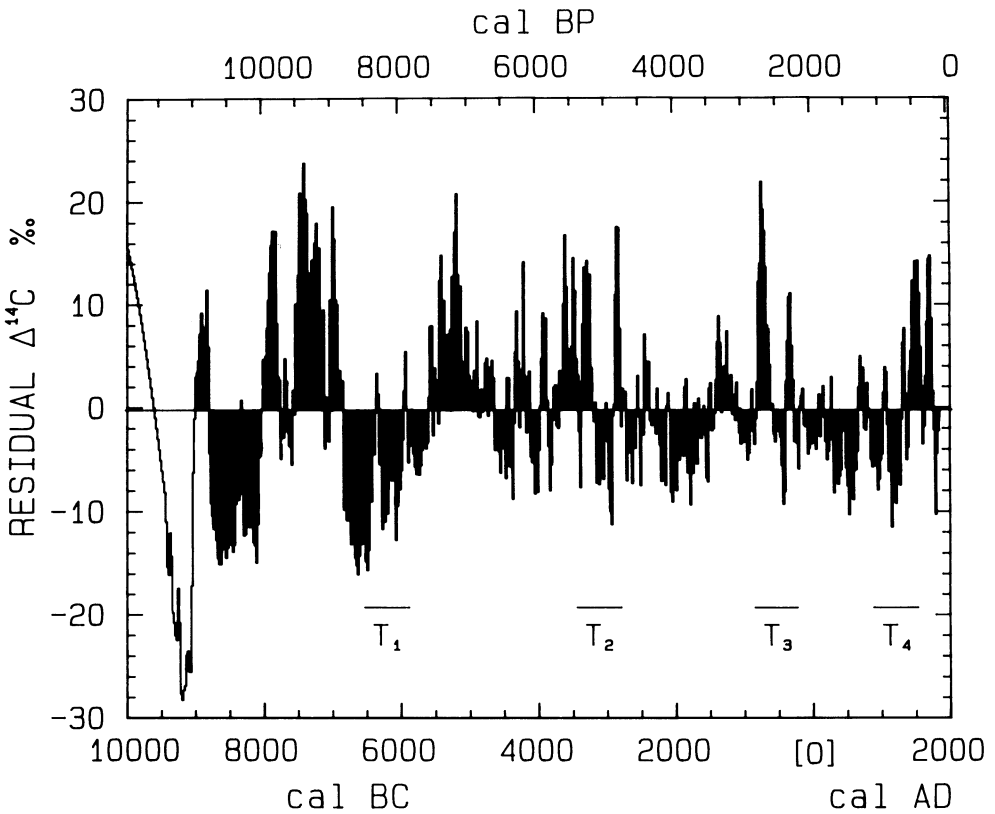

Fig. 11. Residual $\Delta^{14}C$ obtained by deducting the Fig. 10 long-term trend. The $\Delta^{14}C$ trend of the first 500 yr was estimated from coral determinations, the remaining $\Delta^{14}C$ values were derived from tree-ring measurements (see Fig. 1). Lowest residual $\Delta^{14}C$ value following the YD (Younger Dryas) climate oscillation is at 9190 BC (11,140 cal BP); the rapid change (duration *ca.* 150 yr) to Holocene $\Delta^{14}C$ conditions starts at 9060 BC (11,010 cal BP).

In Figures 7 and 8, we present for the AD 1950–10,000 BC interval, respectively, the calculated absolute production rate, Q, and the detrended $\Delta Q/Q_{spline}$ record. Here ΔQ is the difference between Q and the Figure 7 Q_{spline} (the latter approximates, but is not equal to, a 2000-yr moving average).

One interpretation of this record is that solar modulation of the cosmic-ray flux causes a substantial part of the detrended ΔQ variance. Triplets (three successive cycle episodes), T_1 to T_4, are especially notable solar features, and are identified in the figures. These episodes were identified previously, and a best-fit equation was obtained describing these triplet segments (Eq. 1, Stuiver & Braziunas 1989). Figure 9 represents the correlation coefficient, r, between sliding 700-yr portions of the Eq. 1 curve and the detrended ^{14}C production rate record. Although substantial correlation coefficients (0.6–0.7) are found for the T_1–T_4 triplets (Stuiver & Braziunas 1989), the newly added pre-7800 BC part evidently does not contain triplets of the same character, because its correlation coefficients are appreciably lower. Whereas century-type variations of the later part of the ^{14}C record presumably relate mainly to solar forcing (and are dominated by the periodicities of Eq. 1), climate (oceanic) forcing may well have prevailed during the earlier (pre-7000 BC) part of the record.

The oceanic influence has not been accounted for in our marine calibration curves, because the entire atmospheric $\Delta^{14}C$ variablilty was attributed to ^{14}C production rate, Q, change. Whereas Q-

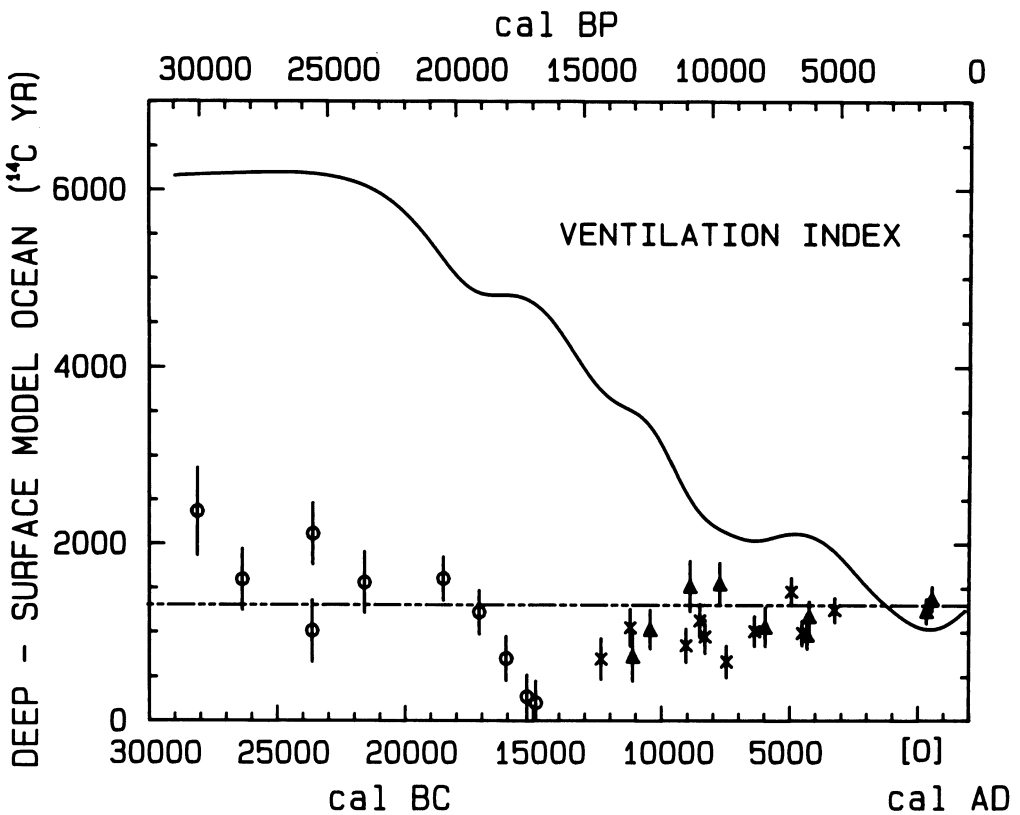

Fig. 12A. Observed ^{14}C age difference of benthic-planktonic species (ventilation index, Andrée *et al.* (1986) ▲ and ×; Shackleton *et al.* (1988) o) compared to model-calculated age difference (top curve). For deriving the age differences, we assumed that ocean-circulation change was solely responsible for the Fig. 10 long-term $\Delta^{14}C$ trend. As in Fig. 4, the South China Sea data have been shifted 295 ^{14}C yr; the East Pacific measurements of Shackleton *et al.* have similarly been shifted by 230 ^{14}C yr to normalize on current conditions. Shackleton *et al.* ^{14}C ages were calibrated using the Stuiver and Reimer (1993) program with ΔR = 180 yr.

related atmospheric $\Delta^{14}C$ perturbations are attenuated in the oceans, oceanic $\Delta^{14}C$ changes must be at least as large as atmospheric changes when oceanic circulation is the cause. The difference in mixed-layer response for century-type variations approaches a factor of two for these scenarios (*ca.* 60 ^{14}C yr, see Stuiver *et al.* 1991). These differences will be less for perturbations of longer durationas the system approaches equilibrium. The postulated oceanic influence is confined to relatively low periodicities (500–3000 yr, see below). Therefore, the impact of our Q-forcing assumption on calibration calculations will be restricted to a few decades.

Figures 10 and 11 depict, respectively, absolute atmospheric $\Delta^{14}C$ and residual $\Delta^{14}C$. The long-term trend in the $\Delta^{14}C$ record can be determined in various ways (sine equations, moving averages, splines, *etc.*). In this instance, we took the Figure 7 production rate spline and calculated the corresponding Figure 10 atmospheric $\Delta^{14}C$ trend; the calculated trend also strongly resembles the 2000-yr $\Delta^{14}C$ moving average. Residual $\Delta^{14}C$ values were obtained by subtracting the Figure 10 long-term trend.

^{14}C production rate variation induced by change in the geomagnetic dipole intensity appears to cause most of the long-term $\Delta^{14}C$ trend (Bard *et al.* 1990; Stuiver *et al.* 1991; Mazaud *et al.* 1991).

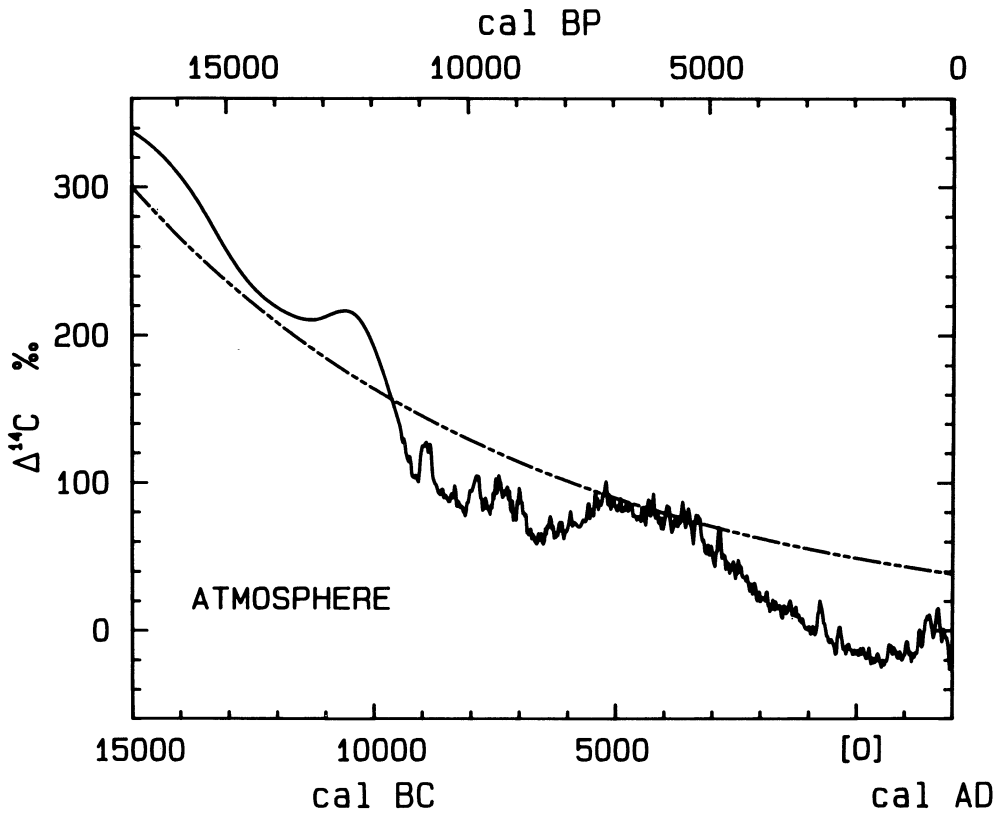

Fig. 12B. Atmospheric $\Delta^{14}C$ compared to decay of excess ^{14}C (– – —, see text).

The incompatibility of the long-term $\Delta^{14}C$ trend with oceanic forcing as an alternative can also be seen in Figure 12A. Here we compare "ventilation indices", representing observed ^{14}C age differences between the deep and surface ocean, to a ventilation history resulting from the ocean circulation changes required to explain the observed long-term atmospheric $\Delta^{14}C$ trend. This ventilation history was calculated using the carbon reservoir model by fixing the ^{14}C production rate at the post-AD 1000 average of the Figure 7 curve. The long-term $\Delta^{14}C$ trend can be explained only by drastic reduction of deep-water formation during the glacial period (K_z about 1/7th of Holocene values), which resulted in a ventilation index value exceeding 6000 ^{14}C yr.

Lower geomagnetic dipole intensity before *ca.* 15,000 yr BP (Mazaud *et al.* 1991) evidently was responsible for elevating $\Delta^{14}C$ up to 50%. The $\Delta^{14}C$ decrease after 15,000 yr BP may be largely the decay of "excess" ^{14}C. The decay curve (dashed line) given in Figure 12B is compatible with a sudden change in steady-state ^{14}C production rate (a reduction by 1.3) at 15,000 BC.

The steep decline in $\Delta^{14}C$ (Fig. 11) between 10,000 and 9190 BC (11,950–11,140 cal BP) is associated with the 10,000 ^{14}C-yr plateau in ^{14}C age *vs.* cal age plots. The termination of the Younger Dryas (YD) interval is not necessarily near the end of this plateau. Although Becker, Kromer and Trimborn (1991) suggest it to be near 11,140 cal BP, annual counting of the Greenland GISP core indicates an age of 11,650 ± 250 cal BP (Alley 1993). Laminated sediments from a Polish lake (Rozanski *et al.* 1992) yield a comparable 11,000–11,700 cal BP range, with a preferred value of 11,200 cal BP. Lehman and Keigwin (1992) place the YD termination near 10,500 ^{14}C BP

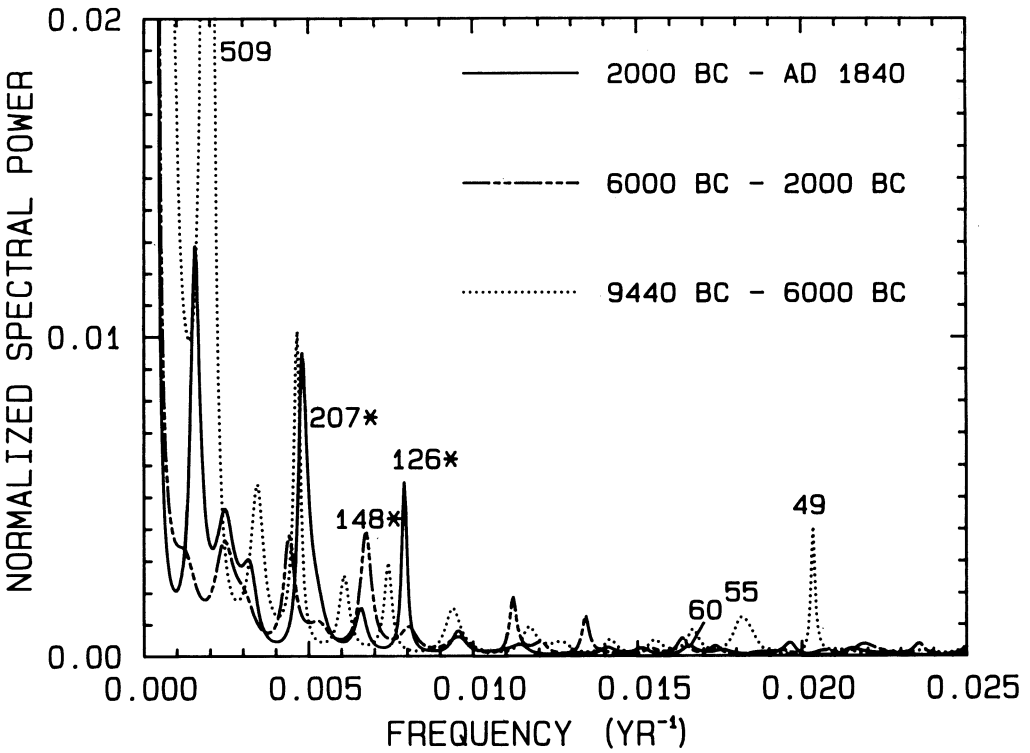

Fig. 13A. MEM power spectrum (AR order *ca.* 50) of Fig. 10 $\Delta^{14}C$ values for the intervals given above. Starred periodicities have spectral power exceeding the 2 σ significance level, the others fall in the 1.5–2.0 σ range. Periodicities for the intervals 2000 BC–AD 1840, 6000–2000 BC, and 9440–6000 BC are, respectively, 60, 126 and 207 yr, 148 yr, and 49, 55 and 509 yr.

(*ca.* 12,420 cal BP, Stuiver & Reimer 1993). We consider the oldest Fig. 11 residual $\Delta^{14}C$ changes, starting with the 12,000–11,140 cal BP decline, to be caused by fluctuations in North Atlantic Deep Water (NADW) formation and transport. The initial $\Delta^{14}C$ decline would be due to an increased rate of upwelling of water relatively low in ^{14}C. Specific details will be published elsewhere.

Adding freshwaters to the surface ocean lowers densities, which, in turn, reduces the potential for sinking of higher-density waters to abyssal depths. A reduced deep-water formation rate agrees with our vertical diffusivity coefficient (K_z) calculations, whereby, according to the carbon reservoir model, K_z values must be reduced by nearly 40% to generate the $\Delta^{14}C$ maximum near 10,900 cal BP (see Fig. 1 inset). However, the timing of the $\Delta^{14}C$ maximum differs from the 11,300 cal BP meltwater pulse discussed by Fairbanks (1990).

In the earliest part of the record, residual $\Delta^{14}C$ amplitudes are among the largest, and durations of the $\Delta^{14}C$ variations among the longest; these lengthened durations are also observed in the spectral properties of the $\Delta^{14}C$ and Q records (both without trend removal). Figures 13A and 13B depict normalized spectral power for three subintervals, each lasting 3.5–4 millennia. We used the maximum entropy method (MEM) or autoregressive (AR) model for AR order n/4, where n = number of data points. The periods where spectral power of atmospheric $\Delta^{14}C$ exceeds the 2 σ significance level, or falls in the 1.5–2.0 σ range (Mitchell *et al.* 1966), change from 60, 126 and 207 yr for the 2000 BC–AD 1840 interval to 49, 55 and 509 yr for the 9440 BC–6000 BC interval. High- and intermediate-frequency production rate variations result in substantially attenuated $\Delta^{14}C$ variations

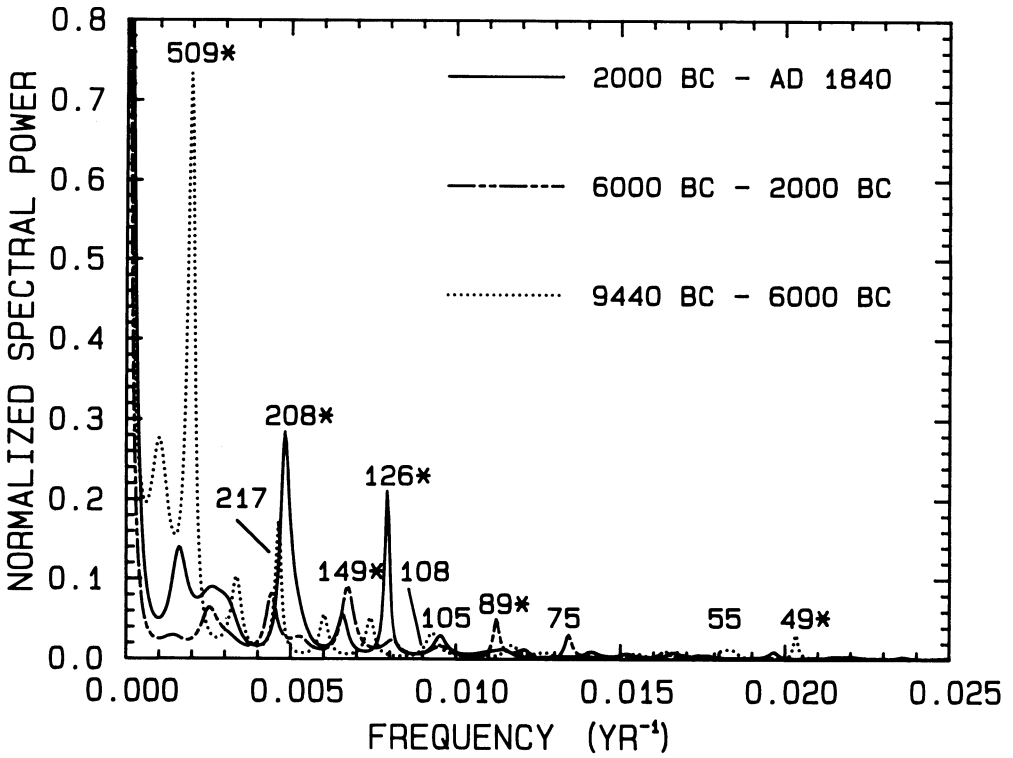

Fig. 13B. MEM power spectrum (AR order *ca.* 50) of the Fig. 7 calculated ^{14}C production rate variations, Q. Starred periodicities have spectral power exceeding the 2 σ significance level, the others fall in the 1.5–2.0 σ range. Periodicities for the intervals listed above are, respectively, 105, 126 and 208 yr, 75, 89 and 149 yr, and 49, 55, 108, 217 and 509 yr.

in the atmosphere, resulting in a loss of frequencies relative to the Q spectrum. Periods where spectral power of Q exceeds or approaches the 2 σ level are 105, 126 and 208 yr for the 2000 BC–AD 1840 interval, and 49, 55, 108, 217 and 509 yr for the 9440–6000 BC interval.

After removal of the long-term trend, the complete detrended $\Delta^{14}C$ record reveals periods with spectral power density exceeding the 2 σ level at 46, 49, 87, 148, 206 and 512 yr. A 2860-yr periodicity was found to be significant in the 1.5 to 2.0 σ range. While the 512- and 2860-yr periodicities may well relate to oceanic (and climate) changes, several higher frequencies appear to be solar-induced. These findings will be discussed elsewhere.

Radiocarbon Age and ΔR Determination

Figure 14 presents model surface-ocean conventional ^{14}C ages *vs.* calendar ages for the post-AD 1500 period. An independent estimate of the calendar age of a sample from a particular location allows the user to determine a model-generated ^{14}C age. This age can be compared to the conventional marine ^{14}C age of the sample from this location. The difference constitutes ΔR, an assumed time-constant offset in ^{14}C ages for that particular region, that should be removed from sample ^{14}C ages before application of the marine calibration curve (see Figs. 16 and 17). The time dependency of reservoir age, R(t), is included in the marine calibration curve.

In some instances, such as with a pair of contemporaneous wood and shell samples from a single location, the reservoir deficiency may be calculated without a direct calibration to the calendar time

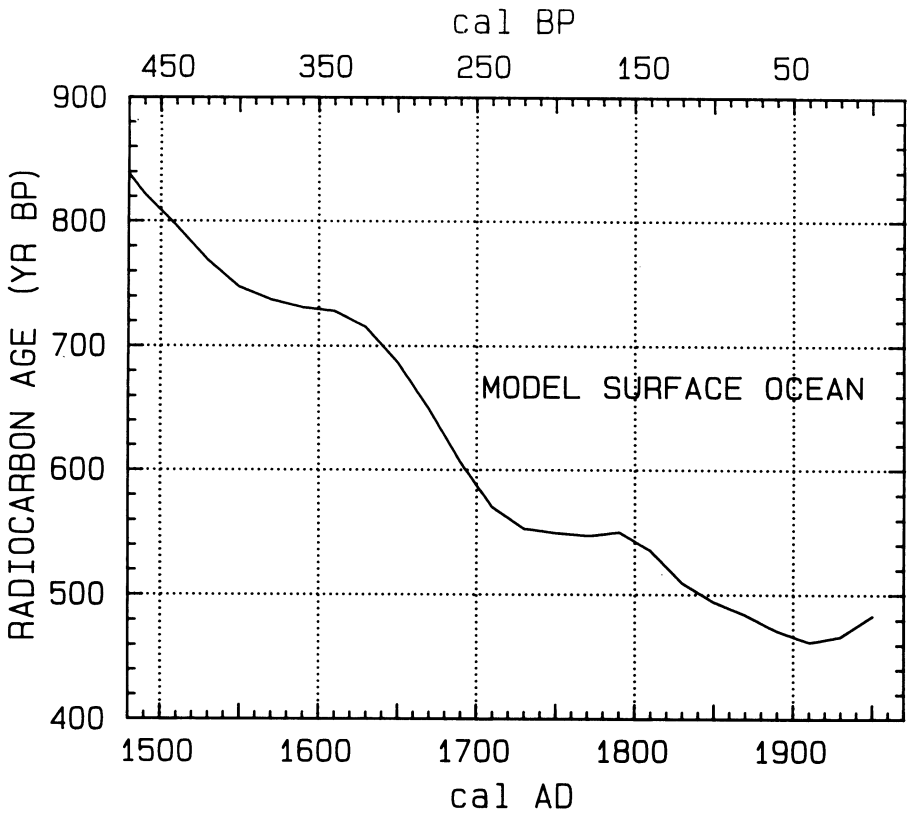

Fig. 14. Post-AD 1500 surface ocean ^{14}C yr *vs.* cal yr

scale. In this case, one can use Figure 15, in which model marine conventional ^{14}C ages are plotted against atmospheric conventional ^{14}C ages. The atmospheric (wood) sample can be initially calibrated using the atmospheric calibration curves (Stuiver & Reimer 1993), and its cal age subsequently applied to the calculation of ΔR by using Figure 14 (or Figure 17); however, one canavoid the middle step in this process by applying Figure 15. The measured wood ^{14}C age is converted through Figure 15 to a model marine ^{14}C age, which, when deducted from the measured shell ^{14}C age, yields ΔR. A 40-yr correction must be applied to the ^{14}C ages of southern hemisphere atmospheric samples before using this figure.

Figure 15 illustrates obvious multiple marine ^{14}C age intercepts for a specific atmospheric ^{14}C age. Similar multiple marine ages (and thus multiple ΔR choices) would also result from using Figure 14 or 17, and by using the cal age derivation of the wood ^{14}C age from the Stuiver and Reimer (1993) atmospheric calibration curves; again, deduct 40 ^{14}C yr for southern hemispheric samples.

A survey of independently calibrated shell ^{14}C samples approximates the geographic distribution of ΔR values for oceanic regions in both hemispheres. A summary of ΔR values, given in the 1986 paper, is augmented in Figure 16 with ΔR data from New Zealand (McFadgen & Manning 1990), South Africa (Talma 1990), Portugal (Soares 1989) and the North American east coast (E. Little, personal communication, 1992). It should be noted that ΔR values for the coast of California, given as 225 ^{14}C yr in Figure 16, are controversial, because recent work indicates values of about 300 $\pm$ 35 ^{14}C yr (Terry Jones, personal communication, 1992) and 500 $\pm$ 100 ^{14}C yr (Bouey & Basgall 1991).

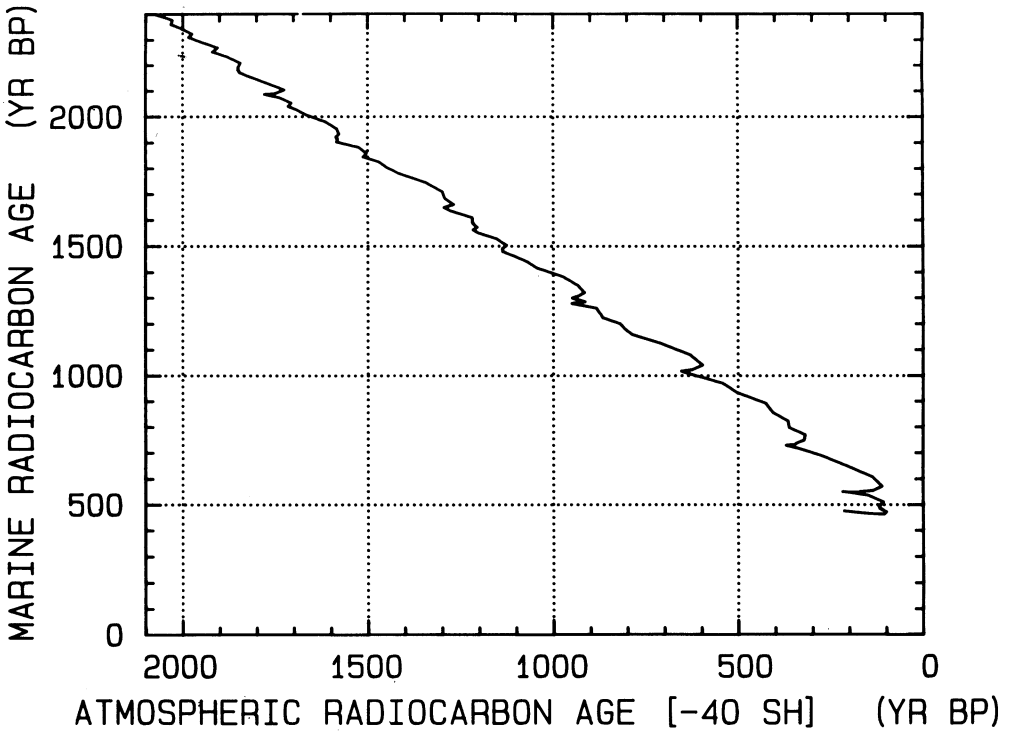

Fig. 15A–C. Holocene surface-ocean ^{14}C ages *vs.* atmospheric ^{14}C ages of the northern hemisphere. Southern hemispheric atmospheric ^{14}C ages should be reduced by 40 yr prior to using the graphs.

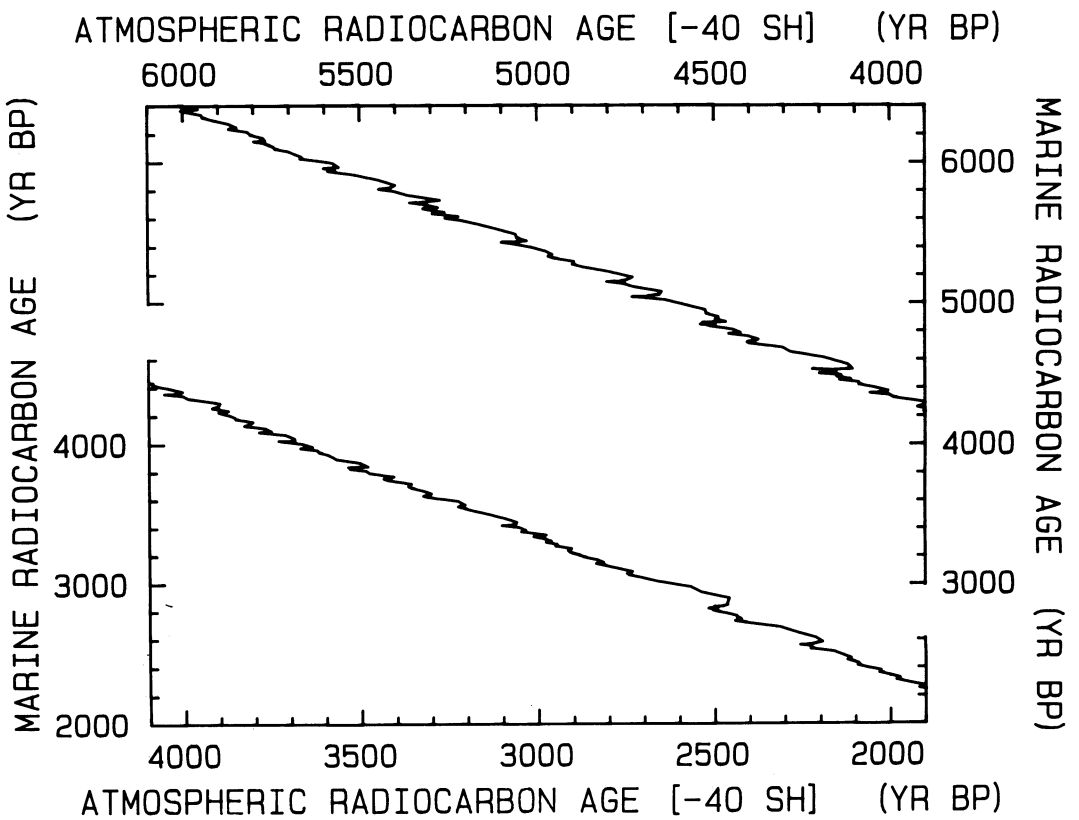

Fig. 15B

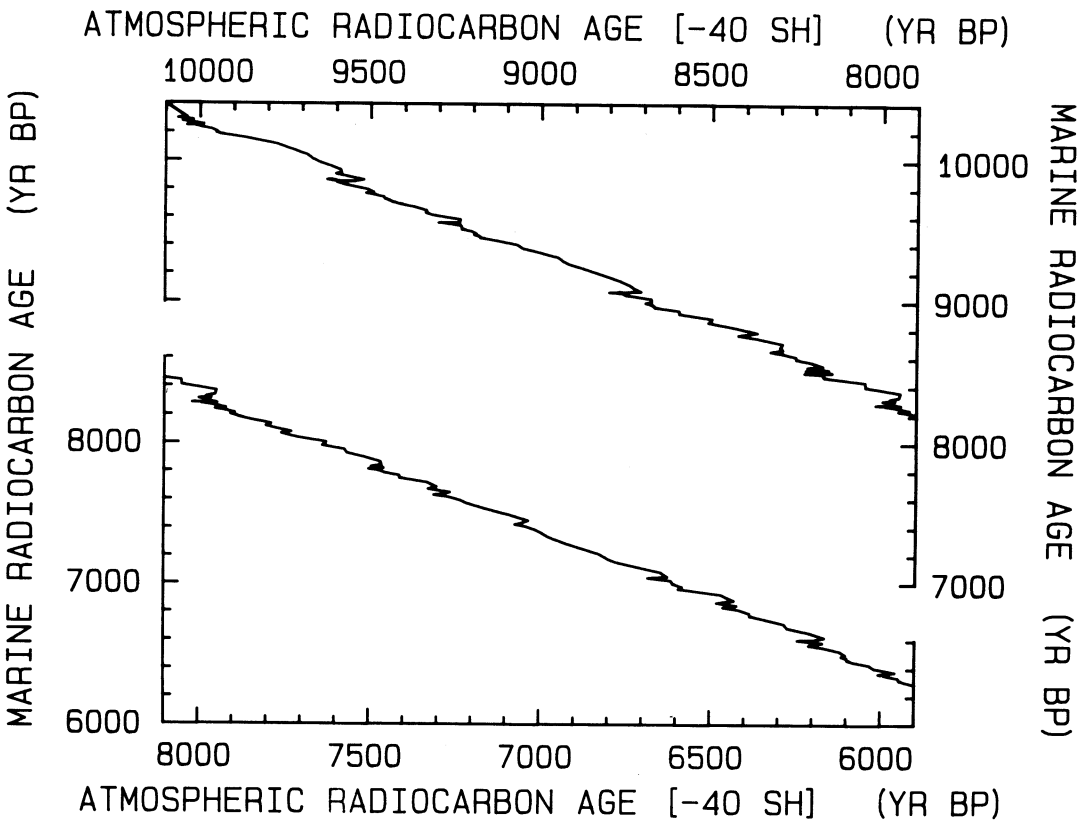

Fig. 15C

Complications may arise (*e.g.*, increase in ΔR) in estuaries, where a mixture of marine and riverine materials are incorporated in the shell. For example, estimated local ΔR values within Long Island Sound (E. Little, personal communication, 1992) vary greatly from the average Sound value of about 120 ± 55 ^{14}C yr; this average value also is distinctly different from the value of -85 ± 75 ^{14}Cyr listed for a single sample in our 1986 paper. Open ocean values from the Massachusetts coast yield ΔR = −95 ± 45 ^{14}C yr (E. Little, personal communication, 1992).

Complications also occur when rates of regional upwelling vary. For example, Soares (1989) determined ΔR of 280 ± 35 ^{14}C yr (38°N – 41°N) and 235 ± 35 ^{14}C yr (37°N) for the coast of Portugal, for samples with conventional ^{14}C ages less than 2000 ^{14}C yr BP. A *ca.* 250-^{14}C-yr reduction in ΔR value is encountered for the earlier part of the Holocene. Such an increase may be related to reduced upwelling of deeper (older) water. Southon, Nelson and Vogel (1990), on the other hand, find, except for one outlier, only minor changes in ΔR for five Holocene determinations from the west coast of British Columbia. Talma (1990) reports, for 15 charcoal-shell sample pairs from the west coast of South Africa (1000 BC–AD 1500 cal age range), that "the spread of ΔR values with age seems fairly random and is probably only the result of measurement imprecision and some natural variability". Figure 16 ΔR values are based on the 1986 calibration curves, with global R(1830) = 409 yr, whereas current calculations yield global R(1830) = 402 yr. No attempt was made to update the regional ΔR determinations, because minor changes in calibration results for the last few centuries would result in corrections about equal to the rounding error (up to 5 yr) of the original data set.

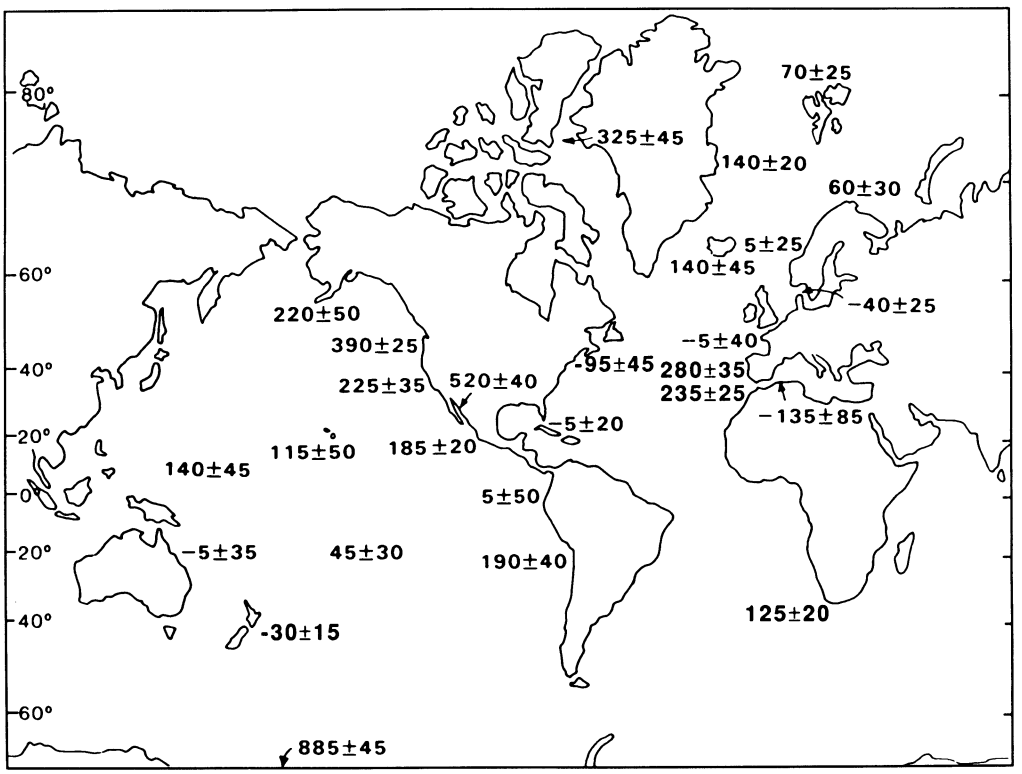

Fig. 16. Geographic distribution of coastal region ΔR values (in ^{14}C yr). The ± values are minimum standard deviations based on the scatter of the data, or the measurement precison, whichever is larger (Stuiver, Pearson & Braziunas 1986). For Long Island Sound ΔR, see text.

A corresponding tabulation of reservoir ages for the AD 1830 bidecade can be derived from the Figure 16 ΔR values by adding 402 and 362 ^{14}C yr for the northern and southern hemispheres, respectively. Such a tabulation gives oceanic ^{14}C levels at one single point in time, and applies to both hemispheres (the southern hemispheric atmosphere was assumed to be 40 yr older than the "global" tree-ring record).

Figure 17 should be used to calibrate surface ocean samples. For such calibration, ΔR must be selected (or, to a first approximation, assume ΔR = 0). The CALIB 3.0 program (Stuiver & Reimer 1993), which incorporates Figure 17 data, also can be used. For marine samples older than 10,500 ^{14}C yr, the Bard *et al.* (1993) calibration curve is applicable. These data are also part of the CALIB 3.0 program, where a smoothing spline is used to approximate the Bard *et al.* information.

To reduce an offset (from 120 to 35 yr at 11,700 cal yr) between the two marine segments (smoothing spline through coral measurements *vs.* our model-calculated part), we changed the pre-tree-derived (Fig. 1) atmospheric $\Delta^{14}C$ model input slightly. This second-order correction allows our model ocean to operate more realistically, in that coral-assigned model reservoir deficiencies prior to 11,700 cal yr BP were allowed to deviate (by 120 yr maximally) from the constant 400-yr reservoir deficiency initially imposed as a simplifying assumption. Specifically, the two marine segments (pre-11,750 cal yr BP smoothing spline through coral measurements *vs.* post-11,650 cal yr BP model-calculated part) are connected by a short (100-yr) linear interpolation to smooth their 35-yr offset.

ACKNOWLEDGMENTS

Talma's (1990) report was an impetus for us to refine our ΔR southern hemispheric concept. E. Little generously provided a draft of her paper, and T. Jones alerted us to the problems with California ΔR values. The ^{14}C research and modeling was supported through National Science Foundation grant BNS-9004492, and NOAA contract NA16RC00081. We are much indebted to P. J. Reimer and P. J. Wilkinson for crucial technical and analytical support. This is JISAO contribution 171.

REFERENCES

Adams, J. M., Faure, H., Faure-Denard, L., McGlade, J. M. and Woodward, F. I. 1990 Increases in terrestrial carbon storage from the Last Glacial Maximum to the present. *Nature* 348: 711–714.

Alley, R. B., Meese, Shuman, C. A., Gow, A. J., Taylor, K., Ram, M., Waddington, E. D. and Mayewski, P. A. 1993 An old, long, abrupt Younger Dryas event in the GISP2 ice core. *Nature*, in press.

Andrée, M., Beer, J., Loetscher, H. P., Moor, E., Oeschger, H., Bonani, G., Hofmann, H. J., Suter, M., Wölfli, W. and Peng, T. H. 1986 Limits on the ventilation rate for the deep ocean over the last 12000 years. *Climate Dynamics* 1: 53–62.

Bard, E. 1988 Correction of accelerator mass spectrometry ^{14}C ages measured in planktonic foraminifera: Paleoceanographic implications. *Paleoceanography* 3: 635–645.

Bard, E., Arnold, M., Fairbanks, R.G. and Hamelin, B. 1993 $^{230}Th/^{234}U$ and ^{14}C ages obtained by mass spectrometry on corals. *Radiocarbon*, this issue.

Bard, E., Hamelin, B., Fairbanks, R. G. and Zindler, A. 1990 Calibration of the ^{14}C timescale over the past 30,000 years using mass spectrometric U-Th ages from Barbados corals. *Nature* 345: 405–410.

Becker, B., Kromer, B. and Trimborn, P. 1991 A stable isotope tree-ring timescale of the Late Glacial/Holocene boundary. *Nature* 353: 647–649.

Bouey, P. D. and Basgall, M. E. 1991 Archaeological patterns along the South-central coast, Point Piedras Blancas, San Luis Obispo County, California. *California Department of Transportation* 05-SLO-1: 39–48.

Braziunas, T. F. 1990 Nature and origin of variations in late-glacial and Holocene atmospheric ^{14}C as revealed by global carbon cycle modeling. Ph.D. dissertation, University of Washington, Seattle.

Broecker, W. S. and Denton, G. H. 1989. The role of ocean-atmosphere reorganizations in glacial cycles. *Geochimica et Cosmochimica Acta* 53: 2465–2501.

Broecker, W. S., Takahashi, T., Simpson, H. J. and Peng, T.-H. 1979 Fate of fossil fuel carbon dioxide and the global carbon budget. *Science* 206: 409–418.

Charles, C. D. and Fairbanks, R. G. 1992 Evidence from Southern Ocean sediments for the effect of North Atlantic deep-water flux on climate. *Nature* 355: 416–419.

Damon, P. E. 1988 Production and decay of radiocarbon and its modulation by geomagnetic field-solar activity changes with possible implications for global environment. *In* Stephenson, F. R. and Wolfendale, A. W., eds., *Secular Solar and Geomagnetic Variations in the Last 10,000 Years*. Dordrecht, The Netherlands, Kluwer Academic Publishers: 267–285.

Fairbanks, R. G. 1990 The age and origin of the "Younger Dryas climate event" in Greenland ice cores. *Paleoceanography* 5: 937–948.

Keeling, C. D. 1973 The carbon dioxide cycle: Reservoir models to depict the exchange of atmospheric carbon dioxide with the oceans and land plants. *In* Rasool, S. I., ed., *Chemistry of the Lower Atmosphere*. New York, Plenum Press: 251–329.

Kromer, B. and Becker, B. 1993 German oak and pine ^{14}C calibration, 7200 BC–9400 BC. *Radiocarbon*, this issue.

Lassey, K. R., Manning, M. R. and O'Brien, B. J. 1990 An overview of oceanic radiocarbon: Its inventory and dynamics. *Reviews in Aquatic Sciences* 3: 117–146.

Lehman, S. L. and Keigwin, L. D. 1992 Sudden changes in North Atlantic circulation during the last deglaciation. *Nature* 356: 757–762.

Lingenfelter, R. E. and Ramaty, R. 1970 Astrophysical and geophysical variations in ^{14}C production. *In* Olsson, I. U., ed., *Radiocarbon Variations and Absolute Chronology*. Proceedings of the 12th Nobel Symposium. New York, John Wiley & Sons: 513–537.

Mazaud, A., Laj, C., Bard, E., Arnold, M. and Tric, E. 1991 Geomagnetic field control of ^{14}C production over the last 80 ky: Implications for the radiocarbon timescale. *Geophysical Research Letters* 18: 1885–1888.

McFadgen, B. and Manning, M. R. 1990 Calibrating New Zealand radiocarbon dates of marine shells. *Radiocarbon* 32(2): 229–232.

Oeschger, H., Siegenthaler, U., Schotterer, U. and Gugelmann, A. 1975 A box diffusion model to study the carbon dioxide exchange in nature. *Tellus* 27: 168–192.

Pearson, G. W., Becker, B. and Qua, F. 1993 High-precision ^{14}C measurement of German oaks to show the natural ^{14}C variations from 7890 to 5000 BC.

Radiocarbon, this issue.

Pearson, G. W. and Stuiver, M. 1993 High-precision bidecadal calibration of the radiocarbon time scale 500–2500 BC. *Radiocarbon*, this issue.

Rozanski, K., Goslar, T., Dulinski, M., Kuc, T., Pazdur, M. F. and Walanus, A. 1992 The Late Glacial-Holocene transition in central Europe derived from isotope studies of laminated sediments from Lake Gosciaz (Poland), *In* Bard, E. and Broecker, W. S., eds., *The Last Deglaciation: Absolute and Radiocarbon Chronologies*. NATO ASI Series I-2. Heidelberg, Springer Verlag: 69–80.

Shackleton, N. J., Duplessy, J.-C., Arnold, M., Maurice, P., Hall, M. A. and Cartlidge, J. 1988 Radiocarbon age of last glacial Pacific deep water. *Nature* 335: 708–711.

Siegenthaler, U. and Münnich, K. O. 1981 $^{13}C/^{12}C$ fractionation during CO_2 transfer from air to sea. *In* Bolin, B., ed., *Carbon Cycle Modeling: SCOPE 16*. New York, John Wiley & Sons: 249-257.

Soares, A. M. M. 1989 O efeito de reservatório oceânico nas águas costeiras de Portugal continental. ICEN-LNETI, Dept. de Quimica: 135 pp.

Southon, J. R., Nelson, D. E. and Vogel, J. S. 1990 A record of past ocean-atmosphere radiocarbon differences from the Northeast Pacific. *Paleoceanography* 5: 197–206.

Stuiver, M. and Braziunas, T. F. 1989 Atmospheric ^{14}C and century-scale solar oscillations. *Nature* 338: 405–408.

Stuiver, M., Braziunas, T. F., Becker, B. and Kromer, B. 1991 Climatic, solar, oceanic, and geomagnetic influences on late-glacial and Holocene atmospheric $^{14}C/^{12}C$ change. *Quaternary Research* 35: 1–24.

Stuiver, M. and Pearson, G. W. 1993 High-precision calibration of the radiocarbon time scale, AD 1950–500 BC and 2500–6000 BC. *Radiocarbon*, this issue.

Stuiver, M., Pearson, G. W. and Braziunas, T.F. 1986 Radiocarbon age calibration of marine samples back to 9000 cal yr BP. *In* Stuiver, M. and Kra, R. S., eds., Proceedings of the 12th International ^{14}C Conference. *Radiocarbon* 28(2B): 980–1021.

Stuiver, M. and Polach, H. A. 1977 Discussion: Reporting of ^{14}C data. *Radiocarbon* 19(3): 355–363.

Stuiver, M. and Reimer, P. J. 1993 Extended ^{14}C data base and revised CALIB 3.0 radiocarbon age calibration program. *Radiocarbon*, this issue.

Talma, A. S. 1990 Radiocarbon age calibration of marine shells. Quarterly Report, Quaternary Dating Research Unit. Pretoria, CSIR: 10 pp.

Toggweiler, J. R. and Sarmiento, J. L. 1985 Glacial to interglacial changes in atmospheric carbon dioxide: The critical role of ocean surface water in high latitudes. *In* Sundquist, E. T. and Broecker, W. S., eds., *The Carbon Cycle and Atmospheric CO_2: –Natural Variations Archean to Present*. Washington D.C., American Geophysical Union. *Geophysical Monograph* 32: 163–184.

Vogel, J. C., Fuls, A., Visser, E. and Becker, B. 1993 Pretoria calibration curve for short-lived samples, 1930–3350 BC. *Radiocarbon*, this issue.

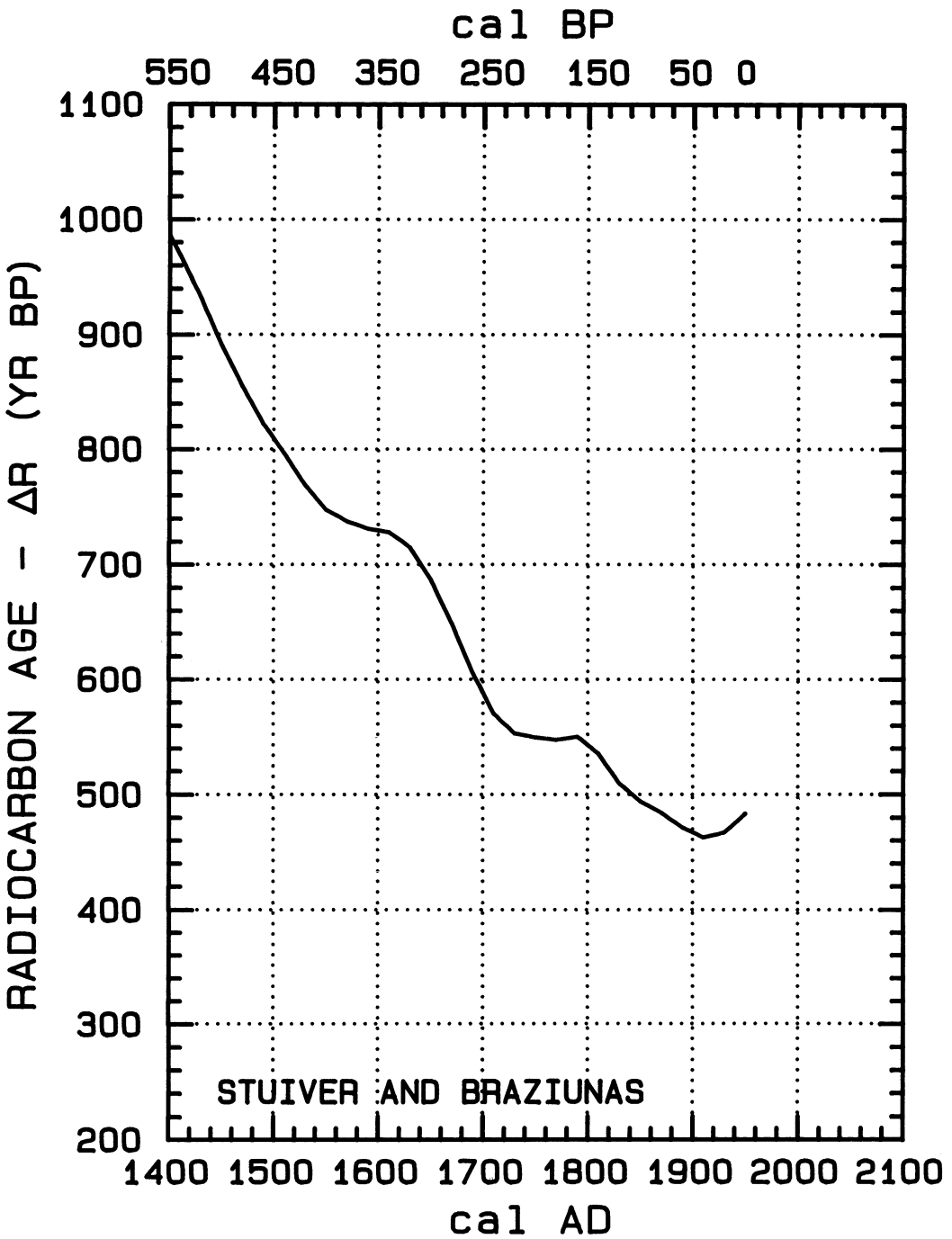

Fig. 17A–X. Calibration curves to be applied for marine (surface ocean) samples. Applicable ΔR values are discussed in the text, and depicted in Fig. 16.

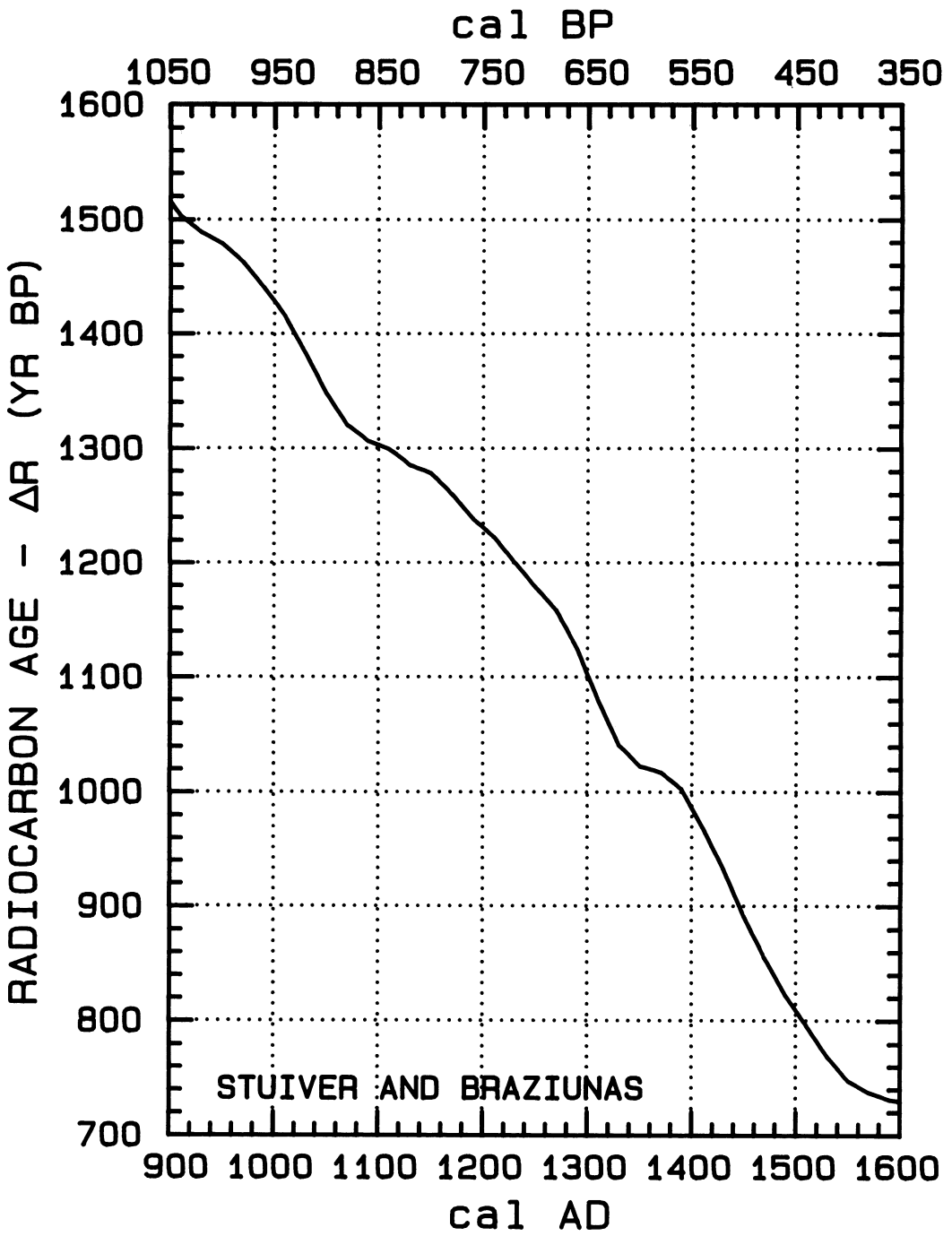
cal BP
1050 950 850 750 650 550 450 350
1600
1500
1400
1300
1200
1100
1000
900
800
700
RADIOCARBON AGE - ΔR (YR BP)
STUIVER AND BRAZIUNAS
900 1000 1100 1200 1300 1400 1500 1600
cal AD

Fig. 17B

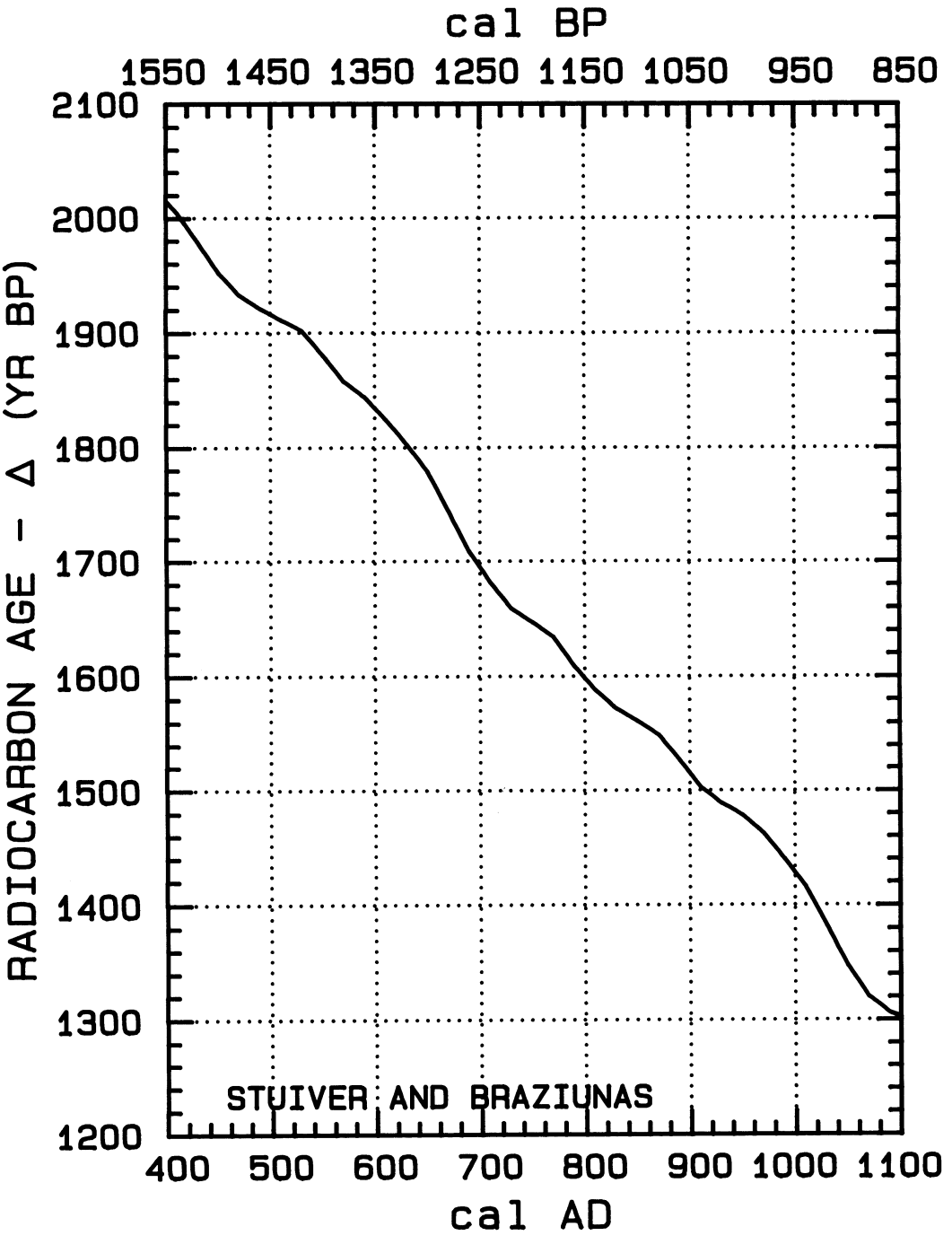
cal BP
1550 1450 1350 1250 1150 1050 950 850
2100
2000
1900
1800
1700
1600
1500
1400
1300
1200
RADIOCARBON AGE - Δ (YR BP)
STUIVER AND BRAZIUNAS
400 500 600 700 800 900 1000 1100
cal AD

Fig. 17C

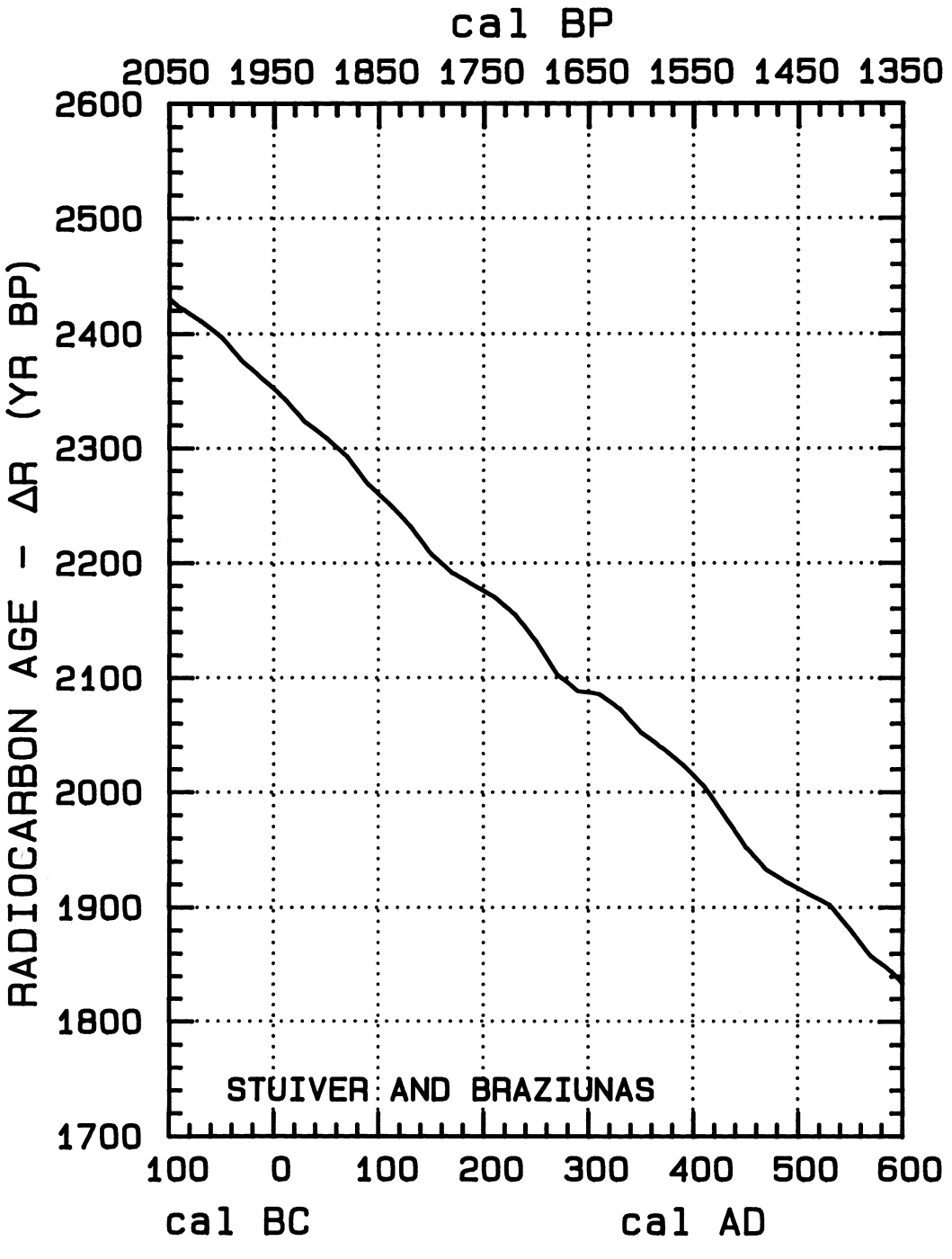
cal BP
2050 1950 1850 1750 1650 1550 1450 1350
2600
2500
2400
2300
2200
2100
2000
1900
1800
1700
RADIOCARBON AGE - ΔR (YR BP)
STUIVER AND BRAZIUNAS
100 0 100 200 300 400 500 600
cal BC
cal AD

Fig. 17D

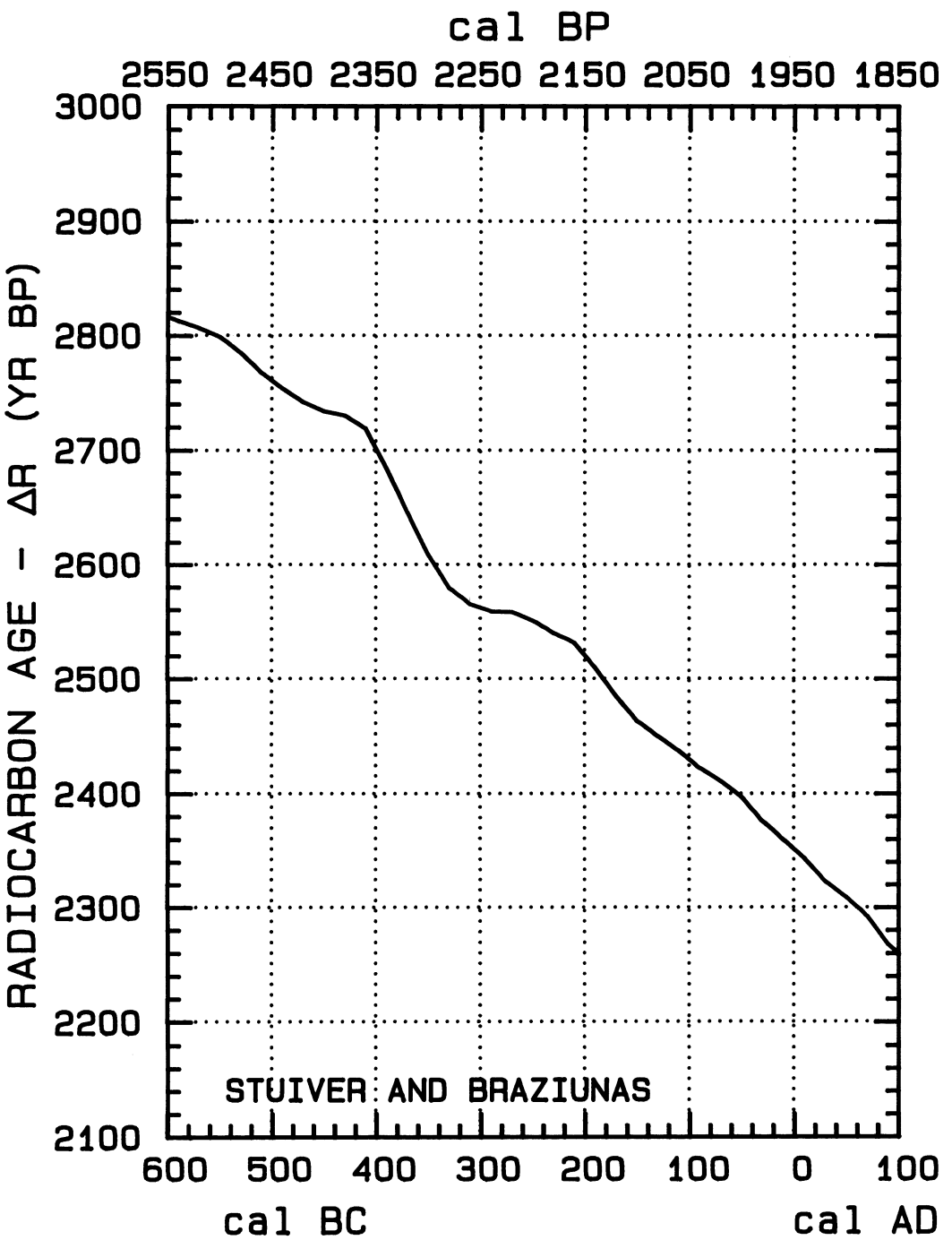
cal BP
2550 2450 2350 2250 2150 2050 1950 1850
3000
2900
2800
2700
2600
2500
2400
2300
2200
2100
RADIOCARBON AGE - ΔR (YR BP)
STUIVER AND BRAZIUNAS
600 500 400 300 200 100 0 100
cal BC
cal AD

Fig. 17E

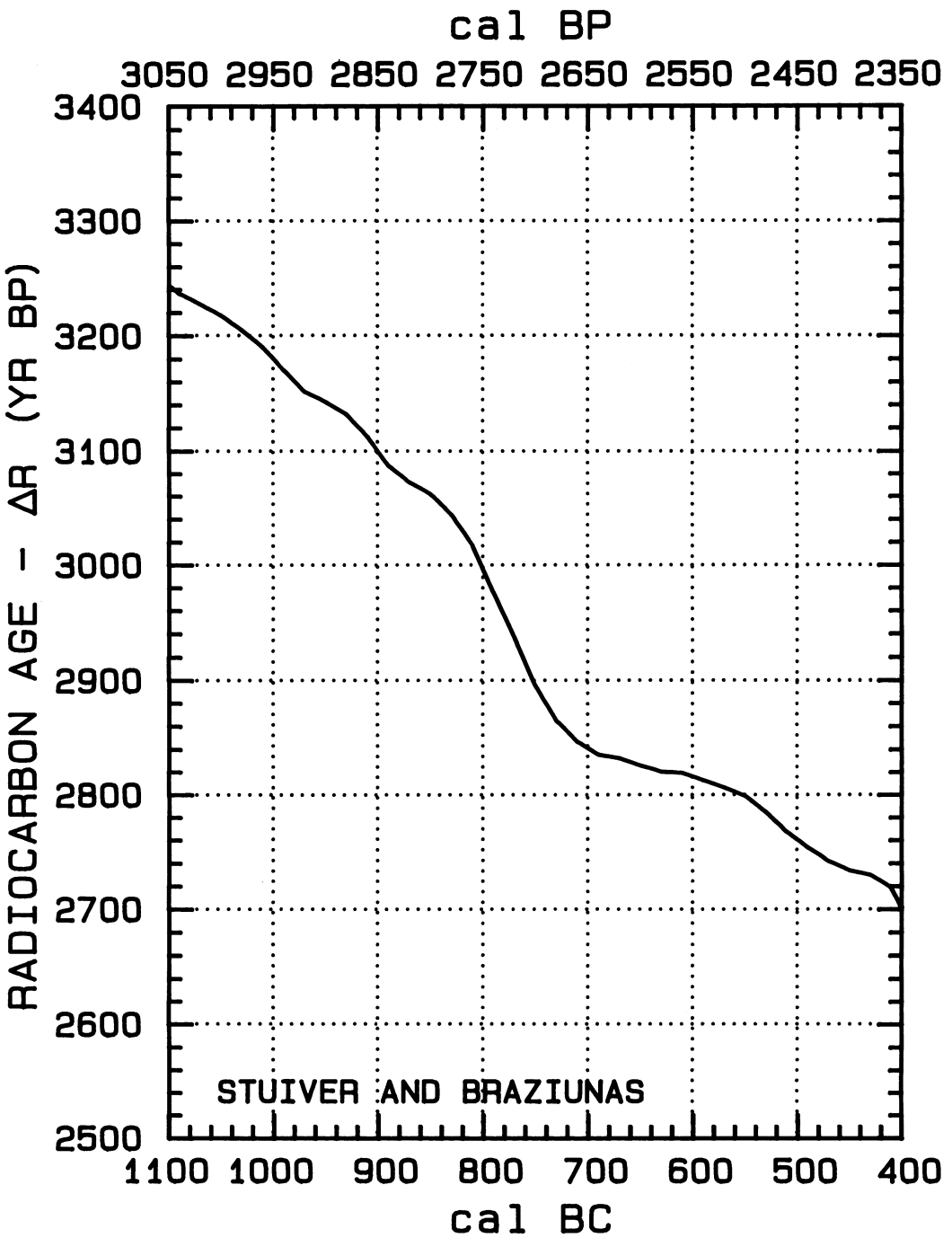
cal BP
3050 2950 2850 2750 2650 2550 2450 2350
3400
3300
3200
3100
3000
2900
2800
2700
2600
2500
RADIOCARBON AGE - ΔR (YR BP)
STUIVER AND BRAZIUNAS
1100 1000 900 800 700 600 500 400
cal BC

Fig. 17F

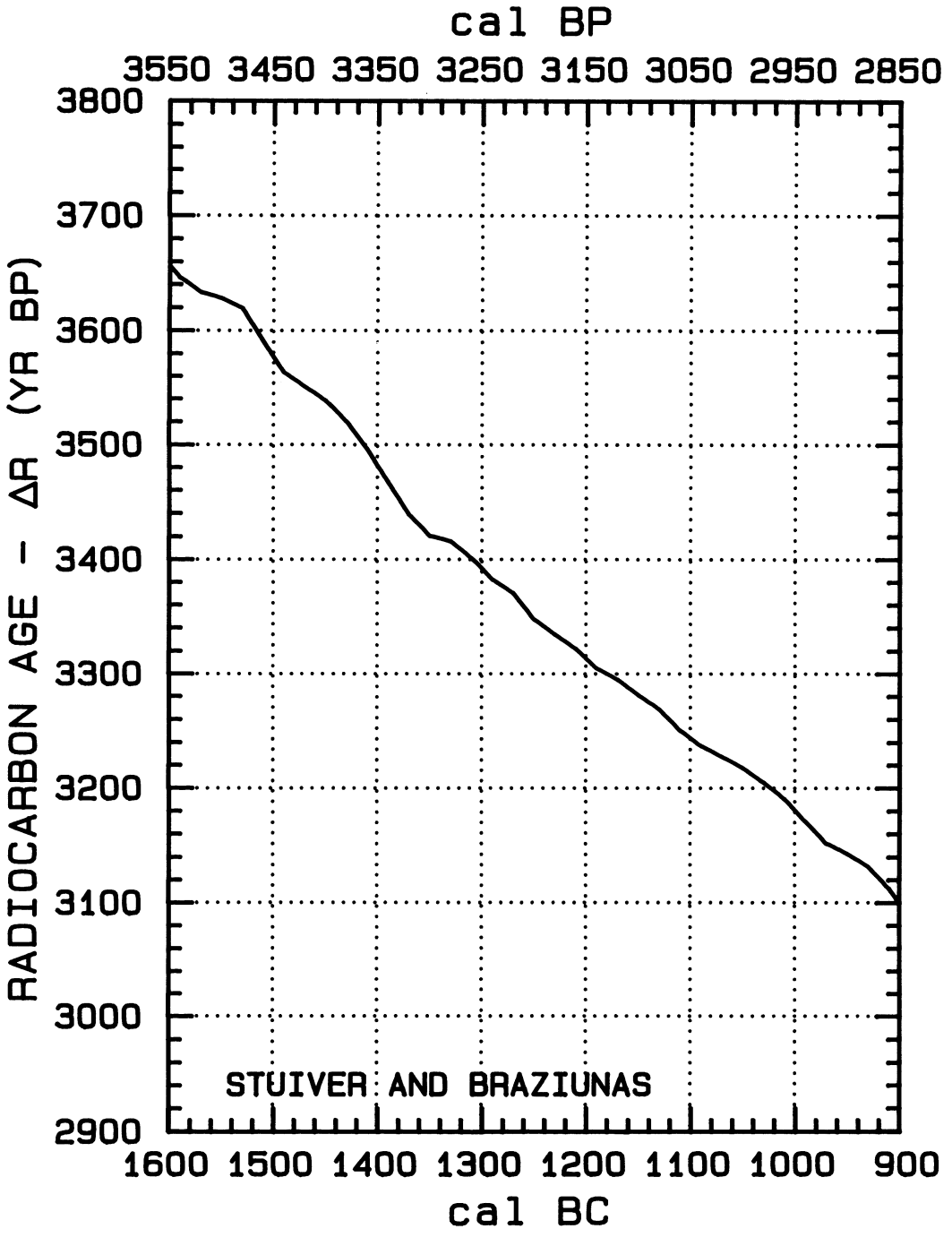
cal BP
3550 3450 3350 3250 3150 3050 2950 2850
3800
3700
3600
3500
3400
3300
3200
3100
3000
2900
RADIOCARBON AGE - ΔR (YR BP)
STUIVER AND BRAZIUNAS
1600 1500 1400 1300 1200 1100 1000 900
cal BC

Fig. 17G

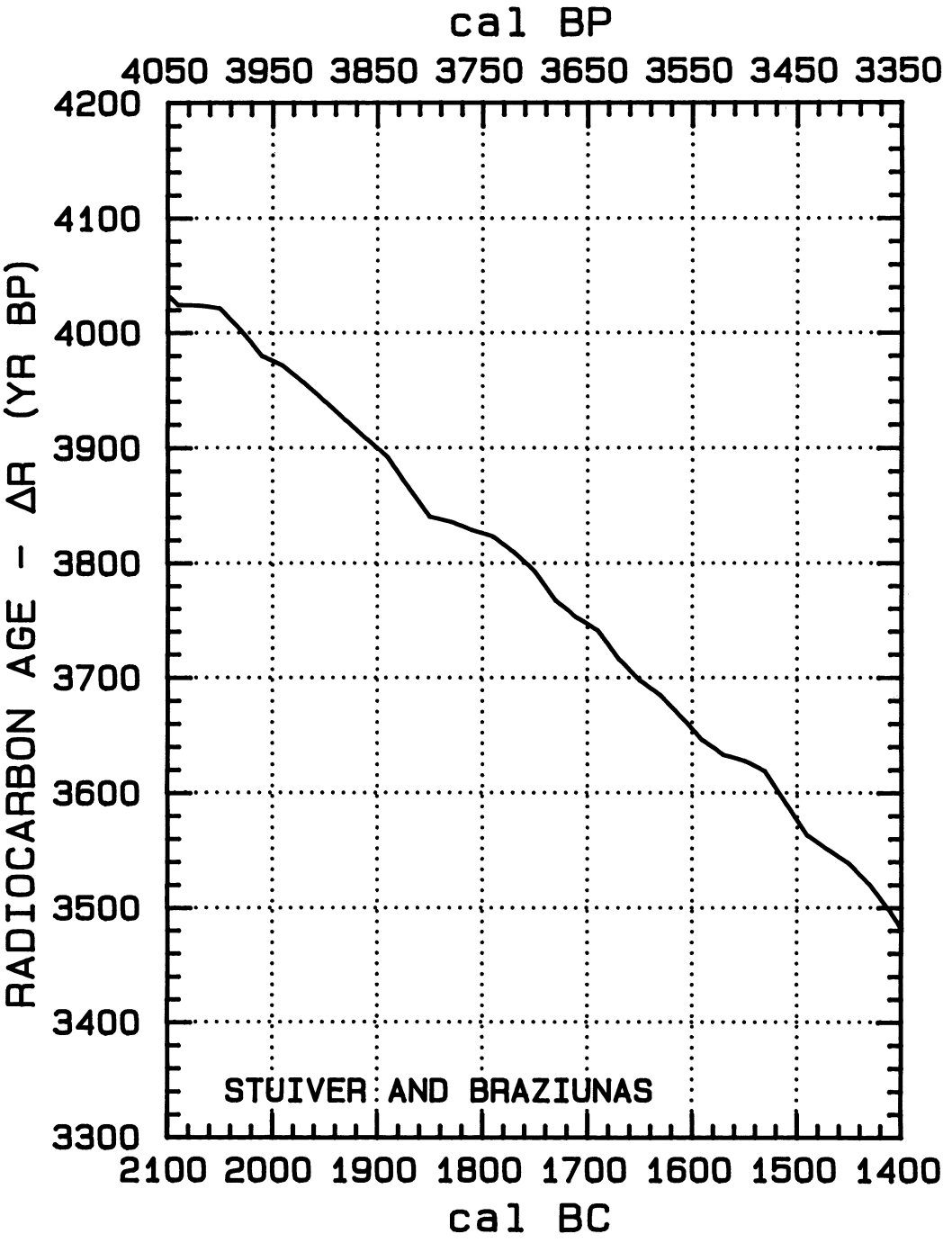
cal BP
4050 3950 3850 3750 3650 3550 3450 3350
4200
4100
4000
3900
3800
3700
3600
3500
3400
3300
RADIOCARBON AGE - ΔR (YR BP)
STUIVER AND BRAZIUNAS
2100 2000 1900 1800 1700 1600 1500 1400
cal BC

Fig. 17H

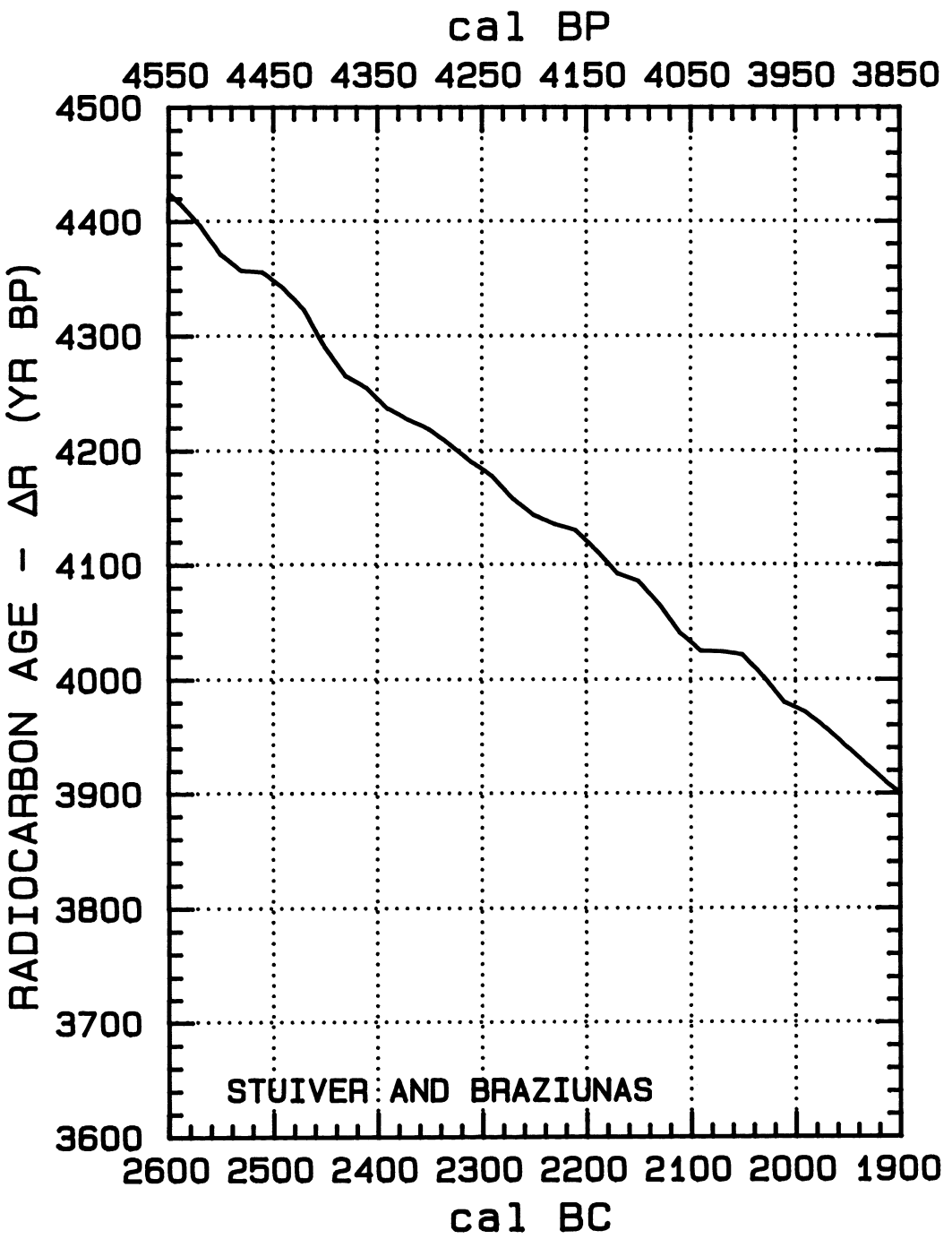
cal BP
4550 4450 4350 4250 4150 4050 3950 3850
4500
4400
4300
4200
4100
4000
3900
3800
3700
3600
RADIOCARBON AGE - ΔR (YR BP)
STUIVER AND BRAZIUNAS
2600 2500 2400 2300 2200 2100 2000 1900
cal BC

Fig. 17I

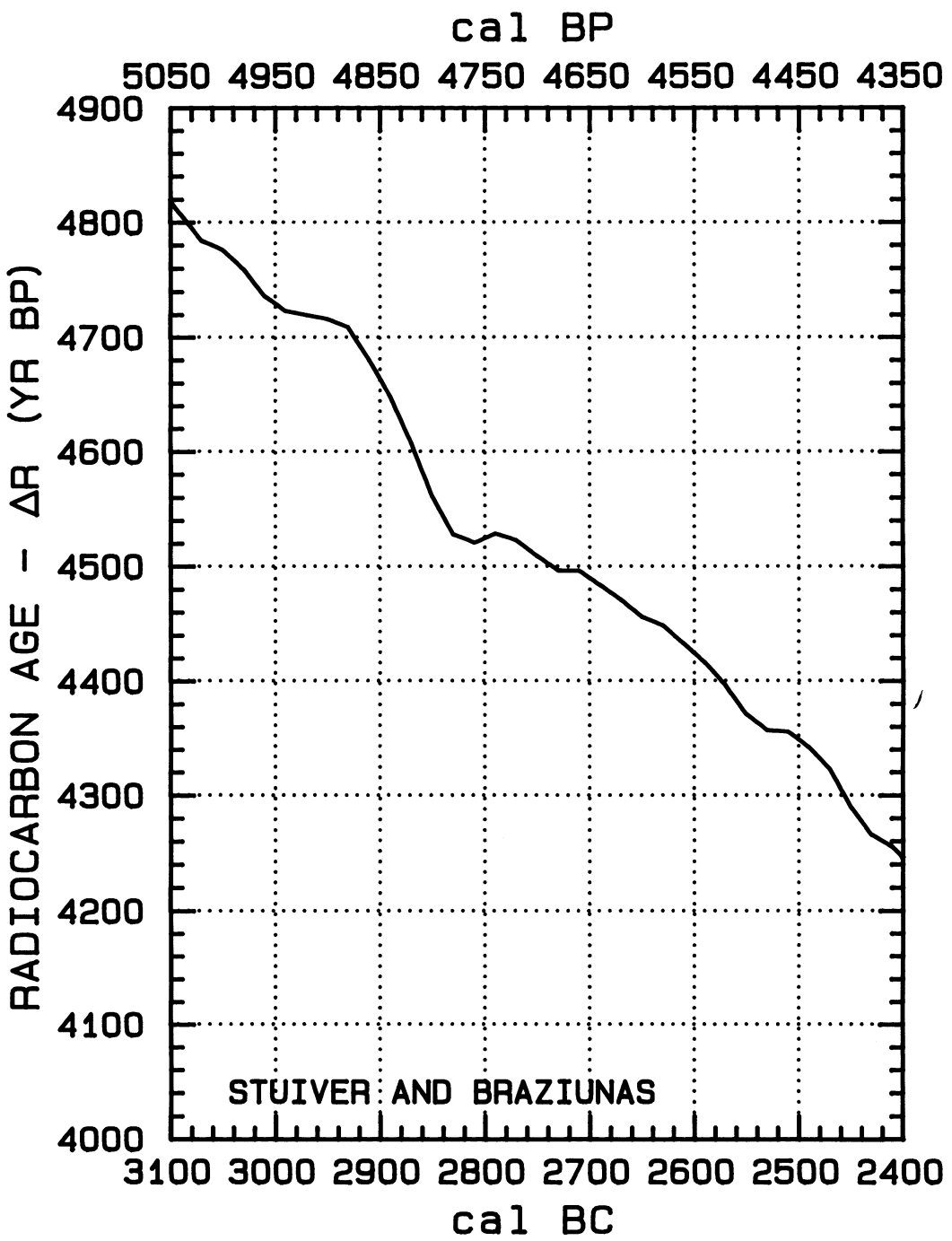
cal BP
5050 4950 4850 4750 4650 4550 4450 4350
4900
4800
4700
4600
4500
4400
4300
4200
4100
4000
RADIOCARBON AGE - ΔR (YR BP)
STUIVER AND BRAZIUNAS
3100 3000 2900 2800 2700 2600 2500 2400
cal BC

Fig. 17J

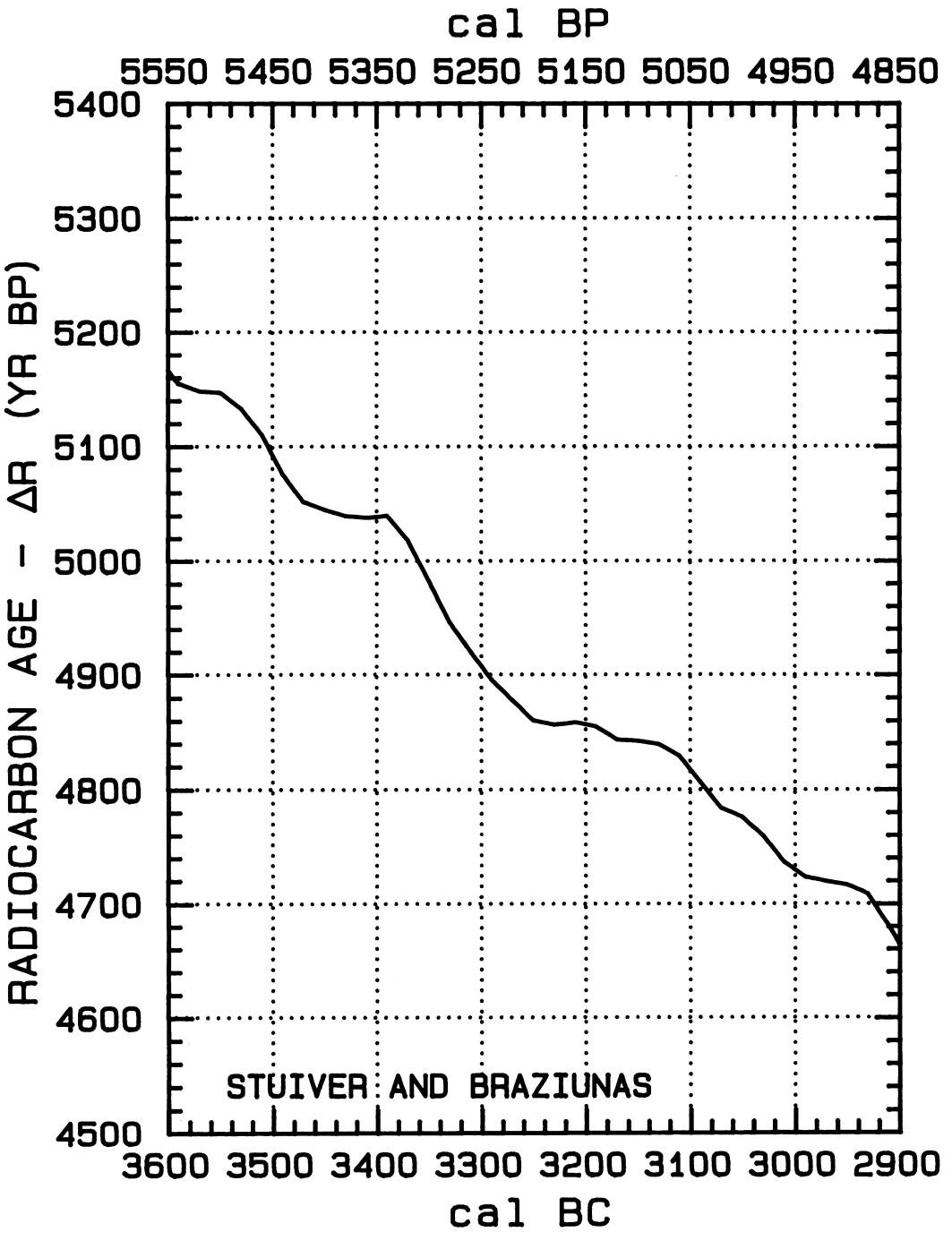
cal BP
5550 5450 5350 5250 5150 5050 4950 4850
5400
5300
5200
5100
5000
4900
4800
4700
4600
4500
RADIOCARBON AGE - ΔR (YR BP)
STUIVER AND BRAZIUNAS
3600 3500 3400 3300 3200 3100 3000 2900
cal BC

Fig. 17K

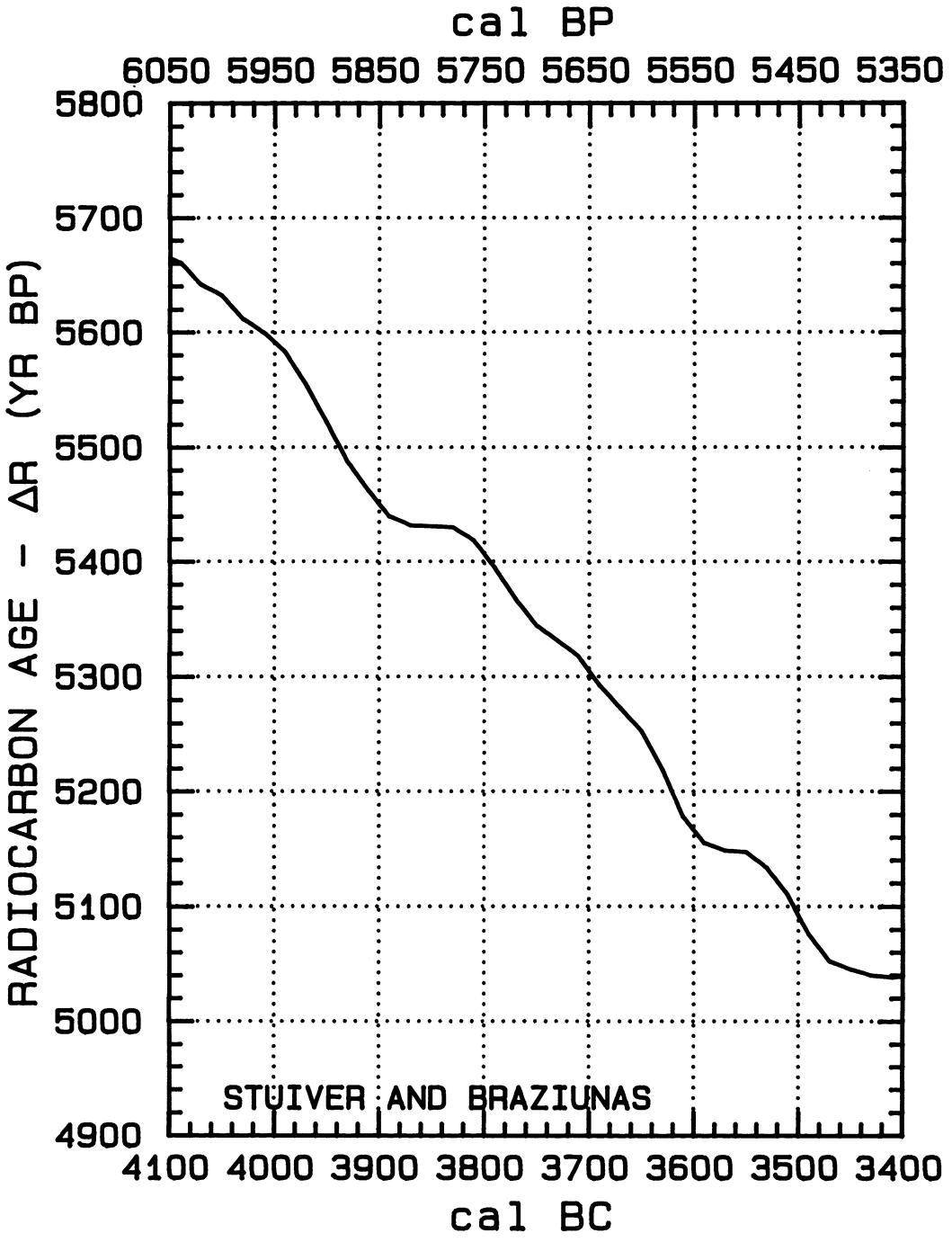
cal BP
6050 5950 5850 5750 5650 5550 5450 5350
5800
5700
5600
5500
5400
5300
5200
5100
5000
4900
RADIOCARBON AGE - ΔR (YR BP)
STUIVER AND BRAZIUNAS
4100 4000 3900 3800 3700 3600 3500 3400
cal BC

Fig. 17L

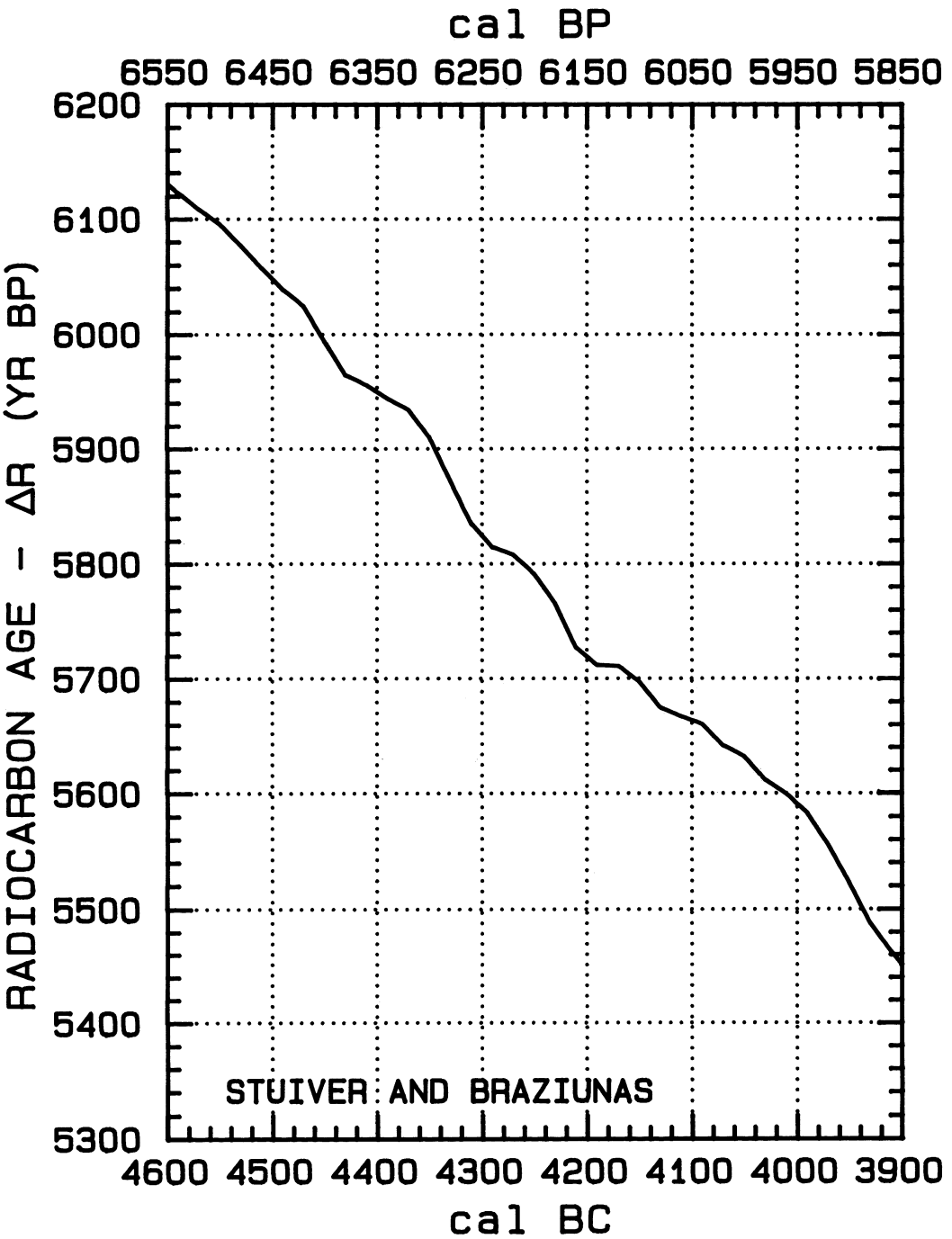
cal BP
6550 6450 6350 6250 6150 6050 5950 5850
6200
6100
6000
5900
5800
5700
5600
5500
5400
5300
RADIOCARBON AGE - ΔR (YR BP)
STUIVER AND BRAZIUNAS
4600 4500 4400 4300 4200 4100 4000 3900
cal BC

Fig. 17M

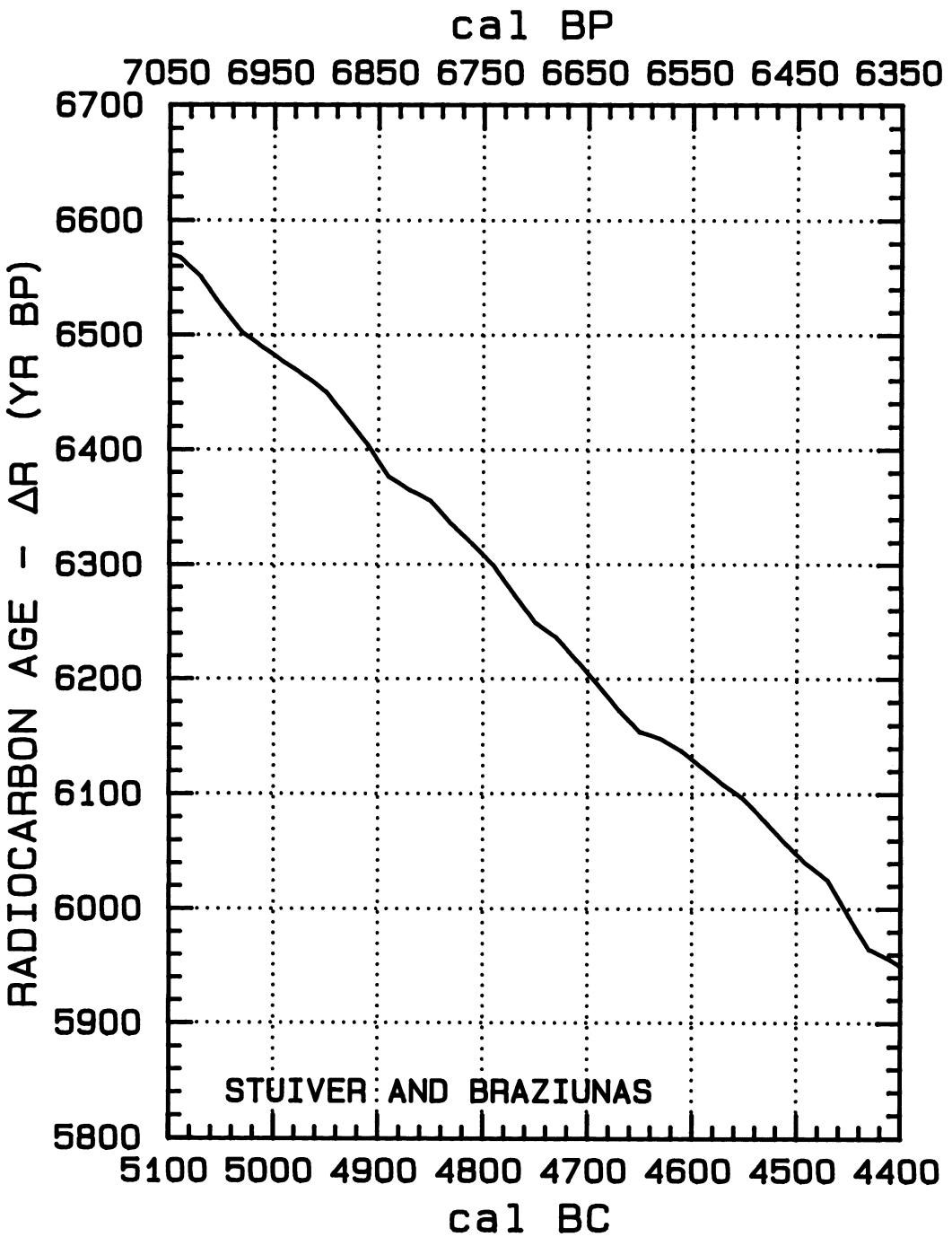
cal BP
7050 6950 6850 6750 6650 6550 6450 6350
6700
6600
6500
6400
6300
6200
6100
6000
5900
5800
RADIOCARBON AGE - ΔR (YR BP)
STUIVER AND BRAZIUNAS
5100 5000 4900 4800 4700 4600 4500 4400
cal BC

Fig. 17N

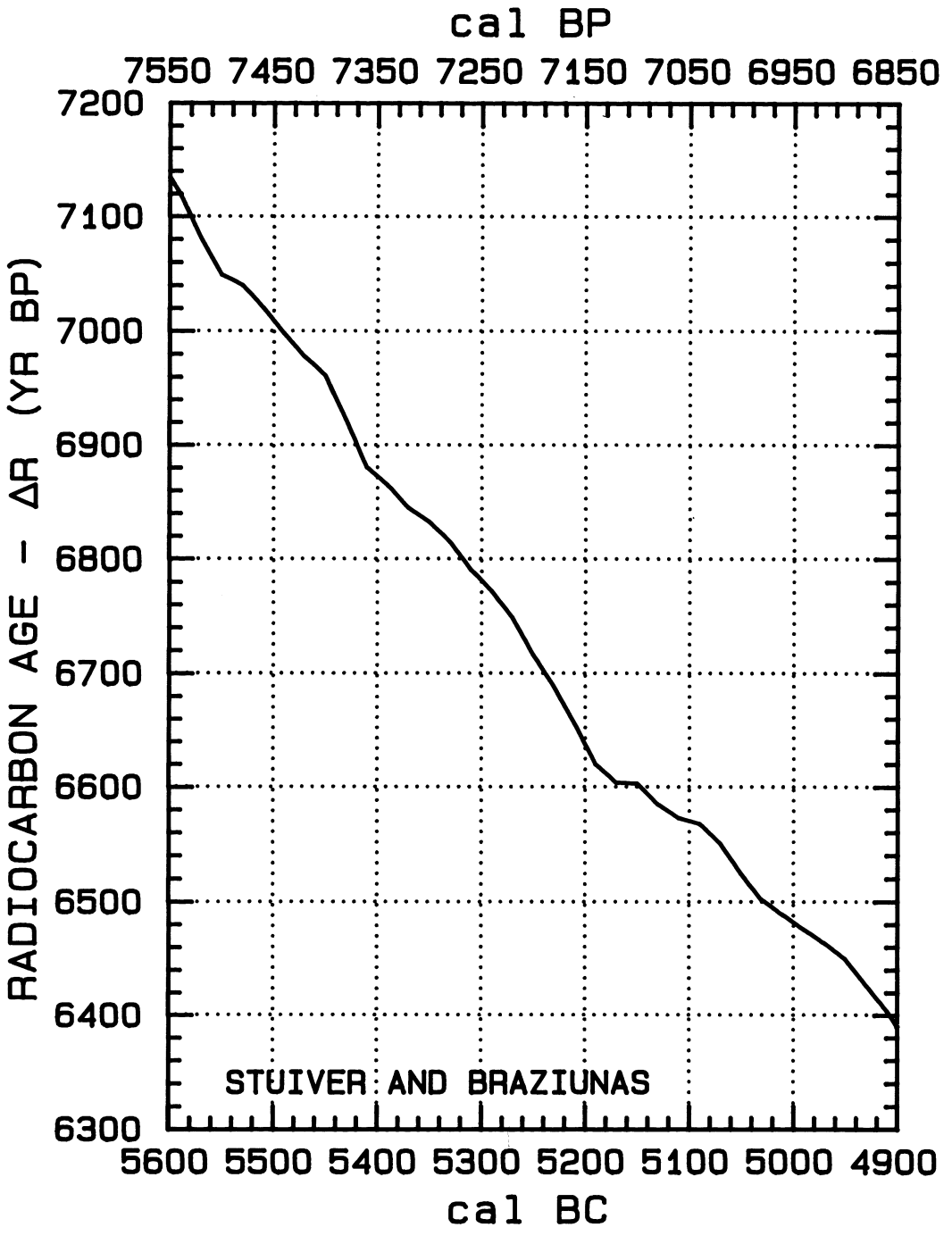
cal BP
7550 7450 7350 7250 7150 7050 6950 6850
7200
7100
7000
6900
6800
6700
6600
6500
6400
6300
RADIOCARBON AGE - ΔR (YR BP)
STUIVER AND BRAZIUNAS
5600 5500 5400 5300 5200 5100 5000 4900
cal BC

Fig. 17O

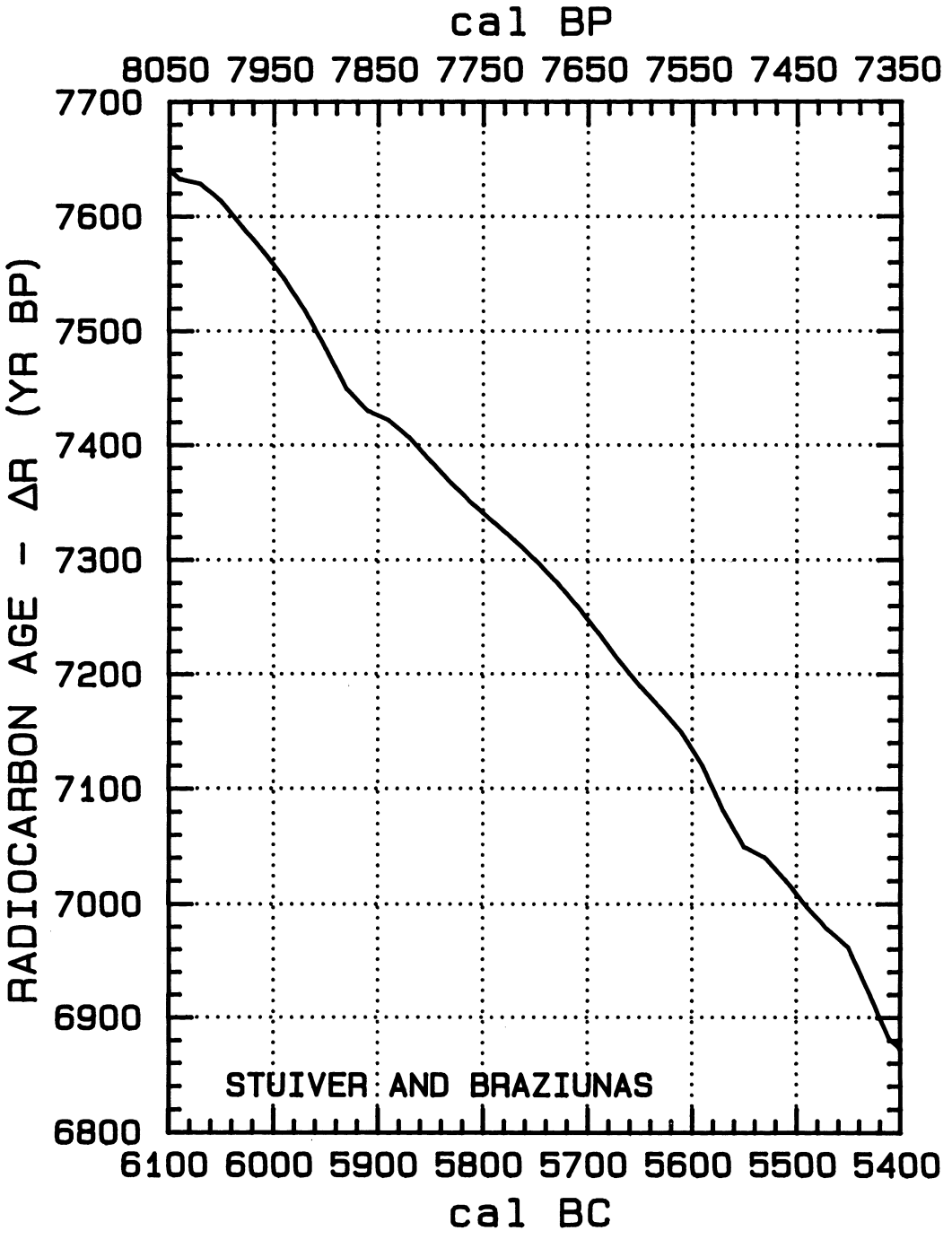
cal BP
8050 7950 7850 7750 7650 7550 7450 7350
7700
7600
7500
7400
7300
7200
7100
7000
6900
6800
RADIOCARBON AGE - ΔR (YR BP)
STUIVER AND BRAZIUNAS
6100 6000 5900 5800 5700 5600 5500 5400
cal BC

Fig. 17P

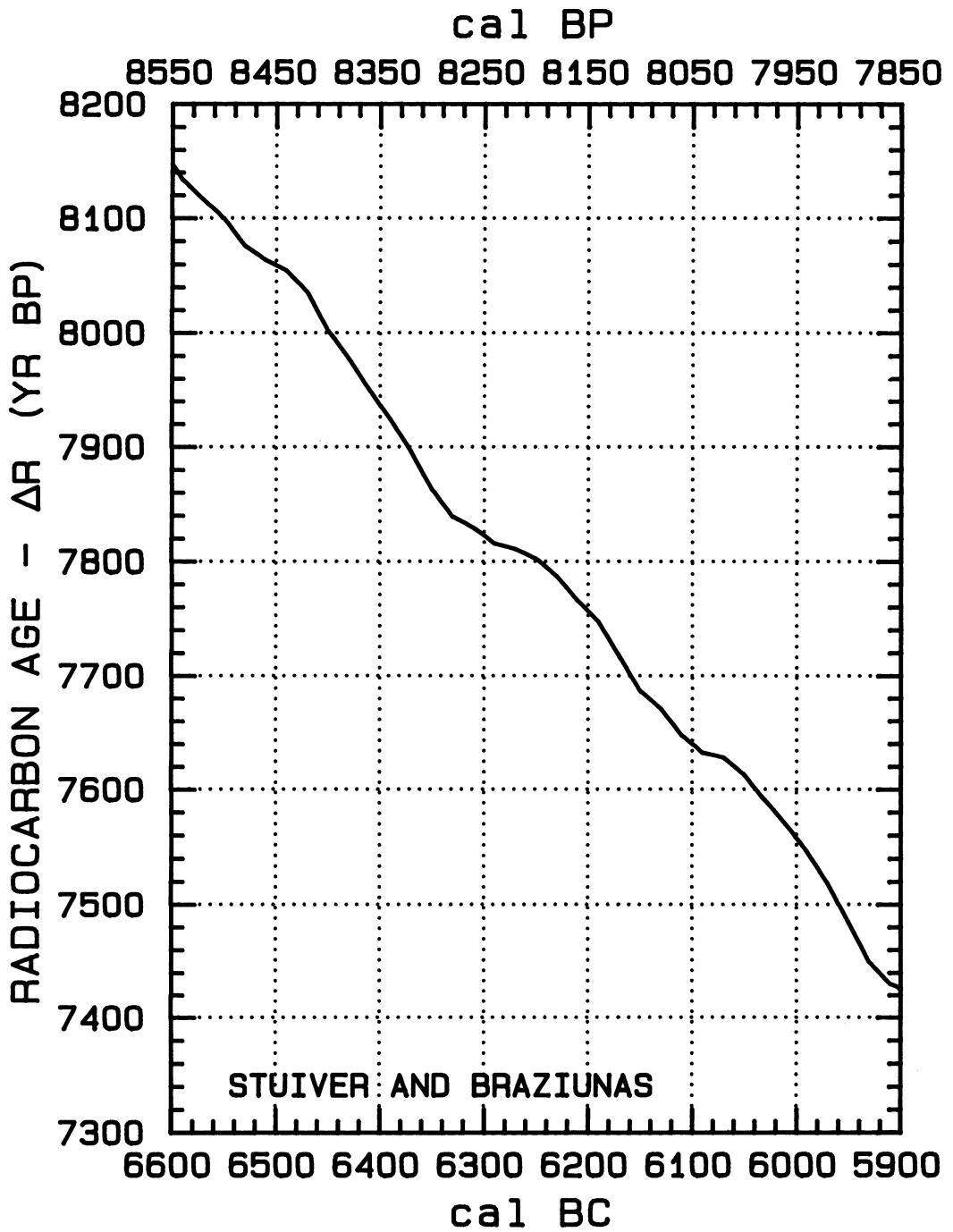
cal BP
8550 8450 8350 8250 8150 8050 7950 7850
8200
8100
8000
7900
7800
7700
7600
7500
7400
7300
RADIOCARBON AGE - ΔR (YR BP)
STUIVER AND BRAZIUNAS
6600 6500 6400 6300 6200 6100 6000 5900
cal BC

Fig. 17Q

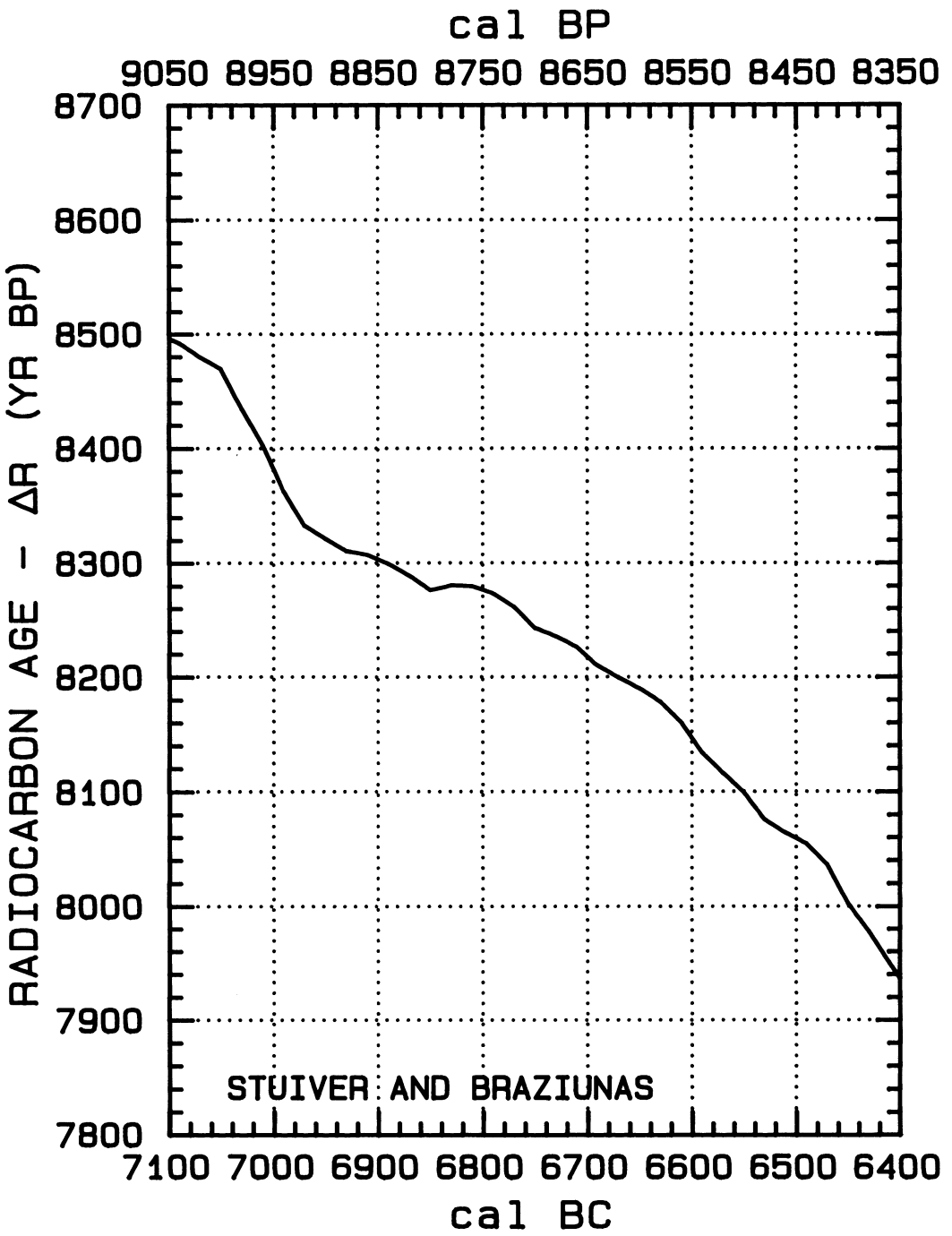
cal BP
9050 8950 8850 8750 8650 8550 8450 8350
8700
8600
8500
8400
8300
8200
8100
8000
7900
7800
RADIOCARBON AGE - ΔR (YR BP)
STUIVER AND BRAZIUNAS
7100 7000 6900 6800 6700 6600 6500 6400
cal BC

Fig. 17R

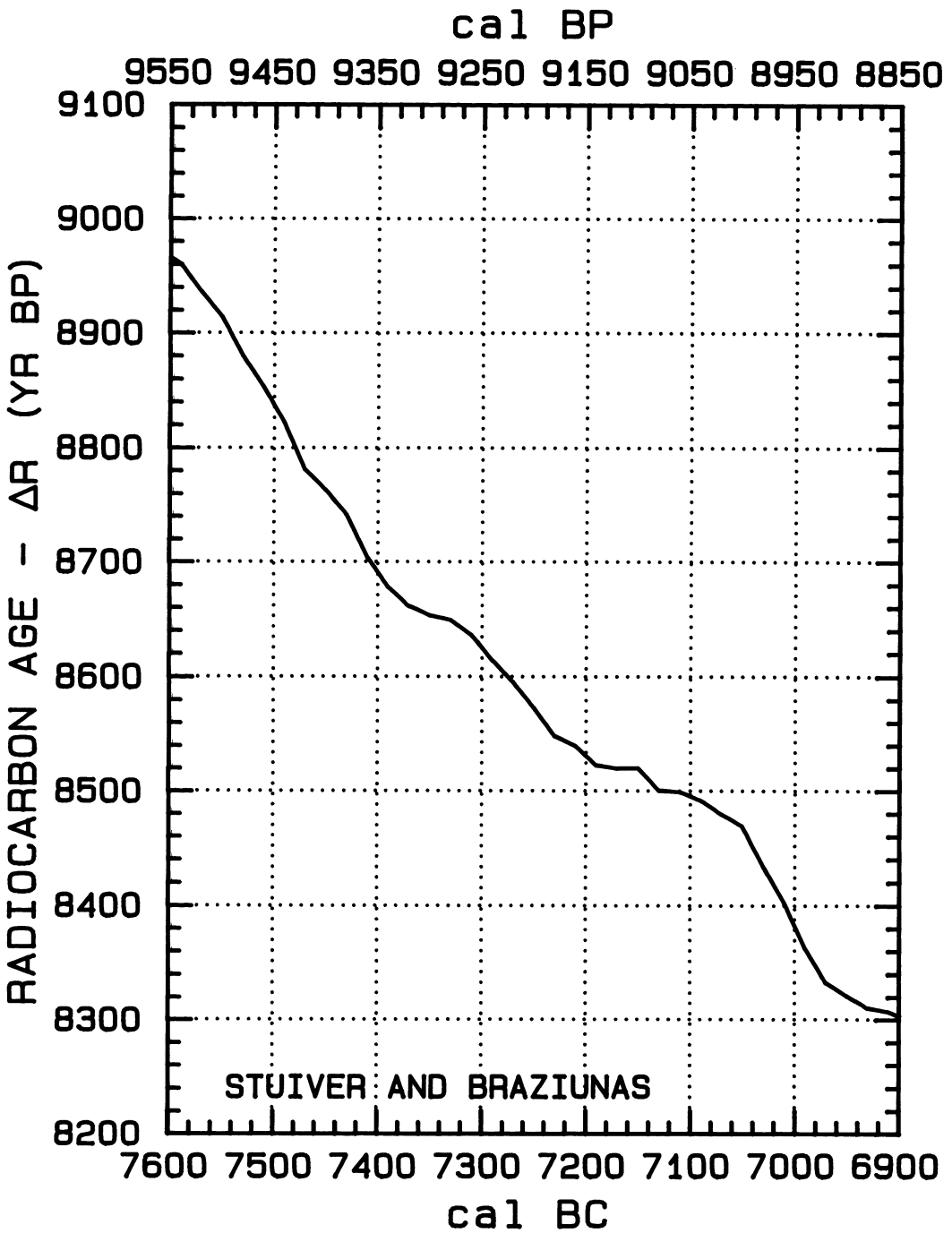
cal BP
9550 9450 9350 9250 9150 9050 8950 8850
9100
9000
8900
8800
8700
8600
8500
8400
8300
8200
RADIOCARBON AGE - ΔR (YR BP)
STUIVER AND BRAZIUNAS
7600 7500 7400 7300 7200 7100 7000 6900
cal BC

Fig. 17S

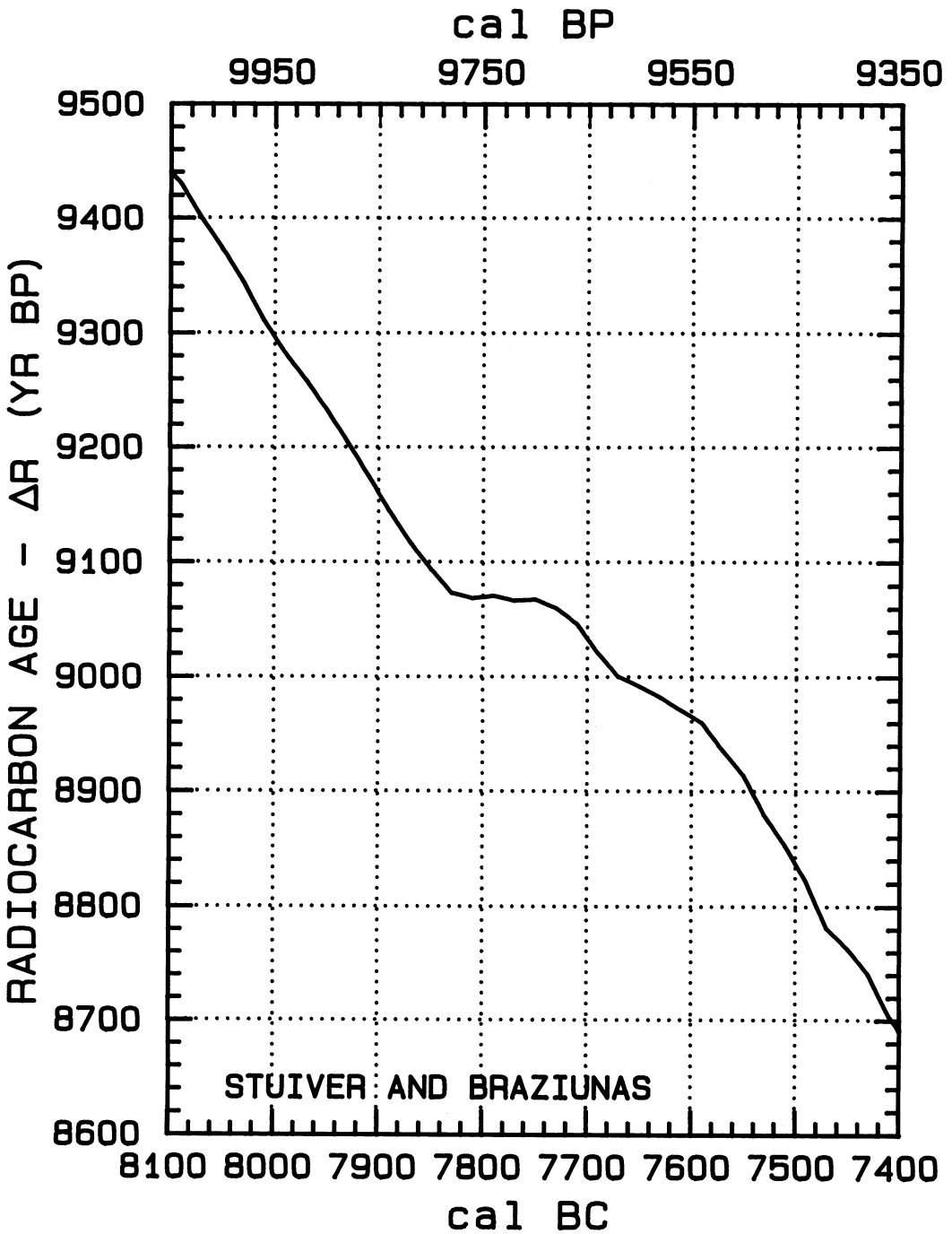
cal BP
9950
9750
9550
9350
9500
9400
9300
9200
9100
9000
8900
8800
8700
8600
RADIOCARBON AGE - ΔR (YR BP)
STUIVER AND BRAZIUNAS
8100 8000 7900 7800 7700 7600 7500 7400
cal BC

Fig. 17T

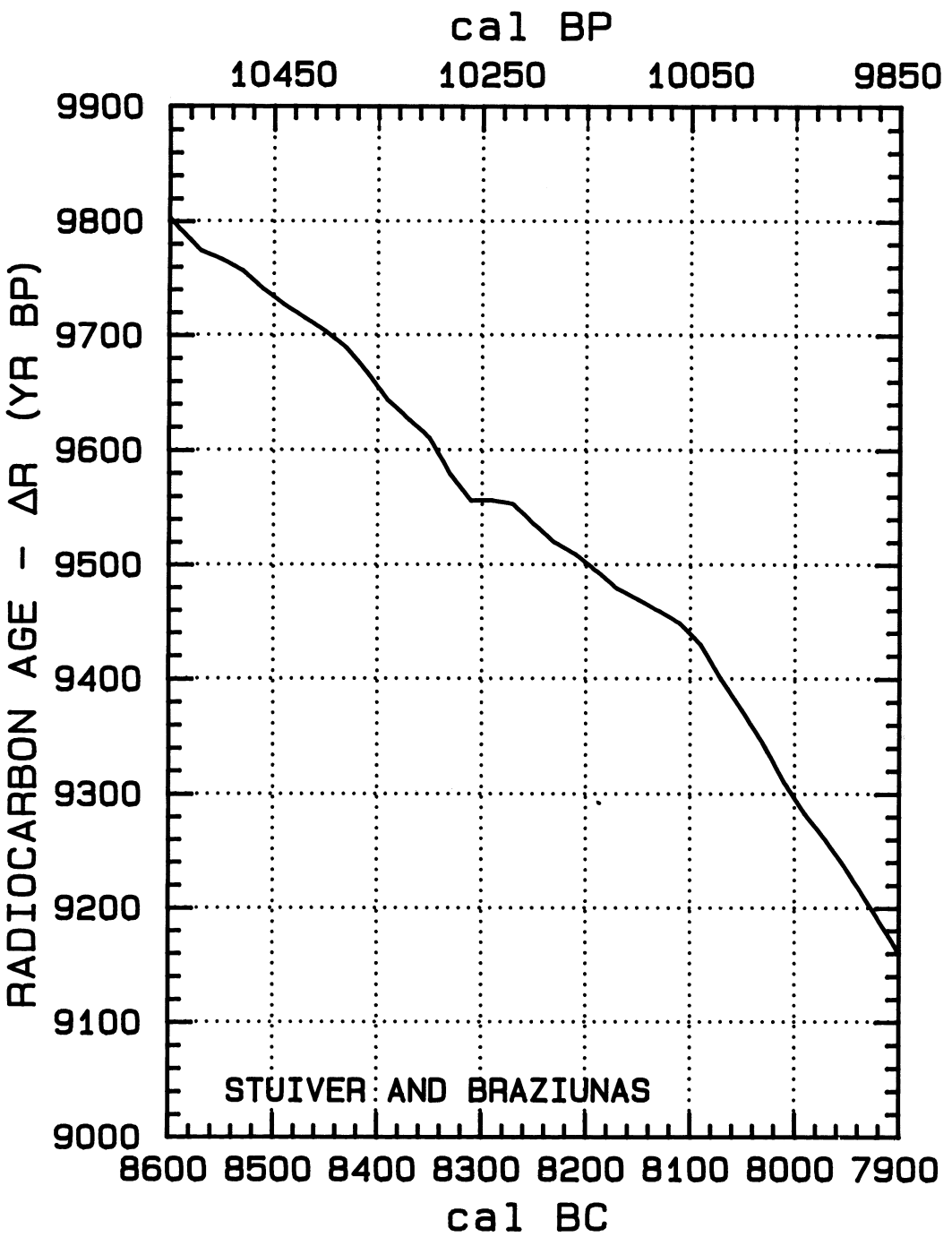
cal BP
10450
10250
10050
9850
9900
9800
9700
9600
9500
9400
9300
9200
9100
9000
RADIOCARBON AGE - ΔR (YR BP)
STUIVER AND BRAZIUNAS
8600 8500 8400 8300 8200 8100 8000 7900
cal BC

Fig. 17U

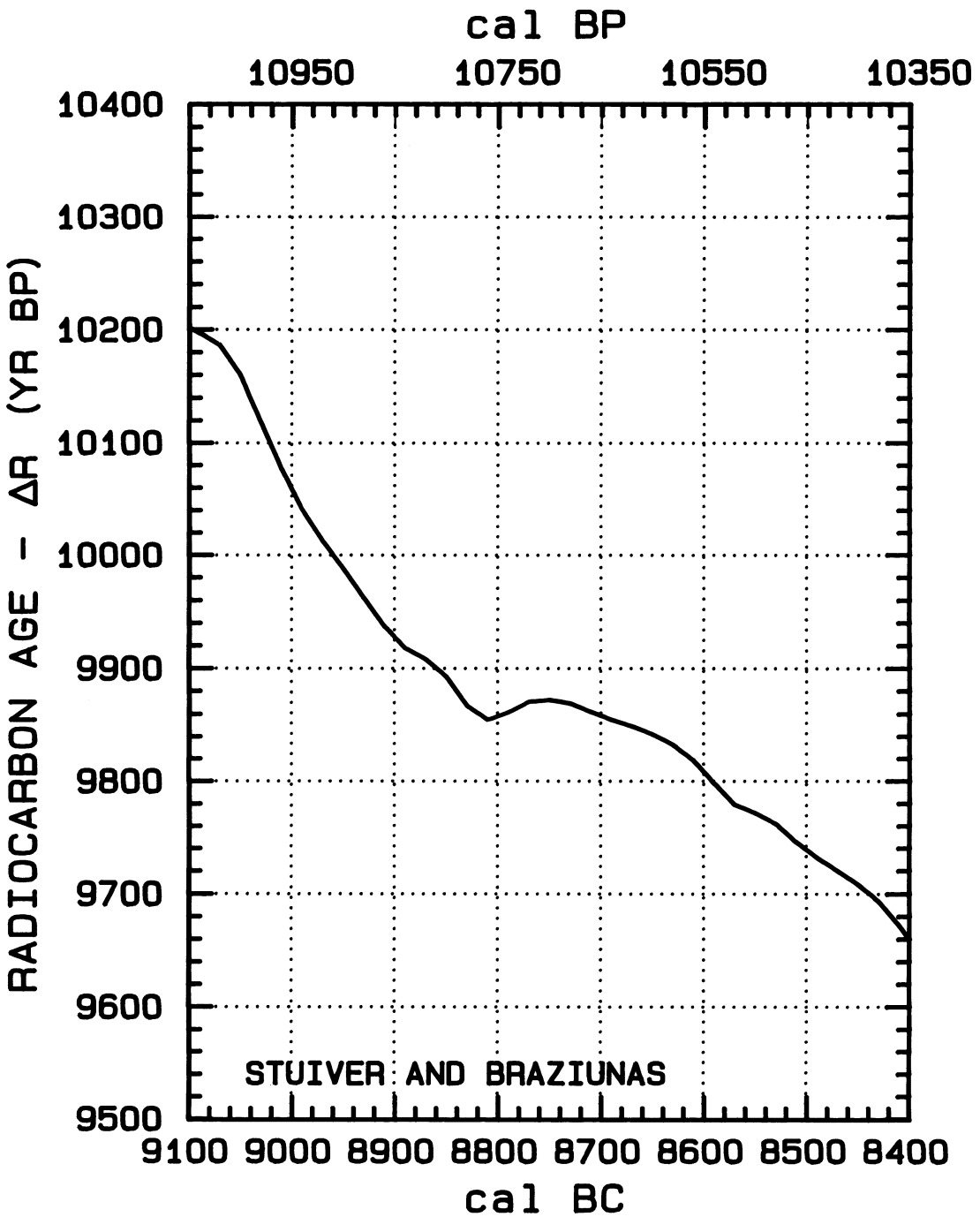
cal BP
10950
10750
10550
10350
10400
10300
10200
10100
10000
9900
9800
9700
9600
9500
RADIOCARBON AGE - ΔR (YR BP)
STUIVER AND BRAZIUNAS
9100 9000 8900 8800 8700 8600 8500 8400
cal BC

Fig. 17V

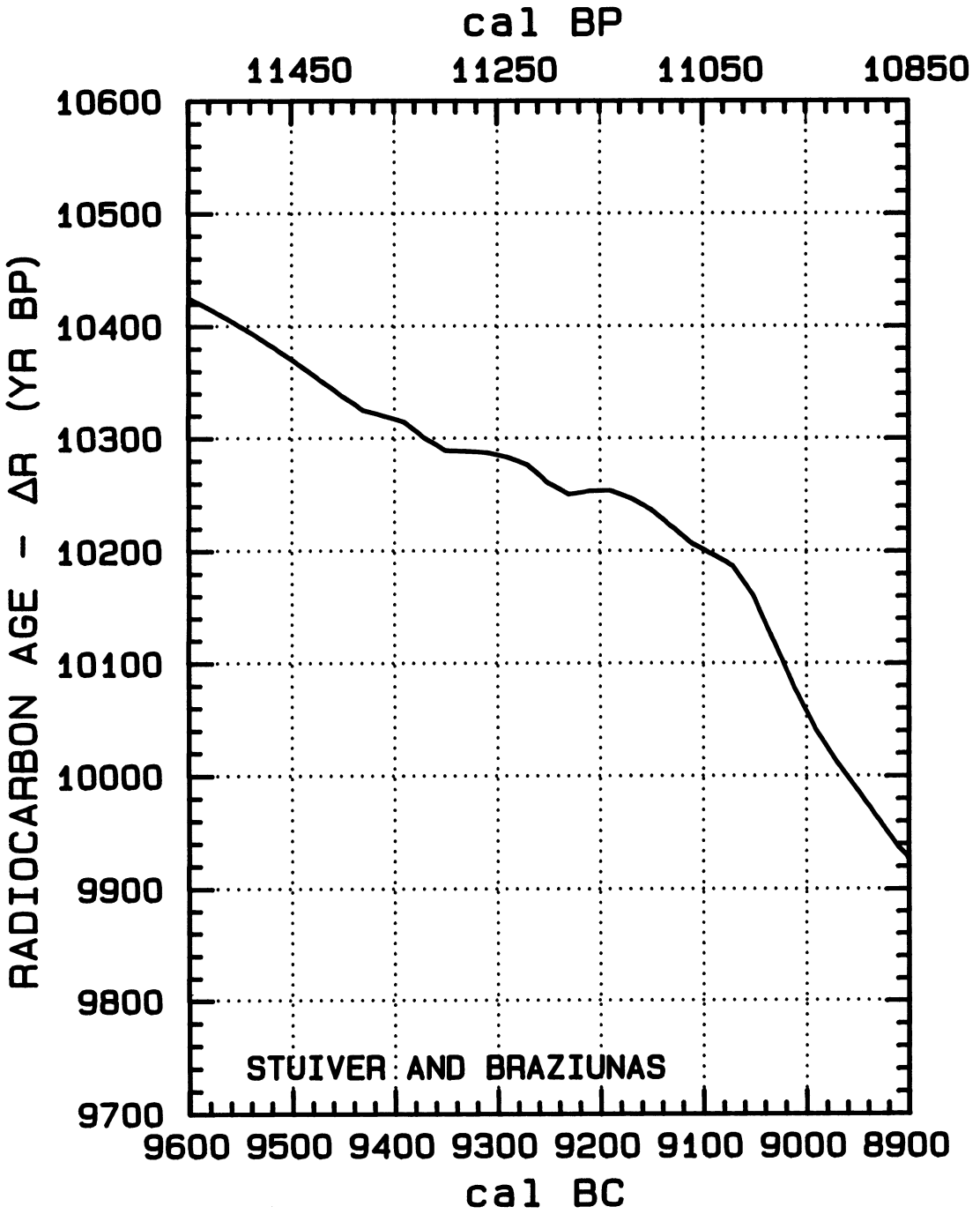
cal BP
11450
11250
11050
10850
10600
10500
10400
10300
10200
10100
10000
9900
9800
9700
RADIOCARBON AGE - ΔR (YR BP)
STUIVER AND BRAZIUNAS
9600 9500 9400 9300 9200 9100 9000 8900
cal BC

Fig. 17W

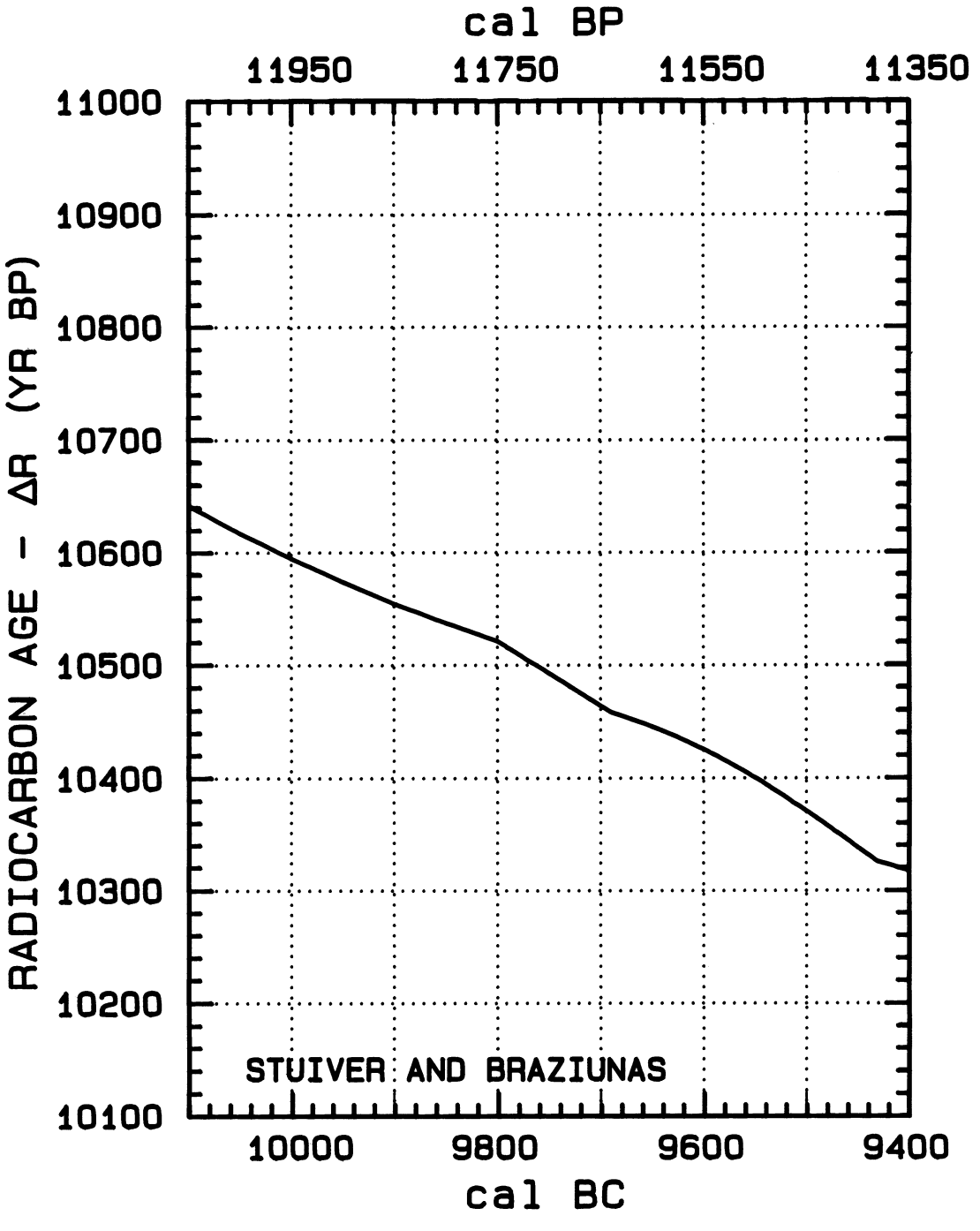
cal BP
11950
11750
11550
11350
11000
10900
10800
10700
10600
10500
10400
10300
10200
10100
RADIOCARBON AGE - ΔR (YR BP)
STUIVER AND BRAZIUNAS
10000
9800
9600
9400
cal BC

Fig. 17X

TABLE 1. Marine model ^{14}C ages (≈460–10,600 ^{14}C yr BP) calculated from the bidecadal atmospheric tree-ring data from AD 1950–9440 BC and a smoothing spline through coral data to 20,000 BC (Bard *et al.*, 1993; Stuiver & Reimer 1993). The pre-10,000 BC part of the spline was only used as a model start-up. The standard deviations in the ages and $\Delta^{14}C$ values reflect the standard deviations in the tree-ring and coral data.

Cal AD/BC	$\Delta^{14}C$ ‰	^{14}C age (BP)	Cal BP	Cal AD/BC	$\Delta^{14}C$ ‰	^{14}C age (BP)	Cal BP
AD 1950	−58.4 ± 1.6	483 ± 13	BP 0	AD 1090	−56.9 ± .9	1306 ± 8	BP 860
AD 1930	−54.2 ± .5	467 ± 4	BP 20	AD 1070	−56.2 ± .9	1320 ± 7	BP 880
AD 1910	−51.3 ± .6	462 ± 5	BP 40	AD 1050	−57.2 ± 1.0	1347 ± 9	BP 900
AD 1890	−50.1 ± .6	471 ± 5	BP 60	AD 1030	−59.0 ± 1.2	1383 ± 10	BP 920
AD 1870	−49.3 ± .5	484 ± 4	BP 80	AD 1010	−60.6 ± 1.2	1416 ± 11	BP 940
AD 1850	−48.2 ± .5	494 ± 4	BP 100	AD 990	−61.1 ± 1.1	1440 ± 9	BP 960
AD 1830	−47.7 ± .6	509 ± 5	BP 120	AD 970	−61.5 ± 1.2	1462 ± 10	BP 980
AD 1810	−48.5 ± .5	535 ± 4	BP 140	AD 950	−61.1 ± 1.5	1479 ± 12	BP 1000
AD 1790	−47.9 ± .5	550 ± 5	BP 160	AD 930	−60.1 ± 1.4	1489 ± 12	BP 1020
AD 1770	−45.3 ± .5	547 ± 4	BP 180	AD 910	−59.4 ± 1.2	1503 ± 10	BP 1040
AD 1750	−43.2 ± .4	549 ± 4	BP 200	AD 890	−60.0 ± 1.2	1527 ± 11	BP 1060
AD 1730	−41.3 ± .5	553 ± 4	BP 220	AD 870	−60.3 ± 1.3	1549 ± 11	BP 1080
AD 1710	−41.1 ± .3	570 ± 3	BP 240	AD 850	−59.4 ± 1.2	1561 ± 10	BP 1100
AD 1690	−43.0 ± .4	606 ± 3	BP 260	AD 830	−58.4 ± 1.3	1572 ± 11	BP 1120
AD 1670	−45.9 ± .5	649 ± 4	BP 280	AD 810	−58.0 ± 1.3	1588 ± 11	BP 1140
AD 1650	−48.0 ± .5	687 ± 4	BP 300	AD 790	−58.2 ± 1.0	1609 ± 9	BP 1160
AD 1630	−49.1 ± .5	715 ± 4	BP 320	AD 770	−58.9 ± 1.1	1634 ± 10	BP 1180
AD 1610	−48.3 ± .5	728 ± 4	BP 340	AD 750	−58.1 ± 1.0	1647 ± 8	BP 1200
AD 1590	−46.3 ± .5	731 ± 5	BP 360	AD 730	−57.2 ± 1.0	1659 ± 8	BP 1220
AD 1570	−44.8 ± .5	737 ± 5	BP 380	AD 710	−57.6 ± 1.1	1681 ± 9	BP 1240
AD 1550	−43.7 ± .5	747 ± 4	BP 400	AD 690	−58.4 ± 1.7	1708 ± 15	BP 1260
AD 1530	−43.9 ± .5	769 ± 4	BP 420	AD 670	−60.4 ± 1.7	1744 ± 14	BP 1280
AD 1510	−44.8 ± .6	796 ± 5	BP 440	AD 650	−62.2 ± 1.3	1779 ± 12	BP 1300
AD 1490	−45.6 ± 1.3	822 ± 11	BP 460	AD 630	−62.7 ± 1.5	1803 ± 13	BP 1320
AD 1470	−47.2 ± 1.6	855 ± 13	BP 480	AD 610	−63.0 ± 1.8	1825 ± 15	BP 1340
AD 1450	−49.2 ± 1.2	891 ± 11	BP 500	AD 590	−63.0 ± 1.6	1844 ± 14	BP 1360
AD 1430	−51.8 ± 1.5	933 ± 13	BP 520	AD 570	−62.3 ± 1.7	1858 ± 14	BP 1380
AD 1410	−53.8 ± 1.4	969 ± 12	BP 540	AD 550	−62.7 ± 1.5	1881 ± 13	BP 1400
AD 1390	−55.5 ± 1.2	1003 ± 10	BP 560	AD 530	−62.9 ± 1.3	1902 ± 12	BP 1420
AD 1370	−54.9 ± 1.2	1017 ± 10	BP 580	AD 510	−61.7 ± 1.5	1911 ± 13	BP 1440
AD 1350	−53.2 ± 1.3	1022 ± 11	BP 600	AD 490	−60.6 ± 1.5	1921 ± 13	BP 1460
AD 1330	−53.1 ± 1.1	1041 ± 10	BP 620	AD 470	−59.7 ± 1.6	1933 ± 14	BP 1480
AD 1310	−55.4 ± 1.1	1080 ± 9	BP 640	AD 450	−59.7 ± 1.6	1952 ± 14	BP 1500
AD 1290	−58.4 ± 1.3	1125 ± 11	BP 660	AD 430	−60.6 ± 1.5	1979 ± 13	BP 1520
AD 1270	−60.0 ± 2.3	1158 ± 20	BP 680	AD 410	−61.4 ± 1.6	2005 ± 14	BP 1540
AD 1250	−60.1 ± 2.3	1178 ± 19	BP 700	AD 390	−61.3 ± 1.3	2024 ± 11	BP 1560
AD 1230	−60.4 ± 1.0	1200 ± 9	BP 720	AD 370	−60.8 ± 1.3	2039 ± 11	BP 1580
AD 1210	−60.8 ± 1.5	1223 ± 13	BP 740	AD 350	−60.0 ± 1.6	2052 ± 14	BP 1600
AD 1190	−60.3 ± 1.4	1239 ± 12	BP 760	AD 330	−60.1 ± 1.7	2072 ± 14	BP 1620
AD 1170	−60.5 ± 1.0	1260 ± 9	BP 780	AD 310	−59.4 ± 1.6	2085 ± 14	BP 1640
AD 1150	−60.4 ± 1.0	1278 ± 9	BP 800	AD 290	−57.4 ± 1.6	2088 ± 13	BP 1660
AD 1130	−59.0 ± 1.2	1285 ± 10	BP 820	AD 270	−56.8 ± 1.4	2103 ± 12	BP 1680
AD 1110	−58.3 ± 1.1	1299 ± 9	BP 840	AD 250	−58.0 ± 1.0	2132 ± 9	BP 1700

TABLE 1. (Continued)

Cal AD/BC	$\Delta^{14}C$ ‰	^{14}C age (BP)	Cal BP	Cal AD/BC	$\Delta^{14}C$ ‰	^{14}C age (BP)	Cal BP
AD 230	−58.4 ± 1.5	2155 ± 13	BP 1720	710 BC	−32.2 ± 1.9	2846 ± 16	BP 2660
AD 210	−57.9 ± 1.5	2170 ± 13	BP 1740	730 BC	−32.0 ± 1.5	2865 ± 12	BP 2680
AD 190	−56.8 ± 1.6	2180 ± 14	BP 1760	750 BC	−33.3 ± 1.6	2895 ± 14	BP 2700
AD 170	−55.8 ± 1.7	2191 ± 15	BP 1780	770 BC	−36.0 ± 1.9	2937 ± 16	BP 2720
AD 150	−55.5 ± 1.6	2207 ± 14	BP 1800	790 BC	−38.4 ± 1.2	2976 ± 10	BP 2740
AD 130	−56.0 ± 1.2	2232 ± 10	BP 1820	810 BC	−41.0 ± 1.6	3017 ± 13	BP 2760
AD 110	−56.0 ± 1.7	2251 ± 15	BP 1840	830 BC	−41.8 ± 1.4	3044 ± 12	BP 2780
AD 90	−55.7 ± 1.4	2268 ± 12	BP 1860	850 BC	−41.7 ± 1.5	3062 ± 13	BP 2800
AD 70	−56.3 ± 1.3	2293 ± 11	BP 1880	870 BC	−40.6 ± 1.5	3072 ± 13	BP 2820
AD 50	−56.0 ± 1.1	2309 ± 9	BP 1900	890 BC	−40.1 ± 1.5	3087 ± 13	BP 2840
AD 30	−55.3 ± 1.3	2323 ± 11	BP 1920	910 BC	−40.7 ± 1.4	3112 ± 12	BP 2860
AD 10	−55.4 ± 1.0	2343 ± 9	BP 1940	930 BC	−40.7 ± 1.6	3132 ± 13	BP 2880
10 BC	−55.2 ± 1.1	2360 ± 9	BP 1960	950 BC	−39.7 ± 1.4	3143 ± 12	BP 2900
30 BC	−54.8 ± .9	2376 ± 8	BP 1980	970 BC	−38.5 ± 1.2	3152 ± 10	BP 2920
50 BC	−55.0 ± 1.0	2397 ± 8	BP 2000	990 BC	−38.4 ± 1.4	3171 ± 11	BP 2940
70 BC	−54.4 ± 1.2	2411 ± 10	BP 2020	1010 BC	−38.4 ± 1.0	3190 ± 9	BP 2960
90 BC	−53.4 ± 1.2	2422 ± 10	BP 2040	1030 BC	−37.9 ± 1.4	3205 ± 12	BP 2980
110 BC	−52.9 ± 1.1	2437 ± 9	BP 2060	1050 BC	−37.1 ± 1.2	3218 ± 10	BP 3000
130 BC	−52.1 ± 1.2	2450 ± 10	BP 2080	1070 BC	−35.9 ± 1.3	3228 ± 11	BP 3020
150 BC	−51.4 ± 1.3	2463 ± 11	BP 2100	1090 BC	−34.7 ± 1.3	3237 ± 11	BP 3040
170 BC	−51.6 ± 1.2	2485 ± 10	BP 2120	1110 BC	−34.0 ± 1.3	3250 ± 11	BP 3060
190 BC	−52.2 ± 1.2	2510 ± 11	BP 2140	1130 BC	−33.8 ± 1.5	3269 ± 13	BP 3080
210 BC	−52.5 ± 1.2	2531 ± 10	BP 2160	1150 BC	−33.0 ± 1.6	3281 ± 14	BP 3100
230 BC	−51.2 ± 1.2	2540 ± 10	BP 2180	1170 BC	−32.3 ± 1.6	3295 ± 13	BP 3120
250 BC	−50.2 ± 1.4	2551 ± 12	BP 2200	1190 BC	−31.2 ± 1.6	3305 ± 14	BP 3140
270 BC	−48.8 ± 1.4	2558 ± 12	BP 2220	1210 BC	−30.9 ± 1.3	3322 ± 11	BP 3160
290 BC	−46.6 ± 1.4	2559 ± 12	BP 2240	1230 BC	−30.1 ± 1.6	3334 ± 13	BP 3180
310 BC	−45.0 ± 1.4	2565 ± 12	BP 2260	1250 BC	−29.3 ± 1.5	3347 ± 12	BP 3200
330 BC	−44.4 ± 1.4	2579 ± 12	BP 2280	1270 BC	−29.7 ± 1.7	3370 ± 14	BP 3220
350 BC	−45.6 ± 1.3	2609 ± 11	BP 2300	1290 BC	−28.8 ± 1.7	3382 ± 14	BP 3240
370 BC	−47.6 ± 1.2	2645 ± 10	BP 2320	1310 BC	−28.8 ± 1.8	3401 ± 15	BP 3260
390 BC	−50.0 ± 1.4	2685 ± 12	BP 2340	1330 BC	−28.2 ± 1.6	3416 ± 13	BP 3280
410 BC	−51.7 ± 1.3	2719 ± 11	BP 2360	1350 BC	−26.4 ± 1.7	3420 ± 14	BP 3300
430 BC	−50.7 ± 1.3	2730 ± 11	BP 2380	1370 BC	−26.2 ± 1.7	3439 ± 14	BP 3320
450 BC	−48.9 ± 1.5	2734 ± 13	BP 2400	1390 BC	−27.3 ± 1.4	3467 ± 12	BP 3340
470 BC	−47.5 ± 1.2	2742 ± 10	BP 2420	1410 BC	−28.5 ± 1.5	3496 ± 13	BP 3360
490 BC	−46.6 ± 1.3	2754 ± 11	BP 2440	1430 BC	−29.0 ± 1.5	3520 ± 12	BP 3380
510 BC	−45.9 ± 1.2	2767 ± 10	BP 2460	1450 BC	−28.9 ± 1.1	3538 ± 9	BP 3400
530 BC	−45.7 ± 1.0	2785 ± 9	BP 2480	1470 BC	−28.0 ± 1.3	3550 ± 11	BP 3420
550 BC	−45.1 ± 1.0	2799 ± 8	BP 2500	1490 BC	−27.2 ± 1.5	3563 ± 13	BP 3440
570 BC	−43.7 ± 1.3	2806 ± 11	BP 2520	1510 BC	−28.2 ± 1.6	3591 ± 14	BP 3460
590 BC	−42.1 ± 1.3	2813 ± 11	BP 2540	1530 BC	−29.3 ± 1.6	3619 ± 13	BP 3480
610 BC	−40.6 ± 1.2	2819 ± 10	BP 2560	1550 BC	−28.0 ± 1.8	3628 ± 15	BP 3500
630 BC	−38.4 ± 1.1	2820 ± 9	BP 2580	1570 BC	−26.2 ± 2.0	3633 ± 17	BP 3520
650 BC	−36.7 ± 1.2	2826 ± 10	BP 2600	1590 BC	−25.4 ± 1.5	3646 ± 12	BP 3540
670 BC	−35.1 ± 1.5	2832 ± 13	BP 2620	1610 BC	−25.5 ± 1.4	3666 ± 12	BP 3560
690 BC	−33.2 ± 1.7	2835 ± 14	BP 2640	1630 BC	−25.4 ± 1.5	3684 ± 12	BP 3580

TABLE 1. (Continued)

Cal AD/BC	$\Delta^{14}C$ ‰	^{14}C age (BP)	Cal BP	Cal AD/BC	$\Delta^{14}C$ ‰	^{14}C age (BP)	Cal BP
1650 BC	−24.6 ± 1.2	3698 ± 10	BP 3600	2590 BC	−.7 ± 1.2	4417 ± 10	BP 4540
1670 BC	−24.5 ± 1.7	3716 ± 14	BP 3620	2610 BC	−.3 ± 1.7	4433 ± 14	BP 4560
1690 BC	−25.2 ± 1.5	3741 ± 12	BP 3640	2630 BC	.1 ± 1.1	4449 ± 9	BP 4580
1710 BC	−24.2 ± 1.8	3752 ± 15	BP 3660	2650 BC	1.6 ± 1.7	4456 ± 14	BP 4600
1730 BC	−23.6 ± 1.5	3767 ± 12	BP 3680	2670 BC	2.1 ± 1.3	4471 ± 11	BP 4620
1750 BC	−24.4 ± 1.5	3793 ± 12	BP 3700	2690 BC	3.0 ± 1.4	4484 ± 11	BP 4640
1770 BC	−24.1 ± 1.4	3810 ± 11	BP 3720	2710 BC	3.9 ± 1.3	4496 ± 11	BP 4660
1790 BC	−23.3 ± 1.4	3823 ± 11	BP 3740	2730 BC	6.3 ± 1.2	4496 ± 10	BP 4680
1810 BC	−21.7 ± 1.4	3829 ± 12	BP 3760	2750 BC	7.1 ± 1.5	4509 ± 12	BP 4700
1830 BC	−20.2 ± 1.8	3836 ± 15	BP 3780	2770 BC	7.8 ± 1.8	4523 ± 14	BP 4720
1850 BC	−18.3 ± 1.6	3840 ± 13	BP 3800	2790 BC	9.5 ± 1.4	4529 ± 11	BP 4740
1870 BC	−19.1 ± 1.4	3866 ± 12	BP 3820	2810 BC	13.0 ± 1.5	4521 ± 12	BP 4760
1890 BC	−20.0 ± 1.5	3892 ± 12	BP 3840	2830 BC	14.6 ± 1.1	4528 ± 9	BP 4780
1910 BC	−19.4 ± 1.8	3908 ± 15	BP 3860	2850 BC	12.8 ± 1.4	4561 ± 11	BP 4800
1930 BC	−19.0 ± 1.4	3924 ± 12	BP 3880	2870 BC	9.4 ± 1.4	4608 ± 12	BP 4820
1950 BC	−18.7 ± 1.5	3940 ± 13	BP 3900	2890 BC	6.6 ± 1.6	4649 ± 13	BP 4840
1970 BC	−18.3 ± 1.7	3957 ± 14	BP 3920	2910 BC	5.2 ± 1.5	4680 ± 12	BP 4860
1990 BC	−17.7 ± 1.4	3971 ± 11	BP 3940	2930 BC	4.0 ± 1.6	4709 ± 13	BP 4880
2010 BC	−16.4 ± 1.6	3980 ± 13	BP 3960	2950 BC	5.5 ± 1.5	4716 ± 12	BP 4900
2030 BC	−16.7 ± 1.4	4002 ± 12	BP 3980	2970 BC	7.5 ± 1.9	4720 ± 15	BP 4920
2050 BC	−16.7 ± 1.4	4021 ± 11	BP 4000	2990 BC	9.5 ± 1.5	4723 ± 12	BP 4940
2070 BC	−14.6 ± 1.6	4024 ± 13	BP 4020	3010 BC	10.4 ± 1.7	4736 ± 13	BP 4960
2090 BC	−12.3 ± 1.6	4024 ± 13	BP 4040	3030 BC	9.9 ± 1.6	4759 ± 13	BP 4980
2110 BC	−11.9 ± 1.6	4040 ± 13	BP 4060	3050 BC	10.2 ± 1.3	4776 ± 11	BP 5000
2130 BC	−12.6 ± 1.8	4065 ± 15	BP 4080	3070 BC	11.7 ± 1.4	4784 ± 11	BP 5020
2150 BC	−12.7 ± 1.2	4086 ± 10	BP 4100	3090 BC	11.3 ± 1.8	4807 ± 15	BP 5040
2170 BC	−11.1 ± 1.6	4092 ± 13	BP 4120	3110 BC	10.9 ± 1.8	4829 ± 15	BP 5060
2190 BC	−11.2 ± 1.1	4112 ± 9	BP 4140	3130 BC	12.0 ± 1.8	4839 ± 14	BP 5080
2210 BC	−11.0 ± 1.4	4130 ± 11	BP 4160	3150 BC	14.1 ± 1.7	4842 ± 13	BP 5100
2230 BC	−9.2 ± 1.4	4135 ± 12	BP 4180	3170 BC	16.4 ± 1.7	4844 ± 14	BP 5120
2250 BC	−7.8 ± 1.3	4143 ± 11	BP 4200	3190 BC	17.4 ± 1.5	4855 ± 12	BP 5140
2270 BC	−7.2 ± 1.8	4158 ± 15	BP 4220	3210 BC	19.4 ± 1.6	4859 ± 12	BP 5160
2290 BC	−7.3 ± 1.5	4178 ± 12	BP 4240	3230 BC	22.1 ± 1.6	4857 ± 12	BP 5180
2310 BC	−6.4 ± 1.8	4190 ± 14	BP 4260	3250 BC	24.2 ± 1.6	4860 ± 13	BP 5200
2330 BC	−5.8 ± 1.4	4205 ± 11	BP 4280	3270 BC	24.4 ± 1.9	4878 ± 15	BP 5220
2350 BC	−5.1 ± 1.6	4219 ± 13	BP 4300	3290 BC	24.6 ± 1.7	4896 ± 14	BP 5240
2370 BC	−3.7 ± 1.4	4227 ± 11	BP 4320	3310 BC	24.0 ± 1.6	4920 ± 12	BP 5260
2390 BC	−2.6 ± 1.6	4237 ± 13	BP 4340	3330 BC	23.1 ± 1.4	4946 ± 11	BP 5280
2410 BC	−2.4 ± 1.3	4255 ± 11	BP 4360	3350 BC	20.9 ± 1.5	4983 ± 12	BP 5300
2430 BC	−1.3 ± .9	4265 ± 7	BP 4380	3370 BC	18.9 ± 2.0	5018 ± 16	BP 5320
2450 BC	−1.9 ± 1.5	4290 ± 12	BP 4400	3390 BC	18.6 ± 1.7	5040 ± 14	BP 5340
2470 BC	−3.6 ± 1.4	4323 ± 12	BP 4420	3410 BC	21.3 ± 2.0	5038 ± 16	BP 5360
2490 BC	−3.6 ± 1.4	4342 ± 12	BP 4440	3430 BC	23.6 ± 1.7	5040 ± 13	BP 5380
2510 BC	−2.8 ± 1.2	4356 ± 10	BP 4460	3450 BC	25.4 ± 2.0	5045 ± 16	BP 5400
2530 BC	−.6 ± 1.3	4357 ± 10	BP 4480	3470 BC	27.0 ± 1.6	5052 ± 13	BP 5420
2550 BC	.1 ± 1.4	4371 ± 11	BP 4500	3490 BC	26.4 ± 1.7	5076 ± 13	BP 5440
2570 BC	−.7 ± 1.2	4397 ± 10	BP 4520	3510 BC	24.5 ± 1.7	5110 ± 13	BP 5460

TABLE 1. (Continued)

Cal AD/BC	$\Delta^{14}C$ ‰	^{14}C age (BP)	Cal BP	Cal AD/BC	$\Delta^{14}C$ ‰	^{14}C age (BP)	Cal BP
3530 BC	24.1 ± 1.7	5133 ± 13	BP 5480	4490 BC	27.5 ± 1.9	6039 ± 15	BP 6440
3550 BC	24.7 ± 1.7	5147 ± 13	BP 5500	4510 BC	27.6 ± 2.0	6057 ± 15	BP 6460
3570 BC	27.1 ± 1.7	5148 ± 13	BP 5520	4530 BC	27.6 ± 2.0	6077 ± 16	BP 6480
3590 BC	28.7 ± 1.5	5155 ± 12	BP 5540	4550 BC	27.7 ± 2.0	6096 ± 16	BP 6500
3610 BC	28.2 ± 1.5	5178 ± 11	BP 5560	4570 BC	28.6 ± 1.7	6109 ± 13	BP 6520
3630 BC	25.4 ± 1.9	5220 ± 15	BP 5580	4590 BC	29.2 ± 1.8	6123 ± 14	BP 6540
3650 BC	23.6 ± 1.7	5254 ± 13	BP 5600	4610 BC	29.8 ± 1.9	6138 ± 15	BP 6560
3670 BC	23.5 ± 1.5	5273 ± 12	BP 5620	4630 BC	30.9 ± 1.6	6148 ± 13	BP 6580
3690 BC	23.5 ± 1.6	5293 ± 13	BP 5640	4650 BC	32.7 ± 1.5	6154 ± 12	BP 6600
3710 BC	22.8 ± 1.6	5318 ± 13	BP 5660	4670 BC	32.8 ± 2.0	6173 ± 16	BP 6620
3730 BC	23.6 ± 1.8	5331 ± 14	BP 5680	4690 BC	32.4 ± 1.5	6195 ± 12	BP 6640
3750 BC	24.4 ± 1.6	5345 ± 12	BP 5700	4710 BC	32.2 ± 1.7	6216 ± 14	BP 6660
3770 BC	23.9 ± 1.6	5368 ± 13	BP 5720	4730 BC	32.1 ± 2.0	6236 ± 16	BP 6680
3790 BC	22.9 ± 1.5	5395 ± 12	BP 5740	4750 BC	32.9 ± 2.0	6249 ± 16	BP 6700
3810 BC	22.3 ± 1.7	5419 ± 13	BP 5760	4770 BC	32.3 ± 2.0	6274 ± 16	BP 6720
3830 BC	23.3 ± 1.8	5430 ± 14	BP 5780	4790 BC	31.5 ± 2.1	6300 ± 16	BP 6740
3850 BC	25.7 ± 1.3	5431 ± 10	BP 5800	4810 BC	31.6 ± 2.1	6318 ± 16	BP 6760
3870 BC	28.1 ± 1.2	5432 ± 9	BP 5820	4830 BC	31.8 ± 1.8	6336 ± 14	BP 6780
3890 BC	29.5 ± 1.4	5440 ± 11	BP 5840	4850 BC	31.8 ± 1.9	6356 ± 14	BP 6800
3910 BC	29.2 ± 1.3	5462 ± 11	BP 5860	4870 BC	33.1 ± 2.1	6365 ± 17	BP 6820
3930 BC	28.4 ± 1.5	5488 ± 12	BP 5880	4890 BC	34.1 ± 1.9	6376 ± 15	BP 6840
3950 BC	26.5 ± 1.4	5523 ± 11	BP 5900	4910 BC	33.0 ± 1.5	6404 ± 12	BP 6860
3970 BC	24.7 ± 1.1	5555 ± 9	BP 5920	4930 BC	32.6 ± 1.3	6427 ± 10	BP 6880
3990 BC	23.7 ± 1.5	5583 ± 12	BP 5940	4950 BC	32.1 ± 1.3	6450 ± 10	BP 6900
4010 BC	24.0 ± 1.6	5600 ± 13	BP 5960	4970 BC	32.8 ± 1.4	6464 ± 11	BP 6920
4030 BC	25.0 ± 1.4	5612 ± 11	BP 5980	4990 BC	33.8 ± 1.5	6476 ± 12	BP 6940
4050 BC	24.9 ± 1.6	5632 ± 13	BP 6000	5010 BC	34.6 ± 1.9	6489 ± 15	BP 6960
4070 BC	26.1 ± 1.6	5642 ± 13	BP 6020	5030 BC	35.4 ± 2.1	6502 ± 16	BP 6980
4090 BC	26.2 ± 1.5	5661 ± 12	BP 6040	5050 BC	35.0 ± 2.0	6525 ± 16	BP 7000
4130 BC	29.3 ± 1.8	5675 ± 14	BP 6080	5070 BC	34.1 ± 1.7	6551 ± 13	BP 7020
4150 BC	28.9 ± 3.3	5697 ± 26	BP 6100	5090 BC	34.4 ± 1.4	6568 ± 11	BP 7040
4170 BC	29.7 ± 1.9	5711 ± 15	BP 6120	5110 BC	36.3 ± 1.5	6573 ± 12	BP 7060
4190 BC	32.1 ± 1.9	5712 ± 14	BP 6140	5130 BC	37.2 ± 1.5	6585 ± 12	BP 7080
4210 BC	32.6 ± 2.0	5727 ± 15	BP 6160	5150 BC	37.4 ± 1.7	6604 ± 14	BP 7100
4230 BC	30.1 ± 1.6	5766 ± 12	BP 6180	5170 BC	39.8 ± 1.5	6605 ± 12	BP 7120
4250 BC	29.3 ± 1.8	5792 ± 14	BP 6200	5190 BC	40.2 ± 1.8	6621 ± 14	BP 7140
4270 BC	29.7 ± 1.8	5808 ± 14	BP 6220	5210 BC	38.1 ± 2.0	6657 ± 15	BP 7160
4290 BC	31.3 ± 1.8	5815 ± 14	BP 6240	5230 BC	36.3 ± 2.0	6689 ± 15	BP 7180
4310 BC	31.2 ± 1.8	5835 ± 14	BP 6260	5250 BC	35.3 ± 1.6	6717 ± 13	BP 7200
4330 BC	28.9 ± 1.7	5873 ± 14	BP 6280	5270 BC	33.6 ± 1.7	6749 ± 13	BP 7220
4350 BC	26.5 ± 1.7	5911 ± 13	BP 6300	5290 BC	33.1 ± 1.7	6773 ± 14	BP 7240
4370 BC	26.0 ± 1.6	5934 ± 13	BP 6320	5310 BC	33.2 ± 1.8	6791 ± 14	BP 7260
4390 BC	27.2 ± 1.9	5944 ± 15	BP 6340	5330 BC	32.6 ± 1.8	6816 ± 14	BP 7280
4410 BC	28.2 ± 1.9	5956 ± 15	BP 6360	5350 BC	32.9 ± 1.7	6833 ± 13	BP 7300
4430 BC	29.6 ± 2.0	5965 ± 15	BP 6380	5370 BC	33.8 ± 2.0	6845 ± 15	BP 7320
4450 BC	28.3 ± 1.9	5994 ± 15	BP 6400	5390 BC	33.7 ± 2.0	6866 ± 16	BP 7340
4470 BC	26.8 ± 1.7	6025 ± 14	BP 6420	5410 BC	34.2 ± 1.8	6881 ± 14	BP 7360

TABLE 1. (Continued)

Cal AD/BC	$\Delta^{14}C$ ‰	^{14}C age (BP)	Cal BP	Cal AD/BC	$\Delta^{14}C$ ‰	^{14}C age (BP)	Cal BP
5430 BC	31.3 ± 1.8	6923 ± 14	BP 7380	6370 BC	23.6 ± 2.6	7897 ± 20	BP 8320
5450 BC	28.8 ± 1.8	6962 ± 14	BP 7400	6390 BC	22.4 ± 2.3	7925 ± 18	BP 8340
5470 BC	29.2 ± 1.8	6978 ± 14	BP 7420	6410 BC	21.6 ± 2.5	7951 ± 19	BP 8360
5490 BC	29.1 ± 2.0	6998 ± 15	BP 7440	6430 BC	20.5 ± 2.7	7979 ± 21	BP 8380
5510 BC	28.7 ± 2.0	7021 ± 15	BP 7460	6450 BC	19.9 ± 2.6	8004 ± 21	BP 8400
5530 BC	28.7 ± 2.0	7041 ± 15	BP 7480	6470 BC	18.1 ± 2.4	8037 ± 19	BP 8420
5550 BC	30.0 ± 1.8	7050 ± 14	BP 7500	6490 BC	18.2 ± 2.5	8056 ± 20	BP 8440
5570 BC	28.4 ± 1.5	7082 ± 12	BP 7520	6510 BC	19.5 ± 2.0	8065 ± 16	BP 8460
5590 BC	25.9 ± 1.7	7121 ± 13	BP 7540	6530 BC	20.4 ± 3.1	8077 ± 25	BP 8480
5610 BC	24.6 ± 1.5	7150 ± 12	BP 7560	6550 BC	19.9 ± 3.2	8101 ± 25	BP 8500
5630 BC	24.4 ± 1.5	7171 ± 12	BP 7580	6570 BC	20.2 ± 4.1	8117 ± 32	BP 8520
5650 BC	24.4 ± 1.4	7190 ± 11	BP 7600	6590 BC	20.5 ± 4.3	8135 ± 34	BP 8540
5670 BC	24.1 ± 1.5	7212 ± 12	BP 7620	6610 BC	19.5 ± 4.1	8162 ± 32	BP 8560
5690 BC	23.4 ± 1.6	7237 ± 12	BP 7640	6630 BC	19.7 ± 4.1	8179 ± 32	BP 8580
5710 BC	22.9 ± 1.6	7261 ± 13	BP 7660	6650 BC	20.7 ± 3.5	8191 ± 27	BP 8600
5730 BC	22.7 ± 1.6	7282 ± 12	BP 7680	6670 BC	22.0 ± 3.5	8200 ± 27	BP 8620
5750 BC	22.8 ± 1.4	7300 ± 11	BP 7700	6690 BC	23.2 ± 3.5	8211 ± 27	BP 8640
5770 BC	23.0 ± 1.5	7318 ± 11	BP 7720	6710 BC	23.5 ± 3.5	8228 ± 27	BP 8660
5790 BC	23.5 ± 1.5	7334 ± 11	BP 7740	6730 BC	24.8 ± 3.5	8237 ± 27	BP 8680
5810 BC	23.9 ± 1.4	7350 ± 11	BP 7760	6750 BC	26.4 ± 4.1	8244 ± 32	BP 8700
5830 BC	24.2 ± 1.5	7367 ± 12	BP 7780	6770 BC	26.4 ± 4.1	8263 ± 32	BP 8720
5850 BC	24.2 ± 1.8	7387 ± 14	BP 7800	6790 BC	27.4 ± 4.1	8275 ± 32	BP 8740
5870 BC	24.1 ± 2.1	7407 ± 16	BP 7820	6810 BC	29.0 ± 4.1	8281 ± 32	BP 8760
5890 BC	24.6 ± 2.0	7422 ± 16	BP 7840	6830 BC	31.4 ± 4.1	8283 ± 32	BP 8780
5910 BC	26.0 ± 1.9	7431 ± 15	BP 7860	6850 BC	34.5 ± 2.6	8278 ± 20	BP 8800
5930 BC	26.0 ± 2.0	7450 ± 15	BP 7880	6870 BC	35.4 ± 4.4	8291 ± 34	BP 8820
5950 BC	24.0 ± 2.1	7485 ± 17	BP 7900	6890 BC	36.6 ± 4.4	8301 ± 34	BP 8840
5970 BC	22.1 ± 2.0	7519 ± 16	BP 7920	6910 BC	38.1 ± 4.4	8309 ± 34	BP 8860
5990 BC	21.0 ± 1.9	7547 ± 15	BP 7940	6930 BC	40.1 ± 4.4	8312 ± 34	BP 8880
6010 BC	20.6 ± 3.0	7571 ± 24	BP 7960	6950 BC	41.2 ± 4.4	8323 ± 34	BP 8900
6030 BC	20.4 ± 4.1	7592 ± 32	BP 7980	6970 BC	42.3 ± 4.4	8334 ± 34	BP 8920
6050 BC	20.0 ± 4.1	7614 ± 32	BP 8000	6990 BC	40.9 ± 4.4	8365 ± 34	BP 8940
6070 BC	20.5 ± 4.1	7629 ± 32	BP 8020	7010 BC	38.2 ± 4.4	8404 ± 34	BP 8960
6090 BC	22.5 ± 3.3	7633 ± 26	BP 8040	7030 BC	36.7 ± 4.4	8436 ± 34	BP 8980
6110 BC	23.0 ± 2.8	7649 ± 22	BP 8060	7050 BC	34.7 ± 2.6	8471 ± 20	BP 9000
6130 BC	22.5 ± 2.8	7672 ± 22	BP 8080	7070 BC	35.8 ± 3.3	8481 ± 26	BP 9020
6150 BC	23.0 ± 2.9	7687 ± 22	BP 8100	7090 BC	36.8 ± 3.3	8494 ± 26	BP 9040
6170 BC	21.5 ± 2.7	7718 ± 21	BP 8120	7110 BC	38.3 ± 3.3	8501 ± 26	BP 9060
6190 BC	20.2 ± 2.3	7749 ± 18	BP 8140	7130 BC	40.6 ± 4.2	8502 ± 32	BP 9080
6210 BC	20.3 ± 2.6	7767 ± 21	BP 8160	7150 BC	40.6 ± 4.2	8522 ± 32	BP 9100
6230 BC	20.0 ± 2.6	7788 ± 21	BP 8180	7170 BC	43.2 ± 4.2	8522 ± 32	BP 9120
6250 BC	20.6 ± 2.7	7803 ± 21	BP 8200	7190 BC	45.3 ± 4.2	8524 ± 32	BP 9140
6270 BC	22.0 ± 2.3	7812 ± 18	BP 8220	7210 BC	45.7 ± 4.2	8541 ± 32	BP 9160
6290 BC	23.9 ± 2.6	7817 ± 21	BP 8240	7230 BC	47.1 ± 4.2	8550 ± 32	BP 9180
6310 BC	24.6 ± 2.8	7830 ± 22	BP 8260	7250 BC	46.4 ± 4.0	8575 ± 31	BP 9200
6330 BC	25.9 ± 2.8	7840 ± 22	BP 8280	7270 BC	45.9 ± 4.0	8598 ± 31	BP 9220
6350 BC	25.3 ± 2.4	7864 ± 19	BP 8300	7290 BC	46.1 ± 3.8	8616 ± 29	BP 9240

TABLE 1. (Continued)

Cal AD/BC	$\Delta^{14}C$ ‰	^{14}C age (BP)	Cal BP	Cal AD/BC	$\Delta^{14}C$ ‰	^{14}C age (BP)	Cal BP
7310 BC	45.7 ± 4.0	8638 ± 31	BP 9260	8250 BC	47.2 ± 5.5	9540 ± 43	BP 10200
7330 BC	46.6 ± 4.4	8651 ± 34	BP 9280	8270 BC	47.5 ± 4.7	9558 ± 36	BP 10220
7350 BC	48.5 ± 4.4	8655 ± 34	BP 9300	8290 BC	49.6 ± 3.8	9560 ± 29	BP 10240
7370 BC	50.0 ± 4.0	8663 ± 31	BP 9320	8310 BC	52.2 ± 4.8	9560 ± 37	BP 10260
7390 BC	50.4 ± 4.4	8680 ± 34	BP 9340	8330 BC	51.7 ± 5.1	9584 ± 39	BP 10280
7410 BC	49.5 ± 3.8	8706 ± 29	BP 9360	8350 BC	50.2 ± 5.6	9615 ± 43	BP 10300
7430 BC	47.2 ± 3.8	8744 ± 29	BP 9380	8370 BC	50.6 ± 5.6	9631 ± 43	BP 10320
7450 BC	46.9 ± 3.8	8766 ± 29	BP 9400	8390 BC	50.9 ± 4.8	9648 ± 37	BP 10340
7470 BC	47.0 ± 3.8	8783 ± 29	BP 9420	8410 BC	50.3 ± 5.7	9672 ± 43	BP 10360
7490 BC	44.2 ± 3.8	8825 ± 29	BP 9440	8430 BC	50.0 ± 4.6	9694 ± 35	BP 10380
7510 BC	42.7 ± 4.0	8856 ± 31	BP 9460	8450 BC	50.7 ± 2.9	9708 ± 22	BP 10400
7530 BC	41.8 ± 4.0	8882 ± 31	BP 9480	8470 BC	51.6 ± 5.0	9720 ± 38	BP 10420
7550 BC	39.9 ± 5.5	8916 ± 43	BP 9500	8490 BC	52.6 ± 6.0	9732 ± 46	BP 10440
7570 BC	39.5 ± 4.0	8939 ± 31	BP 9520	8510 BC	53.4 ± 5.0	9746 ± 38	BP 10460
7590 BC	38.9 ± 4.0	8963 ± 31	BP 9540	8530 BC	53.8 ± 6.6	9762 ± 50	BP 10480
7610 BC	40.0 ± 4.0	8974 ± 31	BP 9560	8550 BC	55.1 ± 7.6	9772 ± 58	BP 10500
7630 BC	41.1 ± 4.0	8985 ± 31	BP 9580	8570 BC	56.6 ± 7.6	9779 ± 58	BP 10520
7650 BC	42.4 ± 4.0	8994 ± 31	BP 9600	8590 BC	56.7 ± 6.0	9798 ± 46	BP 10540
7670 BC	43.8 ± 4.0	9003 ± 31	BP 9620	8610 BC	56.6 ± 5.0	9818 ± 38	BP 10560
7690 BC	43.6 ± 4.0	9024 ± 31	BP 9640	8630 BC	57.3 ± 4.4	9832 ± 33	BP 10580
7710 BC	42.8 ± 4.4	9049 ± 34	BP 9660	8650 BC	58.6 ± 3.8	9842 ± 29	BP 10600
7730 BC	43.6 ± 4.4	9063 ± 34	BP 9680	8670 BC	60.2 ± 4.4	9849 ± 33	BP 10620
7750 BC	45.1 ± 4.4	9071 ± 34	BP 9700	8690 BC	62.0 ± 3.6	9855 ± 27	BP 10640
7770 BC	47.8 ± 4.4	9069 ± 34	BP 9720	8710 BC	63.6 ± 2.9	9862 ± 22	BP 10660
7790 BC	49.7 ± 4.4	9074 ± 34	BP 9740	8730 BC	65.3 ± 3.3	9869 ± 25	BP 10680
7810 BC	52.6 ± 4.0	9072 ± 31	BP 9760	8750 BC	67.4 ± 4.0	9873 ± 30	BP 10700
7830 BC	54.5 ± 4.0	9076 ± 31	BP 9780	8770 BC	70.2 ± 4.6	9871 ± 35	BP 10720
7850 BC	54.4 ± 4.0	9097 ± 31	BP 9800	8790 BC	74.0 ± 4.7	9862 ± 35	BP 10740
7870 BC	53.8 ± 4.0	9121 ± 31	BP 9820	8810 BC	77.6 ± 6.2	9855 ± 46	BP 10760
7890 BC	52.7 ± 4.0	9149 ± 31	BP 9840	8830 BC	78.5 ± 6.4	9867 ± 48	BP 10780
7910 BC	51.3 ± 4.2	9179 ± 32	BP 9860	8850 BC	77.7 ± 4.3	9892 ± 32	BP 10800
7930 BC	50.0 ± 4.4	9208 ± 34	BP 9880	8870 BC	78.3 ± 4.4	9908 ± 33	BP 10820
7950 BC	48.8 ± 4.6	9237 ± 35	BP 9900	8890 BC	79.5 ± 5.4	9918 ± 40	BP 10840
7970 BC	47.9 ± 4.8	9263 ± 37	BP 9920	8910 BC	79.6 ± 5.1	9937 ± 38	BP 10860
7990 BC	47.4 ± 5.2	9286 ± 40	BP 9940	8930 BC	78.8 ± 5.9	9962 ± 44	BP 10880
8010 BC	46.3 ± 5.3	9314 ± 41	BP 9960	8950 BC	78.0 ± 6.8	9988 ± 51	BP 10900
8030 BC	44.4 ± 4.6	9348 ± 36	BP 9980	8970 BC	77.3 ± 4.6	10012 ± 34	BP 10920
8050 BC	43.2 ± 3.6	9377 ± 28	BP 10000	8990 BC	76.1 ± 3.2	10041 ± 24	BP 10940
8070 BC	42.2 ± 3.5	9403 ± 27	BP 10020	9010 BC	73.9 ± 3.2	10077 ± 24	BP 10960
8090 BC	40.9 ± 4.5	9434 ± 35	BP 10040	9030 BC	70.9 ± 3.0	10118 ± 23	BP 10980
8110 BC	40.9 ± 4.8	9452 ± 37	BP 10060	9050 BC	67.9 ± 4.9	10160 ± 37	BP 11000
8130 BC	42.1 ± 4.0	9463 ± 31	BP 10080	9070 BC	67.0 ± 5.6	10186 ± 43	BP 11020
8150 BC	43.3 ± 3.7	9473 ± 29	BP 10100	9090 BC	68.2 ± 5.2	10197 ± 39	BP 11040
8170 BC	44.5 ± 4.5	9483 ± 35	BP 10120	9110 BC	69.5 ± 5.9	10207 ± 44	BP 11060
8190 BC	45.0 ± 5.2	9499 ± 40	BP 10140	9130 BC	70.1 ± 5.4	10222 ± 41	BP 11080
8210 BC	45.7 ± 5.5	9513 ± 43	BP 10160	9150 BC	70.7 ± 4.6	10237 ± 35	BP 11100
8230 BC	46.8 ± 5.5	9524 ± 43	BP 10180	9170 BC	71.9 ± 4.4	10247 ± 33	BP 11120

TABLE 1. (Continued)

Cal AD/BC	$\Delta^{14}C$ ‰	^{14}C age (BP)	Cal BP	Cal AD/BC	$\Delta^{14}C$ ‰	^{14}C age (BP)	Cal BP
9190 BC	73.5 ± 5.0	10254 ± 37	BP 11140	9550 BC	101.2 ± 7.9	10400 ± 58	BP 11500
9210 BC	76.2 ± 4.6	10254 ± 34	BP 11160	9570 BC	102.4 ± 8.0	10410 ± 58	BP 11520
9230 BC	79.2 ± 5.2	10250 ± 39	BP 11180	9590 BC	103.7 ± 8.0	10420 ± 58	BP 11540
9250 BC	80.5 ± 5.5	10260 ± 41	BP 11200	9610 BC	105.1 ± 8.0	10429 ± 58	BP 11560
9270 BC	81.0 ± 4.5	10276 ± 33	BP 11220	9630 BC	106.7 ± 8.1	10438 ± 59	BP 11580
9290 BC	82.7 ± 4.9	10283 ± 36	BP 11240	9650 BC	108.3 ± 8.1	10445 ± 59	BP 11600
9310 BC	84.8 ± 6.1	10287 ± 45	BP 11260	9670 BC	110.1 ± 8.2	10452 ± 59	BP 11620
9330 BC	87.2 ± 7.2	10288 ± 53	BP 11280	9690 BC	111.9 ± 8.2	10458 ± 59	BP 11640
9350 BC	89.8 ± 7.8	10289 ± 57	BP 11300	9710 BC	113.0 ± 8.2	10469 ± 59	BP 11660
9370 BC	90.9 ± 6.5	10300 ± 48	BP 11320	9730 BC	114.1 ± 8.3	10481 ± 60	BP 11680
9390 BC	91.6 ± 5.7	10314 ± 42	BP 11340	9750 BC	115.3 ± 8.3	10492 ± 60	BP 11700
9410 BC	93.5 ± 6.0	10320 ± 44	BP 11360	9770 BC	116.4 ± 8.3	10503 ± 60	BP 11720
9430 BC	95.5 ± 6.5	10325 ± 48	BP 11380	9790 BC	117.5 ± 8.4	10515 ± 60	BP 11740
9450 BC	96.4 ± 7.8	10338 ± 57	BP 11400	9800 BC	118.0 ± 8.4	10521 ± 60	BP 11750
9470 BC	97.2 ± 7.8	10351 ± 57	BP 11420	9850 BC	122.6 ± 8.5	10537 ± 61	BP 11800
9490 BC	98.1 ± 7.8	10364 ± 57	BP 11440	9900 BC	126.9 ± 8.6	10554 ± 61	BP 11850
9510 BC	99.0 ± 7.9	10377 ± 58	BP 11460	9950 BC	131.1 ± 8.7	10573 ± 62	BP 11900
9530 BC	100.0 ± 7.9	10389 ± 58	BP 11480	10000 BC	135.0 ± 8.8	10594 ± 62	BP 11950

[RADIOCARBON, VOL. 35, NO. 1, 1993, P. 191–199]

^{230}Th-^{234}U AND ^{14}C AGES OBTAINED BY MASS SPECTROMETRY ON CORALS

EDOUARD BARD[1,2,3], MAURICE ARNOLD[2], RICHARD G. FAIRBANKS[3] and BRUNO HAMELIN[1,3]

INTRODUCTION

In 1988, Fairbanks conducted a drilling expedition off the south coast of Barbados to recover submerged corals contemporaneous with the last deglaciation. Core recovery was excellent and >30 different samples were dated by conventional β-counting techniques (Fairbanks 1989). At about the same time, we developed, at Lamont, the thermal ionization mass spectrometry (TIMS) technique to obtain precise U-Th ages (Edwards 1988), and to compare them with the ^{14}C estimates measured on the same samples. A surprising result was that the discrepancy between ^{14}C and U-Th ages increased through time to *ca.* 3000–3500 yr at *ca.* 15,000 ^{14}C BP (Bard *et al.* 1990a). Because the three youngest samples yielded U-Th ages in agreement with their calibrated ^{14}C ages, we concluded initially that the TIMS U-Th determinations were not only precise, but also accurate, and that the ^{14}C *vs.* U-Th data set could be used for a first-order ^{14}C calibration.

We replicated ^{14}C measurements through accelerator mass spectrometry (AMS) on very small samples, which enabled us to use strong acid leaching to eliminate surface contaminants (see Bard *et al.* 1990b for technical procedures and the report of initial measurements). To establish global uniformity of the observed phenomenon, we also measured ages in new samples from very different environments, Mururoa Atoll and Isabela Island in the tropical Pacific Ocean.

RESULTS OBTAINED BY AMS AND TIMS ON BARBADOS CORALS

In five runs of the Gif-sur-Yvette Tandetron, we obtained *ca.* 80 new ^{14}C determinations on *ca.* 20 samples previously dated by β-counting (Fairbanks 1989, 1990) and TIMS (Bard *et al.* 1990a). The large quantity of replicates enables us to calculate weighted-mean AMS ^{14}C ages with an improved precision (better than ± 200 yr at 2 σ for the last 15,000 yr). The new AMS results agree to a first order with the β-counting estimates. However, we further confirm our previous observation (Bard *et al.* 1990b) that, for ages beyond the Holocene, the AMS determinations are often slightly older than the β-counting estimates (see Table 1A–C). The samples prepared for AMS were strongly leached with acid (loss of *ca.* 30–40% of the total weight), whereas the samples measured by β-counting were not (except samples RGF7-5-5, RGF7-16-2, RGF9-27-5 and RGF12-30-2). Consequently, a minor (<1pmC) contamination might cause this discrepancy. To illustrate how the calculation of Δ^{14}C is sensitive to old ages, we cite the deepest *A. palmata* sample (RGF 9-27-5), which was AMS-dated 3 times at Gif (weighted mean = 16,360 ± 220 BP [2 σ]), once at Arizona (16,145 ± 240 BP [2 σ], Fairbanks 1990) and twice by TIMS at Lamont (weighted mean = 19,000 ± 70 BP [2 σ]). Thus, the Δ^{14}C of this sample is *ca.* 300 ‰ instead of ca. 350 ‰ initially reported for that period, using β-counting ages obtained without leaching procedures.

Figure 1 shows results obtained by AMS and β-counting *vs.* the ages obtained by TIMS. Figure 2 shows enlarged detail of the intercomparison, which clearly illustrates the concordance between

[1]Laboratoires de Géosciences et d'Environnement, Université d'Aix-Marseille III, 13397 Marseille, France
[2]Centre des Faibles Radioactivités, CNRS-CEA, 91198 Gif-sur-Yvette, France
[3]Lamont-Doherty Geological Observatory, Columbia University, Palisades, New York 10964 USA

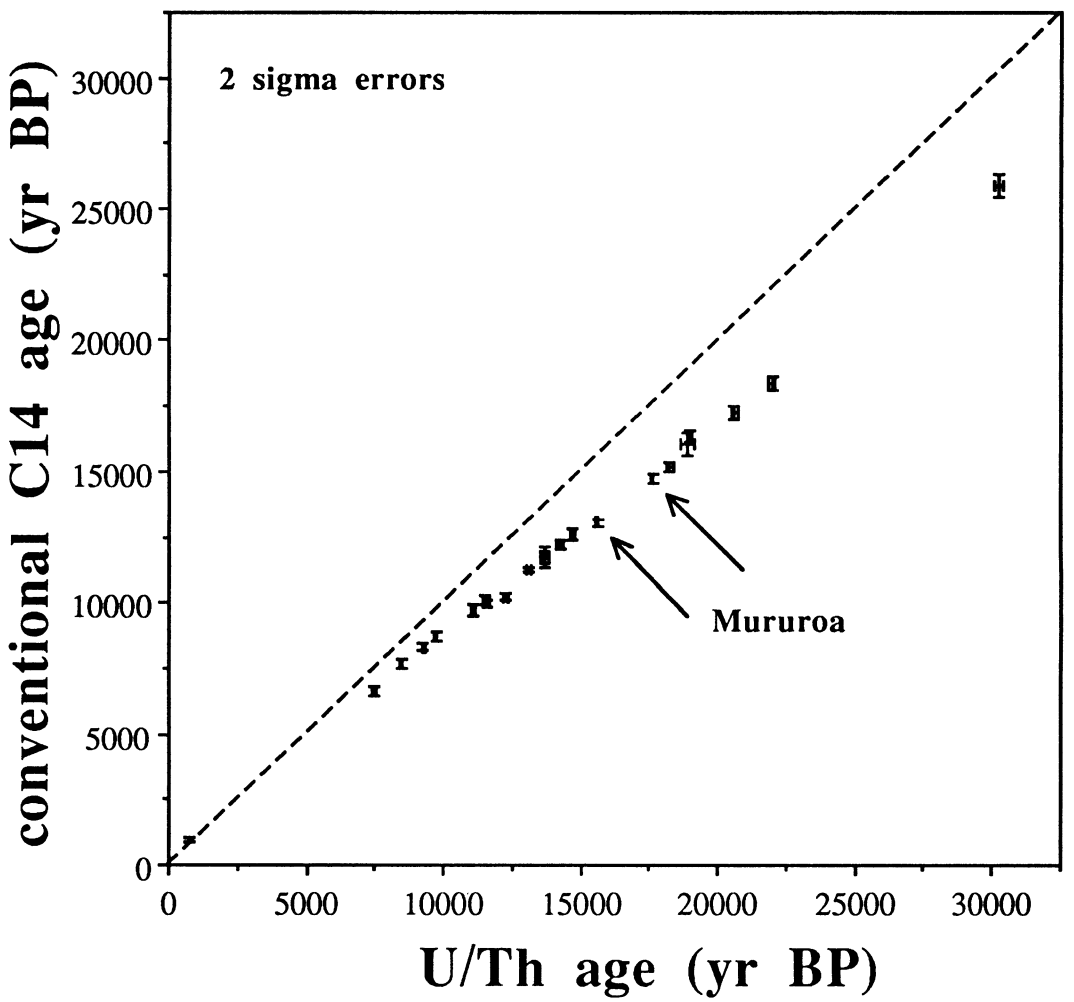

Fig. 1. U-Th ages obtained by TIMS plotted *vs.* AMS ^{14}C ages obtained on corals from Barbados and Mururoa. ^{14}C ages are conventional ages in yr BP with statistical errors given at 2 σ, which does not include the error in the reservoir correction. For the interval between 8500 and 20,000 ^{14}C yr BP, a simple linear calibration is: cal age BP = 1.24(^{14}C age BP) – 840.

our reconstruction and the dendrochronological determinations of Kromer & Becker (1992).

We also studied the 400-yr reservoir age correction by dating a very recent Barbados coral drilled on the flat part of the reef at *ca.* 7 m below the present sea level (RGF B56). The U-Th age is 773 ± 10 BP [2 σ] (weighted mean on 2 replicates); the ^{14}C age is 956 ± 90 BP [2 σ] (weighted mean on 4 measurements), which leads to a calibrated age of 775–957 cal BP, using the "atmospheric" calibration program of the Quaternary Isotope Laboratory, University of Washington. This cal age is in statistical agreement with the U-Th estimate. However, we can also apply the marine ^{14}C calibration of the same program (with $\Delta R = 0 \pm 0$) on the raw ^{14}C age (1356 ± 90 BP [2 σ]). In that case, the calibrated age is 787-967 cal yr BP which is close but slightly older than the U-Th estimate.

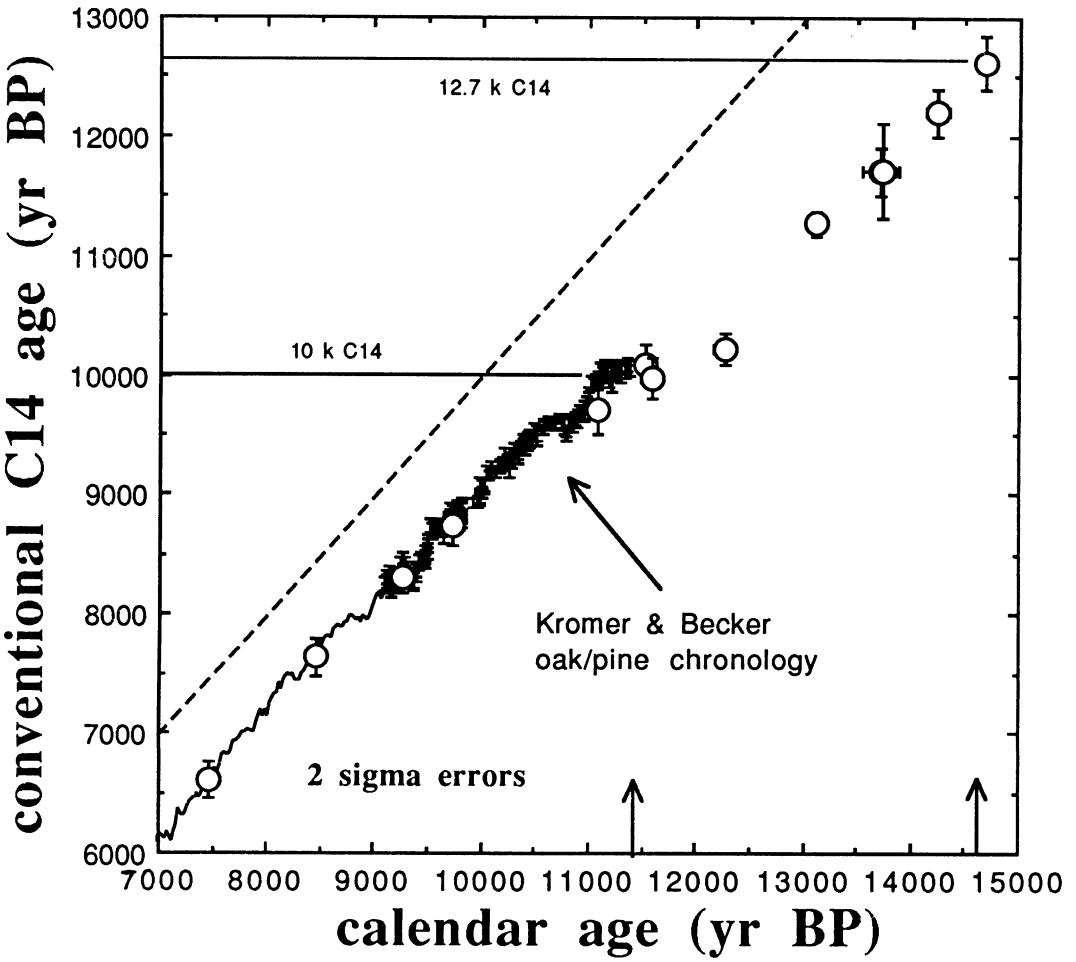

Fig. 2. Enlargement of Figure 1, also showing the tree-ring data base. Until 9100 cal BP, the solid curve is the 20-yr running average of the dendrochronology. Between 9100 and 11,400 cal BP, it comprises German oak and pine data (Kromer & Becker 1992). All errors are given at 2 σ (for ^{14}C ages of corals they do not include the error in the reservoir correction).

Thus, the reservoir age offshore Barbados is not very different from our adopted value of 400 yr (DIC $\Delta^{14}C \approx -50$ ‰), which is a mean for low- and mid-latitude open ocean waters (Bard 1988). However, if we take the results obtained on sample RGF B56 at face value, we could also adopt a different reservoir correction. Indeed, there are still some uncertainties about the pre-anthropogenic $\Delta^{14}C$ of the West Atlantic/Caribbean zone; Druffel & Suess (1983) reported $\Delta^{14}C$ values of −50 ‰ for Belize and Florida corals while Nozaki *et al.* (1978) obtained $\Delta^{14}C$ values of *ca.* −30 ‰ (≈250 yr) for 19th-century annual bands collected from a Bermuda coral head. Perfect agreement should not be expected, and the reservoir age probably exhibits small temporal variations in response to changes of tradewind, temperature and mixed-layer depth (Bard 1988).

Results obtained by AMS and TIMS on Mururoa corals

We measured ages of two coral specimens collected with a land-based deviated drill (≈30°) at *ca.* 170 m below present sea level, offshore Mururoa atoll, French Polynesia. For sample 313, the U-Th age is 17,595 ± 70 BP [2 σ] (weighted mean on 3 replicates), whereas the ^{14}C age is 14,735 ±

TABLE 1A. Comparison of ages obtained by classical ^{14}C β counting, ^{14}C-AMS and U-Th-TIMS. All ages are expressed as yr BP (before 1950). The ^{14}C ages are conventional ages with a reservoir correction of 400 yr. Statistical errors are given at 2 σ, which does not include the error in reservoir correction.

Sample	U/Th (yr BP)	± 2σ	C14 (yr BP) L-DGO	± 2σ	C14 (yr BP) Geochron	± 2σ	Leaching *	Replication **	C14 (yr BP) Gif-sur-Yvette	± 2σ
Galapagos 2#1	283	13								
Galapagos 2#2	265	6								
Galapagos 1#1	295	20								
Galapagos 1#2	269	12								
RGF B56#1	773	11					+		825	180
RGF B56#2	773	28					+	du	1050	180
RGF B56#3							+		995	160
RGF B56#4							+	du	975	180
RGF7-4-2#1	7460	80	6400	200			+		6640	200
RGF7-4-2#2							+	du	6560	220
RGF7-5-5#1	8450	50			7780	220	+		7640	240
RGF7-5-5#2							+	du	7640	220
RGF7-12-2#1	9285	95	8200	200			+		8160	220
RGF7-12-2#2	9250	80					+	du	8080	360
RGF7-12-2#3							+		8410	220
RGF7-12-2#4							+	du	8410	220
RGF7-16-2#1	9730	50			9050	250	+		8750	240
RGF7-16-2#2							+	du	8750	240
RGF7-27-4#1	11090	70	9400	200			+		9690	320
RGF7-27-4#2							+	du	9720	280
RGF12-5-2#1	11590	60	10100	200			+		9760	380
RGF12-5-2#2							+		10070	340
RGF12-5-2#3							+	du	10020	240
RGF12-6-7#1	11530	70	9800	200			+		9730	400
RGF12-6-7#2							+		10080	240
RGF12-6-7#3							+	du	10250	260
RGF12-9-5#1	12260	90	10300	200			+		10320	320
RGF12-9-5#2							+	du	10280	280
RGF12-9-5#3							+		10280	260
RGF12-9-5#4							+	du	10090	220

*+ = strong leaching (>30% weight loss of the sample; for AMS samples only)

**Results obtained by duplicating (du) or triplicating (tri) the AMS runs on 2 or 3 aliquots of the same Fe+C powder.

150 BP [2 σ] (weighted mean on 5 age determinations). For sample 315, the U-Th age is 15,585 ± 50 yr BP [2 σ] (weighted mean on 3 replicates), whereas the ^{14}C age is 13,060 ± 140 yr BP [2 σ] (weighted mean on 5 age determinations). These new results show again a significant difference between the two geochronometers, corresponding to $\Delta^{14}C$ values of 330 ± 30 ‰ and 290 ± 25 ‰ at *ca.* 18,000 and 16,000 Th yr BP, respectively. These values are in excellent concordance with AMS redeterminations of the Barbados ^{14}C ages (*cf.* Fig. 1). This new comparative data set of U-series and ^{14}C ages demonstrates that the large discrepancies first evidenced in Barbados are not caused by local alteration processes.

TABLE 1B. Comparison of ages obtained by classical ^{14}C β counting, ^{14}C-AMS and U-Th-TIMS. All ages are expressed as yr BP (before 1950). The ^{14}C ages are conventional ages with a reservoir correction of 400 yr. Statistical errors are given at 2 σ, which does not include the error in reservoir correction.

Sample	U/Th (yr BP)	± 2s	C14 (yr BP) L-DGO	± 2s	C14 (yr BP) Geochron	± 2s	Leaching *	Replication **	C14 (yr BP) Gif-sur-Yvette	± 2s	C14 (yr BP) other AMS labs	± 2s
RGF12-16-5#1	13220	110	10900	200			+		11640	280		
RGF12-16-5#2	12970	120					+		10940	260		
RGF12-16-5#3							+		11020	240		
RGF12-16-5#4							+		11200	260		
RGF12-16-5#5							+	du	11490	280		
RGF12-16-5#6							+		11570	340		
RGF12-16-5#7							+	du	11190	260		
RGF12-21-6#1	13700	170	11850	200			+		11630	260		
RGF12-21-6#2							+	du	11820	300		
RGF12-21-10#1	13800	140	11800	200			+		11720	400		
RGF12-21-10#2	13660	140										
RGF9-8-2#1	14235	100	11800	400			+		12240	260		
RGF9-8-2#2							+	du	12130	320		
RGF9-13-3#1	14660	160	12500	200			+		12000	420		
RGF9-13-3#2	14700	100					+		12910	340		
RGF9-13-3#3							+	du	12710	380		
RGF9-21-11#1	18240	140	14700	400					14930	400		
RGF9-21-11#2									15390	400		
RGF9-21-11#3							+		15110	320		
RGF9-21-11#4							+	du	15230	340		
RGF9-24-04	18890	250	15400	400			+		16020	420		
RGF9-27-5#1	18980	90			17085	520	+		16260	420	16145	240
RGF9-27-5#2	19030	100					+		16240	360	AMS Arizona	
RGF9-27-5#3							+	du	16550	360		
RGF9-27-4			15200	520							15850 AMS Arizona	240
RGF9-32-4#1	20610	120	16700	600			+		16920	420		
RGF9-32-4#2							+	du	17470	380		
RGF9-34-8#1	21930	150	18200	400			+		18820	520		
RGF9-34-8#2	22130	260					+		18260	420		
RGF9-34-8#3							+	du	18300	400		

*+ = strong leaching (>30% weight loss of the sample; for AMS samples only).

**Results which have been obtained by duplicating (du) or triplicating (tri) the AMS runs on 2 or 3 aliquots of the same Fe+C powder.

RESULTS OBTAINED BY TIMS ON GALAPAGOS CORALS

To further study the reliability of TIMS age estimates on very young samples, we dated samples from a *Pavona clavus* colony collected on Isabela Island (Galapagos). This recent coral head was killed in 1954 due to tectonic uplift from the shelf of Urvina Bay. A high-resolution chronology was previously obtained for this colony through counting of growth bands imaged by x-rays (Shen *et al.* 1991 and references therein). We dated two samples by TIMS: Gal. 2, which has a sclerochronological age of 283–285 cal BP, and yielded a U-Th age of 269 ± 6 BP [2 σ] (weighted mean on 2 replicates), and Gal. 1, dated at 296–298 cal BP with a U-Th age of 277 ± 10 BP [2 σ] (weighted mean on 2 replicates). Thus, the results obtained by TIMS are very close to the true ages, but not in complete agreement if the statistical errors are taken into account.

We made these first attempts to date very young corals on a rather old solid-source mass spectrometer (VG-MM30) equipped with an analog Daly detector. For these analyses, the $^{230}Th+$ ion currents were very close to background, and it would have been preferable to make additional

TABLE 1C. Comparison of ages obtained by classical ^{14}C β counting, ^{14}C-AMS and U-Th-TIMS. All ages are expressed as yr BP (before 1950). The ^{14}C ages are conventional ages with a reservoir correction of 400 yr. Statistical errors are given at 2 σ, which does not include the error in reservoir correction.

Sample	U/Th (yr BP)	± 2σ	C14 (yr BP) Geochron	± 2σ	Leaching *	Replication **	C14 (yr BP) Gif-sur-Yvette	± 2σ	C14 (yr BP) other AMS labs	± 2σ
RGF12-30-2#1	30470	240	27120	1520	+		26290	860	26480	1000
RGF12-30-2#2	30040	210					24600	820	AMS Zürich	
RGF12-30-2#3							25290	840		
RGF12-30-2#4					+		25790	840		
RGF12-30-2#5					+	du	25370	660		
RGF1-17-4#1	70820	600	30080	3520	+		>48000			
RGF1-17-4#2							>48000			
RGF8-27-1#1	79400	700	36240	7980						
RGF8-27-1#2	77800	800								
Mururoa 315#1	15550	100					13160	280		
Mururoa 315#2	15660	90					13160	300		
Mururoa 315#3	15550	80			+		13030	360		
Mururoa 315#4					+		12840	360		
Mururoa 315#5					+	du	12990	300		
Mururoa 313#1	17500	120					14690	320		
Mururoa 313#2	17630	100					14770	340		
Mururoa 313#3	17650	130			+		14630	360		
Mururoa 313#4					+		14620	360		
Mururoa 313#5					+	du	14910	320		
Mururoa Irène 30#1	259000	6000			+		>48700			
Mururoa Irène 30#2					+	du	>48600			
Mururoa Irène 30#3					+	tri	>48400			
Mururoa Irène 30#4					+		>48500			
Ir30 0.25 mg					+		>46700			
Ir30 0.22 mg					+		>47200			
Ir30 0.19 mg					+		>47900			
Ir30 0.13 mg					+		>39700			
stalagmite					+		>48300			
IAEA-C1 marble					+		>48300			

*+ = strong leaching (>30% weight loss of the sample; for AMS samples only).

**Results obtained by duplicating (du) or triplicating (tri) the AMS runs on 2 or 3 aliquots of the same Fe+C powder.

†Quantification of the blank was conducted on three samples: 1) a stalagmite from Orgnac cave (>300 ka by α-counting U-Th dating); 2) the IAEA-C1 marble; and 3) sample Irène-30 dated by TIMS at 259 ± 6 ka. The ^{14}C contamination was also tested on very small aliquots of Irène-30 (0.25 mg C–0.13 mg C). Note that the normal size of the coral samples is always between 1 and 2 mg C. A more comprehensive study of the blank levels on carbonate and organic samples is under preparation and will be published elsewhere (Bard & Arnold, ms. in preparation).

baseline corrections at mass 229.5 and 230.5, instead of using the simpler procedure of measuring a common baseline at mass 227.5. However, this would have caused significant loss in ^{230}Th measurement time, which would have reduced measurement precision. Consequently, we believe that these preliminary results constitute a trade-off between accuracy and precision. Ideally, we will replicate the analyses using the VG Sector-54-30 mass spectrometer recently installed at LGE-Marseille; this instrument is equipped with an ion-counting Daly detector that can decrease significantly the detection limit (by about 100 times) for small ion currents. Another explanation for the 10–20 yr discrepancy could also come from the sclerochronological estimates. It could be caused by problems in correlating different coral sections which had to be corrected for small gaps (Shen *et al.* 1991), or to additional stress bands in response to exceptionally cold years (see, *e.g.*, Druffel & Linick 1978, who showed evidence for three stress bands in a 30-yr section of *Montastera annularis* from the Florida Keys).

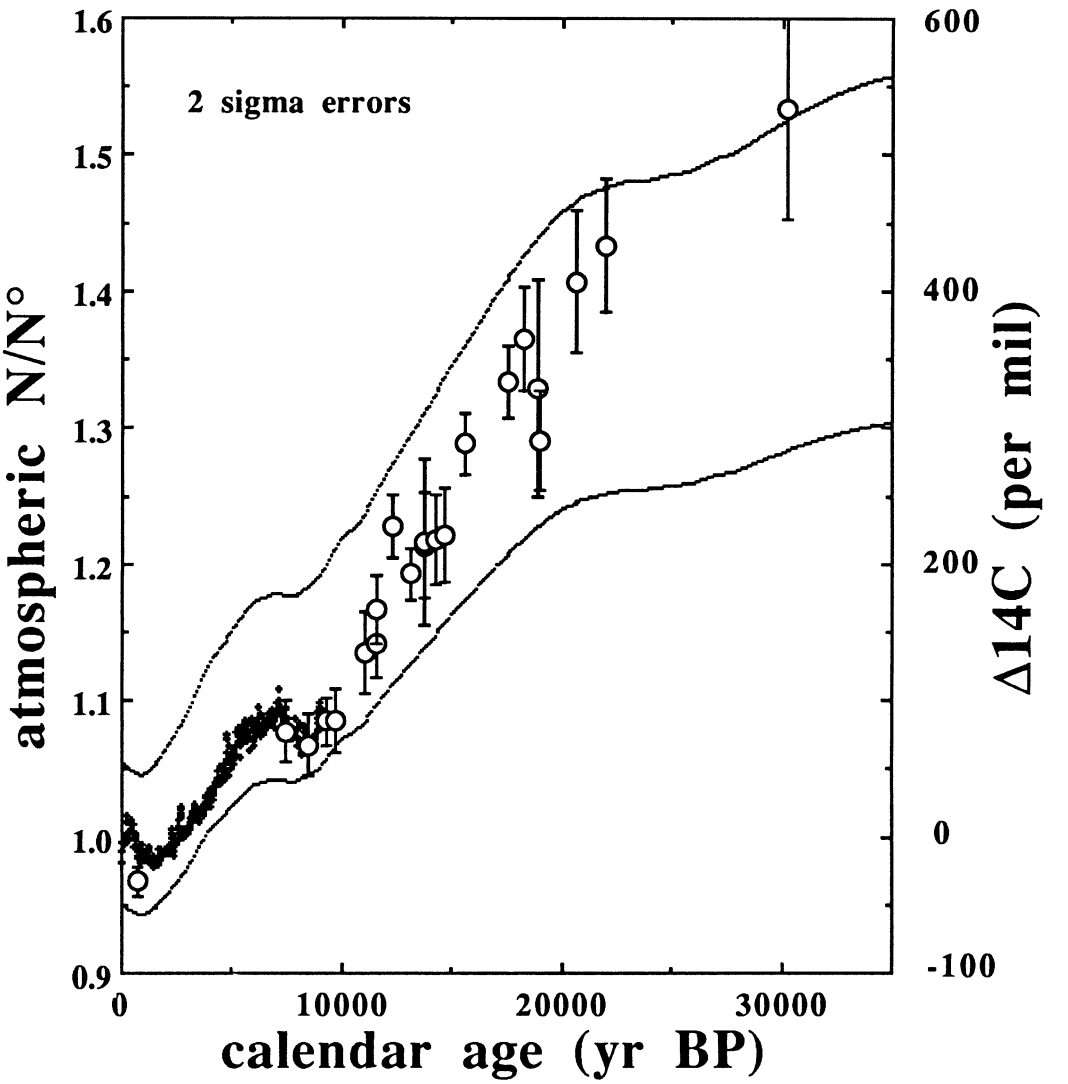

Fig. 3. $\Delta^{14}C$ *vs.* time as calculated by using the AMS-^{14}C *vs.* U-Th comparison. + = dendrochronological calibration. All statistical errors are quoted at 2 σ. For sample RGF12-30-2, we used the ^{14}C replicates obtained by AMS after very strong acid-leaching procedures. The two sets of solid lines correspond to the envelopes of $\Delta^{14}C$ expected as a response to geomagnetic field variations as reconstructed by McElhinny & Senanayake (1982). For those calculations, we used a two-box model and assumed constant errors of ± 10% of the present-day dipole (Bard *et al.* 1990a).

Discussion

The new AMS and TIMS results presented here confirm the precision and accuracy of the U-Th geochronometer applied to scleratinian corals. We show again that the ^{14}C ages are systematically younger than true ages during most of the ^{14}C application range (except for the brief period between 500 and 2500 cal BP). For the 10,000–30,000 ^{14}C yr BP period, other authors found similar discrepancies between ^{14}C and K-Ar dating (Gillot & Cornette 1986), between ^{14}C and thermoluminescence (TL) dating (Valladas & Valladas 1987; Bell 1991) and between ^{14}C ages and U-Th ages obtained in samples from speleothems (Vogel 1983) or corals (Veeh & Veevers 1970; Moore, Normak & Szabo 1990).

On the basis of available data, it is clear that the calendar duration of the Holocene chronozone (0–10,000 ^{14}C yr BP) ranges from 11,200 to 11,500 cal yr, and that the Younger Dryas chronozone (10,000–10,800 ^{14}C yr BP or 10,000–11,000 ^{14}C yr BP) corresponds to *ca.* 1000–1600 cal yr. These results agree with the study of varved sediments from Lake Gosciaz (Rozanski *et al.* 1992; Goslar *et al.* 1992).

If we assume that the ^{2}H and ^{13}C records measured by Becker, Kromer and Trimborn (1991) on German pine sections represents the whole European climate, we estimate an age of *ca.* 9700 ^{14}C yr BP for the midpoint of the Younger Dryas/Preboreal ^{2}H–^{13}C transition. Consequently, the U-Th age of the midpoint can be dated at about 11,100 yr by means of the U-Th *vs.* ^{14}C age comparison (close to sample RGF 7-27-4).

The AMS-^{14}C age of the early Bølling δ^{18}O shift varies between 12,700 BP (Ammann & Lotter 1989) and 12,500 BP (Bard *et al.* 1987), which corresponds to U-Th ages between 14,700 and 14,500 BP. As proposed by Broecker (1992), this benchmark could be used to correlate records obtained from ice cores, tree rings, corals, oceanic and continental sediments, but we should also expect a correlation problem since 12,700 ^{14}C yr BP corresponds to another ^{14}C age plateau (Ammann & Lotter 1989).

Bard *et al.* (1990a) and Stuiver *et al.* (1991) discuss in detail the geophysical interpretation of the difference observed between ^{14}C and U-Th ages obtained in corals. As Figure 3 shows, the results can be explained mainly by changes in cosmogenic nuclide production linked to the gradual decrease of the geomagnetic field, which has been documented by paleomagnetism studies (Barbetti & Flude 1979; McElhinny & Senanayake 1982; Mazaud *et al.* 1991; Salis & Bonhommet 1992). Changes in the carbon cycle also can account for *ca.* 10–20% of the age discrepancy observed between the two geochronometers; these may involve fluctuations in deep-ocean ventilation (Shackleton *et al.* 1988; Broecker *et al.* 1990) and variations in the carbon content of the atmosphere (Berner, Oeschger & Stauffer 1980; Delmas, Ascencio & Legrand 1980) and biosphere (Adams *et al.* 1990).

ACKNOWLEDGMENTS

We thank D. Buigues, D. Aïssaoui and C. T. Hoang for providing information on the samples from Mururoa, which were collected by the LDG-CEA laboratory directed by Y. Caristan. We thank G. Shen for giving us access to the Galapagos samples, B. Kromer and B. Becker for discussions and early release of data and E. Boyle for discussion and review of the manuscript. This work benefitted from the support of NSF, PRCO and DBT.

REFERENCES

Adams, J. M., Faure, H., Faure-Denard, L., McGlade, J. M. and Woodward, F. I. 1990 Increases in terrestrial carbon storage from the last glacial maximum to the present. *Nature* 348: 711–714.

Ammann, B. and Lotter, A. F. 1989 Late-Glacial radiocarbon and palynostratigraphy on the Swiss Plateau. *Boreas* 18: 109–126.

Barbetti, M. and Flude, K. 1979 Geomagnetic variation during the late Pleistocene period andchanges in the radiocarbon timescale. *Nature* 279: 202–205.

Bard, E., 1988 Correction of accelerator mass spectrometry ^{14}C ages measured in planktonic foraminifera: Paleoceanographic implications. *Paleoceanography* 3: 635–645.

Bard, E., Arnold, M., Maurice, P., Duprat, J., Moyes, J. and Duplessy, J.-C. 1987 Retreat velocity of the North Atlantic polar front during the last deglaciation determined by ^{14}C accelerator mass spectrometry. *Nature* 328: 791–794.

Bard, E., Hamelin, B., Fairbanks, R. G. and Zindler, A. 1990a Calibration of ^{14}C timescale over the past 30,000 years using mass spectrometric U-Th ages from Barbados corals. *Nature* 345: 405–410.

Bard, E., Hamelin, B., Fairbanks, R. G., Zindler, A., Arnold, M. and Mathieu, G. 1990b U/Th and ^{14}C ages of corals from Barbados and their use for

calibrating the ^{14}C time scale beyond 9000 years BP. *In* Yiou, F. and Raisbeck, G., eds., Proceedings of the 5th International Conference on AMS. *Nuclear Instruments and Methods* B52 461–468.

Becker, B., Kromer, B. and Trimborn, P. 1991 A stable isotope tree-ring time scale of the Late Glacial/Holocene boundary. *Nature* 353: 647–649.

Bell, W. T. 1991 Thermoluminescence dates for the Lake Mungo aboriginal fireplaces and the implication for the radiocarbon time scale. *Archaeometry* 33: 43–50.

Berner, W., Oeschger, H. and Stauffer, B. 1980 Information on the CO_2 cycle from ice core studies. *In* Stuiver, M. and Kra, R. S., eds., Proceedings of the 10th International ^{14}C Conference. *Radiocarbon* 22(2): 227–235.

Broecker, W. S. 1992 Defining the boundaries of the late glacial isotope episodes. *Quaternary Research* 38: 135–138.

Broecker, W. S., Peng, T. H., Trumbore, S., Bonani, G. and Wölfli, W. 1990 The distribution of radiocarbon in the glacial ocean. *Global Biogeochemical Cycles* 4: 103–117.

Delmas, R. J., Ascencio, J. M. and Legrand, M. 1980 Polar ice evidence that atmospheric CO_2 20,000yr BP was 50% of present. *Nature* 284: 155–157.

Druffel, E. and Linick, T. 1978 Radiocarbon in annual coral rings of Florida. *Geophysical Research Letters* 5: 913–916.

Druffel, E. and Suess, H. 1983 On the radiocarbon record in banded corals: Exchange parameters and net transport of $^{14}CO_2$ between atmosphere and surface ocean. *Journal of Geophysical Research* 88: 1271–1-280.

Edwards, R. L. (ms.) 1988 High precision thorium-230 ages of corals and the timing of sea level fluctuations in the late Quaternary. Ph.D. Thesis. California Institute of Technology.

Fairbanks, R. G. 1989 A 17,000-year glacio-eustatic sea level record influence of glacial melting rates on the Younger Dryas event and deep ocean circulation. *Nature* 342: 637–647.

_____ 1990 The age and origin of the "Younger Dryas climate event" in Greenland ice cores. *Paleoceanography* 5: 937–948.

Gillot, P. Y. and Cornette, Y. 1986 The Cassignol technique for potassium-argon dating, precision and accuracy examples from the late Pleistocene to recent volcanics from southern Italy. *Chemical Geology* 59: 205–222.

Goslar, T., Kuc, T. and Pazdur, M. F., Ralska-Jasiewiczowa, M., Rozanski, K., Szeroczynska, K., Walanus, A., Wicik, B., Wieckowski, K., Arnold, M., Bard, E. 1992 Possibilities of reconstruction of radiocarbon level changes during the late glacial by laminated sequence of the Gosciaz Lake. *In* Long, A. and Kra, R. S., eds., Proceedings of the 14th International ^{14}C Conference. *Radiocarbon* 34(3): 826–832.

Kromer, B. and Becker, B. 1992 German oak and pine ^{14}C calibration, 7200 BC to 9400BC. *Radiocarbon*, this issue.

Mazaud, A., Laj, C., Bard, E., Arnold, M. and Tric, E. 1991 Geomagnetic field control of ^{14}C production over the last 80 ky: Implications for the radiocarbon time-scale. *Geophysical Research Letters* 18: 1885-1888.

McElhinny, M. W. and Senanayake, W. E. 1982 Variations in the geomagnetic dipole I the past 50,000 years. *Journal of Geomagnetism and Geoelectricity* 34: 39–51.

Moore, J., Normak, W. R. and Szabo, B. 1990 Reef growth and volcanism on the submarine southwest rift zone of Mauna Loa, Hawaii. *Bulletin of Volcanology* 52: 375–380.

Nozaki, Y., Rye, D. M., Turekian, K. K. and Dodge, R. E. 1978 A 200 year record of carbon-13 and carbon-14 variations in a Bermuda corals. *Geophysical Research Letters* 5: 825–828.

Rozanski, K., Goslar, T., Dulinski, M., Kuc, T., Pazdur, M. F. and Walanus, A. 1992 The Late Glacial-Holocene transition in laminated sediments of Lake Gosciaz (central Poland). *In* Bard, E. and Broecker, W. S., eds., *The Last Deglaciation: Absolute and Radiocarbon Chronologies.* NATO ASI Series I-2. Heidelberg, Springer-Verlag: 69–80.

Salis, B. and Bonhommet, N. 1992 Variation of geomagnetic intensity from 8-60 Ky BP, Massif Central France. *In* Bard, E. and Broecker, W. S., eds., *The Last Deglaciation: Absolute and Radiocarbon Chronologies.* NATO ASI Series I-2. Heidelberg, Springer-Verlag: 155–162.

Shackleton, N. J., Duplessy, J. C., Arnold, M., Maurice, P., Hall, M. A. and Cartlidge, J. 1988 Radiocarbon age of the last glacial deep water. *Nature* 335: 708–711.

Shen, G. T., Campbell, T. M., Dunbar, R. B., Wellington, G. M., Colgan, M. W. and Glynn, P. W. 1991 Paleochemistry of manganese in corals from the Galapagos Islands. *Coral Reefs* 10: 91–100.

Stuiver, M., Brazunias, T. F., Becker, B. and Kromer, B. 1991 Climatic, solar, oceanic and geomagnetic influences on Late-Glacial and Holocene $^{14}C/^{12}C$ changes. *Quaternary Research* 35: 1–24.

Valladas, H. and Valladas, G. 1987 Thermoluminescence dating of burnt flint and quartz: Comparative results. *Archaeometry* 29: 214–220.

Veeh, H. H. and Veevers, J. J. 1970 Sea level at -175 m off the Great Barrier Reef 13,600 to 17,000 years ago. *Nature* 226: 536–537.

Vogel, J. C. 1983 ^{14}C variations during the Upper Pleistocene. *In* Stuiver, M. and Kra, R. S., eds., Proceedings of the 10th International ^{14}C Conference. *Radiocarbon* 25(2): 213–218.

[RADIOCARBON, VOL. 35, NO. 1, 1993, P. 201–213]

AN 11,000-YEAR GERMAN OAK AND PINE DENDROCHRONOLOGY FOR RADIOCARBON CALIBRATION

BERND BECKER

Institut für Botanik, Universität Hohenheim, D-7000 Stuttgart 70 Germany

INTRODUCTION

Sequences of dendrodated tree rings provide ideal sources for radiocarbon calibration. The wood structure of trees consists of continuous series of annual growth layers, the carbon content of which can be ^{14}C-dated and calibrated to calendar yr. The cellulose and lignin of trees deposited in river gravels or peat-bog sediments below the water table are often very well preserved, even after several millennia. Such tree-trunk deposits are well protected from contamination by younger or older organic materials. Further, the physical and chemical structure of wood allows a strong chemical pretreatment of samples for ^{14}C analysis.

A further advantage of the German oak and pine tree-ring series for ^{14}C calibration is the fact that even single-yr wood samples can be prepared in amounts sufficient for ^{14}C analysis. In this respect, the Hohenheim collection of more than 5000 subfossil, dated cross-sections is a unique source of ^{14}C calibration samples.

The establishment of the German Holocene oak dendrochronology required linking thousands of recent, historic and prehistoric tree-ring records through cross-dating. Aside from the US bristlecone pine, the Irish oak and the Göttingen German oak chronologies, the Hohenheim oak/pine chronologies are the only source for extended dendrochronological ^{14}C calibration measurements. Most of the calibration data presented within this volume are based on our German oak and pine sequences. Thus, a discussion of the validity of this record, focusing on critical links of the chronology, is given here.

Because of the remarkable length of the chronology and the great number of integrated tree-ring patterns, a detailed discussion of all the subsequent linkages would exceed page limitations. Thus, I will demonstrate the reliability of the chronology by presenting the replication of the Holocene master curve. The only valid proof of an absolute dendrochronology is the external replication by significant cross-dating of independently established tree-ring chronologies. In the case of the Hohenheim oak dendrochronology, this can be shown by cross-dating between the Rhine-Main-Danube river oak series, and by comparison with the Irish oak chronology.

Finally, it should be noted that the comparison between the radiocarbon calibration measurements on the German oak and those of US bristlecone pine and Irish oak represent valid corroborative tests; a dendrochronological mismatch between samples at any linkage of each chronology would be detected easily by offsets between the high-precision ^{14}C measurements. In this respect, the absence of anomalies in the ^{14}C intercalibration series, presented in this issue, provides evidence for the accuracy of both European and US dendrochronologies.

THE ESTABLISHMENT OF SUPER-LONG HOLOCENE CHRONOLOGIES

I have described elsewhere the history of dendrochronology with respect to radiocarbon age calibration (Becker 1992). Following the completion of the US bristlecone pine series (Ferguson 1969), research was begun in Ireland and Germany to construct super-long chronologies. After two

decades of intensive field collection and laboratory analyses, three European Holocene oak series have been established:

1. Irish oak, Belfast: Present–5289 BC (Pilcher *et al.* 1984)
2. German oak, Göttingen: Present–6255 BC (Leuschner & Delorme 1988)
3. German oak, Hohenheim: Present–8021 BC

The Belfast group collected subfossil oak trunks from peat-bog deposits, whereas the Hohenheim Laboratory focused on subfossil river oaks from gravel deposits. Researchers from the Göttingen Laboratory used both river and bog oaks for their oak record. Two series, the Belfast Irish oak and the Hohenheim German oak chronologies, became important for radiocarbon age calibration.

THE HOHENHEIM GERMAN OAK CHRONOLOGY

The river oaks of the Hohenheim Laboratory were collected in gravel pits along the upper Rhine, Main and Danube Valleys, and from minor tributaries, such as the Neckar, Iller and Isar Rivers. The subfossil trunks are remnants of riparian Holocene oak forests (*Quercus robur*, probably also *Quercus petraea*). The trees were washed into the rivers by undercutting of meander banks and by erosion of larger river channels during floods. The eroded trees drifted into oxbow lakes, or were immediately deposited in river-channel gravels. Tree-trunk horizons of alluvial terraces were preserved below the water table for >10,000 yr (Becker 1982).

Growth ages of the riparian oaks are surprisingly short; 95% of the trees consist only of 150–400 tree rings. This is related to flood frequency on the alluvial plains. Regularly occurring floods, especially those with drifting ice during the spring, often must have destroyed floodplain forests. Evidently, Holocene river oak stands seldom grew longer than 300–400 yr without disturbance. This explains why >5000 subfossil tree trunks were needed for a continuous Holocene river oak chronology.

The connection of the river oak chronology with present oak series was achieved by using living trees and medieval framework timbers. Further, oak samples associated with the Early Medieval, Roman and Celtic periods in southern Germany became available through archaeological excavations. For the prehistoric part of the chronology, samples from the Bronze Age and Neolithic dwelling sites of Switzerland and southern Germany were used (Becker *et al.* 1985).

For several years before its final linkage, the Hohenheim oak chronology consisted of three parts, namely, the absolute master (to 4000 BC), the middle Holocene floating master (4000 BC–7200 BC), and the earliest part (Main 9 chronology, before 7200 BC). The linkages at 4000 BC and 7200 BC, and a period of lower replication at 6200 BC, are described in detail below. For the present stage of the Hohenheim chronology, >95% of the past 9900 yr are replicated by a minimum of 15–25 cross-dated samples, which is sufficient for significant and reliable cross-dating among the individual curves of the master chronology (see Fig.1).

A first maximum of cross-matched curves occurs during Medieval times. This peak of replication results from numerous dendrodatings of historical buildings in southern Germany. Further maxima exist during AD 700–500, and AD 250–300 BC. Both result from the coincidence of an increased number of oak timbers from archaeological sites and a remarkable number of tree deposits from Late Holocene floods; the floods were induced by widespread forest clearing during Roman times and by Early Medieval settlement activities (Becker 1982). The prehistoric peaks of replication at 1900–2100 BC and at 2400–2600 BC are caused exclusively by increased flooding during the Late Neolithic and Early Bronze Age.

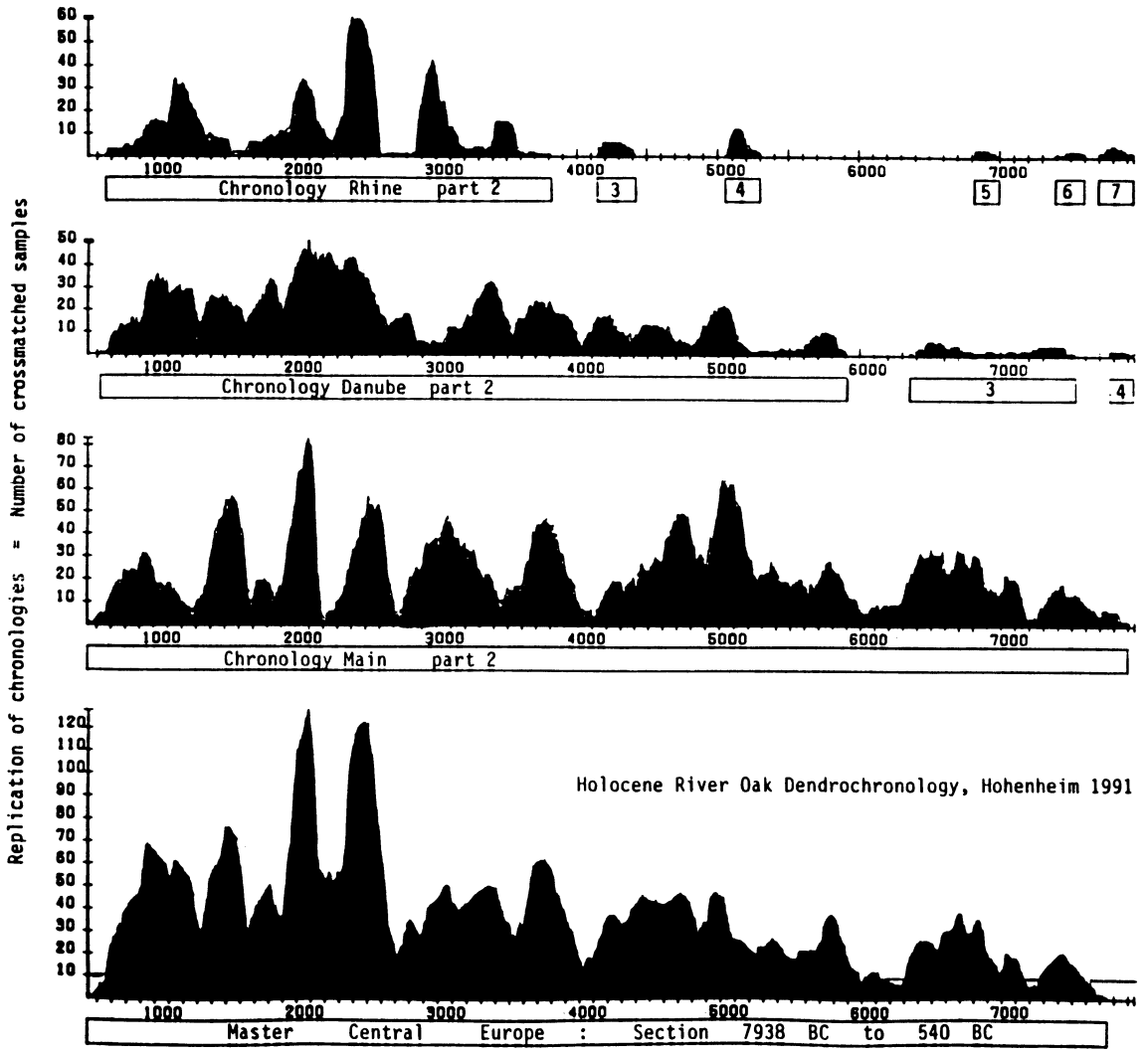

Fig. 1. Replication of the central European oak dendrochronology of the Hohenheim Tree-Ring Laboratory. Shown here is the number of individual samples at each year of the chronologies. The Hohenheim master chronology (bottom) results from matches of the regional series of the Rhine, Main and Danube Rivers, and the series of historical and prehistorical sites in south-central Europe. With the exception of the 6th century BC, the German oak dendrochronology exceeds, at each point, a minimum of 15 cross-dated individual oak samples.

Periods of low replication occur within the Hohenheim oak dendrochronology at 500 BC, 6200 BC and 7200 BC. The only critical linkage of the Hohenheim oak chronology, however, is the "Hallstatt-link" at 500 BC.

THE BRIDGING OF THE HALLSTATT OAK CHRONOLOGY

The gap in the Hohenheim river oak chronology during the later part of the Hallstatt period exists even after 20 years of intensive field sampling, and is still unexplained. On the one hand, continuous overlapping older oak sequences (and in the oldest part, pines) show a unique continuity of flooding events over the entire Holocene. The exception to this is the lack of evidence for tree accumulation in river gravels in south-central Europe between 540 BC (the latest accumulation date

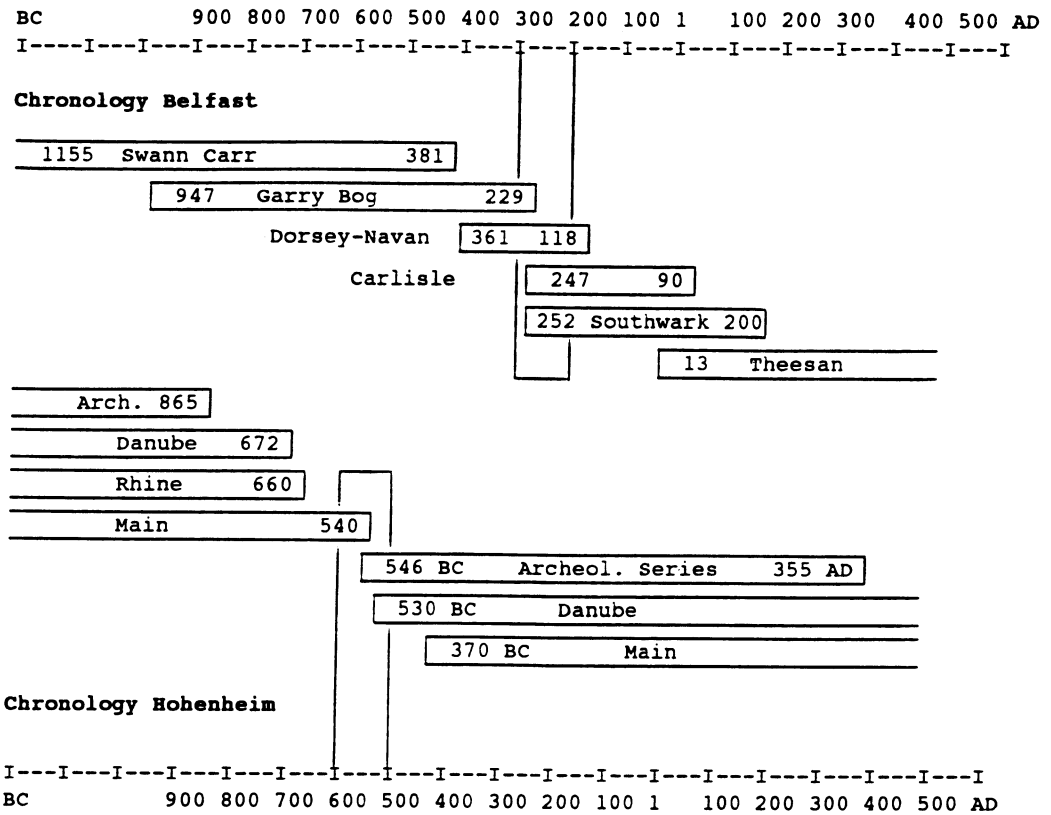

Fig. 2. Linkage of the Hohenheim German oak and the Belfast Irish oak chronologies of the first millennium BC, as published in Pilcher *et al.* (1984). The critical periods at 600–500 BC (German oak) and 300–200 BC (Irish oak) are confirmed by significant cross-datings between both series after their internal linkages (see also Becker *et al.* 1985).

from the Lahn River) and 382 BC (the earliest accumulation date of a series of subfossil trees at the Danube). Because of this lack of evidence, a 10-yr gap in the subfossil river oak series occurs from 540 to 530 BC (see Fig. 2).

Unfortunately, this small gap coincides with a period when finds of archaeological oak samples in southern Germany are also very rare. The early Hallstatt oak samples from archaeological sites end at 684 BC, but the tree-ring curves of the hitherto earliest dendrodated La Tène oak constructions do not start before 546 BC. However, this archaeological series (Thielle, Switzerland) overlaps the prehistoric river oak chronology between 546 and 540 BC. Of course, the resulting six-year link was too short to be detected visually or by cross-dating, but was confirmed in cooperative efforts with the Belfast and Köln laboratories by successful stepwise linkages of German and Irish oak series of the first millennium BC. Figure 2 shows the original overlap among the Hohenheim and Belfast series, and the evidence for the cross-dating by stepwise validation among the master series is indicated by t-test values (see Baillie & Pilcher 1982). The Belfast and Hohenheim chronologies cross-date over 5174–115 BC with a t-value of 7.3.

THE NEOLITHIC LINKAGE AT 4000 BC

In 1985, the Hohenheim master chronology was extended to 4089 BC. This was important for determining the absolute chronology of prehistoric lake and bog dwelling sites north of the Alps;

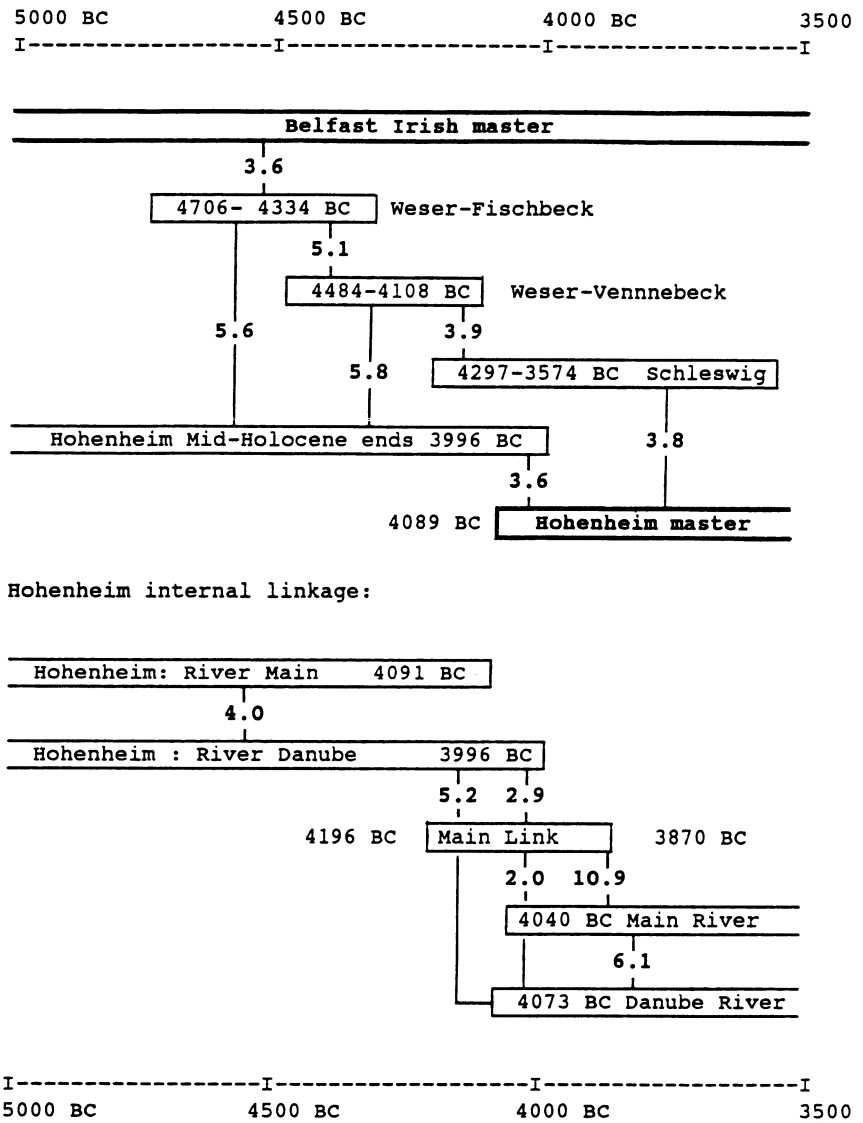

Fig. 3. Linkage of the Hohenheim middle Holocene oak master at 4000 BC. For the first time, the linkage was achieved by stepwise cross-datings among the northern German oaks (Köln) with both the Irish master and the southern German oaks (top). In its actual stage, the Hohenheim master, at 4000 BC, is internally confirmed by a new link of oaks from the Main River, reaching from 4196 to 3870 BC (bottom). The numbers between the blocks show the t-test values of the cross-matches.

it allowed the dendrodating of nearly 100 Neolithic and Bronze Age dwelling settlements of the period 3900–800 BC (Becker *et al.* 1985).

At this stage, a floating mid-Holocene oak sequence also existed, which covered 3242 tree rings (after linkage with the master, this sequence dated from 3996 to 7237 BC). This series was used for calibration measurements by the La Jolla, Seattle and Heidelberg laboratories. Its absolute age was already precisely fixed in 1985 by calibration of its ^{14}C curve with the bristlecone pine ^{14}C curve (Linick, Suess & Becker 1985).

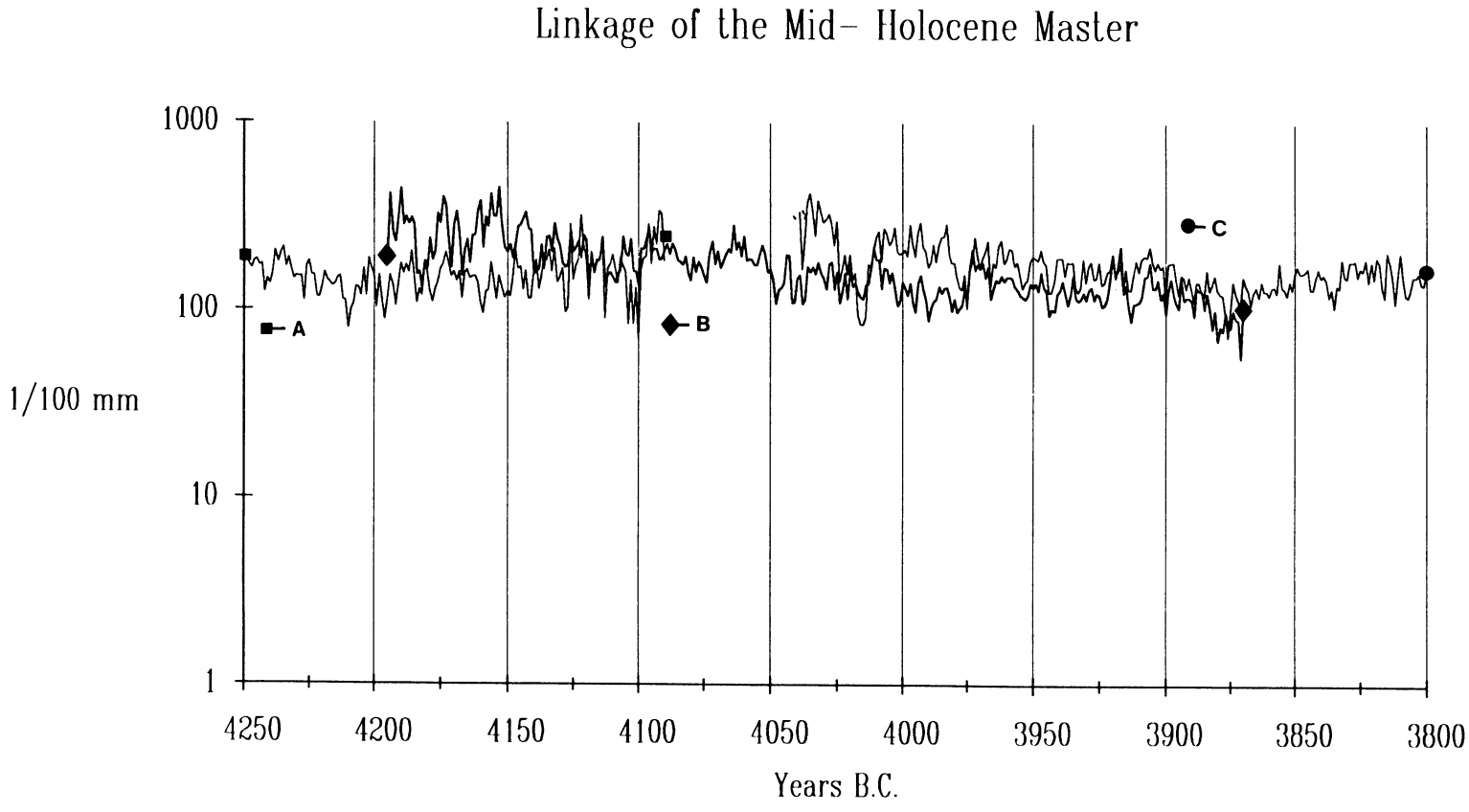

Fig. 4. Linkage of the middle Holocene oak master at 4000 BC. ■–A = end of the middle Holocene master; ◆–B = Link Main River oaks 4196–3870 BC; ●–C = Beginning of the absolute master (see also Fig. 3).

The first linkage of the middle Holocene chronology was again achieved in a cooperative project between the Köln and Hohenheim laboratories. As a result, the absolute German oak chronology was extended continuously back to 7237 BC (Becker & Schmidt 1990). The earliest part of the Köln floating Neolithic master (4706–3574 BC) cross-matches significantly with the Irish master (4706–4334 BC, t = 3.6, see Fig. 3). The Köln oak series was then linked with the end of the middle Holocene Hohenheim master (4706–3996 BC, t = 9.0), and with the beginning of the absolute Hohenheim chronology (4089–3574, t = 3.8). These stepwise cross-matches are confirmed by the final cross-match between the entire Köln Neolithic master, 4706–3574 BC, and the unbroken Hohenheim absolute master; for 1133 yr, the t-test value reaches 9.3.

Since these first successful linkages, the Hohenheim chronology of this part of the curve was further replicated. Figures 3 and 4 show the present status: the middle Holocene Main series (12 trees), ending at 4091 BC, overlaps the Main oak link (4196–3780 BC, 6 trees) with t = 5.2., and the start of the absolute Main sequence cross-matches with this link with t = 10.9. The linkage is also confirmed by the Danube oak series (22 middle Holocene oaks), which also overlaps the Main linkage at both ends. The final chronology, 4200–3900 BC, is now well replicated by at least 25 individual curves.

THE MESOLITHIC LINKAGE OF THE MAIN 9 CHRONOLOGY AT 7200 BC

During the construction of the Hohenheim chronology, a further floating Holocene oak sequence (Main 9 series) was established. It is placed before the middle Holocene master. Before its final linkage, it was already the subject of ^{14}C calibration measurements (by H. E. Suess, La Jolla, B. Kromer, Heidelberg and M. Stuiver, Seattle). This series dates from before the range of the bristlecone pine. For many years, no age determination by ^{14}C calibration was available. After successful cross-match with the master, the sequence was dendrodated from 7751 to 7235 BC. The link was derived from two oaks (7339–7025 BC) which also overlap at the end of the Main 9 series and the beginning of the middle Holocene master, which was slightly enlarged to 7237 BC (see Fig. 5). The link cross-matches Main 9 with t = 5.4, and the beginning of the middle Holocene master with t = 4.4. This extension of the absolute master is also confirmed by two overlapping Danube oak series: 7464–7144 BC and 7195–6743 BC. The validity of this cross-match can be seen from the tree-ring curves of Figure 6.

In 1988, the German Holocene oak chronology was extended by very early oaks of the Main, Rhine and Danube Rivers, which date from the beginning of the Boreal period. This extension of the Boreal oak chronology extends the absolute German oak chronology to 7938 BC. During 1991 field sampling, we found three older oaks from the Main River floodplain, which cross-date with the beginning of the master, and extend the entire absolute master chronology to 8021 BC.

THE 6200–6300 BC LINKAGE

A close look at the replication of the Hohenheim Holocene oak master chronology points to a period of decreased replication between 6200 and 6300 BC. The linkage of the Main oaks of this period can be subdivided into three well-replicated overlapping parts (see Fig. 7). The bridging series of 6402–6057 BC overlaps the end of the older chronology by 122 yr, and the younger chronology, by 131 yr. The corroborative tests yield significant t-values of 7.0 and 6.4, respectively (see also curves of Fig. 8).

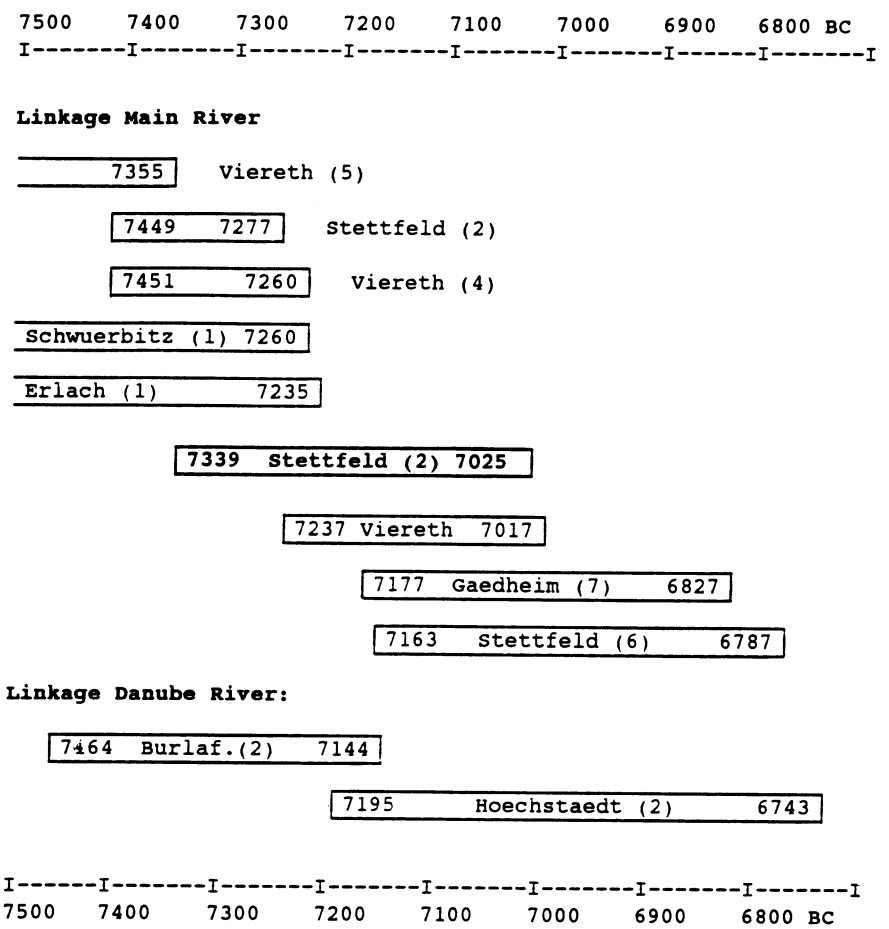

Fig. 5. Linkage of the Main 9 chronology with the absolute master at 7200 BC. Each block represents a site chronology, the numbers in parentheses refer to the replication of the series. The linking series consist of oaks from the Stettfeld site (Main), dating from 7339–7025 BC.

CONFIRMATION OF THE ABSOLUTE HOLOCENE GERMAN OAK CHRONOLOGY BY EXTERNAL REPLICATION

As mentioned above, the validity of a long dendrochronology can be evaluated best by replications between links that have been independently established by samples from different regions or from different sample sources. In the case of the Hohenheim oak chronology, valid cross-matches exist among the river oak chronologies of the Rhine, Main and Danube regions. Further, cross-matches exist between the river oak chronologies and the chronologies from historic to prehistoric oak constructions of south-central Europe. For example, the unbroken 2537-yr oak master curve of modern and Medieval to Iron Age samples (present to 546 BC) is replicated over 2211 yr by the stepwise overlapping river oak chronologies. In its prehistoric section, the 7482-yr unbroken regional series of the Main River (540–8021 BC) is replicated by 3 archaeological oak sample chronologies over 2602 yr, by 8 Rhine River oak series over 3885 yr, and by 5 Danube River oak series over 6440 yr (see Fig. 9).

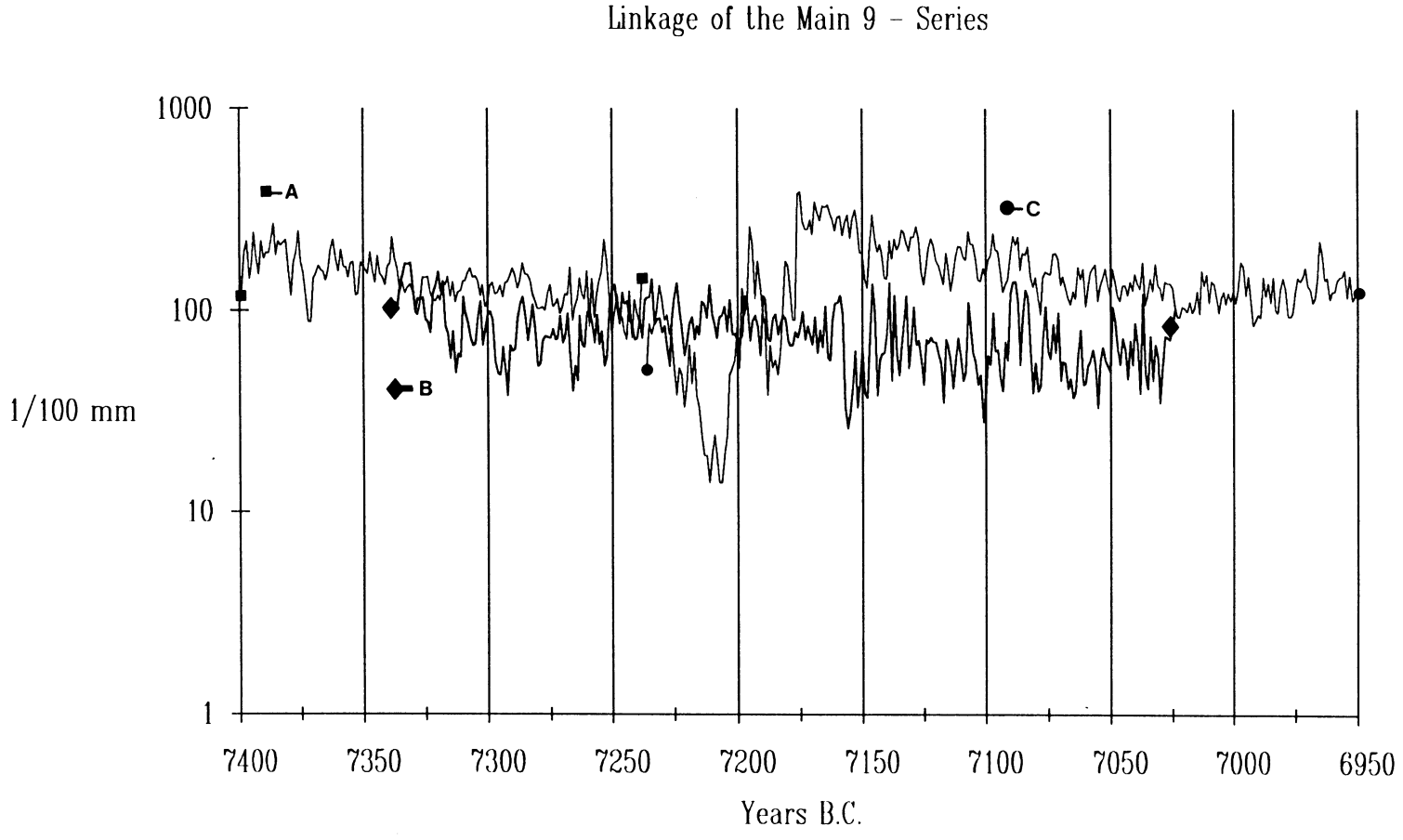

Fig. 6. Linkage of the Main 9 chronology at 7200 BC. ■–A = Main 9 series; ◆–B = Stettfeld link 7339–7025 BC; ●–C = beginning of the absolute master (see also Fig. 5).

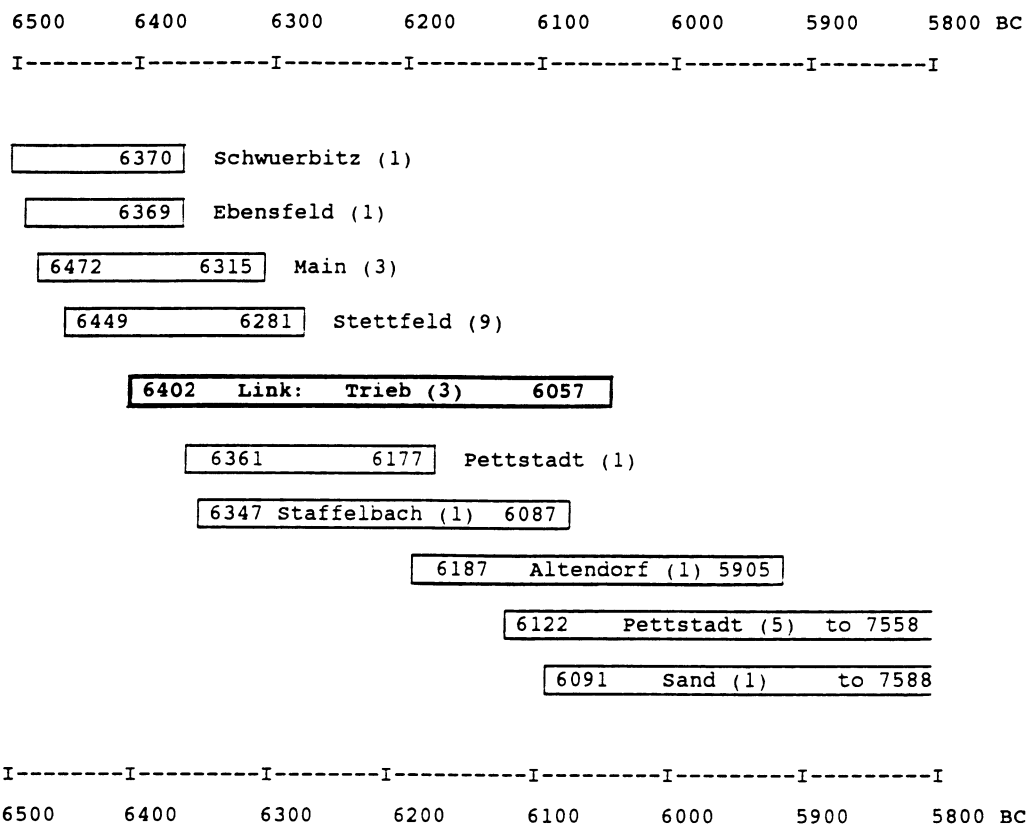

Fig. 7. Linkage at 6200 BC. The linkage consists of three oaks of the Trieb site, dating from 6402–6057 BC, which overlap the older part by 121 yr and the younger part by 131 yr.

THE EARLY HOLOCENE–LATE GLACIAL GERMAN PINE CHRONOLOGY

Along the Danube and Rhine rivers, remnants of well-preserved pine trunks (*Pinus sylvestris*) are frequently dredged from river gravels, along with oaks. When the first ^{14}C dates of H. E. Suess (unpublished data) attributed a surprisingly old age to these pine trees, I started collecting both pines and oaks. This project led to the construction of an unbroken 1768-yr floating late Younger Dryas and early Holocene pine chronology, as well as a 405-yr Allerød pine series.

The subfossil pines are remnants of Late Glacial forests, where both pine and birch (*Betula verrucosa, B. pubescens*) covered the central European valley plains. Pines disappeared when oaks entered the river valleys, displacing the light- demanding pine/birch forests. However, before pines vanished from the Holocene Danube and Rhine valleys, a mixed pine/oak forest must have existed. The temporal overlap of pine and oak trunk deposits of that period provided a unique opportunity to extend further the absolute dendrochronology.

First, we have linked 185 subfossil pines to an unbroken floating record of 1605 tree rings. This sequence crosses the boundary between the early Holocene and the Late Glacial, a boundary recently detected in ^{13}C and ^{2}H records of pine tree-ring cellulose (Becker, Kromer & Trimborn 1991). We derived an absolute minimum age of 11,370 dendroyr BP for the beginning of the pine sequence by linking the end of the pine series with oak at the 8800 BP ^{14}C oscillation, which is visible in both series (Kromer & Becker 1992).

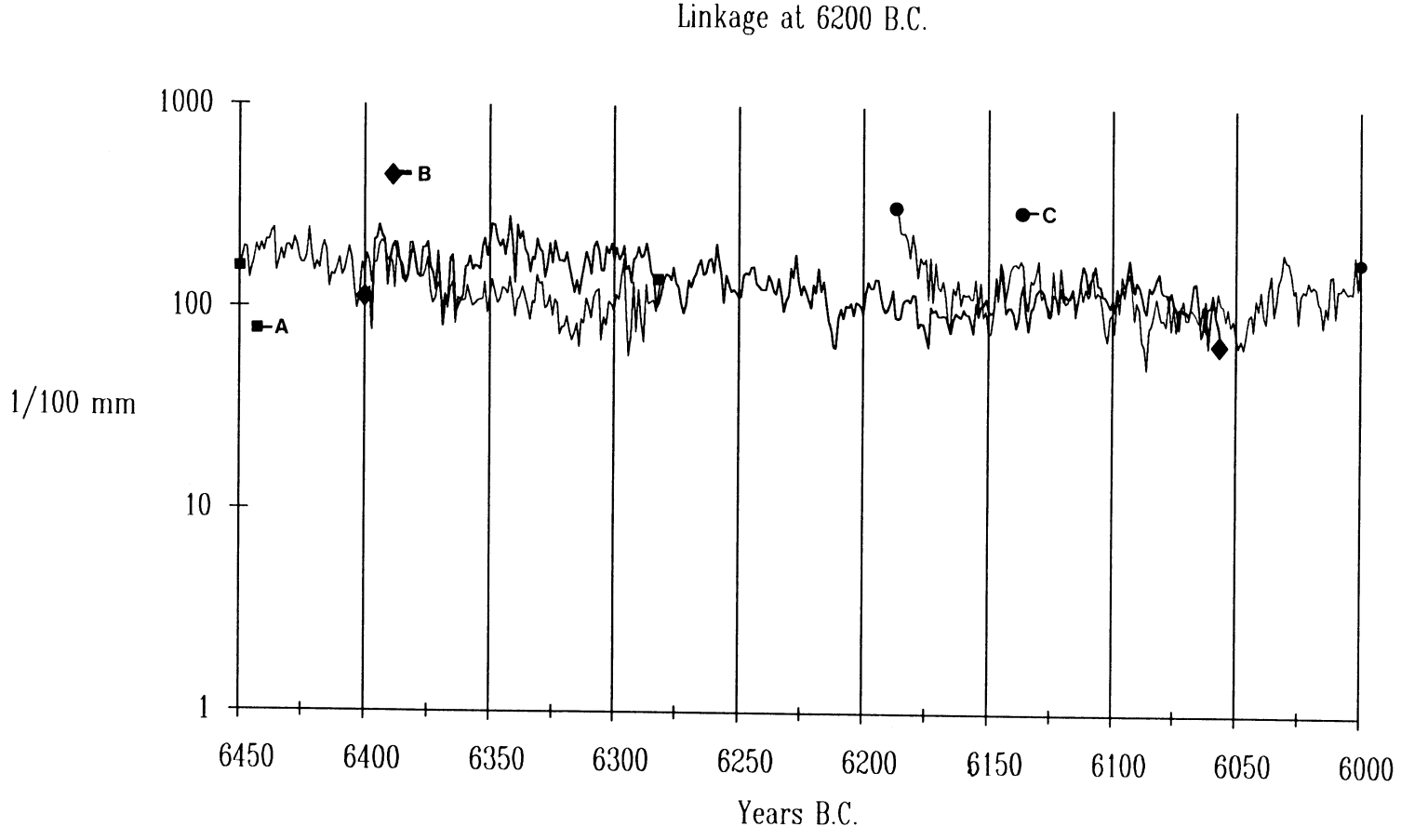

Fig. 8. Tree-ring chronologies of the Hohenheim oak master between 6450 and 6000 BC. The bridging series is ◆–B (Trieb site) (see also Fig. 7).

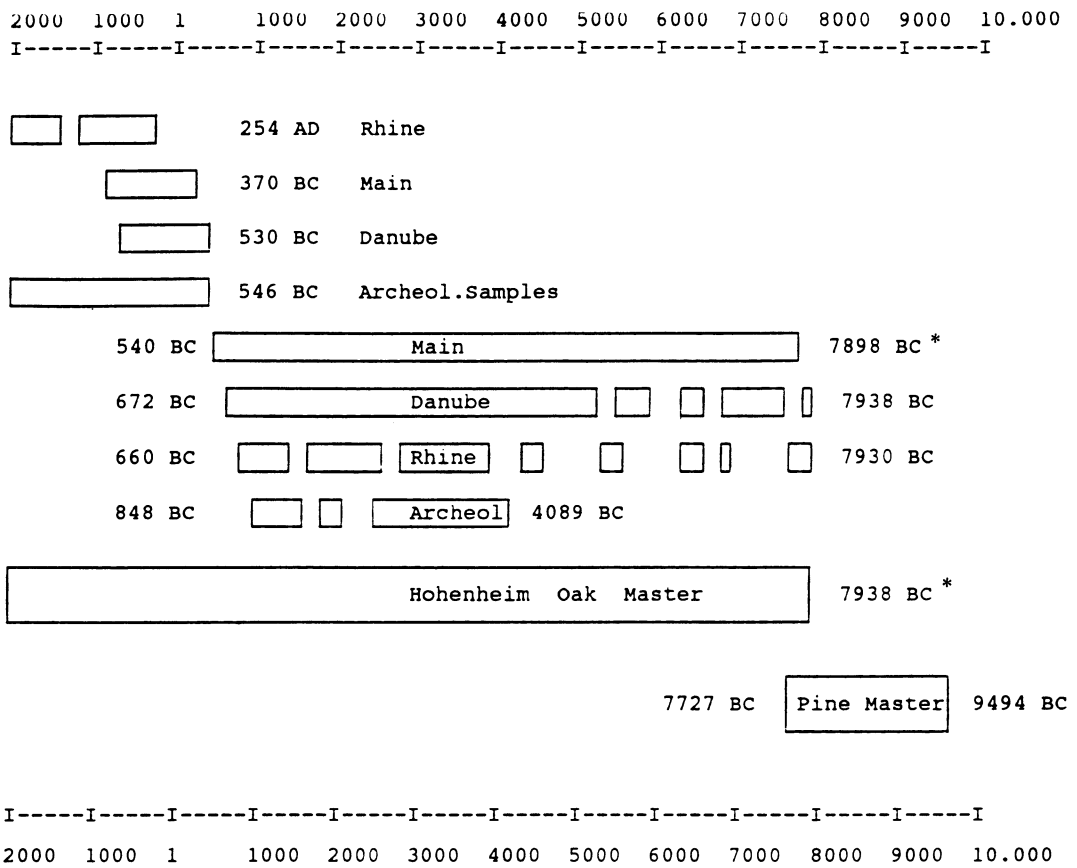

Fig. 9. Compilation of the south central European Holocene/Late Glacial dendrochronology, Hohenheim Laboratory. The blocks represent replicated regional master chronologies. The oak chronology to 546 BC consists of an unbroken series of modern trees, and samples from historic and prehistoric sites. The prehistoric part consists of an unbroken oak record of the Main River valley from 540 to 7898 BC. This chronology is replicated over most sections by archaeological site chronologies, and by series of the Rhine and Danube Rivers. The Danube and Rhine samples extend the master to 7938 BC. The late Preboreal pine chronology overlaps the oak master between 7727 and 8021 BC. A recently detected, but still tentative link of this 1768-yr pine master extends the entire dendrochronology to 9494 BC. The earliest part of the pine series dates from the Younger Dryas and covers the Holocene/Pleistocene boundary (Becker, Kromer & Trimborn 1991). *Recently expanded to 8021 BC, see text.

Very recently, five additional pines covering ^{14}C dates in the 8800 BP range have cross-matched with the end of the pine master chronology, extending the sequence to 1768 tree rings. This series must now overlap the beginning of the oak master near 8800 BP, which meanwhile is extended to 8021 BC. Indeed, a reasonable cross-match between the 8800 BP pine/oak masters is now visible. The overlap between both curves consists of 295 tree rings, but this important linkage is still tentative and must be confirmed by additional ^{14}C measurements. However, this link extends the absolute German oak/pine dendrochronology by an additional 1550 yr, to 9494 BC. The calibration data beyond 7800 BC presented here are derived from this tentative zero point of 9494 BC.

REFERENCES

Baillie, M. G. L. and Pilcher, J. R. 1982 A simple cross-dating program for tree-ring research. *Tree-Ring Bulletin* 33: 7–14.

Becker, B. 1982 Dendrochronologie und Paläoökologie subfossiler Baumstämme aus Flußablagerungen. *Mitteilungen der Kommission für Quartärforschung der Österreichischen Akademie der Wissenschaften* 5: 120 p.

_____1992 The history of dendrochronology and radiocarbon calibration. *In* Taylor, R. E., Long, A. and Kra, R. S., eds., *Radiocarbon After Four Decades: An Interdiscipinary Perspective.* New York, Springer Verlag: 34–49.

Becker, B., Billamboz, A., Egger, H., Gassmann, P., Orcel, A., Orcel, C., and Ruoff, U. 1985 Dendrochronologie in der Ur- und Frühgeschichte. *Antiqua* 11: 1–68.

Becker, B. and Kromer, B. 1991 Dendrochronology and radiocarbon calibration of the Early Holocene. *In* Barton, N., Roberts, A. and Roe, D. A., eds., The Late Glacial in northwest Europe. *CBA Research Report* 77: 22–25.

Becker, B., Kromer, B. and Trimborn, P. 1991 A stable-isotope tree-ring timescale of the Late Glacial/Holocene boundary. *Nature* 353: 647–649.

Becker, B. and Schmidt, B. 1990 Extension of the European oak chronology to the past 9924 years. *In* Waterbolk, H. T. and Mook, W. G., eds., Proceedings of the Second International Symposium, Archaeology and ^{14}C. *PACT* 29: 37–50.

Ferguson, C. W. 1969 A 7104-year annual tree-ring chronology for bristlecone pine, *Pinus aristata*, from the White Mountains, California. *Tree-Ring Bulletin* 29(3–4): 1–29.

Kromer, B. and Becker, B. 1992 Tree-ring ^{14}C calibration at 10.000 BP. In: Bard, E. and Broecker, W. S., eds., The Last Deglacation: Absolute and Radiocarbon Chronologies, *NATO ASI Series* I-2. Heidelberg, Springer Verlag: 3–11.

Leuschner, H. H. and Delorme, A. 1988 Tree-ring work in Göttingen. Absolute oak chronologies back to 6255 BC: *PACT* 22: 123–132.

Linick, T. W., Suess, H. E. and Becker, B. 1985 La Jolla measurements of radiocarbon on South German oak tree-ring chronologies. *Radiocarbon* 27(1): 20-30.

Pilcher, J. R., Baillie, M. G. L., Schmidt, B. and Becker, B. 1984 A 7,272 year tree-ring chronology for western Europe. *Nature* 312: 150–152.

[RADIOCARBON, VOL. 35, NO. 1, 1993, P. 215–230]

EXTENDED ^{14}C DATA BASE AND REVISED CALIB 3.0 ^{14}C AGE CALIBRATION PROGRAM

MINZE STUIVER and PAULA J. REIMER

Department of Geological Sciences and Quaternary Research Center, University of Washington Seattle, Washington 98195 USA

INTRODUCTION

The age calibration program, CALIB (Stuiver & Reimer 1986), first made available in 1986 and subsequently modified in 1987 (revision 2.0 and 2.1), has been amended anew. The 1993 program (revision 3.0) incorporates further refinements and a new calibration data set covering nearly 22,000 cal yr (≈18,400 ^{14}C yr). The new data, and corrections to the previously used data set, derive from a 6-yr (1986–1992) time-scale calibration effort of several laboratories.

One purpose of this paper is to introduce the reader to some features of the IBM-compatible CALIB 3.0 program. As such, it supplements the 26-page CALIB User's Guide (Stuiver & Reimer 1993), which gives the ultimate CALIB details. A Macintosh version of CALIB 3.0 is available upon request.

The CALIB 3.0 program is menu-driven to calibrate ^{14}C ages, provide $\Delta^{14}C$ series and display results. CALIB, the User's Guide, and the calibration data are compressed on the floppy disk enclosed with this *RADIOCARBON* issue; this information should be copied following the instructions printed on the diskette label and in the file, README. The program can also be obtained separately from the Quaternary Isotope Laboratory. $\Delta^{14}C$ series include the data for Figures 2 and 11 of Stuiver and Braziunas (1993).

Although the basic tree-ring calibration data are either decadal or bidecadal, smoothed versions of the calibration curves can be obtained for multiyear samples using the moving average option. These smoothed versions are desirable, as the ^{14}C "wiggles" of the calibration curve play a lesser role in creating cal age uncertainty. Such smoothed versions should be used when samples have grown over intervals longer than 20 yr (*e.g.*, 100 yr for a 5-point moving average of the bidecadal curve).

In the following sections, we evaluate the selection of the calibration (and $\Delta^{14}C$) data, and discuss new CALIB program features.

THE DATA

The ^{14}C data sets used for the CALIB program are given in Table 1. These data sets were constructed from four main categories, as listed below:

A. Bidecadal Data Set (AD 1950–9440 BC; 0–11,390 Cal Yr BP)

The data set utilized in the 1993 CALIB version came from several sources. The entire AD 1950–6000 BC interval is based on averages of ^{14}C ages obtained by the Seattle and Belfast laboratories on 20-yr samples. In the 1987 CALIB version 2.1, we utilized the published bidecadal data of Stuiver and Pearson (1986) and Pearson and Stuiver (1986) for the AD 1950–2500 BC interval. Some minor corrections in the 10–30 ^{14}C yr range (*e.g.*, a radon correction for Quaternary Isotope Laboratory results (Stuiver & Becker 1993)) have since been applied to the published Seattle and Belfast ^{14}C ages. The 1993 program incorporates 1) cor-

TABLE 1. ^{14}C data sets used for the 1993 calibration program. A, B, C and D refer to the subdivisions in the data section.

For atmospheric samples:
Set 1. Limited to 0–18,360 ^{14}C yr BP
Bidecadal tree ring data set A (AD 1955–9440 BC, 0–11,390 cal yr BP)
+ inferred atmospheric spline from D (9450 BC–20,000 BC, 11,400–21,950 cal yr BP)
Set 2. Limited to 0–7210 ^{14}C yr BP:
Decadal tree-ring data set B (AD 1955–6000 BC; 0–7950 cal yr BP)
For marine samples:
Set 3. Limited to 18,760 ^{14}C yr BP
Marine bidecadal model data set C (0–11,400 cal yr BP)
+ marine coral data spline from D (11,400–21,950 cal yr BP), slightly adjusted between 11,400 and 11,750 cal yr BP (Stuiver & Braziunas 1993)

rected averaged bidecadal data of both laboratories for the AD 1950–2500 BC interval, and 2) a new averaged bidecadal data set for the 2500–6000 BC interval (Stuiver & Pearson 1993; Pearson & Stuiver 1993).

The bidecadal ^{14}C age averages of the AD 1950–5000 BC interval are based on separate dendrochronologies (Irish oak for Belfast, and German oak/Northwest Pacific sequoia or Douglas fir for Seattle), which yield ^{14}C results with negligible systematic differences (Stuiver & Pearson 1993). The degree of coherence with other data sets also is discussed in the above paper. Between 5000–5160 BC, a mixture of Irish and German oak is used; for the 5180–6000 BC interval, calibration results are tied solely to the German chronology, with the exception of the 5680–5810 BC interval, where bristlecone pine data (Table 2) were added to the Seattle data set. There is minimal systematic difference between the ^{14}C results of both laboratories between 5500 BC and 6000 BC. For the 5180–5500 BC interval, however, the bidecadal calibration curve may be liable to a 27 ^{14}C-yr offset (see Stuiver & Pearson 1993).

TABLE 2. Radon-corrected ^{14}C ages of Ferguson bristlecone pine samples (Stuiver *et al.* 1986). Standard deviations are based on counting statistics only.

Year (BC)	Year (BP)	No. of rings	^{14}C age	$\Delta^{14}C$
6475	8424	11	7733 ± 26	+57.9 ± 3.4
6360	8309	21	7472 ± 25	+77.9 ± 3.3
5805	7754	11	6968 ± 16	+73.1 ± 2.1
5795	7744	11	6974 ± 22	+71.0 ± 3.0
5785	7734	11	6994 ± 21	+67.0 ± 2.8
5775	7724	11	6976 ± 23	+68.2 ± 3.1
5765	7714	11	6930 ± 17	+73.0 ± 2.3
5755	7704	11	6933 ± 18	+71.3 ± 2.4
5745	7694	11	6946 ± 22	+68.3 ± 2.9
5735	7684	11	6909 ± 22	+71.9 ± 3.0
5725	7674	11	6861 ± 21	+77.0 ± 2.9
5715	7664	11	6895 ± 22	+71.3 ± 3.0
5705	7654	11	6840 ± 21	+77.2 ± 2.9
5695	7644	11	6843 ± 21	+75.6 ± 2.8
5685	7634	11	6844 ± 21	+74.1 ± 2.8

The 6000–8000 BC interval is covered in several data sets. Available intervals are 6016–7885 BC for Heidelberg (Kromer *et al.* 1986; Kromer & Becker 1993), 6436–7160 BC for Seattle (Table 3), 6000–7890 BC for Belfast (Pearson, Becker & Qua 1993), 6393–7199 BC for La Jolla (Linick *et al.* 1985) and 6089–6549 BC for Tucson (Linick, Suess & Becker 1986). Whereas the Tucson laboratory measured samples from the bristlecone pine chronology, all other laboratories worked with samples from the German chronology. Two data sets (Belfast and Tucson) were based on measurements of bidecadal (or decadal) wood samples (indicated below as true bidecadal wood); the other laboratories (Heidelberg, Seattle, La Jolla) measured samples grown over shorter time intervals (usually 1–3 yr).

To compare results from different laboratories, we define an error multiplier, $K_{\text{Lab A-Lab B}}$ (*e.g.*, Stuiver & Pearson 1992, 1993) as the ratio of the actual standard error in the age differences to the average standard deviation of the differences calculated from the quoted errors in the ^{14}C determinations. We define n = number of comparisons, and a = systematic difference with positive values when Lab A dates are older. Comparing Belfast and available Tucson data prior to 6000 BC (6090–6550 BC), $K_{\text{Belfast-Tucson}} = 1.8$, a = 15.8 ± 5.0 yr and n = 24. Application of an error multiplier of 1.8 to both data sets increases the error term in the offset to 9 yr. As the 15.8-yr offset (1.7 σ) is statistically insignificant, we averaged the Belfast and Tucson data over the 6090–6500 BC interval. Our true bidecadal (trueBD) curve for the 6000–8000 BC interval is identical to the Belfast bidecadal data set, except for the 6090–6550 BC interval, where the Belfast and Tucson data averages were used. For comparison with the Heidelberg, Seattle and La Jolla results, we also calculated "bidecadal" data points by averaging the available ^{14}C dates over 20-yr intervals. Often, only part of the bidecade was measured, and the "bidecadal" ^{14}C ages calculated in this manner need not be identical to the ^{14}C ages that would have been obtained by measuring bidecadal wood samples directly. However, the ^{14}C age differences between bidecadal and "bidecadal" samples should, in most instances, be $< \sim 10$ yr, as the scatter of single-year $\Delta^{14}C$ data usually is restricted to a few per mil (*e.g.*, Stuiver 1982).

Comparisons of the trueBD calibration curve to the Heidelberg, Seattle and La Jolla "bidecadal" data reveal some offsets, with $K_{\text{Heidelberg-TrueBD}} = 1.5$, a = 32 ± 4.1 yr, n = 47 (6020–7130 BC), $K_{\text{Heidelberg-TrueBD}} = 1.8$, a = 52 ± 4.8 yr, n = 34 (7190–7870 BC), $K_{\text{Seattle-TrueBD}} = 1.4$, a = 51 ± 4.5 yr, n = 34 (6430–7130 BC) and $K_{\text{LaJolla-TrueBD}} = 1.2$, a = −5 ± 7.8 yr, n = 36 (6390–7190 BC).

The ^{14}C ages of these imperfect "bidecades" can be used to construct a bidecadal data set incorporating all true bidecadal and "bidecadal" data (AllBD). Comparing AllBD with TrueBD, we find a 300-yr interval of substantial offset (6740–7040 BC). Here the mean difference is 43.3 ± 5.7 yr (n = 15, K = 0.84). The minimum proven offset is 43.3 ± 11.4 (2 σ), or ~ 32 yr. Assuming that the average of the Seattle, Heidelberg, Belfast and La Jolla data is more representative of the average trend than the TrueBD data alone, which, for this interval, is Belfast data only, we elected to adjust the TrueBD curve by adding 32 ^{14}C yr to the ^{14}C dates of the 6740–7040 BC interval (the actual midpoints bracket 6750–7030 BC). We also took the trends in the AllBD curve to generate two missing data points in the TrueBD curve, at 7150 and 7170 BC (dashed line in Fig. 1). The resulting bidecadal calibration data set used in CALIB 3.0 for the 6000–7890 BC interval is the Adjusted TrueBD set, with K = 1.7 applied to the quoted standard deviations. The Adjusted TrueBD set is compared to the AllBD set in Figure 1 (offset a = 9.3 ± 2.1 yr, K is only 0.9 and n = 86). The systematic difference averages less than a decade, and is fairly randomly distributed (Fig. 1).

TABLE 3. Corrected data set of previously published (Stuiver *et al.* 1986) cal BC and ^{14}C ages of the unified Donau 6/Main 4/11 German chronology. Ring 1 of this chronology is now matched at 7177 BC and a radon correction (Stuiver & Becker 1993) was applied to the ^{14}C dates. Standard deviations are based on counting statistics only.

Ring no.	Year (BC)	Year (BP)	No. of Rings	^{14}C age	$\Delta^{14}C$
18.5	7159.5	9108.5	2	8306 ± 41	+70.2 ± 5.1
28.5	7149.5	9098.5	4	8236 ± 24	+78.3 ± 3.0
42.0	7136	9085	5	8199 ± 25	+81.5 ± 3.1
52.0	7126	9075	5	8201 ± 25	+80.0 ± 3.1
72.0	7106	9055	5	8238 ± 24	+72.4 ± 3.0
82.5	7095.5	9044.5	6	8168 ± 23	+80.3 ± 2.9
107.0	7071	9020	5	8234 ± 24	+68.4 ± 3.0
132.0	7046	8995	5	8178 ± 23	+72.6 ± 2.8
157.0	7021	8970	5	8151 ± 24	+73.0 ± 3.0
167.0	7011	8960	5	8070 ± 24	+82.5 ± 3.0
187.0	6991	8940	5	8085 ± 24	+77.9 ± 3.0
202.0	6976	8925	5	7908 ± 25	+99.9 ± 3.1
205.0	6973	8922	11	8017 ± 14	+84.7 ± 1.7
217.0	6961	8910	5	7983 ± 32	+87.6 ± 4.0
232.0	6946	8895	5	8048 ± 27	+77.0 ± 3.4
255.0	6923	8872	11	8027 ± 17	+76.8 ± 2.2
257.0	6921	8870	5	8010 ± 26	+78.8 ± 3.3
278.5	6899.5	8848.5	6	8001 ± 24	+77.2 ± 3.0
285.0	6893	8842	11	7994 ± 36	+77.2 ± 4.4
297.0	6881	8830	5	8016 ± 24	+72.8 ± 3.0
317.0	6861	8810	5	8030 ± 24	+68.4 ± 3.0
322.0	6856	8805	5	7973 ± 50	+75.3 ± 6.2
342.0	6836	8785	5	8036 ± 20	+64.3 ± 2.5
347.0	6831	8780	5	8090 ± 25	+56.6 ± 3.1
365.5	6812.5	8761.5	4	8060 ± 26	+58.1 ± 3.2
387.5	6790.5	8739.5	4	8065 ± 26	+54.6 ± 3.2
402.0	6776	8725	5	8008 ± 23	+60.3 ± 2.8
414.0	6764	8713	3	7967 ± 26	+64.1 ± 3.2
431.0	6747	8696	3	7981 ± 26	+60.1 ± 3.2
451.0	6727	8676	3	7982 ± 25	+57.5 ± 3.1
457.0	6721	8670	5	7956 ± 23	+60.2 ± 2.8
462.0	6716	8665	5	7951 ± 25	+60.1 ± 3.1
462.5	6715.5	8664.5	6	7976 ± 24	+56.8 ± 3.0
477.0	6701	8650	5	7940 ± 23	+59.7 ± 2.8
497.0	6681	8630	5	7969 ± 24	+53.3 ± 3.0
502.5	6675.5	8624.5	6	7945 ± 24	+55.8 ± 3.0
517.0	6661	8610	5	7964 ± 23	+51.5 ± 2.8
525.0	6653	8602	11	7938 ± 24	+53.8 ± 3.0
542.5	6635.5	8584.5	6	7872 ± 17	+60.3 ± 2.2
556.5	6621.5	8570.5	6	7928 ± 25	+51.1 ± 3.1
572.0	6606	8555	5	7861 ± 23	+57.9 ± 2.8
589.5	6588.5	8537.5	10	7851 ± 21	+57.0 ± 2.7
618.5	6559.5	8508.5	4	7806 ± 24	+59.2 ± 3.0
641.5	6536.5	8485.5	6	7824 ± 24	+53.9 ± 3.0
663.5	6514.5	8463.5	8	7705 ± 16	+66.8 ± 2.0
680.5	6497.5	8446.5	8	7793 ± 24	+53.0 ± 3.0
704.0	6474	8423	5	7781 ± 17	+51.6 ± 2.1
719.5	6458.5	8407.5	4	7706 ± 17	+59.4 ± 2.1
742.0	6436	8385	5	7640 ± 18	+65.4 ± 2.3

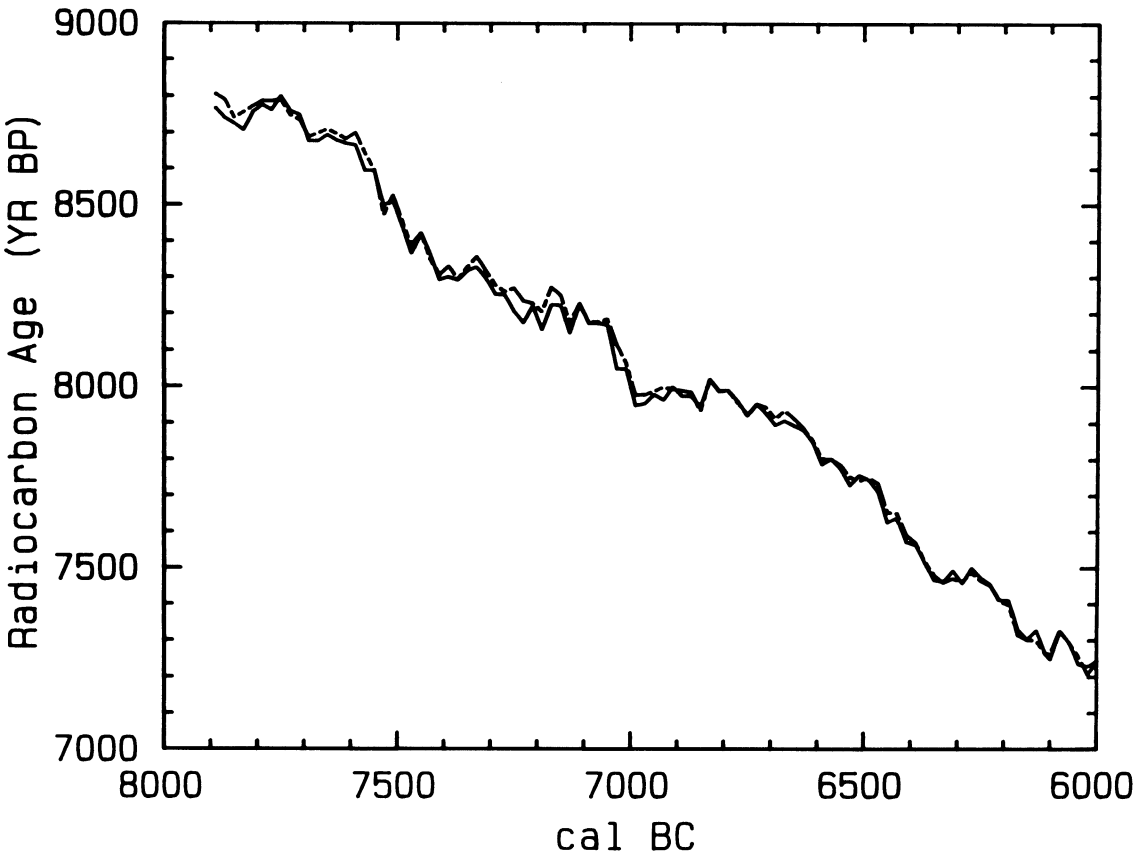

Fig. 1. A comparison of the CALIB 3.0 bidecadal data set (——) and ^{14}C age averages of available data from the Belfast, La Jolla, Heidelberg, Seattle and Tucson laboratories (– –). The CALIB set of the 8000–6000 BC interval derived from Pearson, Becker & Qua (1993) and Linick *et al.* (1986) with adjustments discussed in the text.

Between 7890 and 9440 BC, the CALIB 3.0 program uses Heidelberg measurements (Kromer & Becker 1993) of an early Holocene pine chronology from south-central Europe. The oldest part of the absolute German oak chronology and the youngest portion of the pine chronology have not yet been absolutely matched. The connection by Becker, Kromer and Trimborn (1991) assigns minimum absolute ages to the pine chronology. Bard *et al.* (1993) and Stuiver *et al.* (1991) suggest a shift of 150 and 300 yr, respectively. A very tentative match of overlapping tree-ring patterns by Becker (1993), equivalent to a 74-yr increase in cal ages, leads to the absolute BC ages of Kromer and Becker (1993). These tentative BC dates were adopted for the CALIB 3.0 program. A "bidecadal" record was generated for the 7890–9450 BC interval by taking 20-yr averages of ^{14}C ages reported for shorter-lived samples, with an error multiplier of 1.7 applied to the quoted errors. The CALIB 3.0 tree-ring bidecadal calibration set ends at 11,390 cal yr BP (*ca.* 10,000 ^{14}C yr BP). The corresponding bidecadal $\Delta^{14}C$ profile is given in Figure 2.

Uncertainties and fluctuations in the calibration curve cause the discrete cal ages to broaden into ranges, even for a ^{14}C age with (hypothetical) zero error. The spreads of the cal-yr ranges, obtained from the age calibration of ^{14}C dates between 0 and 10,000 ^{14}C yr BP (bidecadal data set) are given in Figure 3. To generate the graph, the youngest calibrated age of each range

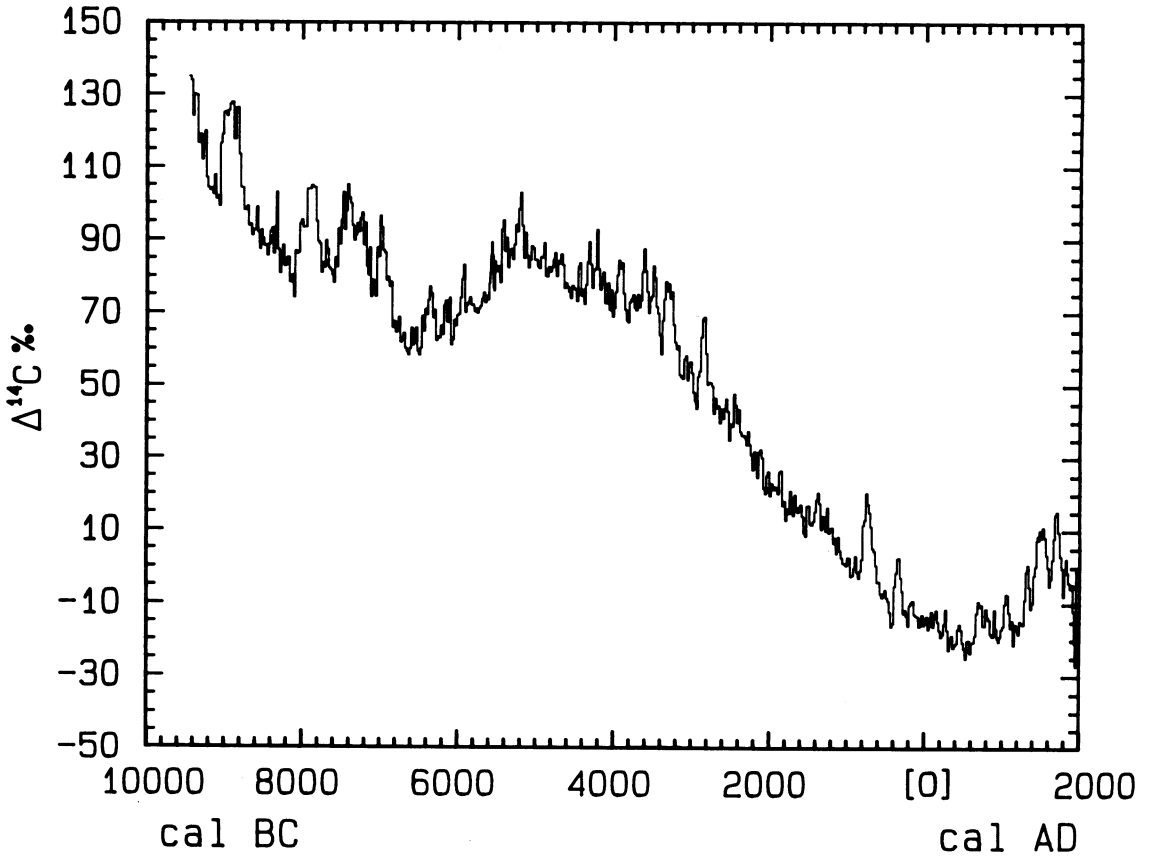

Fig. 2. Bidecadal $\Delta^{14}C$ values (‰) of the CALIB 3.0 data set

of cal ages obtained for each ^{14}C age was set at zero. Each section of the range is represented by a black vertical bar; plotting these vertical bars for each ^{14}C year results in the black shaded areas of Figure 3, which can be used to canvas the ^{14}C ages corresponding to limited cal age ranges. Cal ages will be relatively less precise for ^{14}C dates in the 7500–10,000 ^{14}C yr range, as here the "time warps" (in cal yr) increase in magnitude (Fig. 3).

B. Decadal Data Set (AD 1950–6000 BC; 0–7950 Cal Yr BP)

For users interested in a decade subdivision of time, we have included the decade results of the Seattle laboratory back to 6000 BC (Stuiver & Becker 1993). As discussed above, there is good agreement between the Belfast and Seattle ^{14}C ages for the entire interval, except for 5180–5500 BC, where Seattle ages are, on average, 54 ^{14}C yr younger than Belfast ages. Because the origin of the offset between the laboratories is not known, it is impossible to decide which data set is correct. The decadal cal age calculations of the CALIB 3.0 program do not include offset corrections for the 5180–5500 BC interval, and, therefore, differ from the bidecadal curve by 27 yr.

Fig. 3A–D. The time warps, or ranges, in cal years, obtained from the calibration of ^{14}C ages (for sections covering 0–10,000 ^{14}C BP) when using the CALIB 3.0 bidecadal record. The ranges were produced for an ideal hypothetical case with zero ^{14}C sample standard deviations. The youngest cal age obtained for each ^{14}C age was set at zero. The sample was assumed to have been formed during a 20-yr (or shorter) interval. ——————————→

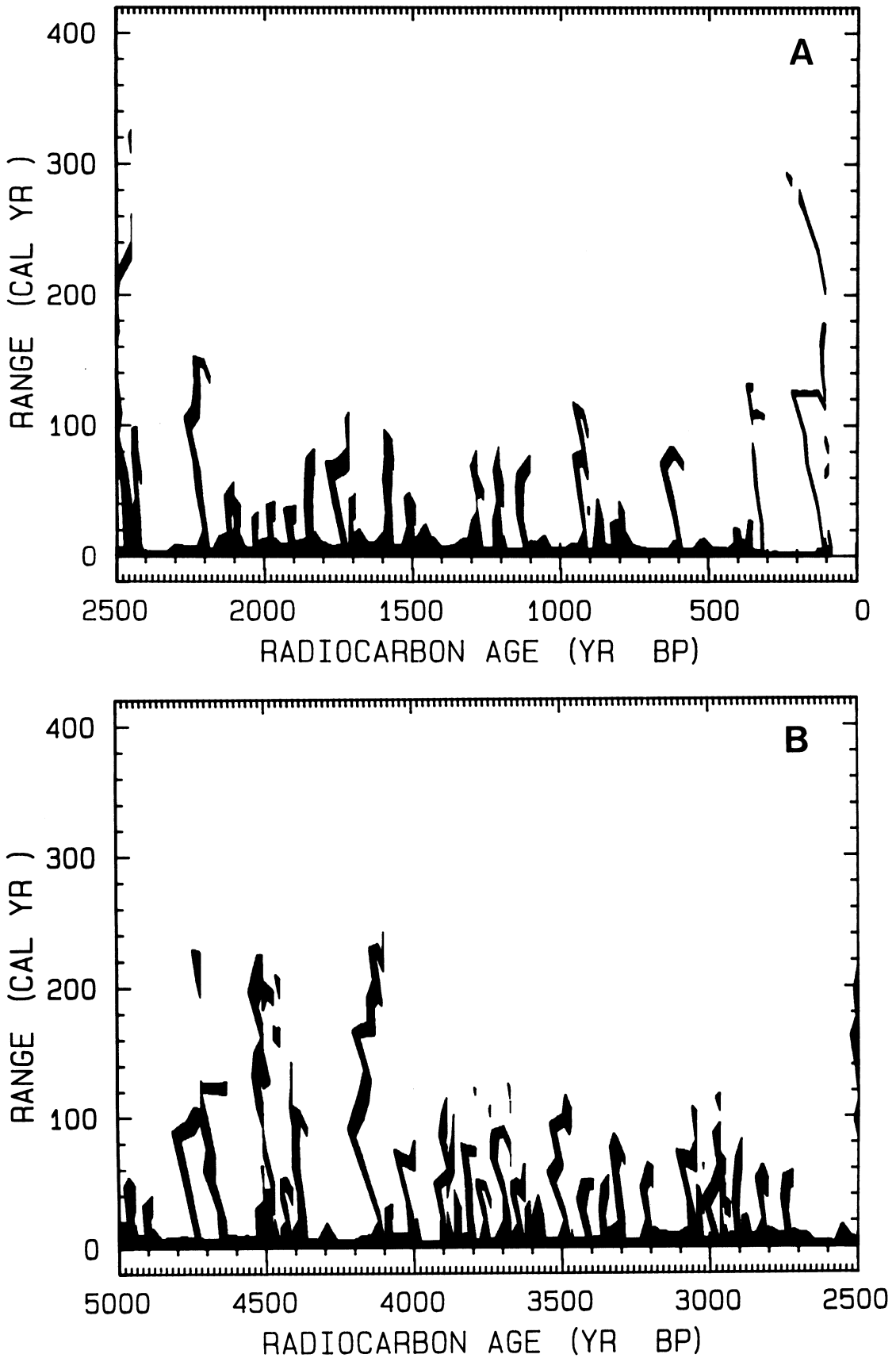
A
400
300
200
100
0
RANGE (CAL YR)
2500
2000
1500
1000
500
0
RADIOCARBON AGE (YR BP)
B
400
300
200
100
0
RANGE (CAL YR)
5000
4500
4000
3500
3000
2500
RADIOCARBON AGE (YR BP)

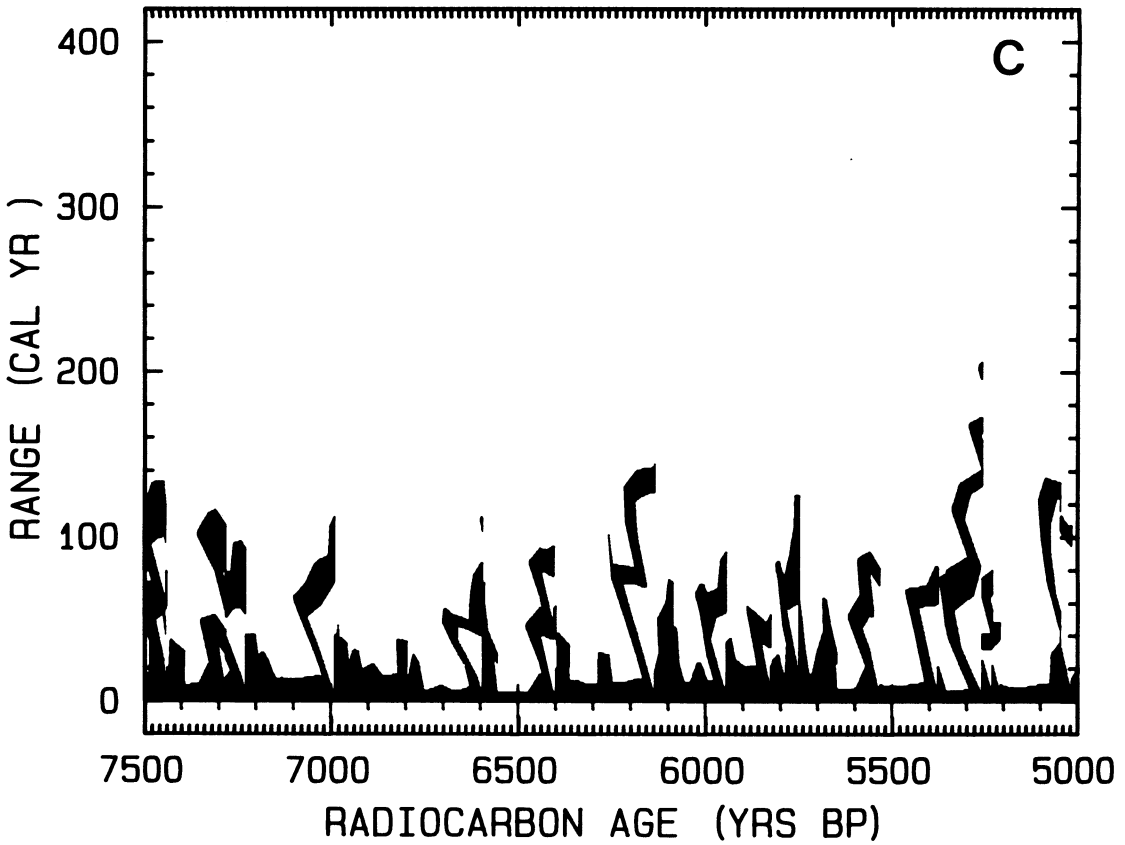
C
400
300
200
100
0
RANGE (CAL YR)
7500
7000
6500
6000
5500
5000
RADIOCARBON AGE (YRS BP)

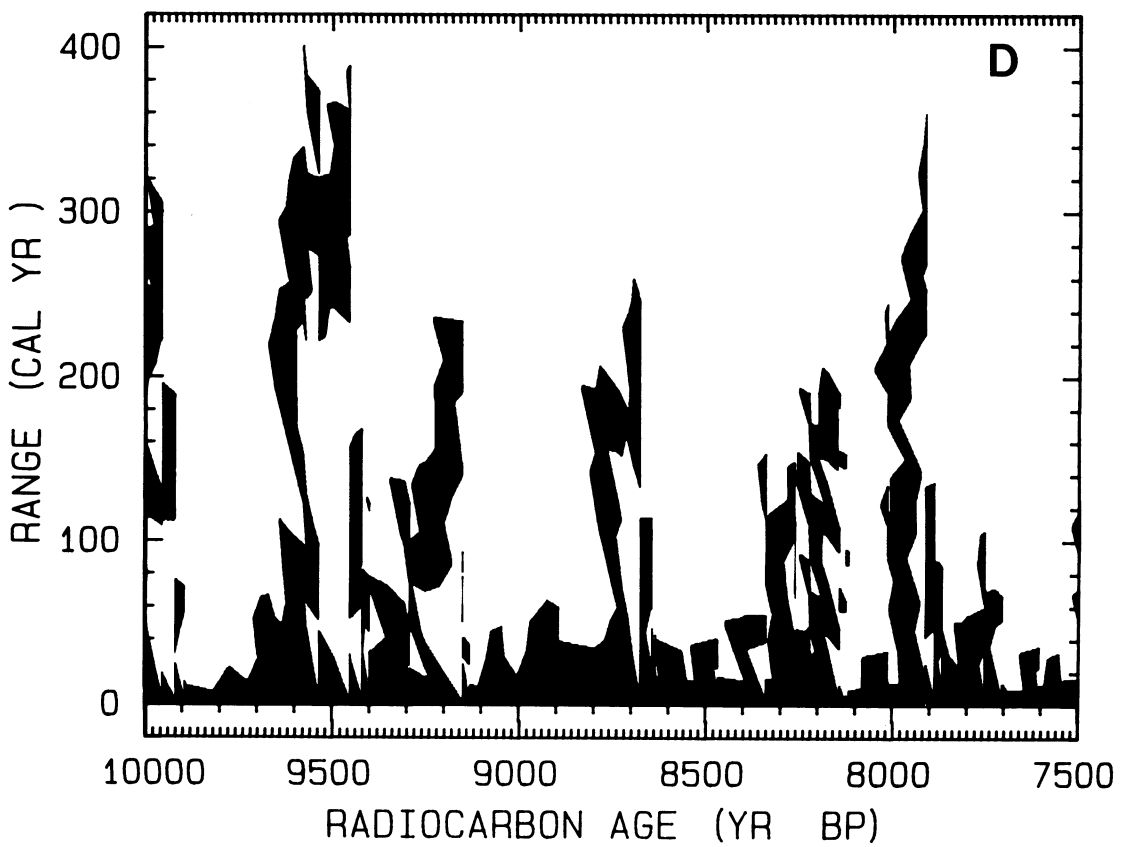
D
400
300
200
100
0
RANGE (CAL YR)
10000
9500
9000
8500
8000
7500
RADIOCARBON AGE (YR BP)

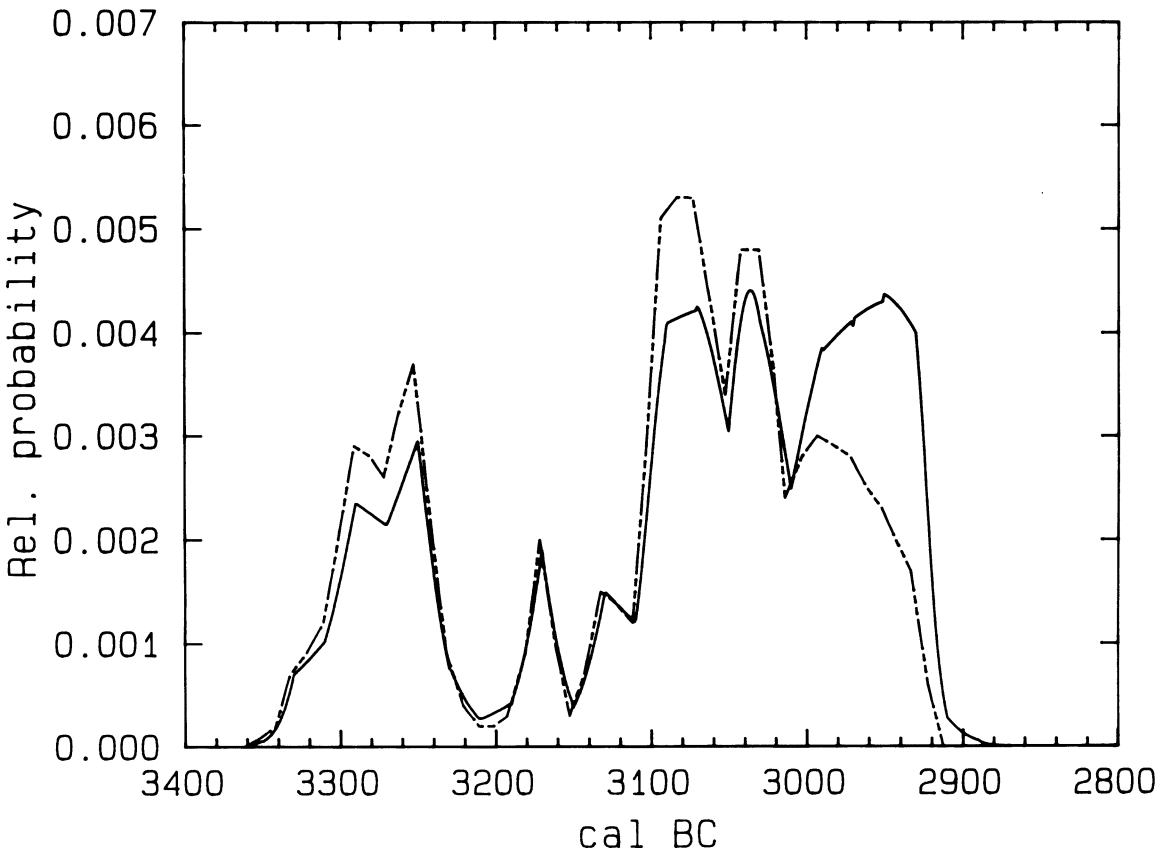

Fig. 4. Alteration of CALIB 3.0 probability diagram (——) when relative position of the sample is taken into account (– –)(Buck *et al.* 1990). Maximum modification is represented by the above example.

C. Marine Bidecadal Data Set (0–11,400 Cal Yr BP)

This calibration for marine samples (Table 1, Stuiver & Braziunas 1993) is based on carbon-reservoir calculations that utilize the bidecadal atmospheric data set as an input. The calculated calibration curve is applicable to the world ocean only, and regional offsets should be accounted for by a ΔR term (see Stuiver & Braziunas 1993). The 1 σ uncertainties assigned to the calculated marine values correspond to the atmospheric bidecadal standard deviations discussed in Section A and below.

D. Atmospheric (Marine) ^{14}C Data for Samples Older Than 10,100 (10,500) ^{14}C Yr BP

U/Th and ^{14}C dating of corals provide ^{14}C age calibration beyond 10,000 ^{14}C yr BP (Bard *et al.* 1993). These data provide measured marine ^{14}C ages. Atmospheric ^{14}C ages are inferred by deducting a 400-yr reservoir age (Bard *et al.* 1993) from the coral ^{14}C ages. Thus, the character of the marine calibration curve changes when moving beyond the Holocene; older samples are calibrated against a curve based on direct measurements, whereas younger samples are calibrated against a model-calculated curve. For atmospheric samples, the situation is the reverse; we use an inferred atmospheric curve for older samples (based on the assumption of a constant 400-yr reservoir age) and a detailed measured calibration curve for the last 11,400 cal yr.

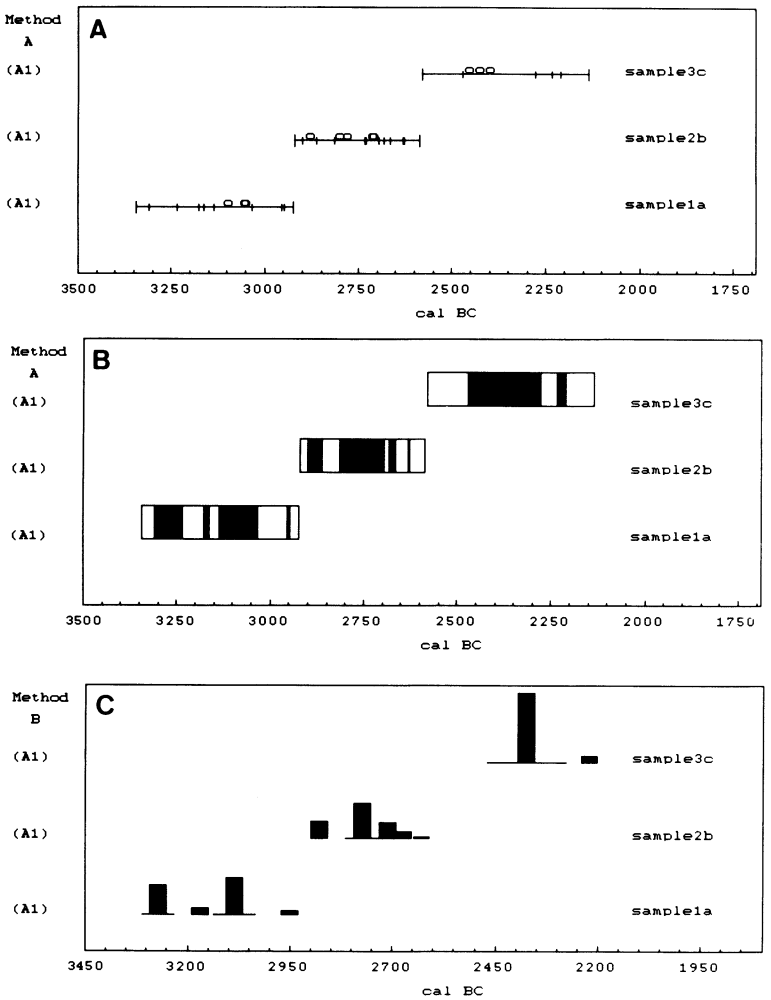

Fig. 5. Calibrated age range plot from CALIB 3.0. The calibration data set used for each sample is indicated in parentheses in the left margin (*e.g.* (A1) = atmospheric Set 1). A. Short, vertical bars indicating the 1 σ ranges, longer vertical bars, the 2 σ ranges, and circles, the calibrated ages. B. Solid blocks representing the 1 σ cal age ranges, and outlined blocks, the 2 σ cal age ranges. C. Cal age ranges represented by horizontal line, and the relative probability, by a column proportional in height to the relative area under the probability curve.

For the CALIB program, the inferred atmospheric data set (11,400–21,950 cal yr BP) is approximated by a smoothing spline (Reinsch 1967) with smoothing parameter = 4. The 1 σ uncertainties assigned to the spline values (one calculated data point for every 50 cal yr) were derived from an interpolation of the reported uncertainties in the ^{14}C ages of the corals. The assigned ^{14}C age errors are an upper limit, as the spline itself is more representative of a moving average. U/Th age errors (about 1/2 the ^{14}C age errors), on the other hand, have not been taken into account. More definite calibration errors, based on the expectation of a much larger future data set, will be assigned in the next CALIB version.

For a smooth connection between the splined curve of inferred atmospheric data and the bidecadal atmospheric data set, we included in the spline derivation a single point (at 11,390 cal BP) of the tree-ring calibration curve. The two marine segments, a pre-11,750 cal yr BP smoothing spline through coral measurements and a post-11,650 cal yr BP model-calculated part, are connected by a short linear interpolation.

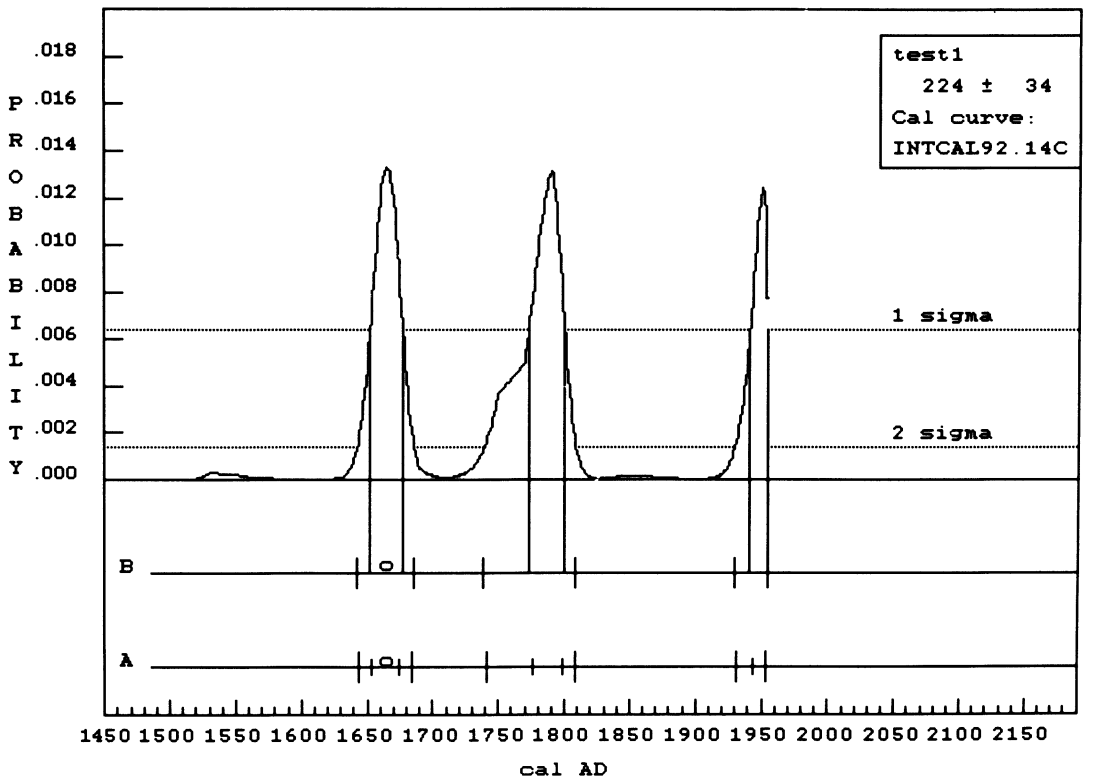

Fig. 6. The probability distribution from CALIB 3.0 for a test sample with Methods A and B cal age ranges marked by vertical lines (see Fig. 5) and cal ages denoted by circles

THE CALIB PROGRAM

CALIB 3.0 runs on any IBM-compatible computer with 640 kb available memory; a hard disk is recommended. The graphics are compatible with VGA, EGA, CGA and HGC (Hercules graphics) cards. To use the program in EGA or VGA mode, MS-DOS 4.0 is required. For older DOS versions, the program will set the mode to CGA or HGC as appropriate. A simplified Macintosh version (requiring >1.5 mb memory) of the IBM program can be obtained from the Quaternary Isotope Laboratory.

The 1993 program (revision 3.0) provides the integrated data (^{14}C age, $\Delta^{14}C$ and standard deviations) for sets 1-3, summarized in Table 1. CALIB 3.0 makes the conversion from a conventional ^{14}C age to calibrated calendar years, and will calculate the probability distribution of the sample's true age. A conventional ^{14}C age implies correction for isotope fractionation through normalization on $\delta^{13}C = -25$ ‰ (Stuiver & Polach 1977). Substantial errors may result if a "radiocarbon date" is not corrected for isotope fractionation. Quite a few commercial "dates" lack $\delta^{13}C$ corrections, and here, the user must estimate $\delta^{13}C$ values based on the type of material. The program will accept an input of either uncorrected "radiocarbon dates", together with an estimated $\delta^{13}C$ value, or conventional ^{14}C ages. Of course, for the latter case, $\delta^{13}C$ should not be entered. Table 1 in Stuiver and Polach (1977) (see also Stuiver & Reimer 1993) illustrates estimated average $\delta^{13}C$ values for various materials.

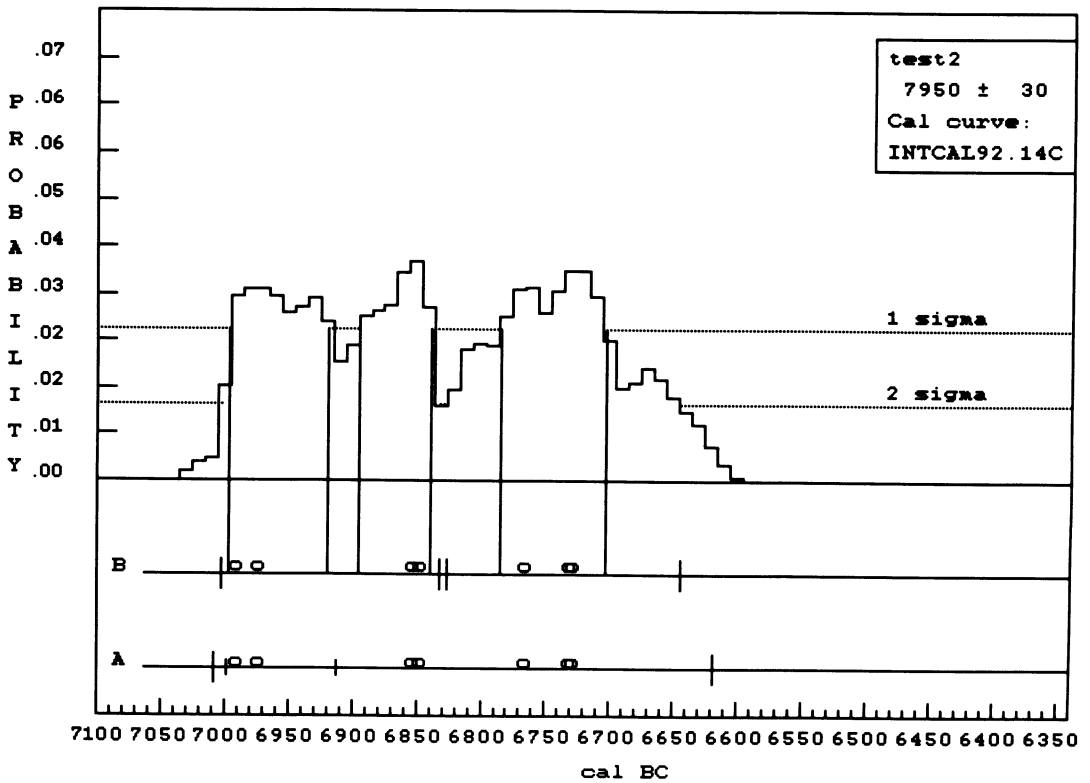

Fig. 7. The probability distribution from CALIB 3.0 for a test sample plotted as a histogram with Methods A and B cal age ranges marked by vertical lines (see Fig. 5) and cal ages represented by circles

An enlargement of the ^{14}C age error will accompany a $\delta^{13}C$ estimate, due to the spread of $\delta^{13}C$ values in nature. The $\delta^{13}C$ uncertainty may differ somewhat for various sample types (Stuiver & Polach 1977). The program assigns, as a first-order approximation, a 2.5 ‰ error to the estimated $\delta^{13}C$ value. This enlarges the reported standard deviation (σ) of the ^{14}C age determination to $(\sigma^2 + 40^2)^{½}$. The fixed 2.5 ‰ $\delta^{13}C$ error can be avoided by entering an estimated $\delta^{13}C$. Of course, those using the conventional ^{14}C age option should avoid the $\delta^{13}C$ error estimate. In this case, only conventional ^{14}C age and error should be entered.

CALIB's Method A yields calibrated ages (intercepts) and age ranges; Method B generates a cal age probability distribution compatible with the ^{14}C age and its Gaussian age distribution (formulation as given in Stuiver & Reimer 1989). In the 1987 version 2.1, the average curve σ of the cal age intercepts was used to calculate the total σ for the range calculations; the 1993 revision 3.0 (Stuiver & Reimer 1993) uses more detailed curve σs found over the full range.

In the 1993 revision, the user can increase the reported standard deviation, σ, by either applying a lab error multiplier, K, or adding variance, f^2 (year^2). The latter approach may be more desirable to some users, as adding sources of variance conforms with standard statistical methods. The sample standard deviation σ increases to either $K\sigma$, or $(\sigma^2 + f^2)$. The curve sigma, σ_c, is added in both cases, so that the total σ of the ^{14}C age prior to its cal age transformation can be either $((K\sigma)^2 + \sigma_c^2)^{½}$ or $(\sigma^2 + \sigma_c^2 + f^2)^{½}$. K values should be available from the laboratory that provides the ^{14}C

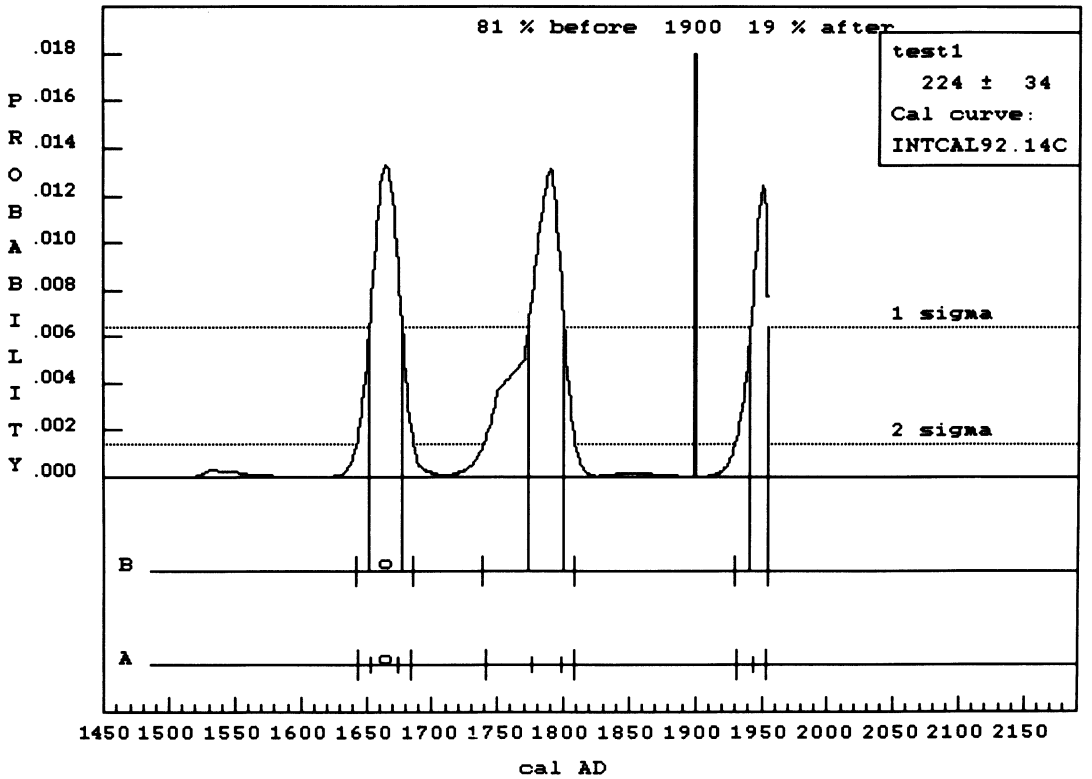

Fig. 8. The probability distribution from CALIB 3.0 for a test sample with a calendar/time marker. The relative area under the probability distribution above and below the marker is labeled.

age determination. A value for f suggested by Clark (1975) for routine ^{14}C dating is 50 yr for samples less than 2700 BP, or 60 yr for samples older than 2700 BP.

CALIB 3.0 allows a series of ^{14}C ages to be checked for consistency through a χ^2 test (Ward & Wilson 1978). If the ^{14}C age differences are judged as insignificant, and if geological, archaeological or other evidence corroborates sample contemporaneity, a pooled ^{14}C age (weighted average) can be used for the age calibration.

When the χ^2 test disproves contemporaneity, the individual probability distributions derived for the sample ages may be summed, if desired. All dates are considered equal, in that the user assumes no *a priori* knowledge of the relative position of the samples. Additional information on sample stratigraphy modifies the summed probability distribution of the group samples to some extent. CALIB does not give information on such modification, but a specific case was discussed by Buck *et al.* (1990), where a series of samples was subdivided into four groups in chronological order. Figure 4 compares the Buck *et al.* (1990) calculated posterior probability with the CALIB probability summation for the sample group experiencing maximum modification of the CALIB distribution. Additional information on estimating the duration of archaeological phenomena is available in Aitchison *et al.* (1991).

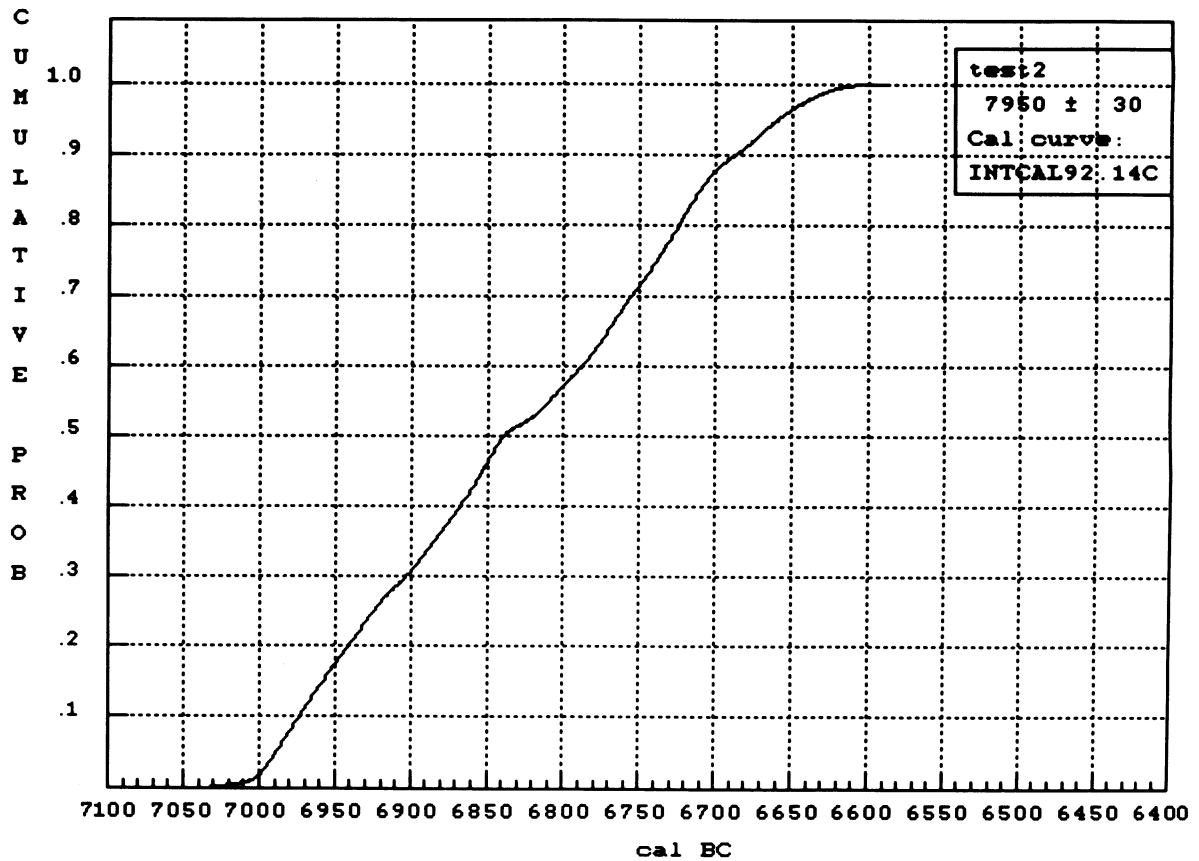

Fig. 9. The cumulative probability plot for a test sample from CALIB 3.0

In the 1987 revision, we did not calculate the ^{14}C ages of any Gaussian distribution (representing the sample σ) falling outside the range of the calibration curve. For the 1993 version, the end of the calibration curve is either extended by a straight-line interpolation between coral data (Sets 1 and 3) or a straight-line estimate (1 ^{14}C yr = 1 cal yr, Set 2). The cal ages exceeding the curve limit are reported as older than the curve limit. The cal age ranges and the probability distribution associated with estimated (beyond the curve limit) cal years are shown as dashed lines in the plots. Plots are displayed in graphics mode, rather than character mode, as in the old version. Three types of plots are available: calibrated age ranges, probability distributions and the calibration curves. The plots may be printed to an IBM-compatible graphics printer or an HP-series printer; for HP, the HPSCREEN driver is required for MS-DOS versions prior to DOS 5.0.

Cal ages and their ranges can be displayed graphically (Figs. 5A and 5B), as can probabilities derived from the age conversion (Figs. 5C–9). Calibrated age ranges may be plotted as: 1) horizontal lines on which circles depict the cal ages, and vertical bars depict the magnitude of 1 (short bars) and/or 2 σ (longer bars) ranges (Fig. 5A); 2) as solid blocks for 1 σ ranges and outlined blocks for 2 σ ranges (Fig. 5B), or 3) as horizontal lines with the relative area under the probability curve for each range, as described in the Fig. 5C legend. The number of samples per plot is set by the user, and samples may be ordered by ^{14}C age.

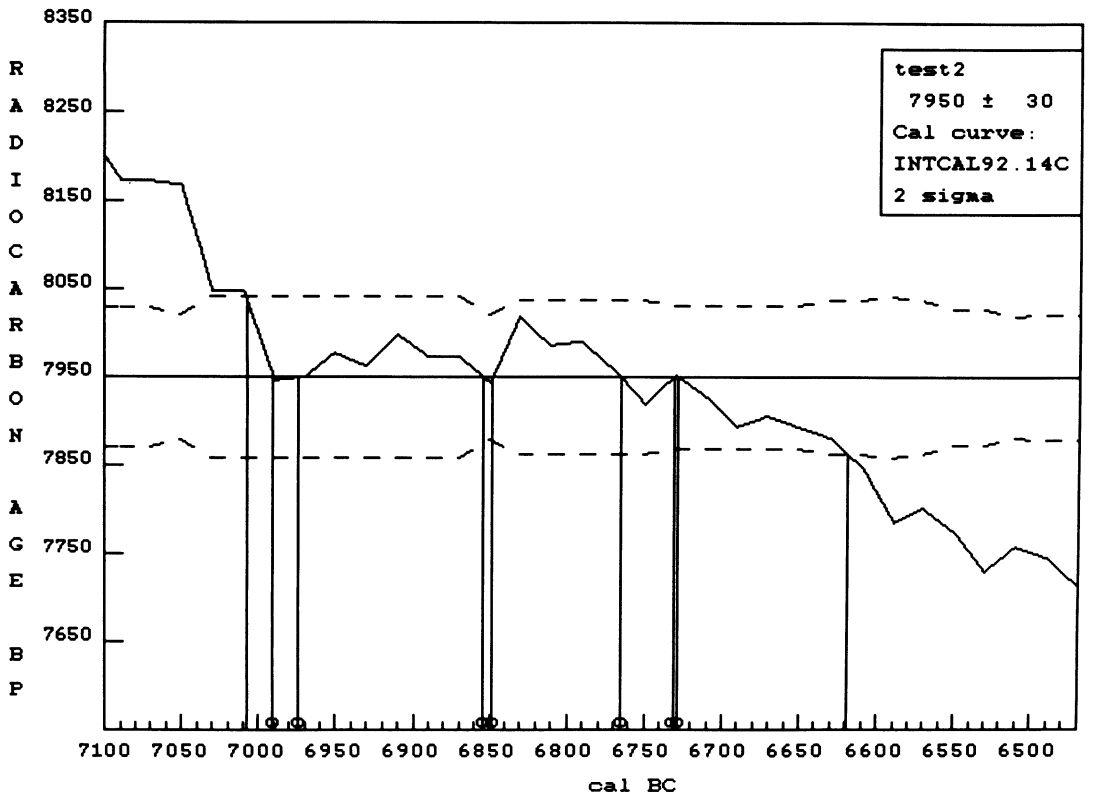

Fig. 10. Bidecadal ^{14}C age BP *vs.* calendar year in the cal age range of the sample. The intersections of the ^{14}C age and ^{14}C age ± total σ (– –) with the calibration curve are marked with vertical lines drawn to the cal yr axis. The calibrated ages are marked with circles.

CALIB 3.0 allows normalization of the probability distributions (Fig. 6), so that total area or the maximum = 1 for the plot. The distribution may be plotted as a histogram (Fig. 7) or a smooth line. The plot may include the Method A and/or Method B cal age ranges. A stratigraphic/calendar marker may be drawn, with the relative area under the probability distribution above and below the marker labeled (Fig. 8). Plotting the cumulative probability (Fig. 9) is another option.

Another CALIB 3.0 feature focuses on the calibration curve, which may be plotted as ^{14}C age BP *vs.* calendar year (Fig. 10), with or without the age ranges for a selected sample, or as $\Delta^{14}C$ ‰ *vs.* calendar year (*e.g.*, Fig. 2). In Figure 10, vertical distance between the dashed lines (representing ^{14}C age ± total σ) varies with cal age, as the σ associated with the calibration curve is not constant.

For additional information, the reader is referred to the CALIB User's Guide (Stuiver & Reimer 1993).

REFERENCES

Aitchison, T., Ottaway, B. and Al-Ruzaiza, A. S. 1991 Summarizing a group of ^{14}C dates on the historical time scale: With a worked example from the Late Neolithic of Bavaria. *Antiquity* 65(246): 108–116.

Bard, E., Arnold, M., Fairbanks, R. G. and Hamelin, B. 1993 ^{230}Th-^{234}U and ^{14}C ages obtained by mass spectrometry on corals. *Radiocarbon*, this issue.

Becker, B. 1993 An 11,000-year German oak and pine dendrochronology for radiocarbon calibration. *Radiocarbon*, this issue.

Becker, B., Kromer, B. and Trimborn P. 1991 A stable isotope tree-ring timescale of the Late Glacial/Holocene boundary. *Nature* 353: 647–649.

Buck, C. E., Kenworthy, J. B., Litton, C. D. and Smith A. F. M. 1990 *Combining Archaeological and Radiocarbon Information: The Betting Man's Guide to Skara Brae*. Nottingham Statistics Group, Department of Mathematics, University of Nottingham, England: 20 p.

Clark, R. M. 1975 A calibration curve for radiocarbon dates. *Antiquity* 49: 251–266.

Kromer, B. and Becker, B. 1993 German oak and pine ^{14}C calibration, 7200–9400 BC. *Radiocarbon*, this issue.

Kromer, B., Rhein, M., Bruns, M., Schoch-Fischer, H., Münnich, K. O., Stuiver, M. and Becker, B. 1986 Radiocarbon calibration data for the 6th to the 8th Millennia BC. *In* Stuiver, M. and Kra, R. S., eds., Proceedings of the 12th International ^{14}C Conference. *Radiocarbon* 28(2B): 954–960.

Linick, T. W., Long, A., Damon, P. E. and Ferguson, C. W. 1986 High-precision radiocarbon dating of bristlecone pine from 6554 to 5350 BC. *In* Stuiver, M. and Kra, R. S., eds., Proceedings of the 12th International ^{14}C Conference. *Radiocarbon* 28(2B): 943–953.

Linick, T. W., Suess, H. E. and Becker, B. 1985 La Jolla measurements of radiocarbon in South German oak tree-ring chronologies. *Radiocarbon* 27(1): 20–32.

Pearson, G. W., Becker, B. and Qua, F. 1993 High-precision ^{14}C measurement of German and Irish oaks to show the natural ^{14}C variations from 7890 to 5000 BC. *Radiocarbon*, this issue.

Pearson, G. W. and Stuiver, M. 1986 High-precision calibration of the radiocarbon time scale, 500–2500 BC. *In* Stuiver, M. and Kra, R. S., eds., Proceedings of the 12th International ^{14}C Conference. *Radiocarbon* 28(2B): 839–862.

_____1993 High-precision bidecadal calibration of the radiocarbon time scale, 500–2500 BC. *Radiocarbon*, this issue.

Reinsch, C. H. 1967 Smoothing by spline functions. *Numerische Mathematik* 10: 177–183.

Stuiver, M. 1982 A high-precision calibration of the AD radiocarbon time scale. *Radiocarbon* 24(1): 1–26.

Stuiver, M. and Becker, B. 1993 High-precision decadal calibration of the radiocarbon time scale, AD 1950–6000 BC. *Radiocarbon*, this issue.

Stuiver, M. and Braziunas, T. F. 1993 Modeling atmospheric ^{14}C influences and radiocarbon ages of marine samples back to 10,000 BC. *Radiocarbon*, this issue.

Stuiver, M., Braziunas, T. F., Becker, B. and Kromer, B. 1991 Climatic, solar, oceanic and geomagnetic influences on Late-Glacial and Holocene atmospheric $^{14}C/^{12}C$ change. *Quaternary Research* 35: 1–24.

Stuiver, M., Kromer B., Becker B. and Ferguson, C. W. 1986 Radiocarbon age calibration back to 13,300 years BP and the ^{14}C age matching of the German oak and US bristlecone pine chronologies. *In* Stuiver, M. and Kra, R. S., eds., Proceedings of the 12th International ^{14}C Conference. *Radiocarbon* 28(2B): 969–979.

Stuiver, M. and Pearson, G. W. 1986 High-precision calibration of the radiocarbon time scale, AD 1950–500 BC. *In* Stuiver, M. and Kra, R. S., eds., Proceedings of the 12th International ^{14}C Conference. *Radiocarbon* 28(2B): 805–838.

_____1992 Calibration of the radiocarbon time scale 2500-5000 BC. In Taylor, R. E., Long, A. and Kra, R. S., eds., *Radiocarbon After Four Decades: An Interdisciplinary Perspective*. New York, Springer Verlag: 19–33.

_____1993 High-precision calibration of the radiocarbon time scale, AD 1950–500 BC and 2500–6000 BC. *Radiocarbon*, this issue.

Stuiver, M. and Polach, H. A. 1977 Discussion: Reporting of ^{14}C data. *Radiocarbon* 19(3): 355–363.

Stuiver, M. and Reimer, P. J. 1986 A computer program for radiocarbon age calibration. *In* Stuiver, M. and Kra, R. S., eds., Proceedings of the 12th International ^{14}C Conference. *Radiocarbon* 28(2B): 1022–1030.

_____1989 Histograms obtained from computerized radiocarbon age calibration. *In* Long, A. and Kra, R. S., eds., Proceedings of the 13th International ^{14}C Conference. *Radiocarbon* 31(3): 817–823.

_____1993 CALIB User's Guide Rev. 3.0. University of Washington, Quaternary Isotope Laboratory.

Ward, G. K. and Wilson S. R. 1978 Procedures for comparing and combining radiocarbon age determinations: A critique. *Archaeometry* 20(1): 19–34.

[RADIOCARBON, VOL. 35, NO. 1, 1993, P. 231–237]

THE GRONINGEN RADIOCARBON CALIBRATION PROGRAM

JOHANNES VAN DER PLICHT

Centre for Isotope Research, University of Groningen, Nijenborgh 4, 9747 AG Groningen, The Netherlands

INTRODUCTION

Variations in atmospheric ^{14}C content complicate the conversion of conventional ^{14}C ages BP (*i.e.*, years before AD 1950) into real calendar ages (AD/BC) (de Vries 1958; Willis, Tauber & Münnich 1960). These variations are indirectly observed in tree rings from European and North American wood. In recent decades, measurements made on dendrochronologically dated wood have resulted in the generally accepted Stuiver and Pearson calibration curves. These curves, together with other calibration data, were published in the first Radiocarbon Calibration Issue (Stuiver & Kra 1986), and are extended in the present Calibration Issue (Stuiver, Long & Kra 1993).

Irregularities in the calibration curve complicate the conversion of a BP ^{14}C age to a real calendar age (cal AD/BC). For example, the ^{14}C age can correspond to more than one real calendar date due to medium-term variations, or "wiggles" (Suess 1970). Consequently, transformation of the Gaussian probability distribution representing the measured ^{14}C age (BP $\pm \sigma$) is not straightforward. The real calendar age probability distribution is no longer Gaussian, unless the calibration curve happens to be a straight line in the time period considered (*i.e.*, there is a linear relationship between cal AD/BC and BP). The calibrated age, then, cannot generally be stated as the most probable result, with an associated error bar.

Recently, several computer programs have been developed to calibrate ^{14}C dates. The most widely distributed programs are those from Seattle (Stuiver & Reimer 1986) and Groningen (van der Plicht & Mook 1987, 1989). The existing programs were compared at the 13th International Radiocarbon Conference in Dubrovnik (Aitchison *et al.* 1989). This comparison was necessary because of the different coding procedures used, mathematical complications caused by calibration curve wiggles, and different interpretations and/or presentations of results. The Groningen program is set up graphically; calibrated age ranges, based on confidence levels used in the Seattle program, have been incorporated, as agreed at the Conference.

The present upgraded version of the program, CAL15, is menu-driven. Previously distributed versions were CAL4 (van der Plicht & Mook 1989) and CAL10. Knowledge of the programming language is not necessary to perform certain options. New features, such as wiggle matching, spline and smoothing (moving average) calculations are incorporated in the program. The mathematical justification for the calibration procedure used is described by Dehling and van der Plicht (1993).

DESCRIPTION OF THE PROGRAM

The present version of the program is written in Turbo Pascal, version 5.0 (Borland 1989). All options and subroutines are accessible through the main menu (Fig. 1). The program runs on XT/AT or compatible computers with either CGA, Hercules, EGA or VGA graphics screens. The graphs can be sent to a color plotter (HP-compatible), laser printer (HP-compatible) or regular printer (Epson-compatible). The graph can also be stored on disk. The latter two options work only from screens in monochrome mode.

```
C.I.O. Groningen Radiocarbon Calibration Program          version july 1992
F1      : interactive calibration      ctr F1 :  change cal. datafile
          (screen)                     alt F1 :  change spline datafile
F2      : interactive calibration      ctr F2 :  change smoothed datafile
          (plotter)                    alt F2 :  read plot from file
F3      : automatic (printer)          ctr F3 :  DOS commands
shf F3  : edit inputdata (F3)          alt F3 :  total restart program
F4      : add calibrations             ctr F4 :  change date/time
shf F4  : edit inputdata (F4)          alt F4 :  options/settings menu
F5      : wiggle matching (hand)       ctr F5 :  calibration data (screen)
shf F5  : edit inputdata (F5)          alt F5 :  calibration data (plotter)
F6      : wiggle matching (auto)       ctr F6 :  spline data (screen)
shf F6  : edit inputdata (F6)          alt F6 :  spline data (plotter)
F7      : spline calculations          ctr F7 :  smoothed data (screen)
                                       alt F7 :  smoothed data (plotter)
F8      : smoothing calculations       ctr F8 :  delta C-14 (screen)
shf F8  : calibration (smoothed)       alt F8 :  delta C-14 (plotter)
F9      : histograms                   ctr F9 :  recent data(>1950) (scr)
shf F9  : edit inputdata (F9)          alt F9 :  recent data(>1950) (plt)
F10     : artificial curves            ctr F10:  calibr data range plot
ESC,Alt_X : exit   alt_H : help/info   date :  9  9 1992  time : 17  7 49
```

Fig. 1. The main menu of the Groningen Radiocarbon Calibration Program, CAL15

Most users will use just the interactive calibration option. One need make only three entries: the ^{14}C age to be calibrated (in BP), its error (σ BP) and an identification label (user-chosen text, such as, *e.g.*, the GrN-number). The calibration procedure will start automatically, resulting in (usually) three graphs and analyzed output. The program uses default options, such as autoscaling the plots, the (recommended) calibration data from Stuiver and Pearson (1986) and the cubic spline function as calibration curve. Program functions are described below.

The Calibration Procedure

The ^{14}C age is the result of a statistical physical measurement, approaching a Gaussian probability distribution with the form

$$\exp\left[-(y-\mathrm{BP})^2/2\sigma_{\mathrm{BP}}^2\right] \quad . \tag{1}$$

The probability distribution along the x-axis (the calendar axis) is not Gaussian; instead, it has the form

$$\exp\left[-(f(x)-\mathrm{BP})^2/2\sigma_{\mathrm{BP}}^2\right] \quad . \tag{2}$$

Here, BP is the ^{14}C age, σ_{BP} its error (standard deviation) and $y = f(x)$ the calibration function.

The computer program selects that part of the calibration curve corresponding to the ^{14}C age, BP $\pm$ 3 σ_{BP}. In the corresponding area along the calendar axis, the function as defined above is calculated. The integration step size (dx) is usually taken as 4 yr (corresponding to 5 steps for the 20-yr intervals in the Stuiver and Pearson data set). In addition, the cumulative distribution:

$$P(x) = \int_{-\infty}^{x} \exp\left[-(f(x) - \mathrm{BP})^2/2\sigma_{\mathrm{BP}}^2\right]dx \qquad (3)$$

is calculated, which is normalized by integrating to $x = \infty$. The calibration function, $y = f(x)$, is determined from the dendrochronologically measured calibration data points. The Groningen program uses a spline function or a smoothed curve calculated through these data points.

Spline Function Calculation

The spline function is calculated according to the procedure of Reinsch (1967). With this procedure, a smooth spline is calculated along a set of data points. The calculation is performed iteratively, such that

$$\sum_i \left[(y(x_i) - y_i)/\sigma(y_i)\right]^2 \leq S \qquad (4)$$

where S is the "smoothing parameter". As discussed by Reinsch (1967), recommended values for S depend on the magnitude of the standard deviations, $\sigma(y_i)$. We have chosen $S = 0$ (no smoothing), where the routine produces the natural cubic spline, *i.e.*, it interpolates the data points. This also means that the error in the calibration data points is not taken into account.

The calculation results in four matrices, a_i, b_i, c_i and d_i, which define the function

$$f(x) = \left[(d_i \cdot h + c_i) \cdot h + b_i\right] \cdot h + a_i \qquad (5)$$

where $h = x - x_i$, and $x_i \leq x \leq x_{i+1}$ are the calibration points. The matrices, a_i, b_i, c_i and d_i (for each calibration data set, and corresponding to the chosen smoothing parameter, S), are stored in a file, and called by the program CAL15. Once the spline function, $y = f(x)$, is calculated, the actual calibration can be performed, *i.e*, the transformation of the ^{14}C age (BP, y-axis) into the real calendar age (cal AD/BC, x-axis) *via* the function, $y = f(x)$, using the formula described above.

Smoothed Calibration Curve

A smoothed calibration curve can be drawn through the calibration data points in various ways. First, the spline function can be calculated using a non-zero value for the smoothing parameter, S (Reinsch 1967). The program also includes alternatively a code that calculates a smoothed curve through the data points with a Gaussian moving average. The curve may consist of several parts separated by a "breakpoint"; outliers may be rejected. The sigma (band width) of the Gaussian moving average is an input parameter, usually taken as three times the average distance between the data points.

Output

As stated, the user can easily perform "standard" calibrations by entering the ^{14}C age and its standard deviation BP. The program uses the Stuiver and Pearson (1986) data points as default calibration data, and a spline function with no smoothing (thus going through the data points) as default calibration function. The standard deviation of the calibration curve is ignored. Three graphs are produced by the program. The first graph shows the selected part of the calibration curve with

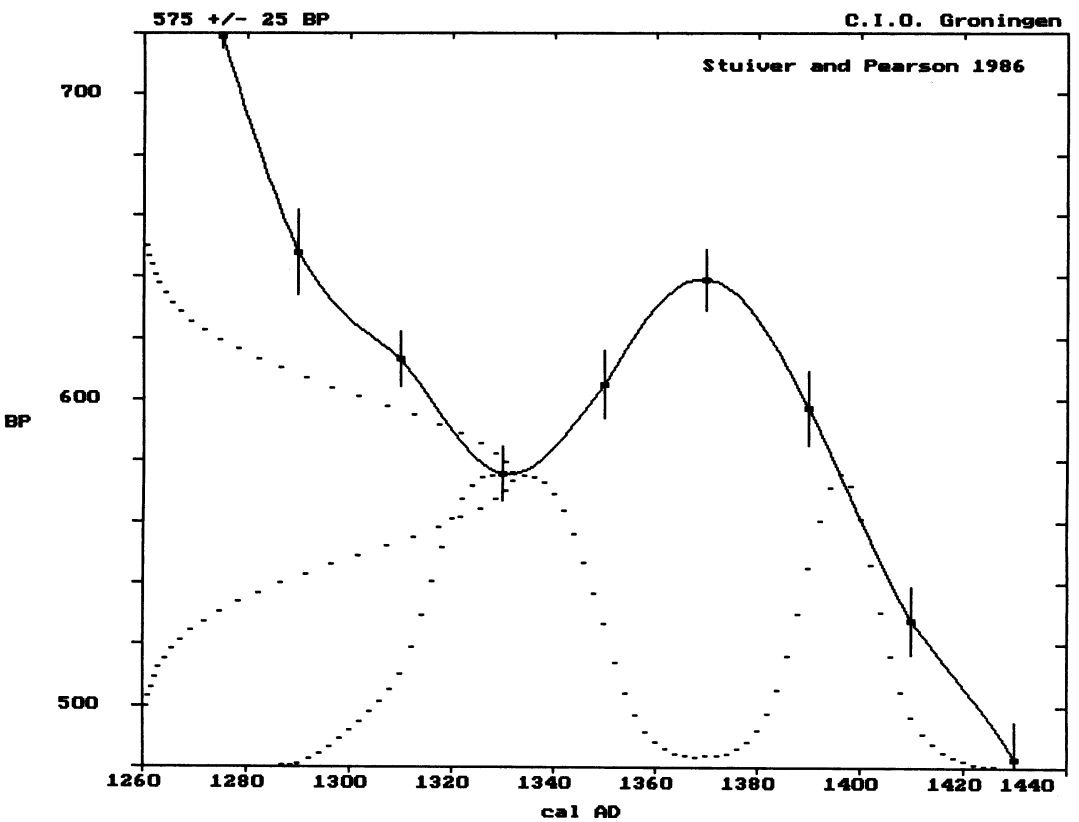

Fig. 2. Calibration of a ^{14}C age, 575 ± 25 BP

the calibration data points, the Gaussian probability distribution of the ^{14}C age along the y-axis, and the resulting calendar age probability distribution along the calendar axis. An example, calibrating 575 ± 25 BP, is shown in Figure 2. Due to a "wiggle", the calibrated distribution has two peaks, centered around 1330 and 1395 cal AD.

The second graph (Fig. 3) shows the cumulative probability, $P(x)$, as defined above. This plot corresponds to an earlier version of the program (van der Plicht, Mook & Hasper 1990). In the example shown here, one may say that the peak around cal AD 1330 has a probability of 65%, and the one around 1395 cal AD, 35%. The cumulative probability, $P(x)$, may be used to determine, *e.g.*, the median, corresponding to $P(x) = 0.5$. The use of "median" and "modus" (= the maximum of the calibrated distribution), however, is not recommended; see the discussion in van der Plicht and Mook (1989).

The third graph (Fig. 4) shows the calibrated calendar age probability distribution with lines indicating the 1 σ (68.3%) and 2 σ (95.4%) confidence intervals. The intercepts indicated by the vertical lines can be taken as calibrated ranges. In this example, the calibrated age ranges correspond to cal AD 1316-1348 and 1390-1402 (1 σ) and cal AD 1300-1358 and 1380-1412 (2 σ).

CAL15 produces output in terms of these calibrated age ranges (1 σ and 2 σ). The graphs can be printed, plotted or saved to disk.

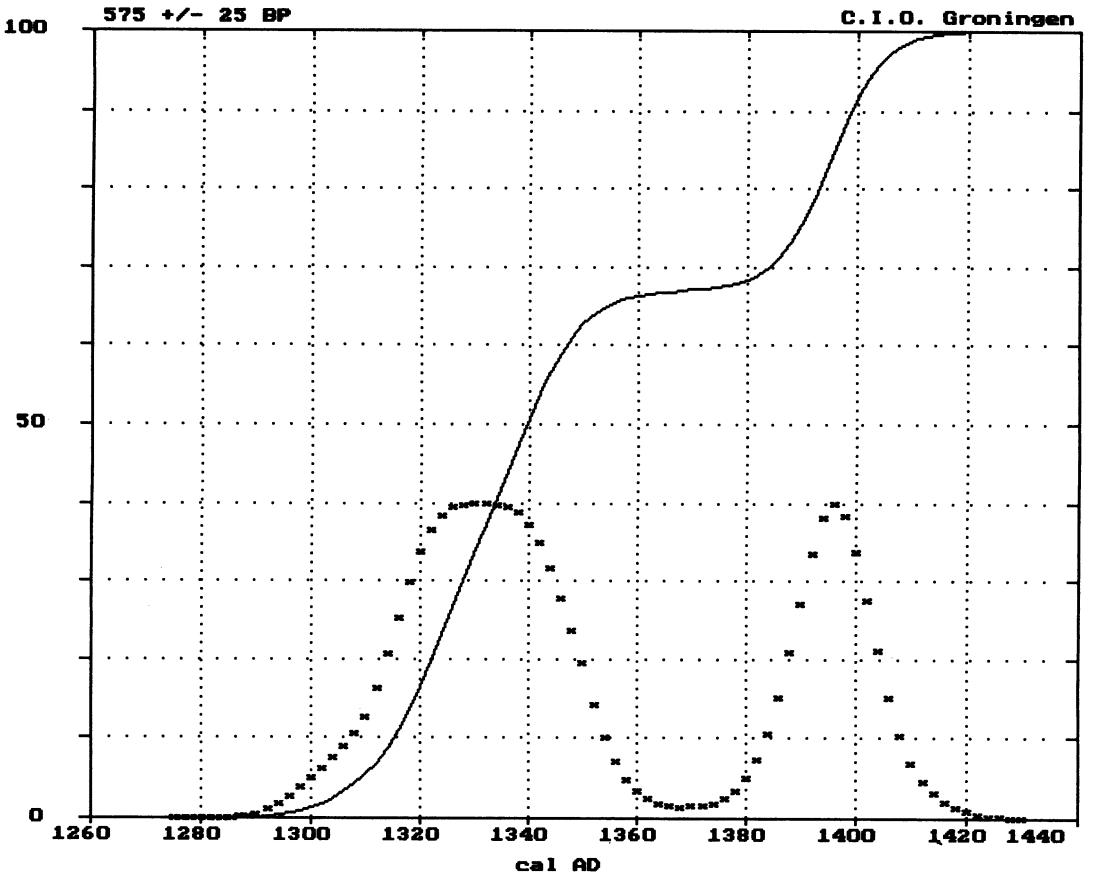

Fig. 3. Cumulative probability distribution for calibrating 575 ± 25 BP

SPECIAL OPTIONS

Calibration of Multiple Dates

A series of ^{14}C dates can be analyzed by the program in several ways, depending on their relation. First, non-related dates read from an input file can be calibrated automatically, without user interaction. The calibrated date ranges (1 σ) can be plotted on an additional graph for this option. Second, the calibrated probability distributions for a series of related dates can be summed together. The results for the individual calibrations are normalized so that the area, $\int(x)dx = 1$. Of the total summed function, $y_{tot}(x)$, the probability distribution is calculated, and analyzed for 1 σ or 2 σ calibrated age ranges as discussed above.

Non-Dendrochronological Calibration Data

Not all calibration data are obtained from dendrochronologically-dated wood. For instance, Stuiver *et al.* (1991) constructed a calibration data set to 30,000 BP, using high-precision U/Th dates from corals and comparing these data with ^{14}C results. From this data set, CAL15 can construct a calibration curve by calculating a smoothed curve through the data points.

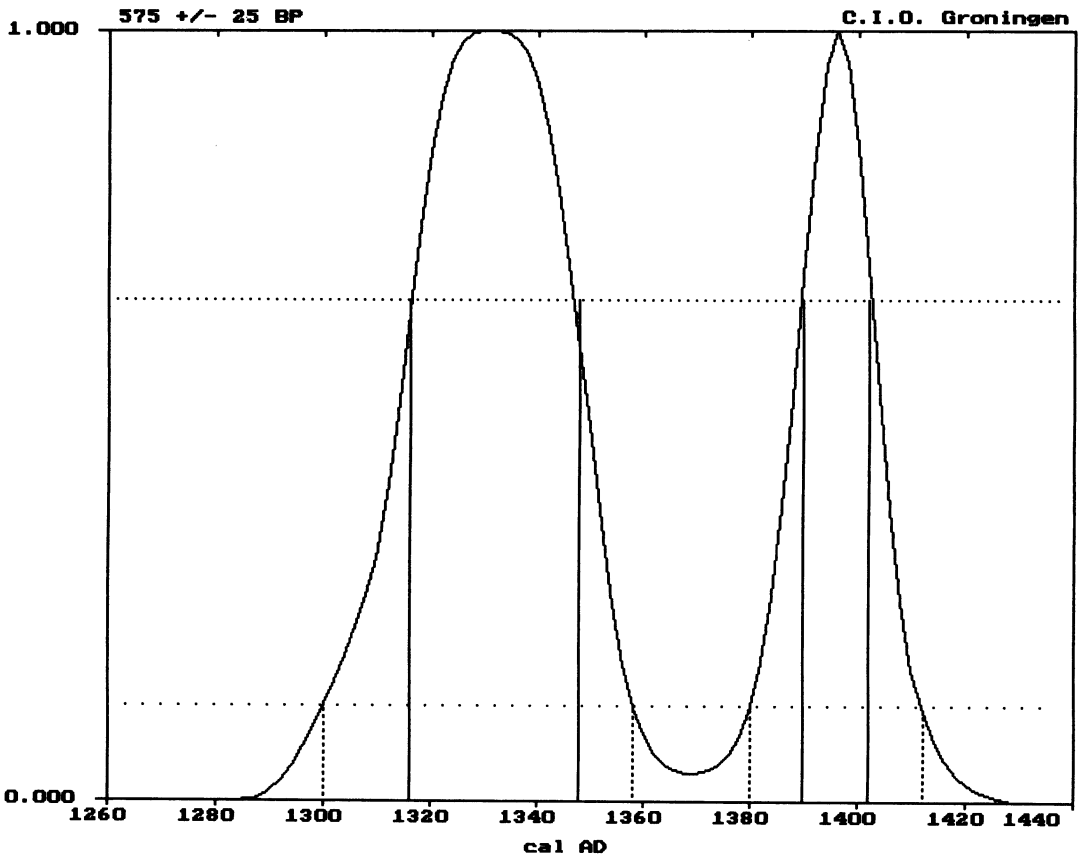

Fig. 4. Calendar axis probability distribution for 575 ± 25 BP, with levels corresponding to 1σ and 2σ confidence

Wiggle Matching

CAL15 has two wiggle matching modes: tree-ring wiggle matching (*i.e.*, data that are fixed along the calendar axis), and wiggle matching for data that are not necessarily fixed along the calendar axis. The latter can be applied where there is variable growth (van Geel & Mook 1989). In the present version of the program, wiggle matching can only be estimated, *i.e.*, the best "fit" of the data to the relevant part of the calibration curve is determined visually; either a mouse or arrow keys can be used. An automatic wiggle-matching procedure will be included in the next release of the program. Wiggle-matching calculations are complex, especially for peat layers with variable growth rates.

Summary and Conclusion

We developed a PC-based computer program, CAL15, for automatic calibration of ^{14}C ages, written in Turbo Pascal (version 5.0). The program uses a spline function generated through the calibration data points, as published in the Radiocarbon Calibration Issues (Stuiver & Kra 1986; Stuiver, Long and Kra 1993). The Gaussian probability distribution of the ^{14}C age is taken at the 3 σ level. The program automatically selects part of the calibration curve and calculates the calibrated probability distribution along the calendar axis; one only enters the date to be calibrated (in BP), the associated

error (σ BP) and a text label, either interactively or through an input file.

The calibrated results are produced mainly in graphical form. The calibrated dates are presented as 1 σ (68.3%) or 2 σ (95.4%) confidence levels. As a default, the recommended calibration data set from Stuiver and Pearson (1986) is used. The default calibration curve is an unsmoothed cubic spline function (Reinsch, 1967) through the calibration data points. Some smoothing, however, may be more realistic, for instance, when the time width of the sample is taken into account (Mook 1983). In CAL15, the user can easily calculate a spline function; the smoothing parameter, S, is entered. The results of the calculation (*i.e.*, the matrices $a_i...d_i$) are stored in a data file, which can be loaded into the main program to perform the calibration with the newly calculated spline function. At present, there is no convention concerning the shape of the calibration curve, calculated through the calibration data points. See also the discussion by Talma and Vogel (1993).

CAL15 also features powerful graphics to display the calibration data sets, calibration functions calculated by spline and smoothing techniques, test curves and $\Delta^{14}C$ values (see the main menu, Fig. 1). The graphs can be printed or plotted, depending on the selection from the menu. CAL15 runs most efficiently from an AT with VGA/color screen and hard disk. Program size is 180 kb. It also works on an XT or without a hard disk, albeit considerably slower. Saving graphs to disk is not practical without a hard disk, since abundant disk space is required (up to 45 kb for VGA screens). The program and necessary data files can be obtained from the Groningen Laboratory.

REFERENCES

Aitchison T. C., Leese, M., Michczynska, D. J., Mook, W. G., Otlet, R. L., Ottaway, B. S., Pazdur, M. F., van der Plicht, J., Reimer, P. J., Robinson, S. W., Scott, E. M., Stuiver M. and Weninger, B. 1989 A comparison of methods used for the calibration of radiocarbon dates. *In* Long, A., Kra., R.S., eds., Proceedings of the 13th International ^{14}C Conference. *Radiocarbon* 31(3): 846–862.

Borland 1989 Turbo Pascal. Scotts Valley, California 95066 USA.

de Vries, H. 1958 Variation in concentration of radiocarbon with time and location on earth. *Proceedings Koninklijke Nederlandse Akademie van Wetenschappen* 61(B): 1–9.

Dehling, H. and van der Plicht, J. 1993 Statistical problems in calibrating radiocarbon dates. *Radiocarbon*, this issue.

Mook, W. G. 1983 ^{14}C calibration curves depending on sample time width. *In* Mook, W. G. and Waterbolk, H. T., eds., Proceedings of the International Symposium on ^{14}C and Archaeology. *PACT* 8: 517–525.

Reinsch, C. H. 1967 Smoothing by spline functions. *Numerische Mathematik* 10: 177–183.

Stuiver, M. and Kra, R. S., eds., 1986 Calibration Issue. Proceedings of the 12th International ^{14}C Conference. *Radiocarbon* 28(2B): 805–1030.

Stuiver, M. and Reimer, P. J. 1986 A computer program for radiocarbon age calculation. *In* Stuiver, M. and Kra, R.S., eds., Proceedings of the 12th International ^{14}C Conference. *Radiocarbon* 28(2B): 1022–1030.

Stuiver, M., Braziunas F., Becker, B. and Kromer, B. 1991 Climatic, solar, oceanic and geomagnetic influences on Late-Glacial and Holocene atmospheric $^{14}C/^{12}C$ change. *Quaternary Research* 35: 1–24.

Stuiver, M., Long A. and Kra, R. S., eds., 1993 Calibration Issue 1993. *Radiocarbon*, this issue.

Suess, H. E. 1970 The three causes of secular C14 fluctuations, their amplitudes and time constants. *In* Olsson, I.U. ed., *Radiocarbon Variations and Absolute Chronology*. Proceedings of the 12th Nobel Symposium. Stockholm, Almqvist & Wiksell, p. 595–605.

Talma, A. S. and Vogel, J. C. 1993 A simplified approach to calibrating ^{14}C dates. *Radiocarbon* 35(3): in press.

van Geel, B. and Mook, W. G. 1989 High-resolution ^{14}C dating of organic deposits using natural atmospheric ^{14}C variations. *Radiocarbon* 31(2): 151–155.

van der Plicht, J. and Mook, W. G. 1987 Automatic radiocarbon calibration: Illustrative examples. *Palaeohistoria* 29: 173–182.

_____ 1989 Calibration of radiocarbon ages by computer. *In* Long, A. and Kra, R. S., eds., Proceedings of the 13th International ^{14}C Conference. *Radiocarbon* 31(3): 805–816.

van der Plicht, J., Mook, W. G. and Hasper, H. 1990 Automatic calibration of Radiocarbon Ages. *In* Mook W. G. and Waterbolk, H. T., eds., Proceedings of the Second International Symposium on ^{14}C and Archaeology. *PACT* 29: 81–94.

Willis, E. H., Tauber, H. and Münnich, K. O. 1960 Variations in the atmospheric radiocarbon concentration over the past 1300 years. *American Journal of Science Radiocarbon Supplement* 2: 1–4.

[RADIOCARBON, VOL. 35, NO. 1, 1993, P. 239–244]

STATISTICAL PROBLEMS IN CALIBRATING RADIOCARBON DATES

HEROLD DEHLING

Mathematics Department, University of Groningen, Blauwborgje 3, 9747 AG, The Netherlands

and

JOHANNES VAN DER PLICHT

Centre for Isotope Research, University of Groningen, Nijenborgh 4, 9747 AG, The Netherlands

INTRODUCTION

The transformation of radiocarbon years to calendar years (cal AD/BC) is not straightforward because of past variations in atmospheric ^{14}C content (de Vries 1958; Suess 1970). A calibration curve, $y = f(x)$, transforms each dendrochronologically dated calendar age (x) to a ^{14}C date (y). By inverting this relationship, one can determine the calibrated calendar age of a given sample. In some time intervals, the calibration curve is problematic in that $f(x)$ is not uniquely invertible (Fig. 1); even an exact measurement of y cannot be converted to a single calendar age (see examples in van der Plicht & Mook (1987)).

The most widely distributed calibration programs are those of Seattle (Stuiver & Reimer 1986) and Groningen (van der Plicht & Mook 1989). Calibration procedures in both programs are essentially the same (Aitchison *et al.* 1989). Questions have been raised about the validity of mathematical procedures underlying the calibrations. Here we discuss problems in the statistical theory to derive correct expressions of the error limits of a calibrated ^{14}C date.

An important purpose of statistical estimation theory is to provide error limits for estimates given. A ^{14}C age, the result of repeated measurements, can be assigned a sample standard deviation, σ, centered around the arithmetic mean. The key question is how one should transform these error limits in the calibration process. The computer program developed in Groningen (van der Plicht & Mook 1989) uses the error function

$$\varepsilon(y) = \frac{1}{\sqrt{2\pi}} e^{-\frac{(y-\hat{y})^2}{2\sigma^2}} \qquad (1)$$

where y is the true ^{14}C date, $\hat{y}$ is the measurement outcome (the mean value), σ is the standard deviation. The error curve for the ^{14}C age is transformed to an error curve for the calibrated age by $\varepsilon^*(x) = \varepsilon(f(x))$. This procedure differs from "classical probability" density transformations according to $\varepsilon^*(x) = |\,dy/dx\,|\,\varepsilon f(x)$.

Figure 2 illustrates problematic consequences of obtaining probability densities under a monotone transformation $y = f(x)$. Here, consider a piecewise monotone function, with a change in slope at $\hat{y}$ (the outcome of the measurement), as transformation function. Figure 2A shows the result of transforming $y \pm \sigma$ along the x-axis, using the Groningen program. Figure 2B shows the result of the classical transformation. The area under the Gaussian curve is symmetric with respect to the measurement outcome $\hat{y}$. For the calibrated distribution, this is also true for the example shown in Figure 2B, whereas this is not true for the example shown in Figure 2A. Although the two resulting distributions are different, one should not conclude that the program is wrong. This is illustrated

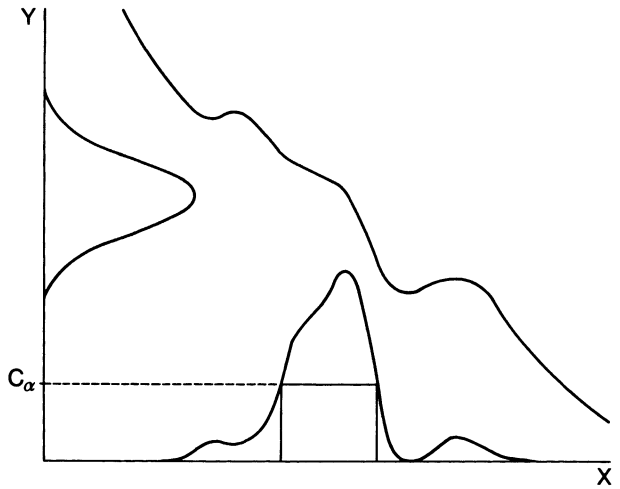

Fig. 1. Example of the ^{14}C calibration procedure: Transformation of a ^{14}C date into a calibrated calendar age probability distribution. The graph shows the calibration curve, $y = f(x)$, the Gaussian probability distribution corresponding to the ^{14}C age along the y-axis, and the calibrated calendar age probability distribution along the x-axis. The confidence limit, c_α, is defined in the text.

in Figure 3, where the transformation function has a horizontal stretch. Figure 3A shows the Groningen result, Figure 3B, the classical result. The latter is counterintuitive; why should the calibrated interval corresponding to the horizontal part of the curve have a near-zero probability, whereas the measurement agrees perfectly with any age in this interval? We aim to resolve this ambiguity by offering a clear interpretation of the error curve being transformed, and shall do this within both classical statistical and Bayesian frameworks.

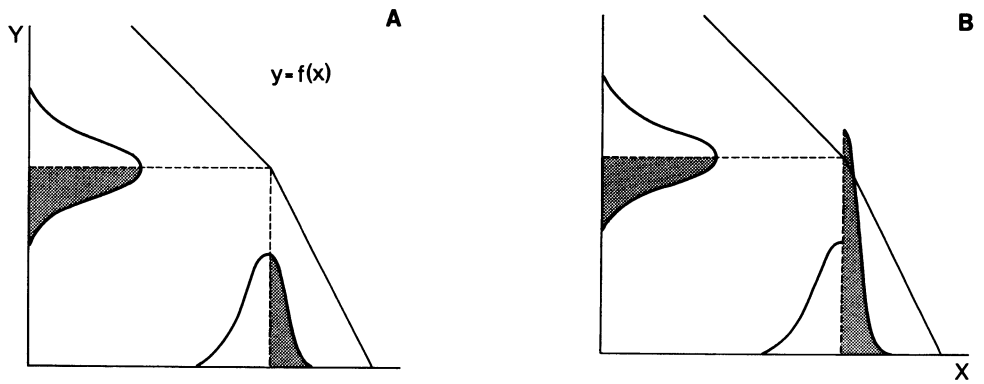

Fig. 2A,B. The calibration paradox (1): Two ways of obtaining a calibrated probability distribution, using an artificial calibration curve

Bayesian methods and classical statistics differ in their approach to statistical inferences. Significance tests, point estimates and confidence limits are essential parts of classical inference, whereas Bayesian inference is expressed as a posterior probability distribution. The fundamental difference between these methods concerns the meaning of probability. The classical objective approach assigns a probability only for events in repeated experiments. In contrast, the Bayesian subjective approach interprets a probability distribution as a degree of belief, in which probabilities can be assigned in situations where the objective approach does not apply.

A Bayesian approach, though subjective, has wider applicability. For instance, two archaeologists examining the same object might have different opinions about the probability that it dates from

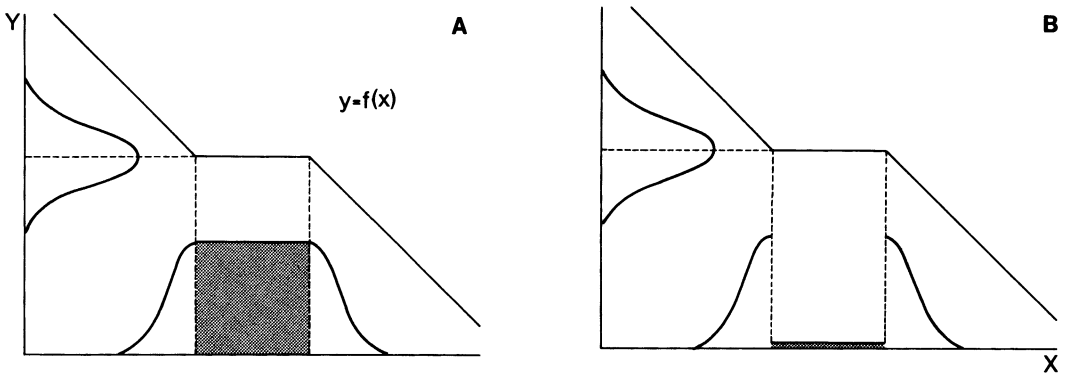

Fig. 3A,B. The calibration paradox (2): Two ways of obtaining a calibrated probability distribution, using an artificial calibration curve

a certain period. If there is no prior information, a common approach would be to assume a uniform distribution. However, the uniform distribution is not invariant under coordinate transformations, so that the choice of coordinate system is somewhat arbitrary. In our calibration example, the uniform distribution along the cal AD/BC axis is different from the uniform distribution along the yr BP axis. This leads to the Bayesian explanation of the aforementioned ambiguity.

A STATISTICAL MODEL FOR ^{14}C MEASUREMENTS

A ^{14}C age measurement is subject to random disturbances. We model this by assuming that the actual measurement, y, is the real value of a random variable with a distribution around the true, but unknown ^{14}C age η. We employ the Gaussian error model, where y has a normal probability density with mean η and variance σ^2:

$$p(y|\eta) = \frac{1}{\sqrt{2\pi\sigma^2}} e^{-\frac{(y-\eta)^2}{2\sigma^2}} \quad . \tag{2}$$

So far, we have viewed the density $p(y|\eta)$ as a function of y for a fixed η. Now, if y is the actual outcome of the measurement, we can study $p(y|\eta)$ as a function of η, given as the so-called likelihood function L. The maximum value of L is the widely used maximum likelihood estimate.

In the Gaussian measurement error model, the likelihood is given by

$$L(\eta) = p(y|\eta) = \frac{1}{\sqrt{2\pi\sigma^2}} e^{-\frac{(\eta-y)^2}{2\sigma^2}} \quad . \tag{3}$$

Note that because of symmetry regarding y and η, the likelihood has exactly the same shape as the density. The Gaussian error curve, drawn along the yr BP axis around y, is the likelihood function.

Using the calibration curve, we reparametrize the model in order to derive calibrated probabilities, relevant to archaeologists. If ξ denotes the true calendar age, the ^{14}C age is given by $\eta = f(\xi)$, and hence, the measured ^{14}C age follows the density:

$$p^*(y|\xi) = p(y|f(\xi)) = \frac{1}{\sqrt{2\pi\sigma^2}} e^{-\frac{(y-f(\xi))^2}{2\sigma^2}} \quad . \tag{4}$$

If we take the calendar age as the model parameter, the likelihood is given by

$$L^*(\xi) = p^*(y|\xi) = p(y|f(\xi)) = L(f(\xi)) \quad . \tag{5}$$

Thus, the likelihood function $L(\eta)$ on the ^{14}C age scale (y-axis) is transformed into the likelihood function $L^*(\xi)$ on the calendar age scale (x-axis).

AN OBJECTIVE APPROACH: CONFIDENCE REGIONS

A point estimate, $\hat{\eta}$ of η, is inadequate in statistical application, because it gives no information about the uncertainty involved. The objective approach expresses this uncertainty as a confidence region R. This function associates, to each outcome y, a set of parameters $C(y) \subset R$. We say that C is a $(1 - \alpha)$ confidence region for η, with $0 < \alpha < 1$, if

$$P_\eta(\{\eta \in C(Y)\}) = \int_{\{y:\eta \in C(y)\}} p(y|\eta)dy = 1-\alpha \tag{6}$$

for all η. This specifies that in a long series of measurements where the true parameter is η, the confidence regions $C(y_1)$, $C(y_2)$, . . . obtained will contain η in about $100(1 - \alpha)\%$ of all cases. For example, for a normal distribution $p(y|\eta)$ with known variance σ^2, the (random) interval $[y - \sigma, y + \sigma]$ is a 68% confidence region, because $C(y)$ will cover the parameter η if the observed value y has a distance less than or equal to σ from η. For any value η of the parameter, the random confidence region, $C(y)$, will cover η with probability $(1 - \alpha)$. From a classical viewpoint, the parameter η either lies in the confidence region C_o or not, but we cannot determine which. Neither could a Bayesian approach compute the probability that $\eta \in C_o$, because this depends essentially on the prior probability.

One approach to obtain confidence limits, based on the likelihood principle, suggests confidence regions given by level sets $C(y) = \{\eta : L_\eta(y) \leq c_\alpha\}$ of the likelihood function. The constant c_α must be chosen in such a way that $C(y)$ is a $(1 - \alpha)$ confidence region.

As observed, error curves drawn on the yr BP and cal AD/BC axes are likelihood functions for ξ and η, respectively. Thus, the $1\ \sigma$ $(2\ \sigma)$ interval on the BP axis, along with the level set on the AD/BC axis, are likelihood-based confidence regions with confidence level 68 (95)%. Now the confidence region for ξ covers the true age ξ if and only if $|f(\xi) - y| \leq \sigma$ $(2\ \sigma)$. But this has again a probability of 68 (95)%, since y follows a normal distribution with mean ξ and variance σ^2.

A BAYESIAN APPROACH

The Bayesian calibration solution provides a basis for interpretation of the error curve (drawn in Figures 2 and 3) as a probability density on the age space. It requires specification of a prior probability density on the parameter space, representing parameter information prior to any measurement. Lindley (1965) and Naylor and Smith (1988) give a thorough treatment of the Bayesian approach. In our situation, either η or ξ must be regarded as the fundamental parameter about which prior assumptions are made. For instance, an archaeologist might, on the basis of

previous samples from a single site, be convinced that this material is from a certain age period. This could be expressed by choosing an appropriate density, either $\pi(\eta)$ for η or $\pi^*(\xi)$ for ξ.

Beginning with $\pi(\eta)$, note that we have a conditional density $p(y|\eta)$, where η is now considered random. If y denotes the observation actually made, we can compute the density of η, given y, using a continuous analog of Bayes' theorem on inverse probabilities

$$\pi(\eta|y) = \frac{p(y|\eta)\pi(\eta)}{\int p(y|\eta)\pi(\eta)d\eta} \quad . \tag{7}$$

$\pi(\eta|y)$ is the posterior density, and it incorporates both our prior information and the measurement result. Alternatively, we can express our prior information with a prior density $\pi^*(\xi)$ on the calendar age. Then the posterior density is given by

$$\pi^*(\xi|y) = \frac{p(y|f(\xi))\pi^*(\xi)}{\int p(y|f(\xi))\pi^*(\xi)d\xi} \quad . \tag{8}$$

A special "improper" case of this is the uniform prior distribution $\pi(\eta) = 1$ ($\pi^*(\xi) = 1$) on the real line, also called the non-informative prior distribution. (Note that this is not a probability density, since $\int_{-\infty}^{\infty} 1\, d\eta = \infty$.) In this case, the posterior probability is formally given by the normalized likelihood function

$$\pi(\eta|y) = \frac{p(y|\eta)}{\int p(y|\eta)\,d\eta} \qquad \left(\pi^*(\xi|y) = \frac{p(y|f(\xi))}{\int p(y|f(\xi))\,d\xi}\right) \quad . \tag{9}$$

In this way, we justify the interpretation of the Gaussian error curve drawn in Figures 2 and 3 as a posterior density on ^{14}C age space, corresponding to a non-informative prior on this space.

As $\pi(\eta|y)$ is a Bayesian density, it must be transformed according to the classical formula for densities

$$\pi^*(\xi|y) = \pi(f(\xi)|y)\cdot|f'(\xi)| \quad . \tag{10}$$

How can we now explain the examples discussed in Figures 2 and 3? As mentioned above, a Bayesian interpretation of the Gaussian error curve (the likelihood function) as a posterior density implicitly assumes a uniform prior distribution $\pi(\eta)$ on the ^{14}C age, and corresponds to a non-uniform prior distribution

$$\pi^*(\xi) = \pi(f(\xi))|f'(\xi)|$$

on the calendar age BC/AD. This accounts for the unusual transformations shown, *e.g.*, in Figure 3B, where the prior $\pi^*(\xi)$ places no mass in the interval where f is constant. Of course, if we choose a prior distribution specifying that the probability of an observation in this range is zero, the posterior density will also place mass zero here. In this light, it seems unreasonable to express the lack of prior information on the age of the sample by a uniform prior distribution on the yr BP axis. However, a uniform prior distribution on the calendar axis would correspond to a non-uniform

prior distribution on yr BP, so that the Gaussian error curve on age BP is no longer the posterior density. But, the curve produced by the calibration programs, being the correct likelihood function, is then, with respect to normalization, the posterior distribution on calendar age, corresponding to the uniform prior on calendar age.

We observe that both the Groningen and classical error curves are posterior densities, the first corresponding to a uniform distribution on cal AD/BC years, the latter to a uniform distribution on yr BP as prior densities. That the latter is an unreasonable prior distribution is evident from Figures 2 and 3.

CONCLUSION

Calibration of radiocarbon dates involves the transformation of a measured ^{14}C age (BP $\pm$ σ) into a calibrated age distribution (cal AD/BC range). Because of the wiggly nature of the calibration curve, the correct procedure to obtain calibrated age ranges and confidence intervals is not straightforward. Mathematical pitfalls can cause calibration procedures to contradict classical formulas.

We show that these ambiguities can be understood in terms of classical and Bayesian approaches to statistical theory. The classical formulas correspond to a uniform prior distribution along the BP axis, the calibration procedure to a uniform prior distribution along the calendar axis. We argue that the latter is the correct choice, *i.e.*, the computer programs used for radiocarbon calibration are correct.

REFERENCES

Aitchison, T. C., Leese, M., Michczynska, D. J., Mook, W. G., Otlet, R. L., Ottaway, B. S., Pazdur, M. F., van der Plicht, J., Reimer, P. J., Robinson, S. W., Scott, E. M., Stuiver M. and Weninger, B. 1989 A comparison of methods used for the calibration of radiocarbon dates. *In* Long, A. and Kra, R. S., eds., Proceedings of the 13th International ^{14}C Conference. *Radiocarbon* 31(3): 846–864.

de Vries, H. 1958 Variation in concentration of radiocarbon with time and location on earth. *Kon. Ned. Acad. Wet. Proc. Ser. B* 61: 1–9.

Lindley, D. V. 1965 *Introduction to Probability Theory and Statistics from a Bayesian Viewpoint.* Cambridge, Cambridge University Press: 2 vols.

Naylor, J. C. and Smith, A. F. M. 1988 An archaeological inference problem. *Journal of the American Statistical Association* 403: 588–595.

Stuiver, M. and Reimer, P. J. 1986 A computer program for radiocarbon age calibration. *In* Stuiver, M. and Kra, R. S., eds., Proceedings of the 12th International ^{14}C Conference. *Radiocarbon* 28(2B): 1022–1030.

Suess, H. E. 1970 The three causes of secular ^{14}C fluctuations, their amplitudes and time constants. In Olsson, I. U., ed., *Radiocarbon Variations and Absolute Chronology.* Proceedings of the 12th Nobel Symposium. Stockholm, Almqvist and Viksell: 595–605.

van der Plicht, J. and Mook, W. G. 1987 Automatic radiocarbon calibration: Illustrative examples. *Palaeohistoria* 29: 173–182.

_____1989 Calibration of radiocarbon ages by computer. *In* Long, A. and Kra, R. S., eds., Proceedings of the 13th International ^{14}C Conference. *Radiocarbon* 31(3): 805–816.

RADIOCARBON Announces the Publication of the Following:

Radiocarbon After Four Decades:
An Interdisciplinary Perspective
Editors: R. E. Taylor, Austin Long and R. S. Kra
Special Hardcover Edition Published by Radiocarbon and
Springer-Verlag, New York
$89.00 List Price; $66.25 for Subscribers to RADIOCARBON

Radiocarbon After Four Decades: An Interdisciplinary Perspective commemorates the 40th anniversary of radiocarbon dating and documents the major contributions of ^{14}C dating to archaeology, biomedical research, earth sciences, environmental studies, hydrology, studies of the natural carbon cycle, oceanography and palynology.

All of the 64 authors played major roles in the development of ^{14}C dating. The 35 chapters provide a solid foundation in the essential topics of ^{14}C dating and include: The Natural Carbon Cycle; Instrumentation and Sample Preparation; Hydrology; Old World Archaeology; New World Archaeology; Earth Sciences; Environmental Sciences; Biomedical Applications; and Historical Perspectives.

Radiocarbon After Four Decades: An Interdisciplinary Perspective serves as a synthesis of past, present and future research in the field. It is offered outside of our regular issues; *RADIOCARBON* subscribers receive a 25% discount off the $89.00 list price and pay only $66.25.

Proceedings of the 14th International Radiocarbon Conference
Tucson, Arizona, 20–24 May 1991
Volume 34, No. 3, 1992 @ $65.00

This Conference Proceedings documents state-of-the-art research in ^{14}C dating and cosmogenic isotopes. It contains papers on recent developments in Sample Preparation and Measurement Techniques, Applied Isotope Geochemistry, Global ^{14}C Production and Variation, Paleoclimatology and Archaeological Applications; Workshop Reports are included. 665 pages. The Proceedings issue is part of the 1992 subscription.

FORTHCOMING . . .

LSC 92: Proceedings of the International Conference on Advances in Liquid Scintillation Spectrometry, 14–18 September 1992, Vienna, Austria. Volume editors: John E. Noakes, Franz Schönhofer and Henry A. Polach.

Applications of Radiocarbon Dating in the Former Soviet Union. Special editor: Jaan-Mati Punning, Tallinn, Estonia. *RADIOCARBON*, Vol. 35, No. 3, 1993.

Late Quaternary Chronology and Paleoclimates of the Eastern Mediterranean. In association with Plenum Publishing Corporation, Interdisciplinary Contributions to Archaeology Series. Volume editors: Ofer Bar-Yosef and Renee Kra.

^{14}C Dynamics in Soils. Special editors: Peter Becker-Heidmann, D. D. Harkness, Eldor Paul and S. E. Trumbore. *RADIOCARBON*, Vol. 36, 1994.

RADIOCARBON
1993 PRICE LIST

New-Calibration 1993 (Vol. 35, No. 1, 1993)	$ 40.00
Proceedings of the 14th International Radiocarbon Conference (Vol. 34, No. 3, 1992)	$ 65.00
Proceedings of the International Workshop on Intercomparison of ^{14}C Laboratories (Vol. 32, No. 3, 1990)	$ 40.00
Proceedings of the 13th International Radiocarbon Conference (Vol. 31, No. 3, 1989)	$ 60.00
Proceedings of the 12th International Radiocarbon Conference (Vol. 28, Nos. 2A & 2B, 1986 – available separately at $30.00 each)	$ 60.00
Proceedings of the 11th International Radiocarbon Conference (Vol. 25, No. 2, 1983)	$ 50.00
Proceedings of the 10th International Radiocarbon Conference (Vol. 22, Nos. 2 & 3, 1980)	$ 60.00
Vol. 35, Nos. 1–3, 1993 (includes NEW Calibration 1993)	**$105.00/vol. Inst.*** **$ 73.50/vol. Ind.** **$ 36.75/vol. Stud.****
Vol. 34, Nos. 1–3, 1992 (includes Proceedings)	$105.00/vol. Inst. $ 73.50/vol. Ind.
Vol. 33, Nos. 1–3, 1991	$ 94.50/vol. Inst. $ 63.00/vol. Ind.
Vol. 32, Nos. 1–3, 1990 (includes Glasgow Proceedings)	$ 94.50/vol. Inst. $ 63.00/vol. Ind.
Vol. 31, Nos. 1–3, 1989 (includes Proceedings)	$ 90.00/vol. Inst. $ 60.00/vol. Ind.
Vol. 30, Nos. 1–3, 1988	$ 85.00/vol. Inst. $ 55.00/vol. Ind.
Vols. 15–29, 1973–1987	$ 75.00/vol. Inst.† $ 50.00/vol. Ind.
Vols. 10–14, 1968–1987	$ 50.00/vol.†
Vols. 1–9, 1959–1967	$ 25.00/vol.
Comprehensive Index (1950–1965)	$ 25.00
Single Issue	$ 25.00
Single copy of out-of-print Issue	$ 35.00

SPECIAL PACKAGE OFFER (now includes 9 out-of-print issues):

Full set, Vols. 1–34 (1959–1992) + *free* subscription for 1993!	$650.00
Postage & handling for Package Offer:	
USA	$ 25.00
Foreign	$ 50.00

***Foreign postage on current volumes $ 10.00**
†Plus additional charge for copy of out-of-print issue(s)
Postage & handling will be added to back orders

****New Student Rate** – with student identification and letter from subscribing sponsor. Back issues available at 1/2 the individual rate.

RADIOCARBON
An International Journal of Cosmogenic Isotope Research

Editor: AUSTIN LONG
Managing Editor: RENEE S. KRA
Assistant Editor: JAMES M. DEVINE
Published by
Department of Geosciences
The University of Arizona

Published three times a year at The University of Arizona, Tucson, AZ 85712 USA.

Subscription rate: $105.00 (for institutions), $73.50 (for individuals), $36.75 (for students with proper identification). Foreign postage is extra. A complete price list, including Proceedings of International Conferences, appears in the back of this issue.

Back issues and price lists may be obtained from the office of *RADIOCARBON*.

All correspondence and manuscripts should be addressed to the Managing Editor, *RADIOCARBON*, Department of Geosciences, The University of Arizona, 4717 East Ft. Lowell Road, Tucson, AZ 85712 USA. Tel: (602) 881-0857; Fax: (602) 881-0554. **Please note our BITNET address: C14@ARIZVMS and INTERNET address: rkra@spider.aml.arizona.edu.**

Offprints. The minimum offprint order for each article will be 100 copies without covers. *No offprints will be furnished free of charge unless page charges are paid.* The cost of additional copies will, of course, be greater if the article is accompanied by plates involving unusual expense. Copies will be furnished with a printed cover giving the title, author, volume, page and year, when specially ordered.

Page charges. Each institution sponsoring research reported in a technical paper or a date list, will be asked to pay a charge of $80.00 per printed page. Institutions or authors paying such charges will be entitled to 100 free offprints without covers. *No charges will be made if the author indicates that the author's institution is unable to pay, and payment of page charges for an article will, in no case, be a condition for its acceptance.*

Missing issues will be replaced without charge only if claim is made within three months (six months for India, New Zealand and Australia) after the publication date. Claims for missing issues will not be honored if non-delivery results from failure by the subscriber to notify the Journal of an address change.

Illustrations should include explanation of symbols used. Copy that cannot be reproduced cannot be accepted. Whenever possible, reduce figures for direct publication. Line drawings should be in black India ink on white drawing board, tracing cloth, or coordinate paper printed in blue and should be accompanied by clear ozalids or reduced photographs for use by the reviewers. Photographs should be positive prints. *Figures* (photographs and line drawings) should be numbered consecutively through each article, using Arabic numerals. **All measurements should be given in SI (metric units).** Tables may be accepted as camera-ready copy.

Citations. A number of radiocarbon dates appear in publications without laboratory citation or reference to published date lists. We ask that laboratories remind submitters and users of radiocarbon dates to include proper citation (laboratory number and date-list citation) in all publications in which radiocarbon dates appear.

Radiocarbon Measurements: Comprehensive Index, 1950–1965. This index covers all published ^{14}C measurements through Volume 7 of *RADIOCARBON*, and incorporates revisions made by all laboratories. It is available at $25.00 per copy.

List of laboratories. Our comprehensive list of laboratories is available upon request. We are expanding the list to include additional laboratories and scientific agencies with whom we have established contacts. The editors welcome information on these or other scientific organizations. We ask all laboratory directors to provide their current telephone, telex, fax numbers and E-mail addresses. Changes in names or addresses, additions or deletions should be reported to the Managing Editor.

NOTICE TO READERS AND CONTRIBUTORS

The purpose of *RADIOCARBON* is to publish technical and interpretative articles on all aspects of ^{14}C and other cosmogenic isotopes, as well as lists of ^{14}C dates produced by various laboratories. In addition, we present regional compilations of published *and unpublished* dates along with interpretative text. Besides the triennial Proceedings of Radiocarbon Conferences, we publish Proceedings of conferences in related fields. Organizers interested in such arrangements should contact the Managing Editor for information.

Our regular issues include NOTES AND COMMENTS, LETTERS TO THE EDITOR, RADIOCARBON UPDATES and ANNOUNCEMENTS. Authors are invited to extend discussions or raise pertinent questions regarding the results of investigations that have appeared on our pages. These sections also include short technical notes to disseminate information concerning innovative sample preparation procedures. Laboratories may also seek assistance in technical aspects of radiocarbon dating. Book reviews are encouraged.

Manuscripts. Papers may be submitted on floppy diskettes and as printed copy. When submitting a manuscript, include three printed copies, double-spaced. When the final copy is prepared after review, please provide a floppy diskette along with one printed copy. We will accept, in order of preference, WordPerfect 5.1 or 5.0, Microsoft Word, Wordstar or any IBM word-processing software program. ASCII files, MS DOS and CPM-formatted diskettes are also acceptable. The diskettes should be either 3½" (720 k or 1.44 mb) or 5¼" (360 k or 1.2 mb). Papers should follow the recommendations in INSTRUCTIONS TO AUTHORS (Radiocarbon, 1992, vol. 34, no. 1, p. 177–185). Offprints are available upon request. Our deadlines for submitting manuscripts are:

For	*Date*
Vol. 35, No. 3, 1993	May 1, 1993
Vol. 36, No. 1, 1994	September 1, 1993
Vol. 36, No. 2, 1994	January 1, 1994

Half-life of ^{14}C. In accordance with the decision of the Fifth Radiocarbon Dating Conference, Cambridge, England, 1962, all dates published in this volume (as in previous volumes) are based on the Libby value, 5568 yr, for the half-life. This decision was reaffirmed at the 11th International Radiocarbon Conference in Seattle, Washington, 1982. Because of various uncertainties, when ^{14}C measurements are expressed as dates in years BP, the accuracy of the dates is limited, and refinements that take some but not all uncertainties into account may be misleading. The mean of three recent determinations of the half-life, 5730 ± 40 yr, (*Nature*, 1962, vol. 195, no. 4845, p. 984), is regarded as the best value presently available. Published dates in years BP can be converted to this basis by multiplying them by 1.03.

AD/BC Dates. In accordance with the decision of the Ninth International Radiocarbon Conference, Los Angeles and San Diego, California, 1976, the designation of AD/BC, obtained by subtracting AD 1950 from conventional BP determinations is discontinued in *RADIOCARBON*. Authors or submitters may include calendar estimates as a comment, and report these estimates as cal AD/BC, citing the specific calibration curve used to obtain the estimate. Calibrated dates should be reported as "cal BP" or "cal AD/BC" according to the consensus of the Twelfth International Radiocarbon Conference, Trondheim, Norway, 1985.

Measuring $\delta^{14}C$. In Volume 3, 1961, we endorsed the notation, Δ (Lamont VIII, 1961), for geochemical measurements of ^{14}C activity, corrected for isotopic fractionation in samples and in the NBS oxalic-acid standard. The value of $\delta^{14}C$ that entered the calculation of Δ was defined by reference to Lamont VI, 1959, and was corrected for age. This fact has been lost sight of, by editors as well as by authors, and recent papers have used $\delta^{14}C$ as the observed deviation from the standard. At the New Zealand Radiocarbon Dating Conference it was recommended to use $\delta^{14}C$ only for age-corrected samples. Without an age correction, the value should then be reported as percent of modern relative to 0.95 NBS oxalic acid (Proceedings of the 8th Conference on Radiocarbon Dating, Wellington, New Zealand, 1972). The Ninth International Radiocarbon Conference, Los Angeles and San Diego, California, 1976, recommended that the reference standard, 0.95 NBS oxalic acid activity, be normalized to $\delta^{13}C = -19‰$.

In several fields, however, age corrections are not possible. $\delta^{14}C$ and Δ, uncorrected for age, have been used extensively in oceanography, and are an integral part of models and theories. Thus, for the present, we continue the editorial policy of using Δ notations for samples not corrected for age.